*Udo Wiesmann, In Su Choi,*
*Eva-Maria Dombrowski*

**Fundamentals of**
**Biological Wastewater Treatment**

*Fundamentals of Biological Wastewater Treatment*. Udo Wiesmann, In Su Choi, Eva-Maria Dombrowski

ISBN: 978-3-527-31219-1

## 1807–2007 Knowledge for Generations

Each generation has its unique needs and aspirations. When Charles Wiley first opened his small printing shop in lower Manhattan in 1807, it was a generation of boundless potential searching for an identity. And we were there, helping to define a new American literary tradition. Over half a century later, in the midst of the Second Industrial Revolution, it was a generation focused on building the future. Once again, we were there, supplying the critical scientific, technical, and engineering knowledge that helped frame the world. Throughout the 20th Century, and into the new millennium, nations began to reach out beyond their own borders and a new international community was born. Wiley was there, expanding its operations around the world to enable a global exchange of ideas, opinions, and know-how.

For 200 years, Wiley has been an integral part of each generation's journey, enabling the flow of information and understanding necessary to meet their needs and fulfill their aspirations. Today, bold new technologies are changing the way we live and learn. Wiley will be there, providing you the must-have knowledge you need to imagine new worlds, new possibilities, and new opportunities.

Generations come and go, but you can always count on Wiley to provide you the knowledge you need, when and where you need it!

*William J. Pesce*
President and Chief Executive Officer

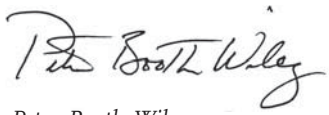

*Peter Booth Wiley*
Chairman of the Board

*Udo Wiesmann, In Su Choi,*
*Eva-Maria Dombrowski*

# Fundamentals of Biological Wastewater Treatment


WILEY-VCH Verlag GmbH & Co. KGaA

**The Authors**

***Prof. Dr.-Ing. Udo Wiesmann***
Technische Universität Berlin
Institut für Verfahrenstechnik
Strasse des 17. Juni 135
10623 Berlin
Germany

***Dr.-Ing. In Su Choi***
Technische Universität Berlin
Institut für Verfahrenstechnik
Strasse des 17. Juni 135
10623 Berlin
Germany

***Prof. Dr.-Ing. Eva-Maria Dombrowski***
Technische Fachhochschule Berlin
Fachgebiet Verfahrenstechnik
und Biotechnologie
Luxemburgerstraße 10
13353 Berlin
Germany



**Library of Congress Card No.: applied for**

**British Library Cataloguing-in-Publication Data**
A catalogue record for this book is available from the British Library.

**Bibliographic information published by the Deutsche Nationalbibliothek**
The Deutsche Nationalbibliothek lists this publication in the Deutsche Nationalbibliografie; detailed bibliographic data are available in the Internet at http://dnb.d-nb.de.



Printed in the Federal Republic of Germany
Printed on acid-free paper

**Typesetting** Fotosatz Detzner, Speyer
**Printing** betz-druck GmbH, Darmstadt
**Bookbinding** Litges & Dopf Buchbinderei GmbH, Heppenheim

**ISBN** 978-3-527-31219-1

# Contents



*Fundamentals of Biological Wastewater Treatment*. Udo Wiesmann, In Su Choi, Eva-Maria Dombrowski

ISBN: 978-3-527-31219-1

# Preface

Clean water is an essential nutrient for humans, animals and plants. Because of its limited resources, especially in countries with low rainfall, little surface water, deep ground water levels and relatively high temperatures, careful use and frequent reuse after appropriate treatment are requirements for healthy life. This awareness is relatively new, because it was not until the late 19th century that the population of larger industrialized cities learned that wastewater must be treated to prevent disease. The reuse of treated water is still a topic of controversial discussions. However, the authors of this book are convinced both that we must learn to develop and continue to promote water recycling systems and also that biological wastewater treatment processes play a highly important role.

The modern concept of industrial wastewater treatment is moving away from the classic "end-of-pipe" technology towards "decentralized effluent treatment processes", "process integrated water management" and ultimately in a number of cases being as close as possible to "fresh water-free processes". The central concept is to save water. In the classic concept, the groups producing intermediate or finished products are relatively isolated from the group which treats the wastewater, frequently treating several different effluents mixed together. This situation characterizes the first period of industrial wastewater treatment. After sampling, the water quality is determined and compared with regulations and the treated water is discharged into surface water. In all but a few exceptional cases, municipal wastewater treatment is performed in this same manner. Frequently, it is more favorable and economical to treat some industrial effluents by using specialized processes ("decentralized effluent treatment"), giving a water quality which makes it possible to reuse one or more water streams and to save fresh water. The next phase of development is to combine production processes and wastewater treatment, often called "process-integrated water management" (sustainable water use, industrial water use, cleaner production, etc.).

Typically, the improvement comes about through a complete change of the production process paradigm to reduce water and energy consumption, as well as waste production. Here, productional and environmental engineers need to cooperate and build one team. In this book, the fundamentals are discussed which are needed to better understand the processes taking place in "end-of-pipe" and

*Fundamentals of Biological Wastewater Treatment*. Udo Wiesmann, In Su Choi, Eva-Maria Dombrowski

ISBN: 978-3-527-31219-1

"decentralized effluent treatment" plants. In the last chapter, examples of "process-integrated water management" and "decentralized treatment" are presented.

Two different wastewater treatment concepts can be followed: either the separation of impurities from water, or the partial or complete mineralization of impurities. Separation processes are based on fluid mechanics (sedimentation, centrifugation, filtration and flotation) or on synthetic membranes (micro-, ultra- and nanofiltration, as well as reverse osmosis). Additionally, physical–chemical processes can be used – like adsorption and coagulation – to separate dissolved or emulsified compounds from water. Impurities can be mineralized by biological and chemical processes (advanced oxidation with ozone, $H_2O_2$, UV, etc.). We want to concentrate our attention on biological processes. Other ones, such as sedimentation or membranes, will be discussed in connection with the activated sludge process and membrane bioreactors.

The main advantages of biological processes in comparison with chemical oxidation are: no need to separate colloids and dispersed solid particles before treatment, lower energy consumption, the use of open reactors, resulting in lower costs, and no need for waste gas treatment.

The advantages of chemical oxidation over biological processes are: no sludge production, mineralization of non-biodegradable compounds and smaller reactor volumes. If it is necessary to remove very large amounts of organics, both processes should be coupled if possible, first the biological step and then the chemical step. We will concentrate our discussion on the fundamentals of biodegradation.

Because of the early development of wastewater technology in industrialized countries, we frequently find "end-of-pipe" treatment plants in industry which simultaneously treat municipal wastewater and vice versa. "Decentralized effluent treatment" plants are initiated only if a large plant would be overloaded or the process would be negatively influenced by hazardous compounds. The main aim is then to optimize the treatment process by using process controls and thereby to reduce the cost of aeration and pumping.

In countries with rapidly growing industries and no municipal treatment plants, the construction and operation of a "decentralized effluent treatment" plant frequently has to be tested for each factory and realized as necessary. An appropriate treatment method should be applied rigorously to enable water reuse in regions with water scarceness or high water prices, for irrigation in agriculture, or as cooling water for power stations or industry. In addition, it is often very important to protect natural water systems used for drinking water supplies, recreation and conservation. Compared with "end-of-pipe" treatment, "decentralized treatment" is often the more economical process.

A better understanding is needed of the biological, physical, ecological, social and economical interactions surrounding water and wastewater. We cannot consider all these aspects, but this book provides important information about the fundamentals and engineering aspects of biological wastewater treatment. The methods used to describe and solve the problems presented are those used by biochemical engineers developing models based on mass balances which are valid for specific systems. The authors made every effort to present mathematical derivations

so comprehensively that at least graduate students can follow. The target group also includes all engineers, biologists and chemists working in the field of wastewater treatment who are interested in learning more about its fundamentals.

After a survey of the historical development of microbiology and wastewater treatment, we give a brief introduction to wastewater characteristics and relevant legislation as well as microbial metabolism and stoichiometry, which is of fundamental importance for mass balances with biological reactions. Gas/liquid oxygen transfer is discussed in detail because of its high importance for all aerobic processes in wastewater treatment. Anaerobic substrate degradation is discussed afterwards as a very interesting alternative for the treatment of high-load effluents. Persistent, industrially produced compounds are not easily treated in biological processes. Therefore, the results of several recent studies are summarized and discussed here. The great significance of nitrogen and phosphorus removal has led us to report about their stoichiometric and kinetic backgrounds individually. In the past two decades, discussions about modelling of the activated sludge process have increased. To gain a better understanding of activated sludge model number 1 (ASM 1) and its description of nitrogen removal, we give detailed explanations. We have dealt with the use of membranes in place of secondary clarifiers to emphasize that new possibilities exist for reusing and recycling water in the future. Therefore, they may be suitable in tandem with the topic of the previous chapters which discuss production-integrated water management and decentralized effluent treatment.

Mrs. Christine Heimerl-Rötsch transcribed our texts several times, as they were updated numerous times. She deserves our high recognition for her thoroughness and punctuality. Dr.-Ing. Gregory Morgan corrected our English. Although we made every effort to compose the text faultlessly, there was still need for improvement. We express our thanks to him.

It would not have been possible to write this book without the numerous discussions with students, graduate students, scientific and chemotechnical co-workers as well as assistants. Thank you all very much for your cooperation!

We realize that not all parts of this book are easy to read, because it was necessary to use a large number of different variables and complicated indices. It was our conviction, however, that this was necessary to avoid misunderstanding and confusion.

Over the past 25 years, many new processes have been tested successfully, a lot of them have gone into operation and a great number of papers have been published in this field. We hope that this book will help provide a better understanding and orientation in the important and interesting field of "Biological Wastewater Treatment".

*The Authors*

## List of Symbols and Abbreviations

| Symbol | Explanation | Unit (example) | Basic unit |
|---|---|---|---|
| A | Surface | $m^2$ | $L^2$ |
| A | Membrane area | $m^2$ | $L^2$ |
| A | Membrane constant | $m\ h^{-1}\ bar^{-1}$ | $L^2\ M^{-1}$ |
| A* | Membrane constant | $g\ m^{-2}\ h^{-1}\ bar^{-1}$ | $L^{-1}$ |
| a | Volume specific surface | $m^2\ m^{-3}$ | $L^2\ L^{-3}$ |
| a | Activity | – | – |
| a | Coefficient | – | – |
| $a_1$, $a_2$, $a_3$ | Constants | – | – |
| B | Membrane constant | $m\ h^{-1}$ | $L\ T^{-1}$ |
| Bi | Biot number | – | |
| $B_v$ | Loading per volume | $g\ m^{-3}\ d^{-1}$ | $M\ L^3\ T^{-1}$ |
| C | Dimensionless concentration | – | – |
| C | Integration constant | | |
| C* | Dimensionless dissolved concentration in equilibrium with gas concentration | – | – |
| C′ | Dimensionless dissolved oxygen concentration | – | – |
| c | Concentration of special gas components in air | $g\ m^{-3}$ | $M\ L^{-3}$ |
| c′ | Dissolved concentration | $g\ m^{-3}$ | $M\ L^{-3}$ |
| c* | Dissolved concentration in equilibrium with gas concentration | $g\ m^{-3}$ | $M\ L^{-3}$ |
| D | Dilution rate | $h^{-1}$ | $T^{-1}$ |
| $D_c$ | Critical dilution rate | $h^{-1}$ | $T^{-1}$ |
| D | Diameter | m | L |
| D | Diffusion coefficient | $m^2\ h^{-1}$ | $L^2\ T^{-1}$ |
| DC | Desorption capacity | $g\ m^{-3}\ h^{-1}$ | $M\ L^{-3}\ T^{-1}$ |
| $D_x$ | Dispersion coefficient in x direction | $m^2\ h^{-1}$ | $L^3\ T^{-1}$ |

*Fundamentals of Biological Wastewater Treatment*. Udo Wiesmann, In Su Choi, Eva-Maria Dombrowski

ISBN: 978-3-527-31219-1

| Symbol | Explanation | Unit (example) | Basic unit |
|---|---|---|---|
| $Da_{II}$ | Damköhler number II (= $\mu_{max} t_v$) | – | |
| d | Diameter | m | L |
| $d_h$ | Hydraulic diameter | m | – |
| E | Efficiency | kg $(kWh)^{-1}$ $O_2$ | $L^{-2} T^2$ |
| E | Density of residence time | – | |
| $E^*$ | Dimensionless efficiency | – | – |
| $e_A$ | Energy of activation | kJ $mol^{-1}$ | $M L^2 T^{-2} N^{-1}$ |
| F | Residence time distribution | – | |
| $F_{O_2}$ | Power of resistence of oxygen molecules | – | |
| $f_i$ | Portion of inert biomass related to the total biomass | – | |
| $f_p$ | Portion of particulate products related to biomass | – | – |
| $\Delta G^0$ | Difference of free reaction enthalpy | kJ $mol^{-1}$ | $M L^2 T^{-2} N^{-1}$ |
| g | Earth acceleration | m $s^{-2}$ | $L T^{-2}$ |
| h | Distance of the stirrer from the bottom | m | |
| $\Delta H^0$ | Difference of enthalpy | kJ $mol^{-1}$ | $M L^2 T^{-2} N^{-1}$ |
| H′ | Henry coefficient | g $L^{-1}$ $bar^{-1}$ | $M L^{-1} T^{-2}$ |
| H | Henry coefficient | – | |
| $H_g$ | Henry coefficient | atm $(mol/l)^{-1}$ | $N L^{-2} M^{-1} L^{-3}$ |
| H | "Height" of deep tanks | | |
| H | Height | m | L |
| I | Strength of a electric current | A | S |
| i | Strength of electric carrent | A | |
| $i_{XB}$ | Nitrogen in bacteria related to mass of bacteria and slowly biod. susbstrate | – | – |
| $i_{XP}$ | Nitrogen in bacteria related to particular inert organic matter | – | – |
| J | Specific mass transfer rate (volume flux) | g $m^{-2}$ $s^{-1}$<br>mol $m^{-2}$ $s^{-1}$ | $M L^{-2} T^{-1}$<br>$N L^{-2} T^{-1}$ |
| $J_D$ | Diffusion flux | g $m^{-2}$ $s^{-1}$ | $M L^{-2} T^{-1}$ |
| $J_{D+C}$ | Flux for diffusion and convection | g $m^{-2}$ $s^{-1}$ | $M L^{-2} T^{-1}$ |
| $J_o$ | Standard volume flux | L $m^{-2}$ $bar^{-1}$ $s^{-1}$ | $M T^{-3}$ |
| K | Total mass transfer coefficient | $h^{-1}$ | $T^{-1}$ |
| K | Bolzmann constant | $1.38 \times 10^{-23}$ J $K^{-1}$ | $M L^2 T^{-2} \theta$ |
| K′ | Saturation coefficient for oxygen | mg $L^{-1}$ | $M L^{-3}$ |
| $K_D$ | Dissoziation constant | – | – |

| Symbol | Explanation | Unit (example) | Basic unit |
|---|---|---|---|
| $K_e$ | Equilibrium constant | – | – |
| $K'_e$ | Equilibrium constant | L $mg^{-1}$ | $L^3$ $M^{-1}$ |
| $K_{iH}$, $K_i$ | Coefficients for excess substrate inhibition | mg $L^{-1}$ | M $L^{-3}$ |
| $K_{iN}$ | Coefficient of non-competitive inhibition | mg $L^{-1}$ | M $L^{-3}$ |
| $K_L$ | Overall mass transfer coefficient | m $h^{-1}$ | L $T^{-1}$ |
| $K_La$ | Specific overall mass transfer coefficient | $h^{-1}$ | $T^{-1}$ |
| $K_m$ | Michaelis–Menten coefficient | mol $L^{-1}$ | N $L^{-3}$ |
| $K_m$ | Equilibrium constant | – | – |
| $K_{OH}$ | Saturation coefficient for hydrolysis | mg $L^{-1}$ | M $L^{-3}$ |
| $K_P$ | Henry coefficient | bar L $g^{-1}$ | M T $L^{-1}$ |
| $K_S$ | Saturation coefficient for substrate | mg $L^{-1}$ | M $L^{-3}$ |
| $K_{SH}$ | Saturation coefficient | – | – |
| k | Coefficient for dry air (= 0.2857) | – | – |
| k | Coefficient of reaction rate | $h^{-1}$ | $T^{-1}$ |
| $k_o$ | Theoretical maximal value of reaction rate for $T \rightarrow \infty$ | – | – |
| $k_L$ | Mass transfer coefficient for liquid boundary | m $h^{-1}$ | L $T^{-1}$ |
| $k_La$ | Specific mass transfer coefficient for liquid boundary | $h^{-1}$ | $T^{-1}$ |
| $k_G$ | Mass transfer coefficient for gaseous boundary | m $h^{-1}$ | L $T^{-1}$ |
| $k_Ga$ | Specific mass transfer coefficient for gaseous boundary | $h^{-1}$ | $T^{-1}$ |
| $k_d$ | Decay coefficient | $h^{-1}$ | $T^{-1}$ |
| $k_s$ | Coefficient of bacteria dying | $h^{-1}$ | $T^{-1}$ |
| $k_e$ | Coefficient of endogeneous respiration | $h^{-1}$ | $T^{-1}$ |
| L | Length | m | L |
| L | Biofilm thickness | m | L |
| $LD_{50}$ | Mass of a compound per mass of living test organism, fatal to one-half of population if delivered rapidly | mg $kg^{-1}$ | – |
| M | Molmass | g $mol^{-1}$ | M $N^{-1}$ |
| m | Mass | g | M |
| N | Amount of moles | mol | N |

| Symbol | Explanation | Unit (example) | Basic unit |
|---|---|---|---|
| n | Speed of a stirrer | $s^{-1}$ | $T^{-1}$ |
| $n_i$ | Number of droplets | – | – |
| $n_R$ | Recycle ratio | – | – |
| $n_E$ | Thickening degree | – | – |
| $n_{PHB}$ | Fraction of PHB inside of bacteria | | |
| n | Number of stages of a cascade | – | – |
| OC | Specific oxygenation capacity | mol $L^{-1}$ $h^{-1}$ | N $L^{-3}$ $T^{-1}$ |
| OTR | Oxygen transfer rate | g $O_2$ $L^{-1}$ $h^{-1}$ | M $L^{-3}$ $T^{-1}$ |
| OTE | Oxygen transfer efficiency | – | – |
| P | Power demand | kW | M $L^2$ $T^{-3}$ |
| p | Pressure | bar | M $L^{-1}$ $T^{-2}$ |
| Q | Flow rate | $m^3$ $h^{-1}$ | $L^{-3}$ $T^{-1}$ |
| R | Radius | m | L |
| R | Gas constant [= 8.314 J (mol K)$^{-1}$] | J (mol K)$^{-1}$ | M $L^2$ $T^{-2}$ $N^{-1}$ $\theta^{-1}$ |
| R | Resistance | $m^{-1}$ | $L^{-1}$ |
| R | Retention coefficient | % | |
| $R_t$ | True retention coeffcient | % | |
| r | Reaction rate | mg $L^{-1}$ $h^{-1}$ | M $L^{-3}$ $T^{-1}$<br>N $L^{-3}$ $T^{-1}$ |
| r′ | Respiration rate | g $L^{-1}$ $h^{-1}$ | M $L^{-3}$ $T^{-1}$ |
| $r_x$ | Growth rate of bacteria | g $L^{-1}d^{-1}$ MLSS | M $L^{-3}$ $T^{-1}$ |
| S | Concentration of substrates | mg $L^{-1}$[1)], mol $L^{-1}$ | M $L^{-3}$, $NL^{-3}$ |
| SOTR | Standardized oxygen transfer rate | mg $L^{-1}$ $h^{-1}$ | M $L^{-3}$ $T^{-1}$ |
| $S^*$ | Dimensionless dissolved oxygen concentration (= S′/K′) | – | – |
| S | Selectivity | – | – |
| T | Temperature | K, °C | θ |
| t | Time | h | T |
| $t_R$ | Mean retention time | h | T |
| $t_{RC}$ | Critical mean retention time | h | T |
| $t_{RX}$ | Mean retention time of bacteria (= sludge age) | h | T |
| $t_{RXC}$ | Critical sludge age | h | T |
| U | Voltage | V | M $L^2$ T $A^{-1}$ |
| V | Volume | $m^3$ | $L^3$ |
| v | Velocity | m $s^{-1}$ | L $T^{-1}$ |
| w | Flow rate | m $s^{-1}$ | L $T^{-1}$ |

[1)] $BOD_5$, COD, DOC etc.

| Symbol | Explanation | Unit (example) | Basic unit |
|---|---|---|---|
| $\bar{w}$ | Gaging void velocity | | |
| $\bar{w}$ | Mean velocity | $m\ s^{-1}$ | $L\ T^{-1}$ |
| X | Concentration of bacteria | $g\ L^{-1}$ MLSS | $M\ L^{-3}$ |
| $X^*$ | Dimensionless bacteria concentration (= X/K′) | – | – |
| x | Local coordinate | m | L |
| x | Mole fraction | – | – |
| y | Mole fraction | – | – |
| $y_{X\text{-}O/X\text{-}C}$ | Mole fraction oxygen/carbon in bacteria | – | – |
| Y | Yield coefficient | – | – |
| $Y^o_{X/S}$ | True yield coefficient growth of bacteria/used substrate | $g\ MLSS\ (g\ COD)^{-1}$ | – |
| $Y^o_{XC/SC}$ | True yield coefficient growth of bacteria carbon/used substrate | $g\ C\ (g\ DOC)^{-1}$ | |
| $Y_{X/S}$ | Apparent yield coefficient growth of bacteria/used substrate | $g\ MLSS\ (g\ COD)^{-1}$ | – |
| Z | Dimensionless local coordinate | – | – |
| z | Local coordinate | m | L |
| Bi | Biot number | $(= w\ d\ D^{-1})$ | |
| Da | Damköhler number | $(\equiv \mu_{max}\ t_R)$ | |
| $Da_{II}$ | Damköhler number II | $(\equiv \mu_{max}\ R^2\ D^{-1})$ | |
| Fr | Froude number | $(\equiv n^2\ d\ g^{-1})$ | |
| Mo | Monod number | $(\equiv S_o\ K_S^{-1})$ | |
| Mo′ | Modified Monod number | $(\equiv c^*\ k'^{-1})$ | |
| Ne | Newton number | $(\equiv P\ d^{-5}\ n^{-3}\ g^{-1})$ | |
| Pe | Peclet number | $(\equiv w\ d\ D^{-1})$ | |
| Pe′ | Modified Peclet number | $(\equiv \bar{w}\ L\ D_x^{-1})$ | |
| Re | Reynolds number | $(\equiv \bar{w}\ d\ v^{-1})$ | |
| Sc | Schmidt number | $(\equiv v\ D^{-1})$ | |
| Sh | Sherwood number | $(\equiv k_L\ d\ D^{-1})$ | |
| Sm | Semenov number | $(\equiv k_L a\ \mu_{max}^{-1})$ | |
| Y | Oxygen transfer number | $\left(\equiv \frac{K_L a V}{d^3}\left(\frac{v}{g^2}\right)^{1/3}\right)$ | |

| Symbol | Explanation | | |
|---|---|---|---|
| **Greek Symbols** | | | |
| $\alpha$ | Conversion, removal ratio | – | – |
| $\alpha_w$ | Relation of specific mass transfer coefficient wastewater/clean water | – | – |
| $\beta$ | Separation coefficient of a settler | – | – |
| $\beta$ | Osmotic coefficient | – | – |
| $\beta_w$ | Relation dissolved oxygen concentration at 20 °C wastewater/clean water | – | – |
| $\gamma$ | Activity coefficient | – | – |
| $\gamma_w$ | $\alpha_w \beta_w$ relation maximal oxygen mass transfer rate at 20 °C wastewater/clean water | – | – |
| $\delta$ | Boundary layer thickness | m | L |
| $\varepsilon$ | Porosity | – | – |
| $\eta$ | Rate of hydrolosis by anoxic bacteria related to rate of hydrolosis by aerobic bacteria | – | – |
| $\eta$ | Efficiency coefficient | – | – |
| $\eta$ | Dynamic viscosity | $g\ m^{-1}\ s^{-1}$ | $M\ L^{-1}\ T^{-1}$ |
| $\theta$ | Coefficient, describing an influence of temperature | – | – |
| $\mu$ | Specific growth rate | $d^{-1}$ | $T^{-1}$ |
| $\mu$ | Tortousity | – | – |
| $\mu_{O_2}$ | Velocity of diffusing oxygen molecules | $m\ s^{-1}$ | $L\ T^{-1}$ |
| $\nu$ | Kinematic viscosity | $m^2\ s^{-1}$ | $L^2\ T^{-1}$ |
| $\xi$ | Resistance coefficient | – | – |
| $\pi$ | Number in analysis of dimensions | – | – |
| $\pi$ | Osmotic pressure | bar | $M\ L^{-1}\ T^{-2}$ |
| $\rho$ | Density | $g\ m^{-3}$ | $M\ L^{-3}$ |
| $\Sigma$ | Sum | – | – |
| $\sigma$ | Surface tension | $N\ m^{-1}$ | $M\ T^{-2}$ |
| $\sigma$ | Dimensionless variance | – | – |
| $\sigma^*$ | Dimensionless surface tension | – | – |
| $\sigma_t$ | Variance according time | s | T |
| $\tau$ | Dimensionless time | – | – |
| $\varphi$ | Phase angle of electric current | – | – |

| Symbol | Explanation |
|---|---|
| **Indices** | |
| arith | Arithmetic mean value |
| A | Active autotrophs |
| A | Air |
| Alk | Alkaline |
| a | Adsorption |
| a | Behind reactor |
| a | Air |
| ae | Aerobic |
| an | Anaerobic |
| ap | Apparent |
| ax | Anoxic |
| b | Back |
| b | Blower |
| c | Cake |
| cat | Catalyst |
| cf | Cross flow |
| C | Convective |
| $CO_2$-O | $CO_2$-oxygen |
| $CO_2$-C | $CO_2$-carbon |
| $CO_2$-C/S-C | $CO_2$-C/substrate-carbon |
| $CO_2$-O/S-O | $CO_2$-O/substrate-oxygen |
| $CO_2$-N | $CO_2$ needed for neutralisation of $H^+$ formed by $NH_4$-N oxidation |
| Σ | Summary |
| d | Daily |
| d | Decay |
| d | Diameter |
| d | Dissolved |
| D | Denitrifyers |
| D | Diffusion |
| DO | Dodecan |
| D+C | Diffusion and convection |
| e | Effluent |
| e | Endogenous |
| eff | Effective |
| ex | Excess |
| E | Enzyme |
| ES | Enzyme–substrate complex |
| ET5 | Emulgin ET5 |

| Symbol | Explanation |
|---|---|
| f | Fouling |
| f | Foreign |
| f | Free of oxygen |
| g | Gear |
| G | Gas |
| G | Generation |
| H | Active heterotrophs |
| H | Hydrolysis |
| i | Impuls |
| i | Inert |
| i | Inhibitor |
| i,j | Component |
| L | Liquid |
| max | Maximal |
| m | Membrane |
| m | Motor |
| M | After mixure |
| M | Mixing point |
| ML | Mixed liquid |
| MLSS | Mixed liquid suspended solids |
| N | Nitrogen |
| N | secondary materials |
| NB | *Nitrobacter* |
| ND | dissolved organic nitrogen |
| NH | Dissolved $NH_3$ and $NH_4$ |
| $NH_4$-$O_2$ | Oxygen used for $NH_4$ oxydation |
| $NH_4$-N | Nitrogen in ammonia |
| NS | *Nitrosomonas* |
| NO | Nitrate and nitrite nitrogen |
| $NO_2$ | Nitrite |
| $NO_3$ | Nitrate |
| NS | Nitrosomonas |
| o Influent | Standardized to $c' = 0$ mg $L^{-1}$ |
| org.P | Dissolved organic phosphorous |
| oTS | Organic dry matter |
| $O_2$ | Oxygen |
| p | Permeate |
| p | Particulate product |
| po | Pore |
| pw | Process water |
| P | Phosphorus |

| Symbol | Explanation |
|---|---|
| PM | Primary materials |
| PO4 | Orthophosphate |
| P-P | Dissolved inorganic polyphosphate |
| rt | Rapid test |
| R | Reactor |
| R | Recycle |
| s | Substrate |
| spec | Specific |
| S | Sewage |
| SC | Substrate-carbon |
| SO | Substrate-oxygen |
| SS | Readily biodegradable substrate |
| St | Standard test |
| t | Total |
| th | Theoretical |
| T | Temperature |
| v | Related to volume |
| VOC | Volatile organic carbon |
| w | Water |
| XA | Biomass of autotrophs |
| XH | Biomass of heterotrophs |
| X | Local coordinate |
| XC | Bacteria mass-carbon |
| XO | Bacteria mass-oxygen |
| XC/XO | Carbon in bacteria mass/oxygen in bacteria mass |
| XC/SC | Carbon in bacteria mass/carbon in substrate |
| $X/O_2$ | Bacteria mass/oxygen |
| X/S | Bacteria mass/substrate |
| z | Local coordinate |
| 0 | Influent |

**Numbers as Indices**

| | |
|---|---|
| 20 | Temperature of 20 °C |
| * | Saturation |
| – | Mean value |
| 20 | Applied to 20 °C |
| 20,0 | Applied to 20 °C and $c' = 0$ mg $O_2$ $L^{-1}$ dissolved oxygen |

| Symbol | Explanation |
|---|---|
| **Abbreviations** | |
| AAO | Anaerobic Anoxic Oxic |
| ADP | Adenosin diphosphate |
| AO | Anaerobic Oxic |
| ASM | Activated sludge model |
| ASCE | American Society of Civil Engineers |
| ATP | Adenosine triphosphate |
| ATV | Abwasser Technische Vereinigung |
| BOD | Biological oxygen demand |
| BWB | Berliner Wasserbetreiber |
| CA | Cellulose acetate |
| CFD | Computational fluid dynamics |
| COD | Chemical oxygen demand |
| CSTR | Completely stirred tank reactor |
| DNA | Deoxyribonucleic acid |
| DMSO | Dimethylsulfonoxide |
| DOC | Dissolved organic carbon |
| DWA | Deutsche Vereinigung für Wasserwirtschaft, Abwasser und Abfall e.V. |
| DVWK | Deutscher Verband für Wasserwirtschaft und Kulturbau e.V. |
| EDS | Endocrine disrupting substances |
| EPA | Environmental Protection Agency |
| EPS | Extracellular polymer substances |
| FM | Ratio of feed to biomass |
| LDS | Lignin degradation system |
| MAP | Magnesium ammonium phosphate |
| MBR | Membrane bioreactor |
| MLSS | Mixed liquor suspended solid |
| MLVSS | Mixed liquor volatile suspended solid |
| NDSA | Naphtalene disulfonic acid |
| NSA | Naphtalene sulfonic acid |
| PA | Polyamide |
| PAN | Polyacrylnitrile acid |
| PAO | Phosphate-accumulating organism |
| PES | Polyethensulphone |
| PFU | Plug-forming unit |
| PHB | Polyhydroxybutyrate |
| PP | Polypropylen |
| PSU | Polysulphone |
| PUDF | Polyvinylidenfluoride |

| Symbol | Explanation |
|---|---|
| RB5 | Reactive black 5 |
| RDR | Rotating disc reactor |
| RNA | Ribonucleic acid |
| SCP | Single-cell protein |
| SRB | Sulfur-reducing bacteria |
| SS | Suspended solid |
| UASB | Upflow anaerobic sludge blanket |
| VFA | Volatile fatty acid |
| VOC | Volatile organic compound |
| WWTP | Wastewater treatment plant |

# 1
# Historical Development of Wastewater Collection and Treatment

## 1.1
## Water Supply and Wastewater Management in Antiquity

One of the most ancient systems of wastewater management was constructed in Mohenjo-Daro near the river Indus (Pakistan) at about 1500 BC. Some centuries later, the river moved its course and obviously the town was given up and covered by sand during the following decades. In the 1930s and 1940s, this early high civilization was newly discovered. Private and public houses were equipped with toilets. Water used for washing and bathing as well as rain water flowed through special grooves into canals which were built with the necessary slope to transport the water into the river Indus. These installations demonstrate a high hygienic standard of an early culture.

The main wastewater collector, the Cloaca Maxima, in Rome presumably follows the course of an old ditch which was used at about 500 BC as a collector for wastewater. But soon it was insufficient to handle the flow of wastewater. Therefore, it was enlarged in the following centuries, extended and roofed over (Lamprecht 1988). Archaeological studies presented a nearly complete picture of its line starting from near the Forum Augustum and flowing into the Tiber near the Ponto Palatino. During the time of the emperors (31 BC to 193 AD), the canal could be traveled by boat and could be entered via manholes. The canal has a breadth up to 3.2 m and a height of up to 4.2 m (Fig. 1.1).

In Hellenistic and Roman times, several water supply systems were constructed for Pergamon castle, which is situated on a rock with an 800 m long plateau, at a height of nearly 300 m over the town situated below it. We are here only interested in one of these systems: the Madradag pipe 2 constructed during the rule of Eumenas II (197–159 BC; Garbrecht 1987). This pipe had a length of 42 km and started in the Madradag mountains at a height of 1230 m, that is 900 m higher than the rock of Pergamon. Three valleys had to be crossed and afterwards the Pergamon rock had to be climbed. Therefore, the pipe had to be operated under pressure. This was an extremely demanding requirement for the quality of pipe manufacturing, laying and sealing. The difference in the height of 900 m (from source to castle) corresponding to a pressure drop of 90 bar (9 MPa) alone for the nonflowing water column. Therefore, very stringent requirements had to be met. The pipes

*Fundamentals of Biological Wastewater Treatment*. Udo Wiesmann, In Su Choi, Eva-Maria Dombrowski

ISBN: 978-3-527-31219-1

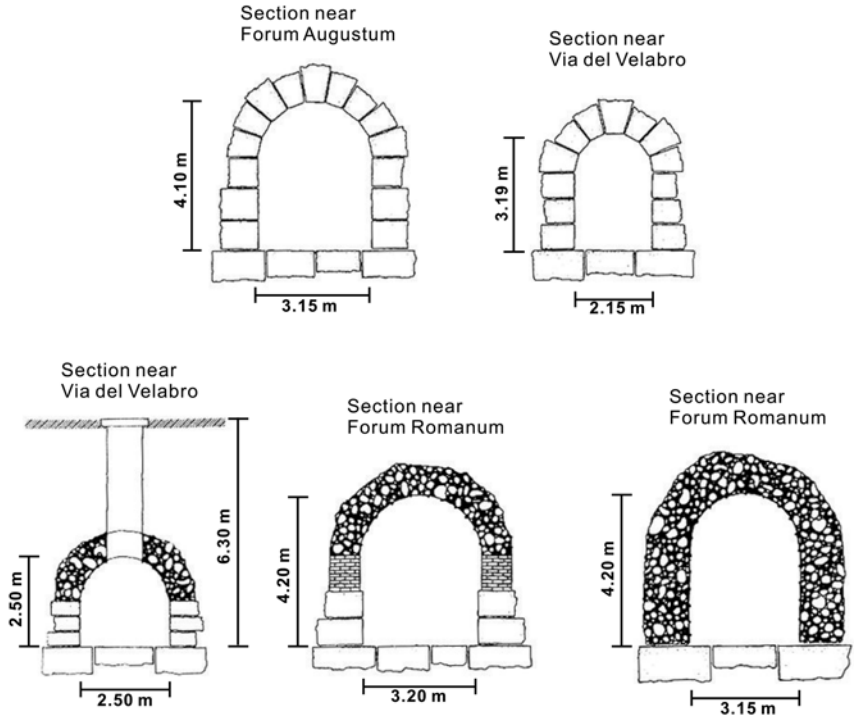


**Fig. 1.1** Cloaca Maxima in Rome, sections of the wastewater collector (Lamprecht 1988).

**Fig. 1.2** Main street with main wastewater collector below the town at the top of the castle of Pergamon (Garbrecht 1987).

were manufactured from fired clay and had a diameter of 16–19 cm. A mean flow rate 15 L $s^{-1}$ can be assumed. Initially, only one pipe was needed, but later on, two further pipes of nearly the same diameter were laid in parallel. This made possible an increase in the flow rate to nearly 45 L $s^{-1}$ or 162 $m^3$ $h^{-1}$.

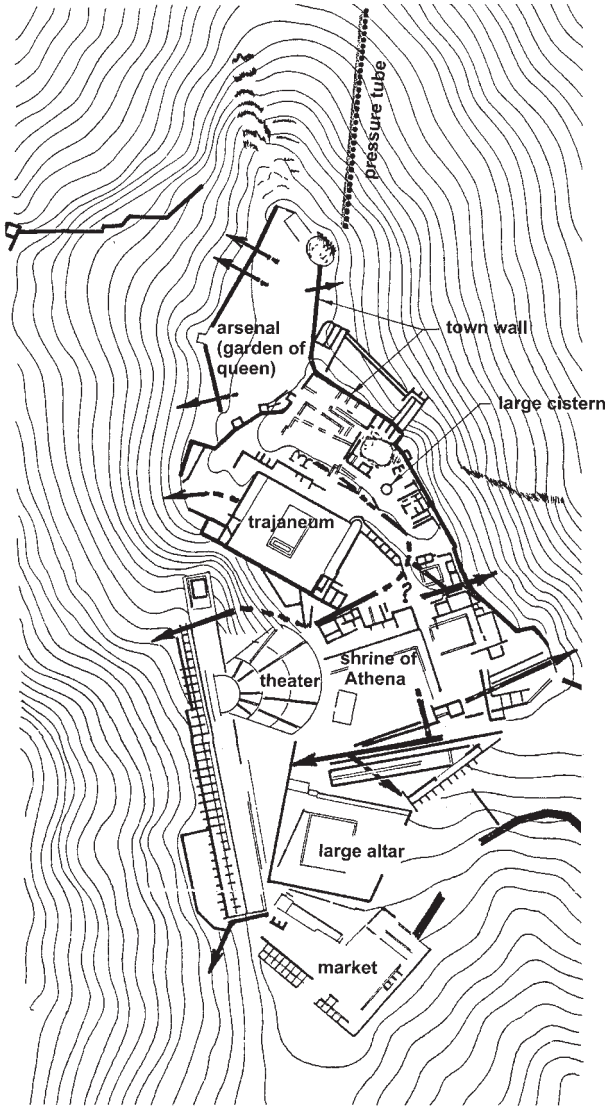


**Fig. 1.3** Main wastewater collector with pipes for wastewater discharge at the castle of Pergamon (Garbrecht 1987).

A system for wastewater management was needed for such a high flow rate of fresh water. The resulting wastewater was collected in carefully masoned collectors laid below a main street covered by rectangular stone plates (Fig. 1.2).

The wastewater flowed from different palaces, temples, public buildings and private houses through clay pipes or open ditches. As a result of the growing flow rate, the cross-section had to be increased from 0.45–0.90 $m^2$ to 1.05–1.70 $m^2$ in places (Garbrecht 1987).

To keep the water from draining away at only one place at the end of the collector, discharge pipes took up the wastewater at various points and conducted it to the edge of the rock. From these points it fell below (Fig. 1.3).

## 1.2
## Water Supply and Wastewater Management in the Medieval Age

Monasteries founded by Cistercians, Premonstratensians and Benedictines in Europe during the 12th and 13th centuries were exemplary business undertakings for that time. Besides the monks and the abbot, numerous lay persons worked and prayed there, all requiring a reliable source of water. Frequently, a monastery was placed near a river and a ditch was dug, which was laid with a necessary gradient through the area of the monastery. Figure 1.4 presents a system for water supply and wastewater discharge as a fundamental concept (Bond 1991).

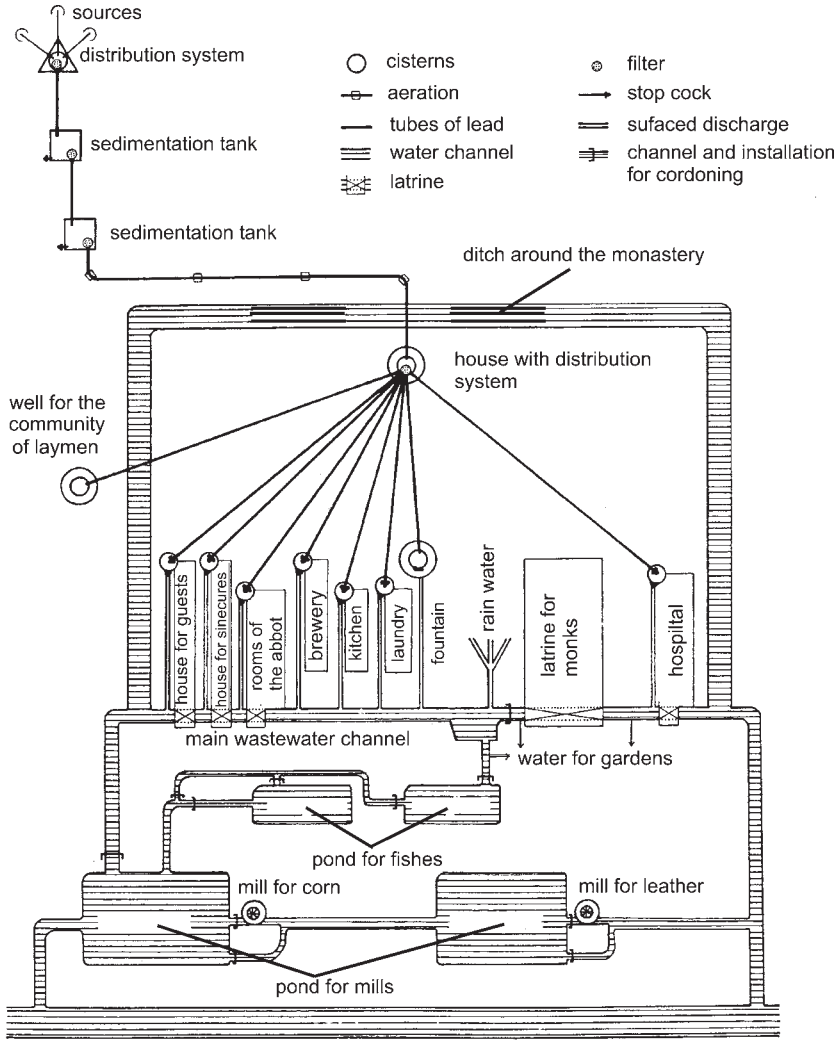


**Fig. 1.4** Fresh water supply and wastewater discharge in monasteries (Bond 1991).

First, the water flowed slowly through two sedimentation basins to a distribution house crossing the main ditch of the monastery. Pipes made either from tree trunks, ceramic material or lead were used for this purpose. From the distribution house, the water flowed to the different consumers, where it was polluted to different degrees; and afterwards it flowed into a wastewater canal, which was divided at two adjustable weirs into two different parts: the smaller one discharging into fish ponds and the larger one flowing below the latrines near the dormitories and afterwards into the river. The not very polluted main ditch was connected with ponds as water reservoirs to drive different mills. For such a demanding water supply, distribution and wastewater discharge, the location of the monastery had to be selected carefully and prepared at great expense.

Figure 1.5 shows an outline of the Cistercian monastery Arnsburg in the Wetterau region of Germany, established there in 1197. There are some differences to the

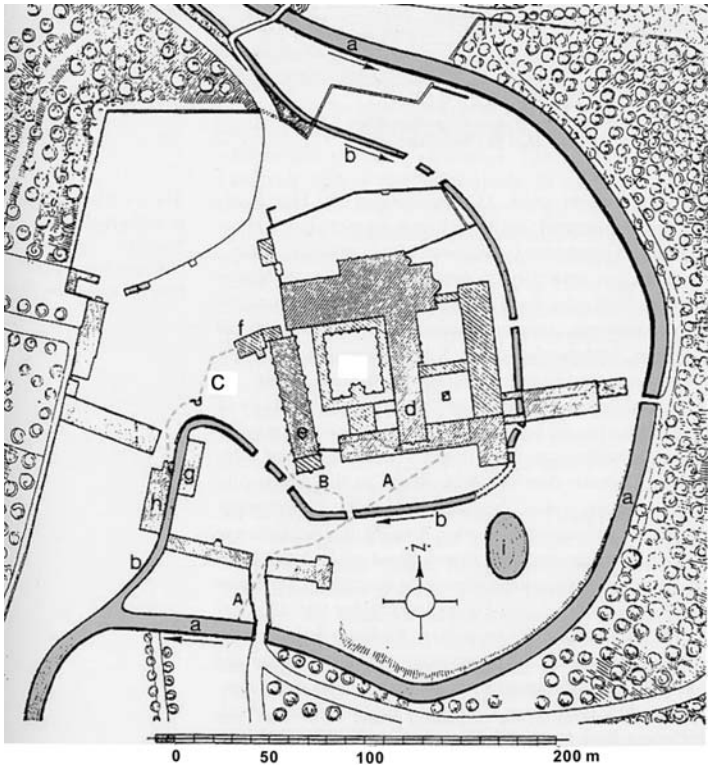


**Fig. 1.5** Cistercian Abbey in Arnsburg (Germany), plan of a medieval system for water use and wastewater discharge (Grewe, 1991). (a) Course of the river Wetter; (b) Branch canal; (c) Courtyard of the cloister with well; (d) Dormitory for the monks; (e) Dormitory for the lay brothers; (f) Rooms for the abbot; (g) Mill; (h) Brewery; (i) Fishpond. Broken lines indicate underground medieval sewers: (A) From the latrine of the monks to the sewer below the canal to the Wetter River; (B) From the lay brothers' latrine to the sewer; (C) From the abbot's rooms to the branch canal downstream from the mill.

fundamental pattern of water supply, but principally we can recognize several elements that correspond. The mill ditch branching off from the Wetter River first went immediately past a building, presumable the kitchen, and then the water drove a mill (g) and was obviously used for brewing beer (h). Starting from the dormitories of the monks and from the wards, pipes crossed the ditch and flowed into the Wetter River. The brewery was connected by a pipe with the rooms of the abbot and we shall leave unanswered whether the pipe was used for the transport of beer or wastewater. Large parts of the monastery are now completely destroyed, but the location of the cloister, the enclosures and the house of the fountain could be reconstructed after excavations. The mill ditch flowed higher than the Wetter River and supplied the water to drive the mills.

The water supply and wastewater management in the castles of that time were simpler, although in the courtyard a deep well was dug to reach the groundwater. The latrines were constructed so that the waste could fall down upon the sloping rock. For palaces, castles and upper chambers lying next to a river, the wastes could be discharged using an underground canal or an open ditch. Figure 1.6 shows such a canal belonging to a palace from the 12th century in Frankfurt near the river Main, Germany (Grewe 1991).

However, inside the towns there was often no system for waste management up to the middle of the 19th century. Frequently, refuse was discarded directly at the streets and paths where swine and chickens then foraged for usable foods and increased the wastes even further. Only after the installation of a water supply, the use of water toilets and the construction of open (Fig. 1.7) and closed wastewater ditches in the middle of the 19th century did the situation improve.

**Fig. 1.6** Wastewater canal of a castle in Frankfurt from the 12th century, with direct discharge into the river Main (Grewe 1991).

**Fig. 1.7** "Freiburger Bächle", initially operated as a wastewater channel, used since the 12th century (Grewe 1991).

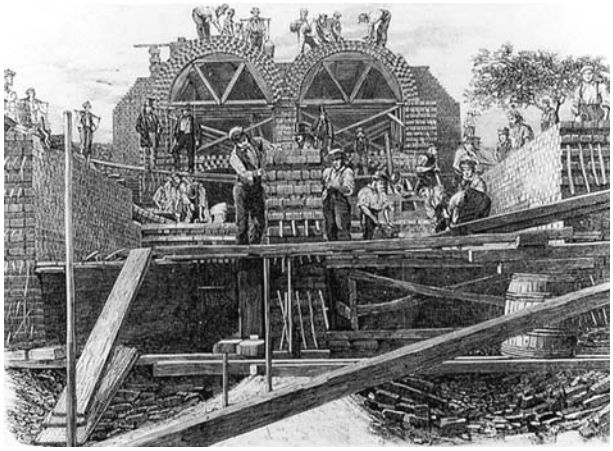

**Fig. 1.8** Construction of main sewage collectors along the river Thames in London (three at the northern and two at the southern bank) in 1865–1868 (Föhl and Hamm 1985).

However, during this period the number of inhabitants in the cities increased considerably. This made it necessary to find a fundamental solution to the problems. In London, for example, they first looked for an interim solution. A large canal was constructed in 1865–1868 along the river Thames (Fig. 1.8), which received most of the countless wastewater streams which were previously disposed directly into the river.

East of London, all the wastes in the canal were again discharged into the Thames. Because of the height difference needed to transport the water, wastewater pumping stations were built at Crossners and Abbey Mills. Fundamentally, this was the same method used in Rome 2000 years earlier: collecting, diverting and discharging.

## 1.3 First Studies in Microbiology

Antoni van Leeuwenhoek (1632–1723) was the first person able to grind simple lenses and who built the first microscopes (Fig. 1.9). The biconvex lens (L) was fastened between two thin metal plates and the object was mounted up on the pin at (P), which was adjustable by moving two screws. He constructed many of these microscopes and all the necessary lenses he ground himself. The best of them magnified about 200 times (Burdon and Williams 1969). With these instruments, he patiently examined numerous natural objects.

Van Leeuwenhoek grew up in Delft, attended school in Leyden, learned the cloth merchants' trade in Amsterdam and subsequently settled in Delft as a cloth merchant. At the age of 28 (1660), he learned to grind lenses and began to study differ-

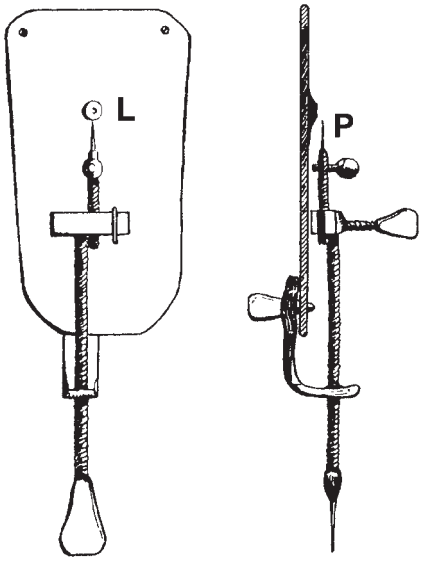


**Fig. 1.9** Front and side views of one of van Leeuwenhoek's microscopes. A lens was fastened between two thin plates at L, and the object was fixed upon the adjustable pin at P. The microscope must be held very close to the eye (Burdon and Williams 1969).

ent small things he found in water droplets. Later on, he started to draw all the things he observed. In 1673, he sent a first letter with some new drawings and descriptions to the Royal Society of London. On 7 September 1674, he reported for the first time about "small animals" (animalcules, protozoa) and small globules (green algae). In his 18th letter, written 9 October 1676, we find the first observations of bacteria, "very small animals", the young of the other animals, as van Leeuwenhoeck assumed (Mockmann and Köhler 1996). In his 39th letter, from 17 September 1683, van Leeuwenhoek enclosed an engraved figure (Fig. 1.10) showing a slide prepared from the film on his own teeth. We recognize cocci, rods and helical bacteria. The Royal Society accepted van Leeuwenhoek as a member in 1680. When he died in 1723, nobody had learned his method for grinding lenses and in

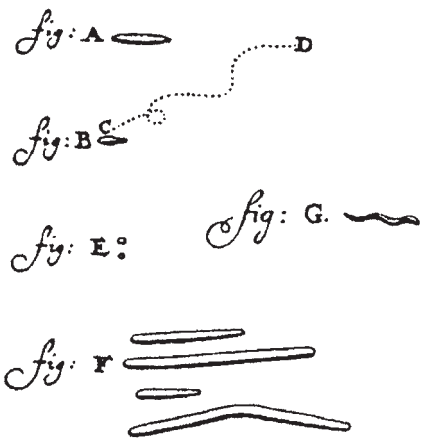


**Fig. 1.10** Van Leeuwenhoek's drawing of bacteria in a letter of 1683 to the Royal Society of London (Mockmann and Köhler 1996).

the following decades only a few microscopes similar to that of Fig. 1.9 were available.

In 1720, an important book was published in London with the title "A new theory of consumption: more specifically on a Phthisis, or consumption of the lungs", written by Benjamin Marten. In contrast to numerous other hypotheses, the cause of the consumption (tuberculosis) was attributed by Marten to small animalcules (microorganisms), which may come in the lungs by the circulation of blood. They may be contained in the air, can be breathed in and can grow in the blood and the lungs.

However, the scholars of that time believed in a phenomenon which was called abiogenesis. This theory of abiogenesis, or "generatio spontanea" (spontaneous generation of living organisms), is an old hypothesis and was not limited to animalcules. The famous alchemist Johann Babtist von Helmont (1577–1644) thought that animals like the mouse, worms and insects could be created by abiogenesis (Helmont 1652).

This period was concluded in part by experiments, carried out by Franceso Redi (Redi 1667), who worked as a personal physician of Ferdinand II de Medici (the grand duke of Toscana). He distributed a snake, some fish, eels and plates of veal into four bottles and closed them with fine porous gauze. The same remains of these animals were placed into open vessels, in which maggots were living after short time, having developed from eggs which were deposited by flies. In the covered bottles no maggots developed.

The abiogenesis of insects had already been refuted and scholars did not perpetuate this idea, but the discussion of abiogenesis started again in connection with animalcules. In their opinion, they must have been produced by abiogenesis.

In 1711, Louse Joblot studied the development of animalcules in hay and water suspensions (Joblot 1718). First, it was boiled for 15 min and distributed into two vessels. One of them was left open and, after some days, many animalcules had grown. The second vessel was closed with moist, oil-impregnated paper. No life could be observed in this vessel. Only after opening the vessel and waiting for some days did the same effect of growing life present itself, probably observed by using van Leeuwenhoek's microscope. But we can assume that he was not able to observe bacteria.

After these experiments, Joblot was convinced that the observed animalcules were descended from small animals living in the air.

The English priest Father John Turberville Needham (1713–1781) tried to refute this opinion experimentally. He was a resolute advocate of abiogenesis. In order to support this hypothesis, he boiled a suspension of mutton meat, bottled it and sealed the flask from the air with a cork. After some days, the suspension was full of living things. Needham and many other scientists were sure that the theory of preformation was conclusively refuted (Needham 1749, 1750).

Charles Bonnet (1720–1793) was one of the first who questioned whether the flasks were really impenetrable for small animal, or whether there were living creatures or eggs which would be able to survive the heating (Bonnet 1762). The Italian priest Abbate Lazzaro Spallanzani (1729–1799) filled different boiled infusions

(1 h) into vessels, which were closed carefully afterwards (Spallanzani 1765). All mixtures remained sterile.

Needham revised this theory: during a heating time of 1 h, a "vegetative power" would be destroyed, which was now introduced into this discussion instead of a biogenesis.

Spallanzani (1776) carried out further experiments in 1776 to test the existence of a "vegetative power". He boiled different infusions, filled them into vessels, closed them and boiled them again for 0.5, 1.0, 1.5 and 2.0 h. Half of them were opened, half of them remained closed. Only in the opened vessels were animalcules observed to be growing. Therefore, a "vegetative power" which could be destroyed after boiling for 1 h could not exist.

Nevertheless, the idea of abiogenesis or generatio spontanea (heterogenesis) as a model for the origin of life from nonliving organics remained a popular theory until 1830. At this point in time, it was shaken more and more by further experiments.

Franz Schulze filled water, meat and vegetables into a glass. At both ends of the glass, vessels were attached which were filled with sulfuric acid (Schulze 1836). From time to time, air was blown into the system (Fig. 1.11a), but all animalcules were restrained and killed off by the strong acid. The organics remained unchanged, no organism was alive. Only after the vessels filled with $H_2SO_4$ were removed did the animalcules penetrate from the air into the flask. Schulze proved with this experiment that germs (molecules or particles) distributed in the air of his breath were retained by washing in $H_2SO_4$, but that they started to digest the organics after entering the open glass.

One year later, Theodor Schwann (1837a) demonstrated that germs could be destroyed by heat. The left bottle in Fig. 1.11b was filled with a heated infusion and connected with a large spherical bottle and a helical tube. Both were heated and the right tube was closed by melting. The organics remained sterile. Obviously, the germs (molecules or particles) could be destroyed by higher temperature.

Schröder and von Dusch (1854) successfully used a layer of cotton as a filter for sterilization (Fig. 1.11c). First, the organic substance in the middle glass was heated and after that a flow of air was adjusted by opening the tap and emptying the left, large bottle slowly. Since then, layers of cotton have been used frequently to sterilize air in microbiology and biotechnology.

Schwann had shown already in 1837 that yeasts are living organisms and that if they grow in aqueous sugar solution and in the absence of oxygen, the sugar is converted to ethanol (Schwann 1837b). This interpretation of fermentation was doubted by scientists over the next 20 years: the conversion of sugar into ethanol must be a purely chemical process!

Nobody was able to describe these germs at this time, but it was known that they grow, that they change organic material and that they multiply. Louis Pasteur (1822–1895) was the first who understood that some germs need oxygen for growing, others do not. If they do not get oxygen, some of them are able to produce lactic acid (Pasteur 1857), ethanol (Pasteur 1860), butyric acid (Pasteur 1861a) and acetic acid (Pasteur 1861b). Pasteur created the foundation of modern *biotechnolo-*

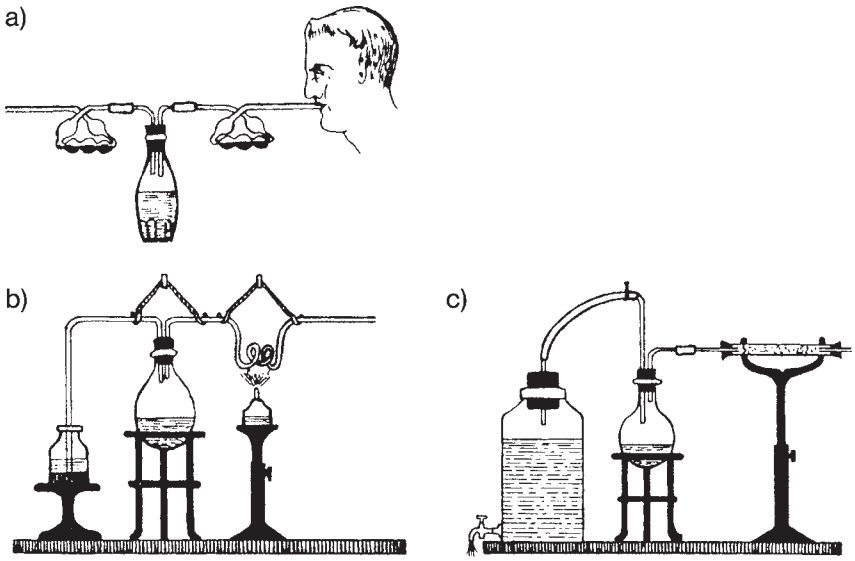


**Fig. 1.11** Early experiments showing activities of microorganisms. (a) Franz Schulze's experiment with a heated suspension of meat and vegetables in the bottle and $H_2SO_4$ in both glasses (Schulze 1836). (b) Theodor Schwann's experiment with a heated glass spiral (Schwann 1837a, b). (c) The Schröder and von Dusch experiment with a glass tube filled with cotton (Schröder and von Dusch 1854).

*gy*, which gained considerably in importance during the following decades. In the next years, Pasteur studied the causes of "wine and beer diseases" (Pasteur 1876) as well as poultry pestilence (Pasteur 1880a), anthrax (Pasteur 1880 b) and rabies (Pasteur 1885). All these works laid the foundation for *medical bacteriology*.

## 1.4 Wastewater Management by Direct Discharge into Soil and Bodies of Water – The First Studies

In the middle of the 19th century, wastewater produced in the fast-growing industrial regions and cities was discharged directly into rivers and canals, as well as into the soil below the toilets at the courtyards of tenement blocks. Frequently, the drinking water pump was located directly next to the toilets. Therefore, it was no wonder that cholera illnesses often occurred, especially in large cities.

Drinking water drawn with these pumps occasionally smelled of $H_2S$; and Rudolf Virchow was the first who assumed that it must be a product of anaerobic reduction of $CaSO_4$ (gypsum) by "microscopic algae" (Virchow 1868).

The situation in English rivers and canals was characterized by Fig. 1.12, a drawing in the satirical journal "Punch" from 1858 (Föhl and Hamm 1985).

**Fig. 1.12** Drawing from the satirical journal *Punch*, demonstrating the extremely polluted river Thames in 1858 with the title "The silent highway man" (Föhl and Hamm 1985).

The first step in solving the problem of river pollution was to describe it by taking samples and making measurements.

Frankland was instructed by the administration of London to present a monthly report about the water supply. In 1868, on the occasion of a meeting of the Royal Institution of Great Britain, he pointed out that the drinking water coming to London from the Cader Idris and Plyalimmon mountains (northern Wales) was polluted by "unhealthy germs" and chemicals (Frankland 1869a). In the same year, Frankland proposed ten analyses of water to characterize the river water quality (Frankland 1869b), but it took a long time to establish regular sampling and measuring.

A similar report and a description of measuring methods and results were published by Finkener and Zinreck, concerning the lakes and rivers in and around Berlin (Finkener 1871; Zinreck 1871). The results cannot be compared with those of today because of the different methods for sampling and measuring. Therefore, we will not report them here.

In 1871, the results of the River Pollution Commission led by Frankland were made available. Of special interest was the condition of the river Irwell and its tributaries. Over a length of 56 km there were 285 factories discharging their effluents into the small river, which was extremely polluted (Reich 1871).

At this time, it was discussed whether the concentration of pollutants could be reduced by chemical oxidation during its transport in a river. Eduard Wiebe, for example, was convinced that all the wastewater of Berlin discharged into the river Spree between Charlottenburg and Spandau was cleaned by "self-purification", a natural chemical process which can be used beneficially (Wiebe 1873).

## 1.5 Mineralization of Organics in Rivers, Soils or by Experiment – A Chemical or Biological Process?

The process of "self-purification" had to be studied experimentally. A commission presumably led by Frankland obtained the order to investigate the problem. Wastewater from the channel was mixed with river water and filled automatically from

one vessel to another after short interruptions. In the course of this filling process, oxygen must be transferred from air if it was necessary for the reaction. But the concentration of the organics was not considerably reduced, even after several weeks. Therefore, the "self-purification" observed was no simple chemical process. Alexander Müller was probably the first who suspected, in 1869, that the degradation of organics must be a microbiological process (Roechling 1899).[1)]

An initial answer resulted from experiments by J. König. A wire mesh was sprayed with wastewater for some weeks and it was observed that a biofilm had formed and that dissolved organics had been removed (König 1883). In this light, the experiments of Wolffhügel and Thiemann are also important, being the first to study the growth of bacteria on culture medium after adding drinking and process water. In these experiments, they were advised by Robert Koch (Wolffhügel and Thiemann 1883).

Between 1885 and 1890, several further studies were published proving that microbiological processes must be responsible for the production of $H_2CO_3$ and $HNO_3$ by the oxidation of organic compounds and $NH_4^+$ (Emich 1885; König 1886; Knauff 1887; Weigmann 1888; Winogradsky 1890).

Nevertheless, another group of chemists could not be convinced by the results of these experiments. Dunbar, the famous director of the Staatliche Hygiene Institut in Hamburg cited Travis in his paper in 1912 (Dunbar 1912), who strongly denied the microbial degradation of organics. Travis presented experimental results on the occasion of the seventh International Congress of Chemists in London in 1907, which should have proved pure chemical oxidation instead of biodegradation by microorganisms. However, Dunbar criticized Travis's methods in his last paper (Dunbar 1912), and obviously the idea of the pure chemical mechanisms was no longer supported in scientific meetings and journals.

We should not conclude this brief description of the birth of environmental microbiology without emphasizing the work of Winogradsky (1890), who carried out fundamental and most important studies on nitrification. In contrast to all the bacteria which use organic compounds as a source of energy and/or carbon, nitrifying bacteria are chemolitho-autotrophs, obtaining energy by the oxidation of $NH_4^+$ and $NO_2^-$ and obtaining carbon from the reduction of $CO_2$ (Chapter 10). He discovered all these facts and much more about this kind of bacteria, catabolism and anabolism during the years prior to 1890; and it is astonishing that the dispute about the oxidation of organic and inorganic compounds as a result of chemical or biological processes was not concluded for several further years.

In 1891, the first textbook on hygiene, "Grundriss der Hygiene" by C. Flügge, was published in its second edition (Flügge 1891). Rightfully, the reader could expect that the very important dictions of the past decade would have been mentioned. But the book, with its 560 pages, did not give any references to the topic. Should we conclude that the papers published in the journal "Gesundheits-Ingenieur", for example, were not noticed by doctors working in the field of hygiene?

---

[1)] A. Müller is mentioned in several other papers. But until now, the original publication has not been found.

## 1.6 Early Biological Wastewater Treatment Processes

The collection of wastewater in canal systems served a purpose, but its discharge into rivers was no solution of the problem, if the amount of wastewater discharged was too great in comparison with the river flow rate. In Berlin, Hobrecht proposed and built a wastewater collecting system consisting of 12 radial arms – five to the south and seven to the north of the river Spree. In each radial system, rainwater and wastewater flowed to a central lowest point by gravity (and the system is still in use today), from where it was pumped in pipes to an irrigation field outside the city. In the middle of each irrigation field, the water exited through a standpipe and gate valves through irrigation ditches in the irrigation fields. The water seeped through the ground and was collected by porous ceramic pipes and flowed into drainage channels and finally into canals or rivers (Hobrecht 1884). Similar irrigation fields were built in the surroundings of several other cities. Data for concentrations measured in the influent and effluent are very rare. Table 1.1 shows some data from 14 April 1891 for the irrigation field in Breslau (Uffelmann 1893). If we compare the values for dissolved organics of 155.9 mg $L^{-1}$ (influent) and 53.2 mg $L^{-1}$ (effluent), we can conclude that about 66% was removed. Nitrification was nearly complete (ammonia 105→7 mg $L^{-1}$).

The cleaning effect of irrigation fields had already been proven in the late 1870s, but in the first decade of operation, the scientific basis for the reduction of organics, which was being monitored by smell (often) and/or by taste (seldom), was largely unclear. During the 1890s, it became more and more certain: it was not a chemical but a biological process performed by aerobic and anaerobic bacteria. Nevertheless, the dispute was not resolved until the beginning of the 20th century (Dunbar 1912).

**Table 1.1** Concentration of samples from the influent and effluent of an irrigation field in Breslau (14 April 1891; Uffelmann 1893, extract).

| Substance | Concentration (mg $L^{-1}$) | |
|---|---|---|
| | Influent[a)] | Effluent[b)] |
| Suspended material | 295.2 | 54.0 |
| Organics | 246.0 | – |
| Inorganics | 49.2 | – |
| Dissolved material | 687.3 | 478.4 |
| Organics | 155.9 | 53.2 |
| Inorganics | 531.4 | 425.2 |
| $KMnO_4$ consumption | 118.1 | 9.7 |
| Ammonia ($NH_3$ + $NH_4^+$) | 105.0 | 7.0 |
| Nitric acid | – | 17.5 |
| Phosphoric acid | 22.4 | – |

[a)] Pump station. [b)] Mean dewatering ditch.

Experiments in ways to increase the specific wastewater load (in $m^3$ (ha day)$^{-1}$) compared with that of irrigation fields resulted in the development of intermittent soil filtration. The following operational conditions had to be met for the first sites: (a) the groundwater level must be low enough, (b) the percolating water must be collected in lateral ditches for recycling and (c) the application of wastewater must be intermittent, so that water levels in the ground recede and allow the simultaneous flow of air downwards to provide oxygen for bacterial growth, respiration and degradation of organics. Although this biological process was not completely understood, it was tested with increasing success.

One of the first of this kind was operated successfully in Lawrence, Massachusetts, USA, in 1888. These first experiments were very successful, showing nearly complete removal of organics and complete $NH_4^+$ oxidation (Dunbar 1899). In London and its surroundings, similar experiments with intermittent soil filtration were carried out by Dibdin in 1894–1896 (Roeckling 1899). In Barking Creek, London, near the river Thames, an area of 4047 $m^2$ was built up with soil that had walls 1 m high, supported by laid bricks. Several solid materials were tested as a contact bed. This filter was periodically filled with wastewater over 2 h, stopped for 1 h and emptied slowly over 5 h; and the cycle was repeated every 8 h. About 70–75% of the dissolved organics were removed. The plants in Sutton and Exeter were different from that of Barking only in one point: the wastewater was biologically pretreated for 24 h – in Sutton apparently aerobically in an open vessel and in Exeter anaerobically in a closed vessel. In both plants, the results were somewhat better than in Barking (Dibdin 1898). Similarly, very early pilot plants for the study of biodegradation went into operation in 1897 in Hamburg (Eppendorfer hospital; Dunbar 1899), in Großlichterfelde near Berlin, in 1898/1899 (Schweder 1901) and in Tempelhof near Berlin in 1900 (Thumm and Pritzkow 1902). After the foundation of the "Königliche Prüfanstalt für Wasserversorgung und Abwasserbeseitigung" in Berlin, pilot experiments were carried out systematically to study intermittent soil filtration, in order to find the best type of contact beds and to improve the process in Tempelhof (Thumm and Pritzkow 1902; Zahn 1902). All these experiments and developments led finally to the development of continuously operated trickling filters (Table 1.2). One of the first large-scale plants was built in the form of contact beds using large pieces of coke and operated with intermittent filtration, in Stahnsdorf near Berlin (Müller 1907).

**Table 1.2** Development of irrigation fields and trickling filters – increase in specific load.

| Year | Process | Specific load [$m^3$ (ha h)$^{-1}$] |
|---|---|---|
| 1860 | Irrigation fields prepared on suitable soil and level area | 0.24–0.36 |
| 1878 | Irrigation fields with drain trenches and soil fields | 4–8 |
| 1884 | Irrigation fields and preliminary sedimentation | 8–10 |
| 1886–1900 | Intermittant soil filtration | 30–40 |
| 1890 | Intermittant filtration with contact beds | 120 |
| 1903 | Trickling filter | 500–2000 |
| 1960 | High-load trickling filter | 8000 |

## 1.7 The Cholera Epidemics – Were They Caused by Bacteria Living in the Soil or Water?

In the rapidly growing European cities of the 19th century, cholera epidemics claimed many thousands of lives. In the time before 1860, nobody had a realistic idea about the cause of these epidemics. It was not until 1883, when Robert Koch discovered the bacteria which caused the illness (Brown 1935) that physicians were able to look for the natural reason of these bacteria. Two different hypotheses characterized the dispute of the following 10 years. Max von Pettenkofer and his followers were convinced that the cholera bacteria lived and grew in the soil and that the infections were caused by contact with soil and dust particles (von Pettenkofer 1882). Robert Koch and his followers supported the opinion that infection by cholera bacteria resulted from surface waters which were often used as sources of drinking water without any processing (Brown 1935).

In 1892, cholera appeared in Hamburg. All the victims of this disease had been supplied with drinking water which came directly from the river Elbe without sand filtration. The central prison and the Attendorfer lunatic asylum with its own groundwater supplies remained completely unaffected by cholera (Kluge and Schramm 1986). In the neighboring town of Altona, the morbidity was significantly lower, although water from the Elbe was used there as well. Was the rate of infection so much lower because the water was sand-filtered in the Altona waterworks? After some months, the number of illnesses was about 18 000 and the number of deaths 7600. But up to this point, the cholera bacillus was only found in the bodies and excrement of those taken ill. But just one year later, the cholera bacillus was also detected in the water of the river Elbe and most notably also in the pumps. After the source of the cholera infection had been identified, an effective solution to the problem had been found: sand filtration in waterworks and wastewater discharge into the river as before (Flügge 1893) or groundwater withdrawal as shore filtrate and wastewater treatment by irrigation fields (Virchow 1868; Hobrecht 1884). Both methods were employed, the first in Hamburg, the second in Berlin. The idea that a river can be loaded with untreated wastewater and then be cleaned by "self-purification" was upheld for the next 80 years. Only in the 1960s did we realize that wastewater must be treated in plants before being discharged into surface waters!

## 1.8 Early Experiments with the Activated Sludge Process

Obviously, nobody before 1913 had the idea to increase the concentration of aerobic bacteria by sludge sedimentation after aerating the sewage in a bottle for several hours, to remove the solids-free water carefully and then add sewage again. The first persons to observe an increase in sludge by repeating this process several times were Edward Arden and William T. Lockett from the River Committee of the Manchester Corporation in 1914. They presented their results on the occasion of a

meeting at the Grand Hotel in Manchester on 3 April 1914 (Arden and Lockett 1914). It was of high importance that the glass bottles filled with 2.27 L of sewage were protected from light for the first time, so that algae could not grow. They filled their bottle with sewage from the Sewage Works at Davyhulme. If the sludge had a volume of 25% after sedimentation, "carbonaceous fermentation" and nitrification could be completed to a high degree within 24 h. It was very important that the sludge was mixed with the sewage and that sufficient air was added. The pH must be controlled by adding a small quantity of alkali. These published results are presented in Fig. 1.13.

In this figure, concentrations are given in "parts per million", which means approximately $200/10^6 = 200$ mg $L^{-1}$. The organics were measured as "Oxygen Abs.". The authors probably used $KMnO_4$ as an oxidizing agent. The nitrification rate was slow compared to the removal rate for organics over the first 8 h. After this time, the situation changed.

Over the following years, this batch process was converted to a continuous process using an aeration tank, a sedimentation tank and sludge recycle system. After several experiments were performed in the UK and in the USA using pilot plants to study the process (Mohajeri 2002), the first technical-scale activated sludge plant was constructed in Sheffield, UK, in 1920 (Haworth 1922). The water flowed in open meandering channels and was aerated, moved and circulated by paddle stirrers. In Indianapolis, USA, compressed air flowed through perforated tubes arranged near the bottom at one side of a long channel, producing a spiral flow of air bubbles (Hurd 1923). The first surface aerator with a vertical shaft was constructed by Bolton. A conducting tube forced the two-phase flow near the bottom, resulting

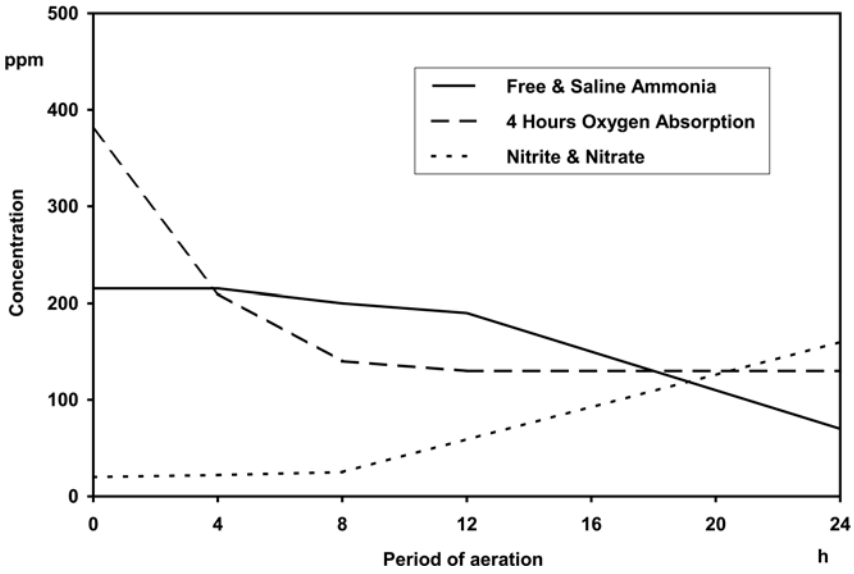


**Fig. 1.13** First batch sewage aeration experiment with enriched activated sludge (Arden and Lockett 1914).

in sufficient oxygen transfer and mixing of the water and sludge (Bolton 1921; Imhoff 1979). In Germany, the first large plants were built in Essen-Rellinghausen in 1926 (Kuhn 1927) and in Stahnsdorf near Berlin in 1929–1931 (Langbein 1930), the latter of which was designed and operated as an experimental plant for the study of different sedimentation tank designs (Mohajeri 2002).

## 1.9 Taking Samples and Measuring Pollutants

There are some important questions which must be answered when studying water technology and pollution control:

- How dirty is the wastewater with respect to specific compounds or total parameters; and how can I measure these parameters or the concentration of these specific compounds?
- What is the best point to take a sample for analysis from a river or treatment plant?
- What is the best method for taking samples (sampling by drawing within a short time, sampling and mixing within a given time period of 1–2 h)?
- How frequently should samples be taken, once per hour, per day, per week or per year?

One of the first methods developed was the measurement of potassium permanganate ($KMnO_4$) consumption for the oxidation of organic compounds dissolved in water (Marqueritte 1846). It took 23 years until Frankland proposed to the Royal Commission of England what else should be measured and how this can be done (Frankland 1869b). Malz in 1999 divided the time which followed into three periods. During the first period (1870–1920), wastewater was mostly characterized by colour and smell, although many methods were available for measuring different compounds. The ability of the wastewater to digest and to form gases ($CH_4$, $CO_2$) was of interest as well as the concentrations of potassium, magnesium and nitrogen to characterize the value for use as fertilizer (Mohajeri 2002). Not until the second period (1920–1970) were some simple methods used for measuring specific compounds ($BOD_5$, COD, dissolved oxygen, pH, conductivity, solid concentration, etc.). The most important problem was that standard methods did not exist. Frequently, one water sample investigated in two different laboratories gave two different results lying considerably beyond the range of confidence. The third period since 1970 is the time of using more and more methods controlled by computers with automatic sampling (COD, DOC, AOX) and the analysis of individual organic and inorganic compounds (different detectors after separation by GC, HPLC, etc.; Malz 1998; Mohajeri 2002). It was very important to standardize the methods of sample-taking, storage and measurement. Often, national standards were agreed upon only after drawn-out discussions. As a result of the development of political and economical confederations, further agreements on standards had to be developed (EU guidelines for prevention of water pollution; Pöppinghaus et al. 1994).

## 1.10
## Early Regulations for the Control of Wastewater Discharge

Initially, solid and liquid wastes were disposed and poured out onto the streets and in the courtyards of medieval towns and villages. The unpaved streets and paths were filled with mud, particularly after a strong rainfall. Since domestic animals also lived in these areas, the mud was mixed with solid and liquid faeces. This situation went unchanged until the first regulations were issued by local authorities (Hösel 1990).

In the 16th and 17th centuries in Berlin, regulations by the Elector and the town council were mostly limited to the sweeping of solid wastes and the formation of heaps. In the 18th century, many tenants who had no toilets in the courtyards still emptied their chamber pots onto the streets. The town council of Berlin forbade this by levying a fine and defining a list of places on the river Spree where chamber pots could be emptied at a certain time of day. After 1830, more and more wastewater channels were constructed, some of them laid underground, some of them as open channels directly near the sidewalks. These were frequently clogged and wastewater could not flow, especially during and after rain or snowfall. In the 19th century, it was forbidden to empty chamber pots into the Spree. Obviously, this law was difficult to enforce (Fig. 1.14; Hösel 1990).

Until the second half of the 19th century, it was common practice to discharge wastewater into the rivers; and it was normal for the communities downstream to have to put up with the polluted water (Driewer 1999). These problems increased dramatically as industrial development took off in the fast-growing cities. In order to avoid epidemics such as cholera and typhus, laws had to be issued for the treatment and discharge of wastewater.

Until 1945 in Germany, water regulations were only issued by the states, some of them even only in the last 32 years of the 19th century (e.g. Oldenburgische Wasserordnung, 10 November 1868; Braunschweigisches Wassergesetz, 20 June 1878). In Prussia, the largest and most highly industrially developed region of Germany, the regulation of water was first established in 1913 (Schlegelberger 1927,

**Fig. 1.14** Berlin: secret emptying of chamber pots into the river Spree. The gases of anaerobic processes (mainly $CH_4$) were used to provide light for the woman during her nightly job. Caricature by Doebeck, dated 1830 (Hösel 1990).

1931), because about 80 single regulations had to be unified which were each valid for only one of the 80 regions of Prussia. This fulminous work of about 1600 pages addressed such problems as ownership rights to waterways and lakes, usufructs, duties for the maintenance of the waterways and the banks as well as flood protection. Limits to volume or concentration of wastewater discharged into surface waters were not fixed. Similar laws were in effect in all German states and were not fundamentally changed until 1945.

Four points were important for the new laws:

- They were passed separately under different conditions in the Federal Republic of Germany (FRG) and in the German Democratic Republic (GDR).
- On 1 March 1960, the Water Resources Policy Act (WRPA) was issued in the FRG; and on 7 April 1963, the Water Act (WA) was issued in the GDR.
- The WRPA was a legal framework in the FRG, supplemented by the legislation of the individual states.
- The WA was a uniform regulation valid in all states.

An important development of the legislation of the FRG was the structure of the "Law governing the payment of fees for disposing of wastewater in surface waters" ("Gesetz über Abgaben für das Einleiten von Abwasser in Gewässer", Abwasserabgabengesetz [AbwAG], from 13 September 1976), which took effect on 1 January 1978. The levying of fees began on 1 January 1981 and only covered the direct discharge of wastewater into surface waters (Direkteinleiter). So-called load equivalents (Schadeinheiten) are calculated according to the yearly disposal load of particular substances (Berendes and Winters 1981). One load equivalent (the untreated domestic wastewater produced by one person in one year) was valued in 1986 at DM 12 (≈ 6 €) and in 1986 at DM 40. Further developments of the AbwAG are described in the appropriate literature.

## References


Arden, E.; Lockett, W.T. **1914**, Experiments on the oxidation of sewage without the aid of filters, *J. Soc. Chem. Ind.* 33, 523–539.

Berendes, K.; Winters, K.-P. **1981**, *Das Abwasserabgabengesetz*, C.H. Beck, Munich.

Bolton, J. **1921**, Activated sludge experiments at Bury, *Proc. Assoc. Mgr. Sewage Disp. Works* 1921, 33–47.

Bond, C.J. **1991**, Mittelalterliche Wasserversorgung in England und Wales, in: *Geschichte der Wasserversorgung*, Bd. 4, ed. Frontinus-Gesellschaft e.V., Verlag Philipp von Zabern, Mainz, p. 149–182.

Bonnet, C. **1762**, *Considérations sur les corps organisés*, Amsterdam.

Brown, L. **1935**, Robert Koch (1842–1910), an American tribute, *Ann. Mus. Hist.* 7, 292–385.

Burdon, K.L.; Williams, R.P. **1969**, *Microbiology*, MacMillan, London, p. 21–33.

Dibdin B. **1898**, *The Purification of Sewage and Water*, 2nd edn., London.

Driewer, G. **1999**, Rechtliche Aspekte der Abwasserentsorgung, in: *Geschichte der Abwasser-Entsorgung, 50 Jahre ATV 1948-1998*, Verlag für Abwasser, Abfall und Gewässerschutz, Hennef.

Dunbar, W.P. **1899**, Die Behandlung städtischer Abwässer mit besonderer Berücksichtigung neuerer Methoden, *Dtsch Vierteljahresschr. öffentliche Gesundheitspfl.* 31, 136–218.

Dunbar, W.P. **1912**, *Leitfaden für die Abwasserreinigungsfrage*, Bd. 17, Oldenbourgs Technische Handbibliothek, München.

Emich, F. **1885**, *Chem. Central Blatt* 33.

Finkener, F. **1871**, Anlage VI Bericht und Analysen, No. 1 zu den "Vorarbeiten zu einer zukünftigen Wasser-Versorgung der Stadt Berlin von L.A. Veitmeyer", in *Auftrage des Magistrats und der Stadtverordneten zu Berlin, angefertigt in den Jahren 1868 und 1869*, Verlag von Dietrich Reimer, Berlin.

Flügge, C.F. **1891**, *Grundriss der Hygiene*, 2. Aufl., Leipzig.

Flügge, C.F. **1893**, Die Verbreitungsweise und Verhütung der Cholera auf Grund der neueren epidemiologischen Erfahrungen und experimentellen Forschungen, *Zeitschr. Hyg.* 14, 122–202.

Föhl, A.; Hamm, M. **1985**, *Die Industriegeschichte des Wassers*, VDI-Verlag, Düsseldorf, p. 151–152.

Frankland, A. **1869a**, *Summary of weakly return of birth, death and causes of death in London during the year 1868*, Eyre and Spottisweek, London.

Frankland, A. **1869b**, Franklands Bericht "über Wasserversorgung an die Royal Institution of Great Britain", *Dtsch Vierteljahresschr. öffentliche Gesundheitspfl.* 1869.

Garbrecht, G. **1987**, Die Wasserversorgung des antiken Pergamon, in: *Geschichte der Wasserversorgung*, Bd. 2, ed. Frontinus-Gesellschaft, Verlag Philipp von Zabern, Mainz, p. 11–48.

Grewe, K. **1991**, Wasserversorgung und -Entsorgung im Mittelalter – ein technikgeschichtlicher Überblick, in: *Geschichte der Wasserversorgung*, Bd. 4, ed. Frontinus-Gesellschaft, Verlag Philipp von Zabern, Mainz, p. 11–81.

Haworth, J. **1922**, Bio-aeration at Sheffield, *Proc. Assoc. Mgr Sewage Disp. Works* 1922, 83–88.

Helmont, J.B. van **1652**, *Ortus medicinae, id es initia physicae inaudita*, Amsterdam.

Hobrecht, J. **1884**, *Die Canalisation von Berlin*, Berlin.

Hösel, G. **1990**, Unser Abfall aller Zeiten – Eine Kulturgeschichte der Städtereinigung, Jehle Verlag, Munich.

Hurd, C.H. **1923**, Design features of the Indianapolis activated sludge plant, *Eng. News-Rec.* 1923.

Imhoff, R. **1979**, Die Entwicklung der Abwasserreinigung und des Gewässerschutzes seit 1868, *Gwf-Wasser/Abwasser* 120, 563–576.

Joblot, L. **1718**, *Descriptions et usage de plusiers nouveaux microscopes tant simples que composez; avec de nouvelles observations faites sur une multitude innombrable d'insects et d'autres animaux de diverses espèces, qui naissant dans le liqueurs préparées et dans celles qui ne le sont point*, Paris.

Kluge, T.; Schramm, E. **1986**, *Wasser Nöte – Umwelt und Sozialgeschichte des Trinkwassers*, Klenkes, Aachen.

Knauff, M. **1887**, Die Reinigung von Spüljauchen durch intermittierende Abwärtsfiltration, *Der Gesundheitsingenieur* 20, 643–648, 687–690, 987–995.

König, J. **1883**, Reinigung von fauligem Abflusswasser aller Art durch Zuführung von Luft beim Herabrieseln an einem Drahtnetz, *Der Gesunheitsingenieur* 4, 121–122.

König, J. **1886**, Die Prinzipien der Reinigung von fauligem und fäulnisfähigem Schmutzwasser, *Dtsch Vierteljahresschr. öffentliche Gesundheitspfl* 121 (Supplement).

Kuhn, P. **1927**, Über die neueren Verfahren der Abwasserbeseitigung, *Gesundheits-Ingenieur* 50, 209–219.

Lamprecht, H.-O. **1988**, Bau und Materialtechnik bei antiken Wasserversorgungsanlagen in *Geschichte der Wasserversorgung*, Bd. 3, ed. Frontinus-Gesellschaft e.V., Verlag Philipp von Zabern, Mainz, p. 150–155

Langbein, F. **1930**, Das Abwasser-Großklärwerk Berlin-Stahnsdorf, *Zeitschr. Ver. Dtsch Ing.* 74, 1349–1358.

Malz, F. **1998**, *Aus der Geschichte der Abwasseranalytik, Geschichte der Abwasserentsorgung, 50 Jahre ATV 1948-1998*, Bonn.

Marqueritte, F. **1846**, Sur un novel procédé de dosage du par la voie humide, *Ann. Chim. Phys.* 18, 244–256.

Mockmann, H.; Köhler, W. **1996**, *Meilensteine der Bakteriologie*, Edition Wötzel, Frankfurt/Main, p. 9–50.

Mohajeri, S. **2002**, *Historische Entwicklung der Wasserversorgung und Abwasserentsorgung in Berlin bis zum Zweiten Weltkrieg*, Dissertation, TU Berlin.

Müller, E. **1907**, Die Entwässerungsanlage der Gemeinde Wilmersdorf, *Zeitschr. d. Vereins Dtsch Ing.* 51, 1971–1982.

Needham, J.T. **1749**, A summary of some late observations upon the generation, composition, and decomposition of animal and vegetable substance, *Phil. Trans. R. Soc. Lond.* 490, 615.

Needham, J.T. **1750**, *Nouvelles observations microscopiques, avec des découvertes interéssantes sur la composition et la décomposition de corps organisés*, Paris.

Pasteur, L. **1857**, Mémoire sur la fermentation appe lée latique, *Compt. Rend. Acad. Sci.* 45, 1032–1036.

Pasteur, L. **1860**, Mémoire sur la fermentation alcoolique, *Ann. Chim. Phys.* 53, 323–426.

Pasteur, L. **1861a**, Expériences et vues nouvelles sur la nature des fermentations, *Compt. Rend. Acad. Sci*, 52, 1260–1264.

Pasteur, L. **1861b**, Animalcules infusoires vivant sans gaz oxygène libre et déferinant des fermentations, *Compt. Rend. Acad. Sci.* 52, 344–347.

Pasteur, L. **1876**, *Études sur la bièra, ses maladies, causes qui le provoquent, procèdè pour la randre inaltèrable avec une thèorie nouvelle de la fermentation*, Paris.

Pasteur, L. **1880a**, Sur les maladies virulentes et en particulier sur la maladie appelèe vulgairement cholèra des poules, *Compt. Rend. Acad. Sci.* 90, 239–248.

Pasteur, L. **1880b**, Sur le choléra des poules. Études des conditions de la nonrécidive de la maladie et de quelques autres de ces caractères, *Compt. Rend. Acad. Sci.* 90, 952–1030.

Pasteur, L. **1885**, Méthode pour prevenir la rage après morsure, *Compt. Rend. Acad. Sci*, 101, 765–773.

Pöppinghaus, K.; Filla, W.; Sensen, S.; Schneider, W. **1994**, *Abwassertechnologie – Entstehung, Ableitung, Behandlung, Analytik der Abwässer*, Springer-Verlag, Berlin, 462–463.

Redi, R. **1667**, *Espoerienze intorno alle generazione degl'insetti*, Florence.

Reich, O. **1871**, Der erste und zweite Bericht der im Jahre 1868 in England eingesetzten Rivers Pollution Commission, *Dtsch Vierteljahresschr. Öffentl. Gesundheitspfl.* 3, 278–309.

Roechling, H.A. **1899**, Coreferat (no title), *Dtsch Vierteljahresschr. Öffentl. Gesundheitspfl.*, 160–201.

Schlegelberger, P. **1927**, *Das Preußische Wassergesetz*, Bd. 1, Karl Heymanns Verlag, Berlin.

Schlegelberger, P. **1931**, *Das Preußische Wassergesetz*, Bd. 2, Karl Heymanns Verlag, Berlin.

Schröder, H.; von Dusch, T. **1854**, Über Filtration der Luft in Beziehungen auf Fäulnis und Gärung, *Ann. Chem. Pharm.* 89, 232–243.

Schulze, F. **1836**, Vorläufige Mitteilung der Resultate einer experimentellen Beobachtung über Generatio aequivoca, *Tilberts Ann. Phys. Chem.* 39, 487–489.

Schwann, T. **1837a**, Versammlung Deutscher Naturforscher und Ärzte zu Jena, 26.9.1836, referiert von Oken, *Isis* 5, 524.

Schwann, T. **1837b**, Vorläufige Mitteilung betreffend Versuche über die Weingärung und Fäulnis, *Tilberts Ann. Phys. Chem.* 41, 184.

Schweder, V. **1901**, Kurzer Bericht über die Versuchsanlage in Großlichterfelde bei Berlin, *17. Jahresbericht über die Fortschritte und Leistungen auf dem Gebiet der Hygiene*, Verlag Vieweg und Sohn, Braunschweig.

Spallanzani, L. **1776**, Osservazioni e sperienze intorno agli animalucci delle infusioni, in: *Opusculi di fisica animale, e vegetabile dell'Abbate Spallanzani*, Modena.

Spallanzani, L. **1765**, *Saggio di osservazioni microscopiche concerneti il sisteme della generatione dei signori Needham e Buffon*, Modena.

Thumm, K.; Pritzkow, A. **1902**, Versuche über die Reinigung der Abwässer von Tempelhof bei Berlin durch das biologische Verfahren, *Mitt. Koenigl. Pruef. Wasserversorgung Abwasserbeseitigung Berlin* 1, 127–163.

Uffelmann, J. **1893**, Zehnter Jahresbericht über die Fortschritte und Leistungen auf dem Gebiet der Hygiene, *Dtsch Vierteljahresschr. Öffentl. Gesundheitspfl.* 25 (Suppl), 143.

Virchow, R. **1868**, Über die angemessenste Art, die Stadt Berlin von den Auswurfstoffen zu reinigen, Gutachten der Wissenschaftlichen Deputation für das Medizinalwesen, *Vierteljahresschr. Ger. Öffentl. Med. Neue Folge* 9, 6.1.

Von Pettenkofer, M. **1882**, *Der Boden und sein Zusammenhang mit der Gesundheit des Menschen*, Berlin.

Weigmann, H. **1888**, Die Reinigung der Abwässer, *Der Gesundheitsingenieur* 1888, 17–19, 41–46.

Wiebe, E. **1873**, Über die Reinigung des Hauswassers, Vortrag am 22.2.1873 im Architekten-Verein zu Berlin, *Dtsch Bauzeit.* 7, 122–123.

Winogradsky, S.N. **1890**, Recherches sur les Organismes de la Nitrification, *Ann. Inst. Pasteur* 4, 213–231.

Wolffhügel, T.; Thiemann, W. **1883**, Über die hygienische Beurteilung der Beschaffenheit des Trink- und Nutzwassers, *Dtsch Vierteljahresschr. Öffentl. Gesundheitspfl.* 15, 552–574.

Zahn, K. **1902**, Weitere Versuche über die Reinigung des Charlottenburger Abwassers auf der Pumpstation Westend durch das biologische Verfahren, *Mitteil. Königl. Prüfanst. Wasserversorgung Abwasserbeseitigung Berlin* 1, 164–171.

Zinreck, K. **1871**, *Anlage VI Bericht und Analysen*, No. 2 zu den "Vorarbeiten zu einer zukünftigen Wasser-Versorgung der Stadt Berlin von L.A. Veitmeyer, im Auftrage des Magistrats und der Stadtverordneten zu Berlin, angefertigt in den Jahren 1868 und 1879", Verlag von Dietrich Reimer, Berlin.

# 2
# Wastewater Characterization and Regulations

## 2.1
## Volumetric Wastewater Production and Daily Changes

Wastewater is typically categorized into one of the following groups:

- Domestic wastewater (only produced in households).
- Municipal wastewater (domestic wastewater mixed with effluents from commercial and industrial works, pre-treated or not pre-treated).
- Commercial and industrial wastewater (pre-treated or not pre-treated).

Table 2.1 presents some average data for the Federal Republic of Germany.

Municipal wastewater is composed of 50% domestic wastewater on average. In some cities it may only amount to 25%, in other municipalities nearly 75%. This is of major significance, concerning the additional substances from certain factories which may be either non biodegradable or toxic. Commercial and industrial wastewater are treated together with domestic wastewater and rainwater in communities with a canal system (wastewater and rainwater). In particular, industrial plants with high water consumption have to treat their effluents in their own treatment plants. This is also required of many commercial and some agricultural works. In

**Table 2.1** Total wastewater and municipal wastewater (Federal Republic of Germany, 60 million inhabitants, 248 534 km$^2$ area; from Pöpel 1997).

| **Total wastewater** | **100%** | **$15.4 \cdot 10^9$ m$^3$ a$^{-1}$** | **694 L (inh. d)$^{-1}$** |
|---|---|---|---|
| Municipal wastewater | 32 | 5.0 | 230 |
| Industrial wastewater | 47 | 7.2 | 320 |
| Agricultural wastewater | 1 | 0.2 | 7 |
| Rainwater drainage in canals | 20 | 3.0 | 137 |
| **Total municipal wastewater** | **100%** | **$5.0 \cdot 10^9$ m$^3$ d$^{-1}$** | **230 L (inh. d)$^{-1}$** |
| Domestic wastewater | 50 | 2.5 | 115 |
| Rainwater | 14 | 0.7 | 32 |
| Commercial and industrial wastewater | 36 | 1.8 | 83 |

*Fundamentals of Biological Wastewater Treatment*. Udo Wiesmann, In Su Choi, Eva-Maria Dombrowski

ISBN: 978-3-527-31219-1

an increasing number of growing cities, domestic wastewater and rainwater are collected separately. Although the rainwater is often highly polluted by several organic and inorganic substances (from car washing, car accidents, high tides, etc.), it is mostly discharged untreated into rivers and canals.

Further information about the mean water consumption (= wastewater production) per inhabitant and per day in different European and North American cities is available (Chow et al. 1979; Pöppinghaus et al. 1994; Pöpel 1997). But we must be very careful when comparing these data, because sometimes they are valid only for one city and sometimes the data are valid only for domestic or for municipal wastewater, with or without rainwater. Therefore, we will not discuss these data here.

Within a 24-h period, the flow rate of domestic or municipal wastewater often changes by a factor of 3–4, causing a corresponding change in the flow rate at the treatment plants, because they most often have no storage tanks. Figure 2.1 shows a typical plot of flow rate versus time for a period of 24 h (Schuchardt 2005).

The minimum value during the night and the maximum at midday and evening are typical for many domestic and municipal treatment plants. In larger plants such as Berlin–Waßmannsdorf (~160 000 $m^3\ d^{-1}$), the profile of flow rate versus time is influenced by the length of the canal system.

The daily and weekly changes in the flow rate are given in Fig. 2.2 (Schuchardt 2005).

Typically, commercial and industrial wastewater flow rates have been published in relation to the mass of specific products (in $m^3\ d^{-1}$; Pöppinghaus et al. 1994; Henze et al. 2002). We will not consider these data here; however, see Section 2.4 where relevant regulations are discussed.

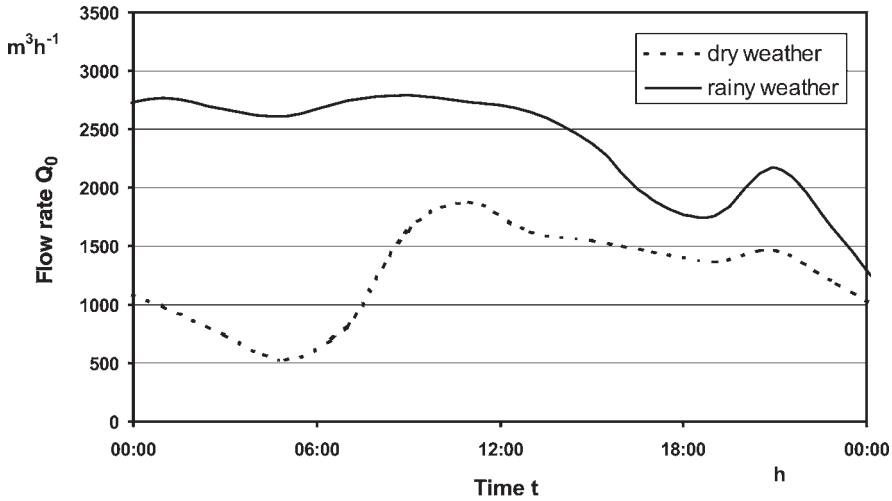


**Fig. 2.1** Daily change in flow rate at the municipal WWTP Waßmannsdorf, near Berlin, BB 12 (basin 12), $Q_o$ from on-line measurements (Schuchardt 2005). Dry weather 6 September 2001; rainy weather 10 September 2001.

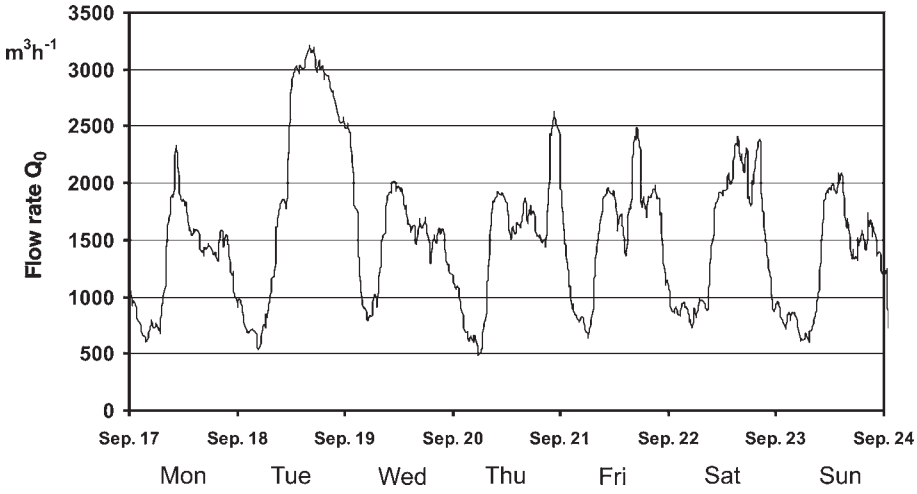


**Fig. 2.2** Daily and weekly change in flow rate at the municipal WWTP Waßmannsdorf, near Berlin, BB 11 (basin 11), 17–24 September 2001, $Q_0$ from on-line measurements.

## 2.2 Pollutants

### 2.2.1 Survey

All wastewater classes (domestic, municipal, commercial or industrial) contain the following groups of pollutants:

**1. Dissolved substances**

a) Organic materials
   – biodegradable substances
   – non-biodegradable substances

b) Inorganic materials
   – nutrients, used in part or totally by microorganisms
   – metal and heavy metal ions, used often only in very small amounts by microorganisms as trace elements (often toxic in slightly higher concentrations)

**2. Colloids**

a) Non-settleable small drops of oil and grease

b) Organic and inorganic small solid particles

**3. Suspended solids**

a) Organic particles
   - microorganisms (bacteria, viruses, worm eggs, protozoa), mostly non-settleable
   - other organic materials (residual particles from fruits, vegetables, meat, etc.), mostly settleable

b) Inorganic particles
   - sand, clay, minerals
   - partly organic and partly inorganic particles

### 2.2.2 Dissolved Substances

#### 2.2.2.1 Organic Substances

The sum of all the different dissolved organic molecules in domestic wastewater can be approximately characterized by the average molecular composition $C_{18}H_{19}O_9N$ (Pöpel 1997) with a mass of 393 g mol$^{-1}$.

The concentration can be measured by chemical oxidation using potassium dichromate. For complete oxidation, the necessary oxygen and the carbon oxidized, measured as $CO_2$, can be calculated from:

$$C_{18}H_{19}O_9N + 17.5\ O_2 + H^+ \rightarrow 18\ CO_2 + 8\ H_2O + NH_4^+ \qquad (2.1)$$

For wastewater with 1 mol m$^{-3}$ $C_{18}H_{19}O_9N$ (or 393 g m$^{-3}$), $17.5 \cdot 32 = 560$ g m$^{-3}$ $O_2$ is needed and $18 \cdot 12 = 216$ g m$^{-3}$ $CO_2$-C is produced.

Therefore, the oxygen consumed and the $CO_2$-C produced can be used as characteristics of the concentration, resulting in:

$S_{th} = 560$ g m$^{-3}$ COD (*c*hemical *o*xygen *d*emand)

or

$S_{th} = 216$ g m$^{-3}$ DOC (*d*issolved *o*rganic *c*arbon)

for

$S_{th} = 393$ g m$^{-3}$ substrate

The theoretical value $S_{th} = 560$ g m$^{-3}$ COD would only be measured for a total oxidation according to Eq. (2.1). Usually, a part of the oxidized mean products cannot be completely oxidized using the standard test. If a rapid test is used, the measured COD is even lower than that of the standard test (Section 2.3.2). For the theoretical value, the standard value would follow as:

$S_{St} = 0.83 \cdot S_{th} = 465$ g m$^{-3}$ COD

giving a rapid test value of only:

$S_{rt} = 0.70 \cdot S_{th} = 392$ g m$^{-3}$ COD (Ramalko 1983)

The oxygen used for biological $CO_2$ and $H_2O$ formation as well as for bacterial growth during a 5-day batch process (Henze et al. 2002; Table 2.1) for this theoretical domestic wastewater is:

$S = 280\ g\ m^{-3}$ $BOD_5$ (*b*iochemical *o*xygen *d*emand over *5* days without nitrification).

The $BOD_5$ is always lower than the COD, although bacteria use oxygen not only for $CO_2$ and $H_2O$ production, but also for growth. We can attribute this to several reasons:

- Only a part of the organics in the wastewater can be used by the bacteria as a carbon and energy source.
- Some substances can only be partly used. Some products of metabolism are excreted.
- Bacteria die and form lysis products, which can only be used in part by living bacteria.
- After 5 days, some biodegradable substances are still left. Therefore, occasionally $BOD_{10}$ or $BOD_{20}$ are used.

The COD and DOC of pure organic substances can be calculated in the same way as shown above, giving the theoretical COD $S_{th}$. Again, the measured values $S_{st}$ and $S_{rt}$ are lower for the reasons mentioned above. Some data have been published for a number of chemicals often used in chemical industry (Busse 1975; Pöppinghaus et al. 1994).

Of more practical importance are the dissolved organics from the processing water of specific products. Mostly, they consist of thousands of specific compounds, as discussed above for domestic wastewater. Table 2.2 presents data on the substrate concentration S measured as COD and $BOD_5$ in processing water from the food industry. Usually the standard method is used to measure COD.

In most cases, the concentrations of COD and $BOD_5$ are considerably higher than in domestic or municipal effluents. Therefore, anaerobic wastewater treatment processes are often preferred. This is also true for effluents from the brewing

**Table 2.2** Some typical concentrations of wastewater from the food industry (Lehr- und Handbuch der Abwassertechnik 1985).

| Product | S (mg $L^{-1}$ COD) | S (mg $L^{-1}$ $BOD_5$) |
|---|---|---|
| Sugar | 7 500 | 5 000 |
| Maize starch | 17 608 | 11 543 |
| Potato starch | 7 416 | 6 333 |
| Wheat starch | | 12 344–18 270 |
| Rice starch | 2 192 | 1 475 |
| Margarine | 1 000–2 000 | 500–1 000 |
| Vegetable refinement | | 5 000–8 000 |
| Fruit juice | 300–800 | 25–1 380 |
| Slaughterhouse | 2 579–6 650 | 1 900 |
| Fish processing | | 1 530–2 567 |

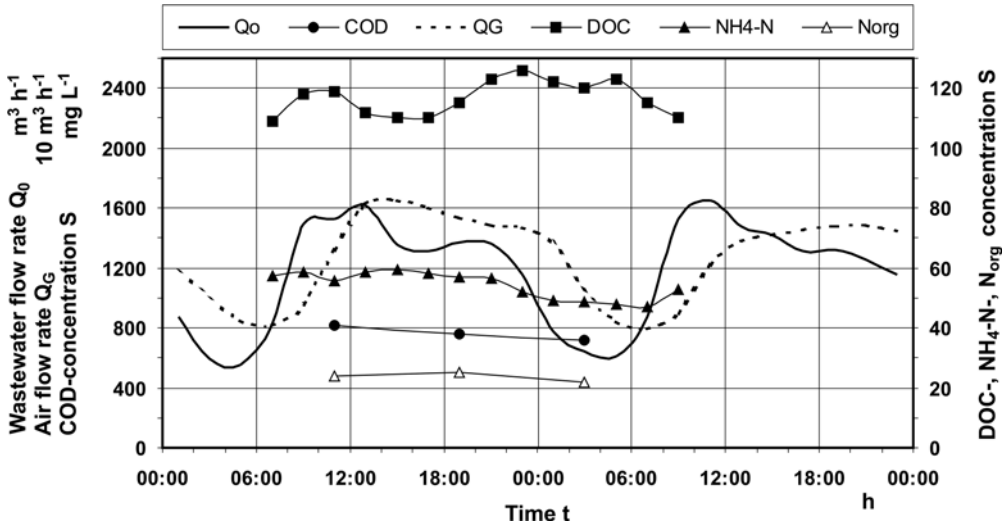


**Fig. 2.3** Daily change in flow rate and concentrations (● COD, ■ DOC, ▲ $NH_4$-N, △ $N_{org}$) at the municipal WWTP Waßmannsdorf, near Berlin, BB 12 (basin 12), 14/15 November 2001, $Q_0$ from on-line measurements, concentrations from 2 h mixed samples.

industry (Lehr- und Handbuch der Abwassertechnik 1985). Wastewater with high loads of organics must be treated separately in other industries such as the chemical industry, oil refineries, paper and cellulose production and the pharmaceutical industry (Lehr- und Handbuch der Abwassertechnik 1985).

In contrast to the flow rate, the concentrations of organics are nearly constant over a 24-h period (Fig. 2.3).

Therefore, the changes in load at municipal treatment plants are defined approximately by their change in flow rate. In contrast, the change in the loads from industries can differ remarkably from the changes in flow rate.

#### 2.2.2.2 **Inorganic Substances**

The most important dissolved inorganic substances are nutrients, metals and heavy metals.

**Nutrients**

Special attention is given to nitrogen and phosphorus compounds which cause the growth of cyanobacteria and microalgae in lakes, rivers and the sea (eutrophication; see Chapter 10). The main dissolved components and their concentrations in municipal wastewater are presented in Table 2.3.

**Table 2.3** Typical content of dissolved nitrogen and phosphorus compounds in municipal wastewater (in mg $L^{-1}$; Henze et al. 2002).

| Nutrient | Concentration | Strong | Medium | Weak |
|---|---|---|---|---|
| Nitrogen | $S_{NH}$, $NH_3 + NH_4$ | 50 | 25 | 12 |
| | $S_{ND}$, organic N. | 35 | 15 | 8 |
| Phosphorus | $S_{PO4}$, orthophosphate | 8 | 4 | 2 |
| | $S_{org,P}$, organic | 5 | 3 | 1 |
| | $S_{PP}$, inorganic | 10 | 5 | 3 |

Dissolved $NH_3 + NH_4$ values for industry and agriculture are given in Table 2.4 (Dombrowski et al. 1989). These concentrations are considerably higher than those for municipal wastewater, resulting in more difficult processing and higher costs.

Higher phosphorus concentrations are observed most frequently in effluents of the fertilizer industry, with up to $S_{PO4} = 50$ mg $L^{-1}$ P.

**Table 2.4** Typical content of nitrogen ($NH_3$-N + $NH_4$-N) in wastewater from industry and agriculture (Dombrowski et al. 1989).

| Industry | $S_{NH}$ (mg $L^{-1}$) | Agriculture | $S_{NH}$ (mg $L^{-1}$) |
|---|---|---|---|
| Coke ovens | 800–1000 | Slaughter houses | 80 |
| Coal gasification | 5–1000 | Intensive livestock farming | |
| Oil refineries | 23.8–752.0 | Swine | 2300 |
| Fertilizer | 200–940 | Cattle | 500–2300 |
| Glass | 196 | Utilization of animal carcasses | 807 |
| Cellulose and paper | 264 | | |

### Heavy Metals

Some heavy metals are important trace elements and necessary for bacterial growth because they are components of some enzymes and other proteins. However, municipal and industrial wastewater contain much higher concentrations. Therefore, their concentrations must be limited by law, so that they are not enriched in the food chain of animals.

Concentrations vary greatly in both municipal and industrial effluents. Therefore, it is senseless to publish areas of different values here. We will come back to this point in Section 2.4.2.

### 2.2.3 Colloids

A colloid is a suspension of small particles, mostly in water. These particles may be small solids and small oil droplets or other liquids insoluble in water. In the latter case, the colloid is called an emulsion. Water-in-oil (fat) emulsions (creams, butter, etc.) are of great practical importance. We must often treat oil-in-water emulsions or solid-in-water colloids (turbid water) as impurities in the environment. Both will be described shortly in this section.

#### 2.2.3.1 Oil-In-Water Emulsions

Part of the oil added to water is suspended as large droplets, which rise to the water surface and form an oil film. Another part forms very small droplets as a result of energy input, for example from a rotating stirrer, and is not able to rise to the surface because of the equilibrium between very low buoyancy forces and downward diffusion. They behave as large molecules and move very slowly. If they collide with other small droplets, they coalesce; and then the diameter of the droplets increases and the emulsion is destabilized.

A stabilized emulsion arises by adsorption of anions at the surface. These anions may already be dissolved as $SO_4^{2-}$, $HCO_3^-$, $Cl^-$, etc., or they may be added as special chemical compounds (emulsifiers). The following results are obtained by experiments with dodecane (not soluble in water) and the emulsifier Eumulgin ET 5 (Henkel AG). In a rotor–stator mixer at a speed of 10 000 $min^{-1}$ and a stirring time of 60 s, a stable emulsion was produced with the droplet size distribution presented in Fig. 2.4.

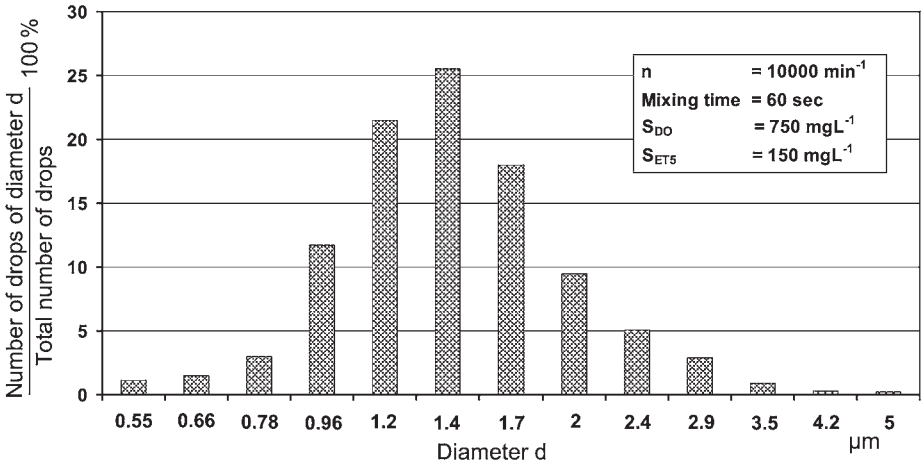


**Fig. 2.4** Size distribution of dodecane droplets in an emulsion stabilized by an emulsifier (Eumulgin ET 5), $S_{D0}$ = 750 mg $L^{-1}$, stirrer speed n = 10 000 $min^{-1}$, $c_{ET5}$ = 150 mg $L^{-1}$, mixing time = 60 s (Cuno 1996).

The diameters of the droplets were measured and the droplets were counted using a microscope (Cuno 1996). In this emulsion, nearly all droplets had diameters between 0.5 µm and 3.5 µm, with a maximum fraction of 25% at 1.5 µm. The fraction describes the number of droplets of this size related to the total number.

Table 2.5 presents some industrial effluents with different oil concentrations. Only a part of the oil concentrations mentioned is really emulsified, while a part is suspended as larger droplets and yet another part may exist as an oil film at the surface.

**Table 2.5** Industrial oil/water suspensions and emulsions (Patterson 1985).

| Wastewater production | Oil concentration (mg $L^{-1}$ COD) |
|---|---|
| Steel rolling mill | 7200 |
| Aluminium rolling mill | 5000–50 000 |
| Ferrous casting | 20–716 |
| Food industry | 3820 |
| Fish processing | 520–13 700 |
| Production of vegetable oil | 4000–6000 |
| Washing water of airplanes | 500–12 000 |
| Textile industry (cleaning of wool and threads) | 1605–12 260 |

It is difficult to measure the concentration of emulsified oil. After separation of nearly all the suspended oil particles by sedimentation (ascending), the oil in the stabilized emulsion can be oxidized and measured as total oxygen demand (TOD), or COD for longer oxidation times. But if there are other dissolved organics, the emulsion must be separated in advance using nano- or ultrafiltration membrane or an extraction method (direct extraction with petrol ether; DIN 38409; Walter 1993).

#### 2.2.3.2 Solid-In-Water Colloids

Small solid particles (minerals, silt, organics, microorganisms) form stabilized colloids after they have adsorbed anions. The light incident on a particle is not transmitted, it is reflected. Depending on the concentration, the mean particle diameter, and particle distribution, turbidity can be observed and measured by using one of two methods: turbidimetry and nephelometry. The latter is widely used. A light beam is directed into the water sample and the light is scattered by the particles (Tyndall effect) and converted to a galvanometric reading. This is compared with a standard such as a formazine polymer colloid (1.25 mg $L^{-1}$ hydrazine sulfate and 12.5 mg $L^{-1}$ hexamethylenetetramine) and set as 1 FTU (*f*ormazine *t*urbidity *u*nit). The colloid standard is used because of its stability and reproducibility (Bratby 1980).

In addition to colloidal solid particles in water, the predominant group of solids is mostly non-settleable. These can be removed by porous membrane filtration of

the total solids (TS) sample (pore size: Denmark, 1.6 µm; Germany, 0.45 µm; Henze et al. 2002). The TS are now separated into a more defined solid-in-water colloid, often called "dissolved solids", and a fraction of suspended solids.

### 2.2.4 Suspended Solids

Unfortunately, in most practical cases, colloids are not separated from suspended solids. Using a graduated Imhoff cone, a sedimentation test yields two fractions: (a) the settleable solids below and (b) the non-settleable solids above, the fraction which now contains the colloid particles.

Mostly, only the settleable solids are measured as X (in mL $L^{-1}$) by reading the scale on the lower part of the Imhoff funnel. More exact data are obtained after separation of the two portions. The organic mass and inorganic mass are definable after filtration, drying, weighing, incineration at 500 °C and re-weighing the ash. Table 2.6 presents some typical data for domestic wastewater.

**Table 2.6** Suspended solids as organics and minerals (Pöpel 1997), Q = 115 L (inh. d)$^{-1}$ (Table 2.1; selected and partly converted data).

| Solids | Unit | Settleable solids | Non-settleable solids | Total |
|---|---|---|---|---|
| Organics | g MLVSS $d^{-1}$ | 40 | 20 | 60 |
| | g $L^{-1}$ MLVSS | 0.350 | 0.175 | 0.525 |
| Minerals | g MLSS $d^{-1}$ | 20 | 10 | 30 |
| | g $L^{-1}$ MLSS | 0.175 | 0.086 | 0.260 |

In municipal wastewater and especially in industrial effluent, the concentration of suspended solids can vary considerably from the data in Table 2.6. For more specific information about different branches of industry, see Pöppinghaus et al. (1994).

## 2.3 Methods for Measuring Dissolved Organic Substances as Total Parameters

### 2.3.1 Biochemical Oxygen Demand

The biochemical oxygen demand ($BOD_n$) is the mass of oxygen which is needed by microorganisms during a test in closed flasks over a period of 5 ($BOD_5$), 10 ($BOD_{10}$) or 20 days ($BOD_{20}$) at a temperature of 20 °C, pH 7–8 and after the addition of nutrients. Additional bacteria have to be injected into samples which contain too few bacteria. In these cases, biologically treated wastewater or contaminat-

ed surface water can be added to domestic wastewater after settling. The $BOD_5$ of these supplements must be taken into account (Fresenius et al. 1988).

Depending on the concentration of biodegradable substances, it may be necessary to dilute with water containing various nutrients. Four different solutions with special nutrients should be prepared, which can be used simultaneously as dilution water. This should be saturated with oxygen.

Predominately, two different methods are used to measure the amount of oxygen needed. The quantity of dissolved oxygen consumed is determined by measuring the difference of dissolved oxygen, either electrometrically using an electrode or manometrically (Ramalko 1983; Fresenius et al. 1988).

In the first case, glass flasks of 110–130 ml or 250–300 ml (with stoppers) are prescribed, which must be totally filled after they are diluted accordingly with water.

In the second case, the sample is put into a vessel leaving a space for air, which can be closed off from the atmosphere. The sample must be stirred or shaken during the measurement in order to avoid any influence of mass transfer on the $O_2$ consumption rate. The $CO_2$ produced, which is not dissolved or converted to $HCO_3^-$, is adsorbed by potassium hydroxide. According to the volume of the air enclosed in the bottle, a certain amount of oxygen is available, so that higher dilutions are not necessary.

Usually, BOD measurements are made after removing the settleable solids from the sample by sedimentation. Therefore, the measurement includes not only the dissolved organics but also the organic colloids and the non-settleable solids, which may partly be hydrolyzed and used by aerobic microorganisms. In addition, bacteria use oxygen by endogenous respiration; and some of them die and thus produce new substrate after cell lysis. The most important disadvantage of the method, however, is its long measuring time. $BOD_5$ is not suitable as a control parameter for treatment plants if rapid measurements are necessary.

Several rapid BOD measuring devices have been developed to improve response time. The ZAW-LAB and ZAW-FIX (GIMAT) are semi-continuous analyzers for the on-line determination of respirometry rates. A sample is saturated with oxygen and mixed with an adapted culture. The oxygen consumption rate is determined from the sinking dissolved oxygen concentration over time and is used for the calculation of the $BOD_5$. The Bio Monitor from LAR (Laser and Analytical Research GmbH) works continuously. Two small, four-step cascades are operated in parallel. One is supplied with air, activated sludge and sample, and another only with air and activated sludge. After a retention time of only 1–4 h, the substrate is nearly completely consumed, resulting in a corresponding oxygen consumption, which is calculated from the difference between the two cascades. The short measuring time results from the elevated temperature of 30–35 °C and the higher bacterial concentration.

### 2.3.2 Chemical Oxygen Demand

The chemical oxygen demand (COD) is defined as the mass of oxygen needed for the complete oxidation of an organic compound present in water. For the oxidation of glucose $(CH_2O)_6$, a representative hydrocarbon, 1 mol $O_2$ $mol^{-1}$ C is needed according to:

$$(COH_2)_6 + 6\ O_2 \rightarrow 6\ CO_2 + 6\ H_2O \tag{2.2}$$

For the standard COD test, a measured sample with a known excess of potassium dichromate ($K_2Cr_2O_7$) is mixed after the addition of $H_2SO_4$ and silver sulfate ($Ag_2SO_4$). The organic matter is oxidized over a 2-h heating period. After this time, the concentration of the remaining dichromate is measured by titration with ferroxine ($Fe^{2+}$) (Ramalko 1983; Fresenius et al. 1988):

$$Cr_2O_7^{2-} + 6\ e^- + 14\ H^+ \rightarrow 2\ Cr^{3+} + 7\ H_2O \tag{2.3}$$

$$Cr_2O_7^{2-} + 6\ Fe^{2+} + 14\ H^+ \rightarrow 2\ Cr^{3+} + 6\ Fe^{3+} + 7\ H_2O \tag{2.4}$$

Equation (2.3) is a reduction reaction, because of the use of electrons. The complete oxidation of glucose is expressed by:

$$(COH_2)_6 + 6\ H_2O \rightarrow 6\ CO_2 + 24\ H^+ + 24\ e^- \tag{2.5}$$

After combining (2.3) and (2.5) we obtain:

$$(COH_2)_6 + 4\ Cr_2O_7^{2-} + 32\ H^+ \rightarrow 6\ CO_2 + 8\ Cr^{3+} + 22\ H_2O \tag{2.6}$$

Four moles of $Cr_2O_7^{2-}$ are needed for the oxidation of six C atoms.

In this special case, all of the carbon in the organic compound is assumed to be oxidized and the COD can be called TOD (total oxygen demand). Usually, the substrate is only partly oxidized by $K_2Cr_2O_7$ and some organic oxidized products remain. These values of the COD may vary between 70% and 95% of the TOD.

In order to reduce the 2 h needed for this measurement, several instruments have been developed and automated. In the on-line continuous COD measurement device made by the company Product Finder the standard method includes mixing the heated sample with $K_2Cr_2O_7$ to drive a reduction of Cr(VI) to Cr(III). The green coloration is measured colorimetrically and is proportional to the amount of Cr(III) formed and the concentration of oxidized organic substance.

Other oxidants are used by other developers. LAR takes advantage of OH° radicals which oxidize the organics at a high rate. These radicals are produced by an electrode, with a rate proportional to the electrical current and therefore the rate of oxidation. Other instruments use the fast oxidation of $H_2O_2$/UV with the measurement of $H_2O_2$ consumption (GIMAT), or $O_3$ consumption with the measurement of $O_3$ in water (PHOENIX-1010 STIP; Isco Inc.) or in air (OXI-JET; UVT-Ingenieurbüro für Umwelt- und Verfahrenstechnik).

### 2.3.3 Total and Dissolved Organic Carbon

Organic substances contained in water samples are oxidized either (a) by UV rays (low-pressure UV lamp) in the water sample, (b) by wet chemical oxidizers in the water sample, or (c) by oxidizing at high temperatures (~950 °C) with or without catalysts.

The amount of $CO_2$ can then be measured, either (a) by using a non-dispersive $CO_2$ infrared analysis device, or (b) by using a flame ionization detector (FID) after conversion of $CO_2$ into $CH_4$ by heterogeneous catalysis.

TOC (total organic carbon) measurement is usually performed on the sample after sedimentation.

If the DOC (dissolved organic carbon) should be measured, the sample has to be separated from suspended non-settleable particles and from some colloids, by using a glass fiber filter or a centrifuge (Fresenius et al. 1988). Both filters and centrifuge glasses must be cleaned carefully with distilled water in advance.

The TC (total carbon) is the sum of organic and inorganic carbon ($CO_2$, $HCO_3^-$, $CO_3^{2-}$ dissolved in water). Often both the organic and the inorganic carbon are measured after heating the sample to 950 °C (reaction tube 1, TC) and only the inorganic carbon at 150 °C (reaction tube 2, TC-TOC). The difference between TC and inorganic carbon is the TOC, if the sample was not filtered, and is equal to the DOC if the sample was filtered (Ramalko 1983).

The measurement of TOC/DOC has been automated since and the time for analysis reduced remarkably. In the Shimadzu TOC-4110, the sample is oxidized catalytically after heating and $CO_2$ is measured by low-pressure infrared analysis.

**Table 2.7** Total concentration parameters for typical raw domestic wastewater and after biological treatment with nitrification (Henze et al. 1995).

| Parameter | Unit | Wastewater | |
|---|---|---|---|
| | | Raw | After treatment |
| Biochemical oxygen demand | | | |
| • after 5 days | mg $L^{-1}$ $BOD_5$ | 280 | 25 |
| • after 20 days (total) | mg $L^{-1}$ $BOD_{20}$ | 400 | 35 |
| Chemical oxygen demand | mg $L^{-1}$ COD | | |
| • easily biodegradable | | 60 | 5 |
| • slowly biodegradable | | 200 | 10 |
| • with $KMnO_4$ | | 180 | 30 |
| • with $K_2Cr_2O_7$ | | 600 | 100 |
| • total (900 °C, Pt catalyst) | | 800 | 230 |
| Total organic carbon | mg $L^{-1}$ TOC | | |
| • at 800 °C | | 200 | 35 |
| Dissolved organic carbon | mg $L^{-1}$ DOC | 160[a)] | 15[a)] |

[a)] WWTP Waßmannsdorf, near Berlin.

The sample is diluted and prepared automatically, resulting in a low measuring time of 3–5 min. In two other developments, the combustion temperature is increased to 1150 °C (TOC-/TC-Analyzer; GIMAT) or to more than 1200 °C (Quick TOC; LAR) without using a catalyst. In all cases, calibration is necessary. Frequently, potassiumhydrogenphthalate is recommended (Fresenius et al. 1988).

Table 2.7 presents some data for total concentration parameters in a typical domestic wastewater.

Several points are worth highlighting:

- The $BOD_5$ is lower than the $BOD_{20}$ because of nitrification, which starts only after several days, and because of the removal of slowly biodegradable substances (see Section 2.3.1).
- The COD depends strongly on the method used. A total oxidation and conversion to $CO_2$, $H_2O$, $NO_3^-$ is only possible by combustion at 900 °C and by using a catalyst or at ~1200 °C without any catalyst.

## 2.4 Legislation

### 2.4.1 Preface

German legislation concerning the discharge of wastewater into public sewers (Ind. VO 1989: Indirekteinleiterverordnung; regulation of indirect introduction) and into surface waters (Mindestanforderungen nach §7a, WHG (2002); minimum requirement, §7a, water resource policy law) places a limit on emissions. This will be presented shortly in the next section.

After that we will briefly discuss EU guidelines for pollution control of waters, which limit immissions, that is, for discharges of treated wastewater into water, not concerning fixed loads or concentrations, but loads which can still be tolerated by the water.

### 2.4.2 German Legislation

#### 2.4.2.1 Legislation Concerning Discharge into Public Sewers

The most important piece of legislation is the "Indirekteinleiterverordnungen der Bundesländer der Bundesrepublik Deutschland (Ind. VO 1989)", regulation of indirect introduction by the states of the Federal Republic of Germany. All industries with discharges of contaminants into public sewer systems which exceed a minimum concentration or hourly load must report this to the local water authority. Effluents with high concentrations and loads coming from specific origins must be treated before being discharged into the public sewers. The Ind. VO of Baden Württemberg (regulation of indirect water disposal for Baden Württemberg, Germany) is presented as an example (Table 2.8).

**Table 2.8** Threshold values required for approval to discharge hazardous materials into public sewer systems (Ind. VO Baden Württemberg; WEKA 2005).

| Material or group of materials | Method of analysis | Thresholds | |
|---|---|---|---|
| | | Concentration (mg $L^{-1}$) | Load (g $h^{-1}$)[a)] |
| Cl total | DIN 38 408-G 4-1/2, June 1984 | 0.2 | 4.0 |
| Cyanide | DIN 38 405-D 13-2, Feb. 1981 | 0.1 | 2.0 |
| As | DIN 38 405-D 18, Sept. 1985 | 0.05 | 1.0 |
| Pb | DIN 38 406-E 6, May 1981 | 0.2 | 8.0 |
| Cd | DIN 38 406-E 19, July 1980 | 0.02 | 0.4 |
| Cr total | DIN 38 406-E 22, March 1988 | 0.2 | 8.0 |
| Cu | DIN 38 406-E 22, March 1988 | 0.3 | 12.0 |
| Ni | DIN 38 406-E 22, March 1988 | 0.2 | 6.0 |
| Hg | DIN 38 406-E 12-3, July 1980 | 0.005 | 0.1 |
| Ag | DIN 38 406-E 22, March 1988 | 0.1 | 6.0 |
| Zn | DIN 38 408-E 22, March 1988 | 0.5 | 20.0 |
| Halogenated hydrocarbon AOX | DIN 38 409-H 18 | 0.5 | 10.0 |
| 1,1,1-trichloroethane, trichloroethene, tetrachloroethene, trichloroethane | Gas chromatography | 0.1 (Cited values are the sum of all mentioned compounds, calculated as Cl) | 2.0 |

[a)] Thresholds in g $h^{-1}$ must be taken from water volume within 1 h.

Several other problems may arise after a discharge of industrial effluents into the public sewer system. Here, only a few are mentioned:

- The settling rate of some solid particles with low density is not sufficient.
- Toxic compounds may decrease the biological activity of bacteria.
- High water temperature may cause an increase of total water temperature to >35 °C and the metabolism of bacteria may be slowed or stopped.
- High, isolated loads of industrial discharges may cause too high a loading of the municipal plant, resulting in non-conformance to the regulations.

In these cases, buffer tanks are often prescribed to protect the treatment processes of the municipal plant. Guidelines are given with ATV-A 115.

#### 2.4.2.2 Legislation Concerning Discharge into Waters

These limiting emission values are valid for effluents from wastewater treatment plants and canals into bodies of water. Naturally, these canals collect treated wastewater from municipalities and industries, but other sources of wastewater may be additionally polluted by agriculture or small communities.

**Table 2.9** AbwV, Appendix 1: municipalities.

| Minimum requirements after §7a, WHG (2002), Appendix 1 (kg $BOD_5$ $d^{-1}$) | $S_S$ (mg $L^{-1}$ COD) | $S_S$ (mg $L^{-1}$ $BOD_5$) | $S_{NH4\text{-}N}$ (mg $L^{-1}$ N) | $S_{Nt}$ (mg $L^{-1}$ N) | $S_{Pt}$ (mg $L^{-1}$ P) |
|---|---|---|---|---|---|
| Class 1: <60 | 150 | 40 | – | – | – |
| Class 2: 60–300 | 110 | 25 | – | – | – |
| Class 3: 300–600 | 90 | 20 | 10 | – | – |
| Class 4: 600–6000 | 90 | 20 | 10 | 18 | 2 |
| Class 5: >6000 | 75 | 15 | 10 | 13 | 1 |

**Table 2.10** AbwV, Appendix 47: washing water for fuel gas from power plants.

| Minimum requirements (after §7a, WHG 2002) | Appendix 47: power plants | | |
|---|---|---|---|
| Specific concentration (mg $L^{-1}$) | Coal (mg $kg^{-1}$ chloride; $Cl^-$) | Lignite coal (mg $kg^{-1}$ $Cl^-$ content at <0.05 mass%) | Domestic refuse (mg $t^{-1}$ waste)[d] |
| COD | 80[a]<br>150[b] | 80[a]<br>150[b] | |
| Filterable material | 30.0 | 30.0 | |
| Pb | 3.6 | 0.2[c] | 30 |
| Cd | 1.8 | 0.1 | 15 |
| Cr, total | 1.8 | 1.0 | 150 |
| Cu | 18.0 | 1.0 | 150 |
| Ni | 18.0 | 1.0 | 150 |
| Hg | 1.8 | 0.1 | 15 |
| Zn | 36.0 | 2.0 | 300 |
| F | 30.0 | 30.0 | |

[a] Using slaked lime.
[b] Using limestone.
[c] Loads given in g $h^{-1}$ for 300 MW electric power.
[d] Discharge of this wastewater is not allowed.

The legislation is called "Rahmen-Abwasser VwV[1] 1992 nach §7a WHG[2] (2002)" (Framework Regulation for Sewage), which was amended by the AbwV[3] (2004). This regulation prohibits the mixing or dilution of wastewater in order to meet the limiting values. In contrast to the Indirekteinleiterverordnung (Section 2.4.2.1), this regulation is valid for all states of the FRG. The rules which apply,

[1] *Verw*altungs*v*orschrift, regulation.
[2] *W*asser*h*aushaltsgesetz, water resource policy law.
[3] *A*bwasser*v*erordnung, regulation for wastewater.

however, depend on the size of the municipalities (Appendix 1) and cover 56 industrial fields (Appendices 2–57). Here, we only want to present two examples: Appendix 1 (municipalities; Table 2.9) and Appendix 47 (washing water containing fuel gases from power plants; Table 2.10).

All the necessary details concerning the collecting of samples, their preparation and analysis are given in AbwV.

In contrast to municipal wastewater (Table 2.9), the effluents of fuel gas washing typically contain high concentrations of heavy metals. According to the regulation, these must now be separated from the washing water. Nutrients such as nitrogen and phosphorus as well as biodegradable substances ($BOD_5$) contained in municipal wastewater are not considered as important pollutants here.

### 2.4.3 EU Guidelines

In these guidelines, the qualities of four different surface waters are described according to their concentration, pH, temperature, color and 42 further parameters, which must not be exceeded (AbwV.; Schulz and Becker 2004). The following guidelines are valid for four different purposes:

- for surface water used for drinking water production,
- for surface water used for swimming and bathing (see Section 12.5),
- for fish farming,
- for mussel farming.

Two types of values are to be distinguished: (a) I-values (which are obligatory = *i*mperative) and (b) G-values (which are guide values = *g*uidelines).

Three types of surface water preparation must be distinguished for drinking water production:

A 1, simple physical methods.
A 2, normal physical and chemical methods.
A 3, advanced physical and chemical methods.

These guidelines for the limitation of *immissions* are characterized by the following advantages compared with such legislation, which is valid for the limitation of emissions (Rahmen-Abwasser VwV 1992):

- A better economical efficiency for all WWTPs; the degree of wastewater treatment is directly linked to the quality demands on the surface water generated, and unnecessary expenditures can be avoided.
- The quality of the treated wastewater can be controlled in such a way to ensure that the surface water can be used as planned.
- The total pollution of the surface water and its capacity of self-purification are considered.
- Different qualities of treated water can be defined in order to stabilize the ecological equilibrium.

The following disadvantages should be considered:

- No experience has been gained with the sampling frequency and the allowed differences of high-tide values from the guideline values.
- There may be problems if the discharged treated wastewater is to be controlled, because the receiving capacity depends greatly on the quality of the receiving water.

## References


AbwV **2004**, Abwasserverordnung: Verordnung über Anforderungen an das Einleiten von Abwasser in Gewässer, Fassung vom 17.6.2004.

ATV-A 115 **1994**, Einheiten von nicht häuslichem Abwasser in eine öffentliche Abwasseranlage, DWA Regelwerk 10.

Bratby, J. **1980**, *Coagulation and Flocculation*, Uplands Press, Croydon.

Busse, H.J. **1975**, Instrumentelle Bestimmung der organischen Stoffe in Wässern, *Z. f. Wasser- und Abwasser-Forschung* 8, 164–176.

Chow, V.T.; Eliassen, R.; Linsley, R.K. (eds) **1979**, *Wastewater Engineering: Treatment Disposal, Reuse*, McGraw-Hill, New York.

Cuno, M. **1996**,: Kinetische Untersuchungen zum biologischen Abbau von Mineralölen und polycyclischen aromatischen Kohlenwasserstoffen, *VDI-Forschungsberichte, Reihe 15, Umwelttechnik*, 148.

Dombrowski, T.; Lompe, D.; Wiesmann, U. **1989**, Biologische Stickstoffeliminierung aus Abwässern, *BioEngineering* 5, 18–27.

Fresenius, W.; Quentin, K.F.; Schneider, W. (eds) **1988**, *Water Analysis*, Springer-Verlag, Berlin.

Henze, M.; Harremoes, P.; Jansen, J.; Arvin, E. **2002**, *Wastewater Treatment, Biological and Chemical Processes*, Springer-Verlag, Heidelberg.

Ind. VO **1989**, Indirekteinleiter-Verordnung: Verordnung über die Genehmigungspflicht für die Einleitung gefährlicher Stoffe und Stoffgruppen in öffentliche Abwasseranlagen und ihre Überwachung vom 14. März 1989, Ind. VO ISBN.

Lehr- und Handbuch der Abwassertechnik **1985**, *Organisch verschmutzte Abwässer der Lebensmittelindustrie*, ed. Abwassertechnische Vereinigung e.V., St. Augustin, Ernst & Sohn Verlag, Berlin.

Patterson, J.W. **1985**, *Industrial Wastewater Treatment Technology*, Butterworths, New York, p. 273–302.

Pöpel, F. (ed) **1997**, *Abwassertechnik und Gewässerschutz*, C.F. Müller Verlag, Heidelberg.

Pöppinghaus, K.; Fresenius, W.; Schneider, W. (eds) **1994**, Chapter 2.2.1: Menge des kommunalen Schmutzwassers, in: *Abwassertechnologie*, Springer-Verlag, Berlin.

Rahmen-Abwasser VwV **1992**, Allgemeine Rahmen-Verwaltungsvorschrift über Mindestanforderungen an das Einleiten von Abwässer in Gewässer (Rahmen-Abwasser VwV vom 25.11.1992), *Bundesanzeiger* 233b.

Ramalko, R.S. **1983**, *Introduction to Wastewater Treatment Processes*, Academic Press, New York (Table 2.1).

Schuchardt, A. **2005**, Bestimmung des dynamischen Sauerstoffeintrags in nitrifizierende Belebtschlammreaktoren einer kommunalen Kläranlage, *VDI-Forschungsberichte, Reihe 3*, 842.

Schulz, R.S.; Becker, B. **2004**, *Deutsche Umweltschutz Gesetze, Bd. 5, Europäisches Umweltrecht*, Verlag R. S. Schulz, Berlin.

Walter, J. **1993**, Vergleichende Untersuchungen zur Druckentspannungsflotation und Begasungsflotation von Emulsionen und Suspensionen in einem pH-Bereich von 6.8 bis 7.3, *PhD Dissertation*, TU Berlin.

WEKA **2005**, Das neue Wasserrecht für die betriebliche Praxis, WEKA Media.

WHG **2002**, Gesetz zur Ordnung des Wasserhaushalts (BGBl. I Nr. 59 vom 23.08.2002, S. 3245; 06.01.2004, S. 2), Wasserhaushaltsgesetz.

# 3
# Microbial Metabolism

## 3.1
## Some Remarks on the Composition and Morphology of Bacteria (Eubacteria)

The elementary composition of bacteria does not vary considerably during their life cycle and between different strains. Table 3.1 presents data for *Escherichia coli* (*E. coli*), left side (Bailey and Ollis 1977) and as mean values for bacteria, right side (Schlegel 1992). The various types of bacteria according to the eighth edition of Bergey's Manual of Determinative Bacteriology (1974) are categorized into 19 groups (Cano and Colomé 1986) or in 17 sections and seven groups (Volk and Wheeler 1986). Detailed information about the most important microorganisms was compiled by O'Leary (1989). The importance of microbial communities in environmental microbiology was the subject of the editors Insam and Rangger (1997). Schön (1978a, b) published an introduction for students.

**Table 3.1** Composition of bacteria (*E. coli*).

| Element | Mass % of dry matter | Substances | Mass % of dry matter |
|---|---|---|---|
| Carbon | 50 | Inorganics | 6 |
| Oxygen | 20 | Grease | 10 |
| Nitrogen | 14 | | |
| Hydrogen | 8 | Micromolecular organics (excluding grease) | 7 |
| Phosphorus | 3 | | |
| Potassium | 1 | Macromolecular organics (polymers)[a)] | 77 |
| Sulfur | 1 | | |
| Sodium | 1 | Proteins | 50 |
| Calcium | 0.5 | Nucleic acids RNA | 16–17 |
| Magnesium | 0.5 | DNA | 3–4 |
| Chlorine | 0.5 | Lipids | 10 |
| Iron | 0.2 | Cell wall | 20 |
| Others | 0.3 | | |

[a)] Polymers recalculated to 100%.

*Fundamentals of Biological Wastewater Treatment*. Udo Wiesmann, In Su Choi, Eva-Maria Dombrowski

ISBN: 978-3-527-31219-1

**1. Cocci, sperical bacteria**

Gram-positive:

| | |
|---|---|
| • aerobic and/or facultative anaerobic: | Lactobacillus<br>*Streptococcus, Leuconostoc, Pediococcus*<br>*Micrococcus, Staphylococcus* |
| • anaerobic | *Peptococcus, Peptostreptococcus, Ruminococcu*<br>*Sarcinas* |

Gram-negative:

| | |
|---|---|
| • aerobic | *Neisseria, Moraxella, Acinetobacter,*<br>*Paracoccus, Lampropedia, Methylococcus* |
| • anaerobic | *Veillonella, Acidaminococcus, Megasphaera* |

**2. Rod-shaped, stretched cylindrical bacteria**

**A) Non-spore forming rods**

Gram-positive:

| | |
|---|---|
| • aerobic and/or facultative anaerobic: | Coryneform bacteria<br>*Corynebacterium, Arthrobacter, Brevibacterium,*<br>*Cellulomonas, Mycobacterium, Nocardia* |
| • anaerobic: | Propionat bacteria<br>Lactobacilla<br>*Lactobacillus, Bifidobacterium* |

Gram-negative:

| | |
|---|---|
| • aerobic: | Pseudomonads<br>*Pseudomonas, Xanthomonas, Zoogloes*<br>*Acetobacter*-Gruppe<br>*Azotobacter*-Gruppe<br>*Azotobacter, Azomonas, Beijerinckia, Derxia* |
| • facultative anaerobic: | Entero bacteria<br>*Escherichia, Salmonella*<br>*Shigella, Klebsiella, Serratia*<br>*Proteus, Erwinia, Enterobacter*<br>*Chromobacterium, Pasteurella* |
| • strictly anaerobic: | *Bacteroides, Fusobacterium* |

**B) Spore forming rods (bacilli)**

| | |
|---|---|
| • aerobic: | *Bacillus, Sporolactobacillus*<br>*Sporosarcina* |
| • anaerobic: | *Clostridium, Desulfotomaculum*<br>*Oscillospira* |

**3. Curved rods**

| | |
|---|---|
| • aerobic: | *Spirillum, Vibrio, Bdellovibrio*<br>*Desulfovibrio* |
| • anaerobic: | *Succinovibrio, Butyrivibrio, Selenomonas* |

**Fig. 3.1** Eubacteria (Schlegel 1992).

Normally, bacteria are divided into ten classes. The first class is that of the eubacteria, which is the most important in environmental microbiology (Schlegel 1992). Therefore, only eubacteria are characterized here in a general manner by Fig. 3.1.

The size of bacteria in comparison to other particles is demonstrated by Fig. 3.2. Because of their small diameter of only $10^{-3}$ mm, bacteria have a large surface per mass. Since the uptake of nutrients occurs via the outer surface, bacteria are characterized by a high growth rate, resulting in a high substrate removal rate.

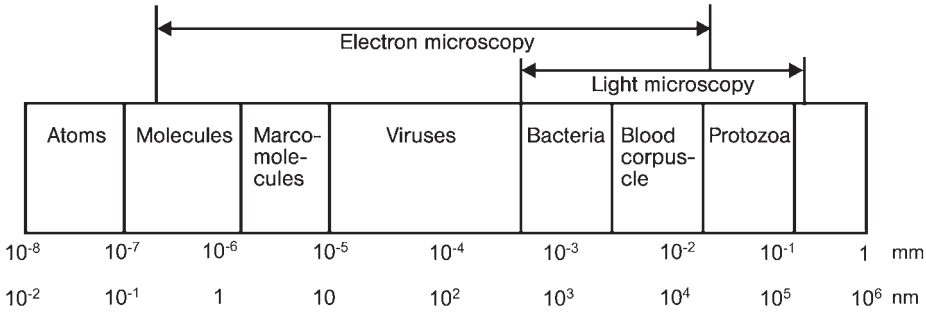


**Fig. 3.2** Mean diameters of particles.

## 3.2
## Proteins and Nucleic Acids

### 3.2.1
### Proteins

#### 3.2.1.1 Amino Acids

As follows from Table 3.1, nearly 50% of bacterial cell mass is protein. Proteins are macromolecules formed by a chain of amino acids. Twenty different amino acids are used in nature for building proteins; and they are all characterized by the same groups, called peptides (Fig. 3.3).

The simplest amino acid is formed with only a hydrogen atom located on a side-chain. It is called glycine (Fig. 3.3a). There exist two isomeric types of glycine, an L-type (Fig. 3.3b) which rotates polarized light to the left in aqueous solution and a

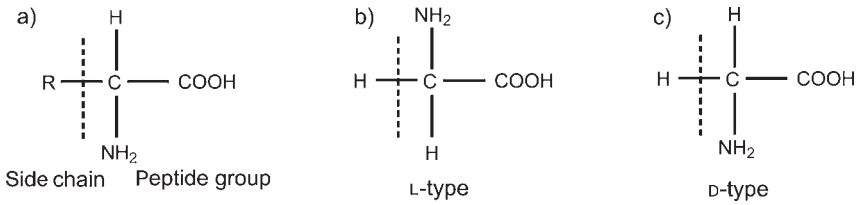


**Fig. 3.3** Amino acids. (a) Structure of an amino acid. (b) L-type: isometric type of the simplest amino acid glycine. (c) D-type: isometric type of the simplest amino acid glycine.

**Table 3.2** Amino acids used for protein synthesis.

| Amino acid | Abbreviation | Side-chain |
|---|---|---|
| Cysteine | Cys | Neutral polar (uncharged) |
| Tyrosine | Tyr | |
| Asparagine | Asn | |
| Glutamine | Gln | |
| Aspartic acid | Asp | Acidic (negatively charged) |
| Glutamic acid | Glu | |
| Glycine | Gly | Neutral polar (uncharged) |
| Serine | Ser | |
| Threonine | Thr | |
| Lysine | Lys | Basic (positively charged) |
| Arginine | Arg | |
| Histidin | His | |
| Alanine | Ala | Nonpolar (hydrophobic) |
| Valine | Val | |
| Leucine | Leu | |
| Isoleucine | Ile | |
| Proline | Pro | |
| Phenylalanine | Phe | |
| Tryptophane | Trp | |
| Methionine | Mat | |

D-type, which rotates it to the right (Fig. 3.3c). Only the L-type is used for protein synthesis; the D-type is used for antibody synthesis. The other 19 amino acids have asymmetric side-chains, each with a number of isomeric types. They are shown in Table 3.2.

The chemical structures of all the 20 amino acids are published in several textbooks of microbiology, for example Cano and Colomé (1986) and Gaudy and Gaudy (1989).

#### 3.2.1.2 **Structure of Proteins**

Amino acids polymerize by forming a polypeptide bond and releasing a water molecule, thereby building a protein molecule (Fig. 3.4). The 20 amino acids can be combined to many permutations in this way to form large protein molecules with a molar mass up to $10^6$ g $mol^{-1}$ and an enormous number of different successions of amino acids. The four atoms of the peptide bond are oriented in one plane, in contrast to all other atoms which lie in different planes.

The primary structure of the protein molecule results from a linear polymerization. $R_1$, $R_2$, ... $R_{20}$ are the different side-chains which are typical for one of the 20 different amino acids.

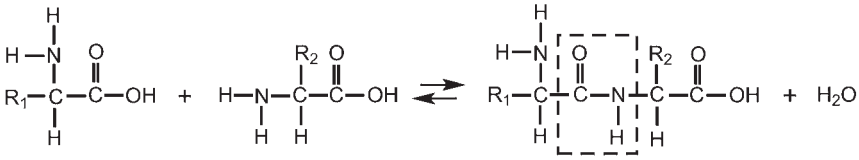

**Fig. 3.4** Formation of a peptide bond.

### 3.2.1.3 Proteins for Special Purposes

Because of the high number of possible structures and varying molar mass, proteins are able to assume different functions. Some of these are described in Table 3.3.

Enzymes are biocatalytic proteins. Nearly all reaction steps in living organisms are catalyzed by enzymes. No organism would be able to live without the effect of enzymes; and each reaction step must be catalyzed by a special enzyme. Therefore, enzymes and their functions will be discussed briefly.

**Table 3.3** Different groups of proteins and examples for special functions.

| Group of proteins | Example | Purpose |
|---|---|---|
| Enzymes | Cytochrome | Transfer of electrons in respiration chain |
| Transport proteins | Haemoglobin | Transport of oxygen in blood |
| Toxins | Poison produced by yeasts | Repulsion of bacteria |
| Hormones | Insulin | Regulation of glucose degradation |
| Structural proteins | Glycoprotein | Components of cell wall |

### 3.2.1.4 Enzymes

The well known Arrhenius equation shows the dependence of the reaction rate on temperature:

$$k = k_o \exp\left(-\frac{E_A}{RT}\right) \tag{3.1}$$

where k is the coefficient of reaction rate, $k_o$ is the theoretical maximal value for $T \rightarrow \infty$ (°C), $E_A$ is the energy of activation (kJ $mol^{-1}$), R is the general gas constant (kJ $mol^{-1}$ $K^{-1}$) and T is the temperature (K).

A reduction in $e_A$ leads to an increase in k. The significance of enzymes is their ability to reduce $e_A$ considerably, which results in high reaction rates at moderate temperatures (Fig. 3.5).

The free energy change of a reaction can be measured as the heat of reaction, resulting in a transfer of energy to the surroundings.

The simplest reaction may be the isomerization of a substrate molecule. This can be described in a very simple way by Fig. 3.6a (Scragg 1988).

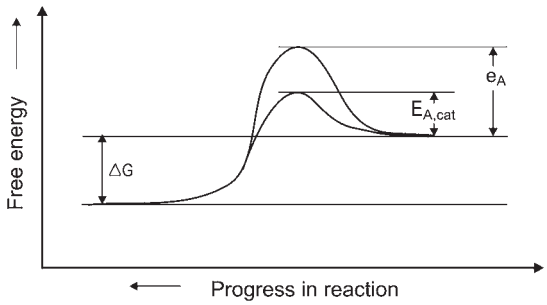


**Fig. 3.5** Reduction of energy of activation by an enzyme (catalyst).

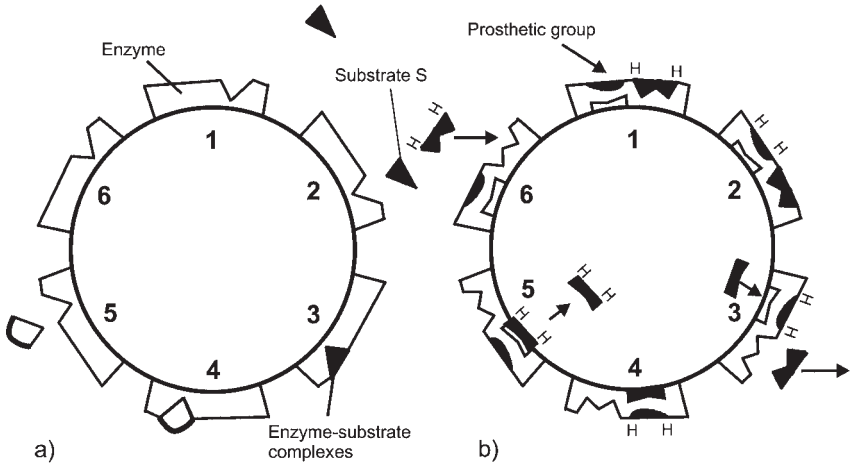


**Fig. 3.6** Models for a better understanding for the effects of enzymes. (a) Model for a one enzyme–one substrate reaction without transfer of atoms or molecules (isomerization). (b) Model for a one enzyme–two substrate reaction with the help of a prosthetic group.

The kinetics of this reaction were modelled by Michaelis and Menten (1913), assuming an adsorption equilibrium for the substrate S at the active site of the enzyme (enzyme/substrate complex ES):

$$S + E \underset{k_2}{\overset{k_1}{\rightleftharpoons}} ES \xrightarrow{k_3} E + P \tag{3.2}$$

A first-order reaction rate is assumed for each step. Writing $r_S = k_3\, S_{ES}$ and $r_{smax} = k_3\, S_{E0}$, we obtain:

$$\frac{r_s}{r_{s\,max}} = \frac{S_{ES}}{S_{E0}} \tag{3.3}$$

and

$$S_{E0} = S_E + S_{ES} \tag{3.4}$$

After a non-stationary period of ES formation, the concentration $S_{ES}$ does not change with time. It is possible to write:

$$\frac{dS_{ES}}{dt} = 0 = k_1 S_E S - k_2 S_{ES} - k_3 S_{ES} \tag{3.5}$$

Considering Eqs. (3.3) to (3.5), the Michaelis–Menten equation follows:

$$r_s = r_{s\,max} \frac{S}{K_m + S} \tag{3.6}$$

with

$$K_m = \frac{k_2 + k_3}{k_1} \tag{3.7}$$

Eq. (3.6) can be transformed easily to linear equations, which are suitable for testing experimental results and for determining $r_{s\,max}$ and $K_m$ (plots called Lineweaver–Burk, Langmuir and Eadie–Hofstee; see Scragg 1988).

A further large group of enzymes called oxidoreductases catalyzes oxidation and reduction reactions (redox reactions) by the transfer of $H^+$ ions from one molecule to another. Enzymes with a prosthetic group are able to take up two different substrate molecules at two different active sites. The transfer of $H^+$ progresses via adsorption at the prosthetic group, which does *not* leave the substrate (Fig. 3.6b).

A further system consists of a pair of two different enzymes, each of them for one of two different substrates. Let us discuss this kind of biocatalysis again for the case of a redox reaction. Now the $H^+$ ions must be transferred from one substrate molecule to the other. For this purpose, a coenzyme is needed as a small part of the substrate molecule which is able to oxidize substrate 1, to leave substrate 1 and to carry the $H^+$ ions to substrate 2, where substrate 2 is then reduced (Fig. 3.7).

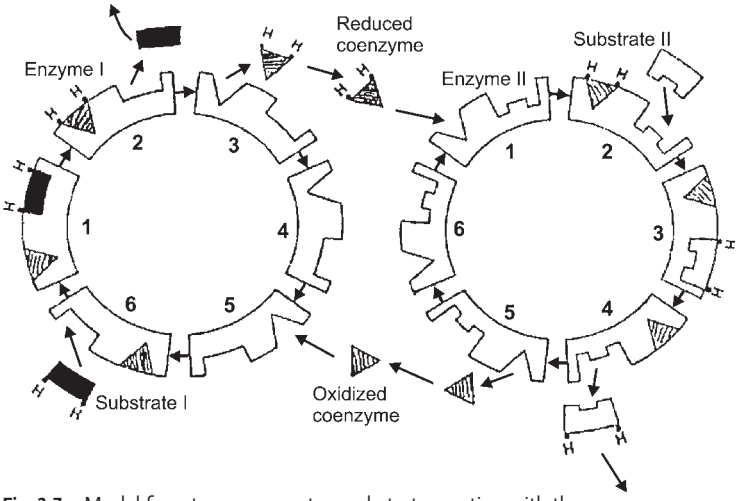


**Fig. 3.7** Model for a two enzyme–two substrate reaction with the help of a coenzyme (e.g. redox reaction).

The most important enzymes can be divided into six large groups, which are listed in Table 3.4.

Although a very large amount of information can be stored and transferred by proteins according to their primary structure, proteins exhibit further distinctions forming secondary, tertiary and quaternary structures. Detailed information is given by Cano and Colomé (1986).

**Table 3.4** Important groups of enzymes.

| Group | Catalyzes the following reaction |
|---|---|
| Isomerase | Reversible conversion of isomeric compounds |
| Oxidoreductase | Oxidation and reduction by transfer of hydrogen ions or electrons |
| Transferase | Transfer of defined groups from one molecule (donor) to another (acceptor) |
| Hydrolase | Hydrolytic reactions |
| Lyase | Separation of groups from molecules (without hydrolysis) |
| Ligase | Combination of two molecules during the splitting of an energy-rich bond |

## 3.2.2 Nucleic Acids

### 3.2.2.1 Desoxyribonucleic Acid

A nucleic acid is formed from a large number of nucleotides via polymerization. Each nucleotide consists of a heterocyclic nitrogen base, a pentose sugar and a phosphate group (Fig. 3.8a).

Besides adenine as the nitrogen base in Fig. 3.8a, three other bases can be connected to carbon atom 1′ of the pentose molecule. Figure 3.8b shows the four nitrogen bases.

One nucleotide is connected with the next by coupling the marked OH bond (see Fig. 3.9) with the OH bond 3′ on the pentose sugar and releasing $H_2O$. Each coupled nucleotide is characterized by one of the four heterocyclic nitrogen bases in Fig. 3.8b. In this way, a polynucleotide is formed. Now, a second nucleotide is constructed parallel to the first in the same manner with the opposite base. Cytosine forms a hydrogen bridge with the guanine on the other side and adenine forms the same bond with thymine, its opposite. Both nucleotides spin around each other in such a way that a helix is formed (Fig. 3.9). This helix is turned a second time round the same axis, but with a longer period, forming a double helix (Watson and Crick 1953; Sayre 1992; Wilson 1988).

Figure 3.10 shows the hydrogen bridge in more detail. Thymine and adenine are coupled by two bonds and guanine and cytosine by three bonds, two between $O^-$ and $H^+$ and one between $N^-$ and $H^+$.

Hydrogen bridges are relatively weak electrostatic bonds which can be opened by special enzymes during transcription. Because of these hydrogen bridge bonds of differing numbers, it is not possible to form other pairs of bases, especially

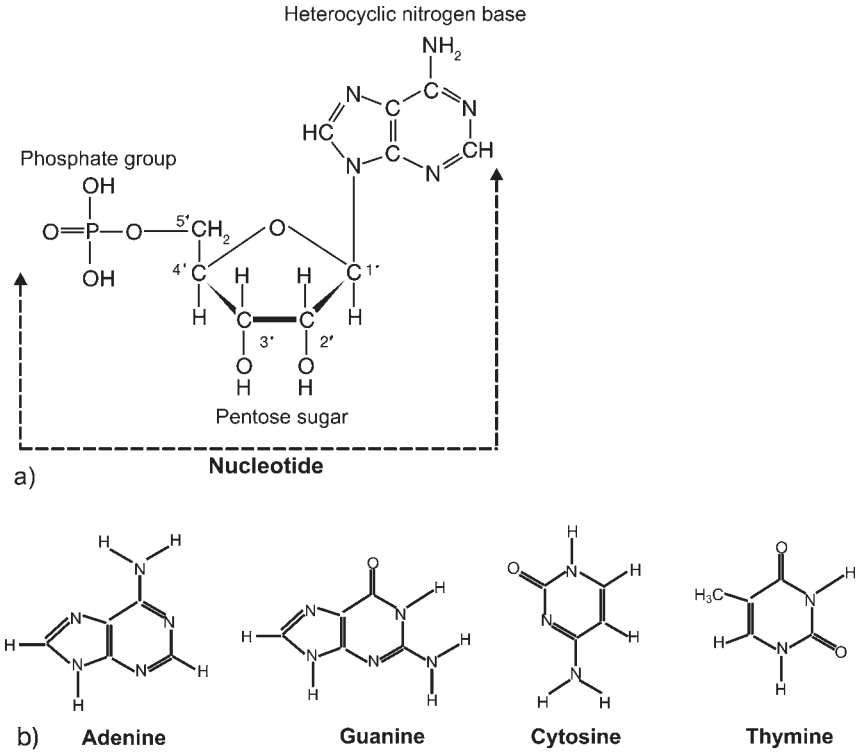


**Fig. 3.8** (a) A nucleotide with adenine as one of four different heterocyclic bases. (b) The four heterocyclic nitrogen bases for four different nucleotides forming DNA.

adenine–guanine. Three bases lying side by side are called a triplet. One possible triplet is:

Adenine
Thymine
Guanine
} ATG

The complementary triplet of the opposite side of the deoxyribonucleic acid (DNA) can only be:

Thymine
Adenine
Cytosine
} TAC

Four bases are used for 64 combinations. All of these are used for the genetic code, the building plan of special compounds. The most important compounds are proteins, particularly enzymes. Only 20 amino acids must be produced (Table 3.2). Actually, only 20 triplets would be necessary. Nevertheless, every amino acid is coded by two, three or four triplets. Some amino acids are coded by two different triplets, e.g. phenylalanine by either TTC or TTT. One such set of triplets is called a *codon*

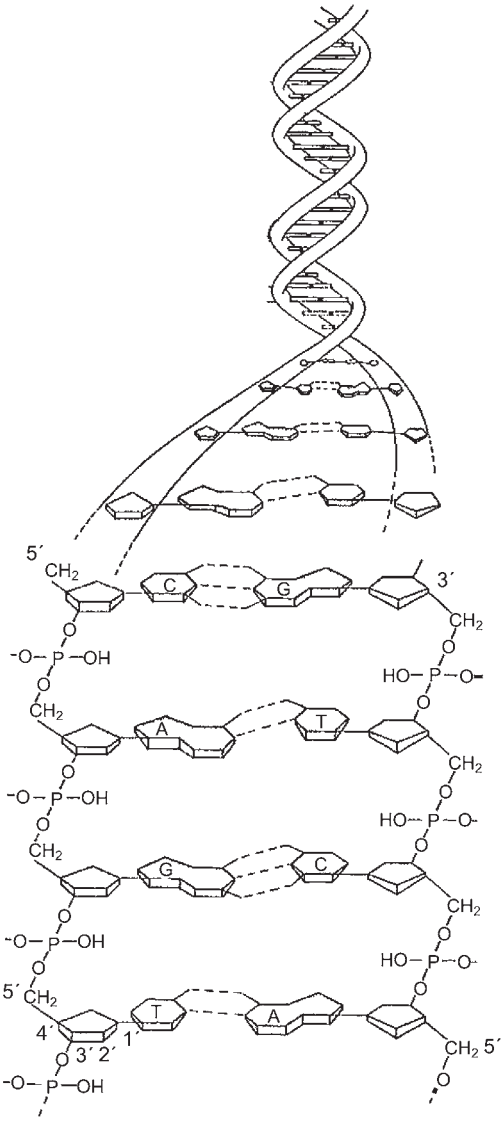


**Fig. 3.9** Two polynucleotides coupled by hydrogen bridges forming a DNA molecule in the form of a double helix (Cano and Colomé 1986).

and the opposite side of the DNA the *anticodon*. Several acids are coded by two different codes (Table 3.5).

Three different codes are used for the order "stop" or "termination site". The reading of the building plan for each protein starts and ends with this code.

A section of the DNA which codes the construction of one protein, consisting of four amino acids, could be (see Table 3.5):

| TGA | TAT | TAC | AAA | AAG | AGA | AGG | ATG | TGA |
|---|---|---|---|---|---|---|---|---|
| stop | Tyr | | Lys | | Arg | | Met | stop |

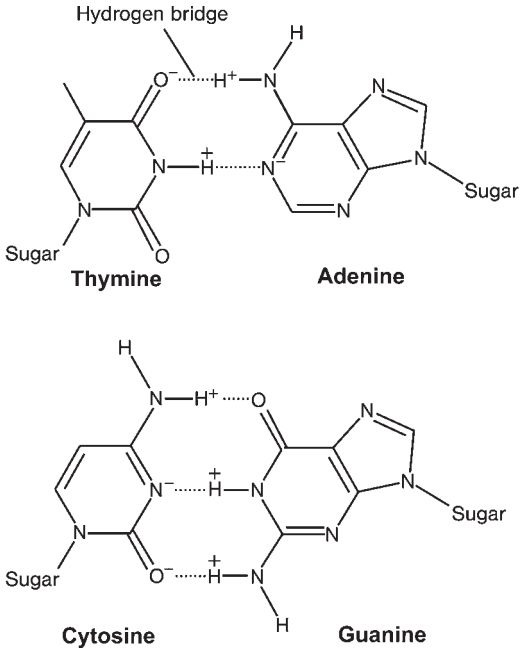


**Fig. 3.10** Hydrogen bridges between both base pairs of DNA (Brown 1999).

**Table 3.5** The genetic code of amino acids (Brown 1999), written for DNA (instead of RNA).

| | | | |
|---|---|---|---|
| TTT, TTC: Phe | TCT, TCC, TCA, TCG: Ser | TAT, TAC: Tyr | TGT, TGC: Cys |
| TTA, TTG: Leu | | TAA, TAG: 'Stop' | TGA 'Stop' |
| | | | TGG Trp |
| CTT, CTC, CTA, CTG: Leu | CCT, CCC, CCA, CCG: Pro | CAT, CAC: His | CGT, CGC, CGA, CGG: Arg |
| | | CAA, CAG: Gin | |
| ATT, ATC, ATA: Ile | ACT, ACC, ACA, ACG: Thr | AAT, AAC: Asn | AGT, AGC: Ser |
| ATG Met | | AAA, AAG: Lys | AGA, AGG: Arg |
| GTT, GTC, GTA, GTG: Val | GCT, GCC, GCA, GCG: Ala | GAT, GAC: Asp | GGT, GGC, GGA, GGG: Gly |
| | | GAA, GAG: Glu | |

### 3.2.2.2 Ribonucleic Acid

The structure of ribonucleic acid (RNA) is similar to that of DNA. It is also formed by the polymerization of nucleotides. There are, however, three important differences:

- Uracil is used instead of the nitrogen base thymine (Fig. 3.11).
- An RNA molecule consists only of one molecule chain and not two as in DNA.
- RNA molecules are much shorter than DNA molecules.

Figure 3.11 shows the primary structure of an RNA molecule.

We distinguish between three different kinds of RNA:

- Messenger RNA (mRNA).
- Transfer RNA (tRNA).
- Ribosomal RNA (rRNA).

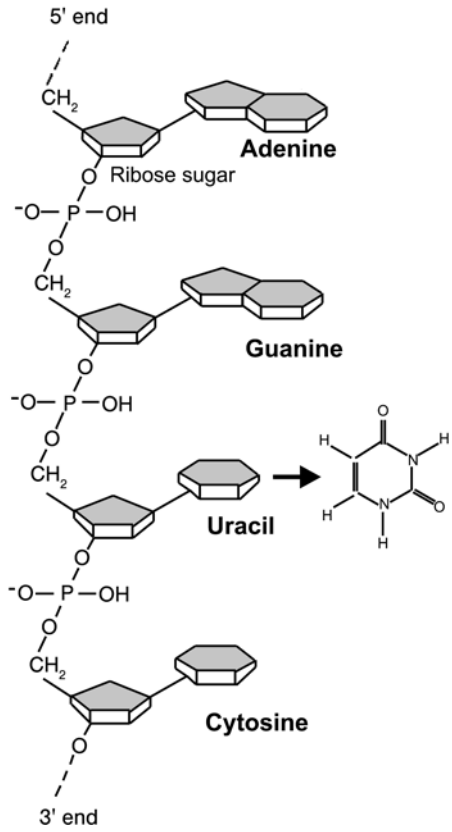


**Fig. 3.11** Primary structure of RNA (Cano and Colomé 1986), showing structure of uracil, a nitrogen base in RNA molecules.

**mRNA**

mRNA arises during the reading of the building plan for a protein which is coded on a section of the DNA, beginning at a triplet coding the promoter side (start) and ending with the termination side (stop; Fig. 3.12a). An enzyme (RNA polymerase) opens both parts of the DNA by cleaving the hydrogen bridges (Fig. 3.12b). Nucleotide molecules diffuse to the complementary nucleotides of the DNA and are coupled together by hydrolysis and reactions at C atoms 3' and 5' of the pentose molecule. The enzyme wanders along the gene, the hydrogen bridges are closed again and the mRNA grows until the termination side is reached (Fig. 3.12c).

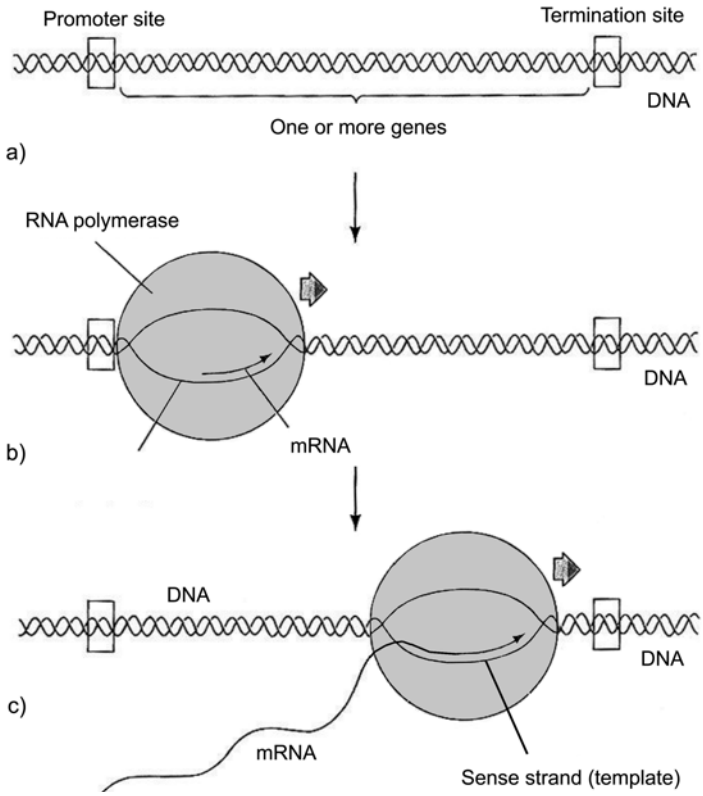


**Fig. 3.12** Transcription steps (a–c), forming an mRNA molecule (Cano and Colomé 1986).

**tRNA**

Compared with mRNAs, which are of different size depending on the size of the coded protein, tRNAs are small polynucleotides and nearly all of the same size. Figure 3.13a gives an impression of the molecule, which is projected in one level. The broken lines show the hydrogen bridges. Figure 3.13b shows that, during reading of the mRNA codon, an anticodon must first be formed which is typical for one amino acid. Thereafter, a second tRNA is joined to the next codon directly left

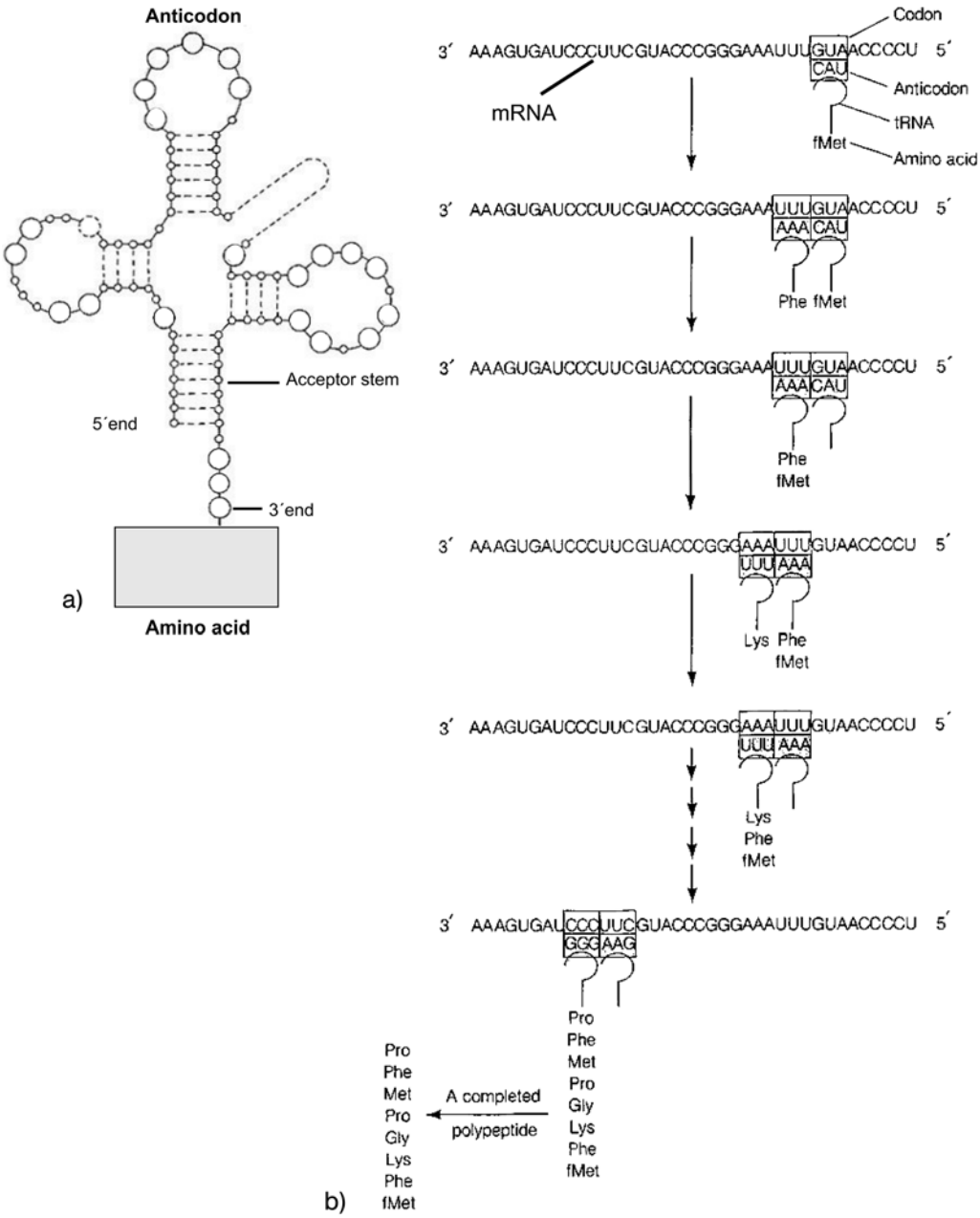


**Fig. 3.13** (a) tRNA with anticodon and the typical end for coupling amino acids. (b) Protein synthesis by reading of mRNA (Cano and Colomé 1985).

to the first to obtain its amino acid. In this way, a protein molecule is made which was coded at the section of the DNA being read. The mRNA is used repeatedly for the production of the same protein every time, but after some time it degrades and a new mRNA must be produced. In a similar way, the mRNA is decoded by the rRNA and the according polypeptide grows inside the ribosomes. In ribosomes, the proteins are manufactured. They exist in the cytoplasm. Ribosomal proteins are assembled together with rRNA before being transported through the nuclear membrane. rRNA makes up the vast majority of RNA found in a typical cell. The reading of the mRNA and protein synthesis by tRNA and rRNA are called transmission.

#### 3.2.2.3 **DNA Replication**

During each cell division, a complete copy of the total DNA must be produced, so that both daughter cells obtain the same genes as the mother cell. This process is called DNA replication. Very high precision must be guaranteed. Even one mistake in $10^4$ nucleotides may cause changes with serious consequences (Brown 1999).

Here, only the fundamental process of DNA replication will be described shortly. In Fig. 3.14, the opening of the DNA molecule, catalyzed by a special enzyme

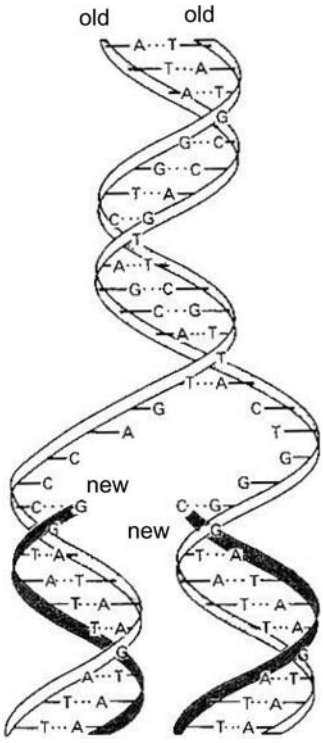


**Fig. 3.14** DNA replication after opening the double helix (Brown 1999).

(not shown), is the first step. After that, the nucleotides already synthesized inside the cell are coupled by hydrogen bridges to the complementary base of the mother DNA (thymine and adenine, guanine and cytosine). The last step is the coupling of the two pentose groups (bond 3′ with 5′) via the phosphate group, thereby splitting off one $H_2O$ molecule (Fig. 3.14).

During the division of a bacterial cell, each of the two DNA molecules will be housed in one of the new cells.

#### 3.2.2.4 **Mutations**

Normally DNA replication occurs without any errors. But, considering the enormous number of cells, e.g. such as bacteria, the short time between two consecutive replications and the length of the DNA, with thousands of genes, errors do occur during replication. These are called *mutations*. A mutation is a change in the nucleotide sequence of the DNA during the process of replication.

We distinguish several kinds of mutations:

- Transition
  - A is replaced by G
  - T is replaced by C
- Transversion
  - A is changed to T
  - T is changed to A
- Addition
  - A is replaced by A C
  - T is replaced by T G
- Deletion
  - A is deleted
  - T is deleted
- Inversion
  - AAA CCC is inverted to GGG TTT
  - TTT GGG is inverted to CCC AAA

In all these cases, one of the two daughter cells has DNA which is not the same as the mother DNA and it may exhibit some new properties.

The rate of mutations can be influenced by chemical reactions between special compounds and DNA. Further, the rate of these reactions is influenced by pH, temperature, concentration and other physical parameters, such as the intensity of UV radiation. These mutations make it possible for microorganisms to degrade new organic substances produced synthetically in the chemical industry (chlorinated benzenes and phenols, dyes, etc.), which never occurred in nature before.

## 3.3
## Catabolism and Anabolism

### 3.3.1
### ADP and ATP

All the processes of synthesis described above need energy, which is provided by catabolic reactions. During these catabolic reactions, chemical energy is stored by forming ATP from a compound with lower energy, ADP; and it is then used partly as chemical energy and is partly converted into thermal energy, resulting in an increase in temperature.

The structures of ADP and ATP are given in Fig. 3.15.

To store energy, a molecule of phosphoric acid ($H_3PO_4$) is coupled to ADP, forming ATP with the help of enzyme A:

$$\mathrm{ADP + H_3PO_4 + 29.97\ kJ\ mol^{-1} \underset{\text{enzyme B}}{\overset{\text{enzyme A}}{\rightleftharpoons}} ATP + H_2O} \qquad (3.8)$$

According to that chemical balance, the same energy is available at a later time when enzyme B is engaged.

There are three mechanisms for the coupling and decoupling of a phosphoric acid group (phosphorylation). The most important for the catabolic pathways discussed later is called substrate-level phosphorylation.

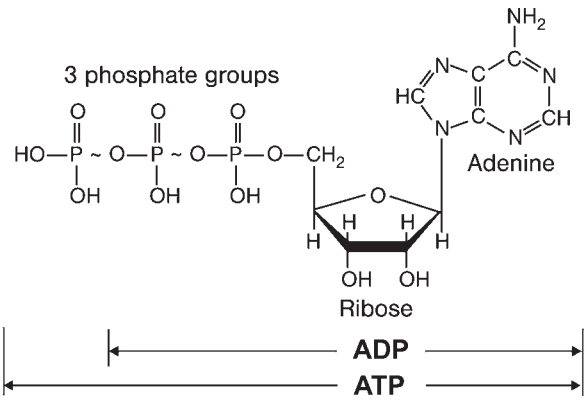


**Fig. 3.15** Adenosinediphosphate (ADP) and Adenosinetriphosphate (ATP).

### 3.3.2
### Transport of Protons

The catalytic effect of enzymes is often combined with a transport of protons or $H^+$ by a coenzyme. This was already explained in Section 3.2.1.4 (Fig. 3.6a, b). Two of the most important coenzymes are nicotine amide adenine dinucleotide (NAD) and flavin adenine dinucleotide (FAD). Figure 3.16a shows NAD in the oxidized

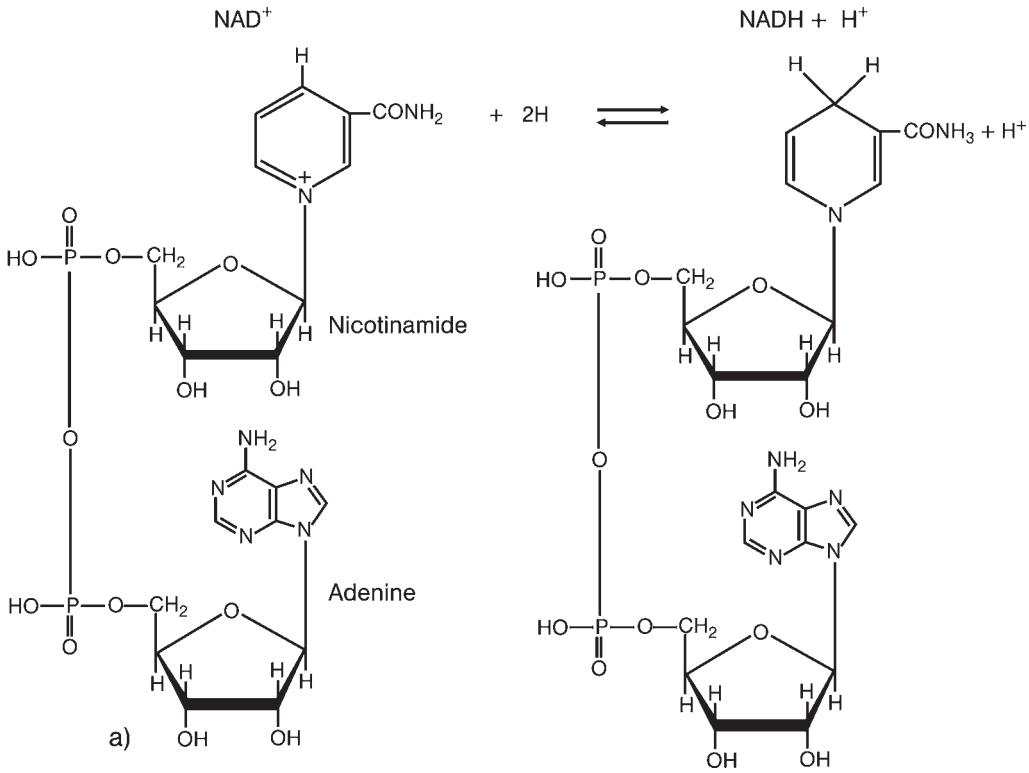


**Fig. 3.16** (a) Equilibrium between $NAD^+$ and $NADH + H^+$ (Cano and Colomé 1986, modified).

form $NAD^+$ and in the reduced form $NADH + H^+$ ($NADH_2$); and Fig. 3.16b shows the coenzyme FAD.

Positively charged $NAD^+$ loses its charge during reduction and is combined with a proton ($NADH + H^+$). This is only possible by reorientation of the double bonds and reduction of the five-valent nitrogen atom of the nicotine amide group to a three-valent one. The FAD molecule is constructed similarly (Fig. 3.16b). The $NADH_2$ coenzyme diffuses to the same enzyme (see Fig. 3.6a) or to another enzyme (see Fig. 3.6b), where another substrate is to be reduced. The importance of NAD and FAD will be discussed in the following catabolic degradation of glucose.

### 3.3.3 Catabolism of Using Glucose

#### 3.3.3.1 Aerobic Conversion by Prokaryotic Cells

Most prokaryotic cells (bacteria) and all eukaryotic organisms obtain their energy from *chemoorgano heterotrophic* metabolism. Part of this energy is stored in ATP molecules and part of it is transformed into heat. The mechanism of ATP produc-

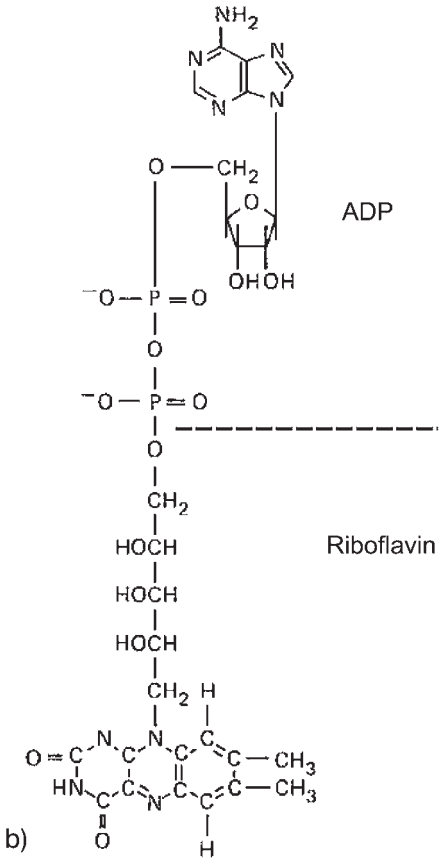


**Fig. 3.16** (b) Structure of FAD (Scragg 1988).

tion is normally described using glucose as an example; and it is divided into three stages:

- the glycolysis or Embden–Meyerhoff pathway,
- the citric acid cycle,
- the respiration chain.

During the first part of glycolysis (Fig. 3.17) two ATPs must be reduced to two ADPs. From one glucose molecule (6 C), two molecules of glycerine aldehyde-3-phosphate (3 C) are produced.

Therefore, the pathway to the end-product of glycolysis pyruvate must be travelled two times, producing 2 $NADH_2$ and 2 ATP:

$$\begin{aligned} &C_6H_{12}O_6 + 2\ H_3PO_4 + 2\ ADP + 2\ NAD \rightarrow \\ &2\ CH_3COCOOH + \boxed{2\ NADH_2} + \boxed{2\ ATP} + 2\ H_2O \end{aligned} \tag{3.9}$$

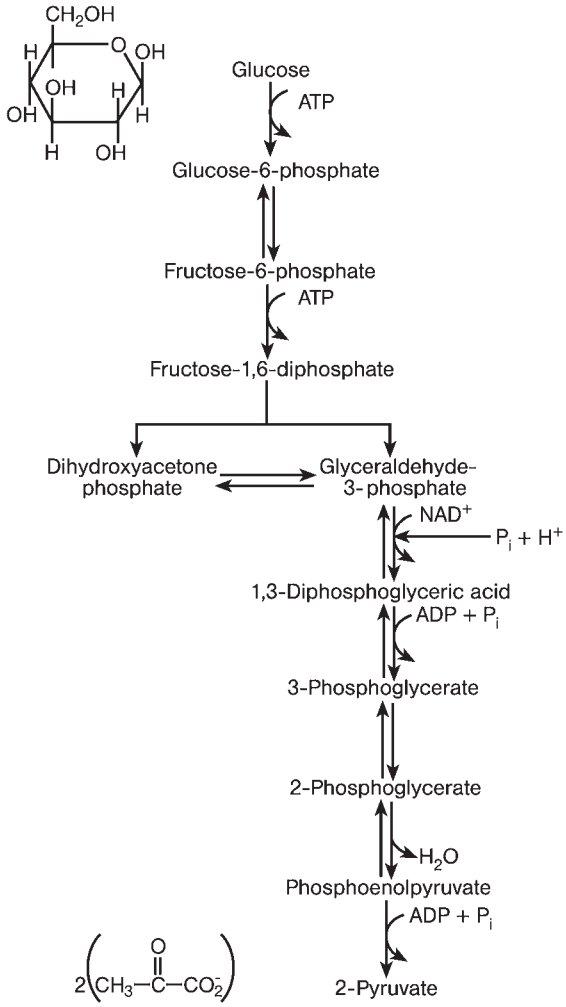


**Fig. 3.17** Glycolysis (Cano and Colomé 1986).

Two pyruvates are now mineralized by the nine steps of the citric acid cycle, after being oxidized by NAD and coupled to coenzyme acetyl CoA (Fig. 3.18):

$$2\ CH_3COCOOH + 2\ NAD + 2\ CoAH \rightarrow$$
$$2\ CH_3CO\text{-}CoA + \boxed{2\ NADH_2} + 2\ CO_2 \qquad (3.10)$$

Only with the help of this coenzyme is it possible for active acetic acid to enter the citric acid cycle and react with oxaloacetic acid (4 C), producing citric acid (6 C). Note that the cycle is passed through two times, producing 2 GTP, 6 $NADH_2$ and 2 $FADH_2$, and that CoA is reduced to CoAH again. It is used repeatedly (see Eq. 3.10) and produced during the two steps from α-ketoglutaric acid to succinic

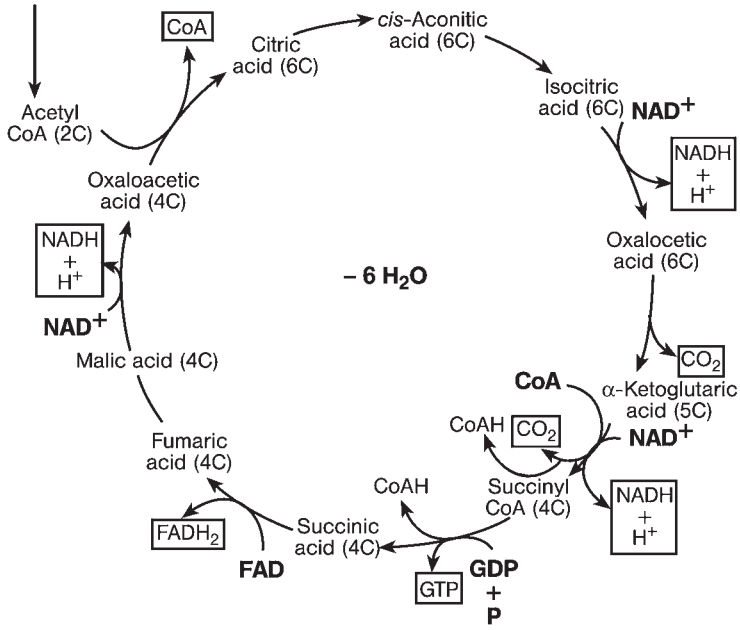


**Fig. 3.18** Citric acid cycle (Cano and Colomé 1986).

acid. GDP is constructed similarly to ATP; and thus we write ATP instead of GTP. The balance for the complete citric acid cycle is:

$$\begin{aligned} &2\ CH_3CO\text{-}CoA + 6\ H_2O + 6\ NAD + 2\ FAD + 2\ ADP + 2\ H_3PO_4 \rightarrow \\ &2\ CoAH + \boxed{6\ NADH_2} + \boxed{2\ FADH_2} + \boxed{2\ ATP} + 2\ H_2O + 4\ CO_2 \end{aligned} \tag{3.11}$$

Note that: $2\ ADP + 2\ H_3PO_4 \leftrightarrow 2\ ATP + 2\ H_2O$ and $FAD^+ + 2H \rightarrow FADH + H^+$ ($FADH + H^+ = FADH_2$).

Altogether, $10\ NADH_2 + 2\ FADH_2$ are now oxidized, passing now eight links of the respiration chain or electron transport system. Figure 3.19 presents a qualitative plot of the energy level versus the course of the reaction. If $NADH_2$ is oxidized, the hydrogen atom is transported from the first link to the last and oxidized by $O_2$ to $H_2O$.

The chemical energy is used to convert 3 ADP to 3 ATP (second and fourth links). The chemical energy of $FADH_2$ is lower by about one-third, resulting in only two ADPs after the uptake by coenzyme Q (third link). The balance of the electron transfer chain can be written as follows:

$$\begin{aligned} &10\ NADH_2 + 2\ FADH_2 + 34\ ADP + 6\ O_2 \rightarrow \\ &10\ NAD + 2\ FAD + 34\ ATP + 46\ H_2O \end{aligned} \tag{3.12}$$

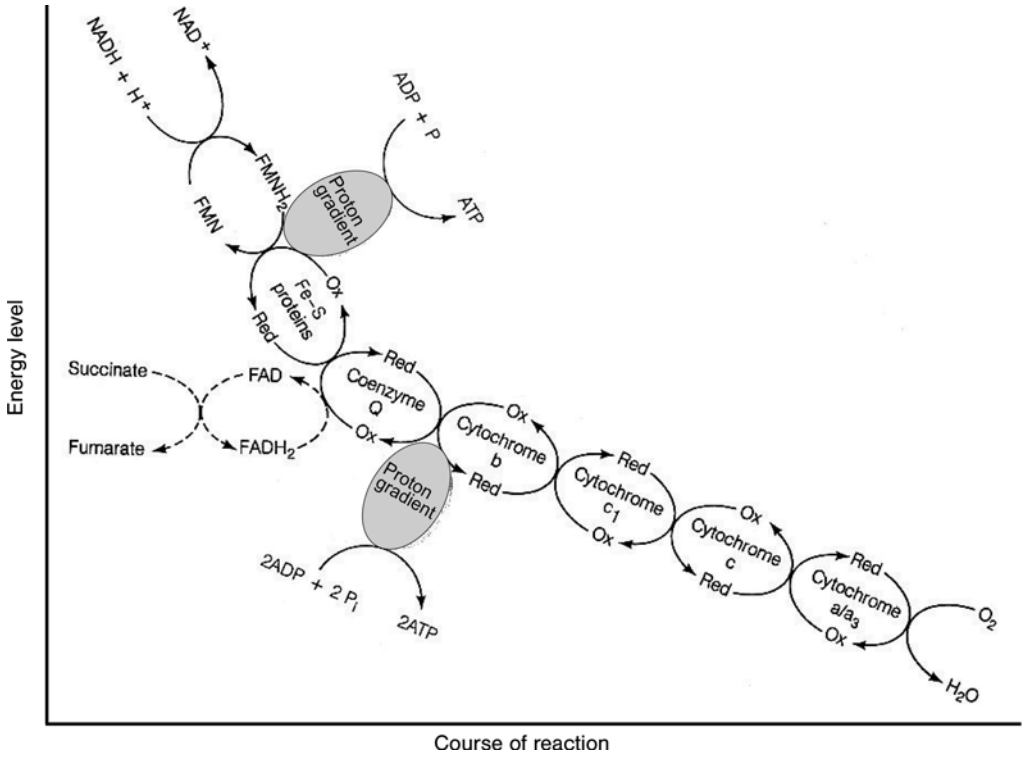


**Fig. 3.19** Electron transport system of respiration chain (Cano and Colomé 1986).

Remember that: 34 ADP + 34 $H_3PO_4 \leftrightarrow$ 34 ATP + 34 $H_2O$.

Alltogether, 2 ATP (Glycolysis) + 2 ATP (Citric acid cycle) + 34 ATP = 38 ATP are produced.

If we summarize Eqs. (3.9) to (3.12), we obtain the known balance for the aerobic catabolic degradation of glucose:

$$C_6H_{12}O_6 + 6\ O_2 \rightarrow 6\ CO_2 + 6\ H_2O + 2826\ \text{kJ mol}^{-1} \tag{3.13}$$

In prokaryotic cells (bacteria), a part of this relatively high amount of energy is stored as ATP, namely 29.97 kJ $mol^{-1}$ per ATP. Therefore, the efficiency of this energy storage is:

$$\eta = \frac{38 \cdot 29.97}{2826} = 0.403 \text{ or } 40.3\%$$

The rest, or nearly 60%, is converted into thermal energy.

#### 3.3.3.2 Anaerobic Conversion by Prokaryotic Cells

If we simply replace oxygen with inorganic electron acceptors ($NO_3^-$, $NO_2^-$, $SO_4^{2-}$) or with hydrogen, catabolism is nearly the same as in the aerobic case, with the exception of the respiration chain. Therefore, a lower amount of ATP is produced. Environmental scientists call this *anoxic* metabolism. We will come back to this topic, when we discuss denitrification in Chapter 10.

*Anaerobic* metabolism (Zehnder 1988) is characterized by a transfer of electrons or hydrogen to organic compounds, resulting in organic products which cannot be used further by the same bacteria. This process, which is at the center of interest for biotechnologists, is called *fermentation*. For this reason, bioreactors are called *fermenters*. Unfortunately, biotechnologists and microbiologists use the term fermenter even if aerobic or anoxic reactions are taking place.

Here, two examples will be discussed briefly:

**Production of Lactic Acid**

Bacteria which produce lactic acid (e.g. *Lactobacillus bulgaricus*) are of great importance for the food industry. Because of their relative insensitivity with regard to low pH, they are used for food sterilization (yoghurt, sauerkraut, pickling, etc.). As the bacteria produce more and more lactic acid and the concentration rises, the pH falls and increasing numbers of bacteria are killed off, until even the lactobacilli themselves die. *L. bulgaricus,* for example, is used to produce buttermilk.

The first stage of catabolism is the glycolysis or Embden–Meyerhoff pathway (Fig. 3.17) if glucose is used. The balance is given by Eq. (3.9). Pyruvate is not coupled to coenzyme CoAH as shown by Eq. (3.10), rather it is reduced directly by $NADH_2$ to lactic acid:

$$2\ CH_3COCOOH + 2\ NADH \rightarrow 2\ CH_3CHOHCOOH + 2\ NAD \tag{3.14}$$

Summarizing Eqs. (3.9) and (3.14), we obtain:

$$C_6H_{12}O_6 \rightarrow 2\ CH_3CHOHCOOH + 2\ H_2O \tag{3.15}$$

and

$$2\ H_3PO_4 + 2\ ADP \rightarrow 2\ ATP + 2\ H_2O \tag{3.16}$$

The greatest part of the chemical energy of 1 mol glucose remains in 2 mol lactic acid, resulting in only 2 mol ATP and a small increase in biomass.

**Production of Ethanol**

Yeasts functioning as eukaryotic cells (e.g. *Sacharomyces cerevisiae*) and bacteria (e.g. *Zymomonas mobilis*) produce ethanol as their end-product of catabolism. After glycolysis, pyruvate is transformed into acetaldehyde and $CO_2$:

$$C_6H_{12}O_6 + 2\ NAD \rightarrow 2\ CH_3CHO + 2\ CO_2 + 2\ NADH_2 \tag{3.17}$$

Acetaldehyde is reduced by $NADH_2$ to ethanol in the final step:

$$2\ CH_3CHO + 2\ NADH_2 \rightarrow 2\ CH_3CH_2OH + 2\ NAD \quad (3.18)$$

Summarizing Eqs. (3.17) and (3.18), we obtain:

$$C_6H_{12}O_6 \rightarrow 2\ CH_3CH_2OH + 2\ CO_2 \quad (3.19)$$

(Zehnder 1988) and:

$$\Delta G^\circ = -244.9\ kJ\ mol^{-1}$$

Because fermentation to ethanol is inhibited by the end-product, only about 18vol% ethanol is attainable (wine, beer, etc.). For more highly concentrated alcoholic drinks, water must be removed by distillation and condensation or by reverse osmosis. Ethanol can also be produced from liquid wastes, which are predominately polluted with mono-, di- and polysaccharides, or renewable raw materials, and then used as a fuel additive to gasoline.

In anaerobic wastewater treatment processes, acetic acid is produced by the fermentation of higher fatty acids. This is discussed in more detail in Chapter 8.

### 3.3.4 Anabolism

Bacteria are characterized by a remarkable achievement during their growth. *E. coli*, for example, synthesizes 1400 protein molecules in 1 s. With 300 peptide bonds in each molecule, this makes 420 000 bonds $s^{-1}$. To reach this rate of protein synthesis, 88% of the energy stored in ATP is needed. Since 6 ATP are used for one peptide bond, $2.5 \cdot 10^6$ ATP must be used every second! The energy stored in an *E. coli* cell is sufficient for only 2 s, with its ATP content of $5.0 \cdot 10^6$ ATP.

Table 3.6 gives an impression of the work rate of *E. coli* biosynthesis per second.

This extremely high capacity can only be realized by very economical synthetic reactions. Therefore, substrates which contain proteins are only hydrolyzed to amino acids, which are then coupled together with new proteins. Only by these and other optimizations are bacteria able to achieve extremely economical anabolism.

**Table 3.6** Biosynthesis capacity of *E. coli* during a 20-min cell division (Lehninger 1965).

| Chemical component | Dry weight (%) | Approximate molar mass | Number of molecules per cell | Number of molecules synthesized per second | Number of molecules of ATP synthesized per second | Total biosynthetic energy required (%) |
|---|---|---|---|---|---|---|
| DNA | 5 | $2 \cdot 10^9$ | 1 | 0.00083 | $60 \cdot 10^3$ | 2.5 |
| RNA | 10 | $1 \cdot 10^6$ | $15 \cdot 10^3$ | 12.5 | $75 \cdot 10^3$ | 3.1 |
| Protein | 70 | $60 \cdot 10^3$ | $1.7 \cdot 10^6$ | 1400 | $2.12 \cdot 10^6$ | 88.0 |
| Lipid | 10 | $1 \cdot 10^3$ | $15 \cdot 10^6$ | 12500 | $87.5 \cdot 10^3$ | 3.7 |
| Polysaccaride | 5 | $2 \cdot 10^5$ | $39 \cdot 10^3$ | 32.5 | $65 \cdot 10^3$ | 2.7 |

## References


Baily, J.E.; Ollis, U.F. **1977**, *Biochemical Engineering Fundamentals*, McGraw-Hill, New York.

Bergey, B. **1974**, *Bergey's Manual of Determinative Bacteriology*, 8th edn., McGraw-Hill, New York.

Brown, T.A. **1999**, *Moderne Genetik*, Spektrum Akademischer Verlag, Heidelberg.

Cano, R.J.; Colomé, J.S. **1986**, *Microbiology*, West Publishing, St. Paul.

Gaudy, Anthony F. Jr.; Gaudy, Elizabeth T. **1989**, *Microbiology for Environmental Scientists and Engineers*, McGraw-Hill, New York.

Insam, H.; Rangger, A. **1997**, *Microbial Communities – Functional versus Structural Approaches*, Springer-Verlag, Berlin.

Lehninger, A.L. **1965**, *Bioenergetic*, 2nd edn., Benjamin, Palo Alto, p. 123.

Michaelis, L.; Menten, M.L. **1913**, Die Kinetik der Invertinwirkung, *Biochem. Zeitschr.* 49, 333–369.

O'Leary, W. **1989**, *Practical Handbook of Microbiology*, CRC Press, Boca Raton.

Sayre, A. **1992**, *Rosalind Franklin and DNA*, Norton, New York.

Schlegel, H.G. **1992**, *Allgemeine Mikrobiologie*, Georg Thieme Verlag, Stuttgart.

Schön, G. **1978a**, *Mikrobiologie*, Herder Verlag, Freiburg.

Schön, G. **1978b**, *Mikrobiologie, Reihe: Studio visuell*, Herder Verlag, Freiburg.

Scragg, A.H. **1988**, *Biotechnology for Engineers, Biological Systems in Technological Processes*, John Wiley & Sons, New York.

Volk, W.A.; Wheeler, M.F. **1986**, *Basis Microbiology*, 6th edn., Harper & Row, New York.

Watson, J.D.; Crick, F.H.C. **1953**, Genetic implications of the structure of deoxyribose nucleic acid, *Nature* 171, 964.

Wilson, H.R. **1988**, The double helix and all that, *Trends Biochem. Sci.* 13, 275–278.

Zehnder, A.J.B. **1988**, *Biology of Anaerobic Microorganisms*, John Wiley & Sons, New York.

# 4
# Determination of Stoichiometric Equations for Catabolism and Anabolism

## 4.1
## Introduction

Chemical reactions can be traced by measuring the concentrations of educts as well as intermediate and final products by continuous or discontinuous measurements after taking samples. One condition is of high importance and can be used for checking the results: balances must be fulfilled for each element.

From a fundamental point of view, the same condition is valid for biological systems. Therefore, it is principally possible to study bioreactors using the same balances of elements. Two points must be considered which are typical for living systems. First, the mass of living organisms can increase by growing, it can decrease by endogenous respiration and by dying and new substrates can be produced by lysis as sources of carbon, hydrogen, nitrogen and phosphorous. The second point is typical for environmental microbiology. In one bioreactor, the number of different strains of bacteria is normally high and the composition may change during the process. Besides that, protozoa and other eukaryotes may grow in the same system as the bacteria and the bacteria are then eaten by protozoa.

Nevertheless, balances of total parameters such as COD, DOC and $BOD_5$, as well as balances of the elements C, O, H, N and P can be very helpful in studying and controlling environmental bioreactors.

First, we will start with simple balances, neglecting endogenous respiration, cell death, lysis, etc.; and we will consider only aerobic chemoorganoheterotrophic bacteria. Later on, we will expand these systems.

Consider that the following balances are totally independent of the kinetics and reaction engineering conditions. The question "How much mass is transferred in what time?" is of great significance, but we will delve into that question later.

*Fundamentals of Biological Wastewater Treatment*. Udo Wiesmann, In Su Choi, Eva-Maria Dombrowski

ISBN: 978-3-527-31219-1

## 4.2
## Aerobic Degradation of Organic Substances

### 4.2.1
### Degradation of Hydrocarbons Without Bacterial Decay

Let us start with the aerobic degradation of glucose, studying the stoichiometry of catabolism and anabolism:

$$C_6H_{12}O_6 + Y^{\circ}_{NH_4-N/S}NH_4^+ + Y^{\circ}_{OH/S}OH^- + Y^{\circ}_{O_2/S}O_2 \rightarrow Y^{\circ}_{X/S}C_5H_7O_2N + Y^{\circ}_{CO_2-C/S}CO_2 + Y^{\circ}_{W/S}H_2O \quad (4.1)$$

and normalizing the glucose and the bacterial mass to *one* C atom:

$$CH_2O + Y^{\circ}_{N/SC}{}^{1)}NH_4^+ + Y^{\circ}_{OH/SC}OH^- + Y^{\circ}_{O_2/SC}O_2 \rightarrow Y^{\circ}_{XC/SC}CH_{1.4}O_{0.4}N_{0.2} + Y^{\circ}_{CO_2/SC}{}^{1)}CO_2 + Y^{\circ}_{W/SC}H_2O \quad (4.2)$$

Equation (4.2) is valid for substrates with the C-standardized composition $CH_2O$ (hydrocarbons) and for bacteria with a mean composition $CH_{1.4}O_{0.4}N_{0.2}$.

Six true yield coefficients $Y^{\circ}$ must be determined. Biomass decay by endogenous respiration and bacterial death are not considered here. To fulfil the charge balance as required, we obtain:

$$Y^{\circ}_{N/SC} = Y^{\circ}_{OH/SC} \quad (4.3)$$

and, because of the following mass balances for four elements, we obtain all together five equations for the calculation of six yield coefficients:

$$\text{C balance:} \quad 1 = Y^{\circ}_{XC/SC} + Y^{\circ}_{CO_2/SC} \quad (4.4)$$

$$\text{H balance:} \quad 2 + 4\,Y^{\circ}_{N/SC} + Y^{\circ}_{OH/SC} = 1.4\,Y^{\circ}_{XC/SC} + 2\,Y^{\circ}_{W/SC} \quad (4.5)$$

$$\text{O balance:} \quad 1 + Y^{\circ}_{OH/SC} + 2\,Y^{\circ}_{O_2/SC} = 0.4\,Y^{\circ}_{XC/SC} + 2\,Y^{\circ}_{CO_2/SC} + Y^{\circ}_{W/SC} \quad (4.6)$$

$$\text{N balance:} \quad Y^{\circ}_{N/SC} = 0.2\,Y^{\circ}_{XC/SC} \quad (4.7)$$

Five yield coefficients can be calculated using Eqs. (4.3) to (4.7):

$$Y^{\circ}_{XC/SC} = 3 - 4\,Y^{\circ}_{O_2/SC} \quad (4.8)$$

$$Y^{\circ}_{CO_2/SC} = 4\,Y^{\circ}_{O_2/SC} - 2 \quad (4.9)$$

$$Y^{\circ}_{N/SC} = 0.6 - 0.8\,Y^{\circ}_{O_2/SC} \quad (4.10)$$

$$Y^{\circ}_{OH/SC} = 0.6 - 0.8\,Y^{\circ}_{O_2/SC} \quad (4.11)$$

$$Y^{\circ}_{W/SC} = 0.4 + 0.8\,Y^{\circ}_{O_2/SC} \quad (4.12)$$

---

[1] Instead of $Y^{\circ}_{CO_2-C/SC}$ we write $Y^{\circ}_{CO_2-SC}$ and instead of $Y^{\circ}_{NH_4-N}$ we write $Y^{\circ}_{N/SC}$.

At first, we conclude that one of the six yield coefficients must be unknown without experiments. But after elimination of $Y^{\circ}_{O_2/SC}$ from Eq. (4.6):

$$Y^{\circ}_{O_2/SC} = 0.2\, Y^{\circ}_{XC/SC} + Y^{\circ}_{CO_2/SC} + 0.5 Y^{\circ}_{W/SC} - 0.5\, Y^{\circ}_{OH/SC} - 0.5 \tag{4.13}$$

and, combining Eqs. (4.8), (4.9), (4.11) and (4.12) into Eq. (4.13), a further equation for the calculation of $Y^{\circ}_{O_2/SC}$ is available:

$$Y^{\circ}_{O_2/SC} = Y^{\circ}_{CO_2/SC} + 0.2\, Y^{\circ}_{XC/SC} + 0.5\,(Y^{\circ}_{W/SC} - Y^{\circ}_{OH/SC} - 1) \tag{4.14}$$

Now the system of the six equations (Eq. (4.3) to (4.7) and (4.14)) can be solved; and we are able to predict all yield coefficients:

$$Y^{\circ}_{XC/SC} = 1/3\ \frac{\text{mol C}}{\text{mol C}};\quad Y^{\circ}_{CO_2/SC} = 2/3\ \frac{\text{mol C}}{\text{mol C}};\quad Y^{\circ}_{N/SC} = 0.067\ \frac{\text{mol N}}{\text{mol C}}$$

$$Y^{\circ}_{OH^-/SC} = 0.067\ \frac{\text{mol OH}^-}{\text{mol C}};\quad Y^{\circ}_{W/SC} = 0.93\ \frac{\text{mol H}_2\text{O}}{\text{mol C}};\quad Y^{\circ}_{O_2/SC} = 2/3\ \frac{\text{mol O}_2}{\text{mol C}}$$

For mol C we can write: mol DOC.

From a fundamental point of view, it should be possible to determine an unknown oxygen and hydrogen content of a substrate $CH_{SH}O_{SO}$, if two yield coefficients are measured, in this case $Y^{\circ}_{XC/SC}$ and $Y^{\circ}_{CO_2/SC}$. Apart from the fact that the $CO_2$ formed is only determined if the change in concentrations of dissolved $CO_2$, $HCO_3^-$ and $CO_3^{2-}$ is known (see Section 4.3), it can be shown that only two equations are available to calculate SH as well as $Y^{\circ}_{W/SC}$, which cannot be measured using aqueous substrate solutions.

Because of the constancy of the elementary composition of most wastewater mixtures, the calculation of SH, SO, SN and SP is mostly only of academic interest.

### 4.2.2 Mineralization of 2,4-Dinitrophenol

2,4-Dinitrophenol (2,4-DNP) is used together with other nitroaromatic compounds for the production of dyes, explosives and photographic materials. It can be mineralized by some aerobic bacteria which need nitroaromatic compounds as a source of not only carbon but also nitrogen. At high concentrations, it is very toxic and acts as an insecticide and fungicide.

Here, only the stoichiometric equation of its aerobic mineralization should be of interest. For this purpose, the catabolic and anabolic reactions are summarized, as already shown for glucose in Section 4.2.1. Writing this equation not as $C_6H_3OH(NO_2)_2$ (2,4-DNP), but for the standardized molecule $CH_{0.67}N_{0.33}O_{0.83}$ (after dividing by the number of C atoms, see Eq. 4.2), the normalized stoichiometric equation is (Heinze 1997):

$$\begin{aligned} &CH_{0.67}N_{0.33}O_{0.83} + Y^{\circ}_{O_2/SC}O_2 + Y^{\circ}_{W/SC}H_2O \rightarrow \\ &Y^{\circ}_{XC/SC}CH_{1.80}O_{0.50}N_{0.19} + Y^{\circ}_{NO_2/SC}HNO_2 + Y^{\circ}_{CO_2/SC}CO_2 \end{aligned} \tag{4.15}$$

Comparing Eq. (4.15) with Eq. (4.2), three differences can be discovered:

- The consideration of the equilibria $HNO_2 = H^+ + NO_2^-$ and $OH^- + H^+ = H_2O$ leads to a stoichiometry equation without ions.
- Nitrogen must not be added because of the high content in the substrate molecule.
- The composition of the bacteria (Behrendt 1994) differs a little from that used in Eq. (4.2).

The five true yield coefficients were calculated in the same way, as described by Heinze (1997). First, four equations are obtained by element balances:

$$\text{C balance:} \quad 1 = Y^{\circ}_{XC/SC} + Y^{\circ}_{CO_2/SC} \tag{4.16}$$

$$\text{H balance:} \quad 0.67 + 2\,Y^{\circ}_{W/SC} = 1.8\,Y^{\circ}_{XC/SC} + Y^{\circ}_{NO_2/SC} \tag{4.17}$$

$$\text{O balance:} \quad 0.83 + 2\,Y^{\circ}_{O_2/SC} + Y^{\circ}_{W/SC} = 0.5\,Y^{\circ}_{XC/SC} + 2\,Y^{\circ}_{NO_2/SC} + 2\,Y^{\circ}_{CO_2/SC} \tag{4.18}$$

$$\text{N balance:} \quad 0.33 = 0.19\,Y^{\circ}_{XC/SC} + Y^{\circ}_{NO_2/SC} \tag{4.19}$$

An additional equation follows if $Y^{\circ}_{XC/SC}$ is eliminated from Eq. (4.18) and (4.19).

$$Y^{\circ}_{O_2/SC} = 0.019 - 0.316\,Y^{\circ}_{N/SC} - 0.5\,Y^{\circ}_{W/SC} + Y^{\circ}_{CO_2/SC} \tag{4.20}$$

This system of five equations with five unknown true yield coefficients can be solved as already discussed in Section 4.2.1, resulting in:

$$Y^{\circ}_{XC/SC} = 0.3\ \frac{\text{mol C}}{\text{mol C}}; \qquad Y^{\circ}_{CO_2/SC} = 0.7\ \frac{\text{mol C}}{\text{mol C}}; \qquad Y^{\circ}_{NO_2/SC} = 0.27\ \frac{\text{mol N}}{\text{mol C}}$$

$$Y^{\circ}_{W/SC} = 0.07\ \frac{\text{mol } H_2O}{\text{mol C}}; \qquad Y^{\circ}_{O_2/SC} = 0.60\ \frac{\text{mol } O_2}{\text{mol C}}$$

Although the substrate is of a completely different type, most of the yield coefficients do not differ remarkably from those of Section 4.2.1.

Heinze (1997) investigated the aerobic mineralization of 2,4-DNP in a bioreactor filled with solid porous particles (polyurethane cubes with sides of 0.9 cm) operated with recycle flow. The particle-free overflow was aerated and dissolved oxygen was measured before and after flowing through the fixed bed. By considering the measured flow rate, the oxygen consumption rate $r_{O_2,\Sigma}$ could be predicted, which changed with the flow rate and was plotted versus the 2,4-DNP removal rate $r_S$ (Fig. 4.1). The observed straight line intersects the ordinate at a positive value, giving the rate of endogenous respiration $r_{O_2,e}$.

The straight line can be described by:

$$r_{O_2,\Sigma} = r_{O_2} + r_{O_2,e} = Y_{O_2/SC} \cdot r_{SC} \tag{4.21}$$

with:

$$Y_{O_2/SC} = \frac{r_{O_2} + r_{O_2,e}}{r_{SC}} \tag{4.22}$$

as the real yield coefficient. Considering:

$$r_{SC} = \frac{\mu X}{Y^0_{XC/SC}} \tag{4.23}$$

$$r_{O_2} = \frac{\mu X}{Y^0_{XC/O_2}} \tag{4.24}$$

$$r_{O_2,e} = \frac{k_e X}{Y^0_{XC/O_2}} \tag{4.25}$$

the following relation between real and true yield coefficient can be applied:

$$Y_{O_2/SC} = Y^\circ_{O_2/SC}\left(1 + \frac{k_e}{\mu}\right) \tag{4.26}$$

If bacteria grow at a high rate μ, the coefficient $k_e/\mu$ can be neglected. Otherwise, a relatively large amount of the oxygen consumed is needed for endogenous respiration. In our stochiometric consideration of Sections 4.2.1 and 4.2.2, it was neglected.

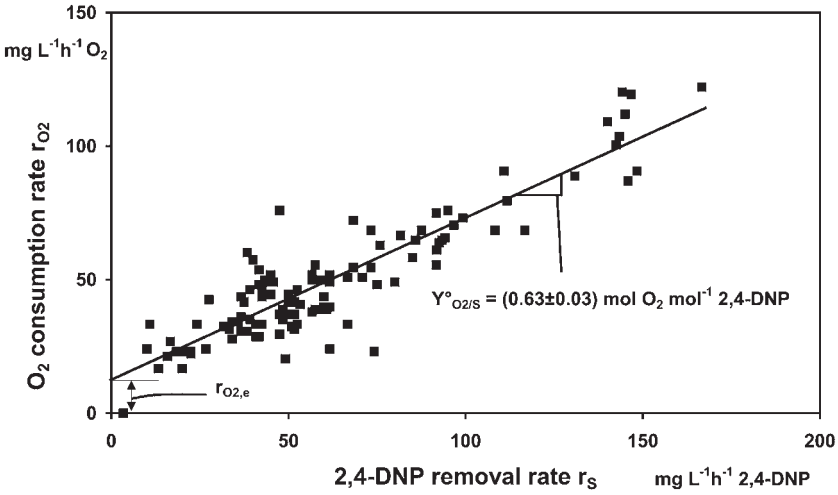


**Fig. 4.1** Biodegradation of 2,4-DNP in a fixed bed reactor: oxygen consumption rate as a function of substrate removal rate (Heinze 1997).

### 4.2.3 Degradation of Hydrocarbons with Bacterial Decay

To this point, endogenous respiration and the death of aerobic bacteria have been neglected, although in Fig. 4.1 the influence of endogenous respiration on total oxygen consumption could be detected. This may be allowed so long as the specific growth rate μ is large compared to the decay rate $k_d$. Otherwise, we must write (Herbert 1958):

$$r_{XC} - r_{XC,d} = \mu X - k_d X = \mu X - (k_e + k_s)\, X \tag{4.27}$$

$$r_{CO_2} + r_{CO_2e} = \frac{\mu X + k_e X}{Y^0_{XC/CO_2}} \tag{4.28}$$

$$r_{SC} = \frac{\mu X}{Y^0_{XC/SC}} \tag{4.29}$$

where μ is the specific growth rate, $k_d$ is the coefficient of decay, $k_s$ is the coefficient of death and $k_e$ is the coefficient of endogenous respiration.

These processes cannot be neglected if the growth rate is reduced as a result of substrate limitation or inhibition. A part of the bacteria will be inactive and no longer involved in substrate consumption and growth. They are dying at rate $k_s X$. Another part loses cell mass at the rate $k_e X$ and uses oxygen at the respiration rate of $k_e X / Y^\circ_{XC/O_2}$ during the consumption of the cell mass (see Eqs. 4.27 and 4.28).

We will assume here that the dying cells do not release organics for the growth of living cells, so that the stoichiometric Eq. (4.2) is not changed, with the exception of the yield coefficients. Instead of the true yield coefficients Y°, now the real yield coefficients Y must be considered, which differ the more greatly the less μ is compared to $k_d$ and $k_e$, respectively.

In the first step, the real yield coefficients are defined as:

$$Y_{XC/SC} = \frac{r_{XC} - r_{XC,d}}{r_{SC}} \tag{4.30}$$

$$Y_{CO_2/SC} = \frac{r_{CO_2} + r_{CO_2,e}}{r_{SC}}\ ^{1)} \tag{4.31}$$

$$Y_{O_2/SC} = \frac{r_{O_2} + r_{O_2,e}}{r_{SC}} \tag{4.32}$$

which can be transformed with the help of Eqs. (4.27) and (4.28) into:

$$Y_{XC/SC} = Y^\circ_{XC/SC} \left(1 - \frac{k_d}{\mu}\right) \tag{4.33}$$

---

[1] We will write $CO_2 - C = CO_2$ only for reasons of simplicity.
All rates r and yield coefficients Y can be written using mol or g.

and:

$$Y_{CO_2/SC} = Y^{\circ}_{CO_2/SC}\left(1 + \frac{k_e}{\mu}\right) \tag{4.34}$$

Starting with Eq. (4.30):

$$r_{SC} - r_{XC,d} = Y_{XC/C} \cdot r_{SC} \tag{4.35}$$

and considering Eq. (4.32) we obtain:

$$r_{XC} - r_{XC,d} = Y^{\circ}_{XC/SC}\left(1 - \frac{k_d}{\mu}\right) r_{SC} \tag{4.36}$$

According to that:

$$r_{CO_2} + r_{CO_2,e} = Y^{\circ}_{CO_2/SC}\left(1 + \frac{k_e}{\mu}\right) r_{SC} \tag{4.37}$$

Equation (4.26) results. Equations (4.35) and (4.36) can be compared with the results of Section 4.2 (Eqs. 4.18 and 4.19). The real growth rate and $CO_2$ production rate differ by the relation of bacterial decay and endogenous respiration to specific growth rate from the true rates.

Using the C balance:

$$r_{SC} = r_{XC} - r_{XC,e} + r_{CO_2} + r_{CO_2,e} \tag{4.38}$$

introducing Eq. (4.30):

$$r_{SC} = r_{SC} Y_{XC/SC} + r_{CO_2,\Sigma} \tag{4.39}$$

$$r_{SC} = \frac{r_{CO_2,\Sigma}}{1 - Y_{XC/SC}} \tag{4.40}$$

and considering Eq. (4.33):

$$r_{SC} = \frac{r_{CO_2,\Sigma}}{1 - Y^{\circ}_{XC/SC}\left(1 - \frac{k_d}{\mu}\right)} \tag{4.41}$$

follows. According to this consideration:

$$r_{SC} = \frac{r_{O_2,\Sigma}}{1 - Y^{\circ}_{XC/SC}\left(1 + \frac{k_e}{\mu}\right)} \tag{4.42}$$

can be obtained from the O balance (C/O = 1 for hydrocarbon molecules).

From Eqs. (4.41) and (4.42) $k_d/\mu$ and $k_e/\mu$ can be easily eliminated after some conversions:

$$\frac{k_d}{\mu} = \frac{Y^o_{XC/SC} + \frac{r_{CO_2,\Sigma}}{r_{SC}} - 1}{Y^o_{XC/SC}} \tag{4.43}$$

$$\frac{k_e}{\mu} = \frac{1 - \frac{r_{O_2,\Sigma}}{r_{SC}} - Y^o_{XO/SC}}{Y^o_{XO/SC}} \tag{4.44}$$

Note that only measurements of DOC for $r_{SC}$ and $O_2$ as well as $CO_2$ reaction rate using gas analysis are needed. However, it is necessary to point out that the $CO_2$ formed is in equilibrium with $HCO_3^-$ and $CO_3^{2-}$, which is influenced by all other ions. This will be discussed in the next chapter.

## 4.3 Measurement of $O_2$ Consumption Rate $r_{O_2,\Sigma}$ and $CO_2$ Production Rate $r_{CO_2,\Sigma}$

As explained in Section 4.2.3, $r_{O_2,\Sigma}$ or $r_{CO_2,\Sigma}$ are needed to measure the substrate removal rate $r_{SC}$ and to calculate real yield coefficients, as well as $k_e/\mu$ and $k_d/\mu$.

The measurement of $r_{O_2,\Sigma}$ is not complicated for closed aeration tanks, conducting a small bypass exhaust air flow through an $O_2$ gas analyzer, such as an ABB Magnos 16. For steady-state conditions and a completely mixed tank, $r_{O_2,\Sigma}$ can be calculated using:

$$r_{O_2,\Sigma} = \frac{Q_G\,(c_{O_2,0} - c_{O_2})}{V_R} \tag{4.45}$$

after measuring $c_{O2}$ in the exhaust gas. The change in the dissolved oxygen concentration is very low compared with the respiration rate because of the high Henry coefficient H, which is defined by Henry's law, see Eq. (5.6):

$$\frac{c_{O_2}}{H} = c^*_{O_2} \tag{4.46}$$

where $c_{O_2}$ is the $O_2$ concentration in the gas and $c^*_{O_2}$ is the $O_2$ concentration at the border gas/liquid at equilibrium.

In comparison to $r_{O_2,\Sigma}$, $r_{CO_2,\Sigma}$ is more difficult to measure for two reasons:

- The solubility of $CO_2$ in water is much higher than that of $O_2$.
- The soluted $CO_{2,L}$ reacts rapidly with water, forming carbonic acid.

$$CO_{2,L} + H_2O \underset{k_2}{\overset{k_1}{\rightleftharpoons}} H_2CO_3 \tag{4.47}$$

However, the equilibrium constant following from:

$$k_1 S_{CO_2,L} \cdot S_{H_2O} = k_2 S_{H_2CO_3} \tag{4.48}$$

$$K'_e = \frac{k_2}{k_1} = \frac{S_{H_2CO_3}}{S_{CO_2,L} \cdot S_{H_2O}} \tag{4.49}$$

$$K_e = S_{H_2O} \cdot K'_e = \frac{S_{H_2CO_3}}{S_{CO_2,L}} = 1.58 \cdot 10^{-3} \tag{4.50}$$

is very low, showing that only ~0.16% of the soluted $CO_2$ is present in the form $H_2CO_3$. Following the concept of Nazaroff and Alvarez-Cohen (2001), we summarize $CO_{2,L}$ and $H_2CO_3$ by writing:

$$r_{H_2CO_3,\Sigma} = r_{CO_2,L} + r_{H_2CO_3} \tag{4.51}$$

or rather as "carbonic acid" concentration, considering Eq. (4.50):

$$S_{H_2CO_3,\Sigma} = S_{CO_2,L} + S_{H_2CO_3} = S_{CO_2,L}(1 + K_e) \tag{4.52}$$

Depending on the pH, "carbonic acid" dissociation reactions display the following equilibria:

$$H_2CO_{3,\Sigma} \rightleftarrows H^+ + HCO_3^- \tag{4.53}$$

$$HCO_3^- \rightleftarrows H^+ + CO_3^{2-} \tag{4.54}$$

which are strongly influenced by $S_{H^+}$ or $pH = -\log S_{H^+}$:

$$K_1 = \frac{S_{H^+} \cdot S_{HCO_3^-}}{S_{H_2CO_3,\Sigma}} = 4.47 \cdot 10^{-7} \text{ mol L}^{-1} \tag{4.55}$$

$$K_2 = \frac{S_{H^+} \cdot S_{CO_3^{2-}}}{S_{HCO_3^-}} = 4.68 \cdot 10^{-11} \text{ mol L}^{-1} \tag{4.56}$$

A fraction $\alpha_i$ of each species $S_{H_2CO_3,\Sigma}$, $S_{HCO_3^-}$ and $S_{CO_3^{2-}}$ related to the total concentration:

$$S_{C\Sigma} = S_{H_2CO_3,\Sigma} + S_{HCO_3^-} + S_{CO_3^{2-}} \tag{4.57}$$

can be calculated using Eqs. (4.55) and (4.56). (Note: $S_{H_2CO_3,\Sigma} \approx S_{CO_2}$):

$$\alpha_{H_2CO_3,\Sigma} = \frac{S_{H_2CO_3,\Sigma}}{S_{C\Sigma}} = \frac{S_{H^+}^2}{S_{H^+}^2 + K_1 K_2 + K_1 S_{H^+}} \tag{4.58}$$

$$\alpha_{HCO_3^-} = \frac{S_{HCO_3^-}}{S_{C\Sigma}} = \frac{K_1 S_{H^+}}{S_{H^+}^2 + K_1 K_2 + K_1 S_{H^+}} \tag{4.59}$$

$$\alpha_{CO_3^{2-}} = \frac{S_{CO_3^{2-}}}{S_{C\Sigma}} = \frac{K_1 K_2}{S_{H^+}^2 + K_1 K_2 + K_1 S_{H^+}} \tag{4.60}$$

For $\alpha_{H_2CO_{3,\Sigma}} = \alpha_{HCO_3^-} = 0.5$ and for $\alpha_{HCO_3^-} = \alpha_{CO_3^{2-}} = 0.5$, the pH values are called $pK_1$ and $pK_2$, showing characteristic values ($pK_1 = 6.33$; $pK_2 = 10.33$).

Equations (4.58) to (4.60) are plotted in Fig. 4.2, presenting some important results:

- At pH < 4.5, all dissolved carbon is in the form of $H_2CO_{3,\Sigma} \approx CO_2$.
- At 4.3 < pH < 8.3, $H_2CO_{3,\Sigma} \approx CO_2$ and $HCO_3^-$ dominates.
- At 8.3 < pH < 12.3, $HCO_3^-$ and $CO_3^{2-}$ dominate.
- At pH > 12.3, all dissolved carbon is in the form of $CO_3^{2-}$.

This equilibrium can be influenced by temperature and the concentration of other anions.

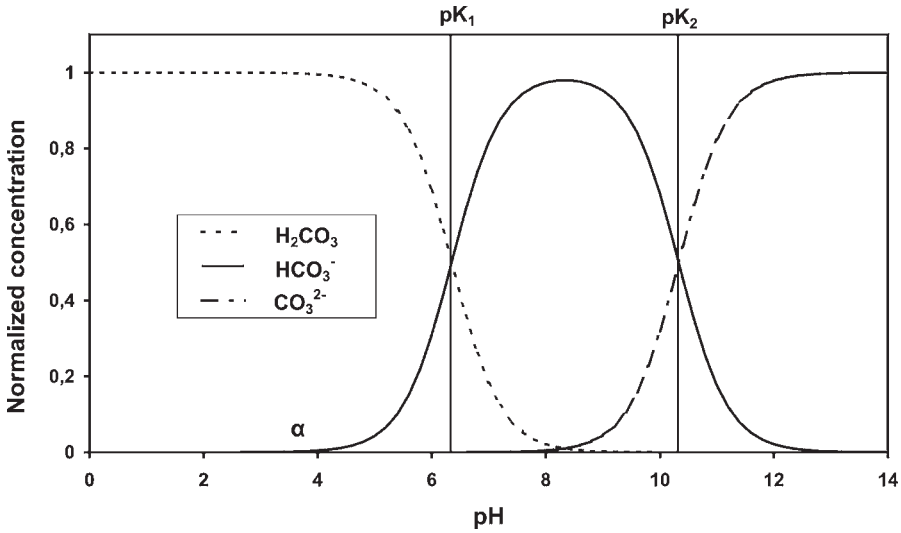


**Fig. 4.2** Normalized concentrations $\alpha_i$ of the dissociation products of "carbonic acid" $H_2CO_{3,\Sigma}$, $HCO_3^-$ and $CO_3^{2-}$ as a function of pH (Nazaroff and Alvarez-Cohen 2001); T = 20 °C.

**PROBLEM 4.1**

An industrial wastewater is polluted mostly by polysaccharides ($C_nH_{2n}O_n$ or for $n = 1$ $CH_2O$, respectively). The composition of the bacteria is given by $C_5H_7O_2N$. The flow rate is 10 000 $m^3\ d^{-1}$, the concentration of the influent is $S_0 = 2000$ mg $L^{-1}$ DOC; and 90% removal should be achieved.

Calculate the amount of nitrogen which must be added.

How much sludge must be treated?

The specific growth rate μ is large compared to the decay coefficient $k_d$.

In Section 4.2.1, $Y^\circ_{N/SC} = 0.067$ mol N (mol DOC)$^{-1}$ and $Y^\circ_{XC/SC} = 1/3$ mol C (mol DOC)$^{-1}$ was calculated for aerobic degradation of hydrocarbons.

**Solution**

$$Y^{\circ}_{N/SC} = \frac{r_N V}{r_{SC} V} = 0.067 \frac{\text{mol N}}{\text{mol DOC}} = 0.067 \cdot \frac{14}{12} \text{ g N (g C)}^{-1} = 0.078 \frac{\text{g N}}{\text{g C}} =$$

$0.078$ t N (t C)$^{-1}$

$r_{SC}V = Q_W (S_o - S) = 10^4\ 1800$ g d$^{-1}$ = 18 t d$^{-1}$ DOC

$r_N V = r_{SC} V \cdot Y^{\circ}_{N/SC} = 18 \cdot 0.078 = 1.4$ t N d$^{-1}$ nitrogen must be added.

$$Y^{\circ}_{XC/SC} = 1/3 \frac{\text{mol C}}{\text{mol DOC}} = 0.33 \text{ g C (g DOC)}^{-1}$$

$$Y^{\circ}_{XC/SC} = \frac{r_{XC}}{r_{SC}};$$

$r_{XC} = r_{SC} Y^{\circ}_{XC/SC}$; $r_{XC} V = r_{SC} V Y^{\circ}_{XC/SC}$

$r_{XC} V = r_{SC} V Y^{\circ}_{XC/SC} = 18{,}000 \cdot 0.33 = 5940$ kg C d$^{-1}$

50% C per mass MLVSS

$r_{MLVSS} V = 2 r_{XC} V \approx 12$ t MLVSS d$^{-1}$ sludge must be treated.

**PROBLEM 4.2**

In a *c*ompletely mixed (*s*tirred) tank *r*eactor (CSTR), a wastewater loaded with organics and without inorganic carbon is treated aerobically. For this process, carried out in a steady state, the following data are given:

Wastewater flow rate $Q_w = 1000$ m$^3$ d$^{-1}$

Air flow rate $Q_A = 7500$ m$^3$ d$^{-1}$

Reactor volume $V = 1000$ m$^3$, pH 8

Henry's law is given by

$p = H_g c^*$

(Nazareff and Alvrez-Cohen 2001).

For $CO_2$ and 25 °C $H_g = 29$ atm (mol/L)$^{-1}$ is given. In order to get Henry coefficiet H in its dimensionless form

$p = RT c$

must be introduced giving

$$c = \frac{H_g}{RT} c^* = H c^*$$

With $R = 8.314$ J mol$^{-1}$ K$^{-1}$ = $82.05 \cdot 10^{-6}$ m$^3$ atm (mol K)$^{-1}$

$T = 273 + 25 = 298$ K

$$H = \frac{29}{82.05 \cdot 10^{-6} \cdot 298} = 1.19 \text{ follows.}$$

$CO_2/HCO_3^-$ equilibrium constant $K_1 = 4.47 \cdot 10^{-7}$ mol $L^{-1}$
$CO_2$ production rate $r_{CO_2} = 9000$ g $m^{-3}$ $d^{-1}$
Calculate the portion of carbon:
produced as $CO_2$ in the air leaving the reactor and
produced as $CO_2$, $HCO_3^-$ and $CO_3^{2-}$ in the water leaving the reactor.

**Solution**

C balance in water:

$$0 = \underbrace{-\frac{Q_W}{V}\left(S_{CO_2} + S_{HCO_3^-} + S_{CO_3^{2-}}\right)}_{\text{dissolved in the effluent water}} \underbrace{-\frac{Q_A}{V} c_{CO_2}}_{\text{stripped out with air}} + \underbrace{r_{CO_2}}_{\text{produced}} \tag{4.61}$$

$S_{CO_3^{2-}}$ can be neglected (pH 8)

$$S_{HCO_3^-} = K_1 \frac{S_{H_2CO_2,\Sigma}}{S_{H^+}} \approx K_1 \frac{S_{CO_2}}{S_{H^+}} \tag{4.62}$$

Henry's law $S_{CO_2} = c^* = \frac{c_{CO_2}}{H}$ (4.63)

From (4.61) we obtain with Eqs. (4.62) and (4.63)

$$S_{CO_2} = \frac{r_{CO_2}}{\frac{Q_w}{V}\left(1 + \frac{K_1}{S_{H^+}}\right) + \frac{Q_A}{V} H} \tag{4.64}$$

$K_1 = 4.47 \cdot 10^{-7}$ mol $L^{-1}$, $M_{HCO_3^-} = 61$ g $mol^{-1}$
$K_1 = 4.47 \cdot 61 \cdot 10^{-7} = 272.67 \cdot 10^{-7}$ g $L^{-1}$
$S_{H^+} = 10^{-8}$ mol $L^{-1} = 10^{-8}$ g $L^{-1}$, $H = 1.19$

$$S_{CO_2} = \frac{9000}{1\left(1 + \frac{272.67 \cdot 10^{-7}}{10^{-8}}\right) + 7.5 \cdot 1.19} = \frac{9000}{2744.6} = 3.29 \text{ g m}^{-3}$$

With Eq. (4.61) the different parts can be calculated

$$\underbrace{9000 \text{ g m}^{-3} \text{ h}^{-1}}_{CO_2 \text{ produced}} \approx \underbrace{3.29}_{CO_2 \text{ transported with water}} + \underbrace{8970.8}_{HCO_3^- \text{ transported with water}} + \underbrace{29.36}_{CO_2 \text{ stripped with air}}$$

In reality two further reactions are of importance, which reduce $HCO_3^-$-concentration:

$$HCO_3^- \rightleftharpoons H^+ + CO_3^{2-}$$

$$Ca^{2+} + CO_3^{2-} \rightleftharpoons \underset{\downarrow}{CaCO_3}$$

## References


Behrendt, J. **1994**, Biologisch-chemische Behandlung von Prozesswässern der Altlastensanierung sowie von kontaminierten Grundwässern, *VDI-Forschungsberichte, Reihe 15, Umwelttechnik* 119.

Heinze, L. **1997**, Mikrobiologischer Abbau von 4-Nitrophenol, 2,4-Dinitrophenol und 2,4-Dinitrotoluol in synthetischen Abwässern, *VDI-Forschungsberichte, Reihe 15, Umwelttechnik* 167.

Herbert, D. **1958**, Some principles of continuous culture, in: *Recent Progress in Microbiology*, ed. Tunevall, G., Almqvist, Stockholm, p. 381–396.

Lax, E. **1967**, *Taschenbuch für Chemiker und Physiker*, Springer-Verlag, Berlin.

Nazaroff, W.W.; Alvarez-Cohen, L. **2001**, *Environmental Engineering Science*, John Wiley & Sons, New York, 96, 114.

# 5
# Gas/Liquid Oxygen Transfer and Stripping

## 5.1
## Transport by Diffusion

Oxygen is needed for all aerobic biological processes. Usually, it consumption rate depends on oxygen mass transfer[1]. If we wish to increase the rate of these processes, we must increase the gas/liquid interfacial area and the rate of the specific mass transfer, which consists of diffusion and convection. The specific mass transport rate of diffusion without convection is given by Fick's law:

$$J_D = -D \frac{dc'}{dx} \text{ mol m}^{-2} \text{ h}^{-1} \tag{5.1}$$

D is the diffusion coefficient. If c′ is the dissolved oxygen concentration in water, then $D = D_{O_2/H_2O}$ is the diffusion coefficient of oxygen in water. It can be calculated by using the Einstein equation (Daniels and Alberty 1955) or the Nernst-Einstein equation (Bird et al. 1962)

$$D = KT \frac{w_{O_2}}{F_{O_2}} \text{ m}^2 \text{ h}^{-1} \tag{5.2}$$

where $K = 1.380\ 10^{-23}$ J K$^{-1}$ (Boltzmann's constant), T is the temperature (K), $w_{O_2}$ is the rate of diffusion of oxygen molecules (mol m h$^{-1}$) and $F_{O_2}$ is the power of resistance of oxygen molecules (J mol m$^{-1}$).

$F_{O_2}$ is obtained from Stokes' law for the motion influenced by high friction forces ($Re \ll 1$):

$$F_{O_2} = 6 \pi \eta w_{O_2} R_{O_2} \text{ J mol m}^{-1} \tag{5.3}$$

where η is the dynamic viscosity of water (g m$^{-1}$ h$^{-1}$) and $R_{O_2}$ is the molecular radius of $O_2$ (m).

Introducing Eq. (5.3) in Eq. (5.2), this follows:

$$D = \frac{KT}{6 \pi R_{O_2} \eta} \text{ m}^2 \text{ h}^{-1} \tag{5.4}$$

[1] Only for very low reaction rates is it not dependent on oxygen mass transfer.

*Fundamentals of Biological Wastewater Treatment*. Udo Wiesmann, In Su Choi, Eva-Maria Dombrowski

ISBN: 978-3-527-31219-1

Wilke and Chang (Reid et al. 1987) calculated for T = 20 °C:

$$D_{20} = 6.48 \cdot 10^{-6}\ m^2\ h^{-1}$$

and recommended that the influence of temperature should be taken into account using:

$$D_T = D_{20}\ \theta^{T-20} \tag{5.5}$$

with $\theta = 1.029$.

At the gas/liquid boundary, the specific transfer rate of oxygen in water calculated by using Eq. (5.1) is low if only diffusion is involved. This follows not only from the low diffusion coefficient, but also from the low solubility of oxygen in water:

$$c = H\ c^* \tag{5.6}$$

Equation (5.6) is called the Henry absorption equilibrium (Henry's law, see Eq. 4.46) and is valid up to oxygen pressures of nearly p = 10 bar (c = p/RT). H decreases with increasing temperature and concentration of chlorides (Table 5.1).

For 20 °C and deionized water H = 32.6 which means that, for an $O_2$ concentration in air of 298.7 mg $L^{-1}$, only 9.17 mg $O_2$ $L^{-1}$ are dissolved in water. Therefore, oxygen transfer into water by diffusion is a slow process, due to the low diffusion coefficient and the low solubility (Fig. 5.1).

If we want to use oxygen for a chemical or biological process in water, we must: (a) use convection in addition to diffusion and (b) increase the gas/liquid interfacial area.

Furthermore, it may be necessary to use pure oxygen instead of air in some cases, resulting in a higher dissolved oxygen concentration at the boundary $c^*$ by a factor of 4.8. But in our further discussion we will only consider the use of air.

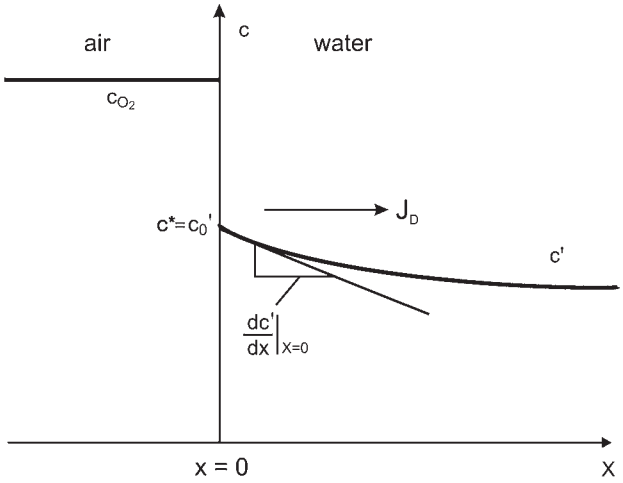


**Fig. 5.1** Transport of oxygen from air into water only by diffusion.

**Table 5.1** Dissolved oxygen concentration in water c′ for different temperatures and chloride concentrations; c = 20.9% $O_2$ in air; $p_{air}$ = 760 bar (Chow et al. 1972).

| Temperature (°C) | Chloride concentration (mg $L^{-1}$) | | | | |
|---|---|---|---|---|---|
| | 0 | 5000 | 10 000 | 15 000 | 20 000 |
| 0 | 14.62 | 13.79 | 12.97 | 12.14 | 11.32 |
| 1 | 14.23 | 13.41 | 12.61 | 11.82 | 11.03 |
| 2 | 13.84 | 13.05 | 12.28 | 11.52 | 10.76 |
| 3 | 13.48 | 12.72 | 11.98 | 11.24 | 10.50 |
| 4 | 13.13 | 12.41 | 11.69 | 10.97 | 10.25 |
| 5 | 12.80 | 12.09 | 11.39 | 10.70 | 10.01 |
| 6 | 12.48 | 11.79 | 11.12 | 10.45 | 9.78 |
| 7 | 12.17 | 11.51 | 10.85 | 10.21 | 9.57 |
| 8 | 11.87 | 11.24 | 10.61 | 9.98 | 9.36 |
| 9 | 11.59 | 10.97 | 10.36 | 9.76 | 9.17 |
| 10 | 11.33 | 10.73 | 10.13 | 9.55 | 8.98 |
| 11 | 11.08 | 10.49 | 9.92 | 9.35 | 8.80 |
| 12 | 10.83 | 10.28 | 9.72 | 9.17 | 8.62 |
| 13 | 10.60 | 10.05 | 9.52 | 8.98 | 8.46 |
| 14 | 10.37 | 9.85 | 9.32 | 8.80 | 8.30 |
| 15 | 10.15 | 9.65 | 9.14 | 8.63 | 8.14 |
| 16 | 9.95 | 9.46 | 8.96 | 8.47 | 7.99 |
| 17 | 9.74 | 9.26 | 8.78 | 8.30 | 7.84 |
| 18 | 9.54 | 9.07 | 8.62 | 8.15 | 7.70 |
| 19 | 9.35 | 8.89 | 8.45 | 8.00 | 7.56 |
| 20 | 9.17 | 8.73 | 8.30 | 7.86 | 7.42 |
| 21 | 8.99 | 8.57 | 8.14 | 7.71 | 7.28 |
| 22 | 8.83 | 8.42 | 7.99 | 7.57 | 7.14 |
| 23 | 8.68 | 8.27 | 7.85 | 7.43 | 7.00 |
| 24 | 8.53 | 8.12 | 7.71 | 7.30 | 6.87 |
| 25 | 8.38 | 7.96 | 7.56 | 7.15 | 6.74 |
| 26 | 8.22 | 7.81 | 7.42 | 7.02 | 6.61 |
| 27 | 8.07 | 7.67 | 7.28 | 6.88 | 6.49 |
| 28 | 7.92 | 7.53 | 7.14 | 6.75 | 6.37 |
| 29 | 7.77 | 7.39 | 7.00 | 6.62 | 6.25 |
| 30 | 7.63 | 7.25 | 6.86 | 6.49 | 6.13 |

There are two possibilities to realize the conditions (a) and (b):

- We can produce small air bubbles, which rise to the surface of the water, causing an oxygen transfer into the water and to the suspended microorganisms.
- We can produce trickling films, which flow downwards at the surface of solids covered by biofilms.

In this chapter we will concentrate only on the transfer of oxygen from bubbles to water by diffusion and convection.

## 5.2
## Mass Transfer Coefficients

### 5.2.1
### Definition of Specific Mass Transfer Coefficients

In contrast to Fig. 5.1, where mass is only transferred by molecular motion (diffusion), we now want to augment it with convective motion (Fig. 5.2).

As a result of the high diffusion coefficient of oxygen in air, the concentration of oxygen in air remains locally constant as before. But in the water, the situation has changed completely: in addition to the molecular motion, total liquid mass is now moved by hydrodynamic forces, i.e. pressure, inertia and friction forces in the direct vicinity of a rising air bubble. This convective transport increases the local slope of the concentration at the boundary $dc'/dx|_{x=0}$ and the specific rate of mass transfer:

$$J_{D+C} = -D \frac{dc'}{dx|_{x=0}} \text{ mol } (m^2\,h)^{-1} \tag{5.7}$$

But the gradient is not measurable and can be calculated only for low liquid flow rates. In contrast, the concentration difference $c^* - c'$ can easily be measured (Fig. 5.2):

$$J_{D+C} = k_L (c^* - c') \text{ mol } (m^2\,h)^{-1} \tag{5.8}$$

where $k_L = \frac{D}{\delta}$ and $\delta$ is the thickness of the boundary (see Fig. 5.3).

The proportionality factor $k_L$ in Eq. (5.8) depends on the diffusion coefficient D as well as the bubble velocity $\overline{w}$, the kinematic viscosity v and the surface tension $\sigma$,

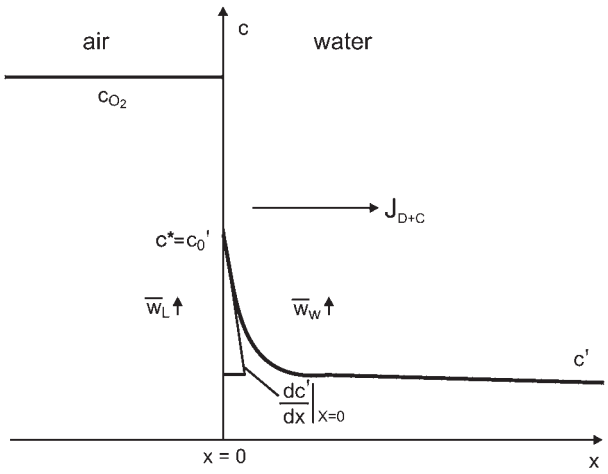


**Fig. 5.2** Transport of oxygen from air into water by diffusion and convection.

for example. We cannot assume that we are able to measure the total boundary surface area A gas/liquid of all the bubbles:

$$J_{D+C}\,A = k_L\,A\,(c^* - c')\ \text{mol h}^{-1} \tag{5.9}$$

Applying Eq. (5.9) to the volume of the system V, the specific oxygenation capacity follows:

$$OC = J_{D+C}\,\frac{A}{V} = k_L a\,(c^* - c')\ \text{mol m}^{-3}\,\text{h}^{-1} \tag{5.10}$$

with $k_L a$ as the specific mass transfer coefficient.

$k_L a$ and $c'$ are dependent on the temperature. For a temperature of 20 °C and $c' = 0$, we obtain the maximum specific standardized oxygenation capacity:

$$OC_{20} = (k_L a)_{20} \cdot c^*_{20} \tag{5.11}$$

$(k_L a)_{20}$ and $c^*_{20}$ are dependent on the concentration of dissolved inorganic and organic substances. Applying the ratio of values effective for wastewater and clean water, we write:

$$\alpha_w = \frac{(k_L a)_{20,w}}{(k_L a)_{20,0}} \tag{5.12}$$

$$\beta_w = \frac{c'_{20,w}}{c'_{20,0}} \tag{5.13}$$

$$\gamma_w = \frac{(k_L a)_{20,w}\,c'_{20,w}}{(k_L a)_{20,0} \cdot c'_{20,0}} \tag{5.14}$$

reflecting the mass transfer coefficients for T = 20 °C gives:

$(k_L a)_{20,w}$ for wastewater
$(k_L a)_{20,0}$ for clean water

and concentrations of dissolved oxygen at the interface:

$c'_{20,w}$ for wastewater
$c'_{20,0}$ for clean water

Especially in industrial wastewater, different components may be dissolved which may desorb during the absorption of oxygen. Because of their low Henry coefficient H, a transport resistance occurs in both phases, in water *and* air. This case will be discussed in the next section.

### 5.2.2 Two Film Theory

Three models have been developed to improve the understanding of gas/liquid mass transfer: the surface renewal model of Higbie (1935) and Danckwerts (1951, 1970); the 'still surface' model of King (1964) and the 'two film' model of Whitman

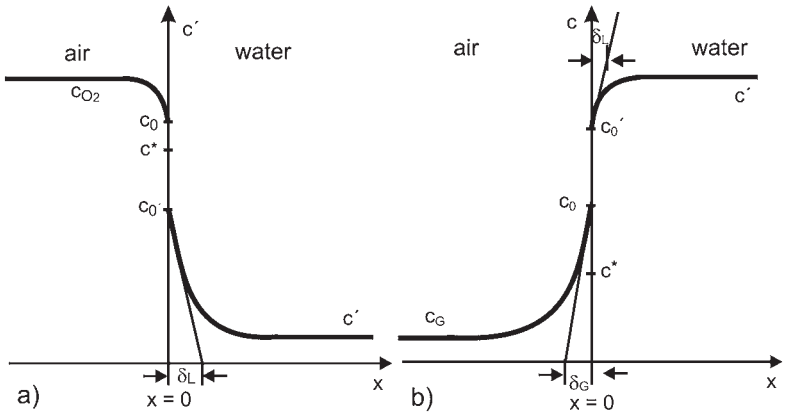


**Fig. 5.3** Absorption and desorption of compounds dissolved in water with a low Henry coefficient, $H = c/c^* = c_0/c_0'$; (a) absorption, (b) desorption.

(1923). We will limit our discussion to the two film theory. A review of all theories is given by Danckwerts (1970).

Let us look at the mass transfer at the boundary water/air for desorption processes and for the case that two films are formed. The desorption of oxygen into an oxygen-free gas film, e.g. nitrogen, is a simple case which follows nearly directly from Fig. 5.2. But such equilibria, which are characterized by a low Henry coefficient, lead to concentration profiles in both water and air for absorption (Fig. 5.3a) and desorption (Fig. 5.3b).

The rate of desorption must now be calculated using the two film theory. Table 5.2 compiles some compounds with low H.

Note that in Fig. 5.3b the concentration c in the air bubble is much lower than $c^*$, the theoretical equilibrium concentration.

An overall mass transfer rate is given using $K_La$. If we define the specific overall mass transfer coefficient $K_La$ by writing:

$$K_La\,(c' - c^*)$$

for the specific overall mass transfer rate, we can conclude that this rate is the same as in the liquid film:

$$K_La\,(c' - c^*) = k_La\,(c' - c_0') \tag{5.15}$$

which also agrees with the rate in the gas film:

$$k_La\,(c' - c_0') = k_Ga\,(c_0 - c_G) \tag{5.16}$$

with:

$$c_0' = \frac{1}{H}\,c_0 \tag{5.17}$$

**Table 5.2** Solubility and Henry coefficient of different compounds (Nyer 1992, supplemented), Henry's law:

$$c^* = \frac{c}{H} \text{ and } c^* = \frac{P\,c_w}{K_P};\ H = \frac{K_P}{RT\,c_w}$$

| | Compound | Maximal solubility ($c^*_{max}$, mg $L^{-1}$) | Henry coefficient ($K_P$, bar) | Henry coefficient (H, –) |
|---|---|---|---|---|
| 1 | Acetone | $1 \cdot 10^6$ | 0 | 0 |
| 2 | Benzene | $1.75 \cdot 10^3$ | 230 | 0.1690 |
| 3 | Bromodichloromethane | $4.4 \cdot 10^3$ | 127 | 0.0934 |
| 4 | Bromoform | $3.01 \cdot 10^3$ | 35 | 0.0257 |
| 5 | Carbon tetrachloride | $7.57 \cdot 10^2$ | 1 282 | 0.943 |
| 6 | Chlorobenzene | $4.66 \cdot 10^2$ | 145 | 0.107 |
| 7 | Chloroform | $8.2 \cdot 10^3$ | 171 | 0.126 |
| 8 | 2-Chlorophenol | $2.9 \cdot 10^4$ | 0.93 | $0.684 \cdot 10^{-3}$ |
| 9 | p-Dichlorobenzene (1,4) | $7.9 \cdot 10^1$ | 104 | 0.0765 |
| 10 | 1,1-Dichloroethane | $5.5 \cdot 10^3$ | 240 | 0.176 |
| 11 | 1,2-Dichloroethane | $8.52 \cdot 10^3$ | 51 | 0.0375 |
| 12 | 1,1-Dichloroethylene | $2.25 \cdot 10^3$ | 1 841 | 1.353 |
| 13 | cis-1,2-Dichloroethylene | $3.5 \cdot 10^3$ | 160 | 0.117 |
| 14 | trans-1,2-Dichloroethylene | $6.3 \cdot 10^3$ | 429 | 0.315 |
| 15 | Ethylbenzene | $1.52 \cdot 10^2$ | 359 | 0.264 |
| 16 | Hexachlorobenzene | $6 \cdot 10^{-3}$ | 37.8 | 0.0278 |
| 17 | Methylene chloride | $2 \cdot 10^4$ | 89 | 0.0654 |
| 18 | Methylethylketone | $2.68 \cdot 10^5$ | 1.16 | $0.853 \cdot 10^{-3}$ |
| 19 | Methyl naphthalene | $2.54 \cdot 10^1$ | 3.2 | $0.235 \cdot 10^{-3}$ |
| 20 | Methyl tert-butyl-ether | 4.8 | 196 | 0.144 |
| 21 | Naphthalene | $3.2 \cdot 10^1$ | 20 | 0.0147 |
| 22 | Pentachlorophenol | $1.4 \cdot 10^1$ | 0.15 | $0.1100 \cdot 10^{-3}$ |
| 23 | Phenol | $9.3 \cdot 10^4$ | 0.017 | $0.0125 \cdot 10^{-3}$ |
| 24 | Tetrachloroethylene | $1.5 \cdot 10^2$ | 1 035 | 0.761 |
| 25 | Toluene | $5.35 \cdot 10^2$ | 217 | 0.160 |
| 26 | 1,1,1-Trichloroethane | $1.5 \cdot 10^3$ | 390 | 0.287 |
| 27 | 1,1,2-Trichloroethane | $4.5 \cdot 10^3$ | 41 | 0.030 |
| 28 | Trichloroethylene | $1.1 \cdot 10^3$ | 544 | 0.400 |
| 29 | Vinyl chloride | $2.67 \cdot 10^3$ | 355 000 | 261.0 |
| 30 | o-Xylene | $1.75 \cdot 10^2$ | 266 | 0.196 |

and:

$$c^* = \frac{1}{H}\,c_G \tag{5.18}$$

$c'_0$ follows from Eqs. (5.15) to (5.18). $c_G$ is the concentration of the desorbed compound in the air and c* is its equilibrium value at the interface:

$$c'_0 = \frac{c' + \frac{k_G a}{k_L a} H c^*}{1 + \frac{k_G a}{k_L a} H} \tag{5.19}$$

After introducing Eq. (5.19) into Eq. (5.15), we obtain:

$$\underset{\text{overall resistance}}{\frac{1}{K_L a}} = \underset{\text{resistance of the air film}}{\frac{1}{k_G a\, H}} + \underset{\text{resistance of the water film}}{\frac{1}{k_L a}} \tag{5.20}$$

Note that:

- This simple equation is only applicable if we use $c' - c^*$ as the driving concentration difference to define the specific overall transfer coefficient $K_L a$.
- The resistance of the air film increases with decreasing Henry coefficient H, i.e. higher dissolution in water at lower concentration in air.
- The influence of H is increased at low $k_G a$ and high $k_L a$.

Looking at Table 5.2 and assuming similar values for $k_G a$ and $k_L a$, mass transfer resistance lies nearly completely on the air film side for compounds with low H (2-chlorophenol, methyl ethyl ketone, phenol and others) and nearly completely on the water film side for vinyl chloride with its very high H.

Although H = 32.6 (T = 20 °C) for oxygen/water (clean water) is relatively high (Section 5.1) and mass transfer is controlled for normal conditions by the resistance of the water film, we want to use the specific overall mass transfer coefficient $K_L a$ as well.

## 5.3 Measurement of Specific Overall Mass Transfer Coefficients $K_L a$

### 5.3.1 Absorption of Oxygen During Aeration

#### 5.3.1.1 Steady State Method

The absorption of oxygen will first be discussed for a *c*ompletely *s*tirred *t*ank *r*eactor (CSTR) filled with clean water and equipped with a perforated annular tube below the stirrer (Fig. 5.4).

Sodium sulfite, $Na_2SO_3$, is dissolved in the clean water together with a cobalt catalyst. Sulfite ions oxidize immediately, consuming the dissolved oxygen:

$$SO_3^{2-} + \frac{1}{2} O_2 \xrightarrow{\text{catalyst}} SO_4^{2-} \tag{5.21}$$

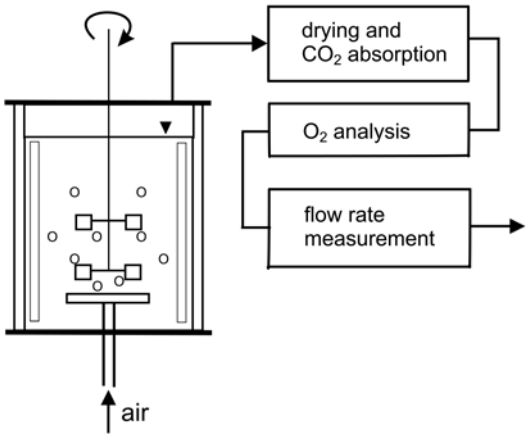


**Fig. 5.4** Installation for measuring the mass transfer coefficient in clean water or wastewater without activated sludge.

Therefore, c′ is zero until the dissolved $SO_3^{2-}$ is totally oxidized to $SO_4^{2-}$. If we want to measure in nearly salt-free water after aeration, only a small amount of $Na_2SO_3$ should be added – just enough for a few experiments. The exhaust air with a low $O_2$ concentration flows through absorption systems for drying and $CO_2$ removal before entering on-line oxygen gas analyzers and flow rate measurement devices.

The steady state oxygen balance in the completely mixed gas is:

$$0 = Q_G\, c_{in} - Q_G\, c_{out} - K_L a\, c^*_{out}\, V \tag{5.22}$$

where V is the water volume, $Q_G$ is the gas flow rate and $c^*_{out} = \dfrac{c_{out}}{H}$ is the saturated dissolved oxygen concentration.

Solving Eq. (5.22) for $K_L a$ gives:

$$K_L a = \frac{Q_G\,(c_{in} - c_{out})\,H}{V\,c_{out}} \tag{5.23}$$

In larger aerated reactors, the $O_2$ gas concentration is often not completely mixed and better results can be obtained if an arithmetic mean value is used for:

$$\overline{c}^{\,*} = \frac{c^*_{in} + c^*_{out}}{2} \tag{5.24}$$

This relatively small simplification is only allowed for small decreases in the percent of oxygen volume inside the air bubbles, e.g. from 20.9 to 19.0%. For a greater decrease, a more complicated evaluation is necessary. Better results follow if a logarithmic mean value is used.

#### 5.3.1.2 **Non-steady State Method**

Only a low amount of $Na_2SO_3$ is added to the water (clean water or wastewater free of activated sludge) using the dissolved $O_2$ for oxidation. After the $Na_2SO_3$ is completely oxidized, c′ increases. It is measured by one or several $O_2$ electrodes, which

are combined with a computer for direct evaluation. For this purpose, the $O_2$ dissolved in the completely mixed water must be balanced:

$$\frac{dc'}{dt} = K_L a\,(c^* - c') \tag{5.25}$$

Considering the initial condition:

$$t = 0 \quad c' = 0$$

the solution of Eq. (5.25) gives:

$$\ln \frac{c^* - c'}{c^*} = -K_L a\, t \tag{5.26}$$

A plot of $\ln (c^* - c')/c^*$ versus t must give a straight line, if the assumption of a completely mixed system is to be met. Frequently, a better linear plot is obtained using an arithmetic mean value for $c^*$. Equation (5.26) should go over at least 1.5 decades of $\left(1 - \frac{c'}{c^*}\right)$.

#### 5.3.1.3 Dynamic Method in Wastewater Mixed with Activated Sludge

The specific overall mass transfer coefficients $K_L a$ can be influenced not only by temperature and pressure (bubble diameter) but also by dissolved and suspended matter, such as minerals and activated sludge (Eqs. 5.12 to 5.14). Therefore, it is necessary to measure $(K_L a)_{20,w}$ in an activated sludge system which can be treated as a CSTR in continuous flow or in batch operation. We will describe this method for a batch system. After a period of continuous operation (Fig. 5.5, period I) and after an input of a given bacteria mass, the flow of wastewater and air is stopped, without reducing the stirrer speed to maintain the activated sludge in suspension. During period II, the concentration of dissolved oxygen c′ is decreased by respira-

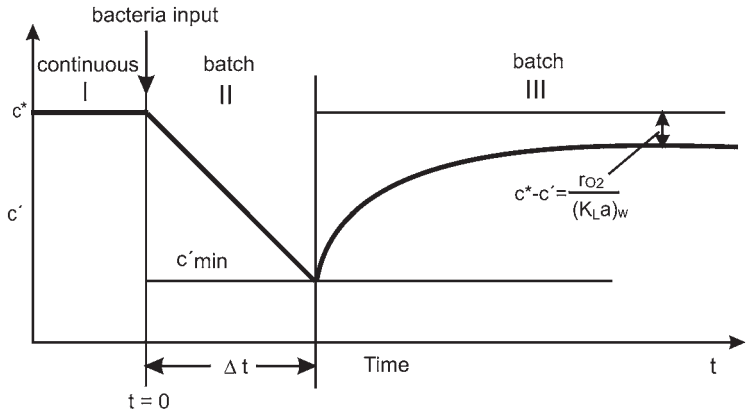


**Fig. 5.5** Non-steady state method for measuring the mass transfer coefficients in wastewater with activated sludge.

tion. Period II is finished as soon as $c'_{min} \approx 2$ mg $L^{-1}$ is reached. In the region of lower c′ values, respiration rate may be limited by oxygen. Now aeration resumes and c′ increases up to a constant value (period III).

The balance for dissolved oxygen in period II and the initial condition are:

$$\frac{dc'}{dt} = - r_{O_2} \tag{5.27}$$

$$\text{at} \quad t = 0 \quad c' = c^*$$

The respiration rate follows as:

$$r_{O_2} = \frac{c^* - c'_{min}}{\Delta t} \tag{5.28}$$

The balance for period III and the initial condition are:

$$\frac{dc'}{dt} = - r_{O_2} + (K_L a)_w \, (c^* - c') \tag{5.29}$$

$$\text{at} \quad t = 0 \quad c' = c'_{min}$$

Equation (5.29) can be solved by the separation of variables. After integration and consideration of the initial condition:

$$\ln \left[ \frac{(K_L a)_w \, c^* - r_{O_2} - (K_L a)_w \, c'}{(K_L a)_w \, c^* - r_{O_2} - (K_L a)_w \, c'_{min}} \right] = - (K_L a)_w \, t$$

can be written, and finally:

$$c^* - c' = \left( c^* - c'_{min} - \frac{r_{O_2}}{(K_L a)_w} \right) \exp \left[ - (K_L a)_w \, t \right] + \frac{r_{O_2}}{(K_L a)_w} \tag{5.30}$$

For higher values of time t:

$$c^* - c' \approx \frac{r_{O_2}}{(K_L a)_w}$$

and $(K_L a)_w$ can be calculated.

The experimental curve in period III is described in the best possible way obtaining a more exact value for $(K_L a)_w$. By comparing this value $(K_L a)_w$ to $K_L a$ measured in clean water, both at 20 °C, $\alpha_w$ can be determined (see Eq. 5.12).

### 5.3.2
### Desorption of Volatile Components During Aeration

Dissolved volatile organic components (VOC) can be divided into two groups, according to their Henry coefficient H (see Table 5.2).

For $H \gg 1$ (e.g. oxygen/water), overall mass transfer resistance is given by liquid mass transfer:

$$\frac{1}{K_L a} = \frac{1}{K_G a\, H} + \frac{1}{k_L a} \tag{5.20}$$

$$K_L a \approx k_L a$$

and usually the desorption capacity for T = 20 °C follows from (see Fig. 5.3b):

$$(DC)_{20} = k_L a\,(c' - c_0') \tag{5.31}$$

If the desorbing component has nearly the same diffusion coefficient as oxygen, the same $k_L a$ can be used. For molar masses of individual VOCs different from oxygen, it is most effective to use a corrected $k_L a$:

$$(DC)_{20} = k_L a \left(\frac{D_{VOC}}{D_{O_2}}\right)^n (c' - c_0') \tag{5.32}$$

$D_{VOC}$ can be measured or calculated using Eq. (5.4). The exponent n is not easily obtainable and depends on the mixing equipment.

For H < 10, the overall mass transfer resistance is normally given by liquid and gas mass transfer rates using the film model (Fig. 5.3 where H < 1). In this case, the desorption capacity at T = 20 °C is:

$$(DC)_{20} = K_L a\,(c' - c^*) \tag{5.33}$$

with:

$$K_L a = \frac{k_G a\, H \cdot k_L a}{k_G a\, H + k_L a} = \frac{k_L a}{1 + \dfrac{k_L a}{k_G a\, H}} \tag{5.34}$$

if the diffusion coefficient of the desorbing component is nearly the same as that of oxygen. Otherwise, Eqs. (5.33) and (5.34) must be corrected in a similar way to Eq. (5.32):

$$K_L a = \frac{k_L a \left(\dfrac{D_{VOC}}{D_{O_2}}\right)^n \cdot k_G a \left(\dfrac{D_{VOC}}{D_{O_2}}\right)^m H}{k_G a \left(\dfrac{D_{VOC}}{D_{O_2}}\right)^m H + k_L a \left(\dfrac{D_{VOC}}{D_{O_2}}\right)^n} \tag{5.35}$$

From Eq. (5.20), follows:

$$\frac{H}{K_L a} = \frac{1}{k_G a} + \frac{H}{k_L a} \tag{5.36}$$

For at least three different components with different Henry coefficients, $H/K_L a$ can be measured in the same mixing system at exactly the same conditions (stirrer speed, flow rate). A straight line must go through the date plotted as $H/K_L a$ versus H. The resulting value of $k_L a$ follows from the slope and $k_G a$ from the ordinate intercept.

Only the results of a few studies are available (Libra 1993) to date.

## 5.4
## Oxygen Transfer Rate, Energy Consumption and Efficiency in Large-scale Plants

### 5.4.1
### Surface Aeration

#### 5.4.1.1 Oxygen Transfer Rate

Principally, the same methods are used for measuring overall specific mass transfer coefficients $K_La$ as described before in Section 5.3, but often the following terms are used:

- OTR oxygenation transfer rate (ASCE 1997: Standard guidelines for in-process oxygen transfer testing).
- OC oxygenation capacity (ATV 1997: Guidelines according to ATV Arbeitsblatt M 209).

We select OTR, which is related to reactor volume V and is calculated from (see Fig. 5.3a):

$$OTR = \frac{Q_G\,(c_{in} - c_{out})}{V} = K_La\,(c^* - c')^{1)} \tag{5.37}$$

However, the air flow rate $Q_G$ as well as the oxygen concentration of the escaping air is normally not measurable. Therefore, the only way to measure $K_La$ is by using data obtained from absorption measurements and the balances for oxygen absorption described in Section 5.3.1.2 (see Eq. (5.27) for period II and Eq. (5.29) for period III).

One problem must be noted: in Section 5.3 the reactors used for laboratory or pilot experiments have a small volume of several liters to 1–2 $m^3$; and, regardless of the aeration method (volume or surface aeration), a nearly completely mixed gas and liquid phase cannot be guaranteed. Large-scale basins of several hundreds to several thousands of cubic meters cannot be completely mixed by surface aerators, such as centrifugal aerators. Therefore $K_La$ as well as c′ are different at several points of a "mixed" tank with one or more aerators.

Nevertheless, the only way to obtain information about OTR in large-scale basins is to evaluate the measurements with Eq. (5.25) for clean water without sludge or Eqs. (5.27) and (5.29) for wastewater with sludge.

Three measures are necessary to standardize OTR:
- Use a fixed temperature (in Europe T = 20 °C).
- Limit the maximum value for the difference of concentration.
- Use clean water (index 0).

For the standardized oxygen transfer rate we write:

$$SOTR = (K_La)_{20,0}\,c^*_{20,0} \tag{5.38}$$

---

[1)] Remember: Only for this definition of $K_La$, it is not influenced by concentration; see Eq. (5.20).

For a measurement in wastewater with or without sludge, we obtain:

$$OTR_{20,w} = (K_L a)_{20}\, c^*_{20} \tag{5.39}$$

$$\alpha = \frac{(K_L a)_{20}}{(K_L a)_{20,0}} \tag{5.40}$$

Figure 5.6 shows a Simplex aerator. Different values of $K_L a$ can be selected via the rotation speed and depth of submersion. Frequently, a transmission makes three speeds possible.

For a Simplex aerator with the dimensions presented in Fig. 5.6, the standardized oxygen transfer rate (SOTR) is plotted versus power consumption P/V (see Fig. 5.7, in the next section).

We will now consider a surface aerator and the power required to achieve a desired oxygen transfer rate.

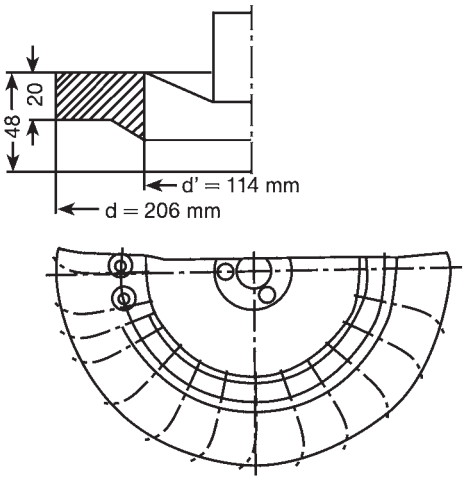


**Fig. 5.6** Simplex aerator, number of blades = 24 (Zlokarnik 1979).

#### 5.4.1.2 Power Consumption and Efficiency

The power consumption of a rotating turbine powered by an electric motor is usually given as the total power consumption $P_t$:

$$P_t = \frac{P}{\eta_m \cdot \eta_g} \tag{5.41}$$

where $\eta_m$ is the efficiency of the electric motor and $\eta_g$ is the efficiency of the transmission.

If we compare different kinds of aerators, we must use the effective power:

$$P = P_t\, \eta_m\, \eta_g \tag{5.42}$$

considering the measurable $P_t$:

$$P_t = \sqrt{3}\, U \cdot I \cos\varphi/(\eta_m\, \eta_g) \tag{5.43}$$

and the values for e.g. $\eta_m = 0.93$ and $\eta_g = 0.93$, or those obtained from the manufacturer (Zlokarnik 1979).

The efficiency of the aerator follows as:

$$E = \frac{OTR}{P/V} \tag{5.44}$$

The total efficiency, which cannot be used in comparisons because of different $\eta_m$ and $\eta_g$, is (see Eq. 5.37):

$$E_t = \frac{OTR}{P_t/V} = \frac{K_L a\,(c^* - c')}{P_t/V} \tag{5.45}$$

$E_t$ provides information about the total energy needed for the aeration of real wastewater with a given system at the effective conditions.

If we wish to compare this system with others with different temperatures and kinds of wastewater, we must use the standardized oxygen transfer rate $OTR_{20}$ = SOTR (see Eq. 5.38) and the power P without considering the energy loss from the motor and the transmission:

$$E_n = \frac{OTR_{20,0}}{P/V} = \frac{SOTR}{P/V} \tag{5.46}$$

and we have to measure in clean water.

Some results for OTR, P/V and E are presented in Fig. 5.7 (Zlokarnik 1979).

In spite of the scattering of the measured data, it can be concluded from Fig. 5.7 that for specific powers P/V = 15 kW $m^{-3}$ and a SOTR = 45 kg $O_2$ $(m^3\,h)^{-1}$ an efficiency of $E \approx 3$ kg $O_2$ $(kWh)^{-1}$ may be attained. However, the total electrical power

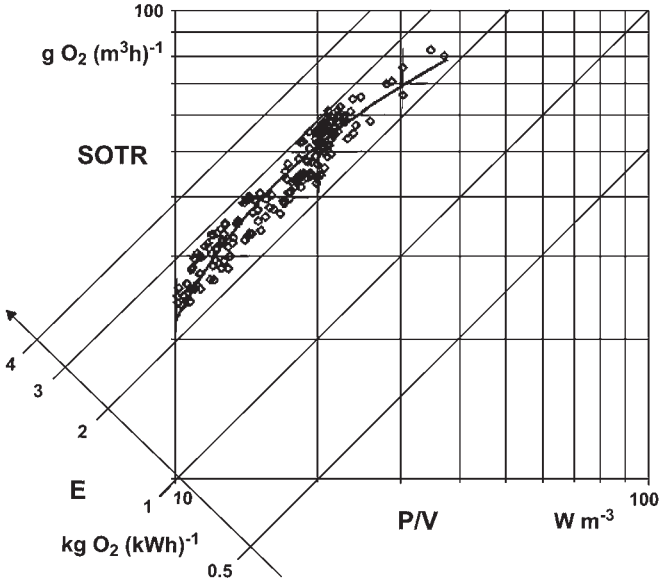


**Fig. 5.7** Standardized oxygen transfer rate, power consumption and efficiency of a Simplex aerator (Schuchardt 2005, data from Zlokarnic 1979).

$P_t$ which must be supplied is higher by the factor $1/\eta_m\ \eta_g = 1.16$, resulting in a lower efficiency of at most:

$$E_t = 2.6 \text{ kg } O_2 \text{ (kWh)}^{-1}$$

In reality $c' = 1–4$ mg $L^{-1}$ and $E_t$ is 10 to 40% lower for e.g. 15 °C water temperature (Eq. 5.45 and Table 5.1). We must not forget that these measurements were carried out in a very small test unit of only 100 L. It is not permissible to transfer these results to a larger tank with a larger aerator without further intermediate studies.

The question should be: can we use these results for a large-scale plant with the same type of aerator if we take the theory of similarity into account?

We will return to this question in Section 5.5.

## 5.4.2 Deep Tank Aeration

### 5.4.2.1 Preliminary Remarks

The aerators mostly used in deep tanks are tubes or plates made of porous ceramics or synthetic materials. We refer to these reactors as deep tanks if the water depth is greater than H = 6 m. Existing tanks frequently have a depth of 4–6 m, but already 6 years ago activated sludge reactors with H = 8–12 m were planned, constructed and commissioned (Pöpel et al. 1998). Reactors with L = 15–25 m have been built for the treatment of industrial effluents (Turmbiologie, Bio-Hochreaktor, deep-shaft reactor). Although most reactors are dug into the ground, some have been built above ground; we speak of "deep tanks" in both cases and use L to indicate the water depth (Turmbiologie, Bayer 1991; Bio-Hochreaktor, Leistner et al. 1979; deep-shaft reactor, Lock 1982).

Let us study mass transfer in deep tanks only in such systems which are approximately characterized by *completely mixed water* and *completely unmixed oxygen* in the rising air bubbles (plug flow). Reactors with L>12 m may be excluded, because nearly complete mixing of the water is not to be expected.

Mass transfer in bubble columns is a complicated process:

1. Oxygen concentration inside the rising bubbles decreases, resulting in a high $\Delta c'$ at the beginning and a lower $\Delta c'$ at the end before the bubbles reach the water surface.
2. The pressure caused by the water column decreases with decreasing depth, which has an effect on both:
   (a) the gas concentration of oxygen and inert components inside the bubble and
   (b) the bubble diameter as well as the velocity of the rising bubble, consequently the specific overall mass transfer coefficient $K_La$.

3. As the result of the mass transfer of oxygen into the water and the mass transfer of $CO_2$ into the bubbles, the molar fraction of $O_2$ changes in a complicated way and the concentration difference between dissolved and gaseous $O_2$ is influenced.

Let us discuss these influences on mass transfer separately.

#### 5.4.2.2 **The Simple Plug Flow Model**

The situation is described in Fig. 5.8: all bubbles rise with the same velocity $\bar{w}$, which is not easy to measure. Therefore, the average void velocity is used:

$$\bar{w} = \frac{Q_G}{A_R} \tag{5.47}$$

with $A_R$ as the cross-sectional area of the reactor (bubble column). We can balance the gaseous oxygen in the total volume of the bubble column; and it is not necessary to determine the total gas volume, which would be nearly impossible in large open tanks.

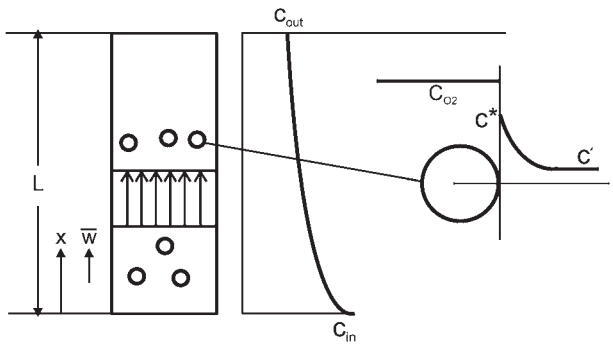


**Fig. 5.8** Upward plug flow of water and flowing bubbles with corresponding diameters.

This steady-state experiment can be carried out:

- with clean water and $Na_2SO_3$, resulting in an oxygen-free liquid system,
- with real wastewater with or without activated sludge.

Let us discuss the first case. For the steady-state oxygen gas balance, we write:

$$0 = -\bar{w}\frac{dc}{dx} - K_L a\, c^* \tag{5.48}$$

and considering Henry's law:

$$c = H\, c^* \tag{5.6}$$

as well as the boundary condition:

$$x = 0 \quad c = c_{in}$$

the result for the concentration profile is:

$$\ln \frac{c}{c_{in}} = -\frac{K_L a}{H\,\overline{w}}\,x \tag{5.49}$$

Frequently, a mean $O_2$ concentration of the bubbles $\overline{c}$ is calculated using:

$$\overline{c} = \int_{c_{in}}^{c_{out}} \ln \frac{c}{c_{in}}\,dc = \frac{c_{in} - c_{out}}{\ln \dfrac{c_{in}}{c_{out}}} \tag{5.50}$$

which is introduced into the integral balance:

$$Q_G\,(c_{in} - c_{out}) = K_L a\,c^*\,V = K_L a\,\frac{\overline{c}}{H}\,V \tag{5.51}$$

Instead of Eq. (5.50), we need to write for the case of a finite dissolved oxygen concentration ($c' \neq 0$):

$$Q_G\,(c_{in} - c_{out}) = K_L a \cdot \left(\frac{\overline{c}}{H} - c'\right) V \tag{5.52}$$

$$\text{with} \quad \overline{c} = \frac{c_{in} - c_{out}}{\ln \dfrac{c_{in} - c}{c_{out} - c}} \tag{5.53}$$

Equations (5.51) and (5.52) are approximations for two reasons:

- A totally mixed liquid system cannot be passed through by gas bubbles flowing with the same velocity and exhibit a detectable decrease in the oxygen concentration.
- A plug-style flow of bubbles cannot be realized precisely when using a swarm of bubbles.

In wastewater technology, this plug flow model is used only seldom. Instead of an exponential decrease in oxygen concentration inside the bubbles, a linear decrease is considered with an arithmetic mean value:

$$\overline{c}_{arith} = \frac{c_{in} + c_{out}}{2}$$

which is a very rough approximation for larger, actual differences $(c_{in} - c_{out})/c_{in}$ (Zlokarnik 1979). Now, the oxygen transfer rate (OTR) can be calculated by using either:

$$OTR = K_L a\,\overline{c}/H \tag{5.54a}$$

or:

$$OTE = K_L a\,\overline{c}_{arith}/H \tag{5.54b}$$

A value of further interest is the oxygen transfer efficiency (OTE):

$$OTE = \frac{c_{in} - c_{out}}{c_{in}} \tag{5.55}$$

Using Eq. (5.55), OTE can be obtained simply. We will now describe the mass transfer in more detail.

#### 5.4.2.3 Proposed Model of the American Society of Civil Engineers

In this advanced kind of evaluation we should consider that the molar fraction of oxygen and the air flow rate $Q_G$ will change as a result of both the consumption of $O_2$ and the uptake of $CO_2$ as well as the change of inert gases. The OTE can be written, while introducing the air flow rate $Q_G$ into Eq. (5.55):

$$OTE = \frac{Q_{G,in}\, c_{in} - Q_{G,out}\, c_{out}}{Q_{G,in}\, c_{in}} \tag{5.56}$$

with:

$$c_{in} = c_{O_2,in} = y_{O_2,in} \cdot \rho_{O_2} \tag{5.57}$$

and

$$c_{out} = c_{O_2,out} = y_{O_2,out}\, \rho_{O_2} \tag{5.58}$$

the $O_2$ concentration in the air flowing in and out of the reactor, Eq. (5.56) gives:

$$OTE = 1 - \frac{Q_{G,out}\, \rho_{O_2}\, y_{O_2,out}}{Q_{G,in}\, \rho_{O_2}\, y_{O_2,in}} \tag{5.59}$$

with the molar fraction:

$$y_{O_2,in} = \frac{N_{O_2,in}}{N_{O_2,in} + N_{CO_2,in} + \sum_{i=1}^{n} N_{inert,in}} \tag{5.60}$$

where $N_{O_2}$ is the number of moles of $O_2$, $N_{CO2}$ is the number of moles of $CO_2$ and $N_{inert}$ is the number of moles of inert components i.

A first approximation is obtained for neglecting the change in the flow rate $Q_G$ ($Q_{G,in} = Q_{G,out}$) respectively:

$$OTE = \frac{y_{O_2,in} - y_{O_2,out}}{y_{O_2,in}} \tag{5.61}$$

If we want to achieve greater precision, we must consider that the air flow rate $Q_G$ changes during the rise of the bubbles. This change is caused by:

- the decrease in oxygen,
- the increase in carbon dioxide,
- the increase in water vapor and all other inert components inside the air bubble.

In the following model, we assume that the water vapor and the concentration of all other inert components do not change. But there is a further problem: it is seldom possible to measure the flow rate of the influent air. Therefore, the air flow rate is replaced by the nitrogen mass flow rate $Q_{N2,in}\,\rho_{N2}$, which must be corrected with Eq. (5.62) (Redmon et al. 1983):

$$Q_{G,in}\,\rho_{O_2}\,y_{O_2,in} = Q_{N_2,in}\,\rho_{N_2}\,\frac{M_{O_2}}{M_{N_2}}\,\frac{N_{O_2}}{N_{N_2}} \tag{5.62}$$

where $Q_{N_2,in}\,\rho_{N_2}$ is the mass flow rate of influent nitrogen (g $N_2$ $h^{-1}$), $\frac{M_{O_2}}{M_{N_2}}$ is the ratio of the molar masses oxygen/nitrogen in influent air ($\frac{gO_2\ mol\ N_2}{gN_2\ mol\ O_2}$) and $\frac{N_{O_2}}{N_{N_2}}$ is the ratio of the moles oxygen/nitrogen in the influent air ($\frac{mol\ O_2}{mol\ N_2}$).

Introducing Eq. (5.62), reflecting whether "in" or "out" into Eq. (5.59) gives:

$$OTE = 1 - \frac{Q_{N_2,out}\,\rho_{N_2}\,\frac{M_{O_2}}{M_{N_2}}\left(\frac{N_{O_2}}{N_{N_2}}\right)_{out}}{Q_{N_2,in}\,\rho_{N_2}\,\frac{M_{O_2}}{M_{N_2}}\left(\frac{N_{O_2}}{N_{N_2}}\right)_{in}} \tag{5.63}$$

or with $Q_{N_2,out} = Q_{N_2,in}$ gives:

$$OTE = 1 - \frac{\left(\frac{N_{O_2}}{N_{N_2}}\right)_{out}}{\left(\frac{N_{O_2}}{N_{N_2}}\right)_{in}} \tag{5.64}$$

with:

$$\left(\frac{N_{O_2}}{N_{N_2}}\right)_{in} = \frac{(N_{O_2}/(N_{O_2} + N_{N_2} + N_{CO_2}))_{in}}{(N_{N_2}/(N_{O_2} + N_{N_2} + N_{CO_2}))_{in}} = \frac{y_{O_2,in}}{y_{N_2,in}} \tag{5.65}$$

$$\left(\frac{N_{O_2}}{N_{N_2}}\right)_{out} = \frac{(N_{O_2}/(N_{O_2} + N_{N_2} + N_{CO_2}))_{out}}{(N_{N_2}/(N_{O_2} + N_{N_2} + N_{CO_2}))_{out}} = \frac{y_{O_2,out}}{y_{N_2,out}} \tag{5.66}$$

as well as:

$$y_{O_2} + y_{N_2} + y_{CO_2} = 1$$

or:

$$y_{N_2,in} = 1 - y_{O_2,in} - y_{CO_2,in}$$

and:

$$y_{N_2,out} = 1 - y_{O_2,out} - y_{CO_2,out}$$

Equation (5.64) can be transformed into:

$$OTE = 1 - \frac{y_{O_2,out}\,(1 - y_{O_2,in} - y_{CO_2,in})}{y_{O_2,in}\,(1 - y_{O_2,out} - y_{CO_2,out})} \tag{5.67}$$

If $CO_2$ is removed before the $O_2$ concentration is measured (e.g. in NaOH), from Eq. (5.67) we obtain:

$$OTE = 1 - \frac{y_{O_2,out}\,(1 - y_{O_2,in})}{y_{O_2,in}\,(1 - y_{O_2,out})} \tag{5.68}$$

Finally, the oxygen transfer rate can be calculated based on Eq. (5.37) by considering the changing gas flow rate and by using:

$$OTR = \frac{Q_{N_2,in}\,\rho_{N_2}\,\frac{M_{O_2}}{M_{N_2}}\left(\frac{N_{O_2}}{N_{N_2}}\right)_{in} - Q_{N_2,out}\,\rho_{N_2}\,\frac{M_{O_2}}{M_{N_2}}\left(\frac{N_{O_2}}{N_{N_2,out}}\right)_{out}}{V} \tag{5.69}$$

and with Eqs. (5.65) and (5.66):

$$OTR = \frac{Q_{N_2,in}\,\rho_{N_2}\,M_{O_2}/M_{N_2}}{V}\left[\frac{y_{O_2,in}}{y_{N_2,in}} - \frac{y_{O_2,out}}{y_{N_2,out}}\right] \tag{5.70}$$

$$OTR = \frac{Q_{N_2,in}\,\rho_{N_2}\,M_{O_2}/M_{N_2}}{V}\left[\frac{y_{O_2,in}}{1 - y_{O_2,in} - y_{CO_2,in}} - \frac{y_{O_2,out}}{1 - y_{O_2,out} - y_{CO_2,in}}\right] \tag{5.71}$$

If $CO_2$ is removed, we obtain:

$$OTR = \frac{Q_{N_2,in}\,\rho_{N_2}\,M_{O_2}/M_{N_2}}{V}\left[\frac{y_{O_2,in}\,(1 - y_{O_2,out}) - y_{O_2,out}\,(1 - y_{O_2,in})}{(1 - y_{O_2,in})\,(1 - y_{O_2,out})}\right] \tag{5.72}$$

With Eq. (5.54a) or Eq. (5.54b), the overall mass transfer coefficient $K_L a$ can be calculated from OTR.

#### 5.4.2.4 Further Models

Zlokarnik (1980) discussed how the increase in the hydrostatic pressure raises the oxygen concentration inside the air bubbles and the equilibrium concentration at the air/water interface, as well as the effects of temperature, which may change in tall bubble columns.

An estimate of the influences of pressure on OTE and OTR as well as the change in bubble surface, mass transfer coefficient and saturation concentration was presented by Pöpel et al. (1998). These considerations were complemented by measurements in a pilot plant with a water depth of up to 12.5 m.

#### 5.4.2.5 Oxygen Transfer Rate

Until now, all systems discussed here have been either completely mixed (Sections 5.3.1.1 to 5.3.1.3, 5.3.2 and 5.4.2.3) or plug flow systems (Section 5.3.1.4). There-

fore, models could be used and $k_L a$ or $K_L a$ could be applied. However, in large-scale tanks, the description of oxygen transfer using the concept of Eq. (5.8) is frequently not allowed because of the different locally structured air/water flows. This is demonstrated by Fig. 5.9 (Mueller et al. 2002).

Porous ceramic tubes are installed in such a way as to promote a secondary water circulation which sucks down a portion of the bubbles rising in the vicinity. But even for a system with a locally constant configuration of diffusers (Fig. 5.10), the oxygen transfer rate may change considerably over time because of the change in load over the course of 24 h and also with location, especially in longitudinal tanks (Schuchardt et al. 2002). We will come back to this point in Section 5.4.2.7.

$K_L a$ can be calculated from Eq. (5.54b):

$$OTR = K_L a \frac{c_{in} + c_{out}}{2\,H} \tag{5.73}$$

and, after introducing $c = Hc^*$, we obtain:

$$OTR = K_L a \frac{c^*_{in} + c^*_{out}}{2} \tag{5.74}$$

OTE was developed in Section 5.4.2.3, resulting in Eq. (5.68); and OTR can be obtained by using Eq. (5.72).

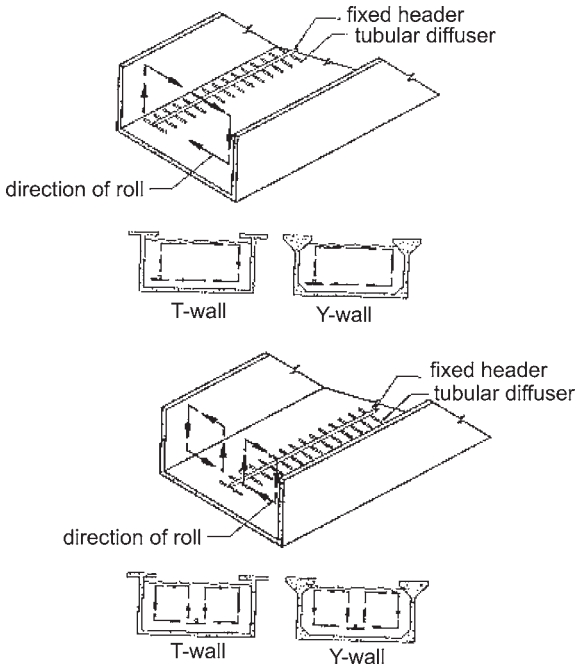


**Fig. 5.9** Configuration of deep tank aeration system (Mueller et al. 2002).

**Fig. 5.10** Porous ceramic tubes in deep tank aeration, second zone of a longitudinal tank at WWTP Waßmannsdorf, near Berlin (Schuchardt et al. 2002).

Considering the influence of temperature on c* at point x by introducing:

$$c^* = c^*_{20,x}\,\theta^{(20-T)} \tag{5.75}$$

with $\theta = 1.024$ (Stenstrom and Gilbert 1981) and the influence of the hydrostatic pressure on $c^*$ at point $x = h$ (h = height of the water column):

$$c^*_{20,x} = c^*_{20,x=L} = \left(1 + \frac{1}{2}\,\frac{x}{10.32}\right) \tag{5.76}$$

we write the standardized oxygen transfer rate for deep tanks:[2)]

$$SOTR = K_L a\, c^*_{20,x=L}\,\theta^{(20-T)}\left(1 + \frac{1}{2}\,\frac{x}{10.32}\right) \tag{5.77}$$

With Eq. (5.77), the influence of aeration, height of the water column and temperature can be considered.

This SOTR value is valid for measurements in clean water. In wastewater, especially with activated sludge, a lower SOTR value is to be expected, resulting in (Stenstrom and Redman 1996):

$$\alpha\,(SOTR) = \frac{SOTR_w}{SOTR} < 1 \tag{5.78}$$

---

[2)] 10.32 m is the height of a water column causing a pressure of 1 bar.
$c^*_{20,x} = p/H_P$ means that $c^*_{20}$ increases linearly with x.

α-Values are dependent upon diffuser configuration, air flow rate, wastewater composition, local position x and temperature T.

We must keep the following simplifications in mind:

- Instead of using the logarithmic concentration difference (5.54a), which followed from the plug flow model, the approximation $\Delta c' = c_T^* - c'$ was applied.
- $K_La$ was assumed to be constant, however there are several influences on both a and $K_L$ (lower pressure, diffusing $CO_2$ into the bubble, coalescence of bubbles and increasing velocity).

#### 5.4.2.6 Power Consumption and Efficiency

We have to distinguish two levels of power consumption:

- The power consumption of the blower P producing compressed air.
- The total power demand $P_T = P/(\eta_b \cdot \eta_m \cdot \eta_g)$, with $\eta_b = 0.8$ for the blower (newer equipment), $\eta_m = 0.95$ for the motor and $\eta_g = 0.95$ for the transmission (Mueller et al. 2002).

The power demanded for compression is:

$$P = \frac{Q_G \rho RT}{k} \left[ \left( \frac{p_{in}}{p_{out}} \right)^k - 1 \right] \text{J h}^{-1} \tag{5.79}$$

where $k = 0.2857$ for dry air, $p_{in}$ is the pressure before compression, $p_{out}$ is the pressure after compression, T is the temperature (K), $R = 8.314$ J (mol K)$^{-1}$ is the gas constant and $Q_G\rho$ is the mass flow rate of air (kg h$^{-1}$).

Considering:

$$1 \frac{\text{J}}{\text{h}} = \frac{1}{3600 \text{ s}} \frac{\text{J}}{\text{s}} = \frac{1}{3600} \text{W} = \frac{10^{-6}}{3.6} \text{kW} = 0.278 \cdot 10^{-6} \text{ kW}$$

we obtain:

$$P = 0.278 \cdot 10^{-6} \frac{Q_G \rho RT}{k} \left[ \left( \frac{p_{in}}{p_{out}} \right)^k - 1 \right] \text{kW} \tag{5.80}$$

Now we calculate the efficiencies using Eqs. (5.77) and (5.80):

$$E = \frac{SOTR}{P/V} \text{ kg } O_2 \text{ (kWh)}^{-1} \tag{5.81}$$

and for the total efficiency:

$$E_t = \frac{SOTR \cdot \eta_b \eta_m \eta_g}{P/V} \text{ kg } O_2 \text{ (kWh)}^{-1} \tag{5.82}$$

#### 5.4.2.7 Monitoring of Deep Tanks

If we want to measure OTE, SOTR and E for a deep tank in operation, we must use the off-gas analysis method (Fig. 5.11).

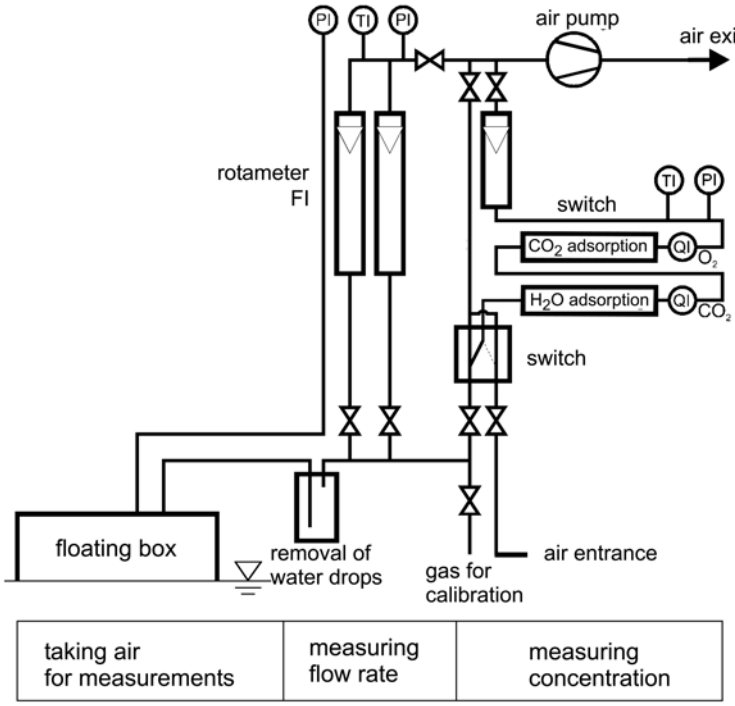


**Fig. 5.11** Instrument for off-gas analysis, apparatus for manual operation (Schuchardt et al. 2002).

An off-gas apparatus consists of an off-gas hood with instruments for the measurement of flow rates and oxygen concentration. The floating hood may have a cross-sectional area of 2–4 $m^2$ (Schuchardt 2005). Air is drawn off by a fan passing first through a rotameter for flow rate measurement of the off-gas. A side-stream is passed through $H_2O$ and $CO_2$ adsorbers and is then analyzed to measure $O_2$ consumption.

The results were obtained from measurements at the aerobic activated sludge basin of the WWTP Waßmannsdorf, near Berlin, equipped with ceramic tubes (see Fig. 5.12). For low and high flow rates of compressed air and specific power demands (P/V), the efficiency E decreases only slightly. Maximum efficiencies ($E = 2.5–2.7$ kg $O_2$ $(kWh)^{-1}$) are obtained only in a narrow band of $11 < P/V < 20$ ($W\ m^{-3}$) with values of $31 < SOTR < 52$ (g $O_2$ $(m^3\ h)^{-1}$) (Schuchardt et al. 2002; Schuchardt 2005). For lower and higher values of P/V, the efficiency decreases slightly, down to $E = 2.1–2.2$ kg $O_2$ $(kWh)^{-1}$. With optimized aeration equipment and optimized automatic process control, great amounts of energy can be saved.

If we compare these results with those presented in Fig. 5.7 for a small Simcar aerator (d = 40 cm) we establish a quite good correspondence. We should not misinterpret these relative small derivatives: We need more studies for the optimization of aeration systems of large WWTP's in a time of arrising costs for energy!

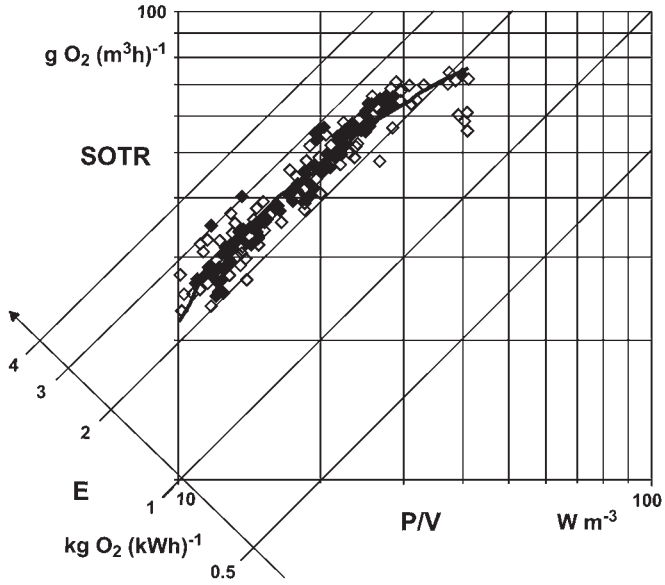


**Fig. 5.12** Standardized oxygen transfer rate, power consumption, and efficiency of a deep tank aeration system equiped with porous aeration tubes of WWTP Waßmannsdorf (see Fig. 5.10) (Schuchardt 2005).

## 5.5 Dimensional Analysis and Transfer of Models

### 5.5.1 Introduction

There are some important questions to answer if we want to study an aeration process in a laboratory-scale or pilot-scale plant and apply the results to large-scale aeration and activated sludge systems. Let us discuss this problem for the example of a surface aerator constructed and processed as a turbine with a vertical shaft. We assume that it is possible to measure the oxygen transfer rate and the power consumption for clean water or wastewater with activated sludge. The volume, the type of tank and the mean residence time (aeration time) are given. Some important questions are:

- The diameter of the aerator in the laboratory-scale plant was 0.25 m, for example. What may be the best diameter for the large-scale plant?
- The range of speeds in the laboratory-scale experiments was 10–100 $min^{-1}$. What may be the suitable range of speeds for the large-scale aerator?
- In the laboratory-scale experiments, an efficiency of nearly E = 3 kg $O_2$ $(kWh)^{-1}$ was obtained. Under what conditions can we expect a relatively high efficiency; and is it possible to find operating conditions yielding E = 3 kg $O_2$ $(kWh)^{-1}$?

- Is it more economical to install two or four aerators instead of one? What is the optimal diameter, speed and depth of submersion?

These questions are not easy to answer. We need two methods, the method of dimensional analysis and the method to transfer models. Both will be explained for a simple case: the stirred non-aerated tank and the stirred aerated tank without suspended solids.

### 5.5.2 Power Consumption of a Stirred, Non-aerated Tank – A Simple Example

The first step is to find all parameters which are relevant to the question (Fig. 5.13). Will this parameter influence the power consumption in the stirred tank if changed?

Looking at Fig. 5.13, we will first mention all the geometric parameters:

D = diameter of the tank
d = diameter of the stirrer
H = height of the water
h = distance of the stirrer from the bottom

The stirrer may be equipped with three plates with a given width and distance from the wall. Usually, the stirrer diameter d is selected as the reference and we can define three dimensionless geometric numbers:

$$\frac{D}{d}, \frac{H}{d}, \frac{h}{d}$$

Tanks of different sizes are considered to be geometrically similar if these values are constant for all tanks.

Furthermore, we will consider a group of tanks with different stirrers of diameter d. Let us now follow the method of Zlokarnik (1999).

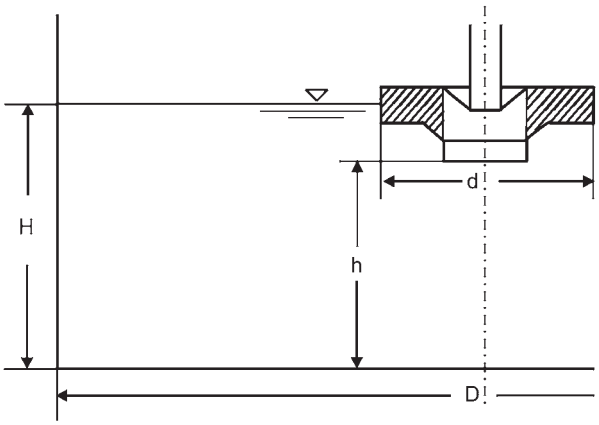


**Fig. 5.13** Cylindrical tank with Simplex rotor, Type A, showing main dimensions.

The next step is to look for parameters which will influence the power input P. These parameters can be divided into:

- Geometric parameters: diameter of the stirrer d.
- Material parameters of the water: density ρ, kinematic viscosity ν.
- Process parameters: stirrer speed n.

Therefore, the list of relevant variables is: {P; d; ρ; ν; n}.

The next step is to formulate the dimensional matrix. Before doing this, we have to decide which parameters should occur only in one dimensionless characteristic number. It is most effective to select P and ν. After making this decision, the dimensional matrix can be formed (Table 5.3), with each number in the matrix representing the power of the unit dimension (length, time, mass) occurring in the variable.

This matrix must be transformed to obtain a unit matrix in the first 3×3 matrix, that is, with a diagonal of ones. To obtain a 0 instead of –3 in the first column (ρ) and a 1 instead of –1 in the third column (n), the Gaussian method is applied by performing linear combinations of the rows. In this manner –3 times the elements of the first row are added to the second row. The exponents listed in the last row need only be multiplied by –1 to obtain a 1 in the proper location (Table 5.4).

The numbers in the remaining matrix to the right of the unit matrix below P and ν give us the exponents of the first three variables which yield dimensionless num-

**Table 5.3** Dimensional analysis of a stirrer, matrix of unit dimensions for relevant parameters with respect to selected P and ν (Zlokarnik 1999).

| | **ρ** | **d** | **n** | **P**[1)] | **ν** |
|---|---|---|---|---|---|
| Mass *M* | 1 | 0 | 0 | 1 | 0 |
| Length *L* | –3 | 1 | 0 | 2 | 2 |
| Time *T* | 0 | 0 | –1 | –3 | –1 |
| | Core matrix | | | Rest matrix | |

[1)] Note: $P = \frac{A}{t} = \frac{Kl}{t}$; $K\,[MLT^{-2}]$; $P\,[ML^2\,T^{-3}]$

A = work, K = force.

**Table 5.4** Transformation of the core matrix into a unit matrix, to obtain two dimensionless numbers with respect to selected P and ν (Zlokarnik 1999).

| | **ρ** | **d** | **n** | **P**[1)] | **ν** |
|---|---|---|---|---|---|
| M | 1 | 0 | 0 | 1 | 0 |
| 3 M + L | 0 | 1 | 0 | 5 | 2 |
| –T | 0 | 0 | 1 | 3 | 1 |
| | Unit matrix | | | Rest matrix | |

bers. The first dimensionless number $\pi_1$ formed with P is known as the Newton number. The second, formed with v, is the Reynold's number:

$$\pi_1 = \frac{P}{\rho^1 n^3 d^5} \equiv \text{Ne (Newton number)} \tag{5.83}$$

and:

$$\pi_2 = \frac{v}{\rho^0 n^1 d^2} = \frac{v}{nd^2} = \text{Re}^{-1} \text{ (Reynolds number)} \tag{5.84}$$

There must be a function of the five parameters for which:

$$f(\text{Ne}, \text{Re}) = 0 \tag{5.85}$$

Another way to find Eq. (5.85) starting from the list of the five variables

$$f(P, \rho, n, d, v) = 0$$

is described below.

Looking for a function, with a reduced number of dimensionless parameter, we have at first to write:

$$\pi_i\ (P^\alpha, \rho^\beta, n^\gamma, d^\delta, v^\varepsilon)$$

and working in the MLT-system (mass, length, time) for the needed dimensions, we introduce P $[ML^2T^{-3}]$, $\rho$ $[M\,L^{-3}]$, n $[T^{-1}]$, d [L], v $[L^2\,T^{-1}]$:

$$\pi_i\ ((ML^2T^{-3})^\alpha\ (ML^{-3})^\beta\ (T^{-1})^\gamma\ (L)^\delta\ (L^2\,T^{-1})^\varepsilon)$$

As can be demonstrated now, this problem can be described by using only two dimensionless numbers resulting from the fact, that we use five parameter with dimensions and three units (5 – 3 = 2). If we want to obtein two dimensionless numbers each with P and v, the exponents of $\rho$, n and d have to be replaced by the exponents of P and v. Writing

$$\pi_i\ ((ML^2T^{-3})^\alpha\ (ML^{-3})^\beta\ (T^{-1})^\gamma\ (L)^\delta\ (L^2\,T^{-1})^\varepsilon)$$

we obtain three equations:

$$\begin{aligned} &\text{M:}\quad \alpha + \beta = 0 \\ &\text{L:}\quad 2\alpha - 3\beta + \delta + 2\varepsilon = 0 \\ &\text{T:}\quad 3\alpha - \gamma - \varepsilon = 0 \end{aligned}$$

and the solutions

$$\begin{aligned} \beta &= -\alpha \\ \gamma &= -3\alpha - \varepsilon \\ \delta &= -5\alpha - 2\varepsilon \end{aligned}$$

which have to be introduced into $\pi_i\ (P^\alpha, \rho^\beta, n^\gamma, d^\delta, v^\varepsilon)$.

$\pi_i$ is only dimensionless, if

$$\left(\frac{P}{\rho\, n^3\, d^5}\right)^\alpha = \text{const} \quad \text{and} \quad \left(\frac{v}{n\, d^2}\right)^\varepsilon = \text{const}$$

giving the numbers Ne and Re (see Eqs. 5.83 and 5.84).

### 5.5.3 Description of Oxygen Transfer, Power Consumption and Efficiency by Surface Aerators Using Dimensionless Numbers

With the results from above, we return to the experimental results during surface aeration with an aeration turbine (see Fig. 5.6). Oxygen transfer rate OTR, power consumption P/V and efficiency E were measured in clean water and plotted in Fig. 5.7. Now we will describe these results for a series of aerators (Simplex, Type A), which are characterized by geometric similarity.

However, the problems to solve are more difficult than those in Section 5.5.2:

- The stirred tank is aerated and buoyancy forces must be considered. Dimensional analysis now yields a set of three dimensionless numbers:

$$f\,(Ne, Re, Fr) = 0 \tag{5.86}$$

with Froude number:

$$Fr \equiv \frac{n^2 d}{g} \tag{5.87}$$

- A further number must be developed which gives information about the rate of oxygen transfer. The relevance list is:

$$K_L a\, V = f\,(d, \rho, \nu, \sigma, D, n, g) \tag{5.88}$$

Using the method described above, we obtain:

$$f\,(Y, Fr, Re, Sc, \sigma^*) = 0 \tag{5.89}$$

with:

$$\frac{K_L a\, V}{d^3}\left(\frac{\nu}{g^2}\right)^{1/3} \equiv Y \text{ (oxygen transfer number)} \tag{5.90}$$

$$\frac{\nu}{D} \equiv Sc \text{ (Schmidt number)} \tag{5.91}$$

$$\frac{\sigma}{\rho\,(\nu^4\, g)^{1/3}} \equiv \sigma^* \text{ (dimensionless surface tension)} \tag{5.92}$$

Let us look at the system air/water and we can conclude that all material coefficients are constant, resulting in:

$$Sc = \text{const}$$
$$\sigma^* = \text{const}$$

Therefore, the set of dimensionless numbers for air/water is:

$$f\,(Y, Fr, Re) = 0 \tag{5.93}$$

If we do not consider aerators with small diameter d and low rotation speed n, $Re \geq 10^4$ is valid (turbulent region of the flow) and Re does not influence Ne and Y remarkably. We can conclude that it must be possible to describe the results using (Zlokarnik 1979, 1980):

$$Ne = f(Fr) \tag{5.94}$$

and:

$$Y = f(Fr) \tag{5.95}$$

Both results obtained by experiments can be represented as straight lines if we use double-logarithmic plots (Figs. 5.14 and 5.15). But the author chose to use a larger region in Fr numbers ($0.02 < Fr < 0.8$) for power measurement (Fig. 5.13) compared with oxygen transfer measurements ($0.08 < Fr < 0.35$; Fig. 5.14).

The straight lines in both figures are given by:

$$Ne = 0.28\ Fr^{-0.78} \tag{5.96}$$

and:

$$Y = 1.25 \cdot 10^{-3}\ Fr^{0.89} \tag{5.97}$$

From these equations a dimensionless efficiency can be defined as:

$$E^* = \frac{Y}{Ne} \tag{5.98}$$

and with Eqs. (5.96) and (5.97):

$$E^* = 4.46 \cdot 10^{-3}\ Fr^{1.67} \tag{5.99}$$

can be used together with Eq. (5.96) and Eq. (5.97) for scale-up calculations, if the dimensionless geometric numbers are (nearly) constant.

### 5.5.4
### Application of Dimensionless Numbers for Surface Aeration

From a fundamental point of view, it is not permissible to exceed the range of experimentally changed parameters considerably, if the results are to be reliable. If we wish to extract information about $K_La$ from Fig. 5.14 for Simplex aerators (Fig. 5.6) of another size, all dimensionless geometric numbers must be constant and we must remain within a range of Fr numbers between $0.08 < Fr < 0.35$.

Using $Fr_{max} = 0.35$ and assuming $n = 1\ s^{-1}$, we can calculate:

$$Fr_{max} = \frac{n^2 d}{g}$$

$$d = \frac{Fr_{max}\, g}{n^2} = \frac{0.35 \cdot 9.81}{l^2} = 3.43\ m$$

Although only a small range of Fr numbers was investigated, a relative high range of diameters d is included. However, is it possible to realize the required $K_La$? We will return to this question in Problem 5.

For practical applications, it is necessary to change geometric numbers and to study their influences. Frequently, the influence of relative small variations (e.g. $d/D = 4.0 \rightarrow d/D = 3.5$) is low and the freedom to move is given.

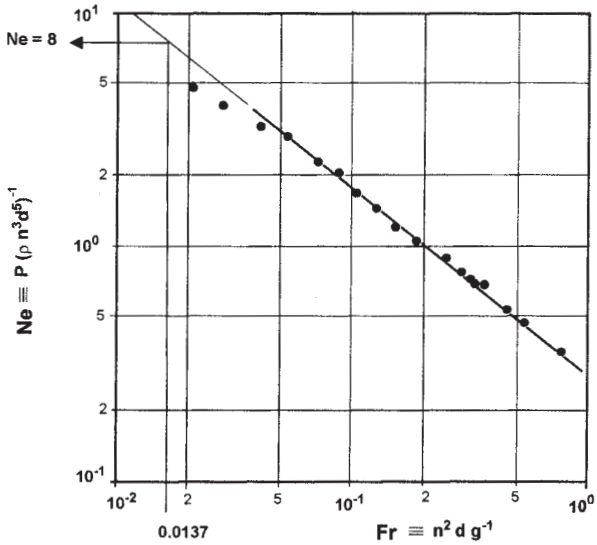


**Fig. 5.14** Power correlation Ne = f (Fr) for surface aerator Symplex Type A, Pushing, H/d = 1.0, D/d = 4.37 (Zlokarnik 1975).

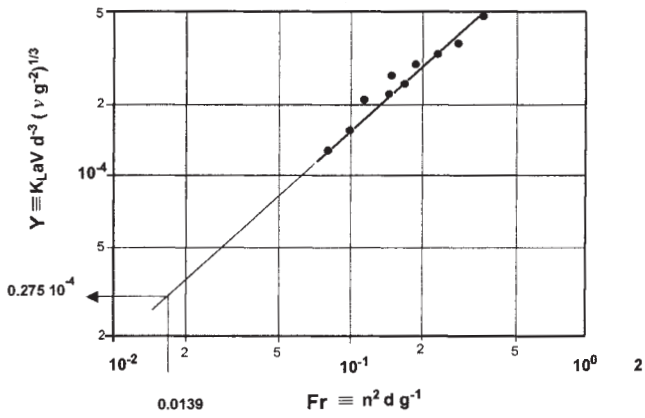


**Fig. 5.15** Sorption correlation Y = f (Fr) for surface Aerator Simplex, Type A, Pushing, H/d = 1.0, D/d = 4.37 (Zlokarnik 1979).

It is very important to prove these methods experimentally with two or three aerators of the same type but different diameters, which differ by a factor of two or three. The same water should be used and all geometric numbers must be the same in all these experiments if the influence of relative small changes has not been studied before. Unfortunately, the expenditure for such experiments is high and such studies are very seldom.

**PROBLEM**

The oxygen transfer rate OTR and power demand P/V of a Simplex aerator (-Type A) with a diameter of d = 0.206 m (Fig. 5.6) was measured for different speeds. The efficiency E was calculated and the results plotted in Fig. 5.7. Following this, the dimensionless numbers Ne, Fr and Y were calculated using Eqs. (5.83), (5.87) and (5.90). First, Ne was plotted versus Fr in Fig. 5.14. In addition, Fig. 5.15 shows the plot of Y as a function of Fr.
A large aerobic tank with a volume of V = 250 $m^3$ and with only one Simplex aerator is to be constructed with an oxygen transfer rate of OTR = 100 g $O_2$ $(m^3\ h)^{-1}$. An aerator with a diameter of 2.0 m is available (Zlokarnik 1979).

1. What is the speed n needed for the demanded oxygen supply?
2. What is the efficiency E of the aeration system?

Constant parameters:

$\nu = 10^{-6}\ m^2\ s^{-1}$, $g = 9.81\ m\ s^{-1}$, $c^* = 8\ mg\ L^{-1}$, $c' = 1\ mg\ L^{-1}$

**Solution**

1. Calculation of the required speed n:

(a) $K_L a = ?$
OTR = $K_L a\,(c^* - c')$ from Eq. (5.37):

$$K_L a = \frac{OTR}{(c^* - c')} = \frac{100}{7}\ \frac{g\ O_2\ m^3}{m^3\ h\ g\ O_2} = 14.3\ h^{-1} = 3.97 \cdot 10^{-3}\ s^{-1}$$

(b) $Y = ?$, $Fr = ?$

$$Y = \frac{K_L a\ V}{d^3}\left(\frac{\nu}{g^2}\right)^{1/3} \quad \text{from Eq. (5.90)}$$

$$Y = \frac{1}{d^3}\left[\frac{3.97 \cdot 10^{-3}\ 250\ 10^{-6/3}}{9.81^{2/3}}\right]\frac{m^3\ m^{2/3}\ s^{4/3}}{m^3\ s\ s^{1/3}\ m^{2/3}} \qquad Y = \frac{1}{d^3} \cdot 0.22 \cdot 10^{-3}$$

$$d = 2.0\ m;\ Y = \frac{0.22 \cdot 10^{-3}}{8.0} = 0.0275 \cdot 10^{-3}$$

From Eq. (5.97) it follows that:

$$Fr = \left[\frac{Y}{1.25 \cdot 10^{-3}}\right]^{\frac{1}{0.89}} = 0.0137$$

(c) The speed n follows from:

$$Fr = \frac{d\,n^2}{g}$$

$$n = \left(\frac{Fr\,g}{d}\right)^{1/2} = \left(\frac{0.0137 \cdot 9.81}{2.0}\right)^{1/2} \left(\frac{m}{s^2\,m}\right)^{1/2} = 0.260\ s^{-1}$$

2. Calculation of the efficiency E:

(a) P/V = ?

Fr = 0.0139 gives Ne = 8

From $Ne = \frac{P}{\rho\, d^5\, n^3}$ (5.83)

we obtain the specific power consumption:

$$\frac{P}{V} = \frac{Ne\,\rho\,d^5\,n^3}{V}$$

$$\frac{P}{V} = \frac{8 \cdot 1000 \cdot 2^5 \cdot 0.26^3}{250}\ \frac{kg\,m^5}{m^3\,m^2\,s^3} = 18\ \frac{kg}{m\,s^3} = 18\ \frac{W}{m^3}$$

(b) With the given $OTR_v = 100\ g\ (m^3\ h)^{-1}\ O_2$ the efficiency follows:

$$E = \frac{OTR}{P/V} = \frac{100}{18}\ \frac{g\ O_2\ m^3}{h\ W\ m^3} = 5.5\ \frac{kg\ O_2}{k\ W\ h}$$

The experimental results in Figs. 5.13 and 5.14 are valid for:

H/d = 1 and D/d = 4.37

For d = 2 m, we obtain H = 2 m and D = 8.74 m for a cylindrical tank with:

$$V = \frac{\pi D^2}{4} \cdot H = 120\ m^3$$

In a tank with V = 250 $m^3$, H and/or D must differ from those values.

For D = 12 m, H follows:

$H = 4\,V/\pi D^2 = 2.21$ m

## References


ASCE **1997**, Standard guidelines for in-process oxygen transfer testing, ASCE Standard, American Society of Civil Engineers, New York.

ATV **1997**, Arbeitsblatt M 209, Messung der Sauerstoffzufuhr von Belüftungseinrichtungen in Belebungsanlagen in Reinwasser und in belebtem Schlamm, ATV, Hennef.

Bayer **1991**, Bayer-Turmbiologie-Verfahren zur Abwasserbehandlung, *Druckschrift der Bayer AG* 1991

Bird, R.B.; Stewart, W.E.; Lightfoot, E.N. **1962**, *Transport Phenomena*, John Wiley & Sons, New York.

Chow, V.T.; Eliassan, R.; Linsley, R.K. **1972**, *Wastewater Engineering*, McGraw-Hill, New York.

Danckwerts, P.V. **1951**, Significance of liquid film coefficients in gas absorption, *Ind. Eng. Chem.* 43, 1460–1473.

Danckwerts, P.V. **1970**, *Gas–Liquid Reactions*, McGraw-Hill, New York.

Daniels, F.; Alberty, R.A. **1955**, *Physical Chemistry*, Wiley, New York, p. 650.

Higbie, R. **1935**, The rate of absorption of a pure gas into a still liquid during short periods, *Trans. Am. Inst. Chem. Engrs.* 31, 365–389.

King, C.J. **1964**, The additivity of individual phase resistances in mass transfer operations, *A. I. Ch. E. J.* 10, 671.

Leistner, G.; Müller, G.; Sell, G.; Bauer, A. **1979**, Der Bio-Hochreaktor – eine biologische Abwasserreinigungsanlage in Hochbauweise, *Chem. Ing. Tech.* 51, 288.

Libra, J.A. **1993**, Stripping of organic compounds in an aerated stirred tank reactor, *VDI-Forschungsberichte, Reihe 15, Umwelttechnik* 102, 1993

Lock, J. **1982**, Deep Shaft, *Water/Engineering & Management*, 1982, 57.

Mueller, J. A.; Boyle, W.C.; Pöpel, H.J. **2002**, *Aeration: Principles and Practice*, Water Quality Management Library vol. 11, CRS Press, Boca Raton.

Nyer, E. **1992**, *Groundwater Treatment Technology*, 2nd edn, Van Nostrand, Reinhold, New York.

Pöpel, H.J.; Wagner, M.; Weidmann, F. **1998**, Sauerstoffeintrag und -ertrag in tiefen Belebungsbecken, *gwf Wasser Abwasser* 139, 189–197.

Redmon, D.; Boyle, W.C.; Ewing, L.: Oxygen transfer efficiency measurements in mixed liquor using off-gas techniques, *Journal WPCF 55, 11*, 1338-1347, 1983

Reid, R.C.; Prausnitz, J.M.; Poling, B.E. **1987**, *The Properties of Gases and Liquids*, McGraw Hill, New York.

Schuchardt, A.; Handschag, J.; Sahlmann, Ch.; Libra, J.; Wiesmann, U. **2002**, Vergleich der Leistungsfähigkeit von Keramik- und Membranbelüftern des Klärwerks Waßmannsdorf und Optimierung der Prozessführung, im *Auftrag der Berliner Wasserbetriebe BWB*, Abschlussbericht, Berlin.

Schuchardt, A. **2005**, Bestimmung des dynamischen Sauerstoffeintrags in nitrifizierende Belebtschlammreaktoren einer kommunalen Kläranlage, *VDI-Forschungsberichte, Reihe 3*, 842.

Stenstrom, M.K.; Gilbert, G. **1981**, Effect of alpha, beta, and theta on specification, design, and operation of aeration systems, *Water Research* 15, 643.

Stenstrom, M.K.; Redman, D.T. **1996**, Oxygen transfer performance of fine pore aeration in ASBs – A full scale review, *Int. Environ. Conf. Exhib.* 1996.

Whitman, W.G. **1923**, The two-film theory of gas absorption, *Chem. Met. Eng. 29*, 146–148.

Zlokarnik, M. **1979**, Scale-up of surface aerators for waste water treatment, *Adv. Biochem. Eng.* 11, 158–180.

Zlokarnik, M. **1980**, Eignung und Leistungsfähigkeit von Oberflächenbelüftern für biologische Abwasserreinigungsanlagen, *Korrespondenz Abwasser* 27, 14–21, 194–209.

Zlokarnik, M. **1983**, Ähnlichkeitstheorie in der Verfahrenstechnik, Bayer AG.

Zlokarnik, M. **1999**, *Rührtechnik – Theorie und Praxis*, Springer, Berlin.

# 6
# Aerobic Wastewater Treatment in Activated Sludge Systems

## 6.1
## Introduction

Since the first experiments performed by Arden and Locket (1914; see Section 1.8), many questions have arisen concerning the activated sludge process:

- What is the best type of reactor?
- Which aeration system is most effective?
- What are the real microbial processes which occur during the decrease in organics and the growth of bacteria?
- What parameters influence the rate of these processes?
- How can we determine the right volumes for reactor and settler to reduce the concentration of organics for a given flow rate?
- How can we feasibly optimize the process?
- Is it possible to treat industrial wastewater containing specific synthetic compounds?

In the first 50 years following Arden's and Locket's invention, the technical realization, and particularly research into the fundamentals, were supported only in a few industrialized countries and to a relatively low extent. Only in the past 40 years has biological wastewater treatment been realized to a greater extent. One of the first textbooks having presented fundamentals of the aerobic activated sludge process was written by Metcalf and Eddy 1972. The pollution of our rivers and lakes caused by society's industrialization endangered nature and reduced the quality of drinking water. Only then were the fundamentals of the activated sludge process studied in more detail. The most important aspects are presented in the next sections.

## 6.2
## Kinetic and Reaction Engineering Models With and Without Oxygen Limitation

### 6.2.1
### Batch Reactors

#### 6.2.1.1 With High Initial Concentration of Bacteria

Monod published the first kinetic studies on the limitation of bacterial growth by substrate concentration. For these experiments he used an aerobic batch reactor,

*Fundamentals of Biological Wastewater Treatment*. Udo Wiesmann, In Su Choi, Eva-Maria Dombrowski

ISBN: 978-3-527-31219-1

glucose as substrate, and a culture of *Escherichia coli* (Monod 1942, 1950). His inspiration came from Michaelis–Menten kinetics (see Section 3.2.1.4), which are only valid for a system consisting of one substrate and one enzyme. Although the biodegradation of one substrate by a pure culture of bacteria and, of course, by a mixed culture is a more complicated process, the standard form of the growth kinetics of bacteria shows the same mathematical structure if the growth is not limited by the concentration of dissolved oxygen:

$$\mu = \mu_{max} \frac{S}{K_S + S} \tag{6.1}$$

and:

$$r_x = \mu X \tag{6.2}$$

where $\mu$ is the specific growth rate ($d^{-1}$), $\mu_{max}$ is the maximal specific growth rate ($d^{-1}$), S is the substrate concentration (g $L^{-1}$), $K_S$ is the saturation coefficient (g $L^{-1}$), $r_x$ is the growth rate (g $L^{-1}$ $d^{-1}$ MLSS) and X is the concentration of bacteria (g $L^{-1}$ MLSS).

Monod's first experiments were carried out in batch reactors. He described his measurements of S and X with respect to time by using the bacterial balance:

$$\frac{dX}{dt} = \mu_{max} \frac{S}{K_S + S} X \tag{6.3}$$

and the substrate balance:

$$\frac{dS}{dt} = -\frac{\mu_{max}}{Y^{o}_{X/S}} \frac{S}{K_S + S} X \tag{6.4}$$

where the substrate consumption rate is:

$$r_S = \frac{r_x}{Y^{o}_{X/S}} \tag{6.5}$$

and $Y^{o}_{X/S}$ is the true yield coefficient.

The initial conditions of Eqs. (6.3) and (6.4) are:

$$t = 0,\ X = X_0 \quad \text{and} \quad t = 0,\ S = S_0$$

The simplest solution can be obtained for a relatively high $X_0$ and a relatively low $S_0$, resulting in a nearly constant $X \approx X_0$. Only Eq. (6.4) must be solved, which is performed by the separation of variables:

$$\int dS \left( \frac{K_S}{S} + 1 \right) = -\frac{\mu_{max}}{Y^{o}_{X/S}} X_0 \int dt + C \tag{6.6}$$

$$K_S \ln \frac{S_0}{S} + (S_0 - S) = r_{S,max}\, t \tag{6.7}$$

with:

$$r_{S,max} = \frac{\mu_{max}}{Y^{o}_{X/S}} X_0 \tag{6.8}$$

The results of an experiment can be tested as a function of $S = f(t)$ and the coefficients $K_S$ and $r_{S,max}$ can be determined by transformation of Eq. (6.7) into:

$$\frac{\ln S_0/S}{S_0 - S} = \frac{r_{S,max}}{K_S} \frac{t}{S_0 - S} - \frac{1}{K_S} \tag{6.9}$$

In order to confirm that the results of the batch experiment correspond with the model used to develop Eq. (6.4), we should plot, e.g.:

$$\frac{\ln S_0/S}{S_0 - S} \quad \text{versus} \quad \frac{t}{S_0 - S}$$

and the points should form a straight line with a positive slope $r_{S,max}/K_S$ and a negative ordinate intercept $-1/K_S$.

For substrate *and* oxygen limitation, Eq. (6.1) must be expanded:

$$\mu = \mu_{max} \frac{S}{K_S + S} \frac{c'}{K' + c'} \tag{6.10}$$

The region where oxygen limitation is significant can be estimated using $K' = 0.2$ mg $L^{-1}$ $O_2$ at T = 20 °C (Putnaerglis 1987). For $S \gg K_S$ the point of limitation may be given as $\mu = 0.9\ \mu_{max}$ (90% of maximal growth rate):

$$\frac{\mu}{\mu_{max}} = 0.9 = \frac{c'}{K' + c'} \tag{6.11}$$

$c' = 9 \cdot 0.2 = 1.8$ mg $L^{-1}$ $O_2$

For $c' \geq 1.8$ mg $L^{-1}$ we do not expect $O_2$ limitation (T = 20 °C, domestic sewage, no influences of mass transfer at the surface or inside of flocs formed by bacteria).

With $K_S = 50–120 \approx 85$ mg $L^{-1}$ $BOD_5$ at T = 20 °C (Sundstrom and Klei 1979), the region of substrate limitation can be estimated roughly to be:

$$\frac{\mu}{\mu_{max}} = 0.9 = \frac{S}{K_S + S} \tag{6.12}$$

$S = 9 \cdot 85 = 765$ mg $L^{-1}$ $BOD_5$

If both concentrations S and c′ decrease to low values during a batch process, the kinetic evaluation is complicated. Therefore, kinetics should be studied considering only under substrate limitation or oxygen limitation. But if we want to study oxygen limitation during a batch process without aeration, the substrate concentration ($BOD_5$, COD, DOC) decreases only about a few milligrams per liter if c′ decreases from 8 mg $L^{-1}$ to 0 mg $L^{-1}$. This kind of batch experiment can be carried out even for low S values.

If we avoid substrate limitation

$$\mu = \mu_{max} \cdot \frac{c'}{K' + c'} \tag{6.13}$$

can be tested.

For $X \approx \text{const}$, the oxygen balance is:

$$\frac{dc'}{dt} = -\frac{\mu_{max}}{Y^{\circ}_{X/S}} \frac{c'}{K' + c'} X \tag{6.14}$$

and a corresponding solution to Eq. (6.9) is obtained which can be linearized as shown before.

#### 6.2.1.2 With Low Initial Concentration of Bacteria

It can be advantageous to start an experiment with a low bacterial concentration. In this case, we must consider the change in X by bacterial growth.

Introducing $r_S = \frac{S_0 - S}{\Delta t}$ and $r_X = \frac{X - X_0}{\Delta t}$ into Eq. (6.5):

$$X = X_0 + Y^{\circ}_{X/S} (S_0 - S) \tag{6.15}$$

is obtained which can be used to eliminate X in the substrate balance (Eq. 6.4):

$$\frac{dS}{dt} = -\frac{\mu_{max}}{Y^{\circ}_{X/S}} \frac{S (X_0 + Y^{\circ}_{X/S} (S_0 - S))}{K_S + S} \tag{6.16}$$

By integrating Eq. (6.16) with $t = 0$, $S = S_0$ and by separating the variables X and t, and by using:

$$a = X_0 + Y^{\circ}_{X/S} S_0 \tag{6.17}$$

we obtain the solution (Winkler 1981):

$$\frac{K_S}{a} \ln \frac{S_0}{S} + \frac{a + K_S}{a} \ln \left(1 + \frac{(S_0 - S) Y^{\circ}_{X/S}}{X_0}\right) = \mu_{max} t \tag{6.18a}$$

After transforming Eq. (6.18a) into:

$$\underbrace{\ln \left(\frac{S}{S_0} + 1 + \frac{(S_0 - S) Y^{\circ}_{X/S}}{X_0}\right)}_{y} = \underbrace{\frac{\mu_{max} a}{(a + K_S)}}_{m} \underbrace{\frac{t}{\ln \frac{S_0}{S}}}_{x} - \underbrace{\frac{K_S}{a + K_S}}_{b} \tag{6.18b}$$

we obtain the coefficients $\mu_{max}$ and $K_S$ which are determined from the slope and ordinate intercept if a straight line with a positive slope m and a negative ordinate intercept b follows.

### 6.2.2 Chemostat

The simple continuous process takes place in a CSTR (*c*ompletely *s*tirred *t*ank *r*eactor) as a steady state process with a bacteria-free influent and with no recycling of settled sludge. This reactor is called a chemostat. The growth of bacteria was initiated by inoculation. After a non-steady period, a constant concentration of bac-

teria and substrate are achieved for mean retention times which are long enough to sustain bacterial growth. Different steady states can be obtained by changing the flow rate, substrate influent concentration or dissolved oxygen concentration at different aeration rates. A very simple solution of the problem follows from a bacterial balance:

$$0 = \underbrace{-\,Q_0\,X}_{\text{flow rate out of the reactor}} + \underbrace{\mu\,X\,V}_{\text{growth rate}} \tag{6.19}$$

With Eq. (6.1) and the mean retention time: $t_R = \dfrac{V}{Q_0}$ (6.20)

or the dilution rate:

$$D = \frac{Q_0}{V} = \frac{1}{t_R} \tag{6.21}$$

we obtain from Eq. (6.19):

$$S = \frac{K_S}{\mu_{max}\,t_R - 1} \tag{6.22}$$

or:

$$S = \frac{DK_S}{\mu_{max} - D} \tag{6.23}$$

With Eq. (6.15), the corresponding equation for X is:

$$X = Y^{\circ}_{X/S}\left(S_0 - \frac{K_S}{\mu_{max}\,t_{RC} - 1}\right) \tag{6.24}$$

with the mean retention time $t_R$ used as a parameter (Fig. 6.1).

It is typical for all bioreactors with suspended microorganisms in continuous operation that the organisms can be washed out at a critical mean retention time ($t_{RC}$) which follows from Eq. (6.24) for X = 0 as:

$$t_{RC} = \frac{K_S + S_0}{\mu_{max}\,S_0} \tag{6.25}$$

and for $S_0 \gg K_S$ as:

$$t_{RC} = \frac{1}{\mu_{max}} \tag{6.26}$$

Using Eq. (6.21), a well known solution is obtained:

$$D_C = \mu_{max} \tag{6.27}$$

All suspended organisms are washed out if the dilution rate is increased beyond a critical value, which corresponds to the maximum specific growth rate, $\mu_{max}$. From a theoretical point of view, a suspended culture of two organisms (1 and 2) with different $\mu_{max}$ can be separated by increasing D up to a value greater than $D_{C1}$ and less than $D_{C2}$.

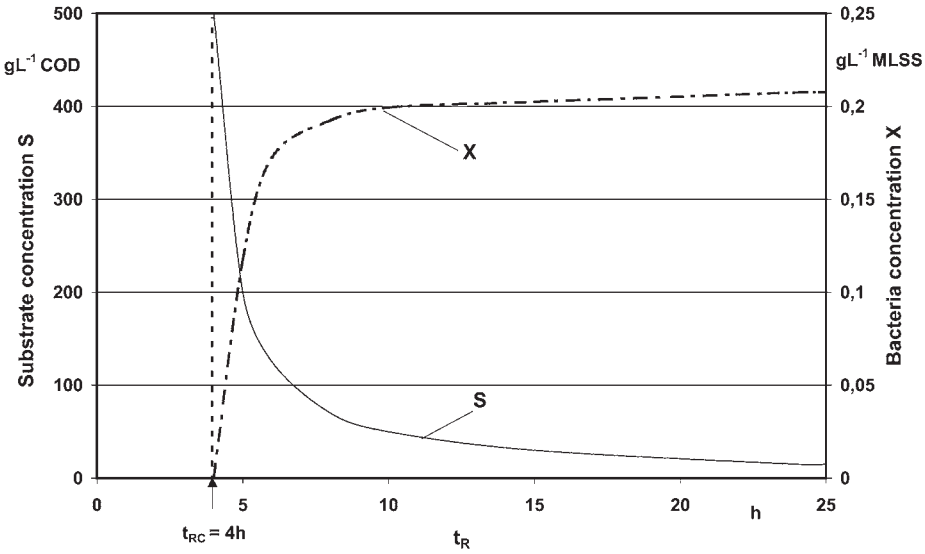


**Fig. 6.1** Effluent COD S and bacterial concentration X of a chemostat versus mean retention time $t_R$. $t_{RC}$ = critical mean retention time, calculated with $\mu_{max} = 7.2\ d^{-1}$, $K_S = 100\ mg\ L^{-1}$ COD.

The growth rate follows directly from Eqs. (6.2) and (6.24):

$$r_x = \mu X \tag{6.28}$$

it increases with increasing $t_R > t_{RC}$, get a maximal value $r_{x,max}$, which can be obtained from: $dr_x/dt_x = 0$ and decreases.

Because the chemostat maintains only a low concentration of microorganisms, it has no practical significance, and as a consequence, it exhibits only a low substrate consumption rate. But experiments can be used to study the reaction kinetics and to determine the coefficients. It can be used to determine S for different $t_R$ values while Eq. (6.22) is linearized as follows:

$$\frac{1}{S} = \frac{\mu_{max}}{K_S} t_R - \frac{1}{K_S} \tag{6.29}$$

A plot of 1/S versus $t_R$ must give a straight line with a negative ordinate intercept $-K_S^{-1}$.

As discussed in Section 6.2.1.1, oxygen limitation must be avoided during these experiments and the dissolved oxygen concentration must be $c' \geq 1.8\ mg\ L^{-1}$ (T = 20 °C, municipal wastewater). The region of oxygen limitation can be studied if an oxygen balance is used:

$$0 = Q_G (c_{O_2,0} - c_{O_2,e}) - \frac{\mu_{max} X}{Y^{\circ}_{X/O_2}} \frac{c'}{K' + c'} V \tag{6.30}$$

and if S is high enough, whereby $S/(K_S + S) \approx 1$ during aeration.

With:

$$r' = \frac{Q_G\,(c_{O2,0} - c_{O2,e})}{V} \tag{6.31}$$

it follows that:

$$\frac{r'}{X} = \frac{\mu_{max}}{Y^{\circ}_{X/O_2}} \frac{c'}{K' + c'} \tag{6.32}$$

Equation (6.32) can be linearized using the Langmuir plot:

$$\frac{c'X}{r'} = \frac{Y^{\circ}_{X/O_2} K'}{\mu_{max}} + \frac{Y^{\circ}_{X/O_2}}{\mu_{max}}\, c' \tag{6.33}$$

Figure 6.2 presents results from measurements at high bacterial concentration $X_0$ and high substrate concentration $S_0$ for 17 °C and 24 °C. $X_0$ was added to the influent wastewater (not chemostat operation).

A good linearization was obtained with $K' = 0.19$ mg $L^{-1}$ (17 °C) and $K' = 0.06$ mg $L^{-1}$ (24 °C; Putnaerglis 1987).

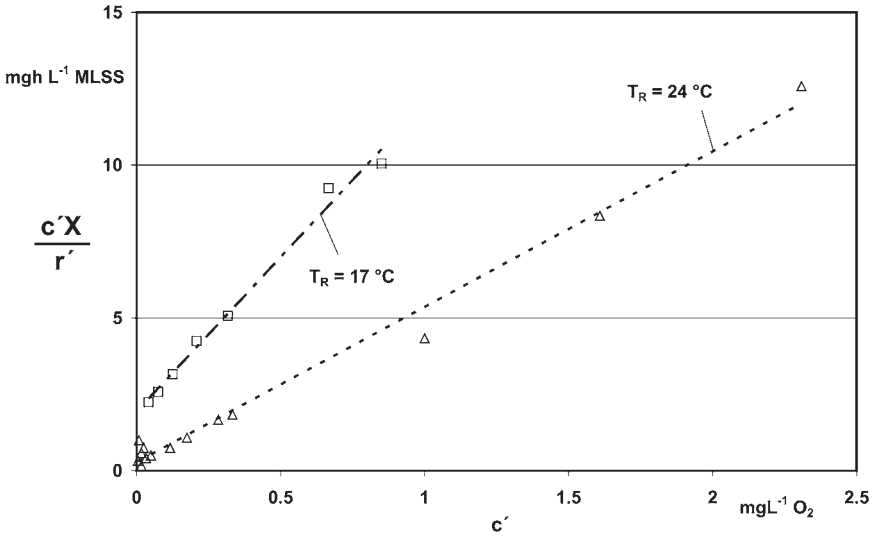


**Fig. 6.2** Plot of Eq. (6.33) in order to test this equation and to determine $K'$ and $\mu_{max}/Y^{\circ}_{X/O_2}$ (Putnaerglis 1987).

## 6.2.3 Completely Mixed Activated Sludge Reactor

### 6.2.3.1 Preliminary Remarks

In the late 1960s and early 1970s, the first models for the activated sludge process were published, which were based on the balances of bacteria and substrate.

Initially, a first-order reaction with regard to substrate concentration S was used (Eckenfelder 1967). Later on, Monod kinetics were considered in most models (Reynolds and Yang 1966; Benedek and Horvath 1967; Lawrence and McCarty 1970; Peil and Gaudy 1971; Chow et al. 1979; Grady et al. 1999).

In some papers, other kinetics were suitable to describe experimental results, for example Contois kinetics (Chen and Hashimoto 1980):

$$\mu = \mu_{max} \frac{S}{KX + S} \tag{6.34}$$

However, we will restrict ourselves to Monod kinetics. In most papers, sludge age (mean retention time of bacteria $t_{RX}$) is the key process parameter, but we want to show that the model first contains three other process parameter (mean retention time of wastewater $t_R$, recycle ratio $n_R$ and thickening ratio $n_E$), which can be replaced by $t_{RX}$.

### 6.2.3.2 Mean Retention Time, Recycle Ratio and Thickening Ratio as Process Parameters

Figure 6.3 presents the flow sheet of an activated sludge plant.

The balance of bacteria X for the CSTR in steady state is:

$$0 = Q_M (X_M - X) + (\mu - k_d)\, X\, V \tag{6.35}$$

Corresponding to Eq. (6.35), the balance of substrate S is:

$$0 = Q_M (S_M - S) - \frac{\mu}{Y^{\circ}_{X/S}}\, X\, V \tag{6.36}$$

with: $k_d = k_s + k_e$ as the decay coefficient.

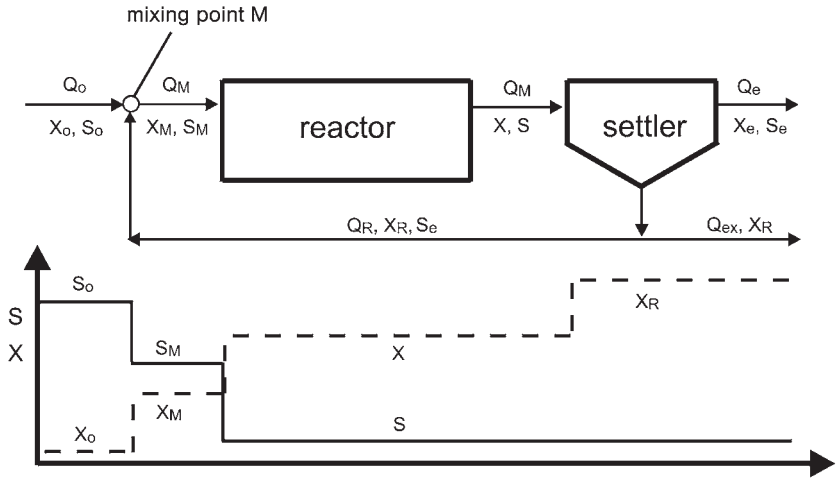


**Fig. 6.3** Flow sheet for a completely mixed (stirred) activated sludge plant (CSTR).

$k_d$ includes both the specific rate of death $k_s$ and that of mass decrease by endogenous respiration $k_e$. The decay coefficient was first proposed by Herbert (1958). $k_d$ and $k_e$ were already introduced in Chapter 4.23 (see Eq. 4.27). Dividing Eq. (6.36) by Eq. (6.35), we obtain:

$$X = X_M + (S_M - S)\, Y^{\circ}_{X/S} \left(1 - \frac{k_d}{\mu}\right) \tag{6.37}$$

For $\mu \gg k_d$, Eq. (6.15) follows from Eq. (6.37), which can be interpreted as a relationship between the substrate used and the bacterial mass formed. After introducing Eq. (6.37) and Monod kinetics (Eq. 6.1) in Eq. 6.36, S can be calculated.

Furthermore, a bacterial balance at the mixing point M is necessary (Fig. 6.3). Neglecting $Q_0X_0$, we obtain:

$$Q_M X_M = Q_R X_R \tag{6.38}$$

With the recycle ratio:

$$n_R = \frac{Q_R}{Q_0} \tag{6.39}$$

and the thickening ratio:

$$n_E = \frac{X_R}{X} \tag{6.40}$$

then we can calculate:

$$X_M = \frac{n_R n_E}{1 + n_R} X \tag{6.41}$$

After introducing Eqs. (6.1), (6.20), (6.37) and (6.41) into Eq. (6.36), we obtain:

$$S = \frac{K_S (1 + n_R - n_E n_R + k_d t_R)}{t_R (\mu_{max} - k_d) - (1 + n_R - n_E n_R)} \tag{6.42}$$

It is interesting that S is not influenced directly by $S_0$.

For $k_d \approx 0$, it follows that:

$$S = \frac{K_S (1 + n_R - n_E n_R)}{t_R \mu_{max} - (1 + n_R - n_E n_R)} \tag{6.43}$$

If we are interested in the bacterial concentration X, we must introduce Eqs. (6.1) and (6.43) into Eq. (6.37).

For $S = S_0$, Eq. (6.43) yields:

$$t_{RC} = \frac{K_S + S_0}{\mu_{max} S_0} (1 + n_R - n_E n_R) \tag{6.44}$$

$t_{RC}$ is the critical mean retention time which was already introduced in Section 6.2.2 for the discussion on the chemostat (see Eq. 6.25). For $n_R = 0$, Eq. (6.44) can be transformed into Eq. (6.25). The higher $n_R$ is, the lower $t_{RC}$ is for $n_E > 1$. This model was published by Mehring (1979) and by Sundstrom and Klei (1979) among others.

#### 6.2.3.3 Sludge Age as Parameter

In activated sludge plants the mean retention time of bacteria (sludge age) $t_{RX}$ is decoupled from that of the water retention time. The sludge age is defined by Eq. (6.45):

$$t_{RX} = \frac{VX}{Q_R X_R + Q_{ex} X_R} \tag{6.45}$$

Because of $Q_R X_R \gg Q_{ex} X_R$, it is often allowed to write:

$$t_{RX} = \frac{VX}{Q_R X_R} \tag{6.46}$$

This is the mass of solids inside the aeration tank applied to the production rate of excess solids. The steady-state balance of solids around the settler gives (see Fig. 6.3):

$$(Q_0 + Q_R)\, X = Q_R X_R + Q_{ex} X_R + Q_e X_e \tag{6.47}$$

Neglecting $Q_e X_e$, transforming Eq. (6.47) and considering Eqs. (6.39), (6.40), (6.46) and (6.20), it follows that:

$$1 + n_R - n_E n_R = \frac{t_R}{t_{RX}} \tag{6.48}$$

If we introduce this result into the solutions with bacterial decay [Eq. (6.42)] and without bacterial decay (Eq. 6.43) we obtain:

$$S = \frac{K_S (1 + k_d t_{RX})}{t_{RX} (\mu_{max} - k_d) - 1} \tag{6.49}$$

and for $k_d = 0$:

$$S = \frac{K_S}{t_{RX} \mu_{max} - 1} \tag{6.50}$$

Substrate removal is only influenced by sludge age $t_{RX}$, which replaces the three parameters $t_R$, $n_R$ and $n_E$. We see here the importance of the parameter "sludge age", which will be used more and more not only in theoretical considerations but also in the practice of activated sludge system control.

The critical sludge age $t_{RXC}$ is the mean retention time of bacteria which must be exceeded in the activated sludge process. Otherwise, the bacteria (the sludge) will be washed out. $t_{RXC}$ follows from Eqs. (6.49) and (6.50) for $S = S_0$:

$$t_{RXC} = \frac{K_S + S_0}{S_0 (\mu_{max} - k_d) - K_S k_d} \tag{6.51}$$

and for $k_d = 0$:

$$t_{RXC} = \frac{K_S + S_0}{\mu_{max} S_0} \tag{6.52}$$

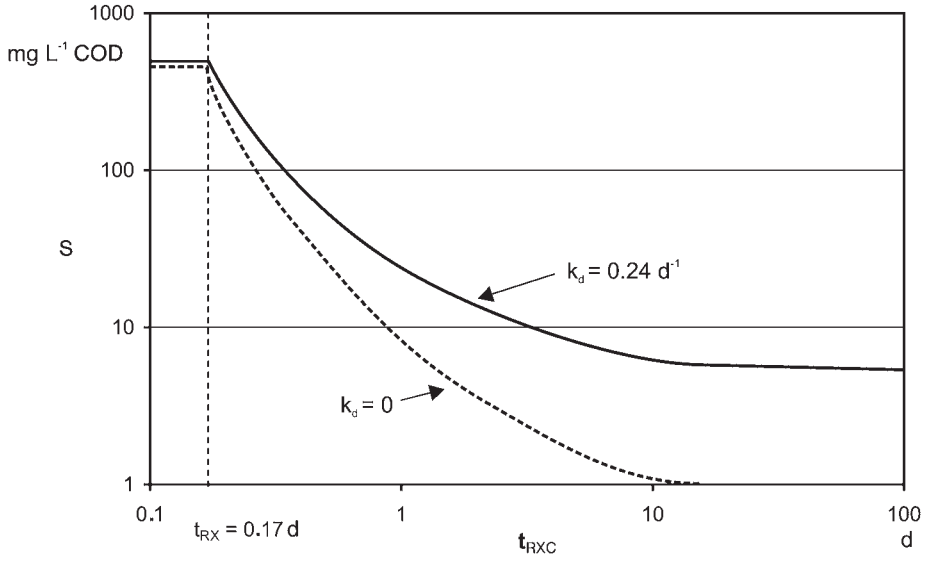


**Fig. 6.4** Effluent COD concentration of a CSTR versus sludge age $t_{RX}$; with bacterial decay ($k_d = 0.24\ d^{-1}$) and without bacterial decay ($k_d = 0\ d^{-1}$) for a one-stage CSTR; $\mu_{max} = 7.2\ d^{-1}$, $K_S = 100\ mg\ L^{-1}$ COD; $S_0 = 500\ mg\ L^{-1}$ COD.

If we introduce Eq. (6.52) into Eq. (6.44), then:

$$1 + n_R - n_E n_R = \frac{t_{RC}}{t_{RXC}} \tag{6.53}$$

follows, the same relationship as calculated for $t_R t_{RX}^{-1}$. After this model with $t_{RX}$ was presented as the only process parameter in the early 1970s, it was published, discussed and applied very frequently (Sunstrom and Klei 1979; Benefield and Randall 1980; Winkler 1981; Nasaroff and Alvarez-Cohen 2001). Figure 6.4 presents some theoretical results which were calculated for $\mu_{max} = 7.2\ d^{-1}$, $K_S = 100\ mg\ L^{-1}$ COD, $k_d = 0.24\ d^{-1}$ and $S_0 = 500\ mg\ L^{-1}$ COD.

For these conditions nearly 90%, that is $S_0 - S = 500 - 50 = 450\ mg\ L^{-1}$ COD are removed, if a sludge age of about $t_{RX} = 0.5\ d = 12\ h$ is selected. The real sludge production is obtained from:

$$Y_{X/S} = Y^{o}_{X/S}\left(1 - \frac{k_d}{\mu}\right) \tag{4.27}$$

for $t_{RX} = 0.5\ d$, $Y^{o}_{X/S} = 0.43\ g\ MLSS\ (g\ COD)^{-1}$ and $\mu_{max} = 7.2\ d^{-1}$

with

$$\mu = \mu_{max}\frac{S}{K_S + S} = 7.2\ \frac{50}{100 + 50} = 2.4\ d^{-1}$$

it follow a real yield:

$$Y_{X/S} = 0.43\left(1 - \frac{0.24}{2.4}\right) = 0.39\ \frac{g\ MLSS}{g\ COD}$$

If we want to consider oxygen limitation, Eq. (6.10) must be introduced into Eqs. (6.41) and (6.42) and we have to add an oxygen balance:

$$0 = \underbrace{Q_G\,(c_{O2,0} - c_{O2,e})}_{\text{O}_2\text{ uptake by exhaust air measurements}} - \underbrace{\frac{\mu_{max}}{Y^o_{X/O_2}}\ X\ \frac{S}{K_S + S}\ \cdot\ \frac{c'}{K' + c'}\ V}_{\text{O}_2\text{ needed for growth}} - \underbrace{\frac{k_e X V}{Y^o_{X/O_2}}}_{\text{O}_2\text{ needed for endogeneous respiration}} \tag{6.54}$$

The difference of dissolved $O_2$ in the influent and effluent water is neglected. We want to continue the calculation of activated sludge plants in Chapter 11.

### 6.2.4 Plug Flow Reactor

The main characteristic of a plug flow reactor (PFR) is that no mixing occurs in the direction of flow; however, complete mixing is assumed within a cross-sectional area of the reactor. Water and all suspended flocs of bacteria move with the same velocity along the tube reactor. In contrast to the CSTR, the PFR exhibits a continuous decrease in substrate concentration and an increase in bacterial concentration in the direction of flow (Fig. 6.5).

Because of the continuous change of concentrations, the balances for bacteria and substrate must be written as differential balances. They can be obtained by writing first an integral balance for the volume element ΔxA in a steady state:

$$0 = Q_M\,(S_1 - S_2) - r_S\,\Delta x A \tag{6.55}$$

with A as cross-sectional area, which is not correct, because of the change of S within Δx; but it can be corrected, by forming the differential:

$$\lim_{\Delta x \to 0} \frac{S_1 - S_2}{x_1 - x_2} = -\lim_{\Delta x \to 0} \frac{S_1 - S_2}{x_2 - x_1} = -\lim_{\Delta x \to 0} \frac{\Delta S}{\Delta x} = -\frac{dS}{dx} \tag{6.56}$$

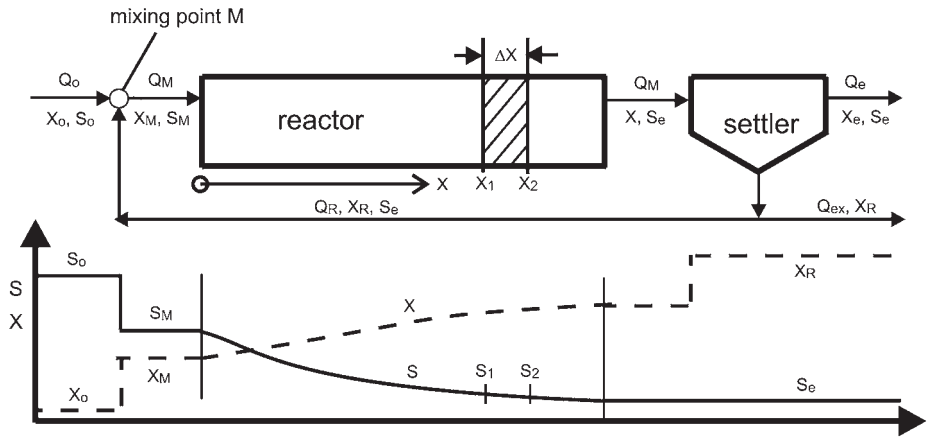


**Fig. 6.5** Flow sheet for a plug flow activated sludge plant (PFR).

with:

$$\bar{w}_M = \frac{Q_M}{A} = \bar{w}\,(1+n_R) \tag{6.57}$$

and Eq. (6.56), then Eq. (6.55) yields:

$$0 = -\,\bar{w}\,(1+n_R)\,\frac{dS}{dx} + r_S \tag{6.58}$$

or for the bacterial balance, it yields:

$$0 = -\,\bar{w}\,(1+n_R)\,\frac{dX}{dx} + r_X \tag{6.59}$$

Assuming Monod kinetics for bacterial growth, then:

$$0 = -\,\bar{w}\,(1+n_R)\,\frac{dS}{dx} - \frac{\mu_{max} X}{Y^{\circ}_{X/S}}\,\frac{S}{K_S + S} \tag{6.60}$$

and:

$$0 = -\,\bar{w}\,(1+n_R)\,\frac{dX}{dx} + \mu_{max} X\,\frac{S}{K_S + S} \tag{6.61}$$

result with the conditions $x = 0$, $S = S_M$ and $x = 0$, $X = X_M$.

If we move along the tube reactor with the flow rate $\bar{w}(1+n_R)$ and measure S and X at time t, the process could be described with Eqs. (6.3) and (6.4). Therefore, by using:

$$\bar{w}\,(1+n_R) = \frac{dX}{dt} \tag{6.62}$$

Equations (6.60) and (6.61) can be transformed into Eqs. (6.3) and (6.4). With the appropriate initial conditions, the solution in Eq. (6.18) is achieved. Batch reactor and plug flow reactor can be described by the same balances if we use the transformation in Eq. (6.62). After consideration of Eq. (6.15) and integration:

$$\frac{K_S}{a}\,\ln\frac{S_M}{S} + \frac{a + K_S}{a}\,\ln\left(1 + \frac{(S_M - S)\,Y^{\circ}_{X/S}}{X_M}\right) = \frac{\mu_{max}\,t_R}{1+n_R} \tag{6.63}$$

with:

$$t_R = \frac{x}{\bar{w}} \tag{6.64}$$

$$S_M = \frac{n_R\,S_e}{1+n_R} \tag{6.65}$$

and:

$$X_M = \frac{n_R\,n_E\,X_e}{1+n_R} \tag{6.66}$$

With Eq. (6.58) the critical sludge age $t_{RXC}$ can be calculated. The critical mean retention time $t_{RX}$ follows from Eq. (6.67):

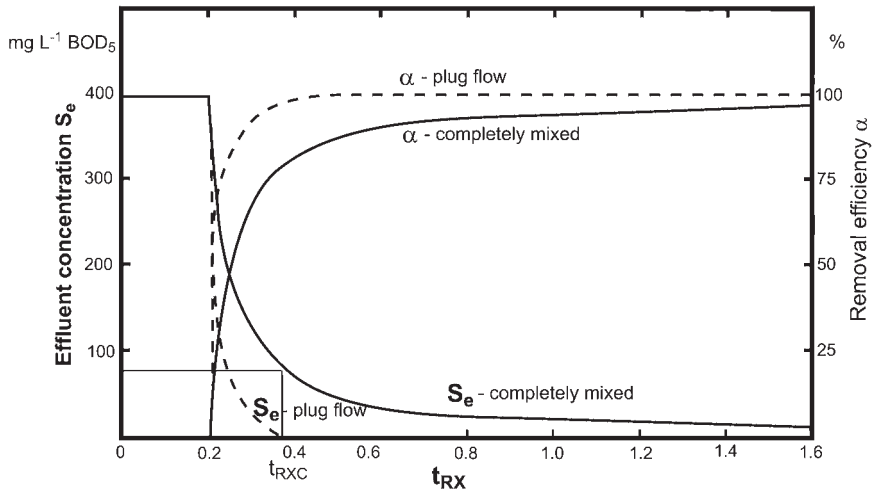


**Fig. 6.6** Comparison of a CSTR with a PFR; effluent concentrations S and treatment efficiency α versus sludge age $t_{RX}$; $\mu_{max} = 16.7\ d^{-1}$, $K_S = 0.1\ g\ L^{-1}$ $BOD_5$, $Y^{\circ}_{X/S} = 0.6$ g MLSS (g $BOD_5)^{-1}$, $k_d = 0.05\ d^{-1}$, $S_0 = 400\ mg\ L^{-1}$ $BOD_5$ (Benefield and Randall 1980; after Lawrence and McCarty 1970).

$$t_{RC} = (1+n_R)\left(\frac{1+K_S/S_0}{\mu_{max}}\right)\ln\left(\frac{1+n_R}{n_E n_R}\right) \tag{6.67}$$

Equation (6.67) was published by Fan et al. (1970), as the mathematical limit of a model of CSTRs in series for $n \rightarrow \infty$, with n as the total number of reactors in the system. This must correspond with the plug flow model. It follows from Eq. (6.67) that $t_{RC}$ and $t_{RX}$ increase with decreasing $n_R$; for $n_R = 0$ (no recycle) $t_{RC}$ is infinitely large. This result is to be expected because there is neither recycle of bacteria into the inlet feed nor mixing of fluid.

Figure 6.6 compares the results of PFR substrate removal and efficiency with those of a CSTR ($S_0 = 400\ mg\ L^{-1}\ BOD_5$, $\mu_{max} = 16.7\ d^{-1}$, $K_S = 100\ mg\ L^{-1}\ BOD_5$, $k_d = 0.05\ d^{-1}$, $Y^{\circ}_{X/S} = 0.6$ g MLSS (g $BOD_5)^{-1}$). These results were published by Benefield and Randall (1980). Equation (6.49) was used for the CSTR and Eq. (6.63) for the PFR. The advantages of a PFR are clear: at $t_{RX} = 0.4$ d, the effluent of the PFR $S_e$ is already very low. By comparison, the CSTR shows an effluent concentration of $S = 70\ mg\ L^{-1}\ BOD_5$. Only at $t_{RX} = 1.6$ d does the CSTR shows an S as low as nearly 10 mg $L^{-1}$ $BOD_5$.

In Fig. 6.6 $t_{RXC}$ for CSTR and PFR are nearly the same, because of the relative high sludge recycle $n_R$. For lower $n_R$, $t_{RC}$ and $t_{RXC}$ increase in PFR systems.

### 6.2.5
### Completely Mixed Tank Cascades With Sludge Recycle

CSTRs and PFRs are reactors idealized as either completely mixed or not mixed at all. In a technical scale, all reactors in continuous operation differ from these extreme cases. In a longitudinal open basin, dispersion effects dominate which

can be reflected, for example, by a dispersion model or by a model of n completely stirred tank reactors coupled in series, which is called a reactor cascade. Frequently, a reactor with longitudinal dispersion can be described as a cascade with a specific number of completely mixed tanks (see Section 6.2.8). In the following, this model will be discussed shortly.

The model consists of n balances each for substrate and bacteria. It is sufficient to write only the balances for stage number n, which shows the structure of all the other balances for stages < n. We write according to Eqs. (6.35) and (6.36) for stage number n and steady-state conditions:

$$0 = Q_M (S_{n-1} - S_n) - \frac{\mu_n}{Y^o_{X/S}} X_n V_n \tag{6.68}$$

$$0 = Q_M (X_{n-1} - X_n) + \mu_n X_n V_n - k_d X_n V_n \tag{6.69}$$

$X_n$ in Eq. (6.68) can be replaced by:

$$X_n = X_{n-1} + (S_{n-1} - S_n)\, Y^o_{X/S} \left(1 \frac{k_d}{\mu_n}\right) \tag{6.37}$$

With:

$$\mu_n = \mu_{max} \frac{S_n}{K_S + S_n} \tag{6.70}$$

$$t^n_R = \frac{V_N}{Q_0} \tag{6.71}$$

$$Q_M = Q_0 + Q_R \tag{6.72}$$

as well as Eqs. (6.38) to (6.41). $S_n$ and $X_n$ can be calculated by coupling the n substrate balances.

The most important property of such a system is the step by step decrease in substrate concentration and increase in bacterial concentration it exibits. For certain conditions of influent substrate concentration and kinetic coefficients, the n-stage cascade is characterized by a higher total reaction rate, compared to a CSTR.

Let us discuss the behavior of a cascade with two stages, without presenting a special figure, but looking at Fig. 6.6 showing a somewhat higher difference because of its plug flow characteristic (infinite number of stages). If S is relative high, e.g. for low mean retention times $t_R$, substrate concentrations S are equivalent in both systems showing nearly the same low removal efficiency because of the zero-order region of Monod kinetics. But for low S values and/or higher $t_{RX}$, the two-stage cascade shows remarkably lower S as a result of the first-order region. In other words: a substrate removal from 5000 mg $L^{-1}$ COD down to 500 mg $L^{-1}$ COD is performed as a reaction with nearly zero order (for $K_S$ = 100 mg $L^{-1}$ COD); and a two-stage cascade is not advantageous. A substrate removal from 100 mg $L^{-1}$ COD to 10 mg $L^{-1}$ COD, however, takes place in the region of the first-order reaction with a remarkably higher reaction rate in a cascade of two or more stages! The influent substrate concentration is 500 mg $L^{-1}$ COD. Here, the region of Monod kinetics is effective, starting from nearly zero order down to a first-order reaction.

For $S_2 = S_0$, the bacteria will be washed out and a critical sludge age $t_{RXC}$ or a critical mean retention time $t_{RC}$ follows from the model for a cascade of n stages:

$$t_{RC}^{n} = \frac{n\left(1 + \frac{K_S}{S_0}\right)\left[1 - \frac{n_E n_R}{1+n_R}\right]^{1/n}(1+n_R)}{\mu_{max} - k_d\left(1 + \frac{K_S}{S_0}\right)} \tag{6,73}$$

With Eq. (6.48), the critical sludge age results:

$$t_{RXC}^{n} = \frac{t_{RC}^{n}}{1+n_R-n_E n_R} \tag{6.74}$$

For $n \to \infty$, Eq. (6.73) transforms to Eq. (6.67) and the critical mean retention time of the PFR with bacterial recycle is:

$$t_{RC} = \frac{(1+n_R)(S_0-K_S)}{\mu_{max} S_0} \ln \frac{1+n_R}{n_R n_E} \tag{6.75}$$

For $n_R = 0$ (no bacterial recycle), $t_{RC}$ is infinitely large: for all mean retention times $t_R$ bacteria are washed out (Fan et al. 1970; Sundstrom and Klei 1979). This property differentiates the cascade with recycle from a chemostat or a cascade system without sludge recycle. In both systems (one stage = chemostat; and n stages = cascade) washing-out situations can occur. With increasing number of stages $t_{RC}$ increases starting from the lowest value for n = 1 (chemostat) to the highest value for n = ∞ (plug flow reactor).

### 6.2.6
### Flow Reactor With Axial Dispersion

In addition to the transport of substrate S and bacteria X by the flow of the water (see Eqs. 6.60 and 6.61), a transport by dispersion will be considered:

$$0 = -\bar{w}(1+n_R)\frac{dS}{dx} + D_x \frac{d^2S}{dx^2} - \frac{\mu_{max} X}{Y^{o}_{B/S}} \frac{S}{K_S+S} \tag{6.76}$$

$$0 = -\bar{w}(1+n_R)\frac{dX}{dx} + D_x \frac{d^2X}{dx^2} + \mu_{max} X \frac{S}{K_S+S} \tag{6.77}$$

The decay rate is neglected here. Two boundary conditions are needed for each balance. Normally, the following conditions are used for a "closed tube" (Danckwerths 1953). They will be written here only for Eq. (6.76) (see Fig. 6.7):

$$x = 0: \quad \bar{w}(1+n_R) S_M = \bar{w}(1+n_R) S - D_x \frac{dS}{dx} \tag{6.78}$$

$$x = L: \quad \frac{dS}{dx} = 0 \tag{6.79}$$

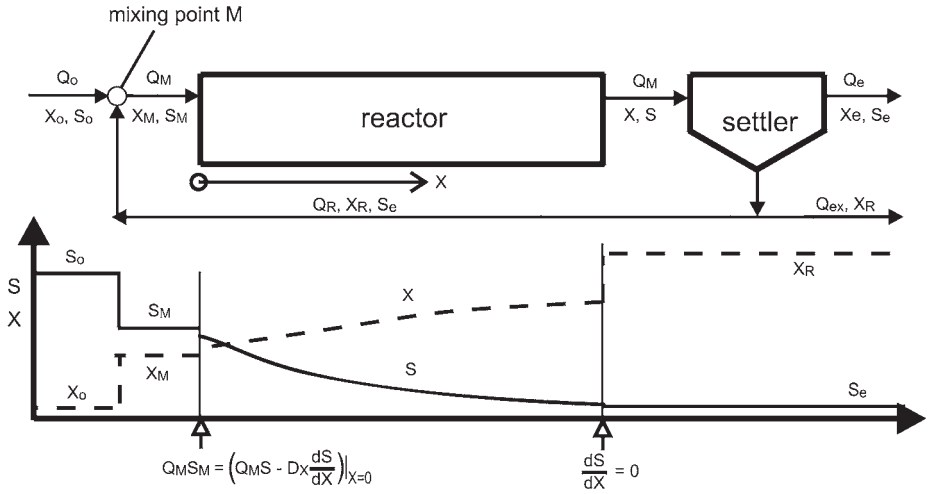


**Fig. 6.7** Flow sheet for a real flow tube reactor (closed tube model).

The same conditions for X can be used to solve Eq. (6.77). As Fig. 6.7 shows at $x = 0$, a discontinuity occurs in S. For very low $D_x$ values, this discontinuity disappears ($\rightarrow$PFR), while for high $D_x$ values, it reaches a maximum ($\rightarrow$CSTR). Dispersion in the tube for $x < 0$ is neglected in this model. Under real conditions, a $dS/dx < 0$ would be correct at $x = L$. But for this "boundary condition" Eq. (6.76) cannot be solved. Danckwerths (1953) introduced Eq. (6.79) and expected a very small error at this point.

Equations (6.76) and (6.77) can be rewritten with dimensionless Peclet or Bodenstein numbers:

$$Pe = \frac{\bar{w}(1+n_R)\,L}{D_x} \tag{6.80}$$

$$0 = -\frac{dS^*}{d(x/L)} + \frac{1}{Pe}\,\frac{d^2S^*}{d(x/L)^2} - \frac{L}{\bar{w}(1+n_R)} \cdot \frac{\mu_{max} X^*}{Y^o_{X/S}}\,\frac{S^*}{1+S^*} \tag{6.81}$$

$$0 = -\frac{dX^*}{d(x/L)} + \frac{1}{Pe}\,\frac{d^2X^*}{d(x/L)^2} + \frac{L}{\bar{w}(1+n_R)}\,\mu_{max} X^*\,\frac{S^*}{1+S^*} \tag{6.82}$$

For $Pe \gg 1$ (high $\bar{w}(1 + n_R)$, high L, low $D_x$), Eq. (6.81) and Eq. (6.82) come close to the balances for a PFR (Eqs. 6.60 and 6.61), for $Pe \ll 1$ (low $\bar{w}(1 + n_R)$, low L, high $D_x$) the ideal CSTR system is nearly reached.

For $S \ll K_S$, the equations can be solved analytically (Lin 1979). For Monod kinetics, a numerical solution is needed (Fan 1970; Vasilin and Vasilyev 1978) even for the case of constant biomass concentration X.

### 6.2.7 Stoichiometric and Kinetic Coefficients

Since Monod's first experiments and kinetic studies in 1942 and 1950 and those by Herbert (1958), a large number of papers concerning the kinetics of bacterial growth and carbon removal have been published. The yield and kinetic coefficients are again typically defined by Eqs. (6.83) to (6.85):

$$r_X = \mu_{max} \frac{S}{K_S + S} \frac{c'}{K' + c'} X - (k_s + k_e) X \tag{6.83}$$

$$r_S = \frac{\mu_{max}}{Y^o_{X/S}} \frac{S}{K_S + S} \frac{c'}{K' + c'} X \tag{6.84}$$

$$r_{O_2} = \frac{\mu_{max}}{Y^o_{X/O_2}} \frac{S}{K_S + S} \frac{c'}{K' + c'} X + \frac{k_e}{Y^o_{X/O_2}} X \tag{6.85}$$

with:

$$k_d = k_s + k_e \tag{6.86}$$

and:

$$Y^o_{X/O_2} = Y^o_{X/S} \cdot Y^o_{S/O_2} \tag{6.87}$$

In contrast to Herbert, Pirt (1965) introduced a kinetic expression considering the endogeneous mass consumption into the balance for substrates. Here, we follow the concept of Herbert, which is usually used in kinetic descriptions of biological wastewater treatment.

Some measurements led to results which are listed in Table 6.1.

Although different substrates and mixed cultures were used, the $\mu_{max}$ values do not differ considerably. However, $K_S$ and $K'$ scatter remarkably. Because of the low values of $K'$, an exact measurement of low dissolved oxygen concentration is necessary. In last time, $O_2$ electrodes with higher precision have become available, so that more exact measurements are possible. We do not want to present here all these results.

Nearly all yield coefficients are influenced by bacterial decay (see Eq. 4.27) or endogenous respiration. More exact studies are needed for us to be able to distinguish the true yield coefficient $Y^\circ$ from the real yield coefficient Y.

Some published ranges of data from several textbooks are compiled in Table 6.2. On the basis of these values, new mean data will be recommended.

**Table 6.1** Published coefficients and recommended ranges of values from some papers for laboratory-scale CSTR measurements.

| Reference | Basis | T (°C) | $\mu_{max}$ ($h^{-1}$) | $K_S$ [b] | $K'$ [b] | $Y_{X/S}$ | $Y_{O2/S}$ | $k_d$ ($h^{-1}$) | $k_e$ ($h^{-1}$) |
|---|---|---|---|---|---|---|---|---|---|
| Reynolds and Yang (1966) | COD[c] | 20 | 0.80 | 345 | – | 0.39 | – | 0.0071 | – |
| Benedek and Horvath (1967) | COD[d] | 18 | 0.16 | 22 | – | 0.67 | – | 0.0029 | – |
| Peil and Gaudy (1971) | COD[d] | 23 | 0.45 | 55 | – | – | – | – | – |
| Strnivasaraghanan and Gaudy (1974)[a] | COD[e] | 25 | 0.49 | 115 | – | 0.59 | – | 0.0058 | – |
| Button and Gurver (1966) | –[f] | 35 | 0.506 | – | 0.45 | – | 1.2–1.8 | – | – |
| Sinclair and Ryder (1972) | –[f] | 35 | 0.54 | 4.6 | 0.084 | 0.55 | 1.41 | – | 0.01 |
| Putnaerglis (1987) | DOC[g] | 17 | 0.32 | – | 0.22 | – | – | – | 0.03 |

[a] Batch, [b] Values given in mg L–1, [c] Synthetic, [d] Municipal, [e] Synthetic, [f] Glycerine, [g] Filtrate of excess sludge after thermal conditioning.

**Table 6.2** Ranges of measured kinetic and stoichiometric coefficients for aerobic degradation of organic compounds in municipal and domestic wastewater.

| Reference | Basis | T (°C) | $\mu_{max}$ ($d^{-1}$) | $K_S$ (mg $L^{-1}$) | $Y_{X/S}$ | $k_d$ ($d^{-1}$) | $K'$ (mg $L^{-1}$ $O_2$) |
|---|---|---|---|---|---|---|---|
| Sundstrom and Klei (1979) | $BOD_5$ | – | 9.6–13.2 | 50–120 | 0.5–0.67[a] | 0.048–0.072 | – |
| Henze et al. (2002) | COD | 20 | 4.0–8.0 | 3–30 | 0.5–0.7[b] | 0.1–0.2 | 0.5–1.0 |
| Chow et al. (1979) | $BOD_5$ | – | 0.8–8.0 | 25–100 | 0.4–0.8[c] | 0.025–0.075 | – |

[a] Value given in g MLSS $(gBOD_5)^{-1}$
[b] Value given in g COD $(gCOD)^{-1}$
[c] Value given in g MLVSS $(gBOD_5)^{-1}$

### 6.2.8 Comparison of Reactors

Batch reactors are used on a technical scale for carbon removal as *s*equencing *b*atch *r*eactors (SBRs) with periods of filling, aerating, settling, part-emptying, filling and so on. We will come back to this system when we discuss the extended process with nitrogen and phosphorus removal (see Chapter 10).

For a completely mixed tank, substrate and bacterial concentrations at the effluent are nearly the same as inside the reactor. The mixed culture of bacteria always comes in contact with a low substrate concentration. The removal rate is relatively low and we do not need to consider large influences of transport processes into

flocs and oxygen limitation. However, in reality, large tanks are frequently not completely mixed. The rotation speed of surface aerators is often adjusted to a needed concentration of dissolved oxygen and not to a certain degree of mixing. Nevertheless, models can help to understand the process and the behavior of the reactor much better.

In PFRs, tube reactors with axial dispersion or cascades, the bacteria returned by the recycled sludge come into contact with substrate of a higher concentration, which decreases during the transport through the tank. Therefore, in the first part, the rate of oxygen consumption is relatively high, resulting in oxygen limitation, particularly inside the flocs. These effects were not described by the relative simple models discussed in Sections 6.2.2 to 6.2.6.

A CSTR is generally more stable to toxic substances as shock loads than all reactors with reduced backmixing, because the toxic material is dispersed rapidly throughout the reactor and the concentration is reduced. In general, a CSTR gives a more uniform effluent for varying loads, but the reactor volume must be larger, because of the lower substrate concentration and the lower carbon removal rate throughout. In axial flow reactors, aeration of the water increases the axial mixing. For a locally constant distribution of aerators (porous ceramic or membrane tubes), the dispersion model may be used successfully. However, to save energy the distribution of aerators should depend on the task: with higher density in the first part at the higher substrate concentration which goes down to a lower density at the end where the concentration and oxygen uptake rate are lower. The model for tanks in series can be here used with more success because of the possibility to change the size of the stages and aeration rates.

## 6.3
## Retention Time Distribution in Activated Sludge Reactors

### 6.3.1
### Retention Time Distribution

To understand and mathematically describe the activated sludge process in continuous operation, information is needed regarding the degree of mixing inside the reactor. Is the reactor completely mixed? Are there short-circuit flows or regions of eddy currents? What is the dispersion coefficient in a selected type of reactor? Such questions can be answered by measurement and mathematical analysis of retention time distributions (Pippel 1978).

Measurement of the distribution is realized by adding tracers at the influent of the investigated system. In principle, any substance can be used as a tracer, as long as it dissolves completely, does not react with other components and does not change state by desorption, adsorption, precipitation or crystallization. In reality, only a few substances are applicable which are cheap enough, can be measured continuously and are not toxic. Frequently, salts, dyes and other substances not found in wastewater are used which can be measured at very low concentrations.

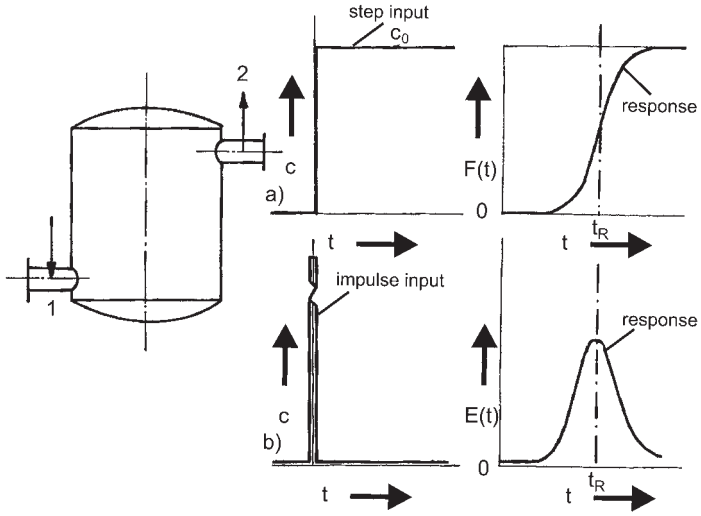


**Fig. 6.8** Explanation for measurement of retention time distribution.
(a) Step input and distribution of retention times F(t) as response.
(b) Impulse input and density distribution of retention time
E(t) = dF/dt as response.

The tracer is added at point 1 (Fig. 6.8) as a step signal or as an impulse signal. At point 2, the signal is deformed in a characteristic way. This response to a step signal is called distribution of retention time and is defined as:

$$F = \frac{c(\tau)}{c_0} = C(\tau) \tag{6.88}$$

with:

$$\tau = \frac{t}{t_R} \tag{6.89}$$

The response to an impulse signal $c_i(\tau)$ is called density distribution of retention time and is defined as:

$$E = \frac{c_i(\tau)}{c_0} \tag{6.90}$$

$c_0$ is here a theoretical concentration, which follows from the mass of the tracer and the volume of the apparatus.

But there is a simple relationship between F and E:

$$E(\tau) = \frac{dF(\tau)}{d\tau} \tag{6.91}$$

The density distribution results from measurements (Fig. 6.8b) and from the distribution by differentiating the dimensionless time.

In the next section we will model some idealized systems and calculate $F(\tau)$.

### 6.3.2 Completely Mixed Tank

The tank is free of tracer at t = 0 and the transport of the tracer concentration starts at t = 0. The tracer balance for the completely mixed tank is:

$$V \frac{dc}{dt} = Q_0 (c_0 - c) \tag{6.92}$$

After separating the variables and considering t = 0, c = 0, the solution is:

$$F(\tau) = \frac{c}{c_0} = 1 - \exp(-\tau) \tag{6.93}$$

or:

$$E(\tau) = \frac{dF(\tau)}{d\tau} = \exp(-\tau) \tag{6.94}$$

Figure 6.9 presents an example of a completely and an incompletely mixed tank reactor with a short circuit flow.

In the incompletely mixed tank, the tracer was measured after only relatively short times at high concentrations in the effluent, as could be expected from a tank (with a short circuit flow) and at a lower concentration after longer times because of the slow transport into eddy flow regions.

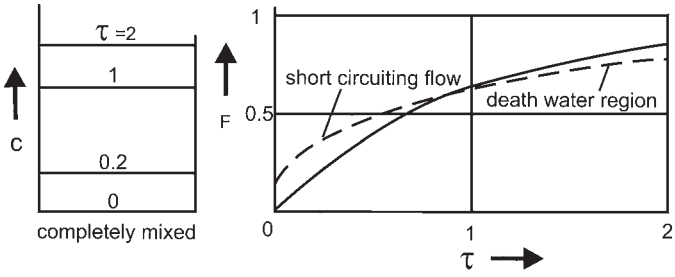


**Fig. 6.9** Retention time distribution F(τ) for a CSTR compared with one from a reactor with a short circuiting flow and eddy water regions.

### 6.3.3 Completely Mixed Tank Cascade

This type of reactor is only rarely utilized in biological wastewater treatment. But we can compare the responses shown in retention time distribution measurements of a tube reactor with axial dispersion with those for a tank cascade. This enables us to calculate the theoretical number of stages which a real tube reactor has (see Section 6.3.5).

The model for n CSTR tanks consists of n tracer balances:

$$V_1 \frac{dc_1}{dt} = Q_0 (c_0 - c_1)$$

$$V_2 \frac{dc_2}{dt} = Q_0 (c_1 - c_2) \qquad (6.95)$$

...

$$V_n \frac{dc_n}{dt} = Q_0 (c_{n-1} - c_n)$$

with the solution for the probability distribution of residence times:

$$F(\tau) = 1 - \exp(-n\tau) \left[ 1 + n\tau + \frac{(n\tau)^2}{2!} + \ldots + \frac{(n\tau)^{n-1}}{(n-1)!} \right] \qquad (6.96)$$

Some results are given in Fig. 6.10.

With increasing n, the probability distribution approaches that of a plug flow reactor, which is the same as a cascade of $n = \infty$ stages (Hill 1977; Chow et al. 1979). By differentiation of Eq. (6.96), the probability density follows:

$$E(\tau) = \frac{dF(\tau)}{d\tau} = n \exp[-n\tau] \frac{(n\tau)^{n-1}}{(n-1)!} \qquad (6.97)$$

(Froment and Bischoff 1979; Chow et al. 1979). With increasing n, the peak becomes more narrow and higher.

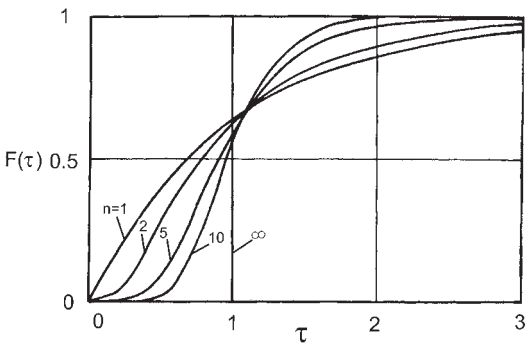


**Fig. 6.10** Retention time distribution F(τ) for a CSTR (n = 1) compared with one from a tank cascade system (n = 2 ... ∞) (Wen and Fan 1975).

### 6.3.4 Tube Flow Reactor With Axial Dispersion

The model for the tank cascade starts with one CSTR coupled with a second stage and so on. Alternatively, we shall begin with a PFR model which is extended by a dispersion term:

$$\frac{dc}{d\tau} = -\bar{w} \frac{dc}{dx} + D_x \frac{d^2c}{dx^2} \qquad (6.98)$$

By using the Peclet number:

$$Pe' = \frac{\bar{w}\, L}{D_x} \tag{6.99}$$

the tracer balance can be written in dimensionless form:

$$\frac{dC}{d\tau} = -\frac{dC}{d(x/L)} + \frac{1}{Pe'}\,\frac{d^2C}{d(x/L)^2} \tag{6.100}$$

For a flow reactor with sludge recycle:

$$Pe = \frac{\bar{w}\,(1+n_R)\,L}{D_x} \tag{6.80}$$

must be introduced instead of Eq. (6.99). One initial and two boundary conditions are needed.

Several different types of boundary conditions exist (Wen and Fan 1975). We want to limit the discussion only to the type of boundary condition "closed, closed". Closed boundary means, that in both tubes at the left and right side of the reactor (see Fig. 6.7) are no concentration gradient because of the low section area compared with that inside the reactor.

These boundary conditions are:

$$t = 0, \quad x \geq 0, \quad c = 0 \tag{6.101}$$

$$t > 0, \quad x = 0, \quad w c_0 = w c - D_x \frac{dc}{dx} \tag{6.102}$$

$$t > 0, \quad x = L, \quad \frac{dc}{dx} = 0 \tag{6.103}$$

The first analytical solution of Eq. (6.98) respectively Eq. (6.100) was published by Danckwerts 1955. We only want to present this solution in graphical form (Wen and Fan 1975):

$$Pe' = \frac{wL}{D_x} = 0$$

characterizes the limit for $D_x \gg wL$, which agrees with the signal of a CSTR, In contrast to that, $Pe' \approx \infty$ shows the signal of a ideal plug flow reactor without an axial mixture.

### 6.3.5
### Comparison Between Tank Cascades and Tube Flow Reactors

How we can compare a tube flow reactor with axial dispersion with a series of tanks in cascade? How many stages of a cascade correspond to the same degree of backmixing of a system with a known Peclet number?

Figure 6.12 presents the response to an impulse-formed input. This response is given by Eq. (6.90). $t = t_R$ follows from the correspondence of $A_1 = A_2$.

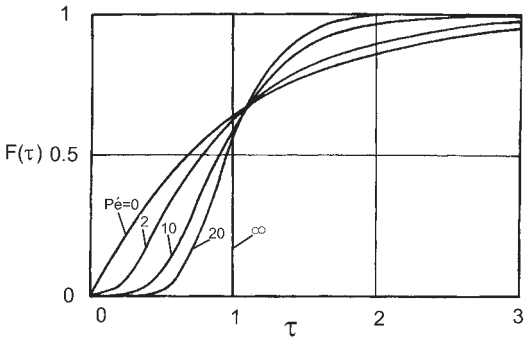


**Fig. 6.11** Retention time distribution F(τ) for a CSTR (Pe′ = 0) compared with one of real tube flow reactors (Pe′ = 2 ... ∞) (Wen and Fan 1975).

The variance according to the property t being investigated is (Froment and Bischoff 1979):

$$\sigma_t^2 = \int_0^\infty E(t)\,(t - t_R)^2\,dt \tag{6.104}$$

Using Eq. (6.104):

$$\sigma^2 = \frac{\sigma_t^2}{t_R^2} = \frac{2}{Pe'} - \frac{2\,(1 - \exp(-Pe'))}{Pe'^2} \tag{6.105}$$

is obtained for a "closed, closed" vessel (Wen and Fan 1975; Levenspiel 1979).

At high Pe′ numbers low dispersion results:

$$\sigma^2 = \frac{2}{Pe'} \tag{6.106}$$

If we consider a tank cascade, Eq. (6.97) must be introduced into Eq. (6.104). A simplified result can be estimated:

$$\sigma^2 = \frac{\sigma_t^2}{t_R^2} = \frac{1}{n} \tag{6.107}$$

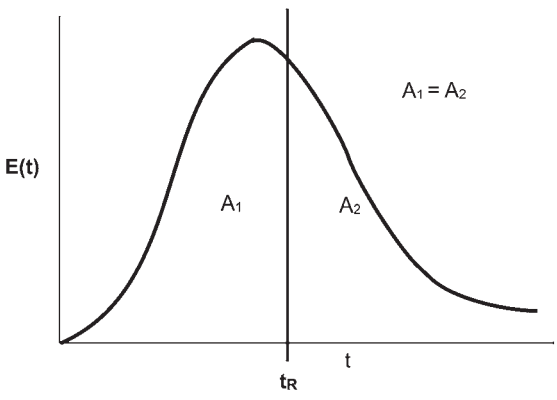


**Fig. 6.12** Retention time density distribution E(t) for a tube flow reactor (qualitative drawing).

Combining Eq. (6.105) and (6.107), we obtain

$$n = \frac{Pe'^2}{2\,(Pe' - 1 + \exp\,(-Pe'))} \tag{6.108}$$

For $Pe' \gg 1$, then

$$n = \frac{Pe'}{2} \tag{6.109}$$

results. This is an approximation and results f.e. in n = 50 for Pe′ = 100. The exact solution from Eq. (6.108) is n = 50.55.

## 6.4 Technical Scale Activated Sludge Systems for Carbon Removal

Based on hydrodynamic properties and the special models needed for the description of bacterial growth, carbon removal and oxygen consumption, activated sludge reactors can be divided into three groups: (a) nearly completely mixed tank reactors (Fig. 6.13a), (b) nearly completely mixed tank reactor cascades (Fig. 6.13b) and (c) tube flow reactors with axial dispersion (Fig. 6.13c).

A large number of reactor types belong to group (a). Figure 6.13a presents a selection of three systems. However, measurements of residence time distribu-

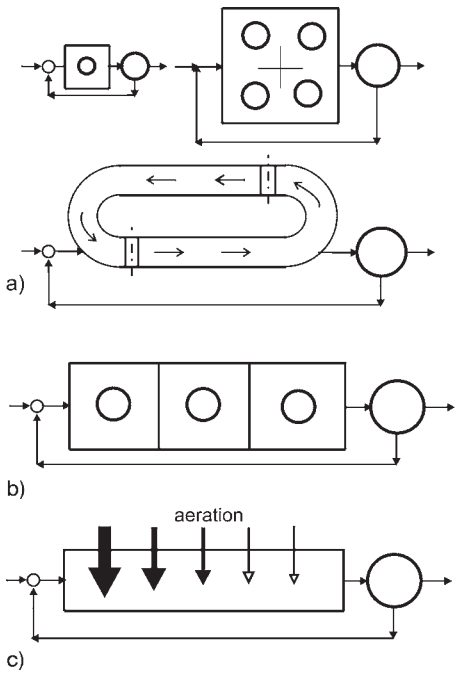


**Fig. 6.13** Standard activated sludge systems. (a) Completely mixed tank reactors. (b) Closed tanks in series, frequently used for pure oxygen. (c) Flow tube reactor with diminishing aeration intensity.

tions are typically not performed. As a result, considerable deviations from the CSTR occasionally exist. In Fig. 6.14, two special types of these reactors are shown: a Bio-Hochreaktor for the treatment of industrial effluents with a height of 20–24 m (Fig. 6.14a) and a Putox-Belebungsanlage for the treatment of municipal wastewater from small housing areas, which is built into the ground (Fig. 6.14b).

Tank reactors connected in series have frequently been used for "pure oxygen WWTPs". The greatest interest was often not the reduction of the degree of mixing, but the more efficient utilization of oxygen. Therefore, the waste gas of the first stage ($O_2$, $N_2$, $CO_2$) is dispersed again to take advantage of the relatively high residual oxygen concentration. Normally, cascades with three or four stages are operated; and both the wastewater and the gas flow in the same direction, resulting in a high removal rate in the first stage and a low removal rate in the last stage, where only a small decrease in $BOD_5$ occurs (see Fig. 6.13b).

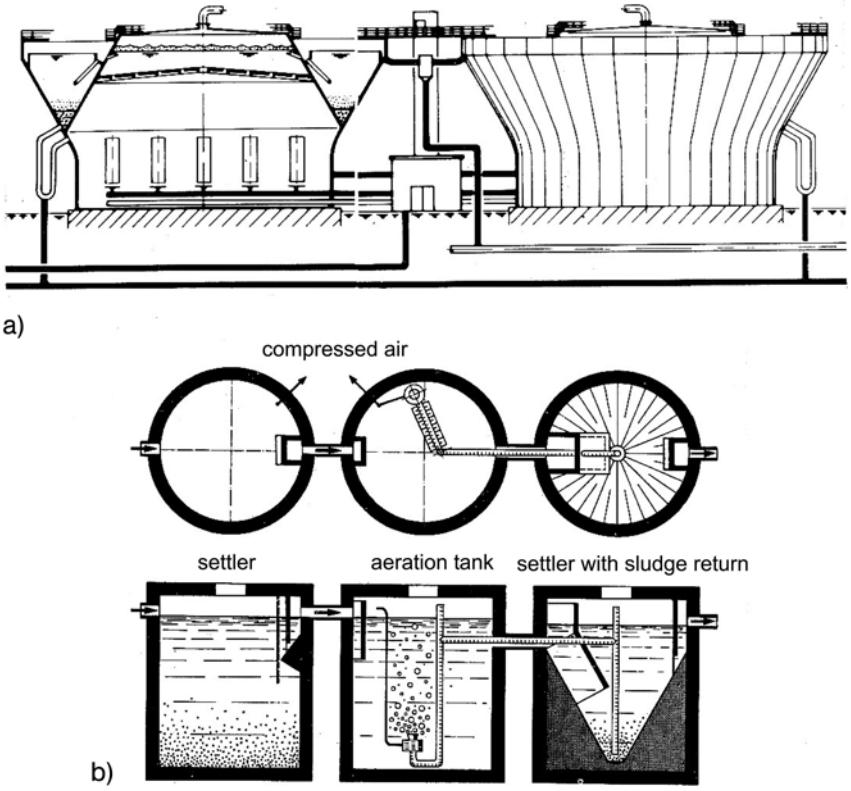


**Fig. 6.14** Special types of completely mixed tank reactors in technical scale. (a) Bio-Hochreaktor for the treatment of high-load effluents (Hoechst AG; Leistner et al. 1979). (b) Putox-Belebungsanlage for domestic effluents (5–1500 inhabitants) (Purator, Vienna).

Tube flow reactors, in contrast, are open systems (Fig. 6.13c). They typically have a length of up to 300 m and are constructed in a meandering form to make better use of the available area and to reduce pipe lengths for sludge return lines. A pressurized aeration system is often used (porous ceramics or membranes) and the number of the aerators per basin area is changed from higher values near the wastewater influent to lower values near the effluent.

**PROBLEM 6.1**

A municipal wastewater ($Q_0 = 10^4$ m$^3$ d$^{-1}$, $S_0 = 500$ mg L$^{-1}$ COD, $X_e = 0$ mg L$^{-1}$) is to be treated by an activated sludge process. The aerobic reactor is completely mixed. For a bacterial concentration of $X = 2$ g L$^{-1}$ MLSS, an effluent COD concentration of $S = 25$ mg L$^{-1}$ COD of dissolved biodegradable substances should be reached.

Coefficients:

$Y^o_{X/S} = 0.43$ g MLSS/g COD
$\mu_{max} = 7.2$ d$^{-1}$
$K_S = 100$ mg L$^{-1}$ COD
$k_d = 0.24$ d$^{-1}$

1. Calculate the sludge age $t_{RX}$ and the critical sludge age $t_{RXC}$.
2. Calculate the reactor volume V.
3. What is the mass flow rate of the surplus sludge which must be removed daily?
4. What is the critical mass flow rate?
5. Calculate the mass of bacteria which will be reduced by bacterial decay daily.

**Solution**

(1) First we have to calculate the sludge age $t_{RX}$ needed, using:

$$S = \frac{K_S\,(1 + k_d\,t_{RX})}{t_{RX}\,(\mu_{max} - k_d) - 1} \tag{6.49}$$

and eliminating:

$$t_{RX} = \frac{K_S + S}{S\,(\mu_{max} - k_d) - K_S\,k_d} = 0.833 \text{ d} = 20 \text{ h}$$

The critical sludge age is:

$$t_{RXC} = \frac{K_S + S_0}{S_0\,(\mu_{max} - k_d) - K_S\,k_d} = 0.173 \text{ d} = 4.16 \text{ h}$$

(2) The reactor volume V follows from the substrate balance:

$$Q_0 (S_0 - S) = \frac{\mu_{max}}{Y^\circ_{X/S}} X \frac{S}{K_S + S} V$$

$$V = \frac{Q_0 (S_0 - S)\, Y^\circ_{X/S} (K_S + S)}{\mu_{max} XS} = 709\ m^3$$

(3) The concentration of excess sludge (without considering sludge thickening by sedimentation) follows from balances for S

$$0 = Q_0 (S_0 - s) - \frac{\mu XV}{Y^\circ_{X/S}}$$

and for X

$$0 = -Q_0 X + \mu XV - k_d XV$$

After elimination of μ:

$$Q_0 X = Y^\circ_{X/S} \frac{Q_0 (S_0 - S)}{1 + k_d}$$

$$= 0.43 \frac{10^4\ 475}{1 + 0.24}\ mg\ MLSS \cdot L^{-1}$$

$$= 1647\ kg\ d^{-1}\ MLSS$$

(4) For $k_d = 0$ and $X_e = 0$ (no bacteria in the overflow of the settler) the mass flow rate for the surplus sludge follows

$$Q_0 X = 2042\ kg\ m^{-3}\ MLSS$$

During biodegradation of $Q_0 (S_0 - S) = 4750\ kg\ h^{-1}$ MLSS a mass of $2042 - 1647 = 395\ kg\ d^{-1}$ MLSS was removed by bacteria decay

(5) Using

$$t_{RXC} = \frac{VX}{Q_{ex,c} X}$$

the critical removal rate of the excess sludge follows:

$$Q_{ex,c} X_R = \frac{VX}{t_{RXC}} = \frac{709 \cdot 2}{0.173} = 8197\ kg\ d^{-1}\ MLSS$$

For a sludge removel of more than 8200 during some days all bacteria of the activated sludge plant were washed out.

**PROBLEM 6.2**

The same municipal wastewater as described in Problem 6.1 must be treated in an activated sludge reactor by extended aeration. The amount of surplus sludge is to be reduced by a factor of 2, compared to the maximum value given by $Y^{\circ}_{X/S} = 0.43$ g MLSS (g COD)$^{-1}$.

The sludge thickening ratio is $n_E = 2.5$.

The recycle ratio is $n_R = 0.8$.

1. Which sludge age must be selected?
2. Calculate the necessary reactor volume.
3. Compare these results with those of Problem 6.1.

**Solution**

(1) From: $$Y_{X/S} = Y^{\circ}_{X/S}\left(1 - \frac{k_d}{\mu}\right) \tag{4.27}$$

and:

$Y_{X/S} = 0.5\ Y^{\circ}_{X/S}$

it follows that: $\mu = 2\ k_d = 0.48\ d^{-1}$

$$\mu = \mu_{max}\frac{S}{K_S + S}$$

The sludge age follows from:

$$t_{RX} = \frac{K_S + S}{S(\mu_{max} - k_d) - K_S k_d} = 4.17\ d$$

(2) The reactor volume V follows from the substrate balance:

$$Q_0(S_0 - S) = \frac{\mu_{max}}{Y^{\circ}_{X/S}}\ X\ \frac{S}{K_S + S}\ V$$

$$V = \frac{Q_0(S_0 - S)\,Y^{\circ}_{X/S}(K_S + S)}{\mu_{max}\,S\,X} = 2208\ m^3$$

(3) Comparison with the results from Problem 6.1:

Problem 6.1: $t_{RX} = 0.833$ d, S = 25 mg L$^{-1}$ COD and V = 709 m$^3$
excess sludge: 1702 kg d$^{-1}$ MLSS

Problem 6.2: $t_{RX} = 4.217$ d, S = 7.14 mg L$^{-1}$ COD and V = 2208 m$^3$
excess sludge: 1065 kg d$^{-1}$ MLSS

## References


Arden, E.; Locket, W.T. **1914**, Experiments on the oxidation of sewage without the aid of filters, *J. Soc. Chem. Ind.* 35, 523–539.

Benedek, P.; Horvath, I. **1967**, A practical approach to activated sludge kinetics, *Water Res.* 1, 663.

Benefield, L.D.; Randall, C.W. **1980**, *Biological Process Design For Wastewater Treatment*, Prentice-Hall, Englewood Cliffs, N.J.

Button, D.K.; Gurver, J.C. **1966**, Continuous culture of *Torulopsis utilis*: a kinetic study of oxygen limited growth, *J. Gen. Microbiol.* 45, 195.

Chen, Y.R.; Hashimoto, A.G. **1980**, Substrate utilization kinetic model for biological treatment processes, *Biotechnol. Bioeng.* 22, 2081–2095.

Chow, V.T.; Eliassan, R.; Linsley, R.K. **1979**, *Wastewater Engineering*, McGraw-Hill, New York.

Danckwerths, P.V. **1955**, Continuous flow systems, distribution of residence times, *Chem. Eng. Sci.* 2.1

Eckenfelder, W.W. **1967**, Comparative biological waste treatment design, *J. Sanit. Eng. Div. S.A.* 6, 157–170.

Fan, L.T. **1970**, Effect of axial dispersion on the optimal design of the activated sludge process, *Water Res.* 4, 271.

Fan, L.T.; Erickson, L.E.; Shah, P.S.; Tsai, B.I. **1970**, Effect of mixing on the washout and steady state performance of continuous cultures, *Biotechnol. Bioeng.* 12, 1019–1068.

Froment, G.F.; Bischoff, K.B. **1979**, *Chemical Reactor Analysis And Design*, John Wiley & Sons, New York.

Grady, C.P.; Daigger, G.T.; Lim, H.C. **1999**, *Biological Wastewater Treatment*, Marcel Dekker, New York.

Henze, M.; Harremoes, P.; Jansen, J.C.; Arvin, E. **2002**, *Wastewater Treatment*, Springer Verlag, Berlin.

Herbert, D. **1958**, Some principles of continuous culture, in: *Recent Progress in Microbiology*, ed. G. Tunevall, Blackwell Scientific, Oxford.

Hill, C.G. **1977**, *An Introduction To Chemical Enginering Kinetics And Reactor Design*, John Wiley & Sons, New York.

Lawrence, A.W.; McCarty, P.L. **1970**, Unified basis for biological treatment design and operation, *J. Sanit. Eng. Div. S.A.* 3, 767–778.

Leistner, G.; Müller, G.; Sell, G.; Bauer, A. **1979**, Der Bio-Hochreaktor – eine biologische Abwasserreinigungsanlage in Hochbauweise, *Chem. Ing. Tech.* 51, 288

Levenspiel, O. **1962**, *Chemical Reaction Engineering*, John Wiley & Sons, New York.

Levenspiel, O. **1979**, The Cemical Reaction, Omnibook, OSU Book Stores, Inc., Corvallis, Oregon, USA.

Lin, S.H. **1979**, Axial dispersion in post-aeration basins, *J. W.P.C.F.* 51, 985–990.

Mehring, A. **1979**, Zur Berechnung des Belebtschlammreaktors als ein- und mehrstufiges Mischbecken unter Berücksichtigung der Sauerstoffbilanz, PhD thesis, TU Berlin.

Metcalf and Eddy **1979**, reviewed by G. Tchobanoglous: *Wastewater Engineering: Treatment, Disposal, Reuse*, McGraw-Hill, New York.

Monod, J. **1942**, Recherches sur la croissance de cultures bactériennes. In: *Actualités Scientifique et Industrielles 911 Microbiologie*, Herrmann & Cie, Paris.

Monod, J. **1950**, La technique of Culture Continue: Theorie et Applications, *Ann. Inst. Pasteur* 79, 390–410.

Nazaroff, W.W.; Alvarez-Cohen, L. **2001**, *Environmental Engineering Science*, John Wiley & Sons, New York.

Peil, K.M.; Gaudy Jr., A.F. **1971**, Kinetic constants for aerobic growth of microbial populations selected with various single compounds and with municipal wastes as substrates, *Appl. Microbiol.* 21, 253.

Pippel, W. **1978**, *Verweilzeitanalyse in technologischen Strömungssystemen*, Akademie-Verlag, Berlin.

Pirt, S.J. **1965**, The maintenance energy of bacteria in growing cultures, *Proc. R. Soc. Lond. B* 163, 224.

Putnaerglis, A. **1987**, Einfluss der Sauerstoffkonzentration und der Stufenzahl auf den aeroben Substratabbau in Belebtschlammreaktor-Kaskaden – Kinetik und reaktionstechnische Modellierung, *VDI-Forschungsberichte, Reihe* 15, 49.

Reynolds, T.D.; Yang, J.T. **1966**, Model of the completely mixed activated sludge process, *Proc. Ind. Waste Conf.* 21, 696.

Sinclair, C.G.; Ryder, D.N. **1972**, Model for the growth of aerobic microorganisms under oxygen limiting conditions, *Biotechnol. Bioeng.* 14, 787.

Strnivasaraghanan, R.; Gaudy Jr., A.F. **1974**, Operational performance of an activated sludge process with constant sludge feedback, *Proc. Ind. Waste Conf.* 24, 197.

Sundstrom, D.W.; Klei, H.E. **1979**, *Wastewater Treatment*, Prentice-Hall, Englewood Cliff, N.J.

Vasilin, V.A.; Vasilyev, V.B. **1978**, Mathematical models of biological waste treatment processes for the design of aeration tanks, *Water Res.* 12, 491–501.

Wen, C.Y., Fan, L.T. **1975**, Models for Flow Systems and Chemical Reactors, Marcel Dekker, Inc., New York.

Winkler, M.A. **1981**, *Microbial Treatment of Wastewater*, Ellis Horwood, Chichester.

# 7
# Aerobic Treatment with Biofilm Systems

## 7.1
## Biofilms

Biofilms are small ecosystems usually consisting of three layers of differing thickness, which change in thickness and composition with location and over time (Meyer-Reil 1996). In the *first phase* of colonization, macromolecules are adsorbed at clean solid surfaces (proteins, polysaccharides, lignin; Wingender and Flemming 1999), because they are transported from the bulk liquid to the solid surface faster than the microorganisms are. As a consequence of this adsorption, the coverage of the solid surface with water is reduced. During the *second phase*, microbial cells attach to this prepared surface. Frequently, they do not form closed layers of uniform thickness, rather they form small attached colonies, which may spread by growth and further attachment. Usually, these cells are supplied with substrate and oxygen and are able to grow at their maximum rate. During this process, they produce organic molecules, which diffuse through the cell wall and to *e*xtracellular *p*olymeric *s*ubstances (EPS) catalyzed by exoenzymes. These EPS molecules are necessary for the formation of a stable biofilm (Wingener and Flemming 1999). In the *third phase*, the biofilm may consist of bacteria and EPS, the thickness of which is a function of growth rate and depends on the stability of the biofilm and the shear stress of the flowing water (Van Loodsrecht et al. 1995). At lower shear stresses, eukaryotic organisms (protozoa, insects, their eggs and larvae) typically establish themselves. All these organisms live in a community. Materials such as substrates and oxygen are transported into the biofilm by diffusion and convection and the products are transported out of the biofilm.

Oxygen may reach only into the exterior part of the biofilm, resulting in a growth of aerobic microorganisms such as nitrifying bacteria and protozoa. Nitrate and nitrite produced in this layer are reduced by anoxic metabolism within a middle layer, resulting in an anaerobic interior layer directly at the solid surface, where acetic acid and sulfate may be reduced (Marshall and Blainey 1991; Fig. 7.1).

Heterogeneous biofilms grow on the sides of ships and on buildings near the water's edge, inside human and animal mouths and within inner organs. They frequently cause damage to these surfaces (biocorrosion) and must be removed. In the area of environmental biotechnology, however, they can be utilized to advantage in certain bioreactors, such as:

*Fundamentals of Biological Wastewater Treatment*. Udo Wiesmann, In Su Choi, Eva-Maria Dombrowski

ISBN: 978-3-527-31219-1

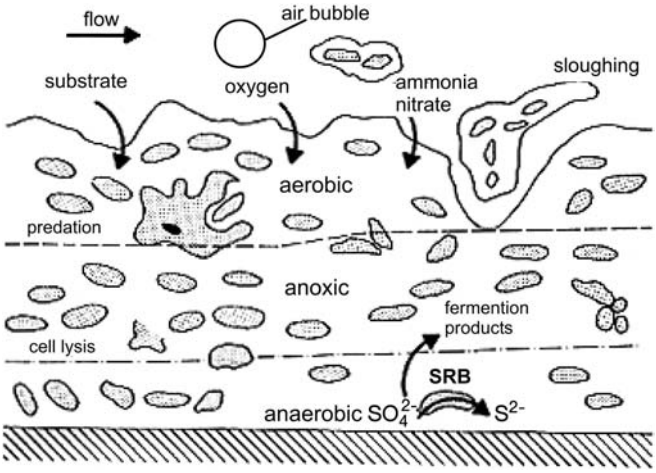


**Fig. 7.1** Biofilm model (according to Marshall and Blainey 1991).

- trickling filters,
- submerged, aerated fixed bed reactors,
- rotating disc reactors.

The formation of biofilms is a requirement for their effectiveness. This chapter will describe these bioreactors and their application and will discuss some models of the processes, which are useful for understanding how they function.

## 7.2 Biofilm Reactors for Wastewater Treatment

### 7.2.1 Trickling Filters

A trickling filter consists of a layer of solid particles or bundles of synthetic material inside a cylindrical (Fig. 7.2) or prismoid container. Wastewater must be distributed uniformly at the top of the fixed bed – frequently by a rotating system of two or four horizontal tubes equipped with many nozzles.

To compensate for the fact that the area of a circular section of the reactor increases with distance from the center, the distance between nozzles must decrease the further they are away from the center in order to have an even distribution of water over the surface. Furthermore, the changes in available pressure in the rotating tubes must be considered as a function of the flow rate. Uniform distribution of the wastewater and uniform packing of the reactor with solid substances are of high importance for a high loading and removal rate. It is critical to ensure that two conditions are met:

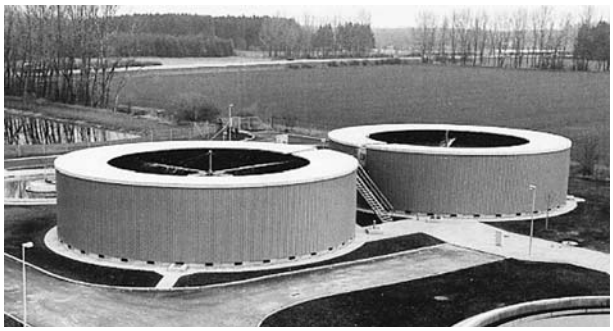

**Fig. 7.2** Trickling filter, BIO-NET, Norddeutsche Seekabelwerke, Germany.

- The downward flowing liquid films must be in direct contact with the biofilm (i.e. the biofilm has to be trickled over all places and at all times) and must be in contact with the upward or downward flowing air (i.e. the trickling filter should not be flooded at any location or time).
- The wastewater must be practically free of solids. It is absolutely necessary that the wastewater passes a primary settler under controlled conditions which is never overloaded.

We distinguish between:

- *Natural aeration* as a result of density differences between the air saturated with moisture inside the trickling filter and the air outside the trickling filter, and
- F*orced aeration* by a ventilator at the top of the trickling filter. In this case, the reactor may have a height of up to 12 m and is filled with packages of synthetic supporting material.

Effective natural aeration can be expected in winter and summer. In winter, the density of cold air is greater than that of the warmer air inside the trickling filter and the air flows upwards. Accordingly, the air flows downwards in summer. In every year, there are some critical situations when water and air temperatures are nearly the same. During those times, the efficiency of trickling filters is reduced.

The composition of the biofilm of a trickling filter varies with the season. In summer, the activity of the organisms is very high. Small filter flies (Psychoda) and other insects, such as water springtails (Podura) and midges (Chironomus) as well as various protozoa lead to a thicker and more porous biofilm (Fair et al. 1986). During the autumn, this third phase of the biofilm is nearly completely sheared off and a thinner film of higher density remains. In every season of the year, smaller parts of the biofilm are rinsed away, but if the ecosystem is changed completely, the biofilm is changed in a characteristic way.

Table 7.1 presents some data for trickling filters. They can be subdivided into four types according to their hydraulic loading, their loading of substrate and their difference from low-rate to super-high-rate trickling filters.

Using these data, one can perform the initial scale concept design for the treatment of municipal wastewater (see Problem 7.1).

**Table 7.1** Design and operation data for trickling filters (Nazaroff and Alvarez-Cohen 2001).

| Parameter | Unit | Type of trickling filter | | | |
|---|---|---|---|---|---|
| | | Low rate | Intermediate rate | High rate | Super-high rate |
| Support material | – | Rock, slag | Rock, slag | Rock | Plastic |
| Specific surface area | $m^2\ m^{-3}$ | 40–70 | 40–70 | 40–70 | 80–200 |
| Porosity | $m^3\ m^{-3}$ | 0.4–0.6 | 0.4–0.6 | 0.4–0.6 | 0.90–0.97 |
| Density of support material[a)] | $kg\ m^{-3}$ | 800–1500 | 800–1500 | 800–1500 | 30–100 |
| Hydraulic loading[b)] | $m^3\ m^{-2}\ d^{-1}$ | 0.5–3.0 | 3–10 | 8–40 | 10–70 |
| Loading per volume | $g\ m^{-3}\ d^{-1}\ BOD_5$ | 100–400 | 200–500 | 500–1000 | 500–1000 |
| Height | m | 1.0–2.5 | 1.0–2.5 | 1.0–2.5 | 3.0–1.02 |
| Recirculation ratio | – | 0 | 0–1 | 1–2 | 1–2 |
| Removal efficiency | % $BOD_5$ | 80–90 | 50–70 | 65–85 | 65–80 |

[a)] Volume includes voids.
[b)] Includes recycled flow (Metcalf and Eddy 1991; Tschobanoglous and Schroeder 1985).

### 7.2.2 Submerged and Aerated Fixed Bed Reactors

In cases of high hydraulic loading, the trickling filter may be operated as a flooded bed and the pressure differential needed for the downwards flow increases. The level of wastewater necessary to overcome the flow resistance depends on the form of the substance used as support material and the thickness of the biofilm. Aerobic fixed beds must be aerated near the bottom, producing a two-phase flow in a three-phase system with an upwards air flow. As a result of friction forces, water is transported upwards in the center of the reactor and flows downwards near its walls. Biomass is attached at the surface of the support material and is also suspended as flocs. It is not easy to avoid blockages in regions of biofilms with a higher thickness and a lower local flow rate. The fixed bed must be cleaned from time to time by considerably increasing the wastewater flow rate.

Synthetic support materials such as BIOPAC (ENVICON, Germany) have been used successfully, especially where nitrifying bacteria with lower growth rates must be immobilized (Fig. 7.3).

In contrast to fixed beds with solid particles, the flow of water and air are more easily controlled and blockages can be avoided in reactors with suspended particles. In contrast to trickling filters, their air flow rates can be adjusted to match the loading of organics and ammonia. The specific surface area can be increased to up to 400 $m^2\ m^{-3}$ (Schulz and Menningmann 1999). Using membrane-type tubular aerators, fine bubbles are produced and the mass transfer rate is increased remarkably. The suspended biological sludge detaches from the surfaces as a result of the friction forces of the flow and is conveyed to the secondary settler. Obviously, blockages do not occur. Table 7.2 presents some operational data.

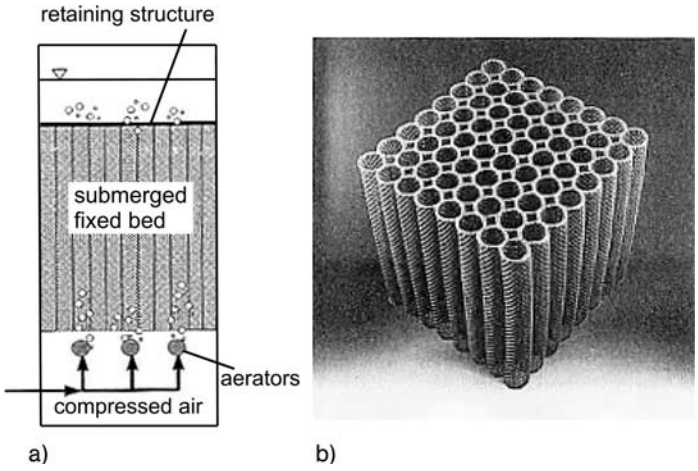


**Fig. 7.3** Submerged aerated fixed bed reactor (a) and BIOPAC (b) (ENVIRON, Germany; Schulz and Menningmann 1999).

Comparing the loading per volume with that of trickling filters (Table 7.1), we can conclude that in this kind of fixed bed reactors the loading can be increased by a factor of three for intermediate and high-rate systems and by a factor of five for super-high-rate systems. This is due to the higher specific surface area of the biofilm and the technological advances which prevent clogging in the BIOPAC system, for example (Schulz and Menningmann 1999).

**Table 7.2** Load, biofilm thickness and application of the BIOPAC system (Schulz and Menningmann 1999).

| Parameter | Type of trickling filter | | | |
|---|---|---|---|---|
| | **Low rate** | **Intermediate rate** | **High rate** | **Super-high rate** |
| Loading per area ($g\ m^{-2}\ d^{-1}\ BOD_5$) | <3 | 3–6 | 6–12 | 12–30 |
| Loading per volume ($g\ m^{-3}\ d^{-1}\ BOD_5$)[a] | <750 | 750–1500 | 1500–3000 | 3000–7500 |
| Thickness of biofilm (mm) | 1.5 | 1–4 | 4–10 | 10–20 |
| Application | Complete nitrification, C elimination | Nitrification, simultaneous C elimination | C elimination, partial nitrification | C elimination |

[a] Specific surface area a = 100–400 $m^2m^{-3}$, here assumed a = 250 $m^2m^{-3}$ (Schulz and Menningmann 1999).

### 7.2.3 Rotating Disc Reactors

In rotating disc reactors (RDR), the principle behind the intense transport of substrates and oxygen to the biofilm is different. In trickling filters and fixed bed reactors, water and air are moved; here, the support material with the biofilm are moved. In rotating disc reactors, circular plates with diameters of 1–2 m are fitted to a horizontal shaft with a spacing of a few centimeters. The system of parallel plates is submerged nearly halfway in a cylindrical tank through which wastewater flows. The packet of plates rotates at a speed of 0.5–5.0 rpm. Bacteria grow on both surfaces of the circular discs. During the portion of the rotation where the biofilm travels through the air, wastewater drips down and oxygen is taken up by convection and diffusion. Parts of the biofilm rinse off from the discs from time to time. Larger pieces settle in the tank and must be removed as surplus sludge, while smaller parts are suspended and involved in aerobic substrate degradation and further growth (carbon removal and nitrification). Figure 7.4 presents a rotating disc reactor.

The development of this kind of biofilm reactor was described in detail by Breithaupt (1997). Its practical application started in the 1960s. The company Stengelin used plates made of low-density synthetic material to decrease the weight which must be born by both bearings. This made it possible to increase the length of the shaft between the bearings to up to 7 m (Breithaupt 1997). Different materials with low density have been utilized in the past 35 years in laboratory- and pilot-scale RDRs (Table 7.3) for carbon removal and nitrification, to test new materials and to optimize the process.

In order to increase the surface area of the support material and to obtain a thicker and more stable biofilm, some authors used special synthetic media. The BIOSURF system was already used commercially in the late 1970s (Benefield and Randall 1980). Tyagi et al. (1993) utilized a polyurethane foam material for the aerobic treatment of a petroleum refinery wastewater. Breithaupt (1997) and Lindemann (2002), experimented successfully with a RDR and plates covered with a structured textile material made from polyethylene styrol.

From Table 7.3, one can see a range for loadings per reactor loading of about 500–4000 g $m^{-3}$ $d^{-1}$ COD for municipal wastewater. This agrees approximately

**Fig. 7.4** Rotating disc reactor, Mecano SA Maschinenfabrik, Schwericon SG, Switzerland.

**Table 7.3** Results for COD removal of different experiments with aerobic treatment of municipal wastewater and rotating disc reactors (Breithaupt 1997).

| Author | Support material | Inlet (mg $L^{-1}$ COD) | Removal (%) | Loading per volume (g $m^{-3}$ $d^{-1}$ COD) | Loading per area (g $m^{-2}$ $d^{-1}$ COD) | $t_R$ (h) | Volume ($m^3$) |
|---|---|---|---|---|---|---|---|
| Clark et al. (1978) | No information | 110 | 96 | 672 | 3.10 | 3.9 | 3.4 |
| Cheng (1982) | Styropor | 130 | 84 | 2136 | 10.27 | 1.5 | 39.7 |
| Gönec and Harremoes (1985) | Polyethylene | 86 | – | 480 | 7.75 | 1.7 | 0.13 |
| Wanner et al. (1990) | Polypropylene | 182 | 92 | 3984 | 11.30 | 1.1 | 1.3 |
| Stegmaier (1993) | Textile structure media | 410 | 87 | 1632 | 20.14 | 6.0 | 0.14 |

with the data from Table 7.2 for the fixed bed reactor (BIOPAC system; Schulz and Menningmann 1999; low rate up to high rate), if we equate $BOD_5$ with COD in this approximation.

Axial mixing is reduced in a RDR and the concentration of COD decreases continuously as in a tube reactor (Fig. 7.5).

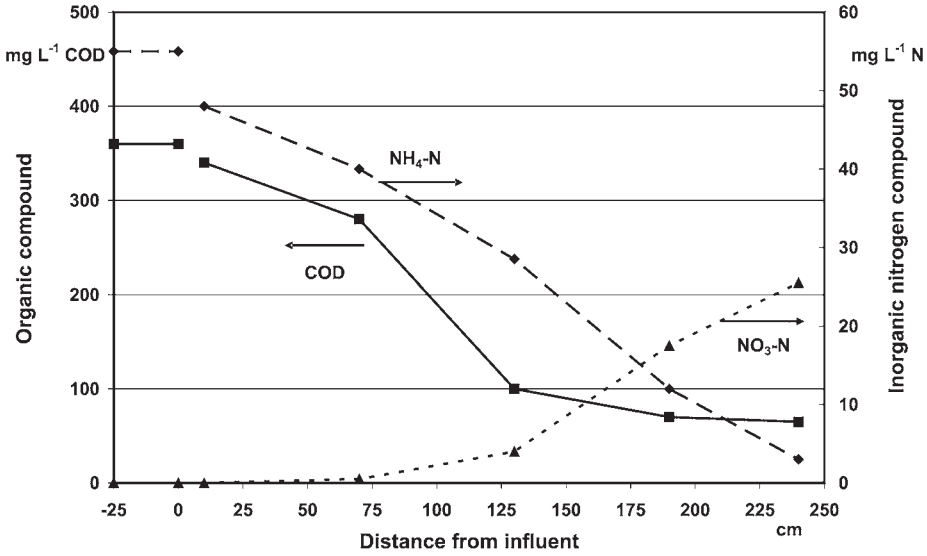


**Fig. 7.5** Decrease in local COD and $NH_4$–N concentration as well as increase in $NO_3$–N concentration during aerobic treatment in a laboratory-scale rotating disc reactor (Breithaupt 1997).

In municipal wastewater containing ammonia, nitrification occurs simultaneously as a result of the immobilization of nitrifying bacteria (see Chapter 10).

## 7.3 Mechanisms for Oxygen Mass Transfer in Biofilm Systems

From a fundamental point of view, the three trickling filter systems discussed, aerated fixed bed reactors and rotating disc reactors can all be modelled according to a mobile air bubble phase, a mobile wastewater film and a mobile biofilm. And it is for the moment unimportant whether:

- the gas-phase does not consist of bubbles (trickling filter),
- the liquid-phase does not form a film (fixed bed reactor and rotating disc reactor),
- the biofilm is moving (rotating disc reactor).

Figure 7.6 describes five situations of rate-limiting cases for the transport of oxygen. Because of the low concentration of dissolved oxygen in tap water at an air pressure of 1 bar ($T = 20\,°C$, $c^* = 9.17$ mg $L^{-1}$ $O_2$), the transport of oxygen is frequently the rate-limiting parameter. Before we study the rate-limiting processes in detail, we will discuss these cases shortly.

(I) Mass transfer gas/liquid (air/water) is rate-limiting. All conditions met for nearly complete oxygen consumption. Substrate concentrations (organics and $NH_4$) are relative high, bacterial concentration inside the biofilm is high and active, but air bubble surface area is low. The dissolved oxygen concentration decreases near the bubble surface to an even lower value. This resulting low oxygen concentration depends nearly entirely upon gas/liquid mass transfer.

(II) Mass transfer liquid/solid (water/biofilm) is rate-limiting. As a result of a high aeration rate and/or a low biofilm surface area and/or high activity, the

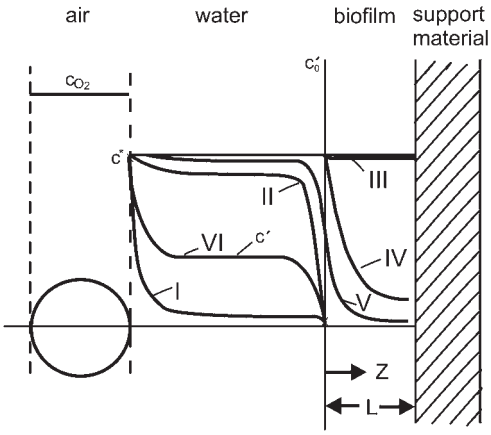


**Fig. 7.6** Oxygen mass transfer in biofilm systems. (I) Mass transfer gas/liquid is rate-limiting. (II) Mass transfer liquid/solid is rate-limiting. (III) Biological reaction is rate-limiting. (IV) Diffusion and reaction inside the biofilm are rate-limiting. (V) Diffusion and reaction inside the biofilm as well as mass transfer liquid/solid are rate-limiting. (VI) Mass transfer gas/liquid and liquid/solid are rate-limiting.

dissolved oxygen concentration is only a little lower than the saturation concentration $c^*$ and decreases near the biofilm surface to a low value. This resulting low oxygen concentration depends nearly entirely on liquid/solid mass transfer.

(III) The biological reaction is rate-limiting.

(IV) Diffusion and reaction inside the biofilm are rate-limiting. As a result of a high aeration rate, a large biofilm surface area and/or activity and a high liquid/solid mass transfer rate, the dissolved oxygen concentration is only a little lower than the saturation concentration. It decreases inside the biofilm to a low value.

(V) Mass transfer at the surface liquid/solid and the diffusion inside the biofilm are rate-limiting as a result of a high aeration rate.

(VI) Mass transfer at both surfaces is rate-limiting.

In the next section we will try to find relatively simple models for the calculation of the oxygen consumption rate for all six situations.

## 7.4 Models for Oxygen Mass Transfer Rates in Biofilm Systems

### 7.4.1 Assumptions

In this section we don't want to describe aerobic bioreactors mathematically. We will only discuss the situations mentioned in Section 7.3 by using mass balances at one point inside the reactor. Further conditions are:

- The concentration of bacteria inside the biofilm is locally constant.
- The substrate concentration should always be high enough and therefore has no influence on the removal rate.
- Endogenous respiration will be neglected.

### 7.4.2 Mass Transfer Gas/Liquid is Rate-limiting

The mass balance for oxygen at the outer surface of the biofilm is:

$$\underbrace{(k_L a)_G\,(c^* - c')}_{\text{rate of transport}} = \underbrace{r'_{max}\,\frac{c'}{K' + c'}}_{\text{rate of consumption}} = r' \qquad (7.1)$$

Using the known yield coefficient:

$$Y^{o}_{S/O_2} = \frac{r_S}{r'} \tag{7.2}$$

we must calculate $r_S$ to obtain $r'$.

In case (a), $c'$ (at the biofilm surface) may be very low compared to $c^*$ but large compared with $K'$ ($c' \gg K'$). Therefore, we can write:

$$(k_L a)_G \, c^* = r'_{max} \tag{7.3}$$

The oxygen consumption rate $r'$ and consequently the substrate removal rate $r_S$ are limited only by mass transfer (Fig. 7.6, curve I).

In case (b), $c'$ may be very low compared with $c^*$ but not large compared with $K'$. For oxygen balance, it follows that:

$$(k_L a)_G \, c^* = r' = r'_{max} \frac{c'}{K' + c'} \tag{7.4}$$

### 7.4.3
### Mass Transfer Liquid/Solid is Rate-limiting

For this case, a similar solution as in Section 7.4.2 can be obtained. Instead of $(k_L a)_G$, we only have to use $(k_L a)_L$ and to consider that the area a in $(k_L a)_L$ is now the specific surface of the biofilm (Fig. 7.6, curve II).

### 7.4.4
### Biological Reaction is Rate-limiting

Oxygen concentration is nearly constant in the liquid as well as insite the biofilm. This situation will occur for very thin biofilms and very low oxygen removal rates. For this case, the oxygen consumption rate requires Henry's law ($c^* = c_{O_2}/H$; see Fig. 7.6, curve III).

$$r' = r'_{max} \frac{c^*}{K' + c^*} = r'_{max} \frac{c_{O_2}}{K' H + c_{O_2}} \tag{7.5}$$

### 7.4.5
### Diffusion and Reaction Inside the Biofilm

In contrast to the two examples discussed above, where mass balances were written for boundary areas, we now need to write the oxygen balance for a thin slice within the biofilm, which is assumed to be smooth and of equal thickness. The oxygen balance is now written as a second-order differential equation (see Problem 7.2):

$$0 = D \frac{d^2 c'}{dz^2} - r'_{max} \frac{c'}{K' + c'} \tag{7.6}$$

The first part is the local change of the rate of diffusion inside a very thin plate of thickness dz; and the second part is the rate of oxygen consumption inside this slice.

We need to integrate twice in order to calculate $c' = f(z)$, the oxygen concentration profile inside the biofilm. For each integral, one unknown constant appears and must be determined. Thus, we need two boundary conditions for the two sides of the film (Fig. 7.6, curve IV)

$$z = 0, \; c' = c'_0 = c^* \tag{7.7a}$$

$$z = L, \; \frac{dc'}{dz} = 0 \tag{7.7b}$$

Now, we will use dimensionless numbers:

$$Mo' \equiv \frac{c^*}{K'} \text{ as the Monod number} \tag{7.8a}$$

$$C' = \frac{c'}{K'} \tag{7.8b}$$

and:

$$Z = \frac{z}{L} \tag{7.8c}$$

as well as the Damköhler-II number (Damköhler 1937, Thiele 1939):

$$Da_{II} \equiv \frac{r'_{max} L^2}{K' D} \equiv \frac{\text{reaction rate}}{\text{diffusion rate inside the biofilm}} \tag{7.9}$$

In literature, the name Thiele modulus $\equiv \sqrt{Da_{II}}$ is more common.

Equations (7.6), (7.7a) and (7.7b) can be written using these dimensionless parameters:

$$0 = \frac{d^2 C'}{dZ^2} - Da_{II} \cdot \frac{C'}{1 + C'} \tag{7.10}$$

$$Z = 0, \; C' = Mo' \tag{7.11a}$$

$$Z = 1, \; \frac{dC'}{dZ} = 0 \tag{7.11b}$$

Only numerical solutions to Eqs. (7.10) and (7.11) are available. Atkinson and Daoud (1968) were two of the first who published a solution for:

$$C' = f(Z, Da_{II}, Mo') \tag{7.12}$$

However, these concentration profiles are of limited interest. More important is to know the part of the biofilm which is supplied with oxygen and which is therefore aerobically active as well as to compare this with the highest possible activity:

$$\eta = \frac{\text{oxygen uptake rate}}{\text{maximal oxygen cosumption rate}} = \frac{r'_{eff}}{r'_{max}} \tag{7.13}$$

with $\eta \equiv$ efficiency coefficient.

The oxygen uptake rate can be calculated using the oxygen concentration profile, Eq. (7.12), and its gradient at z = 0:

$$r'_{eff} = -D \left.\frac{dc'}{dz}\right|_{z=0} \frac{A}{V} = \frac{D}{L} \left.\frac{dc'}{dz}\right|_{z=0} \tag{7.14}$$

where A is the film surface area and V is the film volume = AL; as well as:

$$r' = r'_{max} \frac{Mo'}{1 + Mo'} \tag{7.15}$$

After introducing Eqs. (7.14) and (7.15) into Eq. (7.13) and considering Eqs. (7.8) and (7.9), we obtain:

$$\eta = -\frac{(1 + Mo')}{Da_{II} \cdot Mo'} \left.\frac{dC'}{dZ}\right|_{Z=0} \tag{7.16}$$

Double logarithmic plots are presented in Fig. 7.7, showing the influence of $Da_{II}$ and Mo′. With increasing $Da_{II}$ (reaction rate compared to diffusion rate) and decreasing Mo′ (dissolved oxygen concentration at boundary liquid/solid), a decreasing part of the biofilm can be supplied with oxygen (Atkinson and Davies 1967; Atkinson and Daoud 1968).

For $Mo' \ll 1$, the reaction approximates a first order reaction with:

$$\eta = -\frac{1}{Da_{II} \cdot Mo'} \left.\frac{dC'}{dZ}\right|_{Z=0} \tag{7.17}$$

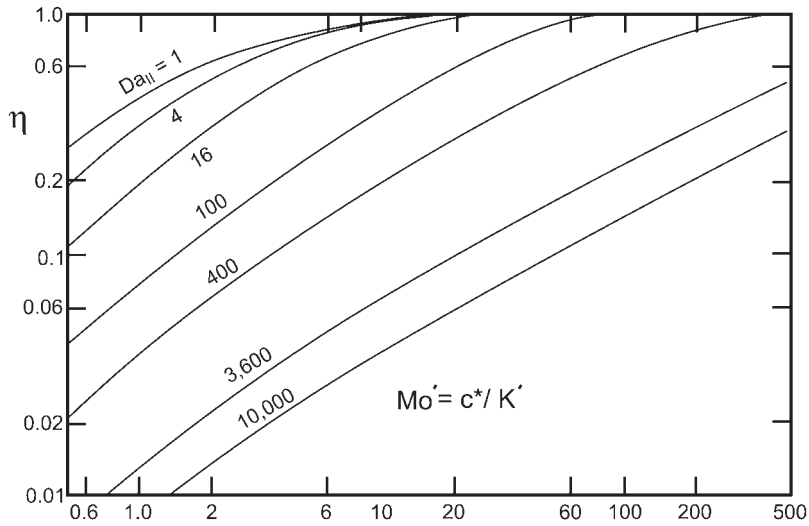


**Fig. 7.7** Diffusion and reaction inside of a plane biofilm without the influence of mass transfer liquid/solid; $Da_{II} = r'_{max} L^2/K' D$, $Mo' = c^*/K'$ (Atkinson and Daoud 1967).

and an analytical solution exists (Damköhler 1937; Thiele 1939):

$$\eta = \frac{\tanh Da_{II}}{Da_{II}} \tag{7.18}$$

which is not influenced by the Monod number.

### 7.4.6 Influence of Diffusion and Reaction Inside the Biofilm and of Mass Transfer Liquid/Solid

The influence of an additional mass transfer resistance at the liquid/solid interface must be considered for the case of low ($k_La$) values (Fig. 7.6, curve V). The required oxygen uptake rate can only be guaranteed for sinking concentrations $c'_0$ at $z = 0$.

The boundary condition, Eq. (7.7a), must be replaced by:

$$z = 0\,, -D\left.\frac{dc'}{dz}\right|_{z=0} \frac{A}{V} = (k_La)_L\,(c^* - c'_0) \tag{7.19}$$

After consideration of Eq. (7.7b) as well as:

$$Bi \equiv \frac{(k_La)_L\,L^2}{D} \tag{7.20}$$

which is called the Biot number as a relation of:

$$Bi \equiv \frac{\text{mass transfer rate liquid/solid}}{\text{diffusion rate inside the biofilm}}$$

then Eq. (7.19) can be rewritten in dimensionless form:

$$Bi\,(Mo' - C'_0) = -\left.\frac{dC'}{dZ}\right|_{Z=0} \tag{7.21}$$

Now, $\eta$ is influenced by three numbers:

$$\eta = f(Da_{II}, Bi, Mo') \tag{7.22}$$

and it is very difficult to present the field of results using only one figure. Therefore, we will not discuss these results in detail. Notice that, with decreasing Biot number (decreasing concentration $c'_0$ as a result of decreasing mass transfer rate liquid/solid), the process is controlled more and more by liquid/solid mass transfer and the efficiency coefficient $\eta$ decreases. Finally, the problem corresponds to that of Section 7.4.3. Also, the problem corresponds to that of Section 7.4.5 for high Bi numbers; and this follows from a high $(k_La)_L$ and biofilm thickness L.

Results for a spherical particle filled with bacteria or enzymes were published by Fink and Schultz (1973).

### 7.4.7
### Influence of Mass Transfer Rates at Gas Bubble and Biofilm Surfaces

A total specific mass transfer rate can be defined by Eq. (7.23):

$$K\,a\,(c^* - c'_0) = (k_L a)_G\,(c^* - c') \tag{7.23}$$

as well as by Eq. (7.24):

$$K\,a\,(c^* - c'_0) = (k_L a)_L\,(c' - c'_0) \tag{7.24}$$

K is the overall mass transfer coefficient.

Notice that $c^*$ is the concentration of oxygen at the bubble surface and $c'_0$ is the concentration of oxygen at the biofilm surface.

We write:

$$c^* - c'_0 = (c^* - c') + (c' - c'_0) \tag{7.25}$$

respectively:

$$\Delta c_\Sigma = \Delta c_1 + \Delta c_2 \tag{7.26}$$

After dividing Eq. (7.23) by Eq. (7.24) and using Eq. (7.25), we obtain:

$$\underbrace{\frac{1}{K\,a}}_{\substack{\text{total resistance}\\ \text{to mass transfer}}} = \underbrace{\frac{1}{(k_L a)_G}}_{\substack{\text{resistance}\\ \text{at gas film}}} + \underbrace{\frac{1}{(k_L a)_L}}_{\substack{\text{resistance}\\ \text{at biofilm}}} \tag{7.27}$$

Equation (7.27) is comparable to the addition of two electrical resistors which are coupled in series. For a high $(k_L a)_G$, only mass transfer liquid/solid at the biofilm is relevant (Section 7.4.2) and vice versa (Section 7.4.3). A possible concentration profile is presented as curve VI in Fig. 7.6.

**PROBLEM 7.1**

A trickling filter should be constructed for the pre-treatment of municipal wastewater. The flow rate is $Q_0 = 10^5\ m^3\ d^{-1}$ and the influent concentration is $S_0 = 250\ mg\ L^{-1}\ BOD_5$. Two different cases should be compared (see Table 7.1):

1. Intermediate loading, supporting material: rock
   Load per volume $B_v = 350\ g\ m^{-3}\ d^{-1}\ BOD_5$
   Hydraulic load $\overline{w} = 7\ m^3\ m^{-2}\ d^{-1}$
2. Super-high-rate, supporting material: plastic
   Load per volume $B_v = 1000\ g\ m^{-3}\ d^{-1}\ BOD_5$
   Hydraulic load $\overline{w} = 40\ m^3\ m^{-2}\ d^{-1}$

Calculate volume V, cross sectional area A and height H.

**Solution**

Loading per volume: $B_v = \frac{Q_0 S_0}{V}$

$$V = \frac{Q_0 S_0}{B_v} = \frac{10^5 \cdot 250}{350} = 7.14 \cdot 10^4 \text{ m}^3$$

Hydraulic loading: $\bar{w} = \frac{Q_0}{A}$

$$A = \frac{Q_0}{\bar{w}} = 1.4 \cdot 10^4 \text{ m}^2$$

$$H = \frac{V}{A} = \frac{7.14}{1.4} = 5.1 \text{ m}$$

Loading per volume: $B_v = \frac{Q_0 S_0}{V}$

$$V = \frac{Q_0 S_0}{B_v} = \frac{10^5 \cdot 250}{1000} = 2.5 \cdot 10^4 \text{ m}^3$$

$$A = \frac{Q_0}{\bar{w}} = \frac{10^5}{40} = 2.5 \cdot 10^3 \text{ m}^2$$

$$H = \frac{V}{A} = \frac{2.5 \cdot 10^4}{2.5 \cdot 10^3} = 10 \text{ m}$$

If this synthetic supporting material is used instead of rock, the volume of the trickling filter can be reduced by a factor of 2.9 and the cross-sectional area by a factor of 5.6.

## PROBLEM 7.2

A biofilm of aerobic bacteria with a thickness of L = 0.2 mm has to be supplied with oxygen to degrade organics in wastewater. The degradation rate is limited by the oxygen concentration inside the biofilm and is not limited by the organic concentration. The concentration of dissolved oxygen is $c' = c^* = 3$ mg $L^{-1}$ $O_2$ and it does not decrease remarkably near the boundary liquid/solid.

Given data:

$\mu_{max}$ = 10 $d^{-1}$, X = 10 g $L^{-1}$ MLSS inside the biofilm, $Y^{\circ}_{X/O_2}$ = 0.5 g MLSS (g $O_2$)$^{-1}$, $K' = 0.1$ mg $L^{-1}$ $O_2$, $D_{O_2} = 10^{-6}$ $cm^2$ $s^{-1}$.

Calculate the efficiency coefficient η.

**Solution**

Damköhler II number: $Da_{II} = \dfrac{r'_{max} L^2}{D_{O_2} K'}$

Maximum oxygen uptake rate inside the biofilm:

$$r'_{max} = \frac{\mu_{max} X}{Y^o_{X/O_2}} = \frac{10 \cdot 10}{0.5} = 200 \frac{g\ O_2}{L\ d}$$

$$Da_{II} = \frac{200 \cdot 0.04}{10^{-6}\ 0.1} \frac{g\ O_2\ mm^2 s\ L}{L \cdot d\ cm^2 mg\ O_2}$$

$$Da_{II} = 80 \cdot 10^6 \frac{10^3}{24 \cdot 3600 \cdot 10^2} = 0.93 \cdot 10^4$$

$$Da_{II} = 9300$$

$$Mo' = \frac{c^*}{K'} = \frac{3}{0.1} = 30$$

From Fig. 7.7 for $Da_{II} = 9300$ and $Mo' = 30$ we find: $\eta = 0.08$.

Therefore, only 8% of the biofilm is sufficiently supplied with oxygen and is thus able to grow and to degrade the organics in the wastewater.

## References


Atkinson, B.; Daoud, I.S. **1968**, The analogy between microbiological "reactions" and heterogeneous catalysis, *Trans. Inst. Chem. Eng.* 46, T19–T24.

Atkinson, B.; Davies, L.J. **1967**, The overall rate of substrate uptake (reaction) by microbial films, part I – a biological rate equation, *Trans. Inst. Chem. Eng.* 45, T257–T264.

Benefield, L.D.; Randall, C.W. **1980**, *Biological Process Design for Wastewater Treatment*, Prentice-Hall, Englewood Cliffs, N.Y.

Breithaupt, T. **1997**, Rotationsscheibenreaktor für die aerobe, anoxische und anaerobe Abwasserreinigung – Praktische Einsatzmöglichkeiten und mathematische Modellierung, *VDI-Forschungsberichte, Reihe 15*, 179.

Cheng, P.-S. **1982**, Biologische Stickstoffelimination mit Tauchtropfkörpern, *Stuttgarter Ber. Siedlungswasserwirtsch.* 73.

Clark, J.H.; Moseng, E.M.; Asano, T. **1978**, Performance of a rotating biological contactor under varying wastewater flow, *W.P.C.F. J.* 50, 896–911.

Damköhler, G. **1937**, Die heterogene Reaktion an schüttgutartigen Kontaktmassen, *Chem. Ing.* 3, 421–434.

Fair, G.M.; Geyer, J.Ch.; Okun, D.A. **1986**, *Water and Wastewater Engineering, Vol. 2: Water Purification and Wastewater Treatment and Disposal*, John Wiley, New York.

Fink, D.J.; Schultz, J.S. **1973**, Effectiveness factor calculations for immobilized enzyme catalysts, *Biotechnol. Bioeng.* 15, 879–888.

Gönec, E.; Harremoes, P. **1985**, Nitrification in rotating disc systems I, *Water Res.* 19, 1119–1127.

Lindemann, J. **2002**, Stickstoffeliminierung in Rotationsscheiben-Biofilmreaktoren, *VDI-Forschungsberichte, Reihe 15*, 179.

Marshall, K.C.; Blainey, B. **1991**, Role of bacterial adhesion in biofilm formation and bio corrosion, in: *Biofouling and Biocorrosion in Industrial Water Systems*, ed. Flemming, H.-C.; Geesey, G.G., Springer-Verlag, Heidelberg, p. 8–45.

Metcalf, Eddy **1991**, *Wastewater Engineering: Treatment, Disposal, And Reuse*, 3rd edn, McGraw-Hill, New York.

Meyer-Reil, L.-A. **1996**, Ökologie mikrobieller Biofilme, in: *Ökologie der Abwasserorganismen*, ed. Lemmer, H.; Griebe, T.; Flemming, H.-C., Springer-Verlag, Berlin, p. 24–42.

Nazaroff, W.W.; Alvarez-Cohen, L. **2001**, *Environmental Science*, John Wiley & Sons, New York, p. 357.

Schulz, J.M.; Menningmann G. **1999**, Submerged fixed bed reactors, in: *Environmental Processes*, (*Biotechnology*, Vol. 11a), Wiley-VCH, p. 349–362.

Stegmaier, K. **1993**, *Inbetriebnahme und Optimierung eines halbtechnischen Rotationsscheibenreaktors für die Nitrifikation von kommunalem Abwasser*, Dissertation (submitted for a diploma), Institut für Verfahrenstechnik, TU Berlin.

Tschobanoglous, G.; Schroeder, E.D. **1985**, *Water Quality: Characteristics, Modelling, Modification*, Addison-Wesley, Reading, Mass.

Thiele, E.W. **1939**, Relation between catalytic activity and size of particle, *Ind. Eng. Chem.* 31, 916–920.

Tyagi, R.D.; Tran, T.T.; Chowdhury, A.K.M.M. **1993**, A pilot study of biodegradation of petroleum refinery wastewater in a polyurethane-attached RBC, *Prog. Biochem.* 28, 75–82.

Van Loodsrecht, M.C.M.; Eickelboom, D.; Gjaltema, A.; Mulder, A.; Tijmuis, L.; Heijnen, J.J. **1995**, Biofilm structure, *Water Sci. Technol.* 32, 35–43.

Wanner, J.; Sykora, M.; Kos, M.; Miklenda, J.; Grau, P. **1990**, Packed-cage RBC with combined cultivation of suspended and fixed-film biomass, *Water Sci. Technol.* 22, 101–111.

Wingender, J.; Flemming, H.-C. **1999**, Autoaggregation of microorganisms: flocs and biofilms, in: *Environmental Processes* I, (*Biotechnology*, Vol. 11a), ed. J. Winter, Wiley-VCH, Weinheim, p. 65–83.

# 8
# Anaerobic Degradation of Organics

## 8.1
## Catabolic Reactions – Cooperation of Different Groups of Bacteria

### 8.1.1
### Survey

In contrast to most widely propagated aerobic degradation processes, the anaerobic conversion of organics down to methane and carbon dioxide is limited to the work of three different groups of bacteria (see Table 8.1 and Fig. 8.1 in the sections below):

1. *Acidogenic* bacteria produce extracellular enzymes (exoenzymes) for the hydrolysis of all organic solid particles and those dissolved colloids and molecules which are too large to diffuse through cell walls and membranes. Carbonhydrates are hydrolyzed down to mono- and disaccharides, proteins into amino acids and lipids into fatty acids. These compounds are transformed to acetate and longer chain fatty acids as well as $CO_2$ and $H_2$.
2. *Acetogenic* bacteria transform lower fatty acids such as butyrate and propionate into acetate, $CO_2$ and $H_2$. It is of great importance that $H_2$ is oxidized by other anaerobic bacteria. Otherwise, propionate concentrations would continually increase.
3. Therefore, hydrogen and acetate must be utilized by *methanogenic* bacteria. They exhibit two main products of catabolic metabolism. Methane is not very soluble in water and carbon dioxide is in equilibrium with $HCO_3^-$ and $CO_3^{2-}$ as a function of pH (see Fig. 4.2). Most of the $CO_2$ and nearly all the methane produced are desorbed, forming biogas bubbles which can be recovered for utilization.

### 8.1.2
### Anaerobic Bacteria

#### 8.1.2.1 Acidogenic Bacteria

The most important organics in wastewater are proteins, lipids and hydrocarbons. All can be utilized by acidogenic bacteria, which encompass a very large group of different, mostly facultative anaerobic bacteria.

*Fundamentals of Biological Wastewater Treatment*. Udo Wiesmann, In Su Choi, Eva-Maria Dombrowski

ISBN: 978-3-527-31219-1

*Proteins* are hydrolyzed into amino acids by proteases which function as exo-enzymes. The amino acids can be taken up by diffusion through cell walls and membranes at a relatively high rate. This process is not rate-limiting for subsequent reactions (Seyfried 1979). A small amount of amino acids is used directly for growth (anabolism), while a large amount is converted to lower fatty acids, $CO_2$, $H_2$ as well as $NH_4^+$ and is excreted (catabolism).

*Lipids* are esters formed from glycerine, an alcohol with three valences, and fatty acids. These have been hydrolyzed previously by lipase enzymes. Glycerine can be partially used for anabolic reactions and is converted in part to lower alcohols (catabolism). The fatty acids cannot be used by acidogenic bacteria and are excreted.

Polymeric *hydrocarbons* are hydrolyzed into monomers (glucose and other sugars) by most facultative anaerobic bacteria via exo-enzymes (McInerney and Bryant 1981). One part is totally used for protein synthesis and bacterial growth, while another part is converted into lower fatty acids. An example is presented by Eq. (8.1), see Fig. 8.1:

$$C_6H_{12}O_6 \rightarrow CH_3CH_2COOH + CH_3COOH + CO_2 + H_2 \quad (8.1)$$

This first reaction step results in a reduction of DOC (16.7%) and the formation of $CO_2$ as well as $H_2$. Mosey (1983) proposed a mechanism for the formation of fatty acids from glucose (Fig. 8.2).

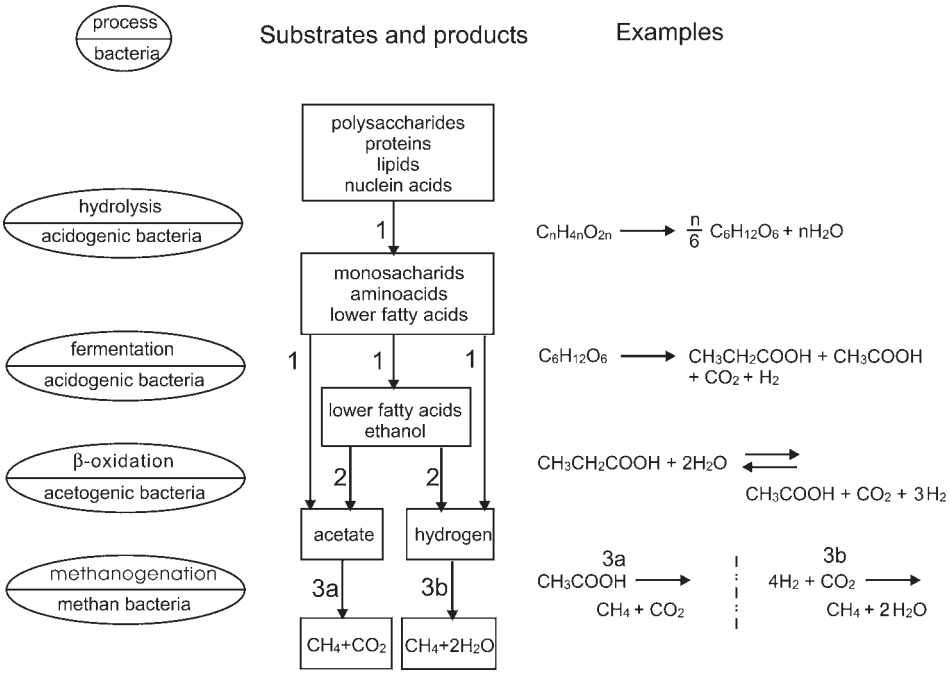


**Fig. 8.1** Anaerobic metabolism.

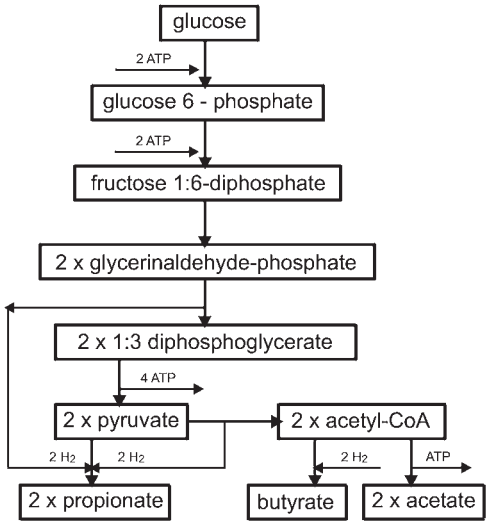


**Fig. 8.2** Fermentation of 1 mol glucose to lower fatty acids and the production of 1 mol ATP (Mosey 1983).

The conversion of chemical energy into ATP during anaerobic fermentation is very low and only 1 mol ATP per 1 mol glucose is converted for growth.

#### 8.1.2.2 **Acetogenic Bacteria**

Only a part of acetate is formed directly during fermentation. Most of it is formed by synthrophic reactions (McInerney 1999). Until now, only a few cultures have been isolated which are capable of this.

*Synthrophobacter wolinii* was described by Boone and Bryant (1980) and is able to convert propionate to acetate.

$$CH_3CH_2COO^- + 3\ H_2O \rightarrow CH_3COO^- + HCO_3^- + H^+ + 3\ H_2$$
$$\Delta G^\circ = 76.1\ \text{kJ mol}^{-1} \qquad (8.2)$$

*Synthrophomonas wolfeii* was first described by McInerney et al. (1979). Butyrate is transformed to acetate:

$$CH_3CH_2CH_2COO^- + 2\ H_2O \rightarrow 2\ CH_3COO^- + H^+ + 2\ H_2$$
$$\Delta G^\circ = 48.1\ \text{kJ mol}^{-1} \qquad (8.3)$$

In both reactions hydrogen is formed. However, problems arise at higher $H_2$ concentrations, as discussed in Section 8.1.3.

#### 8.1.2.3 **Methanogenic Bacteria**

Lower fatty acids such as butyrate and propionate can only be mineralized if two catabolic products of acetogenic bacteria, i.e. hydrogen and acetate, are consumed by methanogenic bacteria.

$$CH_3COOH + H_2O \rightarrow CH_4 + HCO_3^- + H^+ \quad \Delta G^\circ = -31 \text{ kJ mol}^{-1} \tag{8.4}$$

$$4\ H_2 + HCO_3^- + H^+ \rightarrow CH_4 + 3\ H_2O \quad \Delta G^\circ = -135.6 \text{ kJ mol}^{-1} \tag{8.5}$$

The methanogens are very old microorganisms, living on earth since before the oxygen-rich atmosphere was formed. *Methanosarcina* and *Methanothrix* are able to grow using acetate for catabolism; and 70% of the methane formed in digestion processes and elsewhere in nature is produced via Eq. (8.4) (Jeris and McCarty 1965). *Methanosarcina* spp are the most versatile methanogens producing ATP from acetate (Eq. 8.4) and hydrogen (Eq. 8.5). Methanol and methyl amine (Weimer and Zeikus 1978) are further intermediate products which can be biodegraded down to $CH_4$ and $CO_2$.

Four spherical cell species of *Methanosarcina barkeri* often grow in a close community (Fig. 8.3a). In contrast with *Methanosarcina, Methanotrix* does not use $H_2$. It was first isolated by Zehnder et al. (1980) and is rod-shaped, similar to *Methanobacterium bryantii* (Fig. 8.3d). *M. ruminantium* (Fig. 8.3b) and *M. bryantii* (Fig. 8.3d)

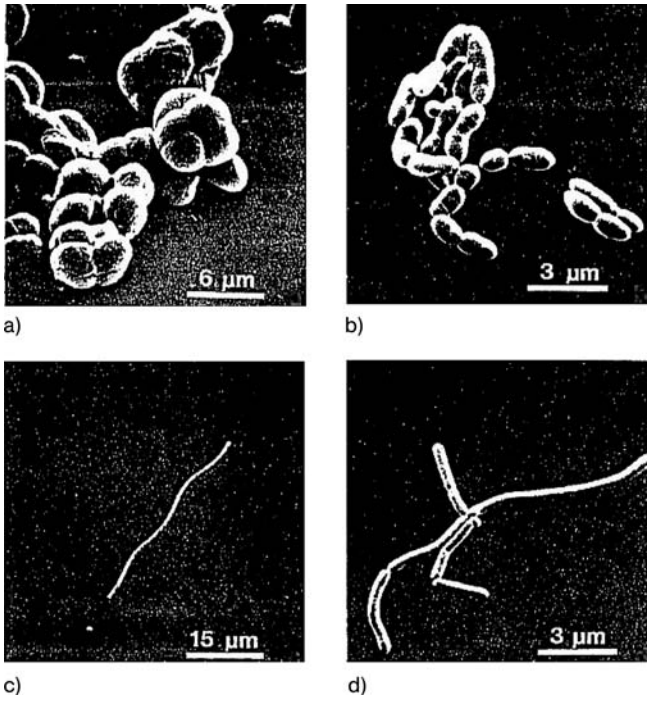


**Fig. 8.3** Electron microscopic photographs of methanogenic bacteria. (a) *Methanosarcina barkeri*; (b) *Methanobacteria ruminantium*; (c) *Methanospirillum hungatii*; (d) *Methanobacterium bryantii* (Zehnder and Wuhrmann 1977).

are able to produce ATP using $H_2/CO_2$ and formicate HCOOH, but both do not grow on acetate (Balch et al. 1979). $H_2/CO_2$-using Methanobacteria produce considerably more ATP than bacteria using acetate. They have a correspondingly higher maximum growth rate.

Although only about 30% of all $CH_4$ is produced from $H_2/CO_2$, Methanobacteria are very important for the regulation of anaerobic wastewater treatment processes. This will be explained in the next section.

Detailed information about anaerobic bacteria has been published by Zehnder and Wuhrmann (1977) and by Zehnder (1988).

### 8.1.3
### Regulation of Acetogenics by Methanogenics

Table 8.1 presents several catabolic reactions which yield acetate and $H_2$. First we shall have a look at Eq. (8.2), the degradation of propionate to acetate. It is interesting to note how far the concentration of hydrogen must be decreased to make the degradation of propionate possible.

This makes it necessary to study the equilibrium of Eq. (8.2). First, we write for the equilibrium constant:

$$K_e = \frac{S_{Pr^-} S^3_{H_2O}}{S_{Ac^-} S_{HCO_3^-} S_{H^+} \cdot c^3_{H_2}} \tag{8.6}$$

**Table 8.1** Arrangement of some important catabolic anaerobic reactions for oxidation (electron-donating reaction) and respiration (electron-accepting reaction). In part from Harper and Pohland (1986) and Pohland (1992).

| Process | Reaction | $\Delta G^\circ$ (kJ mol$^{-1}$) |
|---|---|---|
| Fermentation by acidogenic bacteria | $C_6H_{12}O_6 \rightarrow CH_3CH_2COOH + CH_3COOH + CO_2 + H_2$<br>$C_6H_{12}O_6 \rightarrow CH_3CH_2CH_2COOH + 2\ CO_2 + 2\ H_2$ | |
| β-Oxidation by acetogenic bacteria (synthrophic reactions) | $CH_3CH_2CH_2COO^- + 2\ H_2O \rightarrow 2\ CH_3COO^- + H^+ + 2\ H_2$<br>$CH_3CH_2COO^- + 3\ H_2O \rightarrow CH_3COO^- + H^+ + HCO_3^- + 3\ H_2$<br>$CH_3CH_2OH + H_2O \rightarrow CH_3COO^- + H^+ + 2\ H_2$<br>$CH_3CHOH\ COO^- + 2\ H_2O \rightarrow CH_3COO^- + H^+ + HCO_3^- + 2\ H_2$ | 48.1<br>76.1<br>9.6<br>–4.2 |
| $CH_4$ formation by methanogenic bacteria | $HCO_3^- + H^+ + 4\ H_2 \rightarrow CH_4 + 3\ H_2O$<br>$CH_3COO^- + H_2O \rightarrow CH_4 + HCO_3^-$ | –135.6<br>–31.0 |
| Further respiration reactions | $2\ CH_3CHOH\ COO^- + SO_4^{2-} \rightarrow 2\ CH_3COO^- + 2\ HCO_3^- + 2\ H^+ + S^{2-}$<br>$CH_3COO^- + SO_4^{2-} \rightarrow 2\ HCO_3^- + H^+ + S^{2-}$<br>$4\ H_2 + SO_4^{2-} \rightarrow 2\ H_2O + S^{2-}$<br>$2\ NO_3^- + 5\ H_2 + 2\ H^+ \rightarrow N_2 + 6\ H_2O$ | –1120.5 |

After introducing partial pressures for:

$$c_{H2} = \frac{p_{H_2}}{RT} \tag{8.7}$$

$$K_c = (RT)^3 \frac{S_{Pr^-} S^3_{H_2O}}{S_{Ac^-} S_{HCO_3^-} S_{H^+} \cdot p^3_{H_2}} \tag{8.8}$$

$$K_c = (RT)^3 \, k \frac{S_{Pr^-}}{S_{Ac^-} S_{HCO_3^-} S_{H^+} \cdot p^3_{H_2}} \tag{8.9}$$

where R is the ideal gas constant and:

$$k = S^3_{H_2O} \tag{8.10}$$

The equilibrium constant is a function of the free enthalpies of reaction:

$$K_c = \exp\left(-\frac{(\Delta G^\circ - \Delta G)}{RT}\right) \tag{8.11}$$

where $\Delta G$ is the free enthalpy of reaction and $\Delta G^\circ$ is the standard free enthalpy for T = 0 K.

From Eqs. (8.9) and (8.10), it follows that:

$$\Delta G = \Delta G^\circ + RT\,(3 \ln RT + \ln k + \ln S_{Pr^-} - \ln S_{Ac^-} - \ln S_{HCO_3^-} - \ln S_{H^+} - 3 \ln p_{H_2}) \tag{8.12}$$

For given values of $S_{Pr^-}$, $S_{Ac^-}$, $S_{HCO_3^-}$, pH and T, the reaction enthalpy can be calculated as a function of $p_{H_2}$ (McInerney and Bryant 1981; Pohland 1992; McInerney 1999). Curve 1 in Fig. 8.4 presents some results.

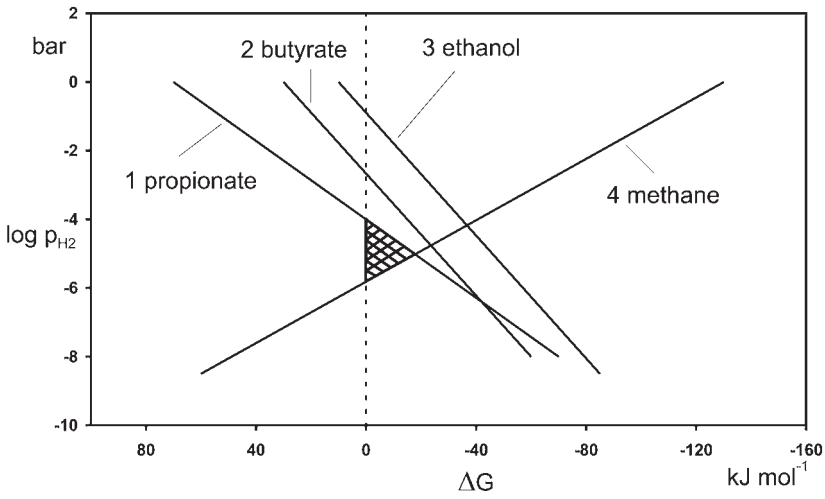


**Fig. 8.4** Influence of hydrogen partial pressure $p_{H2}$ on free enthalpy $\Delta G$ for anaerobic degradation of propionate (curve 1), butyrate (curve 2), ethanol (curve 3) and for $CH_4$-formation from $H_2$ (curve 4). Curve 1 is calculated from Eq. (8.12) using $S_{Pr^-}$ = 1 mmol $L^{-1}$, $S_{Ac^-}$ = 1 mmol $L^{-1}$, $S_{HCO_3^-}$ = 50 mmol $L^{-1}$, pH 7, T = 25 °C (McInerney and Bryant 1981).

Only at partial pressures $p_{H_2} < 10$ Pa or $p_{H_2} < 10^{-4}$ bar is $\Delta G$ negative at the given conditions and the equilibrium constant $K_c$ increases, resulting in a higher rate of propionate conversion. Compared with that, for $p_{H_2} > 10$ Pa or $p_{H_2} > 10^{-4}$ bar $\Delta G$ is positive, $K_c$ decreases and the propionate concentration increases. But there is an important catabolic reaction utilized by some methanogenic bacteria which produces $CH_4$ from $H_2$ (see Eq. 8.5).

This cooperation of acetogenic bacteria which produces $H_2$ from butyrate and propionate (Eqs. 8.2 and 8.3), but which is not able to transfer hydrogen to other β-oxidation products and methanogenics using $H_2$ is called β-oxidation (Stronach et al. 1986).

If the thermodynamic equilibrium is calculated using the same method as described above, a straight line with a positive slope follows, resulting from the negative free enthalpy $\Delta G° = -135.6$ kJ mol$^{-1}$ (Fig. 8.4, curve 2).

For $p_{H_2} = 2 \cdot 10^{-6}$ bar, the difference of reaction enthalpies is nearly zero. Methane cannot be produced via the reaction in Eq. (8.5) and $p_{H_2}$ must increase. The reaction can only "move along the two sides of the triangle" formed by curves 1, 4 and the vertical line for $\Delta G = 0$. But for other T, pH and concentrations of propionate, acetate and $CO_2$, the triangle with the two paths of reaction is moved somewhat and a somewhat higher or lower $p_{H2}$ must be reached.

Following the same thermodynamic consideration, curve 2 can be obtained for butyrate and curve 3 for ethanol. For given conditions (not shown here) $\Delta G$ is already negative for $p_{H_2} \approx 10^{-1}$ bar (ethanol) and $p_{H_2} \approx 10^{-3}$ bar (butyrate). The fermentation of butyrate or ethanol, in each case by a pure culture, is inhibited by higher partial pressures of $H_2$. However, for experiments with mixed cultures the lowest value of $p_{H_2} = 10^{-4}$ bar is crucial for the whole process. In nature this problem was solved billions of years ago by forming communities which included methanogenic bacteria able to use $H_2$ and acetate.

### 8.1.4
### Sulfate and Nitrate Reduction

Sulfate-reducing bacteria of the genera *Desulfovibrio* and *Desulfotomaculum* grow in anaerobically treated wastewater that contains sulfate (Zeikus 1979). Several organic compounds can be mineralized or partly used with lactate, i.e. *Desulfovibrio desulfuricans* (Gottschalk 1986; Yoo 2000):

$$2\ CH_3CHOHCOO^- + SO_4^{2-} \rightarrow 2\ CH_3COO^- + 2\ HCO_3^- + 2\ H^+ + S^{2-} \qquad (8.13)$$

and acetate by *Desulfobacter postgateii* (Widdel and Pfennig 1981):

$$CH_3COO^- + SO_4^{2-} \rightarrow 2\ HCO_3^- + H^+ + S^{2-} \qquad (8.14)$$

Beside these chemoorganoheterotrophic sulfate reducers even chemolitho-autotrophics have been isolated (Brandis and Thauer 1981; Nethe-Jaenchen and Thauer 1984):

$$4\ H_2 + SO_4^{2-} \rightarrow 4\ H_2O + S^{2-} \qquad (8.15)$$

Depending on the pH, the sulfur exists mainly in the form of $S^{2-}$ (high pH) or $H_2S$ (low pH):

$$S^{2-} + H^+ \rightleftarrows HS^- \quad (8.16)$$

$$HS^- + H^+ \rightleftarrows H_2S \quad (8.17)$$

The formation of $H_2S$ is a serious problem because of its corrosive effects and its smell. Therefore, it must be separated from biogas, e.g. by reaction with iron sharings. Another disadvantage of sulfate reduction is the consumption of acetate (Eq. 8.14) and hydrogen (Eq. 8.15). Via these reactions, sulfate-reducing and some denitrifying bacteria compete with the methanogenic bacteria for hydrogen:

$$2\ NO_3^- + 5\ H_2 \rightarrow N_2 + 2\ OH^- + 4\ H_2O \quad (8.18)$$

and the $CH_4$ content of the biogas is reduced.

## 8.2 Kinetics – Models and Coefficients

### 8.2.1 Preface

We must distinguish between the hydrolysis of solids and that of dissolved organics. The anaerobic treatment process of solids and sludge stabilization are frequently used in municipal WWTPs in order to obtain residual solids which cannot be utilized further by microorganisms as their carbon and energy source. It is to a large extent odorless and can be dewatered easily. About 25–30% of dry mass is converted thereby into sludge gas containing $CH_4$. Therefore, it can be used as a form of gaseous energy. This process will not be discussed here in detail.

The hydrolysis of dissolved organics is the first step of anaerobic wastewater treatment. Higher-loaded wastewater, such as that generated by breverage and food industries, offers the possibility to separate, concentrate and recycle the anaerobic bacteria from the treated wastewater or to immobilize the bacteria on solid support materials (Section 8.4). The efficiency of these processes can be increased and the processes can be optimized considerably. Micro- and macrokinetics are the foundation of process construction and control. In the next section we will discuss the present knowledge of anaerobic microkinetics.

### 8.2.2 Hydrolysis and Formation of Lower Fatty Acids by Acidogenic Bacteria

The formation rate of amino acids from proteins, glycerine and fatty acids from lipids and monosaccharides from higher hydrocarbons depends on:

- the mole mass of polymers,
- their stability during hydrolysis,
- the portion of colloids,
- the concentration of enzymes.

Normally, a high enzyme concentration is assumed in relation to the total amount of substrates, measured as COD or DOC, resulting in a first-order reaction with regard to substrate concentration:

$$r_H = k_H S \text{ mg (L h)}^{-1} \text{ COD} \tag{8.19}$$

where $k_H$ is the rate coefficient ($h^{-1}$) and S is the polymer concentration (mg $L^{-1}$ COD).

For most types of wastewater, hydrolysis and the formation of lower fatty acids by acidogenic bacteria are not rate-limiting for the total process. This follows from kinetic studies of hydrolysis of polymers and glucose fermentation to lower fatty acids (Table 8.2).

A relatively high amount of energy can be supplied for ATP production and anabolism. A yield coefficient $Y^{\circ}_{X/S}$ = 0.162–0.310 g MLSS (g COD)$^{-1}$ has been measured. The mean value of $Y^{\circ}_{X/S}$ = 0.236 is about 50% of that for the aerobic mineralization of glucose. The influence of the glucose concentration on the growth rate is described by Monod kinetics:

$$r_X = \mu_{max} X \frac{S}{K_S + S} - k_d X \tag{8.20}$$

with $\mu_{max}$ = 10.9–64.8 $d^{-1}$

Values of $K_S$ = 24.1 mg $L^{-1}$ COD and 73.4 mg $L^{-1}$ COD were obtained for the saturation coefficient, which points to the useable range of substrate limitation. Only one $K_S$ value is very high and could be confirmed by other measurements. These degradation reactions of hydrolysis products (i.e. glucose) to butyrate and propionate are called fermentation. These coefficients and others from the literature are compiled in Table 8.2.

### 8.2.3
### Transformation of Lower Fatty Acids by Acetogenic Bacteria

In order to study the formation of acetate from butyrate and propionate by acetogenic bacteria, it is necessary to reduce the partial pressure of $H_2$ down to $p_{H2}$ = $10^{-3}$ bar (butyrate) or between $10^{-4}$ bar and $2 \cdot 10^{-6}$ bar (propionate; Fig. 8.4). It is useful to investigate the growth of *Synthrophobacter wolinis* on *n*-butyrate (Eq. 8.2) or the growth of *Synthrophomonas wolfeii* on propionate (Eq. 8.3) in mixed culture with methanogenic bacteria, as they reduce the $p_{H_2}$ (Eq. 8.5) and the acetate concentration (Eq. 8.4). The removal of acetate is absolutely necessary to prevent product inhibition. Two results of butyrate transformation to acetate in experiments are presented in Table 8.2. The yield coefficient $Y^{\circ}_{X/S}$ = 0.0094 ... 0.022 = 0.014 g MLSS (g COD)$^{-1}$ and the maximum specific growth rate $\mu_{max}$ = 0.17 ... 0.39 = 0.28 $d^{-1}$ are considerably lower than those of acidogenic bacteria: the $\mu_{max}$ is lower by a factor of about 100 and $Y^{\circ}_{X/S}$ by a factor of about 15. From these values, the following specific maximal substrate removal rates are obtained for butyrate:

$$r_S/X = \mu_{max}/Y^{\circ}_{XS} = 0.28/0.014 = 20 \text{ g COD (g MLSS} \cdot \text{d)}^{-1}$$

**Table 8.2** Fermentation, β-oxidation and methanization – stoichiometric and kinetic coefficients.

| Bacterial substrate | Ref. | Reactor (pH) | T (°C) | $Y^{\circ}_{X/S}$ [a] | $\mu_{max}$ [b] | $K_S$ [c] | $K_{SH}$ [d] | $K_{iH}$ [e] | $k_d$ [b] |
|---|---|---|---|---|---|---|---|---|---|
| Fermentation of glucose to lower fatty acids by acidogenics | Ghosh and Pohland (1974) | Chemostat | 35 | 0.162 | 30.1 | 24.1 | | | 1.06 |
| | Massey and Pohland (1978) | Chemostat | 35 | 0.31 | 64.8 | 2583 | | | 1.56 |
| | Hanaki et al. (1985) | Chemostat | 35 | 0.212 | 10.9 | 73.4 | | | 4.13 |
| β-Oxidation of *n*-Butyrate | Lawrence and McCarty (1969) | Chemostat (pH 7.0) | 35 | 0.0094 | 0.39 | 48.3 | | | 0.027 |
| | Chang (1982) | Batch | 35 | 0.022 | 0.17 | 47.0 | | | 0.005 |
| β-Oxidation of propionate to acetate and $H_2$ by acetogenics | Andrews (1969) | Chemostat (pH 7.0) | 38 | 0.05 | 0.4 | | 3 | 60 | |
| | Lawrence and McCarty (1969) | Chemostat (pH 7.0) | 35 | | 0.4 | | 0.36 | | |
| | Gujer and Zehnder (1983) | Chemostat (pH 7.0) | 33 | 0.025 | 0.155 | 248 | | | |
| Methanization from $H_2$ | Shea et al. (1968) | Chemostat pH 7.8) | 37 | 0.043 | 1.06 | 556[f] | | | 0.009 |
| | Zehnder and Wuhrmann (1977) | Chemostat (pH 7.0) | 33 | | 1.4 | | | | |
| | Bryer (1985) | | 55 | 0.038 | 1.4 | 37.5 | | | 0.1 |
| Methanization from acetate | Graef and Andrews (1973) | Chemostat (pH 7.0) | 38 | 0.057 | 0.4 | | 2.13 | 42.7 | |
| | Carr and O'Donell (1977) | | 35 | 0.027 | 0.11 | | 1.15 | 35.6 | 0.006 |
| | Bolle et al. (1986) | Chemostat (pH 7.0) | 35 | 0.037 | 0.038 | | 2.1 | 16.9 | 0.0036 |

[a] g MLSS (g COD)$^{-1}$, [b] d$^{-1}$, [c] mg L$^{-1}$ COD, [d] mg L$^{-1}$ COD, [e] mg L$^{-1}$ COD, [f] µmol L$^{-1}$.

and for propionate:

$$r_S/X = 0.0028/0.001 = 2.8 \text{ g COD (g MLSS)}^{-1}$$

if the results of three studies are considered (Table 8.2). The maximum specific removal rate of propionate is lower than that of butyrate nearly by a factor of 7. But in reality, the reaction in Eq. (8.2) is very sensitive to the following influences:

- As mentioned in Section 8.13, $p_{H2}$ must be reduced by methanogenic bacteria down to $10^{-4}$ bar.
- The conversion of propionate to acetate can be inhibited by higher concentrations of non-ionized propionate $S_{HPr}$. As shown by several authors, the influence of $S_{HPr}$ on the specific growth rate can be described by Haldane kinetics (Andrews 1969; Attal et al. 1988; Fukuzaki et al. 1990):

$$\mu = \mu_{max} \frac{S_{HPr}}{K_{SH} + S_{HPr} + S_{HPr}^2/K_{iH}} \tag{8.21}$$

- In addition to $S_{HPr}$, the concentration of non-ionized acetate $S_{HAC}$ influences μ by non-competitive inhibition (Mosey 1983; Denac 1986; Fukuzaki et al. 1990; Kus 1993):

$$\mu = \mu_{max} \frac{S_{HPr}}{K_{SH} + S_{HPr} + S_{HPr}^2/K_{iH}} \cdot \frac{K_{iH}}{K_{iH} + S_{HAc}} \tag{8.22}$$

Therefore, the formation of methane from $H_2$ and acetate should not be disturbed. Otherwise, propionate and butyrate cannot be biodegraded.

### 8.2.4
### Transformation of Acetate and Hydrogen into Methane

As described by Fig. 8.4, the hydrogen partial pressure must be reduced down to $p_{H_2} < 10^{-4}$ bar by *Methanosarcina* and *Methanobacterium* to enable conversion of propionate to acetate (see Section 8.1.3). The specific growth rate was described using Monod kinetics (Table 8.2). If the rate of $H_2$ oxidation is measured as COD, the mean specific removal rate follows as:

$$r_S/X = \mu_{max}/Y^\circ_{X/S} = 32.5 \text{ g COD (g MLSS d)}^{-1}$$

with mean values of $\mu_{max} = 1.3\ d^{-1}$ and $Y^\circ_{X/S} = 0.04$ g MLSS (g COD)$^{-1}$. This specific rate is higher than that of propionate degradation (see Section 8.2.3). If there are no toxic effects from heavy metal ions, these bacteria grow rapidly and propionate degradation is not inhibited by higher $p_{H_2}$.

Methane formation from acetate by *Methanosarcina* and *Methanotrix* (Eq. 8.4) is a much slower reaction. From three studies (Table 8.2), a mean specific removal rate can be calculated as:

$$r_S/X = \mu_{max}/Y^\circ_{X/S} = 4.9 \text{ g COD (g MLSS d)}^{-1}$$

with $\mu_{max} = 0.18\ d^{-1}$ and $Y^{\circ}_{X/S} = 0.037$ g MLSS (g COD)$^{-1}$. This is low compared to acetate formation from propionate. Therefore, it is the most important step of anaerobic digestion and is more frequently studied. All authors mentioned in Table 8.2 considered Haldane kinetics with non-ionized acetate as the substrate:

$$\mu = \mu_{max} \frac{S_{HAc}}{K_{SH} + S_{HAc} + S^2_{HAc}/K_{iH}} \tag{8.23}$$

The frequently observed disruption of digestion processes with sinking pH and enrichment of lower fatty acids can be explained in part by substrate inhibition. As shown in Eq. (8.22), some authors observed an inhibition of methane formation by propionate described as a non-competitive inhibition.

Because we have to distinguish three totally different groups of anaerobic bacteria, we actually have to measure the concentration of these groups X. This is very difficult and often not realized although it is a requirement for correct determinations of $\mu_{max}$ values. Normally, the unit g L$^{-1}$ MLSS or MLVSS (mixed liquid volutile suspended solids) is used (Table 2.6).

### 8.2.5 Conclusions

The anaerobic degradation of organics is a rather complicated process. Even if we only wish to discuss the digestion of glucose, we must take into account three different groups of bacteria. It is not easy to separate them and, in the case of conversion of propionate to acetate and hydrogen, the acetogenic and methanogenic bacteria are dependant upon each other. Although it is important to know the value of X, the bacterial concentration responsible for one interesting catabolic reaction, measurements are frequently impossible and X must be obtained by calculations using mass balances.

In many studies the concentrations:

$$S_{Ac} = S_{HAc} + S_{Ac^-} \quad \text{and} \quad S_{Pr} = S_{HPr} + S_{Pr^-}$$

are used in Monod or Haldane kinetics instead of $c_{HAc}$ and $c_{HPr}$ in recent publications.

Let us write:

$$\mu_{max} \frac{S_{Ac}}{K_S + S_{Ac} + S^2_{Ac}/K_i} = \mu_{max} \frac{S_{HAc}}{K_{SH} + S_{HAc} + S^2_{HAc}/K_{iH}} \tag{8.24}$$

and $CH_3COOH \leftrightarrow CH_3COO^- + H^+$

Then, respectively:

$$K = \frac{S_{Ac^-}\, S_{H^+}}{S_{HAc}} \tag{8.25}$$

as well as:

$$S_{Ac} = S_{Ac^-} + S_{HAc} \tag{8.26}$$

and:

$$S_{HAc} = \frac{S_{Ac}}{1 + K\,10^{pH}} \tag{8.27}$$

After introducing Eq. (8.27) into Eq. (8.24), we obtain:

$$K_{SH} = \frac{K_S}{1 + K\,10^{pH}} \tag{8.28}$$

and:

$$K_{iH} = \frac{K_i}{1 + K\,10^{pH}} \tag{8.29}$$

Note that, in contrast to $K_S$ and $K_i$, $K_{SH}$ and $K_{iH}$ are *not* functions of pH, because of Eq. (8.25), which yields:

$$K = \frac{S_{Ac^-}}{S_{HAc} \cdot 10^{pH}} \tag{8.30}$$

The next important point is to calculate how much methane is produced if 1 mol $CH_3COOH$ or 1 mol $C_6H_{12}O_6$ is degraded anaerobically. We can compare both substrates according to their COD. Let us start with $CH_3COOH$.

For chemical oxidation of $CH_3COOH$ we write:

$$CH_3COOH + 2\,O_2 \rightarrow 2\,CO_2 + 2\,H_2O$$

and therefore 1 mol $CH_3COOH$ needs 2 mol $O_2$; or 60 g HAc give 64 g COD.

Methane production from $CH_3COOH$ can be calculated using:

$$CH_3COOH \rightarrow CH_4 + CO_2$$

giving a yield coefficient of:

$$Y^{o}_{CH_4/HAc} = \frac{r_{CH_4}}{r_{HAc}} = \frac{1\ \text{mol}\ CH_4}{1\ \text{mol HAc}} = \frac{22.4}{64}\ \frac{Nm^3}{kg}\ \frac{CH_4}{COD} = 0.35\ Nm^3\ (\text{kg COD})^{-1} \tag{8.31}$$

Now we calculate the yield of $CH_4$ from glucose: for the chemical oxidation of $C_6H_{12}O_6$, it follows that:

$$C_6H_{12}O_6 + 6\,O_2 \rightarrow 6\,CO_2 + 6\,H_2O$$

Therefore, 1 mol $C_6H_{12}O_6$ needs 6 mol $O_2$; or 180 g $C_6H_{12}O_6$ is equivalent to 192 g COD.

Methane production from $C_6H_{12}O_6$ can be calculated by summarizing Eqs. (8.1), (8.2), (8.4) and (8.5)

$$C_6H_{12}O_6 \rightarrow 3\ CH_4 + 3\ CO_2$$

giving a yield coefficient of:

$$Y^{o}_{CH_4/C_6H_{12}O_6} = \frac{r_{CH_4}}{r_{Glu}} = \frac{3\ \text{mol}\ CH_4}{1\ \text{mol}} = \frac{22.4}{64}\ \frac{Nm^3\ CH_4}{kg \cdot COD} \tag{8.32}$$

$$= 0.35\ Nm^3\ CH_4\ (kg\ COD)^{-1}$$

Conclusion: from wastewater loaded with hydrocarbons ($CH_2O$) and a given reaction rate of kg COD $(m^3\ d)^{-1}$, which can be mineralized by anaerobic processes (digestion), the maximum rate of methane production can be calculated using Eq. (8.31):

$$r_{CH_4} = 0.35\ r_{COD}\ Nm^3\ CH_4\ (kg\ COD)^{-1}$$

regardless of whether polysaccharides, monosaccharides or acetate are present in the wastewater.

## 8.3 Catabolism and Anabolism

The catabolic conversion of acetate into $CH_4$ and $CO_2$ (Eq. 8.4) is a very simple reaction. We will use the method realized by methanogenic *Methanotrix* bacteria as an example for the evaluation of the stoichiometric equation describing catabolism and anabolism.

Starting from a general form considering only carbon, hydrogen and oxygen as elements of bacterial mass, we do not need to add nutrients and we can write:

$$CH_{SH}O_{SO} \rightarrow Y^{o}_{X-C/S-C}CH_{BH}O_{BO} + Y^{o}_{CH_4-C/S-C}CH_4 + Y^{o}_{CO_2-C/S-C}CO_2 + Y^{o}_{H_2O-H/S-C}H_2O \tag{8.33}$$

Note that the substrate molecule and the "bacteria molecule" are each standardized relative to one carbon atom, resulting in the yield coefficients, three of which can be measured:

$$Y^{o}_{XC/SC} \equiv \frac{\text{C for growth}}{\text{C of total substrate removal}}$$

$$Y^{o}_{CH_4-C/SC} \equiv \frac{\text{C for } CH_4 \text{ formation}}{\text{C of total substrate removal}}$$

$$Y^{o}_{CO_2-C/SC} \equiv \frac{\text{C for } CO_2 \text{ formation}}{\text{C of total substrate removal}}$$

According to these formulas, the content of hydrogen and oxygen in the substrate molecule and the "bacteria molecule" are given by SH and SO as well as BH and BO, respectively. Now, we already know that we will obtain three mass balances for the three elements C, H and O. Therefore, we can calculate only three of the four yield coefficients. In order to complete the stoichiometric equations describing catabolism and anabolism, one of the four yield coefficients must be measured (however, see Section 4.2.1).

Let us use acetate as the substrate with $CH_2O$ ($CH_3COOH$, written as $C_2H_4O_2$ and divided by two, gives $CH_2O$) and $CH_{1.8}O_{0.5}$ as a mean composition for the bacterial mass. Instead of Eq. (8.33), we now write:

$$CH_2O \rightarrow Y^{o}_{XC/SC}CH_{1.8}O_{0.5} + Y^{o}_{CH_4-C/SC}CH_4 + Y^{o}_{CO_2-C/SC}CO_2 + Y^{o}_{H_2O-H/SC}H_2O \tag{8.34}$$

The balances for each of the three elements are:

$$\text{C balance: } 1 = Y^{o}_{XC/SC} + Y^{o}_{CH_4-C/SC} + Y^{o}_{CO_2-C/SC} \tag{8.35}$$

$$\text{H balance: } 2 = 1.8\, Y^{o}_{XC/SC} + 4\, Y^{o}_{CH_4-C/SC} + 2\, Y^{o}_{H_2O-H/SC} \tag{8.36}$$

$$\text{O balance: } 1 = 0.5\, Y^{o}_{XC/SC} + 2\, Y^{o}_{CO_2-C/SC} + Y^{o}_{H_2O-H/SC} \tag{8.37}$$

From these three balances, three of the four yield coefficients can be calculated. To find the stoichiometry of Eq. (8.34), one of these yields must be measurable. Let us assume that we measure $Y^{o}_{CH_4-C/S-C}$ and we obtain:

$$Y^{o}_{CH_4-C/SC} = 0.48 \text{ mol } CH_4 \text{ (mol C)}^{-1}$$

Remember that, for catabolism alone, we would write $Y^{o}_{CH_4-C/SC} = 0.5$ and $Y^{o}_{CO_2-C/SC} = 0.5$. The solution of the three balances gives:

$$Y^{o}_{XC/SC} = \frac{1 - 2\,Y^{o}_{CH_4-C/SC}}{1.2} = 0.03 \text{ mol X–C (mol S–C)}^{-1}$$

$$Y^{o}_{CO_2-C/SC} = 0.167 + 0.67\, Y^{o}_{CH_4-C/SC} = 0.49 \text{ mol } CO_2 \text{ (mol S–C)}^{-1}$$

$$Y^{o}_{H_2O-H/SC} = 0.01 \text{ mol } H_2O\text{–H (mol S–C)}^{-1}$$

The reaction describing the elements used for anabolism and catabolism is obtained after multiplying by a factor of two, considering the 2 C atoms in one acetate molecule:

$$CH_3COOH \rightarrow 0.060\, CH_{1.8}O_{0.5} + 0.96\, CH_4 + 0.98\, CO_2 + 0.026\, H_2O \tag{8.38}$$

Only 3% of the acetate carbon is used for growth!

## 8.4 High-rate Processes

### 8.4.1 Introduction

Compared with anaerobic sludge treatment, anaerobic wastewater treatment allows us to increase the concentration of bacteria remarkably, resulting in an increase in reaction rate (high-rate processes). Three different mechanisms are effective at increasing the bacterial concentration:

- Sedimentation of floc-forming bacteria and recycling of the thickened sludge into the bioreactor.
- Sedimentation and suspension of particles formed from bacteria and minerals inside the bioreactor.
- Immobilizing the bacteria at the surface of either fixed or suspended solid materials, as well as at rotating solid plates.

Comparing the specific maximum removal rate:

$$\frac{r_{s\,max}}{X} = \frac{\mu_{max}}{Y^{\circ}_{X/S}} \tag{8.39}$$

for an aerobic and an anaerobic process (degradation of acetate by methanogenic bacteria) and using mean values for $\mu_{max}$ and $Y^{\circ}_{X/S}$ from Table 6.2 (aerobic bacteria) and Table 8.2 (methanogenic bacteria) for unlimited substrate removal, we obtain for aerobics:

$$\frac{r_{s\,max}}{X} = \frac{\mu_{max}}{Y^{\circ}_{X/S}} = \frac{12}{0.6} = 20 \text{ g COD (g MLSS d)}^{-1}$$

and for anaerobics:

$$\frac{r_{s\,max}}{X} = \frac{\mu_{max}}{Y^{\circ}_{X/S}} = \frac{0.2}{0.04} = 5 \text{ g COD (g MLSS d)}^{-1}$$

This real difference of only a factor of four is remarkably low because:

- The higher sludge density results in a higher bacterial concentration inside anaerobic reactors.
- There is less influence from mass transfer and diffusion than in aerobic aerated reactors, which can be limited by low dissolved oxygen levels.

Some effective and economical high-rate anaerobic treatment processes which take advantage of these benefits have gone into operation over recent decades (Dauber 1993).

In all these high-rate processes, the temperature is increased to about 35 °C. It is therefore absolutely necessary to construct the bioreactor with a thermal insulation and a preheating system for the inflowing and recycled wastewater and the settled

sludge, especially in northern climates. The biogas produced should be used nearly completely and only a very low amount should be burned off in a bypass flame.

The lowest substrate concentrations which can be reduced anaerobically in an economical way are about $S_o$ = 2000–3000 mg $L^{-1}$ COD.

About 80–90% of the $BOD_5$ can be removed:

$$\alpha = \frac{S_o - S_1}{S_o} \cdot 100 = 80 - 90\%$$

If it is intended to discharge the treated water into surface water, it must be treated aerobically in a second stage to adhere to local legislation.

### 8.4.2 Contact Processes

In the anaerobic contact process, the higher bacterial concentration is most often obtained in an incompletely mixed tank reactor (suspended growth) as a result of recycling sludge after settling in a sedimentation tank (Fig. 8.5), similar to an activated sludge reactor.

The reactor is mixed using:

- stirrers,
- the distribution of recycled external wastewater near the reactor bottom,
- the recycling of compressed biogas (not presented in Fig. 8.5).

In some reactors, two or three of these mixing processes are applied. Nevertheless, the case of nearly ideal mixing is rarely obtainable. It is absolutely necessary to install a system for degasifying the mixed liquor, i.e. the treated wastewater, suspended bacterial flocs and gas bubbles, before sedimentation. Several methods are available. In most degasifying systems, the water flows through tanks kept under a partial vacuum. In addition, the mass transfer rate and the gas/liquid interfacial surface are increased by the use of rotating stirrers or the formation of falling drops or trickling films. Temperatures fall during the degasification, resulting in lower $CH_4$ and $CO_2$ production rates and higher saturation concentrations of both gases. This significantly reduces the amount of gas bubbles which form during sedimentation.

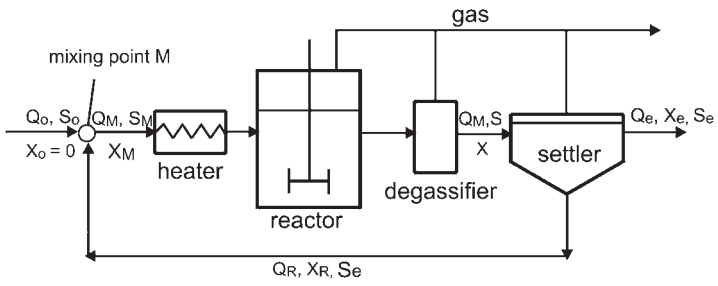


**Fig. 8.5** Contact process.

An anaerobic wastewater treatment process can be calculated easily if the following conditions are met:

- The process is controlled by acetate degradation.
- It is a steady-state process.
- The reactor is completely mixed.
- The surplus bacteria are removed with the overflow.
- Bacterial decay is neglected.

We want to estimate the acetate concentration $S_e$ depending on the mean hydraulic retention time $t_R$. Looking at Fig. 8.5, we write the bacterial balance for the reactor:

$$0 = Q_M\,(X_M - X) + \mu\,X\,V \tag{8.40}$$

For the bacterial concentration at mixing point M, we obtain:

$$X_M = X_R\,\frac{n_R}{1+n_R} \tag{8.41}$$

with:

$$n_R = \frac{Q_R}{Q_0} \text{ as the sludge recycle ratio} \tag{6.39}$$

The concentration of bacteria in the recycled sludge $X_R$ must be calculated from the balance of a settler:

$$(Q_0 + Q_R)\,X = Q_0 X_e + Q_R X_R \tag{8.42}$$

with $Q_0 X_e$ as the overflow mass flow rate and $Q_R X_R$ as the mass flow rate of recycled sludge.

It is useful to define β, the separation coefficient of the settler:

$$\beta = \frac{(Q_0+Q_R)\,X - Q_0 X_e}{(Q_0+Q_R)\,X} \tag{8.43}$$

and considering Eq. (6.39):

$$\beta = \frac{(1+n_R)\,X - X_e}{(1+n_R)\,X} \tag{8.44}$$

then, respectively:

$$X_e = X\,(1-\beta)\,(1+n_R) \tag{8.45}$$

which is introduced into Eq. (8.43):

$$X_R = X\beta\,\frac{1+n_R}{n_R} \tag{8.46}$$

Eq. (8.47) in Eq. (8.41) gives:

$$X_M = \beta\,X \tag{8.47}$$

introducing this into the balance of the reactor (Eq. 8.40) and considering $Q_M = Q_0 + Q_R$, we can write:

$$0 = (1 + n_R)\,(\beta - 1) + \mu\, t_R \tag{8.48}$$

Using Monod kinetics:

$$\mu = \mu_{max}\frac{S}{K_S + S} \tag{6.1}$$

The acetate concentration in the effluent is represented by:

$$S_e = \frac{K_S\,(1-\beta)\,(1+n_R)}{\mu_{max}\,t_R - (1-\beta)\,(1+n_R)} \tag{8.49}$$

and the critical mean retention time follows for $S_e = S_0$:

$$t_{RC} = \frac{(1-\beta)\,(1+n_R)\,(K_S + S_0)}{\mu_{max}\,S_0} \tag{8.50}$$

For $\beta = 0$, $n_R = 0$, $S_0 \gg K_S$, we obtain the simple solution valid for a chemostat:

$$t_{RC} = \frac{1}{\mu_{max}} \tag{6.26}$$

In large-scale contact reactors, the mixing energy is not sufficient to realize locally constant conditions (concentrations, temperature, pH), which means that considerable discrepancies exist between theory and practice. Nevertheless, the influence of $t_R$, $\beta$ and $n_R$ can be discussed fundamentally and can often be compared successfully with operational data.

Two-stage anaerobic contact processes can be advantageous, with a first stage predominately for the formation of lower fatty acids at a lower pH 5.5–6.5 and a second stage predominately for the methanization process at a higher pH 6.5–7.5. Because of the higher yield coefficient of acidogenic bacteria (Table 8.2; $Y^{\circ}_{X/S}$ = 0.23 g MLSS (g COD)$^{-1}$) compared with that of methanization ($Y^{\circ}_{X/S}$ = 0.04 g MLSS (g COD)$^{-1}$) and the higher reaction rate in the first stage, sludge concentrations are frequently high enough and must not be increased by sedimentation and sludge recycle.

In all systems described below, the bacteria are retained directly inside the reactor.

### 8.4.3
### Upflow Anaerobic Sludge Blanket

In the upflow anaerobic sludge blanket (UASB) type of reactor, the gas/solid/liquid separation system is integrated into the vessel (Fig. 8.6).

This reactor can only be used if large, dense, readily settleable particles are formed – a granular sludge which allows high concentrations of suspended solids between 20 g L$^{-1}$ MLSS and 30 g L$^{-1}$ MLSS (Lettinga and Hueshoff 1991, 1992).

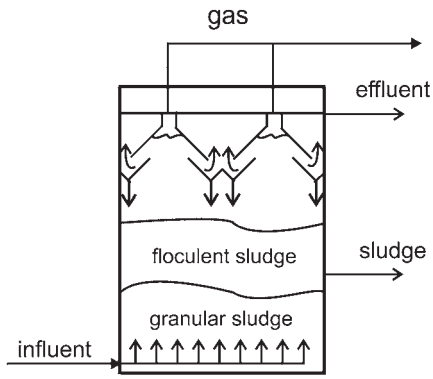


**Fig. 8.6** Upflow anaerobic sludge blanket.

The influent wastewater is distributed at the bottom by a system of tubes which provides a flow through a blanket of granular sludge. Inside these porous particles, fatty acids and biogas are formed. The reaction rate of the process is controlled by diffusion, convection and reaction inside the pores. Ascending biogas bubbles keep the particles partially fluidized. Depending on the kind of wastewater, the sludge tends to be more or less flocculating, which determines how well it is suspended in the fluidized sludge (Fig. 8.6). At the top of the UASB, the gas bubbles are separated from the water in hoods and the rising flocs which show a lower settling rate are carried up by the gas/liquid flow. Gas is collected in the hoods and removed. Liquid/solid separation takes place in the settler section. The treated water flows over weirs while discharging into a wastewater canal system for further treatment either together with municipal wastewater or directly by subsequent dedicated processes, such as aerobic purification. The mass of flocculent and granular sludge must be controlled by siphoning off excess sludge. Depending on the wastewater, hydraulic retention times of $t_R$ = 0.2–2.0 d are typical for a load of $B_V$ = 2–25 kg COD $m^{-3}$ $d^{-1}$ (Grady et al. 1999).

### 8.4.4
### Anaerobic Fixed Bed Reactor

A fixed bed reactor is filled with solid media to facilitate the formation of biofilms with anaerobic bacteria. Frequently, the synthetic media used are the same as those in trickling filters (Fig. 8.7a; Young 1991) or, alternatively, they are porous polyurethane particles with a diameter between 0.3 cm and 1.0 cm and are used with inner surfaces for bacteria immobilization (Fig. 8.7b; Spieß 1991; Kus 1993).

Examples of such support materials are shown in Fig. 8.7. The surface area for bacterial growth is about 100 $m^2$ $m^{-3}$ with a void volume fraction of 90–95% (Grady et al. 1999). The formation of biofilms and the two-phase flow must facilitate liquid/gas separation and must avoid blockage by thick biofilms or large suspended sludge particles. For these reasons, the wastewater is recycled to increase the flow rate and shear stress inside the fixed bed (Fig. 8.8a).

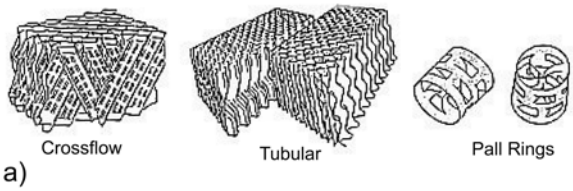


a)

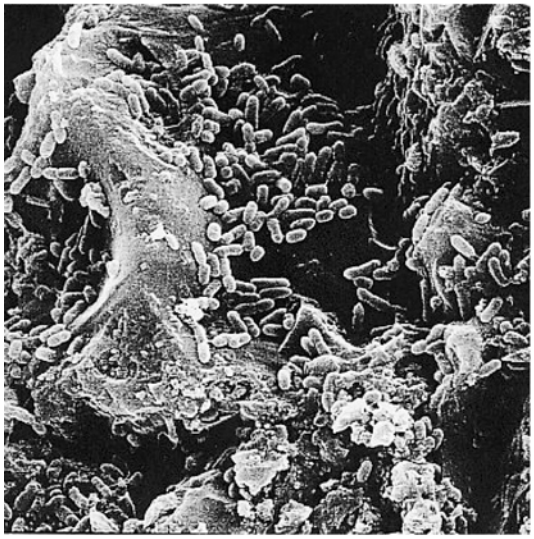

b)

**Fig. 8.7** Media for immobilization of anaerobic bacteria.
(a) Non-porous synthetic media (Young 1991).
(b) Immobilized bacteria on porous polyurethane particle.

Excess sludge is normally rinsed out with the effluent. If blockages occur, the flow rate of the recycle flow must be increased temporarily.

In some cases, the advantages of the UASB and the fixed bed reactor – the establishment of high bacteria concentrations by granular particles and the formation of biofilms near the effluent to reduce the loss of bacteria – are combined (Fig. 8.8b).

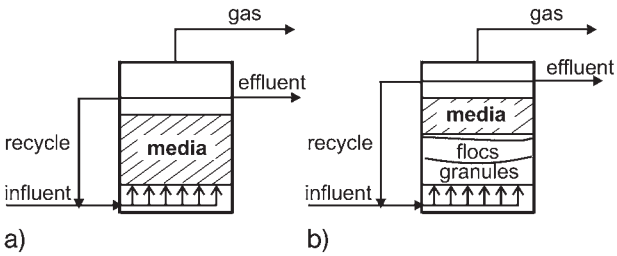


**Fig. 8.8** Anaerobic fixed bed reactor (a), Hybrid USAB (b).

On the top of an UASB, a fixed bed reactor with a relatively short bed of synthetic media is installed (hybrid UASB).

### 8.4.5 Anaerobic Rotating Disc Reactor

Anaerobic rotating disc reactors (RDR) are characterized by a horizontal wheel that, on a technical scale, can have a diameter of up to 2 m and a length of about 5 m (Fig. 8.9). With a plate spacing of 5 cm, about 100 plates can be installed, giving a total surface area of about 630 $m^2$.

An anaerobic RDR has a double wall for heating and temperature control, has a closed top and is combined with a gas collection system. The plates are completely submerged in the wastewater. Surplus sludge is collected at the bottom and must be removed periodically. The discs rotate with a speed of 0.5–2.0 $min^{-1}$.

Several authors have published results obtained by laboratory-, pilot- and large-scale studies (Tait and Friedman 1980; Laquidara et al. 1986; Ware and Pescod 1989; Ware et al. 1990; Breithaupt 1997; Breithaupt and Wiesmann 1998).

Breithaupt (1997) used plates with a covering made from a synthetic structural material which made it possible to form biofilms with a higher area and thickness. In these anaerobic RDR both a high total COD removal and a high COD removal rate could be realized for wastewater with high acetate concentrations.

The reactor is not completely mixed: the concentration of immobilized bacteria increases in the first 25% of the total length up to 10 g $L^{-1}$ MLSS and decreases in the last 75% down to 2.5 g $L^{-1}$ MLSS. The pH increases due to the methanization of acetate. Using an acetate balance and considering axial dispersion, Haldane kinetics and the influence of locally changing pH, mathematical models were used to calculate the acetate concentration profile (Breithaupt 1997).

Anaerobic RDRs are particularly suitable for moderate amounts of highly loaded wastewater. Low amounts of <10 $m^3$ $d^{-1}$ wastewater are more appropriate for aero-

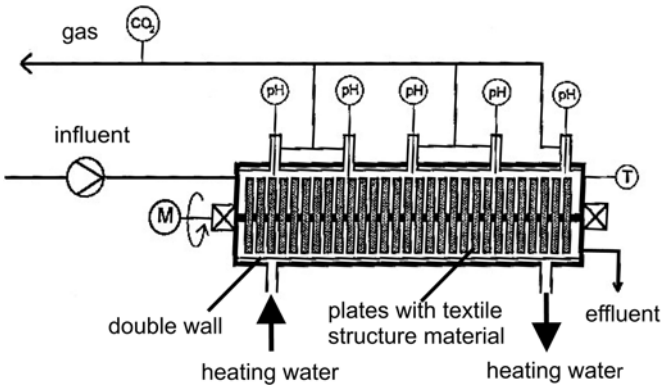


**Fig. 8.9** Anaerobic rotating disc reactor (Breithaupt 1997).

bic treatment; and high amounts of >$10^3$ $m^3$ $d^{-1}$ should be treated by using one of the other anaerobic processes described above.

### 8.4.6
### Anaerobic Expanded and Fluidized Bed Reactors

In both systems, small particles are used as carriers for biofilms (bioparticles). Frequently, silica sand with a diameter of 0.2–0.5 mm and a specific density of 2.65 g $cm^{-3}$ or activated carbon particles with somewhat higher diameters and a lower density are used. The upward flow rate must be high enough to expand the bed and the wastewater must be recycled at a much higher rate than in fixed bed reactors (Fig. 8.10).

Expanded beds are expanded by 15–30% and fluidized beds by 30–300%, relative to the volume at rest. Because of the very high surface area of the biofilms (9000–11 000 $m^2$ $m^{-3}$), their low thickness and the high mass transfer rate in the mobile bed, the biogas production rate is very high and the mean retention time of the wastewater is often only about 6 h and sometimes remarkably lower.

High biomass concentrations of 15–35 g $L^{-1}$ MLSS are possible, similar to those achieved with the UASB process (Hall 1992), but the load rates achieved of more than 20 kg COD $m^{-3}$ $d^{-1}$ can be significantly higher than that of the UASB process (2–25 kg COD $m^{-3}$ $d^{-1}$; Grady et al. 1999) because of the reduced limitation of mass transfer by diffusion and convection. The upper segment of the reactors above the expanded and fluidized beds serves to separate the gas bubbles from the water (which is recycled to a large degree) and from the bacterial flocs which have sheared off the biofilms.

In recent times, new anaerobic systems have been investigated and proposed for technical use which are equipped with integrated membranes for retaining and increasing the amount of bacteria.

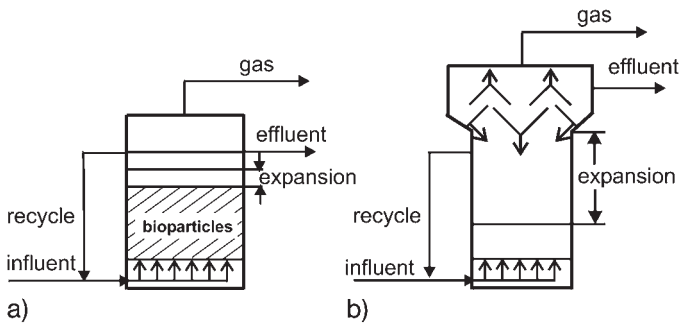


**Fig. 8.10** Anaerobic expanded and fluidized bed reactors: (a) expanded bed, (b) fluidized bed

**PROBLEM**

An industrial wastewater with a substrate concentration of $S_o = 2000$ mg $L^{-1}$ DOC = 5000 mg $L^{-1}$ COD and a flow rate of $Q_o = 1000$ $m^3$ $d^{-1}$ is to be treated anaerobically by a one-stage contact process at steady state for a temperature of 35 °C, with a removal efficiency of 90% and a concentration of X = 1 g $L^{-1}$ MLSS methanogenic bacteria. The wastewater is free of $SO_3^{2-}$ and $NO_3^-$. The reaction is neither limited nor inhibited by low or high concentrations of acetate.

Given coefficients:

$\mu_{max} = 0.18\ d^{-1}$

$Y^{\circ}_{X/S} = 0.037$ g MLSS (g COD)$^{-1}$

Calculate:
1. The necessary volume of the bioreactor V.
2. The volume of methane produced daily $r_{CH_4}$ V in $Nm^3\ d^{-1}$.

**Solution**

1. First we have to balance the substrate. As demonstrated in Section 8.2.4, the organics and the $CO_2$ formed are all converted into acetate. Although intermediate compounds are formed by other bacteria, they do not reduce the COD or DOC.

$$0 = Q_0(S_0 - S) - \frac{\mu_{max} X \cdot V}{Y^{\circ}_{X/S}}$$

$$V = \frac{Q_0(S_0 - S)\,Y^{\circ}_{X/S}}{\mu_{max} X} = \frac{10^3 \cdot 4.5 \cdot 10^3 \cdot 0.037}{0.18 \cdot 1} = 925\ m^3$$

2. As demonstrated in Section 8.25, the yield is:

$Y^{\circ}_{CH_4/S} = 0.35\ Nm^3\ CH_4$ (kg COD)$^{-1}$

or: $r_{CH_4} = 0.35\ r_S\ Nm^3\ CH_4$ (kg COD)$^{-1}$

$$r_S = \frac{Q_0(S_0 - S)}{V} = \frac{10^3 \cdot 4.5 \cdot 10^3}{925}\ g\ (dm^3)^{-1} = 4.86\ kg\ COD\ (m^3\ d)^{-1}$$

$r_{CH_4} = 0.35 \cdot 4.86\ Nm^3\ CH_4\ (m^3\ d)^{-1} = 1.70\ Nm^3\ CH_4\ (m^3\ d)^{-1}$

$r_{CH4} \cdot V = 925 \cdot 1.70 = 1.572\ Nm^3\ d^{-1}$

## References


Andrews, J.F. **1969**, Dynamic model of the anaerobic digestion process, *Am. Soc. Civil Eng.* 95, 95–116.

Attal, A.; Ehlinger, F.; Audic, J.M.; Faup, G.M. **1988**, pH-Inhibition mechanism of acetogenic, acetoclastic and hydrogenophilic populations, Proc. Int. Symp. Anaerobic Digestion, 5, 22–26.

Balch, W.E.; Fox, F.E.; Magrum, L.J.; Woese, C.R.; Wolfe, R.S. **1979**, Methanogens: reevaluation of an unique biological group, *Microbiol. Rev.* 43, 260–296.

Bolle, W.L.; Breugel, J.; Gils, W. **1986**, Kinetics of anaerobic purification of industrial wastewater, *Biotechnol. Bioeng.* 28, 542–548.

Boone, D.R.; Bryant, M. **1980**, Propionate degrading bacterium *Synthrophobacter wolinii* sp. nov. gen. nov. from methanogenic ecosystem, *Appl. Environ. Microbiol.* 40, 626–632.

Brandis, A.; Thauer, R.K. **1981**, Growth of *Desulfovibrio* species on hydrogen and sulfate as sole energy source, *J. Gen. Microbiol.* 126, 249–252.

Breithaupt, T. **1997**, Rotationsscheibenreaktor für die aerobe, anoxische und anaerobe Abwasserreinigung. Praktische Einsatzmöglichkeiten und mathematische Modellierung, *VDI-Forschungsberichte, Reihe 15*, 197.

Breithaupt, T.; Wiesmann, U. **1998**, Konzentrationsprofile in Rotationsscheibenreaktoren und deren Modellierung am Beispiel des anaeroben Acetatabbaus mit experimenteller Überprüfung, *Acta Hydrochem. Hydrobiol.* 26, 288–295.

Bryer, J.D. **1985**, Structured modelling of the anaerobic digestion of biomass particulates, *Biotechnol. Bioeng.* 27, 638–649.

Carr, A.D.; O'Donell, R.C. **1977**, The dynamic behavior of an anaerobic digester, *Prog. Water Technol.* 9, 727–738.

Chang, J. **1982**, *Studies On Methanogenic Phase In Anaerobic Digestion*, PhD thesis, Tohoku University, Tohoku.

Dauber, S. **1993**, in: *Anaerobtechnik*, ed. B. Böhnke, W. Bischofsberger, S.F. Seyfried, Springer-Verlag, Berlin.

Denac, M. **1986**, *Anaerober Abbau gelöster organischer Stoffe in Festbett- und Wirbelschichtreaktoren*, PhD thesis, ETH Zurich.

Fukuzaki, S.; Nishio, N.; Nagai, S. **1990**, Kinetics of the methanogenic fermentation of acetate, *Appl. Environ. Microbiol.* 56, 3158–3163.

Ghosh, S.; Pohland, F.G. **1974**, Kinetics of substrate assimilation and product formation in anaerobic digestion, *J. W.P.C.F.* 46, 748–759.

Gottschalk, G. **1986**, *Bacterial Metabolism*, 2nd edn, Springer-Verlag, Berlin.

Grady, C.P.L. Jr.; Daisser, G.T.; Lin, H.C. **1999**, *Biological Wastewater Treatment*, 2nd edn, Marcel Dekker, New York, p. 611.

Graef, S.P.; Andrews, J.F. **1973**, Mathematical modelling and control of anaerobic digestion, *AIChE Symp. Ser.* 70, 101–131.

Gujer, W.; Zehnder, A.J.B. **1983**, Conversion processes in anaerobic digestion, *Water Sci. Technol.* 15, 127–167.

Hall, E.R. **1992**, Anaerobic treatment of wastewaters in suspended growth and fixed film processes, in: *Design of Anaerobic Processes for the Treatment of Industrial and Municipal Wastes*, ed. Malina, J.F. Jr.; Pohland, F.G., Technomics Publishing, Lancaster, Penn., p. 41–118.

Hanaki, K.; Noike, T.; Matsumoto, J. **1985**, Mathematical modelling of the anaerobic digestion process, in: *Mathematical Models in Biological Waste Water Treatment*, ed. Jörgensen, S.E.; Gromiec, M.J., Elsevier-Verlag, Berlin, p. 41–118.

Harper, S.R.; Pohland, F.G. **1986**, Recent developments in hydrogen management during anaerobic biological wastewater treatment, *Biotechnol. Bioeng.* 27, 585–602.

Jeris, J.S.; McCarty, P.C. **1965**, Biochemistry of methane fermentation using $^{14}C$ tracers, *J. W.P.C.F.* 37, 178.

Kus, F. **1993**, Kinetik des anaeroben Abbaus von Essig- und Propionsäure in Bioreaktoren mit immobilisierten Bakterien, *VDI-Forschungsberichte, Reihe 15*, 115.

Laquidara, M.J.; Blanc, F.C.; O'Shaughnessy, J.C. **1986**, Developtment of biofilm, operating characteristics and operational control in the anaerobic rotating biological contactor process, *Water Pollut. Control Fed.* 58, 107–114.

Lawrence, A.W.; McCarty, P.L. **1969**, Kinetics of methane fermentation in anaerobic treatment, *J. W.P.C.F.* 41, 2.

Lettinga, G.; Hulshoff, L.W. **1991**, UASB process design for various types of wastewaters, *Water Sci. Technol.* 24, 87–108.

Lettinga, G.; Hulshoff, L.W. **1992**, UASB process design for various types of wastewaters, in: *Design of Anaerobic Processes for the Treatment of Industrial and Municipal Wastes*, ed. Malina, J.F. Jr.; Pohland, F.G., Technomics Publishing, Lancaster, Penn., p. 119–145.

Massey, M.L.; Pohland, F.G. **1978**, Phase separation of anaerobic stabilization by kinetic controls, *J. W.P.C.F.* 50, 2204–2222.

McInerney, M.J. **1999**, Anaerobic metabolism and its regulation, *Biotechnology* 11a, 455–478

McInerney, M.J.; Bryant, M.P. **1981**, Review of methane fermentation fundamentals, in: *Fuel Gas Production from Biomass*, ed. Wise, D.L., CRC Press, Boca Raton, p. 19–46.

McInerney, M.J.; Bryant, M.P.; Pfennig, N. **1979**, Anaerobic bacterium that degrades fatty-acids in syntrophic association with methanogenes, *Arch. Microbiol.* 122, 129–135.

Mosey, F.E. **1983**, Mathematical modelling of the anaerobic digestion process: regulatory mechanisms for the formation of short chain volatile acids from glucose, *Water Sci. Technol.* 15, 209–232.

Nethe-Jaenchen, R.; Thauer, R.K. **1984**, Growth yields and saturation constant of *Desulfovibrio vulgaris* in chemostat culture, *Arch. Microbiol.* 137, 236–240.

Pohland, F.G. **1992**, Anaerobic treatment: fundamental concepts, applications, and new horizons, in: *Design of Anaerobic Processes for the Treatment of Industrial and Municipal Wastes*, ed. Malina, J.F.; Pohland, F.G., CRC Press, London, p. 1–33.

Seyfried, C.F. **1979**, Reinigung organisch hochverschmutzter Abwässer mit dem anaeroben Belebungsverfahren am Beispiel von Abwässern aus der Nahrungsmittelherstellung, Veröffentlichung des Instituts für Siedlungswasserwirtschaft, Universität Hannover.

Shea, T.G.; Pretorius, W.A.; Cole, R.D.; Pearson, E.A. **1968**, Kinetics of hydrogen assimilation in the methane fermentation, *Water Res.* 2, 833–848.

Spieß, A. **1991**, Anaerobe Abwasserreinigung in neuen Bioreaktoren mit Polyurethanpartikeln zur Immobilisierung der Bakterien, *VDI-Forschungsberichte, Reihe 15*, 85.

Stronach, S.M.; Rudd, T.; Lester, J.N. **1986**, *Anaerobic Digestion Processes in Industrial Wastewater Treatment*, Springer-Verlag, Berlin, p. 32–33.

Tait, S.J.; Friedman, A.A. **1980**, Anaerobic rotating biological contactor for carbenous wastewater, *J. W.P.C.F.* 52, 2256–2269.

Ware, A.J.; Pescod, M.B. **1989**, Full-scale studies with an anaerobic/aerobic RBC unit treating brewery wastewater, *Water Sci. Technol.* 21, 197–208.

Ware, A.J.; Pescod, M.B.; Storch, B. **1990**, Evaluation of alternatives to conventional disc support media for rotating biological contactors, *Water Sci. Technol.* 22, 113–117.

Weimer, P.J.; Zeikus, J.G. **1978**, Acetate metabolism in *Methanosarcina barceri*, *Archiv. Microbiol.* 119, 175–182.

Widdel, F.; Pfennig, N. **1981**, Studies on dissimilatory sulfate reducing bacteria that decompose fatty acids I. Isolation of new sulfate reducing bacteria enriched with acetate from saline environments. Description of *Desulfobacter postgatei* gen. nov., sp. nov., *Arch. Microbiol.* 129, 395–400.

Yoo, E.S. **2000**, *Biological and Chemical Mechanisms of Reductive Decolorization of Azo Dyes*, PhD thesis, TU Berlin.

Young, J.C. **1991**, Factors effecting the design and performance of up flow anaerobic filters, *Water Sci. Technol.* 24, 133–156.

Zehnder, A.J. **1988**, *Biology of Anaerobic Microorganisms*, John Wiley & Sons, New York.

Zehnder, A.J.; Wuhrmann, K. **1977**, Physiology of a Methanobacterium Strain AZ, *Arch. Microbiol.* 111, 119.

Zehnder, A.J.; Huser, B.A.; Brock, T.D.; Wuhrmann, K. **1980**, Characterisation of an acetic-decaroxylation, non-hydrogen-oxidizing methane bacteria, *Arch. Microbiol.* 124, 1–11.

Zeikus, J.G. **1979**, Microbial populations in digesters, in: *Proc. 1st Int. Symp. Anaerobic Digestion*, Applied Science Publications, London.

# 9
# Biodegradation of Special Organic Compounds

## 9.1
## Introduction

Until today, industrial effluents loaded with particular organic compounds, which are difficult to biodegrade, have frequently been mixed with other effluents and "treated" together in WWTPs. Over time, the disadvantages of this technology have become obvious:

- The chemical oxygen demand (COD) of the effluent is considerably higher than legal limits, resulting in high discharge fees or the requirement to supplement the process with activated carbon treatment.
- Stripping of a part of the organic volatile compounds leads to air pollution problems and the necessity to cover the aerated basins and to treat the waste air.
- Certain effluents are only diluted, such as those from chemical plants with a high concentration of non-biodegradable compounds.
- Effluents containing toxic compounds reduce the removal rate in activated sludge plants.
- Endocrine-disrupting compounds discharged into wastewater can pass through WWTPs and enter aquatic environments.

Many more reasons can be cited for the need to turn away from end-of-the-pipe technology. New approaches are necessary, especially when new production units are to be constructed or old units have to be modernized. Furthermore, local circumstances have to be taken into consideration. In industrialized countries, a large percentage of industrial effluent is discharged into municipal WWTPs. But a significant number of large cities around the world do not have any municipal WWTP, so that industrial wastewater treatment is absolutely necessary to protect ground water reservoirs and to guarantee a minimum quality of raw water for the production of clean drinking water. Since clean water is also an essential raw material for industry and agriculture, many national economies will be affected by the need for clean water in the near future.

This makes it necessary for industry to conserve water by reducing its consumption. In principle, there are essentially three ways to conserve water:

*Fundamentals of Biological Wastewater Treatment*. Udo Wiesmann, In Su Choi, Eva-Maria Dombrowski

ISBN: 978-3-527-31219-1

1. Design new production processes with lower water consumption.
2. Recycle cooling and process water.
3. Develop economical solutions for the treatment of effluents with different types and strengths of problematic and non-problematic compounds (see Chapter 13).

The treatment of wastewater and process water should be carried out in most cases in the immediate proximity of the production unit. Both production and waste management have to be designed and optimized by a single team; and both units have to be operated by a single team. Wastewater treatment must be integrated into the production process!

Physical, chemical and biological processes must all be considered to find the best solution. Biological and chemical oxidation and reduction processes are of special interest if almost complete transformation to compounds such as $CO_2$, $H_2O$, $N_2$ and $CH_4$ is possible. The pollution in the effluents from such optimized processes is no longer characterized by thousands of different chemicals, rather there are often only three or four single compounds which dominate; and a knowledge of stoichiometry as well as kinetic coefficients may be helpful for a better understanding and optimization of the biodegradation processes.

Before we pick up this topic in Chapter 13, this chapter will discuss groups of problematic dissolved materials, which are not easily mineralized by microorganisms.

## 9.2 Chlorinated Compounds

### 9.2.1 Chlorinated *n*-Alkanes, Particularly Dichloromethane and 1,2-Dichloroethane

#### 9.2.1.1 Properties, Use, Environmental Problems and Kinetics

Chlorine, a by-product from the electrolysis of chloroalkalis, was used in the beginning of the 20th century for the production of chloroorganic compounds and is known for its high reactivity with organics. Of the 114 organic priority pollutants listed by the United States Environmental Protection Agency (EPA) in 1975, 22 are chlorinated alkanes (Patterson 1985). Some of these are cited in Table 9.1. Because of their toxicity and tendency to bioaccumulate in animals, they must be removed as completely as possible from all liquid and gaseous effluents.

Inspection of the compound properties listed in Table 9.1 (Wiesmann and Libra 1999) shows that, with increasing chlorine content, the Henry coefficient rises, whereas solubility and biodegradability show a reversed trend. Therefore, tri- and tetrachloroethene are normally air pollutants and are removed from water and air by activated carbon adsorption. The discussion here will concentrate on dichloromethane (DCM) and 1,2-dichloroethane (DCA).

The maximum concentration permitted in drinking water for DCM is 20 μg $L^{-1}$ and for DCA is 30–50 μg $L^{-1}$ (WHO 1987). Toxicity experiments with rats led to a

**Table 9.1** Some chlorinated n-alkanes, their properties and uses (Patterson 1985).

| Compound | $c^*$ (mg $L^{-1}$)[a] | H[b] | $LD_{50}$[c] | Uses | EPA No.[d] |
|---|---|---|---|---|---|
| Dichloromethane ($CH_2Cl_2$) | 16 700 | 0.13 | 167–2400 | Solvent for intermediate products<br>Cleaning agent for metal surfaces<br>Propellent for polyurethane production | |
| 1,2-Dichloroethane ($C_2H_4Cl_2$) | 8 700 | 0.046 | 730 | Intermediate product in the production of polyurethane solvent<br>Fuel additive | 10 |
| Trichloromethane ($CHCl_3$) | 7 800 | 0.14 | 450–800 | Solvent in pharmaceutical industry | |
| 1,1,1-Trichloroethane ($C_2H_3Cl_3$) | 4 800 | 0.21 | 10 000–14 300 | Solvent for dyes and ink<br>Cleaning agent for cars and textiles | 11 |
| Trichloroethene ($C_2HCl_3$) | 1 000 | 0.49 | 4 200–7 200 | Solvent for dyes and ink<br>Cleaning agent for cars and textiles | 87 |
| Tetrachloroethene ($C_2Cl_4$) | 150 | 1.2 | 4 000–5 000 | Solvent for dyes and ink<br>Cleaning agent for cars and textiles | 85 |

[a] Solubility, 20 °C.
[b] Henry coefficient, 20 °C.
[c] Rat, oral (mg $kg^{-1}$ body weight).
[d] EPA list of organic pollutants (EPA 1975).

$LD_{50}$ of 0.167–2.4 g $kg^{-1}$ live weight. The $LD_{50}$ value gives the mass of the toxic compound per mass of the animal for which there is a 50% probability that the animal would die within a given time. Mutagenic effects in rats could not be proven (Jongen et al. 1978). Loew et al. (1984) and Rannug (1980) indicate that DCA may be carcinogenic. Data on the worldwide production of DCA during 1960–1981 show an increasing production from $93 \cdot 10^3$ t $a^{-1}$ to $825 \cdot 10^3$ t $a^{-1}$, however, production decreased in Germany from $137 \cdot 10^3$ t $a^{-1}$ to $67 \cdot 10^3$ t $a^{-1}$ in the 3-year period 1990–1993 (Herbst 1995). Study of the mechanism and the kinetics of DCM degradation began in the late 1970s. Studies of the catabolic reactions were first published by Leisinger (1988).

The influence of DCM concentration on the specific growth rate can be described by Haldane kinetics, and the influence of oxygen by Monod kinetics. These two influences are combined by multiplication:

$$\mu = \mu_{max} \frac{S}{K_S + S + S^2/K_i} \cdot \frac{c'}{K' + c'} \tag{9.1}$$

The kinetic and stoichiometric coefficients are listed in Table 9.2. The variability of the values can be explained by the use of different methods for kinetic measurements and different microbial cultures. Some authors used pure cultures, some mixed.

**Table 9.2** Kinetic and stoichiometric coefficients for aerobic and anoxic degradation of DCM and DCE (Herbst 1995, expanded).

| Compound; reference | Bacteria | $Y_{O_2/S}$ (mol mol$^{-1}$) | $Y_{B/S}$ gMLSS (g DCM)$^{-1}$ | $\mu_{max}$ (d$^{-1}$) | $K_S$ (mg L$^{-1}$ DCM) | $K_i$ (mg L$^{-1}$ DCM) | $K'$ (mg L$^{-1}$ $O_2$) |
|---|---|---|---|---|---|---|---|
| DCM | | | | | | | |
| Brunner (1982) | *Pseudomonas* | | 0.158 | 2.6 | 17.0–42.5 | 995 | |
| Dirks and Ottengraf (1991) | *Hyphomicrobium* | | 0.17 | 2.6 | | 300 | 0.055 |
| Hauschild et al. (1992) | *Pseudomonas* | | | 5.3 | 4 | 1470 | |
| Niemann (1993) | Mixed culture | 0.62 | | | 3–10 | 200–2500 | 0.5–0.9 |
| Herbst (1995) | Mixed culture | 0.56 | 0.105 | 0.77 | 11.6 | | |
| Freedman et al. (1997) | *Acinetobacter* sp. | | 0.118[a)] | 1.1 | | 405 | |
| DCA | | | | | | | |
| Freedman et al. (1997) | Mixed culture | 0.58[b)] | 0.087 | 0.77 | | | |
| Janssen et al. (1985) | *Xanthobacter* | | | | 109 | | |
| Sallis et al. (1990) | *Rhodococcus* | | | 2.5 | 26 | | |
| Rudek (1992) | *Xanthobacter* | 1.12 | 0.12 | 3.4 | | | 0.055 |
| Freitas dos Santos and Livingston (1995) | *X. autotrophicus* | 1.65 | 0.166 | 4.6 | 7.6 | | 0.1 |
| Herbst (1995) | Mixed culture | 1.7 | 0.17 | 4.6 | 57 | 125 | 0.5 |

[a)] g MLVSS (g DCM)$^{-1}$. [b)] $Y_{NO_3/S}$ mol mol$^{-1}$.

We can conclude from a mean $K_S$ value of 10 mg L$^{-1}$ DCM that very low DCM concentrations below 1 mg L$^{-1}$ can only be obtained by a physical or chemical second step, e.g. adsorption on activated carbon or ozonation.

A hypothetic pathway for the catabolism of 1,2-dichloroethane oxidation was published by Janssen et al. (1985).

#### 9.2.1.2 Treatment of Wastewater Containing DCM or DCA

DCM balances in activated sludge systems show that DCM is almost totally stripped by air (Gerber et al. 1979). Therefore, trickling filters are also unsuitable.

Only 11% of the DCM added were biodegraded, 75% were desorbed into the air and 14% remained in the effluent (Winkelbauer and Kohler 1989).

In further laboratory- and pilot-scale studies, fixed and fluidized bed reactors with solid particles as support material for bacteria were used. In fixed-bed reactors, a high fluid recycle rate is necessary for aeration in external absorption tanks (Kästner 1989) or for the addition of $H_2O_2$ by mixing (Stucki et al. 1992). Similarly, in two-phase fluidized-bed reactors, a high recycle rate must be used for oxygen addition and fluidization (Gälli 1986; Burgdorf et al. 1991; Stucki et al. 1992; Niemann 1993; Herbst 1995). In order to avoid total substrate desorption, oxygen can be added in the absorption tank using non-porous membranes (Herbst 1995). Figure 9.1 presents a laboratory-scale fluidized bed reactor for the mineralization of DCA and DCM. The production of HCl makes it necessary to control the pH to 7–8 by adding NaOH.

During growth, bacteria formed pellets with a diameter of 3–5 mm, which were kept fluidized in the reactor with the upflowing water containing the DCM or DCA. The pellets settled inside the enlarged head of the reactor; and the solid-free water passed a non-porous tubular membrane where oxygen was taken up by diffusion. This water was mixed with inflowing wastewater containing DCA or DCM before being recycled into the reactor.

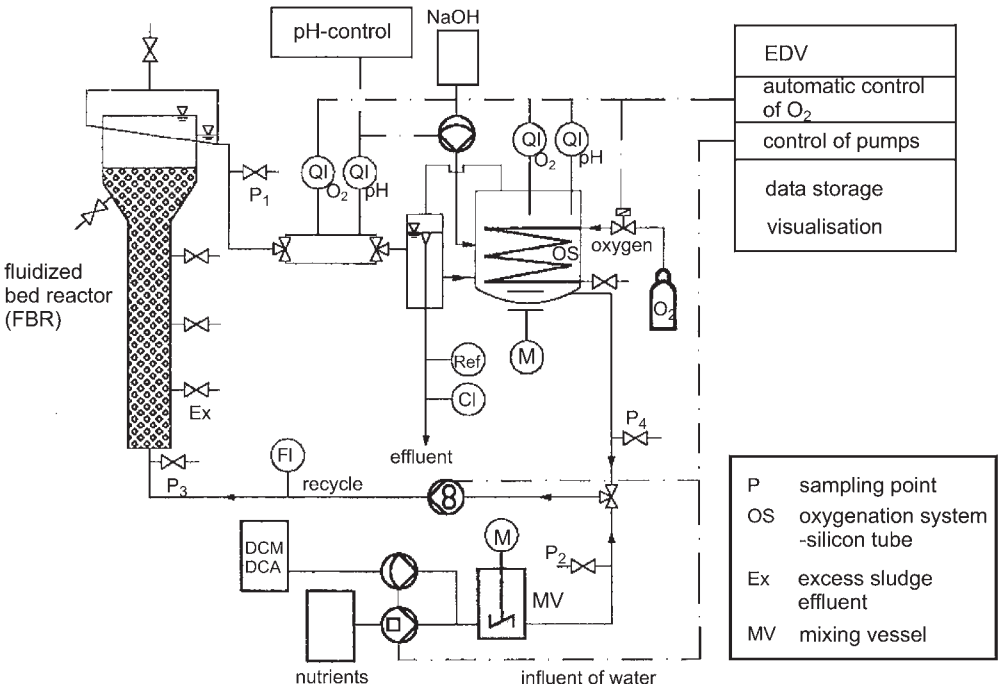


**Fig. 9.1** Laboratory-scale plant with fluidized-bed reactor and oxygenation membrane for bubble-free aerobic mineralization of dichloromethane (DCM) and dichloroethane (DCA; Herbst and Wiesmann 1996).

The avoidance of direct aeration by using a membrane prevented desorption of the volatile substrates. A special membrane bioreactor to mineralize DCA has been tested successfully (Freitas dos Santos and Livingston 1995). DCA was kept separated from the biofilm by a membrane and only the part of the reactor with the biofilm and without DCA was aerated. This kept the DCA concentration inside the region of the membrane and biofilm so low that almost none was stripped by air bubbles.

High bacterial concentrations growing on the surface of small sand particles (Gälli 1986; Stucki et al. 1992; Niemann 1993), in porous glass particles (Burgdorf et al. 1991) or in dense flocs weighted by $CaCO_3$ (Herbst 1995; Herbst and Wiesmann 1996) yielded high mean reaction rates of up to 1400 mg $L^{-1}$ $h^{-1}$ DCM and 400 mg $L^{-1}$ $h^{-1}$ DCA. HCl was formed during the reaction and a relatively large amount of NaOH or $Ca(OH)_2$ had to be dosed. Lonjaret (1996) successfully tested a biotrickling filter for the treatment of DCM-loaded exhaust air.

## 9.2.2 Chlorobenzene

### 9.2.2.1 Properties, Use and Environmental Problems

Of the 12 known chlorobenzenes, six are of commercial importance (MCB, 1,2-DCB, 1,4-DCB, 1,2,4-TCB, 1,2,4,5-TeCB and HCB). Compounds with less chlorine are characterized by higher water solubility and higher vapor pressure or Henry coefficient (Table 9.3).

The toxicity of the chlorobenzenes also increases with increasing number of chlorine atoms. German production decreased steadily through the 1980s and 1990s as a result of stricter regulations. Emissions in the state of North-Rhine-Westphalia (Bayer Leverkusen, Germany) were estimated at 2886 t $a^{-1}$ MCB and 1055 t $a^{-1}$ DCB for 1992 (Döpper and Stock 1995). Three years earlier (1989), these emissions for the state of Hessen (Hoechst AG, Germany) were higher by a factor of nearly ten (Döpper and Stock 1995). These reductions result from the decrease in production and increase in efficiency of wastewater treatment.

### 9.2.2.2 Principles of Biological Degradation

A suitable auxiliary substrate is necessary to facilitate anaerobic dechlorination (acetate, acetone and others). The anaerobic degradation of MCB and benzene is obviously possible only in combination with the reductive dechloronation of higher-chloronated benzenes. The hydrogen replacing the chlorine atom probably comes from water (Nowak 1994).

Some papers report the production of the stable intermediate 1,2,3-TCB (Bosma et al. 1988; Ramanand et al. 1993). An example of the formation of intermediates during the anaerobic dechlorination of a mixture of 1,2,3-TCB, 1,3,4-TCB and 1,3,5-TCB in batch experiments (20 mg $L^{-1}$ of each compound, 1-L flask tests) is presented in Fig 9.2.

**Table 9.3** Some chlorobenzenes, their properties and uses at T = 25 °C. For symbols used, see Table 9.1.

| Compound | $c^*$ (mg $L^{-1}$) | H | $LD_{50}$ for rat (mg $kg^{-1}$) | Uses | EPA No. |
|---|---|---|---|---|---|
| Monochlorobenzene (MCB) | 460[a] T = 20–30 °C | 0.16[a] | 2900[a] | – Intermediate in the production of dyes, agrochemical, synthetics, aids for textile industry[a] | 7 |
| 1,2-Dichlorobenzene (1,2-DCB) | 130[a] T = 20–30 °C | 0.10[a] | 1500 | – Intermediate in the production of 3,4-dichloroaniline decolorizer, degreaser[a] | |
| 1,4-Dichlorobenzene (1,4-DCB) | 73[a] T = 20–30 °C | 0.079[a] | 500 | – Deodorizer, moth repellent<br>– Intermediate in production of dyes[a] | |
| 1,2,4-Trichlorobenzene (1,2,4-TCB) | 30[b] | 0.059 | | – Intermediate in the production of trichloronitrobenzene, etc.<br>– Solvent | 8 |
| 1,2,4,5-Tetrachlorobenzene (1,2,4,5-TeCB) | 0.5–2.4[c] T = 25 °C | $K_p$ = 0.12 kPa $m^3$ $mol^{-1}$[c] | | – Intermediate in the production of tetrachloronitrobenzene and trichlorophenol[c] | |
| Hexachlorobenzene (HCB) | 0.006[b] | 0.071 | | – Intermediate in the production of pentachlorothiophenol and PCP production (in Germany until 1985)[c] | 9 |

[a] Rippen (1991). [b] Patterson (1985). [c] Nowak (1994).

The mixed culture performing this degradation was obtained from methanogenic sediments of the Saale River near Jena, Germany. Acetone was used as an auxiliary substrate. It is remarkable that all three DCBs were observed in different amounts, presumably as a result of different degradation rates. Special cultures of aerobic bacteria seem to be capable of mineralizing all chlorinated benzenes from 1,2,4,5-TeCB (Sander et al. 1991) and 1,2,3,4-TeCB (Feidieker 1993) to MCB. Prieger-Kraft (1995) proved that both compounds were mineralized as the only source of carbon and energy. Currently, there is no confirmation of the aerobic elimination of PCB and HCB. In contrast to anaerobic dechlorination, during aerobic reactions the ring of the MCB is opened and chloro-*cis* together with *cis*-muconic acid are formed. Only then can the chlorine atom be separated.

Aerobic pure cultures use chlorinated benzenes as the only source of carbon and energy, with $\mu_{max}$ = 13.2 $d^{-1}$ with MCB (Reineke and Knackmuss 1984), $\mu_{max}$ = 4.3 $d^{-1}$ with 1,2-DCB (Haigler et al. 1992) and $\mu_{max}$ = 1.7 $h^{-1}$ with 1,3-DCB (De Bont et al. 1986).

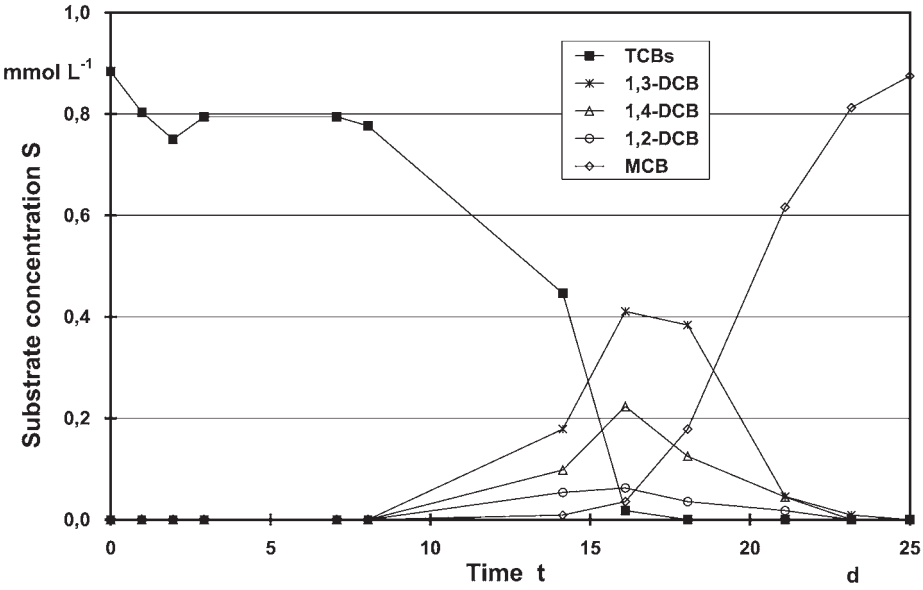


**Fig. 9.2** Anaerobic reduction of three tetrachlorobenzenes (three isomeric TCBs, 20 mg $L^{-1}$ of each), T = 28 °C, pH 7.28, auxiliary substrate: acetone (Adrian et al. 1995).

#### 9.2.2.3 **Treatment of Wastewater Containing Chlorobenzene**

In all known continuous biological processes: (a) only laboratory-scale experiments have been carried out and (b) the pure or mixed bacterial cultures used were immobilized on solid particles.

As shown above, the dechlorination of HCB and PCB is only possible by using anaerobic conditions and auxiliary substrates. Fathepure and Vogel (1991) used a biofilm reactor and were able to transform HCB to 1,2,3,4-TeCB with methanol and to 1,2,3-TCB and 1,2-DCB with acetate as an auxiliary substrate. Nowak (1994) was successful in reducing 1,2,3,4-TeCB, all three TCBs and all three DCBs as well as MCB in a fluidized bed reactor with a mixture of methanol, acetate, acetone, ethanol, propanol and a mixed culture from a sediment of the Saale River.

Aerobic mineralization of MCB, the three DCBs and 1,2,4-TCB were achieved in fixed bed reactors by Bouwer and McCarthy (1982) with small glass beads for biofilm growth, by Van der Meer et al. (1987) with sand particles from the Rhine River and by Schäfer (1994) with polyurethane foam particles with and without activated carbon as carriers for mixed cultures, or *Pseudomonas* sp. (Van der Meer et al. 1987). In the experiments by Schäfer (1994), no auxiliary substrates were needed as the source of energy or carbon.

### 9.2.3 Chlorophenols

Of the ten known chlorophenols, five are produced as intermediates or end-products in the chemical industry (Table 9.4). Compared with chlorobenzenes, chlorophenols have a higher solubility in water and a lower Henry coefficient of nearly two orders of magnitude. Because of its high toxicity and its low biodegradability, pentachlorophenol (PCB) was used during the 1970s as an herbicide, fungicide and disinfectant worldwide in amounts of several 10 000 t $a^{-1}$. As a result of stronger regulations, production decreased during the 1980s (BRD in 1983 produced 1800 t $a^{-1}$, EU in 1989 produced 1000 t $a^{-1}$; Rippen 1991).

Khandker (1992) studied the aerobic degradation of 4-MCP as the only source of carbon and energy by a culture with three strains of bacteria ($Y^{\circ}_{X/S}$ = 0.63 MLSS $(gMCP)^{-1}$, $\mu_{max}$ = 3.6 $d^{-1}$, $K_S$ = 21.1 mg $L^{-1}$ MCP). The relatively high $K_S$ value points to a large region of substrate limitation.

The oxidation of 2-CP, 3-CP, 4-CP and 2,4-DCP by $H_2O_2$ was catalyzed by an immobilized peroxidase (Siddique et al. 1993). High oxidation rates were obtained, but high-molecular-weight polymerization products arose which precipitated as small solid particles.

**Table 9.4** Some chlorophenols, their properties and use. For symbols used, see Table 9.1.

| Compound | $c^*$ (mg $L^{-1}$; at 20 °C) | H (at 20 °C) | $LD_{50}$ for rat (mg $kg^{-1}$) | Uses | EPA No. |
|---|---|---|---|---|---|
| 2-Monochlorphenol (2-CP) | 29.0 | 0.49 | 670 | Intermediate in the production of phenols, phenol resins, dyes, bactericide, fungicide | 24 |
| 4-Monochlorophenol (4-CP) | 27.0 | $0.025 \cdot 10^{-3}$ | 250–670 | Intermediate in the production of 2,4-DCP, TCP and TeCP solvent for mineral oil industry | |
| 2,4-Dichlorophenol (2,4-DCP) | 4.4 | $0.131 \cdot 10^{-3}$ | 580 | Intermediate in the production of 2,4-dichlorophenoxy acetate herbicide, toxin for moths | 31 |
| 2,4,5-Trichlorophenol (2,4,5-TCP) | 1.2 | $0.28 \cdot 10^{-3}$ | 820 | Intermediate in the production of 2,4,5-trichlorophenoxyacetate herbicide, fungicide, preservation aid | 8 |
| Pentachlorophenol (PCP) | 19 | $0.029 \cdot 10^{-3}$ | 50 | Herbicide, fungicide Wood preserver Disinfectant | |

## 9.3 Nitroaromatics

### 9.3.1 Properties, Use, Environmental Problems and Kinetics

The most prominent compound of this group is 2,4,6-trinitrotoluene (TNT). It has been produced in large amounts since 1900 and is used particularly as an agent of warfare. The soil of nearly all production sites is polluted by TNT and the products of its slow, natural biodegradation. Cleaning of these sites will be a task for many years to come. Because of its relatively low solubility in water (130 mg $L^{-1}$), TNT causes mainly soil pollution problems.

In contrast, several other nitroaromatics are characterized by a higher solubility in water (Table 9.5). 2,4-Dinitrotoluene (2,4-DNT) and 4-nitrophenol (4-NP), for example, are intermediates in the production of TNT. Therefore, they are more likely to be found in wastewater; and our knowledge about their biodegradability will be discussed briefly below.

Rippen (1991) reported an annual worldwide production of 60 000 t $a^{-1}$ and a German production of 10 000 t $a^{-1}$ TNT. Usually, 4-NP is produced in batch reactors on the basis of purchase orders. After each production run, the reactor, pipes and stirring vessels are washed with water and the remaining raw materials, prod-

**Table 9.5** Some nitroaromatic compounds, their properties and uses. For symbols used, see Table 9.1.

| Compound | $c^*$ (mg $L^{-1}$) | H | Uses | EPA No. |
|---|---|---|---|---|
| Nitrobenzene, | 2000, | 0.0029 | Intermediate in the production of aniline | |
| $C_6H_5NO_2$ | 20 °C | | Intermediate in the production of dyes Rubber, pharmaceutical products, photochemicals | |
| 4-Nitrophenol, $C_6H_4OHNO_2$ | 13 700, 20 °C | $0.021 \cdot 10^{-6}$ | Intermediate in the production of pesticides, azo and sulfur dyes, as well as chemicals for photo industry | 58 |
| 2,4-Dinitrophenol, $C_6H_3OHN_2O_4$ | 200, 12.5 °C | $0.65 \cdot 10^{-6}$ | Pesticide, fungicide Intermediate in the production of dyes, explosives and chemicals for photo industry | |
| 2,4-Dinitrotoluene, $C_7H_6N_2O_4$ | 250, 20–25 °C | $2.4–200 \cdot 10^{-6}$ | Intermediate in the production of polyurethane and of 2,4,6-dinitrotoluene | |
| 2,4,6-Trinitrotoluene $C_7H_5N_3O_6$ | 130, 20 °C | $0.30 \cdot 10^{-8}$ | Explosive Intermediate in the production of dyes and pharmaceuticals | |

ucts and by-products enter the wash water, which is eventually discharged to the next wastewater treatment plant. Because of the multiple dilution processes, the concentration of 4-NP in water is normally relatively low and specialized cultures of bacteria cannot establish themselves in activated sludge plants. Therefore, 4-NP must be removed from the concentrated industrial effluents near the source by biological or physico-chemical processes. Its human toxicity is based on damage caused to the function of liver, kidney and central nervous system (Thiem and Booth 1991). The respiration rate of activated sludge is inhibited by 50% at a 4-NP concentration of 110 mg $L^{-1}$ (Pagga et al. 1982).

With 660 000 t $a^{-1}$ worldwide and 97 000 t $a^{-1}$ in Germany, the annual production of 2,4-DNT is much higher than that of 4-NP (Rippen 1991). 2,4-DNT is mainly used as an intermediate in the production of TNT and polyurethane. Rippen (1991) reported concentrations of 9.7 mg $L^{-1}$ in TNT production effluents and about 14 mg $L^{-1}$ in the wastewater of special production processes for organic chemicals. Biodegradation experiments with anaerobic bacteria have been unsuccessful (Hu and Shieh 1987; Battersby and Wilson 1989).

Table 9.6 shows published stoichiometric coefficients for the description of aerobic catabolism and anabolism. It follows from these coefficients that 67.5% of the carbon is used for catabolism (formation of $CO_2$) and 24% of the nitrogen for anabolism, resulting in 76% being transformed to $NO_2$ ($Y^{\circ}_{NO_2/S\text{-}N}$ = 0.76 mol $NO_2$–N (mol S-N)$^{-1}$).

The low value of $\mu_{max}$ = 0.072 $d^{-1}$ (Heinze 1997) for 4-NP degradating bacteria results in a long generation time of $t_G$ = 9.6 d, but this value obtained with a mixed culture is considerably longer than that obtained by Schmidt et al. (1987) with *Pseudomonas* sp.

**Table 9.6** Stoichiometric and kinetic coefficients for aerobic degradation of 4-NP (Heinze et al. 1995; Heinze 1997).

| Compound, reference | Bacteria | $Y^{\circ}_{O_2/S}$ [mol $O_2$ (mol C)$^{-1}$] | $Y^{\circ}_{X/S}$ [g MLSS (g DOC)$^{-1}$] | $Y^{\circ}_{NO_2/S-N}$ [mol N (mol S-N)$^{-1}$] | $Y^{\circ}_{CO_2/S}$ [mol $CO_2$ (mol C)$^{-1}$] | $\mu_{max}$ ($d^{-1}$) | $K_S$ (mg $L^{-1}$ DOC) |
|---|---|---|---|---|---|---|---|
| 4-NP | | | | | | | |
| Jensen and Lautrup-Larsen (1967) | *Pseudomonas* sp. | | | 0.52 | | | |
| Jakobezyk et al. (1984) | Mixed culture | | | 0.76 | | | |
| Schmidt et al. (1987) | *Pseudomonas* sp. | | | | | 7.4 | 1.1±0.2 |
| Ou and Sharma (1989) | *Pseudomonas* sp. | | | | 0.675 | 0.048 | |
| Heinze (1997) | Mixed culture | 0.82 | 0.41 | 0.76 | | 0.072 | <1.0 |
| 2,4-DNT | | | | | | | |
| Bausum et al. (1992) | Mixed culture | | | | 0.64 | | |
| Heinze (1997) | Mixed culture | 0.71 | 0.62 | 0.80 | | 2.4 | 2.6–4.9 |

Bausum et al. (1992) carried out measurements with 2,4-DNT labelled by $^{14}C$. Offgas measurements of $^{14}CO_2$ made it possible to determine $Y^{o}_{CO_2/S}$ = 0.64 mol $CO_2$ (mol C)$^{-1}$ (Table 9.6). The same authors used first-order kinetics to describe the influence of 2,4-DNT concentration, but their results for the reaction rate showed a relatively high degree of scattering. Further kinetic results were published by Heinze et al. (1995) and Heinze (1997; Table 9.6). It is remarkable that the maximum growth rate $\mu_{max}$ = 2.4 d$^{-1}$ is higher by a factor of 33 than for the mineralization of 4-NP. Additionally, the higher $Y^{o}_{X/S}$ and the lower $Y^{o}_{O_2/S}$ show that a higher amount of carbon was used in anabolism, although two $NO_2^-$ ions have to be separated from one 2,4-DNT molecule!

### 9.3.2
### Treatment of Wastewater Containing 4-NP or 2,4-DNT

Laboratory-scale experiments were successfully carried out with an activated sludge reactor at an influent concentration of 400 mg L$^{-1}$ 4-NP by Jakobezyk et al. (1984). If very low effluent concentrations (μg L$^{-1}$ range) are required, bioreactors must be used (e.g. fixed-bed reactors) which have activated carbon as a support material for bacteria (Speitel et al. 1989). For the treatment of highly loaded synthetic wastewater (630–2500 mg L$^{-1}$ 4-NP), Heitkamp et al. (1990) used a fixed-bed reactor with an immobilized culture of *Pseudomonas* sp. At a mean retention time of only 2.3 h, they obtained a mineralization efficiency of 93%. These experiments show that high reaction rates are possible after some time if slow-growing bacteria are immobilized. An effluent from a 2,4-DNT production plant of BASF Schwarzheide GmbH has been treated since 1995 by a two-step anoxic/aerobic activated sludge plant. In the first step, 2,4-DNT is most likely reduced to amino-nitrotoluene and 2,4-diaminotoluene, which are mineralized in the second step (Socher 1997).

## 9.4
## Polycyclic Aromatic Hydrocarbons and Mineral Oils

### 9.4.1
### Properties, Use and Environmental Problems

Polycyclic aromatic hydrocarbons (PAHs) are contained mainly in the tar of hard coals and in all kinds of mineral oils. During the various preparation processes for intermediate products in the chemical industry and for numerous fuels, PAHs enter the wastewater, groundwater and solid wastes. Because of their toxicity, 13 PAHs are included in the EPA list. Four of these and two further PAHs are presented in Table 9.7. Two characteristics are of notable importance: their low solubility in water, but high solubility in mineral oil, and their toxicity ($LD_{50}$). With increasing number of rings and molecular mass, their solubility in water decreases and their toxicity increases dramatically.

**Table 9.7** Some polycyclic aromatic compounds, their properties, and use (Rippen 1991). For symbols used, see Table 9.1.

| Compound | $c^*$ (mg $L^{-1}$) | $LD_{50}$ (mg $kg^{-1}$) | Use | EPA No. |
|---|---|---|---|---|
| Naphthalene | 25 (20 °C) | Rat: 1780 | Raw material for the production of dyes | |
| Anthracene | 0.048 (20 °C) | *Daphnia magna*: 3 mg $L^{-1}$ | Intermediate in the production of dyes and anthrachinone | 78 |
| Phenanthrene | 0.95 (20 °C) | Rat: 700 | Raw material for the production of explosives, pharmaceutical products, drugs, herbicides, tanneries | 81 |
| Benzo(e)pyrene | 0.0038 (25 °C) | | | |
| Benzo(k)fluorethene | 0.0006 (25 °C) | | | 75 |
| Acenaphthene | | Rat: 10 000 | Raw material for the production of textile pigment dyes and synthetics, insecticides and fungicides | 77 |

Therefore, toxic PAHs are mostly dissolved in other organics such as mineral oils. Mineral oils and their biodegradability will be discussed first before continuing with the biodegradability of PAHs.

### 9.4.2 Mineral Oils

Mineral oils are composed of the following compounds (Berwick 1984):

- saturated hydrocarbons, *n*-alkanes, branched alkanes, cyclic alkanes,
- unsaturated hydrocarbons,
- heterocyclic alkanes,
- asphalts.

Saturated hydrocarbons can be mineralized by bacteria and yeasts and have been used as an energy and carbon source for the production of single-cell protein (SCP). *n*-Alkanes are very important components; and their content in distillation products increases as their boiling points decrease. The solubility in water is only about 0.002 mg $L^{-1}$ for compounds with 12 or more C-atoms (Mackay and Shiu 1981). For solutions with concentrations above solubility, the oil phase can be dispersed as small droplets with adequate energy input, e.g. with a rotor-stator system. A stable oil–water emulsion can be produced with high energy input and the addition of an emulsifier.

An emulsion produced from *n*-dodecane (750 mg $L^{-1}$) with a surfactant (Eumulgin ET5, Henkel; 150 mg $L^{-1}$) and at a rotational speed of 10 000 $min^{-1}$ for 1 min was designated as a standard emulsion (Cuno 1996). The distribution of oil droplets of this standard emulsion is presented in Fig. 9.3.

It could be demonstrated by biodegradation experiments of emulsions with mean droplet diameters between 1 and 15 µm that the bacterial growth rate was completely independent of the droplet size (Fig. 9.4).

These results can only be understood if the following mechanism of the oil biodegradation is assumed: the bacteria were covered by oil layers during collisions and then oil diffused into the cells. It is probable that the microkinetics of oil biodegradation is rate-limiting.

The following results of a kinetic biodegradation study were obtained with the standard emulsion mentioned above (Cuno 1996): T = 20 °C, $Y^{\circ}_{X/S}$ = 1.34 g MLSS (g DOC)$^{-1}$, $\mu_{max}$ = 4.08 $d^{-1}$, $K_S$ = 22.9 mg DOC $L^{-1}$, $k_d$ = 0.96 $d^{-1}$.

The result makes it probable that, in these experiments, mass transfer was not rate-limiting.

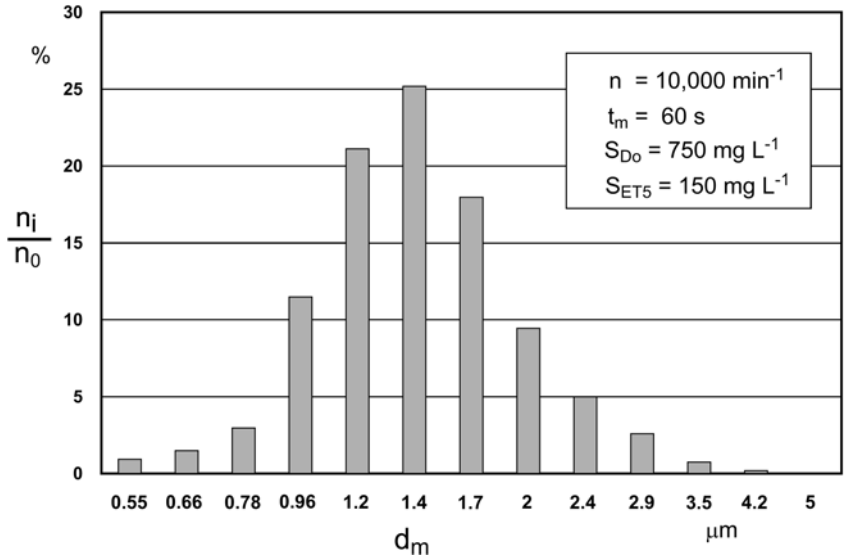


**Fig. 9.3** Oil droplet distribution of the standard emulsion (Cuno 1996). n = stirrer speed, $S_{Do}$ = concentration of *n*-dodecane, $n_i$ = number of droplets of each size range, $n_0$ = total number of droplets, $t_m$ = mixing time, $S_{ET5}$ = concentration of the emulsifier, $d_m$ = mean diameter of droplets.

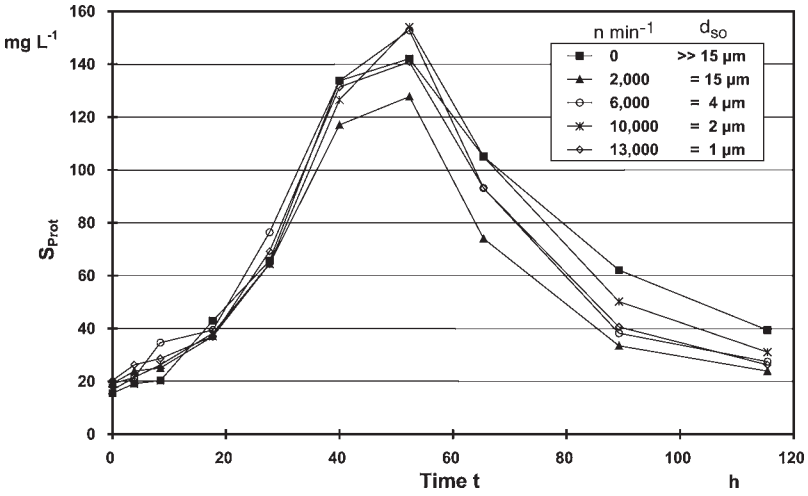


**Fig. 9.4** Concentration of protein $S_{prot}$ from growing bacteria for *n*-dodecane emulsions with different mean diameter of the droplets (Cuno 1996). n = stirrer speed, $d_{50}$ = diameter of 50% of the droplet distribution, t = time, $S_{prot}$ = concentration of protein.

9.4.3
## Biodegradation of PAHs

### 9.4.3.1 PAHs Dissolved in Water

Because of their low solubility in water and the frequently rate-limiting dissolution of crystals, PAH biodegradation can be more easily studied by using solving agents such as dimethylsulfonoxide (DMSO; Cuno 1996). With the help of DMSO, the solubility of acenaphthene can be increased remarkably. Figure 9.5 shows the results of a batch experiment with a mixed culture of PAH-degrading bacteria. The concentration of the culture using acenaphthene as an energy and carbon source could not be measured. Therefore, in the solution of the model:

$$\frac{dX}{dt} = \mu_{max} \frac{S}{K_S + S} X - k_d X \tag{9.2}$$

$$\frac{dS}{dt} = -\frac{\mu_{max}}{Y^{\circ}_{X/S}} \frac{S}{K_S + S} X \tag{9.3}$$

assumptions must be made for $Y^{\circ}_{X/S}$ and $k_d$. The line in Fig. 9.5 shows the solution which agrees with the experimental data very well. Table 9.8 shows some further kinetic coefficients for the aerobic biodegradation of acenaphthene and other PAHs. The maximum growth rate decreases from naphthalene over phenanthrene, acenaphthene to anthracene. Further results for PAHs with four rings were published by Cuno (1996).

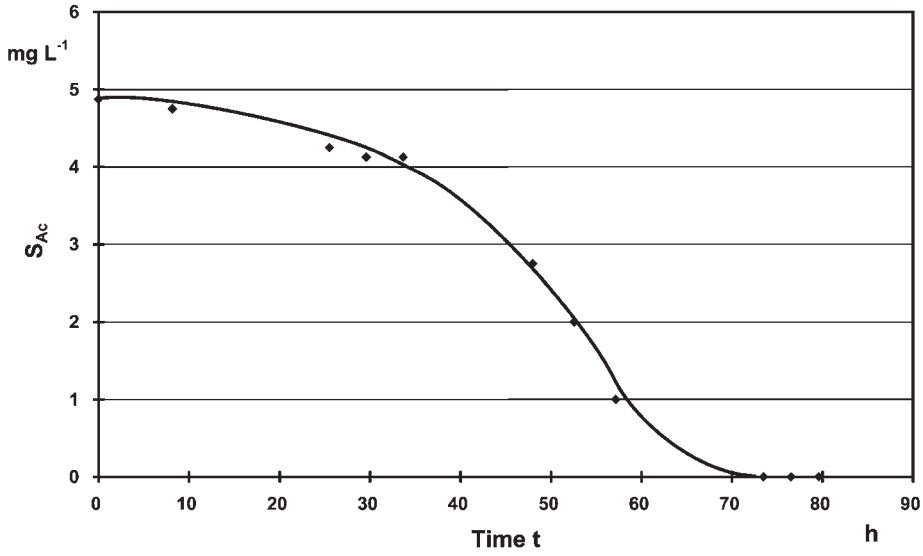


**Fig. 9.5** Biodegradation of acenaphthene dissolved in water using a solving agent (5 vol% dimethylsulfonoxide; Cuno 1996), modelled using Eqs. (9.2) to (9.3).

**Table 9.8** Stoichiometric and kinetic coefficients for aerobic degradation of some PAHs.

| Reference | Bacteria | Compound | $Y^{\circ}_{X/S}$ | $\mu_{max}$ ($d^{-1}$) | $K_S$ (mg $L^{-1}$ S) | $k_d$ ($d^{-1}$) |
|---|---|---|---|---|---|---|
| Wodzinski and Johnson (1968) | *Pseudomonas* sp. | Naphthalene | 0.5[a)] | 7.2 | | |
| Guha and Jaffé (1996) | Mixed culture | Phenanthrene | 0.3[a)] | 0.026 | 0.09 | |
| Springfellow and Aitken (1995) | *P. stutzeri* | Phenanthrene | | | 0.24 | |
| Komatsu et al. (1993) | *Pseudomonas* sp. | Acenaphthene | | 2.8 | | |
| Cuno (1996) | Mixed culture | Acenaphthene | 0.7[b)] | 1.48 | 0.065 | 0.0048 |
| Breure et al. (1990) | *Pseudomonas* sp. | Anthracene | | 0.072 | | 0.048 |
| Cuno (1996) | Mixed culture | Anthracene | | 0.55 | 0.18 | |

[a)] g MLVSS (g S)$^{-1}$, [b)] g Pr (g S)$^{-1}$

The cometabolism of two PAH by a pure culture was studied by Springfellow and Aitken (1995). *Pseudomonas stutzeii* is able to use both naphthalene and phenanthrene as the only source for carbon and energy. The influence of both substrates on the oxygen consumption rate could be described by using a model for competitive inhibition:

$$\frac{r_{O_2}}{r_{O_2,max}} = \frac{S}{K_S\left[1 + \frac{S_i}{K_i}\right] + S} \tag{9.4}$$

with S as the concentration of phenanthrene and $S_i$ as the concentration of naphthalene.

#### 9.4.3.2 PAHs Dissolved in n-Dodecane Standard Emulsion

An interesting question regarding the biodegradation of *n*-dodecane droplets (standard emulsion, Section 9.4.2) and the biodegradable PAHs dissolved inside the droplets is: *will both be oxidized at the same reaction rate?*

Indeed, the results published by Cuno (1996) seem to confirm this assumption. Although *n*-dodecane, acenaphthene and anthracene are biodegraded by bacteria at different growth rates (Tables 9.7 and 9.8), the results in Fig. 9.5 can be described approximately by Eqs. (9.2) and (9.3), using the same kinetic coefficients for all three substrates.

A possible model to gain insight into these results is the transfer of very small oil droplets with dissolved PAHs into the bacterial cell. PAHs such as pyrene, dissolved in non-biodegradable, and in water-insoluble substances such as heptamethylnonane, can be used by bacteria such as *Rhodococcus* sp. at a considerably higher rate than those dissolved in the aqueous medium (Bouchez et al. 1997). PAHs need a solving agent which may be biodegradable (*n*-alkanes) or not (heptamethylnonane). Naphthalene and phenanthrene as well as the solving agent hexadecane can also be mineralized by sulfate-reducing bacteria, which could be proven with $^{14}C$-labeled substances (Coates et al. 1997; Zhang and Young 1997).

## 9.5 Azo Reactive Dyes

### 9.5.1 Properties, Use and Environmental Problems

Nearly half of the dyes being used in textile finishing processes are reactive dyes which are soluble in water (Schönberger 1996). The molecular structure is characterized by three functional parts:

- a hydrophilic group,
- a group which produces the colour,
- a group which reacts with the textile fiber.

Figure 9.6 demonstrates the fixation of a reactive dye at a textile fiber. $HSO_4^-$ is first separated from the reactive anchor group (step 1) before the vinyl sulfate group is hydrolyzed (step 2) and reacts directly with the fiber (step 3).

But a part of the vinyl sulfate groups formed is hydrolyzed and is not able to react with the fiber (step 4). It is lost for this dyeing process and remains as an impurity in the wastewater arising from the washing processes. The most important groups of reactive dyes are azo dyes. They are characterized by an azo group: –N=N–. Reactive black 5 (RB 5) is the most commonly used azo dye. It is a diazo dye with two azo groups. Figure 9.7 presents RB 5 in its vinyl sulfonic form, before fixation to the fiber and before hydrolysis. In this form with two vinyl sulfonic anchor groups, the RB 5 molecule can be fixed at one or two points on the fiber.

One vinyl sulfonic group can be hydrolyzed, resulting in a weaker fixation. No reaction with the fiber occurs if both groups are hydrolyzed.

Azo dyes occur in wastewater from textile works and also occur together with naphthalene sulfonic acids (NSA) in wastewater from the production of azo dyes. Let us discuss briefly some experiences showing the biodegradation of NSA.

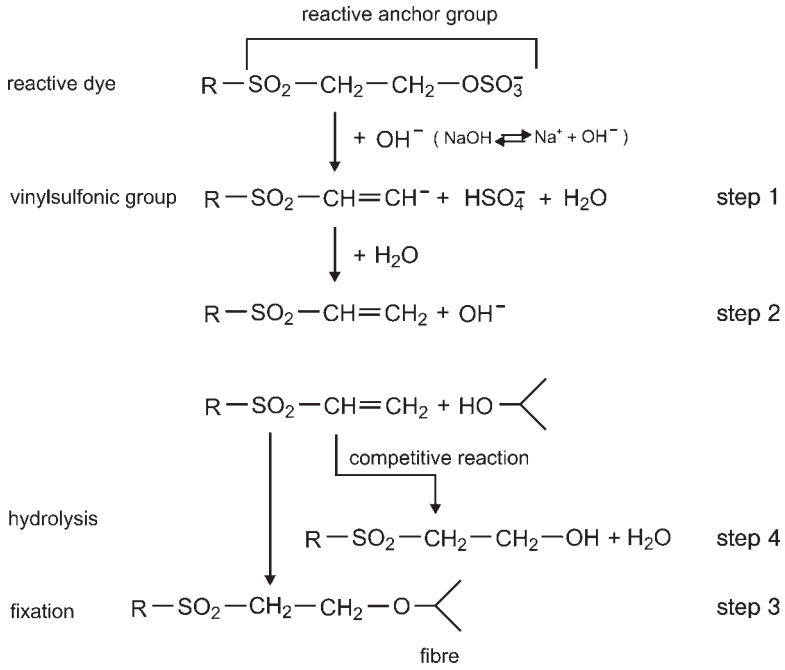


**Fig. 9.6** Formation of the vinyl sulfonic group in reactive dyes, fixation at textile fibers and hydrolysis.

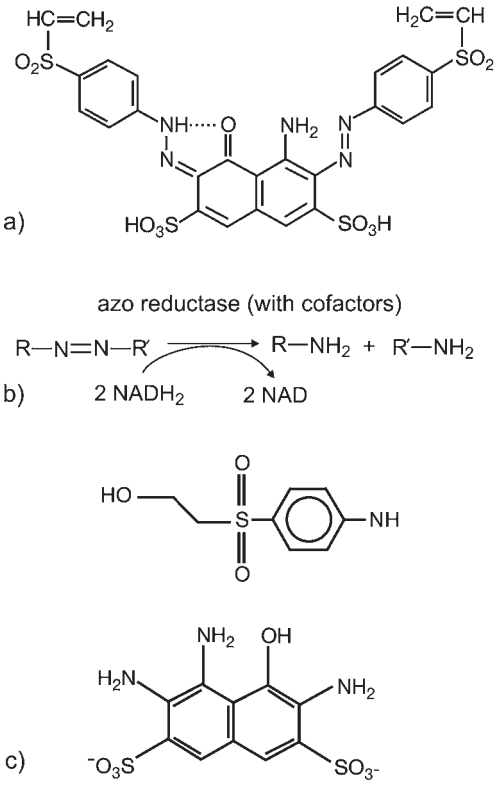


**Fig. 9.7** Reactive black 5 (RB 5) and metabolites of anaerobic treatment. (a) RB 5 with two vinyl sulfonic groups, ready for fixation on textile fibers. (b) Reduction of an azo dye. (c) Metabolites formed by anaerobic treatment: aminobenzene-2-hydroxyethylsulphonic acid (above; p-Base) and naphthalene metabolite (below; TAHNDS). (After Sosath 1999; Borchert 2002; Wiesmann 2002).

### 9.5.2
### Production of Azo Dyes in the Chemical Industry – Biodegradability of Naphthalene Sulfonic Acids

NSAs and their substituted analogs are commonly found in the wastewater from the production of azo dyes together with 1-hydroxonaphtalene, wetting agents, dispersants and other surfactants (Nörtemann and Hempel 1991) at concentrations up to 4300 mg $L^{-1}$ COD (Krull and Hempel 1993). Naphthalene sulfonic acids which are of high significance for the production of azo dyes are, for example, naphthalene-2-sulfonic acid (2 NSA) or 6-amino naphthalene 2-sulfonic acid (6-A 2-NSA; Fig. 9.8a). In aerobic WWTPs they are non-biodegradable because bacteria which are able to use these compounds as a source of carbon, nitrogen or energy are washed out because of their low growth rates. Nörtemann and Hempel (1991) were successful in obtaining aerobic enrichment cultures of adapted bacteria with 6-A 2-NSA as the only substrate. Results for different dilution rates (D) are presented in Fig. 9.8b (Diekmann et al. 1988).

In Fig. 9.8b, the experimental results are compared with a model on the basis of Monod kinetics (solid line). With a dilution rate $D = D_C = 0.2\ d^{-1}$, a maximal growth rate of $\mu_{max} = 4.8\ d^{-1}$ follows (see Table 9.9; Diekmann et al. 1988; Diekmann and

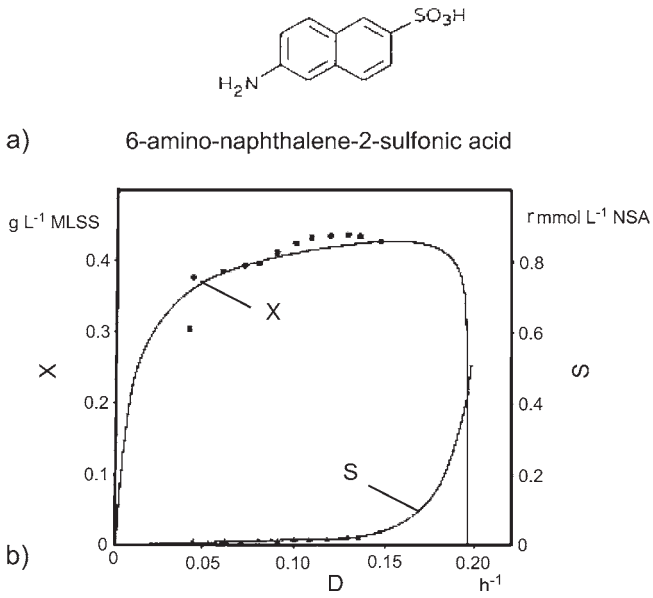


**Fig. 9.8** Concentration of 6-aminonaphthalene-2-sulfonic acid (6-A-2-NSA) and bacterial concentration depending on dilution rate D.

Hempel 1989). Experiments with an airlift-loop reactor and sand as support material for bacteria were very successful (Diekmann et al. 1988).

Table 9.9 includes other kinetic coefficients regarding the biodegradation of naphthalene sulfonic acids obtained by the same group.

Some NSAs seem to be non-biodegradable. Until now, it has not been possible to transform some NDSAs, e.g. 1,5-naphthalene disulfonic acid. Breithaupt et al. (2001b) were successful in mineralizing this compound only by a two-step process of ozonation and biodegradation (Wiesmann 2002).

**Table 9.9** Stoichiometric and kinetic coefficients for aerobic degradation of naphthalene sulfonic acids.

| Reference | Bacteria | Compound | $Y^{\circ}_{X/S}$ [a] | $\mu_{max}$ [b] | $K_S$ [c] | $m_S$ [d] |
|---|---|---|---|---|---|---|
| Krull et al. (1998) | *P. testosteroni* A3 | 1NS/2NS | 0.84 | 12 | 3 | 0.034 |
| Krull and Hempel (1993) | Defined mixed culture | 1NS/1,6 2,6NDS | 0.37 | 0.89 | 41 | 0.004 |
| Diekmann et al. (1988) | Defined mixed culture | 6-A-2-NSA | 1.47 | 4.8 | 2 | 0.009 |
| Diekmann and Hempel (1989) | Defined mixed culture | 6-A-2-NSA | 1.28 | 4.8 | 2 | 0.007 |

[a] g MLSS (g COD)$^{-1}$; [b] d$^{-1}$; [c] mg L$^{-1}$ COD; [d] Maintenance coefficient, g COD (kg MLSS · d)$^{-1}$.

Only about 70–90% of the azo dye is fixed to the fiber during the colorization process. The rest is hydrolyzed by a competitive reaction and remains in the wastewater generated by washing and rinsing with clean water (Fig. 9.6). We distinguish three main effluents with different concentrations of dyes and other compounds, such as fixers and surfactants (Sosath 1999):

- wastewater produced by the first rinsing processes, with concentrations of 4000–12 000 mg $L^{-1}$ COD (60–70%);
- wastewater produced by the following processes, with concentrations of 200–2000 mg $L^{-1}$ COD;
- used dye bath liquors.

The COD of the dye liquor is very high, but it cannot be used for further dying because of its excessive water content and various impurities. It is separated, transported and often incinerated with solid wastes. Dye houses with a direct discharge into surface water have to treat the wastewater after mixing with other waste streams. An activated sludge process is often used without a noticeable degree of mineralization of the used dyes. Dye houses with an indirect discharge into the sewerage system are generally not required to pretreat the wastewater.

We are convinced that this situation must be changed in future. Suitable pretreatment processes have to be developed (Sosath and Libra 1997).

### 9.5.3 Biodegradation of Azo Dyes

#### 9.5.3.1 Direct Aerobic Degradation

The aerobic degradation of azo dyes by adapted bacteria has been reported (Meyer et al. 1979; Kulla et al. 1984; Blümel et al. 1997), but the relevance of such specialized bacteria to textile wastewater treatment is probably very limited. The aerobic decolorization of a number of azo dyes by different species of white-rot fungi has been demonstrated successfully (Spadaro et al. 1992; Ollikka et al. 1993; Heinfling et al. 1997; Borchert and Libra 2001; Borchert 2002). Their lignin-degrading systems (LDS) are relatively non-specific and so are able to oxidize and decolorize a variety of high-molecular-weight compounds. However, the complete mineralization of azo dyes by white-rot fungi seems impossible.

The most common approach to the biological treatment of azo dyes is the combination of anaerobic reduction with aerobic degradation of the aromatic amines. This will be discussed in more detail.

#### 9.5.3.2 Anaerobic Reduction of Azo Dyes

It has long been known that azo dyes can be reduced by anaerobic bacteria in the human intestine to aromatic amines (Dieckhues 1960). The reduction equivalents gained by the oxidation of an auxiliary substrate through $NADH_2$ reduce the azo bond to form aromatic amines and thus decolorize the solution (Fig. 9.7b). We use

the simplified notation of the energy carrier here as $NADH_2$, as opposed to the proper notation as $NAD(P)H + H^+$ (see Chapter 3).

Putting it into the perspective of the classic three-step anaerobic degradation of complex carbon substrates, the anaerobic reduction of the dye is thought to take place in the first of the three steps by acidogenic bacteria.

The hypothesis for the mechanism of the biological reduction of azo dyes through the redox equivalents varies, depending on the enzyme (azo reductase) which participates in the decolorization. The enzymatic reduction theory was proposed by Zimmermann et al. (1982), Rafii et al. (1990), Haug et al. (1991), and Chung and Stevens (1993). Although most of the microorganisms reported to produce azo reductase are facultative anaerobic bacteria (Chung and Stevens 1993), some obligate anaerobic bacteria have been isolated from human intestinal microflora which produce azo reductase (Rafii et al. 1990). They found that the enzyme was extracellular and did not require induction by an azo dye for production.

Yoo et al. (2000) presented evidence that sulfur-reducing bacteria (SRB) can play an important role in the reduction of azo dyes. The azo bond is most likely chemically reduced through the sulfide produced by *Desulphovibri* from the sulfate often found in dye wastewaters. The biomediated chemical reduction rate was much faster than the rate found for fermenting bacteria.

The inhibition of *Vibrio fischeri* by the products of anaerobically treated RB 5 was studied by Libra et al. (2004). The $EC_{50}$ value was decreased from 29.6 mg $L^{-1}$ (completely hydrolyzed RB 5) to 1.5 mg $L^{-1}$ (partly hydrolyzed RB 5; Libra et al. 2004).

#### 9.5.3.3 Aerobic Degradation of Metabolites

Various authors have investigated the pathways of aromatic amine degradation in pure cultures (Meyer et al. 1979; Nörtemann et al. 1986; Haug et al. 1991). However, determination of the degree of degradation in mixed cultures is difficult. An auxiliary substrate is usually added to facilitate anaerobic decolorization, often in concentrations (measured as DOC) very much higher than that of the metabolites. Reduction in the effluent DOC is usually not a reliable indication of metabolite degradation. It is possible to follow the metabolites analytically, e.g. with HPLC; however, some of the metabolites are instable in the presence of oxygen and are not measurable for a longer time as a result of auto-oxidation, although no change in the DOC concentration occurs (Sosath and Libra 1997).

Using the commercial preparation of the RB 5 metabolite p-Base (Fig. 9.7c), Soewondo (1997) showed nearly complete mineralization in aerobic batch experiments. The results could be described using Monod kinetics.

### 9.5.4 Treatment of Wastewater Containing the Azo Dye Reactive Black 5

Sosath (1999) used a laboratory-scale two-step process with an anaerobic step and a subsequent aerobic step. In both reactors, bacteria were immobilized on the surface of rotating discs. He used a mixture of yeast extract and acetate as an auxiliary sub-

strate. In step 1, 66% decolorization was observed without remarkable consumption of the auxiliary substrate DOC, which was removed nearly completely in step 2, down to the remaining DOC of the dye. Obviously, the metabolites of decolorization are not biodegradable in this system. The mineralization of RB 5 seems only to be possible by chemical oxidation or a combination of chemical oxidation and biodegradation. Krull et al. (1998) treated a highly concentrated dyehouse effluent by using combination of biological and chemical methods. Breithaupt et al. (2001a) were successful in using a recycle reaction system consisting of an aerobic biological rotation disc reactor and an ozone batch reactor with automatic process control. Nearly 88% of the DOC could be removed. Approximately 66% of the ozone which would be needed for a 90% chemical oxidation could be saved (Wiesmann 2002).

An oxidation step with $H_2O_2$/UV and subsequent aerobic biodegradation operating in recycle mode was suitable to reduce the RB 5 DOC of 450 mg $L^{-1}$ to about 33% by chemical oxidation and to reduce it by a further 33% by biological oxidation (Mohey El-Dein 2002). Of more practical interest is the treatment of more realistic dyehouse effluent, a mixture of RB 5 (18% DOC), a fixer (e.g. Akrofil PGM, 75%) and a surfactant (7%). Because of the biodegradability of these latter compounds, the most effective reactor system would consist of a first aerobic biological stage, followed by an ultrafiltration membrane to hold back microorganisms, an ozone reactor and an aerobic rotating disc reactor to mineralize products of chemical oxidation. The DOC could be reduced down to about 18% ($\alpha$=82%), including the remaining molecules of all three model components (Rapp and Wiesmann 2003; Rapp 2005).

## 9.6 Final Remarks

In this chapter, we discussed some of the problems which arise from products of chemical industry, e.g.:

- chlorinated organics,
- nitro aromatics,
- polycyclic aromatic hydrocarbons,
- azo dyes.

It is very seldom that any of these are produced in nature. Nevertheless, some bacteria and yeasts “learn” to use their carbon, nitrogen and/or energy for growth after going through mutations, which can occur within a relatively short time due to the brevity of each generation. However, the processes of mineralization are often very difficult; and several different strains must cooperate. In some cases, toxic compounds are produced which are more dangerous to animals and human beings than the original compounds.

Most of these compounds cannot be removed in activated sludge plants or trickling filters; and thus it is necessary to develop tailored processes for their treatment. For high removal efficiencies it is necessary to combine different processes.

One alternative is to utilize precipitation, adsorption and membrane separation to obtain concentrates which can be disposed by other methods, such as incineration. Another alternative is the use of biological and chemical oxidation processes which result in the production of biomass and $CO_2$. We have shown some examples in which the combination of both can be successful. However, in nearly all cases the treatment costs are relatively high.

The best way to avoid these problems, therefore, is to use more and more natural dyes (Seweko 1988) and thus stop the production of water-polluting products by the chemicals industry which cannot be biodegraded, or only with great difficulty. The production of chlorinated organics was remarkably reduced in Europe over the past two decades. The production of azo dyes, however, is still increasing. We shall need much time to reach this goal, but we must start.

## References


Adrian, L.; Manz, W.; Szewzyk, U.; Görisch, H. **1995**, Anaerober Abbau von Trichlorbenzonen in hochangereicherter Mischkultur, *Schriftenreihe Biologische Abwasserreinigung* 6, 81–103.

Battersby, N.S.; Wilson, V. **1989**, Survey of the anaerobic biodegradation potential of organic chemicals in digesting sludge, *Appl. Environ. Microbiol.* 55, 433–439.

Bausum, H.T.; Mitshell, W.R.; Major, M.A. **1992**, Biogradiation of 2,4- and 2,6-dinitrotoluene by fresh water microorganisms, *J. Environ. Sci. Health* A 27, 663–695.

Berwick, P.G. **1984**, Physical and chemical conditions for microbial oil degradation, *Biotechnol. Bioeng.* 26, 1294–1305.

Blümel, S.; Kudlich, M.; Stolz, A. **1997**, Mögliche Strategien für den mikrobiellen Abbau sulfonierter Azofarbstoffe, in: *Treatment of Wastewaters from Textile Processing* (*7 Kolloquium des Sonderforschungsbereiches 193*), Technical University Berlin.

Borchert, M. **2002**, Transformation von Reaktivfarbstoffen durch den Weißfäulepilz *Trametes versicolor* und bakterielle Mischkulturen (PhD thesis), *VDI-Forschungsberichte, Reihe 15*, 240.

Borchert, M.; Libra, J.A. **2001**, Decolorization of reactive dyes by the white rot fungus *Trametes versicolor* in sequencing batch reactors, *Biotechnol. Bioeng.* 75, 313–321.

Bosma, T.N.P.; van der Meer, J.R.; Schraa, G.; Tros, M.E. **1988**, Reductive dechlorination of all trichloro- and dichlorobenzene isomers, *FEMS Microbiol. Ecol.* 53, 223–229.

Bouchez, M.; Blanchet, D.; Vandecasteele, J.R. **1997**, An interfacial uptake mechanism for the degradation of pyrene by a *Rhodococcus* strain, *Microbiology* 143, 1087–1092.

Bouwer, E.J.; McCarty, P.L. **1982**, Removal of trace chlorinated organic compounds by activated carbon and fixed film bacteria, *Environ. Sci. Technol.* 16, 836–843.

Breithaupt, T.; Choi, I.S.; Wiesmann, U. **2001a**, Optimierung eines Systems aus Bioreaktor und Ozonreaktor zur Abwasserreinigung und Prozesswasseraufbereitung, *DFG Abschlussbericht*, 2001.

Breithaupt, T.; Reemtsma, T.; Jekel, M.; Storm, T.; Wiesmann, U. **2001b**, Combined biological treatment/ozonation of wastewaters for the mineralization of non-biodegradable naphtalene-1,5-disulphonic acid, *Acta Biotechnol.* 23, 321–333.

Breure, A.M.; Volkering, F.; van Andel, J.G. **1990**, Biodegradation of polycyclic aromatic hydrocarbons, in: *DECHEMA Biotechnology Conferences 4*, VCH, Weinheim.

Brunner, W. **1982**, *Bakterieller Abbau von Dichlormethan und 1,2 Dichlorethan*, PhD thesis, ETH Zurich.

Burgdorf, R.; Donner, C.; Weber, A.; Wiesmann, U. **1991**, Bakterien knacken CKW – Biologischer Abbau im Wirbelschichtreaktor, *Chem. Ind.* 11, 13–18.

Chung, K.-T.; Stevens, S.E., Jr. **1993**, Degradation of azo dyes by environmental microorganisms and helminths, *Environ. Toxicol. Chem.* 12, 2121–2132.

Coates, J.D.; Woodward, J.; Allen, J.; Philipp, P.; Lovley, D.R. **1997**, Anaerobic degradation of polycyclic aromatic hydrocarbons and alkanes in petroleum-contaminated marine harbor sediments, *Appl. Environ. Microbiol.* 63, 3589–3593.

Cuno, M. **1996**, Kinetische Untersuchungen zum biologischen Abbau von Mineralölen und polyzyklischen aromatischen Kohlenwasserstoffen (PhD thesis), *VDI-Forschungsberichte, Reihe 15*, 148.

De Bont, J.A.M.; Vorage, M.J.A.W.; Hartmann, S.; von den Tweel, W.J.J. **1986**, Microbial degradation of 1,3-dichlorobenzene, *Appl. Environ. Microbiol.* 52, 677–680.

Dieckhues, B. **1960**, Untersuchungen zur reduktiven Spaltung der Azofarbstoffe durch Bakterien, *Zbl. Bakteriol. Parasitenkd. Infektionskr. Hyg.* 1, 244–249.

Diekmann, R.; Hempel, D.C. **1989**, Production rates of $CO_2$ by suspended and immobilized bacteria degrading 6-aminonaphthalene-2-sulphonic acid, *Appl. Microbiol. Biotechnol.* 32, 113–117.

Diekmann, R.; Nörtemann, B.; Hempel, D.C.; Knackmuss, H.-J. **1988**, Degradation of 6-aminonaphthalene-2-sulphonic acid by mixed cultures: kinetic analysis, *Appl. Microbiol. Biotechnol.* 29, 85–88.

Dirks, R.; Ottengraf, P. **1991**, Verification of a simplified model for the removal of dichloromethane from waste gases using a biological trickling filter, *Bioprocess Eng.* 6, 93–99.

Döpper, M.; Stock, W. **1995**, Herkunft, Eintrag und Verbleib von Chloraromaten in der Umwelt, in: Mikrobielle Eliminierung chlororganischer Verbindungen, Vol. 6, *Schriftenreihe Biologische Abwasserreinigung Sonderforschungsbereich* 193, Berlin.

EPA **1975**, Development document for effluent limitation guidelines, in: *New Source Performance Standards for the Pressed and Blow Glass Segment of the Glass Manufacturing Point Source Category* (US EPA 440/1-75/034-a), U.S. Environmental Protection Agency, Washington, D.C.

Fathepure, B.Z.; Vogel, T.A. **1991**, Complete degradation of polychlorinated hydrocarbons by a 2-stage biofilm-reactor, *Appl. Environ. Microbiol.* 57, 3418–3422.

Feidieker, D. **1993**, *Untersuchungen zur mikrobiologischen Sanierbarkeit eines mit Chlorkohlenwasserstoffen kontaminierten Industriestandortes*, PhD thesis, Technical University Berlin.

Freedman, D.L.; Smith, C.R.; Noguera, D.R. **1997**, Dichloromethane biodegradation under nitrate-reducing conditions, *Water Environ. Res.* 69, 115–122.

Freitas dos Santos, L.M.; Livingston, A.G. **1995**, Novel membrane bioreactor for detoxification of VOC wastewaters: biodegradation of 1,2-dichloroethane, *Water Res.* 29, 179–194.

Gälli, R. **1986**, Optimierung des mikrobiellen Abbaus von Dichlormethan, in: *BUA-Stoffbericht 6*, VCH, Weinheim.

Gerber, V.; Gorobets, L.; Loakimis, E. **1979**, Effects of urea and dichloromethane on biochemical treatment of refinery wastewater, in: *Chemistry and Technology of Fuels and Oils, vol. 1,5 no. 3/4*, Consultens Bureau Enterprise, New York, p. 269–272.

Guha, S.; Jaffé, P. **1996**, Determination of Monod kinetic coefficients for volatile hydrophobic organic compounds, *Biotechnol. Bioeng.* 50, 693–699.

Haigler, B.E.; Pettigrew, C.Y.; Spain, J.C. **1992**, Biodegradation of mixtures of substituted benzenes by *Pseudomonas* sp. strain JS150, *Appl. Environ. Microbiol.* 58, 2237–2244.

Haug, W.; Schmidt, A.; Nörtemann, B.; Hempel, D.C.; Stolz, A.; Knackmuss, H.-J. **1991**, Mineralization of the sulfonated azo dye Mordant Yellow 3 by a 6-aminonaphthalene-2-sulfonate-degrading bacterial consortium, *Appl. Environ. Microbiol.* 57, 3144–3149.

Hauschild, I.; Horn, T.; Rudek, M.; Safak, T.; Starnick, J. **1992**, The effect of substrate and product inhibition on the microbial degradation of chlorinated hydrocarbons, in: *DECHEMA Biotechnology Conferences 5*, VCH, Weinheim, p. 1061–1967.

Heinfling, A.; Bergbauer, M.; Szewzyk, U. **1997**, Biodegradation of azo and phthalocyanine dyes by *Trametes versicolor* and *Bjerkandera adusta*, *Appl. Microbiol. Biotechnol.* 48, 261–266.

Heinze, L. **1997**, Mikrobiologischer Abbau von 4-Nitrophenol, 2,4-Dinitrophenol und 2,4-Dinitrotoluol in synthetischen Abwässern, (PhD thesis), *VDI-Forschungsberichte, Reihe 15*, 167.

Heinze, L.; Brosius, M.; Wiesmann, U. **1995**, Biologischer Abbau von 2,4-Dinitrotoluol in einer kontinuierlich betriebenen Versuchsanlage und kinetische Untersuchungen, *Acta Hydrochim. Hydrobiol.* 23, 254–263.

Heitkamp, M.A.; Camel, V.; Reuter, T.J.; Adams, W.J. **1990**, Biodegradation of p-nitrophenol in an aqueous waste stream by immobilized bacteria, *Appl. Environ. Microbiol.* 56, 2967–2973.

Herbst, B. **1995**, Biologischer Abbau von Dichlormethan und Dichlorethan durch Mischkulturen im Wirbelschichtreaktor (PhD thesis), *VDI-Forschungsberichte, Reihe 17*, 126.

Herbst, B.; Wiesmann, U. **1996**, Kinetics and reaction engineering aspects of the biodegradation of dichloromethane and dichloroethane, *Water Res.* 30, 1069–1076.

Hu, L.Z.; Shieh, W.K. **1987**, Anoxic biofilm degradation of monocyclic aromatic compounds, *Biotechnol. Bioeng.* 30, 1077–1083.

Jakobezyk, J.; Kwiatkowski, M.; Ostrowska, J. **1984**, Untersuchung der biologischen Zersetzung aromatischer Nitroverbindungen in Abwässern, *Chem. Tech.* 36, 112–116.

Janssen, D.B.; Scheper, A.; Dijkhizen, L.; Witholt, B. **1985**, Degradation of halo-organic compounds by *Xanthobacter autotrophicus* GJ10, *Appl. Environ. Microbiol.* 49, 673–677.

Jensen, H.L.; Lautrup-Larsen, G. **1967**, Microorganisms that decompose nitro-aromatic compounds, with special reference to dinitro-ortho-cresol, *Acta Agric. Scand.* 17, 115–126.

Jongen, W.; Alink, G.; Koeman, J. **1978**, Mutagenic effect of dichloromethane on *Salmonella typhimurium*, *Mutat. Res.* 56, 245–248.

Kästner, M. **1989**, Biodegradation of volatile chlorinated hydrocarbons, in: *DECHEMA Biotechnology Conferences 3B*, DECHEMA, Frankfurt, p. 909–912.

Khandker, S.A.K. **1992**, *Mikrobieller Abbau von aromatischen und chloraromatischen Verbindungen unter aeroben und denitrifizierenden Bedingungen*, PhD thesis, Technical University Berlin.

Komatsu, T.; Omori, T.; Kodama, T. **1993**, Microbial degradation of the polycyclic aromatic hydrocarbons acenaphthene and acenaphthylene by a pure bacterial culture, *Biosci. Biotechnol. Biochem.* 54, 864–865.

Krull, R.; Hempel, D.C. **1993**, Biodegradation of naphthalene-sulphonic acid-containing sewages in a two-stage treatment plant, *Bioprocess. Eng.* 10, 229–234.

Krull, R.M.; Hemmi, P.O., Hempel, D.C. **1998**, Combined biological and chemical treatment of a highly concentrated residual dyehouse liquors, *Water Sci. Technol.* 36, 339–346.

Kulla, H.G.; Krieg, R.; Zimmerman, T.; Leisinger, T. **1984**, Experimental evolution of azo dye-degrading bacteria, in: *Current Perspectives in Microbial Ecology*, ed. Klug, M.J.; Reddy, C.A., American Society of Microbiology, Washington, D.C., p. 663–667.

Leisinger, T. **1988**, Mikrobieller Abbau problematischer Komponenten in Abluft, in: *Biosensors and Environmental Biotechnology* (Biotech. Ser. Vol. 2), ed. Hollenberg, C.; Sahm, H., Gustav Fischer, Stuttgart, p. 125–133.

Libra, J.A.; Borchert, M.; Vigelahn, L.; Storm, T. **2004**, Two stage biological treatment of a diazo reactive textile dye and the fate of the dye metabolites, *Chemosphere* 56, 167–180.

Loew, G.; Regbagatti, M.; Poulsen, M. **1984**, Metabolism and relative carcinogenic potency of chloroethanes: a quantum chemical structure–activity study, in: *Cancer Biochemistry and Biophysics*, Vol. 7, Gorden and Breach, New York, p. 109–132.

Lonjaret, J.-P. **1996**, *Entwicklung und mathematische Modellierung eines Biotropfkörperfilters für den biologischen Abbau von Dichlormethan in Abluft*, Wissenschaft und Technik Verlag, Berlin.

Mackay, D.; Shiu, W.J. **1981**, A critical review of Henry's law constants for chemical environmental interest, *J. Phys. Chem. Ref. Data* 10, 1175–1199.

Meyer, U.; Overney, G.; Wattenwyl, A. **1979**, Über die biologische Abbaubarkeit von Azofarbstoffen, *Textilveredelung* 14, 15–20.

Mohey El-Dein, A.A. **2002**, Oxidation kinetics of the azo dye Reactive Black 5 using $H_2O_2$/UV and aerobic biological treatment (PhD thesis), *VDI-Forschungsberichte, Reihe 3*, 762.

Niemann, D. **1993**, *Biologische Abluftreinigung mit Biofilm-Wirbelschicht-Reaktoren*, PhD thesis, ETH Zurich.

Nörtemann, B.; Hempel, D.C. **1991**, Application of adapted bacterial cultures for the degradation of xenobiotic compounds in industrial wastewaters, in: *Biological Degradation of Wastes*, ed. Martin, A.M., Elsevier Applied Science, London, p. 261–279.

Nörtemann, B.; Baumgarten, J.; Rast, H.G.; Knackmuss, H.-J. **1986**, Bacterial communities degrading amino- and hydroxynaphthalenesulphonates, *Appl. Environ. Microbiol.* 52, 1195–1202.

Nowak, J. **1994**, *Umsatz von Chlorbenzolen durch methanogene Mischkulturen aus Saale-Sediment in Batch- und Reaktorversuchen*, PhD thesis (Berichte zur Siedlungswasserwirtschaft Nr 4), Technical University Berlin.

Ollikka, P.; Alhonmäki, K.; Leppänen, V.; Glumoff, T.; Raijola, T.; Suominen, I. **1993**, Decolorization of azo, triphenyl methane, heterocyclic, and polymeric dyes by lignin peroxidase isoenzymes from *Phanerochaete chrysosporium*, *Appl. Environ. Microbiol.* 59, 4010–4016.

Ou, L.T.; Sharma, A. **1989**, Degradation of methyl parathion by a mixed bacterial culture and a *Bacillus* sp. isolated from different soils, *J. Agric. Food Chem.* 37, 1514–1518.

Pagga, U.; Haltrich, W.G.; Günthner, W. **1982**, Untersuchungen über die Wirkung von 4-Nitrophenol auf Belebtschlamm, *Vom Wasser* 59, 51–65.

Patterson, J.W. **1985**, *Industrial Wastewater Treatment Technology*, Butterworth, Boston, Mass., p. 305–306.

Prieger-Kraft, A. **1995**, *Mikrobieller Abbau von 1,2,3,4- und 1,2,3,5-Tetrachlorbenzol*, PhD thesis, Technical University Berlin.

Rafii, F.; Franklin, W.; Cerniglia, C.E. **1990**, Azoreductase activity of anaerobic bacteria isolated from human intestinal microflora, *Appl. Environ. Microbiol.* 56, 2146–2151.

Ramanand, K.; Balba, M.T.; Duffy, J. **1993**, Reductive dehalogenation of chlorinated benzenes and toluenes under methanogenic conditions, *Appl. Environ. Microbiol.* 59, 3266–3272.

Rannug, U. **1980**, Genotoxic effects of 1,2-dibromomethane and 1,2-dichloroethane, *Mutat. Res.* 76, 269–295.

Rapp, T. **2005**, Untersuchungen zur biologischen Behandlung und Ozonisierung eines synthetischen Textilabwassers (PhD thesis), *VDI-Forschungsberichte, Reihe 15*, 53.

Rapp, T.; Wiesmann, U. **2003**, Biologisch-chemische Verfahrenskombination zur Reinigung von Mischabwässern der Textilveredlung, *Chem. Ing. Tech.* 75, 453–457.

Reineke, W.; Knackmuss, H.-J. **1984**, Microbial metabolism of haloaromatics: isolation and properties of a chlorobenzene-degrading bacterium, *Appl. Environ. Microbiol.* 47, 395–402.

Rippen, G. **1991**, *Handbuch Umweltchemikalien: Stoffdaten, Prüfverfahren, Vorschriften, Landsberg/Lech*, Ecomed, Berlin.

Rudek, M. **1992**, *Mikrobieller Abbau von 1,2-Dichlorethan*, PhD thesis, Technical University Berlin.

Sallis, P.; Armfield, S.; Bull, A.; Hardman, D. **1990**, Isolation and characterization of a haloalkane halidohydrolase from *Rhodococcus erythropolis* Y2, *J. Gen. Microbiol.* 136, 115–120.

Sander, P.; Wittich, R.M.; Fortnagel, P.; Wilkey, H.; Franke, W. **1991**, Degradation of 1,2,4-trichloro- and 1,2,4,5-tetrachlorobenzene by *Pseudomonas* sp. strains, *Appl. Environ. Microbiol.* 57, 1420–1440.

Schäfer, M. **1994**, *Untersuchungen zum Abbau chlorierter Benzole durch Mischkulturen in kontinuierlich betriebenen Reaktoren*, PhD thesis, Technical University Berlin.

Schmidt, S.K.; Scow, K.M.; Alexander, M. **1987**, Kinetics of p-nitrophenol mineralization by a *Pseudomonas* sp.: effects of second substrates, *Appl. Environ. Michrobiol.* 53, 2617–2623.

Schönberger, H.: Zur Abwässerfrage der Textilveredlungsindustrie (PhD thesis), *VDI-Forschungsberichte, Reihe 15*, 196.

Seweko, U. **1988**, Naturfarbstoffe – eine Alternative zu synthetischen Farbstoffen, *Melliand Textilberichte* 4, 271–276.

Siddique, M.H.; St. Pierre, C.C.; Biswas, N.; Bewtra, J.K.; Taylor, K.E. **1993**, Immobiliz-

ed enzyme-catalyzed removal of 4-chlorophenol from aqueous solution, *Water Res.* 27, 883–890.

Socher, R. **1997**, personal communication, BASF Schwarzheide.

Soewondo, P. **1997**, *Zweistufige anaerobe und aerobe biologische Behandlung von synthetischem Abwasser mit dem Azofarbstoff C.I. Reactive Orange 96*, PhD thesis, Technical University Berlin.

Sosath, F. **1999**, Biologisch-chemische Behandlung von Abwässern der Textilveredelung mit Reaktivfarbstoffen (PhD thesis), *VDI-Forschungsberichte, Reihe 15*, 215.

Sosath, F.; Libra, J.A. **1997**, Biologische Behandlung von synthetischen Abwässern mit Azofarbstoffen, *Acta Hydrochim. Hydrobiol.* 25, 259–264.

Spadaro, J.T.; Gold, M.H.; Renganathan, V. **1992**, Degradation of azo dyes by the lignin-degrading fungus *Phanerochaete chrysosporium*, *Appl. Environ. Microbiol.* 58, 2397–2401.

Speitel, G.E. Jr; Luc, C.-J.; Turakhia, M.; Zhu, X.-J. **1989**, Biodegradation of trace concentrations of substituted phenols in granulated activated carbon columns, *Environ. Sci. Technol.* 23, 68–74.

Springfellow, W.T.; Aitken, M.D. **1995**, Competitive metabolism of naphthalene, methylnaphthalene, and fluoriene by phenanthrene-degrading *Pseudomonas*, *Appl. Environ. Microbiol.* 61, 357–362.

Stucki, G.; Thüer, M.; Bentz, R. **1992**, Biological degradation of 1,2-dichloroethane under groundwater conditions, *Water Res.* 26, 273–278.

Thiem, K.-W.; Booth, G. **1991**, Nitro compounds, aromatic, in: *Ullmann's Encyclopedia of Industrial Chemistry*, Vol. A17, 5th edn, VCH, Weinheim.

Van der Meer, J.R.; Roelofsen, W.; Schraa, G.; Zehnder, A.J.B. **1987**, Degradation of low concentrations of dichlorobenzenes and 1,2,4-trichlorobenzene by *Pseudomonas* sp. strain P51 in non-sterile soil columns, *FEMS Microbiol.* 27, 1538–1542.

WHO **1987**, *Methylene Chloride Health and Safety Guide, Environmental Health Criteria, No. 32: Methylene Chloride IPCS (International Program on Chemical Safety)*, Wissenschaftliche Verlagsgesellschaft, Stuttgart, p. 42.

Wiesmann, U. **2002**, Versuche zur Entfärbung und Mineralisierung des Azo-Farbstoffs C.I.Reactive Black 5, *GWF Wasser Abwasser* 134, 329–335.

Wiesmann, U.; Libra, J.A. **1999**, Special aerobic wastewater and sludge treatment processes, *Biotechnology* 11a, 373–415.

Winkelbauer, W.; Kohler, H. **1989**, Biologischer Abbau von leichtflüchtigen Chlorkohlenwasserstoffen im offenen System am Beispiel von Dichlormethan in einem Tauchtropfkörper, *GWF Wasser Abwasser* 130, 13–20.

Wodzinski, R.; Johnson, M. **1968**, Yields of bacterial cells from hydrocarbons, *Appl. Microbiol.* 16, 1886–1891.

Yoo, E.S.; Libra, J.A.; Wiesmann, U. **2000**, Reduction of azo dyes by *Desulfovibrio desulfuricans*, *Water Sci. Technol.* 41, 15–22.

Zhang, X.; Young, L.Y. **1997**, Carboxylation as an initial reaction in the anaerobic metabolism of naphtaline and phenanthrene by sulfidogenic consortia, *Appl. Environ. Microbiol.* 63, 4759–4764.

Zimmermann, T.; Kulla, H.G.; Leisinger, T. **1982**, Properties of purified orange II azoreductase, the enzyme initiation of azo dye degradation by *Pseudomonas* KF46, *Eur. J. Biochem.* 129, 197–203.

# 10
# Biological Nutrient Removal

## 10.1
## Introduction

Nutrient compounds frequently present in wastewater are valuable substances which act as fertilizers. They are becoming increasingly significant in water and wastewater management because the discharge of nutrients such as nitrogen and phosphorus into rivers and lakes can cause adverse influences on our environment and life. An excessive increase in the quantities of these nutrients in the aquatic surroundings disturbs the ecological balance, resulting in severe damage to environment (e.g. eutrophication).

It is probable that either nitrogen or phosphorus will be the limiting nutrient controlling eutrophication because of the relatively large quantities required for biomass growth compared to other nutrients, such as sulfur, potassium, calcium and magnesium.

Nitrogen is dissolved in water as ammonia, nitrite and nitrate and is present in organic molecules such as amino acids, which are formed by the hydrolysis of proteins and are transformed to ammonia during biodegradation. Ammonia and organic nitrogen compounds are most closely associated with plants and animals. An example of an organic nitrogen compound is urea ($NH_2CONH_2$), which is a major chemical component of urine. Urea is produced from ammonia in fauna and converted to ammonium by hydrolysis.

Several problems result from discharging wastewater with ammonia and nitrate into rivers and lakes:

- Ammonia is oxidized by bacteria to nitrite and nitrate, leading to a decrease in the dissolved oxygen concentration and to fish killing.
- Uncontrolled nitrification of ammonia causes a decrease in pH in the receiving stream.
- Ammonia and ammonium are in chemical equilibrium; with increasing temperature and pH more and more ammonia is produced which is toxic to fish.
- Nitrate stimulates the growth of algae, contributing to the eutrophication of open bodies of water.

*Fundamentals of Biological Wastewater Treatment*. Udo Wiesmann, In Su Choi, Eva-Maria Dombrowski

ISBN: 978-3-527-31219-1

- Nitrite and nitrate may reach groundwater resources which are used for producing drinking water. High concentrations of nitrate and nitrite in drinking water cause methemoglobinemia in babies and promote the formation of carcinogenic nitrosamines. As a result, the water must be denitrified in drinking water plants.
- In oxygen-free soil layers, denitrification can cause sludge build-up and anaerobic decomposition, resulting in the generation of methane.

In order to solve these problems, nitrogen must be removed from water. Biological nitrification and denitrification are an alternative.

Phosphorus is a key element in all known forms of life and a common earth element which can be induced into aquatic ecosystems by natural and human-caused erosion of soil materials and by human activity, e.g. the use of fertilizer in agriculture. It exists in different forms, such as dissolved inorganic orthophosphate, dissolved organic phosphorus found in algae, dissolved inorganic polyphosphate and non-dissolved particulate phosphorus (Fig. 10.1):

- Dissolved organic phosphorus is found as a lysis product of algae and bacteria in water and is used for industrial products like pesticides, complex binders and antiknock agents. They are difficult to biodegrade and pass through bank filtration and the filtration of water purification plants (Klinger 1999).

- Two types of dissolved inorganic phosphates are orthophosphate and polyphosphate. Orthophosphate takes the form of $PO_4^{3-}$, $HPO_4^{2-}$ or $H_2PO_4^-$, depending on the pH value. $PO_4^{3-}$ plays a major role in organic molecules such as DNA and RNA, where it forms part of their structural backbone (see Fig. 3.8 in Chapter 3). Living cells also utilize phosphate to transport cellular energy via adenosine triphosphate (ATP; see Fig. 3.15). Existing orthophosphate facilitates algal growth. This is followed by algal death, lysis of algae and biodegradation by aerobic bacteria, which leads to oxygen depletion in lakes (eutrophication). Orthophosphate is stored in algae as polyphosphate. Polyphosphate is formed by polymerization of orthophosphate linked between hydroxyl groups and hydrogen atoms.

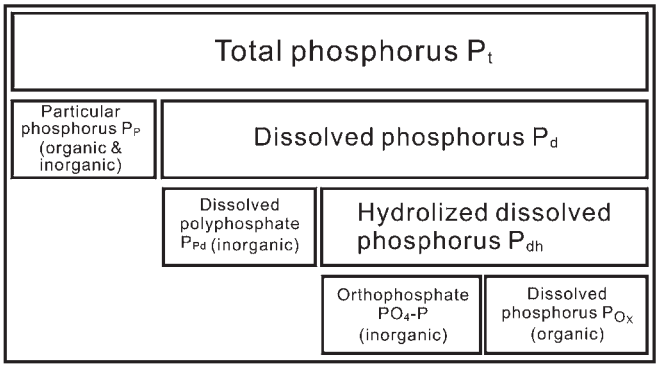


**Fig. 10.1** Different forms of phosphorous in wastewater (Klein 1988; DIN 38405, D11).

- Non-dissolved organic phosphorus particles are found in organisms and their cell refuse. A part of these phosphorus particles is separated by sedimentation and filtration; the colloid particles are eliminated only after flocculation and membrane processes.

To avoid problems with nitrogen and phosphorus, more and more limitations are being placed on the discharge permits of WWTP.

The minimum requirements for the discharge of municipal wastewater into inshore waters are laid down by the Wastewater Framework Regulation (Abwasserverordnung: Verordnung über Anforderungen an das Einleiten von Abwasser in Gewässer) of the Federal Republic of Germany from 17 June 2004 (AbwV 2004) which was recently renewed, going into effect from 1 January 2005.

The $NH_4$-N concentration of a 2-h mixed sample of domestic and municipal wastewater must be less than 10 mg $L^{-1}$ $NH_4$-N for $BOD_5$ loads greater than 300 kg $d^{-1}$ (Appendix 1 in AbwV 2004). That means that all treatment plants with flow rates greater than 4000 $m^3$ $d^{-1}$ have to be expanded to include a nitrification stage. An expansion is made necessary by the limit on the total inorganic nitrogen content (ammonia, nitrite and nitrate) and total phosphorus content. For $BOD_5$ loads from 600 kg $d^{-1}$ to 6000 kg $d^{-1}$, the total N and P concentrations of a 2-h mixed sample must be less than 18 mg $L^{-1}$ N and 2 mg $L^{-1}$ P respectively. For $BOD_5$ loads greater than 6000 kg $d^{-1}$, both limit values are even lower, i.e. 13 mg $L^{-1}$ N and 1 mg $L^{-1}$ P (see Table 2.9).

The German Wastewater Framework Regulation also sets limits for industrial effluents for their direct discharge into inshore waters. The limit for total N ranges from 18 mg $L^{-1}$ N for the food industry to 70 mg $L^{-1}$ N for landfill leachate water. The limits for phosphorus and ammonium nitrogen are mostly fixed at 2 mg $L^{-1}$ $P_t$ and 10 mg $L^{-1}$ $NH_4$-N, respectively (Table 10.1).

The different limits for various branches of industry depend on the raw materials used. For example, most food producers have the same limits of total N and P concentration as those for domestic and municipal wastewater at the 6000 kg $d^{-1}$ $BOD_5$ level.

The European Union passed Directive 91/676/EEC (EU 1991a) concerning the protection of waters against pollution caused by nitrates from agricultural sources to reduce or prevent water pollution. The member states are obliged to take measures against the discharge of nitrate into surface waters and groundwater. Moreover, a framework for European Community action in the field of water policy was established in the form of Directive 2000/60/EC from 23 October 2000 which aims at maintaining and improving the aquatic environment in the EC. It was completed and amended by Decision No. 2455/2001/EC from 20 November 2001 to establish a list of priority substances (Annex X) in the field of water policy.

In addition, Directive 91/271/EEC (EU 1991b) requires the collection and treatment of wastewater, with P removal in sensitive areas and effectively in almost all large urban areas. Application of this Directive is essential to protect the quality of surface waters (see Chapter 2 for regulations concerning wastewater and Chapter 12 for hygienic standards for bathing water).

**Table 10.1** German legal requirements for direct discharge of specific industrial effluents to inshore waters regarding nitrogen, phosphorus, COD and $BOD_5$ (AbwV 2004).

| Industry/products | $S_{NH4-N}$ (mg $L^{-1}$ N) | $S_{Nt}$ (mg $L^{-1}$ N) | $S_{Pt}$ (mg $L^{-1}$ P) | S (mg $L^{-1}$ COD) | S (mg $L^{-1}$ $BOD_5$) |
|---|---|---|---|---|---|
| Food production[a)] | 10 | 18 | 2 | 110 | 25 |
| Sugar production | 10 | 30 | 2 | 200 | 25 |
| Edible oil refinery | – | 30 | 4.5 | 200 | 38 |
| Leather production | 10 | – | 2 | 250 | 25 |
| Biological treatment of waste | – | 70 | 3 | 200 | 20 |
| Meat meal industry | – | 50 | – | 150 | 25 |
| Cellulose production | – | 10 | 2 | 25 | 30 |
| Gelatine production | 10 | 30 | 2 | 110 | 25 |
| Paper production | – | 10 | 2 | 50 | 25 |
| Textile production | 10 | 20 | 2 | 160 | 25 |
| Petroleum processing | – | 40 | 1.5 | 82 | 25 |
| Laundry | – | 20 | 2 | 100 | 25 |
| Animal and plant production | – | – | 2 | 110 | 25 |

[a)] This includes milk, brewery, potatoes, meat, fish, drinks, alcohol and alcoholic drinks, fruits and vegetables.

In domestic wastewater, one major problem is that the ratios of N:C and P:C of many organic compounds in wastewater are much higher than those needed by heterotrophic bacteria for catabolism and anabolism. Therefore, inorganic and organic N and P compounds are left in the treated wastewater. The processes for nitrogen and phosphorus removal are generally applied for domestic wastewater treatment. In industrial effluents, the contents of N and/or P are usually too low, so that N and/or P must be supplemented via additives. If the wastewater has a high N concentration, it is removed by stripping with steam or air at higher pH which must be cleaned afterwards, e.g. by absorption and reaction in sulfonic acid. The process of nitrification and denitrification has been used here only seldom.

The typical mean $NH_4$-N and total N concentrations in raw municipal wastewater range is 44.5–75.9 mg $L^{-1}$ $NH_4$-N and 74.5–103.5 mg $L^{-1}$ N in Berlin wastewater (WWTP Ruhleben). The total P concentrations range is 11.7–18.9 mg $L^{-1}$ P (BWB 2004; see also Table 2.3). But sometimes industrial effluents are heavily loaded with ammonia; and its concentration varies depending on the production processes responsible (see Table 2.4).

Chemical systems have frequently been used to remove phosphorus in wastewater treatment. Biological processes to remove nitrogen and phosphorus from wastewater have become more or less standard technology in wastewater treatment. The utilization of biological nutrient removal processes for the treatment of wastewater has environmental, economical and operational benefits. We will return to this topic later.

## 10.2
## Biological Nitrogen Removal

### 10.2.1
### The Nitrogen Cycle and the Technical Removal Process

The relationship between the various nitrogen compounds and their transformation is presented in Fig. 10.2 as the nitrogen cycle. The transformation reactions include fixation, ammonification, assimilation, nitrification and denitrification. The principle compounds in the nitrogen cycle are nitrogen gas, ammonium, organic nitrogen and nitrate (De Renzo 1978).

The atmosphere serves as a reservoir of $N_2$ gas which is naturally transformed by electrical discharge (lightning) and by nitrogen-fixing organisms. Moreover, $N_2$ gas is fixed by a technical manufacturing process known as the Haber–Bosch synthesis process since 1915. Industrial fixation was initially developed for the production of fertilizers and explosives:

$$N_2 + 3H_2 \rightarrow 2NH_3 \tag{10.1}$$

$$NH_3 + 2O_2 \rightarrow HNO_3 + H_2O \tag{10.2}$$

$$C_6H_5CH_3{}^{1)} + 3\,HNO_3 \rightarrow C_6H_2CH_3(NO_2)_3{}^{2)} + 3\,H_2O \tag{10.3}$$

In the fixed state, nitrogen can continue through various reactions. Nitrogen gas is returned to the atmosphere by an explosive reaction of a mixture from $NaNO_3$ and $Ca(NO_3)_2$ with $NH_4Cl$ to $N_2$ gas (Foerst 1965). Nitrogen gas is also formed by the biological reduction through denitrification. The nitrogen cycle is applicable to surface water and the soil/groundwater environment, where many transforming reactions can occur. Nitrogen can be added by precipitation and dustfall, surface runoff, artificial fertilizers and the direct discharge of wastewater (Fig. 10.2).

Domestic wastewater contains organic nitrogen compounds and ammonium. These originate from protein metabolism in the human body. In fresh domestic wastewater, approximately 60% of the nitrogen is in the organic and 40% is in the inorganic form, such as $NH_4^+$. The organic compounds include amino acids, proteins, ADP/ATP and urea as the basic organic sources of nitrogen and phosphorus.

Biological nitrification and denitrification together make up the most useful processes to remove nitrogen. During nitrification, ammonium is first oxidized to nitrite or nitrate by aerobic chemolitho-autotrophic bacteria. Nitrite and nitrate are then reduced to $N_2$ gas in the denitrification process by chemoorgano-heterotrophic denitrifying bacteria under anoxic conditions. Nitrification and denitrification occur inside living bacteria in nature and in biological wastewater treatment processes.

In Sections 10.2.2 to 10.2.5 we discuss the microbiology, basic reactions, kinetics and performance of biological nitrogen removal processes by nitrification and denitrification.

---

[1)] Toluene, [2)] TNT = 2,4,6-Trinitrotoluene

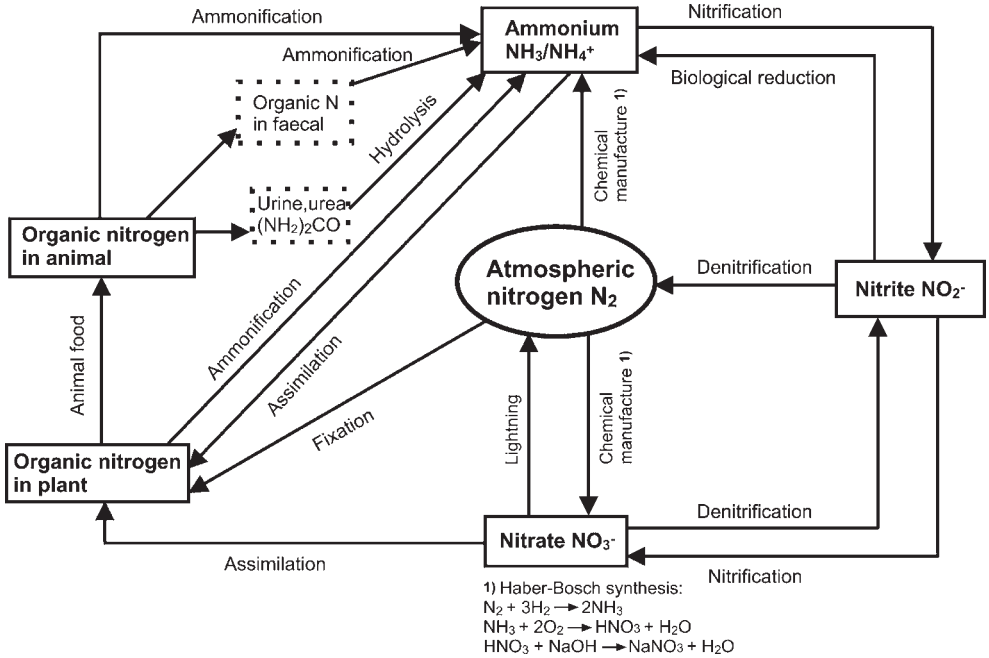


**Fig. 10.2** Principal compounds in the nitrogen cycle are nitrogen gas, ammonium, organic nitrogen and nitrate.

## 10.2.2 Nitrification

### 10.2.2.1 Nitrifying Bacteria and Stoichiometry

The autotrophic bacteria oxidize inorganic nitrogen components to obtain energy for growth and maintenance, while they obtain carbon for cell building by the reduction of $CO_2$. The principal genera in the activated sludge process, *Nitrosomonas* and *Nitrobacter*, are responsible for the oxidation of ammonium to nitrite (nitritification) and of nitrite to nitrate (nitratification), respectively.

Basic physiological and structural characteristics of *Nitrosomonas* and *Nitrobacter* are presented in Table 10.2.

The stoichiometry for catabolism of $NH_4$ and $NO_2$ oxidation are:

$$NH_4^+ + 1.5O_2 \rightarrow NO_2^- + H_2O + 2H^+ + \Delta G^o \quad (10.4)$$

$$NO_2^- + 0.5O_2 \rightarrow NO_3^- + \Delta G^o \quad (10.5)$$

with $\Delta G^o = -240 \ldots -350$ kJ mol$^{-1}$ for *Nitrosomonas* and $\Delta G^o = -65 \ldots -90$ kJ mol$^{-1}$ for *Nitrobacter* (Halling-Sørensen and Jørgensen 1993; Wiesmann and Libra 1999).

**Table 10.2** Basic comparison between nitrifying and denitrifying bacteria (Gerardi and Michael 2002; Halling-Sørensen and Jørgensen 1993).

| Indication | Nitrifiers | | Denitrifiers |
|---|---|---|---|
| | *Nitrosomonas* | *Nitrobacter* | |
| Carbon source | Inorganic ($CO_2$) | Inorganic ($CO_2$) | Organic carbon |
| Cell shape | Coccus (spherical) | Bacillus (rod-shaped) | – |
| Cell size | 1.0 · 1.5 µm | 0.5 · 1.0 µm | – |
| $O_2$ requirement | Strictly aerobic | Strictly aerobic | Facultative aerobic |
| pH range | 5.8–8.5 | 6.5–8.5 | 6.5–8.5 |
| $t_G$ | 8–36 h | 12–60 h | 0.25–0.5 h |
| Growth range of temperature | 5–30 °C | 5–40 °C | |

The overall oxidation of ammonium by both groups is obtained by adding Eqs. (10.4) and (10.5):

$$NH_4^+ + 2O_2 \rightarrow NO_3^- + 2H^+ + H_2O \tag{10.6}$$

in which a large amount of oxygen is needed and the pH decreases in water with low buffer capacity if no pH control is performed.

Compared to the catabolism of nitrification, anabolism has more complex stoichiometric reactions. Due to the use of carbon dioxide as the carbon source, a much lower growth rate of nitrifying biomass results and it is difficult to study cell-building compared to aerobic heterotroph growth, especially if the cell-building of both nitrifying genera must be determined separately. Therefore, there are significant deviations among equations describing the metabolism of nitritification and nitratification (Sherrad 1977; Dombrowski 1991; US EPA 1993; Grady et al. 1999; Henze et al. 2002).

The stoichiometric reactions for the anabolism of $NH_4^+$ and $NO_2^-$ oxidation are as follows, assuming that the empirical formulation of bacterial cells is $C_5H_7O_2N$ (Halling-Sørensen and Jørgensen 1993; Henze et al. 2002):

$$13NH_4^+ + 15CO_2 \rightarrow 10NO_2^- + \underset{\text{bacteria}}{3C_5H_7O_2N} + 23H^+ + 4H_2O \tag{10.7}$$

$$10NO_2^- + 5CO_2 + NH_4^+ + 2H_2O \rightarrow 10NO_3^- + \underset{\text{bacteria}}{C_5H_7O_2N} + H^+ \tag{10.8}$$

When compared to the catabolism of $NH_4^+$, less energy is available for the growth of *Nitrobacter* in comparison to *Nitrosomonas* (see Eqs. 10.4 and 10.5). Both anabolic reactions usually take place at $5.5 < pH < 8.3$; therefore, Eq. (10.9) must be considered (see also Section 4.3):

$$CO_2 + H_2O \leftrightarrow HCO_3^- + H^+ \tag{10.9}$$

The stoichiometric reactions of $NH_4^+$ and $NO_2^-$ oxidation for catabolism and anabolism applied to 1 mol $NH_4^+$ and $NO_2^-$ are given by Eq. (10.10) and Eq. (10.11) respectively (Wiesmann and Libra 1999):

$$NH_4^+ + 1.98HCO_3^- + 1.3O_2 \rightarrow 0.0182C_5H_7O_2N + 0.98NO_2^- + 1.04H_2O + 1.89H_2CO_3 \quad (10.10)$$

$$NO_2^- + 0.02H_2CO_3 + 0.48O_2 + 0.005NH_4^+ + 0.005HCO_3^- \rightarrow 0.005C_5H_7O_2N + NO_3^- + 0.015H_2O \quad (10.11)$$

Ammonium and nitrite are used as energy sources and $CO_2$ as a carbon source for nitrifying bacteria. Ammonium is oxidized to nitrite over three steps and the oxidation of nitrite to nitrate is a single step (Eq. 10.12). The intermediate between hydroxylamine and nitrite is not known (Henze et al. 2002).

$$NH_4^+ \xrightarrow{a} NH_2OH \xrightarrow{b} NOH? \xrightarrow{c} NO_2^- \xrightarrow{d} NO_3^- \quad (10.12)$$

It is assumed that, for every reaction step, almost the same amount of energy is produced. The energy produced by the oxidation from ammonium to nitrite is a factor of about 3.0–3.8 greater than that of the transformation from nitrite to nitrate (see Eqs. 10.4 and 10.5). Based on this fact, the biomass yield coefficient of $Y^o_{XA/NH_4}$ or $Y^o_{XA/NO_2}$ has to correspond to this relation (see Eqs. 10.18 and 10.19). Many authors have measured the growth of *Nitrosomonas* and *Nitrobacter* and described its stoichiometry, but the values are very different. The growth of new cells in the activated sludge process is referred to as an increase in the mixed liquor volatile suspended solids (MLVSS). Nitrifying bacteria obtain a relatively small amount of energy from the oxidation of ammonium and nitrite, resulting in long generation times and a small population MLVSS.

The specific growth rate of the nitrifying bacteria in activated sludge is much lower than that of aerobic organo-heterotrophs. Nitrifiers' poor ability to form flocs and the risk of being washed out of the system with their low growth rate can be overcome by the likelihood that they are adsorbed onto the surface of other floc particles. This characteristic is normally used for nitrification in biofilm reactors (see Chapter 7). Using membrane bioreactors (see Chapter 12) for nitrification is also very beneficial. The growth of nitrifying bacteria is affected by a number of environmental parameters such as dissolved oxygen concentration c′, pH and the presence of inhibitors (see Section 10.2.2.3).

In order to determine the rate of $NH_4$ oxidation in a CSTR, assuming steady state, the following expressions are used:

$$0 = Q_0 (S_{NH_4-N,0} - S_{NH_4-N}) - r_{NH_4-N} V \quad (10.13)$$

$$r_{NH_4-N} = \frac{\mu_A X_A}{Y^o_{XA/NH_4-N}} \quad (10.14)$$

$$r_{O_2} = \frac{\mu_A X_A}{Y^o_{XA/O_2}} \quad (10.15)$$

In the next section, the yield coefficients and specific growth rate of nitrifying bacteria μ are discussed.

#### 10.2.2.2 Stoichiometry and Kinetics of Nitrification

From the catabolic stoichiometric reactions Eqs. (10.4) and (10.5) for *Nitrosomonas* and *Nitrobacter* respectively, the true yield coefficients are:

$$Y^{\circ}_{O_2/NH_4-N} = 1.5\,\frac{M_{O_2}}{M_N} = 1.5\,\frac{32\ \text{g mol}^{-1}\ O_2}{14\ \text{g mol}^{-1}\ N} = 3.43\,\frac{\text{g } O_2}{\text{g N}} \tag{10.16}$$

$$Y^{\circ}_{O_2/NO_2-N} = 0.5\,\frac{M_{O_2}}{M_N} = 0.5\,\frac{32\ \text{g mol}^{-1}\ O_2}{14\ \text{g mol}^{-1}\ N} = 1.14\,\frac{\text{g } O_2}{\text{g N}} \tag{10.17}$$

The stoichiometric coefficients show the true oxygen requirements, with the exception of the amount for endogenous respiration. From the sum of both coefficients we obtain $Y^{\circ}_{O_2/N} = 4.57\ \text{g } O_2\ (\text{g N})^{-1}$. Thus, 4.57 g $O_2$ are required for each g $NO_3$-N produced (see Section 11.3.3). If anabolism is considered, the yield coefficients are only a little lower.

The true yield coefficients follow directly from Eqs. (10.10) and (10.11):

$$Y^{\circ}_{XA/NH_4-N} = \frac{0.0182\ M_{C_5H_7O_2N}}{M_{NH_4-N}} = \frac{0.0182 \cdot 115\ \text{g mol}^{-1}\ C_5H_7NO_2}{14\ \text{g mol}^{-1}\ NH_4-N} = 0.147\,\frac{\text{g MLVSS}}{\text{g N}}\ ^{1)} \tag{10.18}$$

$$Y^{\circ}_{XA/NO_2-N} = \frac{0.005\ M_{C_5H_7NO_2}}{M_{NO_2-N}} = \frac{0.005 \cdot 113\ \text{g mol}^{-1}\ C_5H_7O_2N}{14\ \text{g mol}^{-1}\ NO_2-N} = 0.04\,\frac{\text{g MLVSS}}{\text{g N}} \tag{10.19}$$

The total yield values without accumulation of $NO_2^-$ for the growth of *Nitrosomonas* and *Nitrobacter* are 0.187 g MLVSS per g $NH_4$-N oxidized or g $NO_3$-N produced. Lindemann (2002) and Choi (2005) presented and compared some yield coefficients. Averaged values of $Y^{\circ}_{XA/NH_4-N}$ and $Y^{\circ}_{XA/NO_2-N}$ were calculated from values of different authors, as follows (Larsen-Vefring 1993):

$$Y^{\circ}_{XA/NH_4-N} \approx 0.142\ \text{g MLVSS}\ (\text{g } NH_4\text{-N})^{-1}$$

$$Y^{\circ}_{XA/NO_2-N} = 0.02 \text{ to } 0.084 \approx 0.048\ \text{g MLVSS}\ (\text{g } NO_2\text{-N})^{-1}$$

---

1) The total parameter MLVSS (mixed liquor volutile suspended solids) includes here only the mass of Nitrosomonas or Nitrobacter, respectively.

The influence of the decay rate (death and endogenous respiration) was not considered. The yield coefficients for the growth of nitrifyers with respect to oxygen consumption are calculated as follows:

$$Y^{o}_{XA/O_2} = \frac{Y^{o}_{XA/NH_4-N}}{Y^{o}_{O_2/NH_4-N}} = \frac{0.147}{3.43} = 0.043 \frac{\text{g MLVSS}}{\text{g } O_2} \tag{10.20}$$

$$Y^{o}_{XA/O_2} = \frac{Y^{o}_{XA/NO_2-N}}{Y^{o}_{O_2/NO_2-N}} = \frac{0.04}{1.14} = 0.035 \frac{\text{g MLVSS}}{\text{g } O_2} \tag{10.21}$$

As the yield coefficients show, nitrification is characterized by high oxygen consumption and low biomass production. From Eqs. (10.20) and (10.21) it can be seen that almost the same amounts of oxygen are used for the cell multiplication of *Nitrosomonas* and *Nitrobacter*.

Ammonia and nitric acid are believed to be the real electron donor (substrate) of *Nitrosomonas* and *Nitrobacter*, respectively, because less energy is required for its transport into the cell compared to the transport of an ionised molecule like $NH_4^+$ or $NO_2^-$ (Suzuki et al. 1974; Bergeron 1978; Wiesmann 1994). $NH_3$ and $HNO_2$ are formed by dissociation which can be described based on a dissociation equilibrium depending on pH and temperature:

$$NH_4^+ \underset{k_2}{\overset{k_1}{\rightleftharpoons}} NH_3 + H^+ \tag{10.22}$$

$$NO_2^- + H^+ \underset{k_4}{\overset{k_3}{\rightleftharpoons}} HNO_2 \tag{10.23}$$

The concentration of $NH_3$ and $NH_4^+$ can be expressed via the dissociation constant $K_{D,NH_3} = k_2/k_1$ from Eq. (10.22) as follows:

$$K_{D,NH_3} = \frac{S_{NH_4^+-N}}{S_{NH_3-N} \cdot S_{H^+}} \tag{10.24}$$

with:

$$S_{NH_4^+-N} + S_{NH_3-N} = S_{NH_4-N,\Sigma} \tag{10.25}$$

Introduction of Eq. (10.25) into Eq. (10.24) gives:

$$K_{D,NH_3} = \frac{S_{NH_4-N\Sigma} - S_{NH_3-N}}{S_{NH_3-N} \cdot S_{H^+}} \tag{10.26}$$

or:

$$S_{NH_3-N} = \frac{S_{NH_4-N\Sigma}}{1 + K_{D,NH_3} \cdot 10^{-pH}} \tag{10.27}$$

where:

$$pH = -\log S_{H^+};\ S_{H^+} = 10^{-pH}$$

Note, that $S_{NH_4^+-N,\Sigma}$ is approximately the same as $S_{NH_4^+-N}$ for 6.0 < pH < 7.8, the pH range at which wastewater is usually treated. Finally, this results in (Anthonisen et al. 1976; Wiesmann 1994):

$$S_{NH_3-N} = \frac{S_{NH_4^+-N}}{1 + K_{D,NH_3} \cdot 10^{-pH}} \tag{10.28}$$

with:

$$K_{D,NH_3-N} = \exp\left(\frac{6344}{273 + T}\right) \tag{10.29}$$

The concentration of $HNO_2$-N is described using a similar calculation method:

$$S_{HNO_2-N} = \frac{S_{NO_2-N}}{1 + K_{D,HNO_2} \cdot 10^{pH}} \tag{10.30}$$

with:

$$K_{D,HNO_2} = \exp\left(-\frac{2300}{273 + T}\right) \tag{10.31}$$

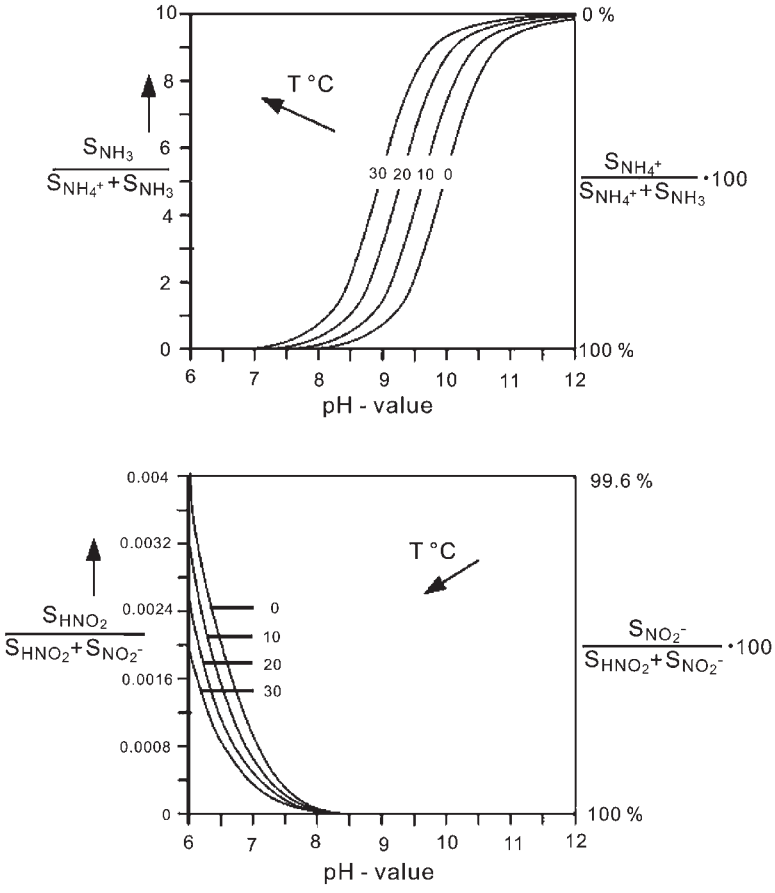


**Fig. 10.3** Influence of the temperature and pH value on the dissociation equilibrium of $NH_3$ and $HNO_2$.

The dissociation equilibria of $NH_3/NH_4^+ + S_{NH_4}$ and $HNO_2/NO_2^- + S_{HNO_2}$ with regard to the influence of temperature and pH are presented in Fig. 10.3.

It is very important to recognize that $S_{NH_3}$ increases and $S_{HNO_2}$ decreases with increasing pH.

A kinetic description of nitrification is proposed based on Haldane kinetics. Both equations are valid for ammonium and nitrite-rich wastewater where both ammonium and nitrite oxidations are inhibited by substrate surplus (see Eq. 10.32 and Eq. 10.33).

$$\mu_{NS} = \mu_{max,NS} \cdot \frac{S_{NH_3-N}}{K_{S,NH_3} + S_{NH_3-N} + \frac{S^2_{NH_3-N}}{K_{iH,NS}}} \cdot \frac{c'}{K'_{NS} + c'} \tag{10.32}$$

$$\mu_{NB} = \mu_{max,NB} \cdot \frac{S^3_{HNO_2-N}}{K_{S,HNO_2} + S_{HNO_2-N} + \frac{S^2_{HNO_2-N}}{K_{iH,NB}}} \cdot \frac{c'}{K'_{NB} + c'} \tag{10.33}$$

For higher values of $S^3_{NH_3-N}$ (higher pH) or $S^3_{HNO_2-N}$ (lower pH) the reactions are inhibited.

For lower values of $S_{NH_3-N}$ or $S_{HNO_2-N}$, e.g. in municipal wastewater treatment plants, the inhibition according to Haldane kinetics can be neglected. Oxygen limitation can be disregarded for $c' \gg K'$. According to these assumptions, Eqs. (10.32) and (10.33) result in simplified kinetic descriptions which are used for nitrification in the WWTP loaded with a low ammonia and nitrite concentration, respectively:

$$\mu_{NS} = \mu_{max,NS} \cdot \frac{S_{NH_3-N}}{K_{S,NS} + S_{NH_3-N}} \tag{10.34}$$

$$\mu_{NB} = \mu_{max,NB} \cdot \frac{S_{HNO_2-N}}{K_{S,NB} + S_{HNO_2-N}} \tag{10.35}$$

Table 10.3 presents the kinetic and yield coefficients of nitrification.

Usually, ammonium oxidation to nitrite is regarded as the bottleneck of nitrification to nitrate. However at low pH, low $c'$ and low temperature, the oxidation rate of $NO_2^-$ is considerably lower than that of $NH_4^+$. $NO_2^-$ accumulation can be observed (see Section 10.2.4). It is beneficial if $NH_4^+$ is oxidized only to $NO_2^-$, which is subsequently denitrified in biological nitrogen-removal systems. Nitrogen removal via the nitrite pathway is also an environmentally cleaner process which reduces the cost of aeration and carbon sources (e.g. methanol as an electron donor). Moreover, it has been reported that denitrification rates with nitrite are 1.5–2.0 times faster than with nitrate (Abeling and Seyfried 1992). The concept of nitrogen removal via nitrite accumulation will be explained in Section 10.2.4 in detail.

If $CO_2$ is added as the carbon source in effluents with low concentrations of organics resulting in low $CO_2$ formation, its concentration may be a rate-limiting factor, especially if high $NH_4^+$ concentrations are to be oxidized in higher pH regions (Green et al. 2002; Carrera et al. 2003).

**Table 10.3** Kinetic and yield coefficients of autotrophic nitrification.

| Reference | T (°C) | $\mu_{max}$ ($h^{-1}$) | $K_{NH_4\text{-}N}$ (mg $L^{-1}$ N) | $K_{iH}$ (mg $L^{-1}$ N) | K′ (mg $L^{-1}$ $O_2$) | $Y^{\circ}_{X_{A/N}}$ [a] |
|---|---|---|---|---|---|---|
| **$NH_4$ oxidation** | | | | | | |
| Knowles et al. (1965) | 30 | 0.0822 | 0.084 | – | – | – |
| Bergeron (1978) | 25 | 0.0064 | 0.138 | 35 | 1.8 | – |
| Nyhius (1985) | 15–17 | 0.04 | 0.056 | 33 | 0.5 | – |
| Dombrowski (1991) | 20 | 0.0138 | 0.714 | 540 | 0.29 | – |
| Wiesmann (1994) | 20 | 0.032 | 0.028 | 540 | 0.3 | 0.147 |
| Horn and Hempel (1996) | 20–22 | 0.0063 | 0.5 | – | 0.5 | 0.062 |
| Pirsing (1996) | 25 | 0.038 | 0.03 | 200 | 0.3 | 0.142 |
| Lindemann (2002) | 22.5 | 0.0074 | 0.079 | 16.5 | 0.25 | 0.142 |
| **$NO_2$ oxidation** | | | | | | |
| Knowles et al. (1965) | 30 | 0.058 | $1.9 \cdot 10^{-4}$ | – | – | – |
| Bergeron (1978) | 25 | 0.005 | $2.5 \cdot 10^{-4}$ | 35 | 1.4 | – |
| Nyhius (1985) | 15–17 | 0.016 | $1.7 \cdot 10^{-4}$ | 0.15 | 0.75 | – |
| Dombrowski (1991) | 25 | 0.019 | $0.39 \cdot 10^{-4}$ | 0.25 | 1.1 | – |
| Wiesmann (1994) | 20 | 0.045 | $0.32 \cdot 10^{-4}$ | 0.26 | 1.1 | 0.042 |
| Okabe et al. (1995) | 20 | 0.034 | $0.94 \cdot 10^{-4}$ | – | 0.68 | 0.083 |
| Pirsing (1996) | 25 | 0.041 | $0.55 \cdot 10^{-4}$ | 0.1 | 1.3 | 0.048 |
| Lindemann (2002) | 22.5 | 0.019 | $3.0 \cdot 10^{-4}$ | 0.26 | 1.27 | 0.048 |

[a] For $NH_4$ oxidation: g MLVSS (g $NH_4$-N)$^{-1}$; for $NO_2$ oxidation: g MLVSS (g $NO_2$-N)$^{-1}$.

#### 10.2.2.3 Parameters Influencing Nitrification

There are several parameters which influence the ability of a population of nitrifying bacteria to perform nitrification, such as c′, pH, T, $t_R$ and $t_{RX}$. Of all these parameters, c′ and pH are the most important.

Nitrifying bacteria are strict aerobes. The nitrification rate is limited entirely if oxygen is not supplied. Equations (10.32) and (10.33) show the influence of oxygen on the nitrification rate. For example, the region of oxygen limitation can be estimated using $K'_{NB}$ = 1.1 mg $L^{-1}$ $O_2$ (see Table 10.3). The point of limitation may be given as $\mu = 0.9\ \mu_{max}$ (90% of maximal growth rate) which is already reached at c′ = 9.9 mg $L^{-1}$ $O_2$ (see also Eq. 6.11). This means that there is always a limiting effect of the oxygen concentration on the nitrification rate when aerating with air.

For effective nitrification, the amount of c′ maintained in the aeration tank should be monitored as a control parameter to ensure permanent effluent concentrations for $NH_4^+$, $NO_2^-$ and $NO_3^-$. The practice of over-aeration is expensive and can even contribute to shearing of nitrifying bacterial flocs and/or enhance foam production.

A relationship between growth rate and pH was given by Eqs. (10.28) and (10.32) for ammonium oxidation and by Eqs. (10.30) and (10.33) for nitrite oxidation. The optimum pH for the growth of nitrifying bacteria is generally assumed to be pH 7.2–8.0, depending on $S_{NH_4}$ (see Eq. 10.28). If the pH of the aeration tank drops

below pH 5.5 or goes above pH 9.0, a significant decrease in nitrification occurs as a result of protein damage. A low wastewater pH has the primary effect of inhibiting nitrifiers' enzymatic activity and has a secondary effect on the availability of alkalinity.

A drop in temperature results in a remarkable reduction in the growth rate of nitrifying bacteria. Some authors (Hopwood and Downing 1965; Knowles et al. 1965; Painter and Loveless 1983) described the temperature dependence of nitrification. To describe the influence of temperature on nitrification as well as denitrification, we use the Arrhenius equation for biochemical reactions (see Eq. 3.1).

The temperature dependence of the maximum growth rate during nitrification was already published by Knowles et al. (1965):

$$\mu_{max,NS} = 0.042 \exp(0.0351\,T - 2.174) \tag{10.36}$$

$$\mu_{max,NB} = 0.042 \exp(0.0587\,T - 1.13) \tag{10.37}$$

The nitrification rate is a function of temperature between 8 °C and 30 °C. Low wastewater temperatures in winter negatively affect the nitrification. Therefore, many regulatory agencies in temperate regions have different ammonia discharge limits according to the season.

Figure 10.4 shows the optimal range of nitrification with respect to the growth rate of nitrifying bacteria in relation to pH and temperature (Larsen-Vefring 1993).

Excursions to low temperatures, temporary and long-term drops in c′ and/or extreme pH values lead to incomplete nitrification which results in operational disruptions.

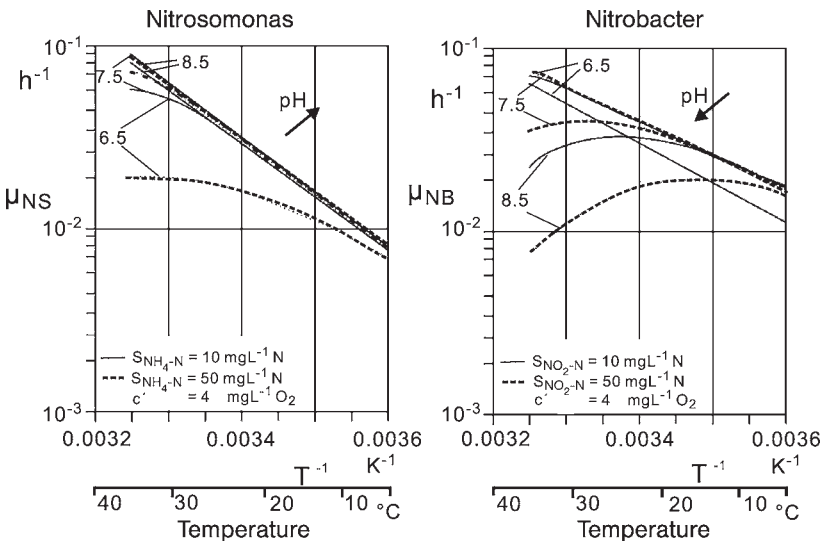


**Fig. 10.4** Specific growth rate of nitrifying bacteria in relation to pH and temperature (Larsen-Vefring 1993, calculated).

**Table 10.4** Operational parameters influencing nitrification.

| Parameters | Optimal range/value and comments |
|---|---|
| $c'$ | 2–3 mg $L^{-1}$ $O_2$, $c'$ limits nitrification |
| pH | pH 7.2–8.0, pH <5.5 and >9.0 critical |
| Temperature | T = 28–32 °C, T <5 °C and >40 °C critical |
| $S_{NH3}$ | Inhibits *Nitrosomonas* >10 mg $L^{-1}$, *Nitrobacter* >0.1 mg $L^{-1}$ |
| $S_{HNO2}$ | Inhibits *Nitrosomonas* and *Nitrobacter* >1.0 mg $L^{-1}$ |
| $S_{NH4}$ | inhibits nitrification > 400–500 mg $L^{-1}$ |
| $t_{RX}$ | > 4–6 days, increases with decreasing temperature |
| $t_R$ | > 10 h at low temperatures |
| X | > 2 g $L^{-1}$ MLVSS |
| Ratio of FM[a)] | ~ 0.5 g $NH_4$-N (g MLVSS)$^{-1}$ recommended |

[a)] Ratio of feed to biomass.

Table 10.4 summarizes the operational parameters favoring nitrification. Generally, increasing T, $t_R$, $S_N$ and a sufficiently high $t_{RX}$ are beneficial for nitrifying bacteria. They result in sufficient MLVSS. A sludge age of $t_{RX}$ > 4–6 days is needed to achieve nitrification. The presence of healthy and adequate nitrifying bacteria is the basic requirement for successful nitrification. The influences of $t_R$ and $t_{RX}$ on removal or removal rate are discussed in Chapter 6.

## 10.2.3 Denitrification

### 10.2.3.1 Denitrifying Bacteria and Stoichiometry

Denitrifying bacteria are capable of removing oxidized nitrogen from wastewater by converting it to $N_2$ gas which escapes to the atmosphere. Most denitrifying organisms are facultative aerobic chemoorgano-heterotrophic bacteria which make up approximately 80% of the bacteria within an activated sludge environment. Under anoxic conditions nitrite and nitrate serve as electron acceptors instead of $O_2$ and organic substrates as electron donors for ATP production at very low oxygen concentration.

Denitrifying bacteria are common soil and water microorganisms and are associated with fecal waste. They enter an activated sludge process as fecal organisms in domestic wastewater and use free molecular oxygen if it is available. The energy produced with $O_2$ as the electron acceptor is only 7% more than with $NO_2^-$ and $NO_3^-$ if the same C source is used (McKinney and Conway 1957).

Besides heterotrophic denitrification, denitrification can also be performed by chemolitho-autotrophic bacteria with $H_2$ or with reduced sulfate compounds as electron acceptors (Lompe 1992; Beller et al. 2004). Kuai and Verstraete (1998) showed the occurrence of oxygen-limited autotrophic nitrification–denitrification. The reduction of $NO_2^-$ and $NO_3^-$ to gases such as NO, $N_2O$ or $N_2$ in suspended sludge or biofilm under low $c'$ and/or anoxic condition is possible, even in the ab-

sence of organic carbon as endogeneous denitrification (Bernet et al. 2001). Autotrophic denitrification is used in some waterworks for treating groundwater containing $NO_3^-/NO_2^-$ (Lompe 1992). We will not discuss these processes here.

There are five main nitrogenous compounds in denitrification (see Eq. 10.38). Nitrate is the initial substrate for denitrification and molecular $N_2$ is the end-product. Other intermediates like NO and $N_2O$ can be emitted if incomplete denitrification occurs due to very high nitrate concentrations and relatively low organic substrate concentrations (Sümer et al. 1996).

$$NO_3^- \xrightarrow{1} NO_2^- \xrightarrow{2} NO \xrightarrow{3} N_2O \xrightarrow{4} N_2 \tag{10.38}$$

The reduction of $NO_3^-$ is carried out by one organism in four steps. Each step can conditionally be inhibited; and intermediate products can escape by being dissolved in water and by being subsequently desorbed and transported by mass transfer into gas bubbles and then into the air. The kinetics of the intermediate steps are still not known in detail. Until now, no exact nitrogen balance has been able to show how much NO and $N_2O$ are built. It is very important to balance exactly by measurements, but it is very difficult to perform.

Nearly all denitrifiers are able to use $NO_2^-$ and $NO_3^-$. The catabolism of denitrification that provides two growth- and energy-yielding steps is described in simplified form using methanol as the energy source (Halling-Sørensen and Jørgensen 1993; Lawrence and McCarty 1969):

$$6NO_3^- + 2CH_3OH \rightarrow 6NO_2^- + 2CO_2 + 4H_2O \tag{10.39}$$

$$6NO_2^- + 3CH_3OH \rightarrow 3N_2 + 3CO_2 + 3H_2O + 6OH^- \tag{10.40}$$

$$6NO_3^- + 5CH_3OH \rightarrow 3N_2 + 5CO_2 + 7H_2O + 6OH^- + \Delta G^0 \tag{10.41}$$

with $\Delta G^0 = -783$ kJ mol$^{-1}$.

However, this is in contrast to aerobic catabolism, during which the hydroxyl ion is not produced:

$$3O_2 + 2CH_3OH \rightarrow 2CO_2 + 4H_2O \tag{10.42}$$

The organic substrate is completely oxidized to $CO_2$ and $H_2O$. The produced $OH^-$ (see Eqs. 10.40 and 10.41) is alkaline; and some of the $CO_2$ produced is returned to the nitrification tank. The ion is compensated in part or completely depending on $NH_4^+$ influent concentration and is consumed during nitrification of soft water.

In order to maintain adequate alkalinity in the activated sludge, various chemicals or alkalics can be added to the water. These chemicals include bicarbonates ($HCO_3^-$), carbonates ($CO_3^{2-}$) and hydroxides ($OH^-$) of calcium, magnesium and sodium. The following chemicals for buffering alkalinity are commonly added: sodium bicarbonate ($NaHCO_3$), calcium carbonate ($CaCO_3$), sodium carbonate ($Na_2CO_3$), calcium hydroxide ($Ca(OH)_2$) and sodium hydroxide (NaOH). Sometimes this is not needed if, for example, hard water such as the water from Berlin (Beelitzhof) is being treated, which has a total hardness of 15.3 °dH and a carbonate hardness of 10.8 °dH (BWB 2004).

#### 10.2.3.2 Stoichiometry and Kinetics of Denitrification

Nearly all organics can be used as substrate. For this discussion of stoichiometry for catabolism and anabolism methanol is suitable. Related to one C atom of methanol, we can write (Lawrence and McCarty 1969):

$$0.926\,NO_3^- + CH_3OH + 0.22\,H_2CO_3 \rightarrow 0.051\,C_5H_7O_2N + 0.435\,N_2 + 0.926\,HCO_3^- + 1.56\,H_2O \quad (10.43)$$

$$1.49\,NO_2^- + CH_3OH + 0.79\,H_2CO_3 \rightarrow 0.059\,C_5H_7O_2N + 0.72\,N_2 + 1.49\,HCO_3^- + 1.84\,H_2O \quad (10.44)$$

In accordance with Eq. (10.13), the substrate utilization and denitrification rates are calculated as:

$$r_{NO_3\text{–}N} = \frac{\mu X}{Y^{\circ}_{XC/NO_3\text{–}N}} \quad (10.45)$$

$$r_{SD} = \frac{\mu X}{Y^{\circ}_{XC/SC}} \quad (10.46)$$

The corresponding equations for $NO_2$ can be obtained.

From Eq. (10.43) the true yield coefficients $Y^{\circ}_{XC/SC}$ and $Y^{\circ}_{SC/NO_3\text{–}N}$ follow:

$$Y^{\circ}_{XC/SC} = \frac{0.051\,M_{XC}}{M_{SC}} = \frac{0.051 \cdot 12 \cdot 5\ g\ mol^{-1}\ C_5H_7O_2N\text{–}C}{1.0 \cdot 12\ g\ mol^{-1}\ CH_3OH\text{–}C} = 0.255\,\frac{gXC}{gSC} \approx 0.51\,\frac{gMLVSS^{1)}}{gDOC} \quad (10.47)$$

$$Y^{\circ}_{SC/NO_3\text{–}N} = \frac{M_{SC}}{0.926\,M_{NO_3\text{–}N}} = \frac{1.0 \cdot 12\ g\ mol^{-1}\ CH_3OH\text{–}C}{0.926 \cdot 14\ g\ mol^{-1}\ NO_3\text{–}N} = 0.89\,\frac{gSC}{gNO_3\text{–}N} \quad (10.48)$$

From Eq. (10.47) and Eq. (10.48), then Eq. (10.49) follows:

$$Y^{\circ}_{XC/NO_3\text{–}N} = Y^{\circ}_{XC/SC} \cdot Y^{\circ}_{SC/NO_3\text{–}N} = \frac{gXC}{gNO_3\text{–}N} \approx 0.454\,\frac{gMLVSS}{gNO_3\text{–}N} \quad (10.49)$$

and, respectively, for $NO_2$ from Eq. (10.44):

$$Y^{\circ}_{XC/NO_3\text{–}N} = Y^{\circ}_{XC/SC} \cdot Y^{\circ}_{SC/NO_2\text{–}N} = \frac{gXC}{gNO_3\text{–}N} \approx 0.34\,\frac{gMLVSS}{gNO_3\text{–}N} \quad (10.50)$$

[1)] It is assumed that the MLVSS consists of 50% carbon.

**Table 10.5** Kinetic and yield coefficients of heterotrophic denitrification (Wiesmann 1994).

| Symbol | Unit | $NO_3$ reduction | $NO_2$ reduction |
|---|---|---|---|
| $\mu_{max}$ | $d^{-1}$ | 2.6 | 1.5 |
| $Y^{o}_{X/S}$ | g MLVSS (g DOC)$^{-1}$ | 1 | 1 |
| $Y^{o}_{X/N}$ | g MLVSS (g $NO_X$-N)$^{-1}$ | 1.2 | 0.8 |
| $k_d$ | $d^{-1}$ | 0.1 | 0.1 |
| $K_S$ | mg $L^{-1}$ DOC | 62.5 | – |
| $K_{NO_X\text{-}N}$ | mg $L^{-1}$ $NO_X$-N | ≤ 0.14 | ≤ 0.12 |

Thus, 0.454 g MLVSS is produced for 1 g $NO_3$-N removed by denitrification; and 25.5% of the $CH_3OH$-C is used for anabolism and 74.5% for catabolism (see Eq. 10.49). However, the production of biomass depends on substrate used, resulting in different $Y^{o}_{X/N}$. Denitrifying bacteria can use most organic compounds commonly found in domestic wastewater. Several organic substrates such as methanol, acetic acid, ethanol, glucose, molasses or a part of the influent wastewater are often added to a denitrification tank if post-denitrification is run (see Section 10.4.2).

Table 10.5 presents some kinetic and yield coefficients of denitrification.

The specific growth rate of bacteria is influenced by both the concentration of the organic substrate and the concentration of $NO_2^-$ or $NO_3^-$. The kinetics of denitrification can be described by a double Monod kinetic model and an additional term to include the inhibiting effect of dissolved $O_2$ concentration on denitrification for $NO_3^-$ (Batchelor 1982; IAWPRC 1986):

$$\mu_{NO_3\text{–}N} = \mu_{max,NO_3\text{–}N} \frac{S}{K_S + S} \cdot \frac{S_{NO_3}}{K_{NO_3} + S_{NO_3}} \cdot \frac{K_{iO_2}}{K_{iO_2} + c'} \tag{10.51}$$

and for $NO_2^-$:

$$\mu_{NO_2\text{–}N} = \mu_{max,NO_2\text{–}N} \frac{S}{K_S + S} \cdot \frac{S_{NO_2}}{K_{NO_2} + S_{NO_2}} \cdot \frac{K_{iO_2}}{K_{iO_2} + c'} \tag{10.52}$$

Note that all three saturation coefficients can differ if different substrates are used.

#### 10.2.3.3 Parameters Influencing Denitrification

From the kinetic observation in Eqs. (10.51) and (10.52) it can be seen that denitrification needs certain favorable conditions, such as the presence of organic substrate, very low c′ ($c' \approx 0$), correct pH and T.

Sufficient organic substrate is one of the main control parameters for denitrification. From Eq. (10.48) the optimal ratio of organic carbon to nitrate is approximately $Y^{o}_{SC/NO_3\text{-}N}$ = 0.89 g DOC (g $NO_3$-N)$^{-1}$ where complete denitrification is possible. For lower ratios, the $NO_3$ effluent concentration is increased. The value for $NO_2$ is somewhat lower at $Y^{o}_{SC/NO_2\text{-}N}$ = 0.58 g DOC (g $NO_2$-N)$^{-1}$. This is one of the advantages of nitrification via $NO_2$ accumulation (see Section 10.2.4). A high denitrification rate can be achieved if the concentration of readily biodegradable organic matter is controlled.

Free molecular oxygen inhibits denitrification because the oxygen suppresses the formation of the enzyme nitrate reductase (Payne 1973). Wheatland et al. (1959) found that the denitrification rate at $c' = 0.2$ mg $L^{-1}$ was about one-half of the rate at $c' = 0$ mg $L^{-1}$ ($K_{iO} = 0.2$ mg $L^{-1}$ $O_2$).

Denitrification results in an increase in the alkalinity. The $OH^-$ produced in Eqs. (10.40) and (10.41) is used for building $H_2O$ with the $H^+$ produced during nitrification. Denitrification can occur over a wide range of pH values. Most studies show the highest rates of denitrification occurring at pH 7.0–7.5 (Halling-Sørensen and Jørgensen 1993).

The growth rate of the organism and removal rate of nitrate are both affected by temperature. For wastewater below 5 °C, denitrification is highly limited because biological metabolism is too slow. Table 10.6 summarizes the operational factors favoring denitrification.

Within a redox potential range of +50 mV to –50 mV, oxygen is either absent or present only at a relatively small concentration. Above +50 mV, aerobic conditions dominate.

If it is possible for the carbon source for denitrification to be depleted, endogenous denitrification can occur. Adam (2004) observed a constant denitrification rate over a long time (>30 h) in a post-denitrification process without Bio-P organisms. This means that the kind of carbon source was not changed and/or depleted during this experiment. This is a typical characteristic of endogenous denitrification. Based on Eq. (10.51), $r_{NO_3}$ can be described to reflect endogenous respiration:

$$r_{NO_3} = \mu_{NO_3-N} X + k_e X \approx k_e X \tag{10.53}$$

where: $\mu_{NO_3-N} X \approx 0$

Endogenous denitrification rates are normally lower than when using external carbon sources. However, if the bacterial concentration in the anoxic zone is increased, the denitrification rate increases as a result (Adam 2004). The increase in ammonium concentration and decrease in bacterial concentration could be observed during endogenous denitrification and bacterial lysis.

**Table 10.6** Operational parameters influencing denitrification.

| Parameters | Optimal range/value and comments |
|---|---|
| Organic carbon | Main control parameter, ratio of 3 : 1 (organics as COD to $NO_2$ and $NO_3$) is optimal for complete denitrification, and above 3:2 causes increase in $NO_2$ and $NO_3$. |
| $c'$ | Inhibits denitrification, obvious inhibition of denitrification at $c' > 0.2$ mg $L^{-1}$ $O_2$. |
| pH | Affects enzymatic activity of denitrifying bacteria, 7.0 < pH optimum <7.5. |
| Temperature | Denitrification rate increases with increasing T, until T=35 °C; very low rate below 5 °C. |
| Redox potential | +50 to –50 mV, above +50 mV aerobic conditions dominate. |

### 10.2.4
### Nitrite Accumulation During Nitrification

Nitrite is accumulated under certain process conditions which promote the ammonium oxidation rate to a point that it exceeds the nitrite oxidation rate. Finding and optimizing these process conditions are the key points for nitrite accumulation. The following parameters are favorable for high nitrite concentrations:

- Limited dissolved oxygen concentrations due to a lower $K'_{NS} = 0.3$ mg $L^{-1}$ $O_2$ for *Nitrosomonas* compared with $K'_{NB} = 1.1$ mg $L^{-1}$ $O_2$ for *Nitrobacter* (see Table 10.3).
- Controlling the pH to obtain certain concentration levels of $HNO_2$ and $NH_3$ (see Section 10.2.2.2).
- Higher temperature favors *Nitrosomonas* (T = 28–35 °C; see Section 10.2.5).

The different K′ values of *Nitrosomonas* and *Nitrobacter* (Dombrowski 1991; Wiesmann 1994; Pirsing 1996) show that nitrite oxidation to nitrate is more limited at low oxygen concentrations than ammonium oxidation. In aerobic biofilm reactors with high biomass concentrations, the conversion rate is usually limited by the oxygen transfer from liquid to biofilm (see Chapter 7). The limited oxygen transfer to a biofilm causes a very low dissolved oxygen concentration at the surface of the biofilm, so that the nitrite oxidation to nitrate is limited more effectively due to the lower K′ values of *Nitrosomonas* compared to *Nitrobacter*. To take advantage of this characteristic, most research done on nitrite accumulation has centered on biofilm reactors (Abeling and Seyfried 1992; Garrido et al. 1997; Bernet et al. 2001; Antileo et al. 2003).

In some cases the oxidation of ammonia stops at the nitrite stage, even though c′ is high enough not to limit nitrite oxidation. This can be explained by the fact that nitrite accumulation is also linked to inhibition by ammonia. Anthonisen et al. (1976) found that ammonia inhibition of *Nitrosomonas* first becomes evident at concentrations of 8–124 g $m^{-3}$ $NH_3$-N (see Eq. 10.28), while the selective inhibition of *Nitrobacter* by $HNO_2$ already occurs at concentrations of 0.1–1.0 g $m^{-3}$ $NH_3$-N.

By using both the characteristics of low oxygen concentration and the different ammonia inhibitions of *Nitrosomonas* and *Nitrobacter*, 74% nitrite accumulation was observed in a suspended membrane bioreactor (Choi 2005).

Figure 10.5 shows the schematic of nitrification and denitrification for achieving nitrite accumulation.

Sustained nitrite accumulation via the nitrite pathway ($NH_4^+ \rightarrow NO_2^- \rightarrow N_2$) offers several benefits for nitrogen removal of wastewater, compared to the nitrate pathway ($NH_4^+ \rightarrow NO_2^- \rightarrow NO_3^- \rightarrow NO_2^- \rightarrow N_2$):

- faster kinetics of the nitrification and denitrification processes,
- up to 25% energy savings during aeration,
- up to 40% savings from reduced demand for organic substrate,
- a higher rate of denitrification,
- lower biomass production (up to one third of former amount).

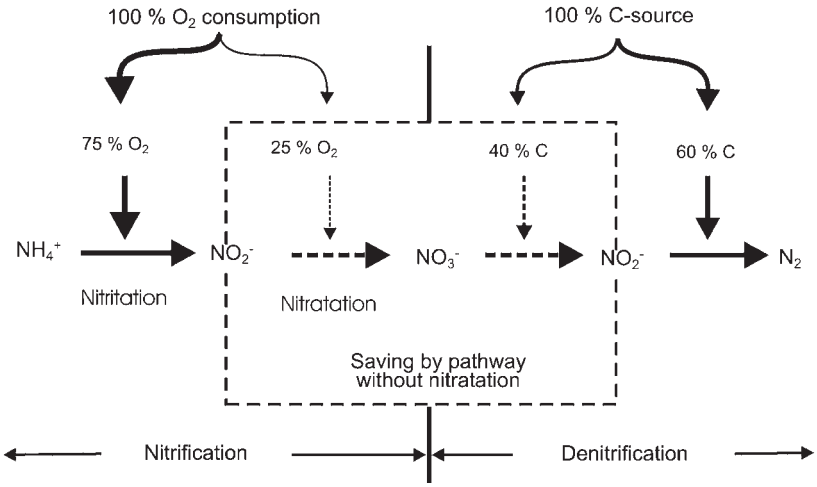


**Fig. 10.5** Schematic for the accumulation of nitrite by nitrification and denitrification.

As disadvantages it can be mentioned:

- nitrification must be operated and controlled precisely,
- automatic measurement of $NO_2$ concentration in effluent of the anoxic step results in increasing operating costs.

### 10.2.5
### New Microbial Processes for Nitrogen Removal

The ANAMMOX process – an acronym for *an*aerobic *amm*onium *ox*idation – has been described as a new way for biological nitrogen removal. Certain chemolithoautotrophic bacteria are capable of oxidizing the electron donor ammonium to nitrogen gas, with nitrite as the electron acceptor under anoxic conditions (Mulder 1992; Mulder et al. 1995; Jetten et al. 1998; Helmer et al. 2001):

$$NH_4^+ + NO_2^- \rightarrow N_2 + 2H_2O + \Delta G^0$$

where: $\Delta G^0 = -359$ kJ ... $-380$ kJ $(\text{mol } NH_4^+)^{-1}$

The bacteria belong to the rare order of the Planctomycetes, of which *Planctomyces* and *Pirellula* are the most important members. Current genera are *Brocadia* and *Kuenenia* (both freshwater species) and *Scalindua* (marine species). The bacteria catalyzing the ANAMMOX reaction are autotrophic, which means the conversion of nitrite to $N_2$ proceeds without the use of organic carbon. The process is characterized by low sludge production and a substantial reduction in aeration energy by 60% and chemicals for neutralization. The net $CO_2$ emissions are strongly reduced. The cost reduction compared to conventional N removal should be considerable (Van Dongen et al. 2001).

The SHARON process (acronym for *s*ingle reactor system for *h*igh activity *a*mmonia *r*emoval *o*ver *n*itrite) was conceived to promote biological nitrogen removal over nitrite in concentrated wastewater (Van Dongen et al. 2001) and provides several advantages (see Section 10.2.2). Its pH control is very important. Nitrite oxydation can be inhibited in regions of lower pH (higher $HNO_2$ concentration) and limited in regions of lower oxygen concentration (Van Kempen et al. 2001). The process is operated at high temperatures (>25 °C), which selectively promote the fast-growing ammonium oxidizers, while *Nitrobacter* can be washed out of the system. It is characterized by a complete absence of sludge retention ($t_{RX} = t_R$), because the growth and washout of sludge are in equilibrium (Hellinga et al. 1998; Van Kempen et al. 2001).

Processes based on this autotrophic nitrogen removal concept have been described and investigated intensively in a sequencing batch reactor SBR (Strous et al. 1998; Fux et al. 2002), in a continuous flow moving-bed pilot plant (Helmer et al. 2001), in a fluidized-bed reactor (Van de Graaf et al. 1996) and in suspended SHARON–ANAMMOX systems (Hellinga et al. 1998; Van Dongen et al. 2001). This combined new way for nitrogen elimination can be applied technically to industrial wastewater with high ammonium concentrations but no DOC.

Cost estimates for the classic method of autotrophic nitrification/heterotrophic denitrification and for partial nitritation/autotrophic anaerobic ammonium oxidation (ANAMMOX) with anaerobic sludge digestion demonstrate that partial nitritation/ANAMMOX is more economical than classic nitrification/denitrification (Fux and Siegrist 2004). A full-scale cost estimation of different techniques for N removal from rejection water was carried out based on STOWA (1996) for WWTP capacity of 500 000 inh.

## 10.3 Biological Phosphorus Removal

### 10.3.1 Enhanced Biological Phosphorus Removal

Enhanced biological phosphorus removal in activated sludge systems was first reported in the late 1960s (Vacker et al. 1967). *Acinetobacter* sp. and especially the strain *L. woffii* were identified as the organisms responsible for accumulating excess phosphates in their cells, if they have short-chain volatile fatty acids (VFAs) available, especially acetate, as feed stock (Fuhs and Chen 1975).

Biological phosphorus removal is realized by creating conditions favorable for the growth of phosphate-accumulating organisms (PAOs). An initial anaerobic zone allows the PAOs to take up VFAs into their cells and store them as poly-β-hydroxybuterate (PHF). The polyphosphate stored just prior to this is oxidized and used as an energy source, producing ATP; and it is thereby released into the liquid phase (Fig. 10.6). The anaerobic uptake of organic matter is inherently related to the accumulated polyphosphate.

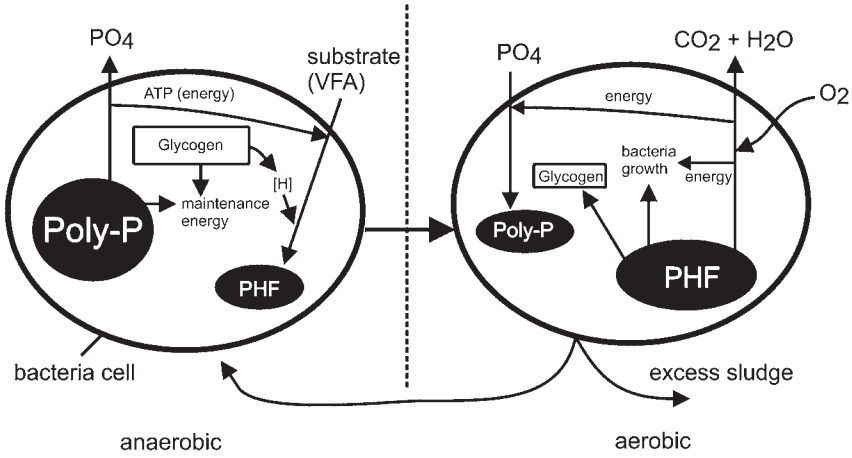


**Fig. 10.6** Mechanism of enhanced biological phosphorus removal; shown is each time the beginning of the process (Wentzel et al. 1991).

After the mixed liquor reaches the aerobic zone, the stored PHF is used by the PAOs for cell growth and to provide energy for reforming polyphosphate from all the available orthophosphate and also for the synthesis of polyglucose (glycogen). By going through both anaerobic and aerobic conditions, PAOs are adequately established and become predominant in the biomass community after several weeks. The PAO's are the only bacteria being able to store substrate in a first anaerobic reactor and to oxidize them in a second aerobic reactor. This is only possible by enrichment of the Poly–P storage. This enrichment of the PAOs containing a high concentration of polyphosphate leads to the establishment of biological phosphorus removal. The net elimination of the process results from the bacterial cell growth and the removal of surplus sludge at the point when the phosphate is taken up to a higher level than that released in the anaerobic stage (see Fig. 10.7, below).

### 10.3.2 Kinetic Model for Phosphorus Removal

#### 10.3.2.1 Preliminary Remarks

Obtaining kinetic and stoichiometric information requires that we make some assumptions, as follows:

- the reactors are operated as CSTRs (see Section 6.2.2),
- the process is in steady state,
- acetate is used as the substrate.

The biochemical pathway of the organic substrate metabolism is closely associated with polyphosphate storage. There is an apparent relationship between two parameters: organic substrate and polyphosphate. Substrate uptake and phosphorus release in the anaerobic phase can be described by the balances of acetate and $PO_4$-P (Fig. 10.7).

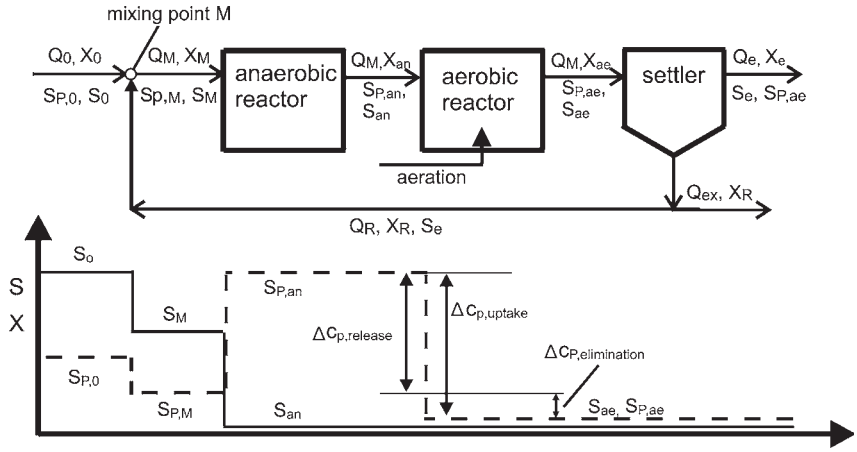


**Fig. 10.7** Two-stage biological phosphorus removal in CSTR (AO process, Phoredox) with concentration profiles for phosphorus and substrate.

The process diagram is expanded compared to Fig. 6.3 by installing an anaerobic reactor in front of the aerobic one.

### 10.3.2.2 Anaerobic Zone

The following balances are valid for an anaerobic CSTR volume $V_{an}$:

for acetate S:

$$0 = Q_M (S_M - S_{an}) - r_{S,an} V_{an} \tag{10.54}$$

for $PO_4$-P:

$$0 = Q_M (S_{P,M} - S_{P,an}) + \frac{r_{S,an}}{Y^o_{SC/PO_4-P}} V_{an} \tag{10.55}$$

for biomass X:

$$0 = Q_M (X_M - X_{an}) + \frac{r_{S,an}}{Y^o_{SC/XC}} V_{an} \tag{10.56}$$

with:

$$Y^o_{SC/PO_4-P} = \frac{S_M - S_{an}}{S_{P,an} - S_{P,M}} = \frac{S_M - S_{an}}{S_{PP,an} - S_{PP,M}} \tag{10.57}$$

and:

$$Y^o_{XC/SC} = \frac{X_{an} - X_M}{S_M - S_{an}} \tag{10.58}$$

where $S_M$ is the concentration of acetate after mixing with returned sludge, $S_{an}$ is the concentration of acetate in the anaerobic reactor, $S_{P,an}$ is the concentration of $PO_4$-P in the anaerobic reactor, $S_{P,M}$ is the concentration of $PO_4$-P after mixing with returned sludge, $r_{S,an}$ is the rate of acetate uptake, $S_{PP,an}$ is the concentration

of polyphosphate in bacterial cells in the anaerobic reactor and $S_{PP,M}$ is the concentration of polyphosphate in bacterial cells after mixing with returned sludge.

In order to determine $S_{P,an}$ with a known reactor volume $V_{an}$ and flow rate $Q_M$, it is first necessary to know the dependency of the substrate conversion rate $r_{S,An}$ on the concentrations of acetate $S_{an}$ and orthophosphate-P $S_{P,an}$ in the anaerobic stage. The specific maximum growth rate $\mu_{max}$ and yield coefficient $Y^{\circ}_{XC/SC}$ are replaced by the rate coefficient k. The modified double-Monod kinetics could be verified by experiments (Wentzel et al. 1987; Gao 1995; Romanski 1999):

$$r_{S,An} = \frac{\mu_{max}}{Y^{\circ}_{XC/SC}} X_{an} \frac{S_{an}}{K_S + S_{an}} \frac{n_{PP}}{K_{PP} + n_{PP}} \tag{10.59}$$

with:

$$n_{PP} = \frac{S_{PP,an}}{X_{an}} \tag{10.60}$$

If $n_{PP} = 0$, no substrate can be taken up. For $n_{PP} \gg K_{PP}$, the acetate uptake rate $r_{S,an}$ is only a function of $S_{an}$ and $X_{an}$; and for $S_{an} \gg K_S$ it depends only on $X_{an}$.

### 10.3.2.3 Aerobic Zone

The following balances are valid for an aerobic CSTR volume $V_{ae}$:

for acetate S:

$$0 = Q_M (S_{an} - S_{ae}) - r_{S,ae} V_{ae} \tag{10.61}$$

for $PO_4$-P:

$$0 = Q_M (S_{P,an} - S_{P,ae}) - \frac{r_{S,ae}}{Y^{\circ}_{SC/PO_4-P}} V_{ae} \tag{10.62}$$

for biomass X:

$$0 = Q_M (X_{an} - X_{ae}) + \frac{r_{S,ae}}{Y^{\circ}_{SC/XC}} V_{ae} \tag{10.63}$$

with:

$$Y^{\circ}_{SC/PO_4-P} = \frac{S_{an} - S_{ae}}{S_{P,ae} - S_{P,an}} = \frac{S_{an} - S_{ae}}{S_{PP,ae} - S_{PP,an}} \tag{10.64}$$

and:

$$Y^{\circ}_{XC/SC} = \frac{X_{ae} - X_{an}}{S_{an} - S_{ae}} \tag{10.65}$$

In the aerobic zone, phosphorus uptake and substrate transformation rates are influenced by orthophosphate in the liquid phase and by the carbon source stored as PHB in bacterial cells. They are very closely connected with each other and it is assumed that the bacterial growth occurs based on intracellular PHB:

$$r_{P,ae} = \frac{\mu_{max}}{Y^{o}_{XC/PO_4-P}} X_{ae} \frac{S_{P,Ae}}{K_{P,Ae} + S_{P,Ae}} \frac{n_{PHB}}{K_{PHB} + n_{PHB}} \frac{c'}{K' + c'} \quad (10.66)$$

$$r_{S,ae} = -\frac{\mu_{max}}{Y^{o}_{XC/PHB}} X_{ae} \frac{S_{P,ae}}{K_{P,ae} + S_{P,ae}} \frac{n_{PHB}}{K_{PHB} + n_{PHB}} \frac{c'}{K' + c'} \quad (10.67)$$

with:

$$n_{PHB} = \frac{S_{PHB}}{X_{an}} \quad (10.68)$$

Note that the substrate is now stored as PHB inside the cells.

Various models have been developed for the biological phosphorus removal by several authors (Wentzel et al. 1986; Tsuno et al. 1987; Ante and Voß 1995; Gao 1995; Henze et al. 1995; Romanski 1999). But today there is no standard model to describe the kinetics of biological phosphorus removal. Its rate depends primarily on the concentration of polyphosphate-accumulating bacteria in both anaerobic and aerobic reactors and the concentrations in the Eqs. (10.59), (10.66) and (10.67). These equations have not been sufficiently validated and further investigations are needed.

### 10.3.3
### Results of a Batch Experiment

Figure 10.8 shows concentration profiles of S and $S_P$ in a batch experiment, presenting a net elimination of phosphorus (Romanski 1999).

In the anaerobic period, the obligatorily aerobic poly-P bacteria (PAOs) take up substrate (e.g. acetate) and store it as lipid reserve material (PHB). Simultaneous-

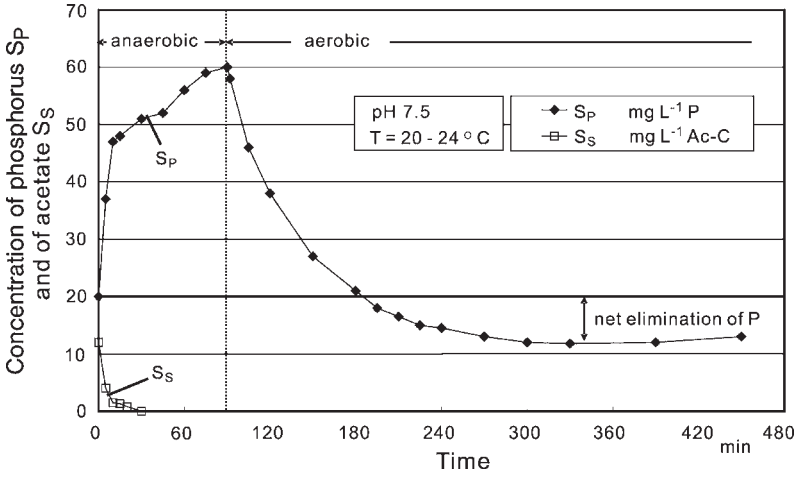


**Fig. 10.8** Concentration profiles of $S_S$ and $S_P$ in a batch experiment (Romanski 1999).

ly, the polyphosphate in the cells is partly utilized as an energy source and is released, resulting in an increase in $S_P$ from 20 mg $L^{-1}$ to 60 mg $L^{-1}$ $PO_4$-P, which is closely correlated with the synthesis of PHB. The polyphosphate is released with a high rate as long as the acetate exists. Afterwards, other substrates being formed by lysis of bacteria are partly converted into lower fatty acids, resulting in a slower P-release.

In the following aerobic phase, the orthophosphate is taken up into the bacterial cells while the PHB is utilized for growth. The orthophosphate concentration $S_P$ decreases from the initial concentration of 20 mg $L^{-1}$ at the beginning of the anaerobic batch test down to 12 mg $L^{-1}$ $PO_4$-P. The difference of 8 mg $L^{-1}$ $PO_4$-P is the net elimination of phosphorus. More phosphate is taken up aerobically than is released anaerobically because it is enriched in the biomass due to bacterial growth which is removed with the excess sludge.

### 10.3.4
### Parameters Affecting Biological Phosphorus Removal

An adequate supply of VFAs is one of the key factors for successful biological phosphorus removal, due to its very strong relation to polyphosphate release or phosphate uptake. VFAs either are a part of the readily biodegradable substrate in the influent or are formed from it by fermentation in the anaerobic zone by facultative aerobic bacteria. In comparison, methanogenic bacteria are not able to grow in a system with changes from anaerobic to aerobic conditions.

If adequate dissolved oxygen is present, PAOs can grow in the aerobic zone at adequate rates. But the introduction of $O_2$ or $NO_2$ and $NO_3$ to the anaerobic zone should be minimized because it is used preferentially as a terminal electron acceptor, which reduces the amount of VFAs available for uptake by the PAOs (Hascoet and Florentz 1985). As a result, phosphate uptake in the aerobic zone is reduced.

The solid retention time $t_{RX}$ must be adequate to allow PAOs to grow and can remarkably affect the phosphorus removal rate. Increasing the anaerobic $t_{RX}$ will allow increased fermentation of organic matter, resulting in increased production of VFAs and total removal rate. A low hydraulic retention time $t_R$ is beneficial in optimizing the process. The main parameters affecting biological phosphorus removal performance are summarized in Table 10.7.

Decreasing temperature in the anaerobic zone reduces the rate of fermentation. PAOs are less affected by decreasing pH than nitrifying bacteria are (US EPA 1993). Overall phosphate removal may fall with decreasing pH values because more energy is needed to take up acetates against a higher $H^+$ concentration, because the concentration of undissociated acetate decreases.

The phosphorus content of the bacteria $n_{PP}$ may have a remarkable influence on the phosphorus removal rate because it is very closely linked to the capacity of PAOs for P release and uptake. The typical average $n_{PP}$ value is 5–7% of the bacterial mass and values as high as 12–15% are obtained in some cases, depending on the process configuration. The $n_{PP}$ for conventional activated sludge will typically range from 1.5% to 2.0% (Grady et al. 1999).

**Table 10.7** Parameters affecting BPR process.

| Parameters | Optimal range/value and comments |
|---|---|
| Concentration of VFAs[a)] | Adequate concentration of VFAs is beneficial. Low VFA concentration reduces the P release in anaerobic zone resulting in corresponding low P uptake in aerobic zone. |
| $t_{RX}$ | $t_{RX}$ = 1.0–1.5 d is recommended for a growing of PAOs. |
| c′ | c′ limits the formation of VFAs because VFAs are properly formed under strictly anaerobic conditions. |
| Temperature | Low temperatures can reduce the formation of VFAs and the activity of PAOs. |
| pH | PAOs are less sensitive to pH changes than nitrifying bacteria. Decreasing pH adversely affects the P removal rate. |
| Presence of $NO_3$ | $NO_3$ in anaerobic zone reduces P release resulting in decreasing P uptake in aerobic zone. |
| P content of MLSS | Very closely connected with capacity of PAOs for P-release and uptake. |

[a)] Volatile fatty acids.

## 10.4 Biological Nutrient Removal Processes

### 10.4.1 Preliminary Remarks

Biological nutrient removal processes are modifications of the activated sludge process that combine anoxic and/or anaerobic zones with aerobic zones to provide nitrogen and/or phosphorus removal. Many configurations are possible, resulting in a wide range of performance capabilities and operational characteristics, which are presented in Table 10.8.

This section describes and discusses biological removal systems which provide removal of either nitrogen or phosphorus, or both components.

### 10.4.2 Nitrogen Removal Processes

The primary process for biological nitrogen removal consists of an aerobic stage for nitrification and an anoxic stage for denitrification. Figure 10.9a shows a two-stage biological nitrogen removal system (Ludzack and Ettinger 1962) called a modified Ludzak–Ettinger (MLE) process. They were the first to propose a single sludge nitrification–denitrification process using biodegradable organics in the influent wastewater.

**Table 10.8** Characteristics of different zones in the biological nutrient removal process.

| Zone | Biochemical transformation | Function | Removed component |
|---|---|---|---|
| Anaerobic | Phosphorus release | Enrichment of PAOs[a)] | Phosphorus |
| | Formation of readily biodegradable organic matter by fermentation | | Carbon |
| | Uptake and storage of volatile fatty acids by PAOs | | |
| Anoxic | Denitrification | Reduction of $NO_3$-N to $N_2$ | Nitrogen |
| | Metabolism of exogenous substrate by facultative heterotrophs | Selection of denitrifying bacteria | Carbon |
| | Production of alkalinity | Uptake of $PO_4$[b)] | Phosphorus |
| Aerobic | Nitrification | Oxidation of $NH_4$-N to $NO_2$-N and/or $NO_3$-N | Nitrogen |
| | Consumption of alkalinity | Nitrogen removal via gas stripping | |
| | Phosphorus uptake | Formation of polyphosphate | Phosphorus |
| | Metabolism of stored and exogenous substrate by PAOs | Uptake of $PO_4$[c)] | |
| | Metabolism of exogenous substrate by heterotrophs | | Carbon |

[a)] Phosphate-accumulating organism.
[b)] In the presence of easily biodegradable organics, nearly all the $PO_4$-P is taken up.
[c)] If all the easily biodegradable organics are used in the anoxic stages without complete $PO_4$-P uptake, additional $PO_4$-P is removed within the aerobic stage using organic lysis product.

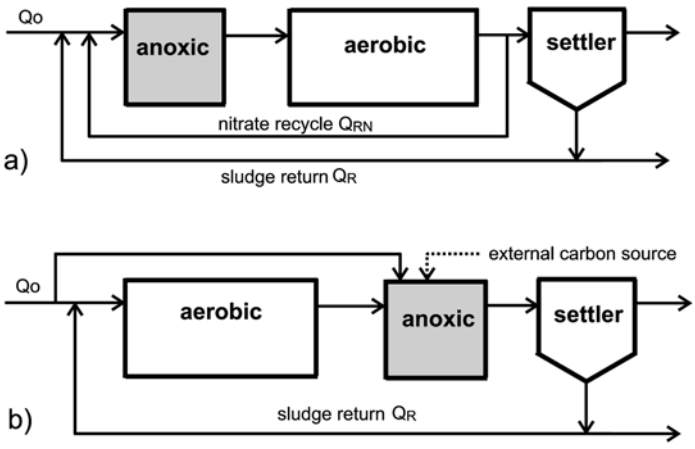


**Fig. 10.9** Biological nitrogen removal process for (a) pre-denitrification and (b) post-denitrification.

The anoxic stage for denitrification is located in front of the aerobic stage where $NO_3^-$ is formed. Both recycle streams $Q_{RN}$ and $Q_R$ have the target effluent amount of nitrate which restrains the possible amount of the denitrification. The real effluent nitrogen concentration is determined by the total nitrogen influent concentration to the process and the relation of total recycle flow $Q_{Rt}$ to the influent flow $Q_0$ as $n_{RN}$.

It is advantageous that the organic matter contained in the wastewater is consumed while no additional organic substrate is added. One drawback of this process is the remaining $NO_3^-$ which is discharged after formation because a typical maximum recycle flow rate is $Q_{RN} \approx 5\,(Q_0 + Q_R)$. At higher $Q_{RN}$, the energy consumption for pumping is too high, resulting in high operational costs without a noticeable increase in N removal. This process enables excellent nitrification and a good degree of denitrification down to $S_N \approx 4$–$8$ mg $L^{-1}$ $N_t$. In order to increase removal efficiency down to effluent levels of $S_N < 3.0$ mg $L^{-1}$ $N_t$, the MLE process was developed further, yielding the four-stage Bardenpho process by Bardard (1973). It involves the expansion of the process by a secondary anoxic and a small aerobic reactor.

In contrast to the MLE process (Fig. 10.9a), the aerobic zone is located in front of the anoxic zone (Fig. 10.9b). To use the biodegradable organic matter in the wastewater, a part of the influent bypasses the first stage and is introduced to the anoxic stage. Only the sludge is returned to the initial aerobic process. The energy consumption for pumping $Q_{RN}$ is saved. If in some cases sufficient organic matter is not present in the influent or in the effluent from the aerobic nitrifying stage, a supplemental N-free carbon source, such as methanol or acetate, is added to the anoxic stage. This configuration may be useful if the price of added supplemental substrate is low and very low $NH_4$ concentrations are required. This configuration can be expanded beyond the anoxic stage by a smaller aerobic zone to remove the remaining carbon and $NH_4$ (in the case of a bypass of wastewater) from the anoxic stage. The addition of a supplemental N-free carbon source results in an improvement in the process efficiency, but increases chemical costs.

### 10.4.3 Chemical and Biological Phosphorus Removal

Before discussing the biological P removal process, we will briefly explain chemical P elimination by precipitation. The main part of phosphorus in domestic wastewater is orthophosphate $PO_4$-P (Fig. 10.1). It can be separated from wastewater by precipitation with $Al^{3+}$ and $Fe^{3+}$ salts. Mostly two different processes are used: simultaneous precipitation occurs in the aerobic tank of an activated sludge plant, where $Fe^{3+}$ is produced by the very fast oxidation of the cheaper $Fe^{2+}$. If $FeSO_4$ is applied, we write:

$$PO_4^{3-} + FeSO_4 \rightarrow FePO_4 \downarrow + SO_4^{2-} + e^- \qquad (10.69)$$

The insoluble $FePO_4$ forms flocs mostly inside the activated sludge particles and can be separated as excess sludge.

In some northern countries, post-precipitation is preferred behind the secondary clarifier, using a reactor for precipitation and a settler for floc separation. The reactor is not aerated. Therefore instead of $Fe^{2+}$ salts, $Al^{3+}$ and $Fe^{3+}$ salts are applied. If $Fe_2(SO_4)_3$ is used, we write:

$$2PO_4^{3-} + Fe_2(SO_4)_3 \rightarrow 2FePO_4 \downarrow + 3SO_4^{2-} \quad (10.70)$$

To obtain larger flocs with higher settling rate, polymers as flocculation aids are added.

As shown in Table 10.1, dissolved inorganic polyphosphates and organic phosphorus as well as particulate phosphorus are further components of municipal wastewater. They can only be separated partly by adsorption and co-precipitation.

The anaerobic and aerobic (or oxic) process (AO process, also called Phoredox) is a method for biological phosphorus removal (see Fig. 10.7). The placement of an anaerobic reactor in front of the conventional activated sludge process leads to the use of influent organic matter for the anaerobic formation of PHB. High rates of phosphorus removal are obtained by minimizing nitrification and maximizing the production of poly-P-storing bacteria. High solids production is beneficial if usage in agriculture is planned because the production of high phosphorus content biomass is maximized. The anaerobic zone is contained in the main process stream and is thus regarded as a mainstream biological phosphorus removal process.

### 10.4.4 Processes for Nitrogen and Phosphorus Removal

#### 10.4.4.1 Different Levels of Performance

Many configurations have been developed as combined processes for biological nitrogen and phosphorus removal, including anaerobic, anoxic and aerobic zones. Due to the negative influence of nitrate on phosphorus removal, recycling of the nitrate into the anaerobic zone should be minimized and controlled; it is a key consideration in the selection and design of these processes.

The AAO process (Fig. 10.10a) is a combination of the anoxic and oxic MLE process (Fig. 10.9a) for nitrogen removal and the anaerobic and oxic Phoredox process (see Fig. 10.7) for phosphorus removal. The internal recycle flow rate is usually $Q_{RN} \approx (2\text{–}4) \cdot (Q_0 + Q_R)$. The nitrogen removal rate is similar to that of the MLE process, but the phosphorus removal is sometimes a little lower than that of the AO Phoredox process.

Some nitrate is introduced with the return sludge into the anaerobic zone, resulting in an adverse impact on the phosphorus removal if $Q_{RN}$ is too low. The greatest influence on the phosphorus removal is the organics content of the influent. If the organics content is high enough for both phosphorus and nitrogen removal, then the nitrate recycle will only have a slight impact on effluent quality, but if it is low then there would be serious influence on the removal rate. Denitrification for conversion of nitrate to $N_2$ can be also carried out in part within a sludge blanket in the settler, which reduces the nitrate recycle to the anaerobic zone and leads to bacterial flocs being washed out of the system. Improper design of the

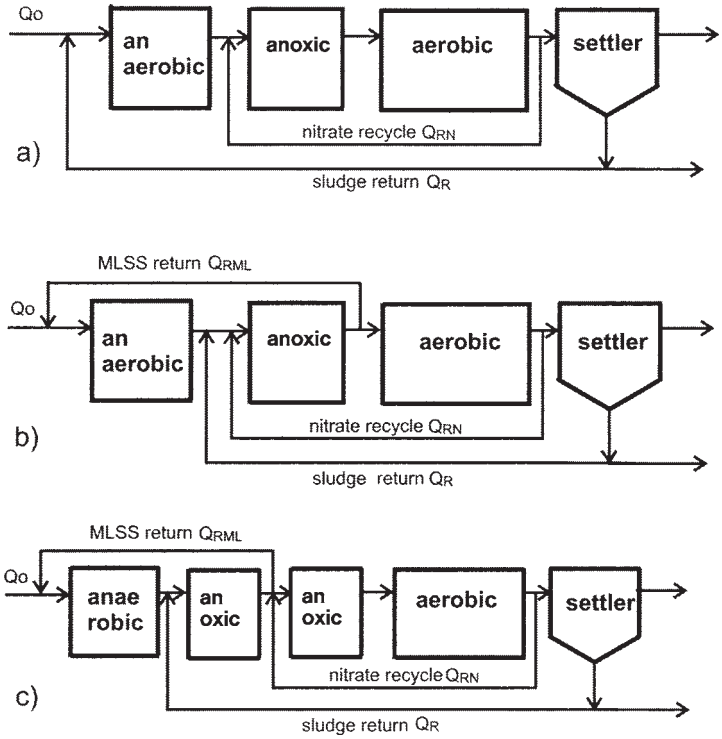


**Fig. 10.10** Processes for removal of both nitrogen and phosphorus: (a) the AAO process; (b) sludge return only into the anoxic stage, partly return of $O_2$- and $AlO_3$-free activated sludge from the anoxic to the anaerobic stage; (c) two anoxic stages.

sludge blanket can lead to bulking, clumping and floating sludge, which reduces system effectiveness.

In order to eliminate the negative influences of the nitrate recycling to the phosphorus removal rate, a process was developed where the sludge was only returned to the anoxic stage in order to avoid the input of some oxygen into the anaerobic stage (Fig. 10.10b). Behind the anoxic stage a partial flow with $NO_3$-free, non-thickened sludge was recycled into the anaerobic stage.

In addition to that, the anoxic zone can be divided into two (up to four) reactors (Fig. 10.10c). The first anoxic reactor receives and denitrifies the return sludge stream and the second receives and denitrifies the nitrate recirculation stream. The denitrified mixed liquor is recirculated from the effluent of the first anoxic reactor to the anaerobic zonein order to provide the influent wastewater with bacteria. The advantage is the protection of the second anoxic stage for influences of recycled nitrate with sludge return.

Many other biological nutrient removal processes for both nitrogen and phosphorus have been developed (Randall et al. 1992; Grady et al. 1999). The kind of pro-

cess and plant design used depends on the treatment goal, the legislation, the composition of the wastewater to be treated and the costs for operation as well as the costs for the modification of the existing plant.

#### 10.4.4.2 WWTP Waßmannsdorf

The primary principle of the AAO process is applied in the Waßmannsdorf wastewater treatment plant near Berlin, Germany (Schuchardt 2005). This WWTP eliminates organic substrate, nitrogen and phosphorus. Figure 10.11 presents the layout and sampling points of the WWTP.

The influent wastewater has about 100 mg $L^{-1}$ DOC, 56 mg $L^{-1}$ $NH_4$-N and 9.5 mg $L^{-1}$ $PO_4$-P (Fig. 10.12), which fluctuate according to a daily cycle.

In the anaerobic zone, approximately half of the DOC is removed when the PAOs take up PHB into the bacterial cells (see Fig. 10.6). The PHF is used for the reduction of nitrate in the anoxic zone. The measured DOC concentration of 16 mg $L^{-1}$ in the effluent from the aerobic stage corresponds to the inert organic matter.

The change in the orthophosphate concentration shows the typical course of biological P elimination. It increases in the anaerobic stage due to the $PO_4$-P release from the Bio-P bacterial cells, the uptake of $PO_4$-P begins in the anoxic zone by denitrification with polyphosphate uptake and continues in the aerobic zone. No $PO_4$-P is detected in the aerobic effluent. Phosphorus precipitants are dosed as needed at the beginning of the third aerobic zone to compensate for the extreme daily fluctuations in phosphorus loads and also the high flows associated with storm drainage.

First, in the aerobic zone, the $NH_4$-N concentration is decreased in the course of nitrification. Its effluent concentration is about 0.81 mg $L^{-1}$ $NH_4$-N and a nearly complete nitrification to nitrate is observed already in the first and/or second aerobic zone (Fig. 10.13).

The amount of aeration following the first and/or second aerobic zone can be reduced if, for example, precise measurement of the nitrogen fractions is used to control c′ exactly, depending on the time of day (see Problem 10.2).

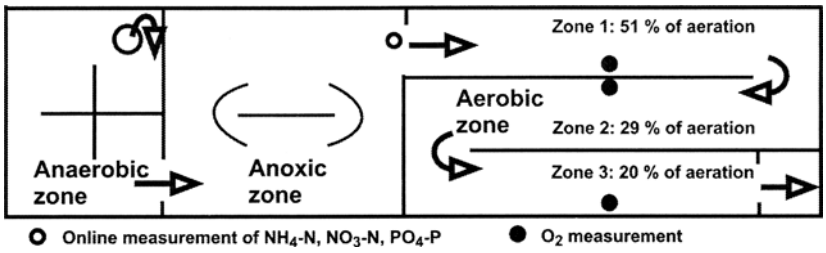


**Fig. 10.11** Processes for removal of organics, nitrogen and phosphorus by the AAO process in WWTP Waßmannsdorf near Berlin (Schuchardt 2005).

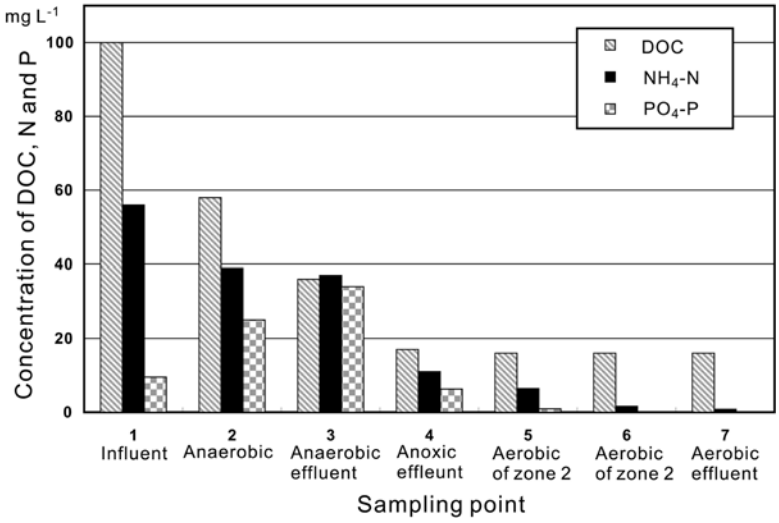


**Fig. 10.12** Concentration profiles of DOC, ammonium and phosphate in WWTP Waßmannsdorf, 3.5.2000 ($13^{00}$–$16^{50}$) (Schuchardt et al. 2002).

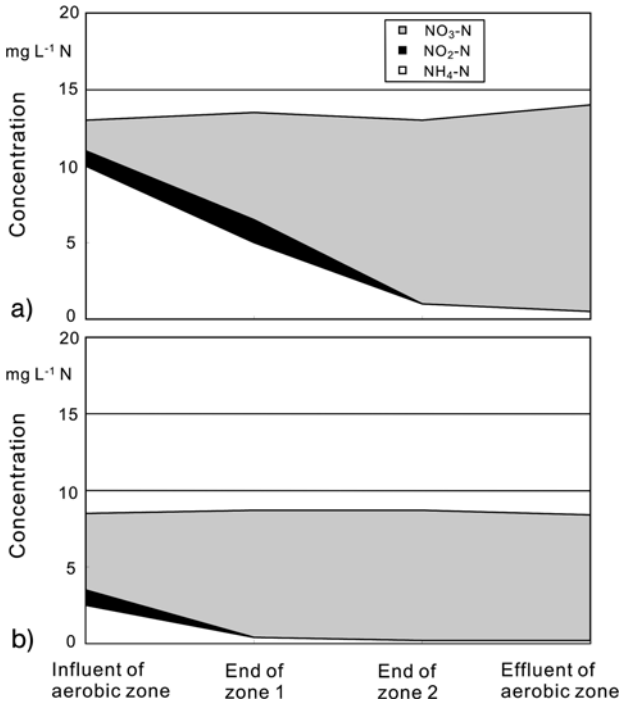


**Fig. 10.13** Concentrations of nitrogen fractions in the aerobic zone of basin BB-K in WWTP Waßmannsdorf (Schuchardt 2005).
a) 14.11.2001, $14^{20}$–$16^{05}$; b) 15.11.2001, $6^{15}$–$8^{05}$.

#### 10.4.4.3 Membrane Bioreactors (MBR)

The process of biological removal of nitrogen and phosphorus has been adapted to MBR technology. Modern membrane applications allow us to carry out the process without secondary clarifiers and to increase the sludge concentration to values of 10–20 g $L^{-1}$ MLVSS, which cannot be attained by sedimentation, resulting in high sludge ages, higher metabolic rates and better nutrient removal.

Although they have increased energy consumption, higher initial investment costs and operating costs, various accounts of practical experience and data are available on MBR processes and increasing numbers of full-scale plants are going into operation. Recently, post-denitrification and enhanced biological phosphorus removal have emerged in the form of MBR processes (Kraume et al. 2005). A MBR bench-scale plant was successfully operated performing biological phosphorus removal in both pre- and post-denitrification configurations without additional carbon and with different sludge retention time $t_{RX}$ values of 15 d and 26 d (Adam et al. 2002; Lesjean et al. 2003).

Chapter 12 presents the principles and applications of membrane technology in biological wastewater treatment.

## 10.5 Phosphorus and Nitrogen Recycle

### 10.5.1 Recycling of Phosphorus

High-grade deposits of phosphate rock are utilized as the main source for the production of fertilizers and other industrial phosphates. Until now, phosphorus has been utilized as a non-renewable resource. The end-products of the phosphate industry are introduced in the environment via sewage and manure with hardly any of it being reused. It is clear that known reserves have a limited lifetime of about 50–100 years (Steen 1998). If the current practice does not change, we may face the depletion of one of the most important elements of all living beings. This problematic situation could be prevented by the recycling of phosphates into the agricultural fertilizer industry and/or the phosphate industry. Closing the phosphorus cycle is the answer.

With the focus on wastewater treatment, there are various methods to recycle phosphorus, such as biological P removal and spreading sludge in agriculture, as well as chemical P precipitation.

Bio-P-containing sludges have average phosphorus concentrations of 2.9% (STOWA 2001), which can be increased by the incineration process (up to 8% P in ash). In spite of the increase in P concentration achieved, the quality is still not sufficient for use in the phosphorus industry because of the levels of impurities such as copper and zinc (Lijmbach et al. 2002).

The most widely developed techniques for recovering phosphorus are calcium phosphate formation and precipitation of struvites (i.e. magnesium ammonium phosphates, MAP, or potassium ammonium phosphates; CEEP 1998).

First, the formation of calcium phosphate can be induced with high calcium concentrations and elevated pH by the addition of lime. Up to 80% P recovery has been achieved, but 50–60% may be more common. The calcium phosphate formed is very similar to mined phosphate rock and can readily be used in the manufacture of agricultural fertilizers or by the phosphate industry. But the main disadvantage of this technique is the low efficiency of P formation compared to the calcium input.

The MAP process is suitable for high-strength wastewater, like digester supernatant or manure wastewater (Lijmbach et al. 2002). Magnesium forms a relatively insoluble complex together with ammonium and phosphate (MAP). The formation reaction is well known for analyzing magnesium:

$$Mg^{2+} + NH_4^+ + PO_4^{3-} \rightarrow MgNH_4PO_4 \tag{10.71}$$

Normally, struvites produced by precipitation can be used as an agricultural fertilizer; and recycling is possible in certain phosphate industry processes, such as in phosphorus furnaces (CEEP 1998). A number of full-scale struvite recovery plants are operating in Japan, producing material that is sold to the local fertilizer industry (Ueno and Fujii 2001).

The struvite technique is characterized not only by removing $PO_4$ and $NH_4$ from the wastewater but also by its reuse.

### 10.5.2 Recycling of Nitrogen

Wastewater with high $NH_4$ concentration can be treated according to the reaction in Eq. (10.71) (Schulze-Rettmer 1993). To reduce the consumption of magnesium and phosphate, magnesium must be recycled. Struvite is treated by heat drying and by injecting steam under basic conditions in the presence of NaOH:

$$MgNH_4PO_4 + NaOH \rightarrow MgNaPO_4 + NH_3 + H_2O \tag{10.72}$$

The concentrated ammonia from Eq. (10.72) is separated and reused, while the $MgNaPO_4$ can be used again for precipitation of the $NH_4$ in the MAP process:

$$NH_4^+ + MgNaPO_4 + OH^- \rightarrow MgNH_4PO_4 + NaOH \tag{10.73}$$

The MAP process is suitable for high-strength ammonium-rich wastewater (see Table 2.4) and operates at high efficiency of ammonium elimination (up to 99%; Schulze-Rettmer 1993). Moreover, there are various possible techniques to recycle ammonium nitrogen from wastewater, such as the application of biosolids (sludge from WWTP) in agriculture, adsorption of ammonium by zeolites, stripping of ammonia and chemical precipitation in the MAP process (Maurer et al. 2002). The produced $NH_3$ in Eq. (10.72) can be further used for the synthesis of nitrate (see Eqs. 10.2 and 10.3).

**PROBLEM 10.1**

Domestic wastewater containing ammonium is to be treated. An effluent total nitrogen concentration of $S_{Nt,e} = 10$ mg $L^{-1}$ is given. A pre-denitrification step (Fig. 10.14) is available for the removal of ammonium.

It is assumed that 99% of the ammonium is oxidized to nitrate without nitrite accumulation. Enough carbon is available to ensure complete denitrification (100%). The anoxic and aerobic reactors are completely mixed and operated in steady state.

The following conditions and data are given: no additional formation of $NH_4$ during the anoxic and aerobic process, wastewater influent flow rate $Q_0 = Q_R = 100$ $m^3$ $d^{-1}$, $Q_{RN} = 4\ Q_0$ resulting in $n_{RN} = 4$, $S_{NH_4\text{-}N,0} = 50$ mg $L^{-1}$ before mixing point, $S_{NO_3\text{-}N,ax} = 1$ mg $L^{-1}$; and the bacterial concentration is $X_{NS} = 0.05$, respectively $X_D = 0.2$ g $L^{-1}$ MLVSS.

Calculate the volumes of the anoxic and aerobic reactors.

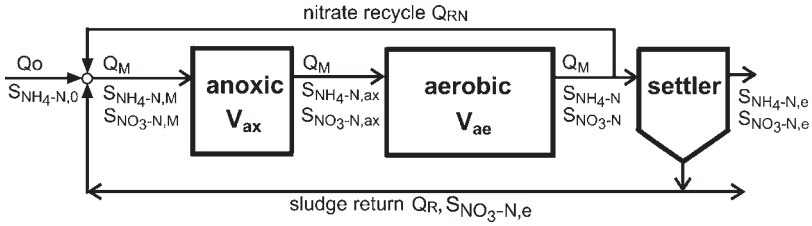


**Fig. 10.14** Configuration for post-denitrifification with internal recycle.

**Solution**

First, we obtain the following values from known data above:

$Q_{RN} = 4\ Q_0 = 4 \cdot 100$ $m^3$ $d^{-1} = 400$ $m^3$ $d^{-1}$

$Q_M = Q_0 + Q_R + Q_{RN} = 100 + 100 + 400$ $m^3$ $d^{-1} = 600$ $m^3$ $d^{-1}$

$Q_M \equiv$ flow rate after mixing point

$S_{NH_4\text{-}N} = S_{NH_4\text{-}N,e} = 0.5$ mg $L^{-1}$ due to the 99% degree of ammonium oxidation

$S_{NO_3\text{-}N} = S_{NO_3\text{-}N,e} = 9.5$ mg $L^{-1}$ based on $S_{Nt,e} = 10$ mg $L^{-1}$ N $= S_{NH_4\text{-}N,e} + S_{NO_3\text{-}N,e}$

The following coefficients are valid:

$\mu_{max,NS} = 0.48$ $d^{-1}$

$\mu_{max,D} = 2.6$ $d^{-1}$

$K_{NH_4\text{-}N} = 0.5$ mg $L^{-1}$ N

$K_{NO_3\text{-}N} = 0.14$ mg $L^{-1}$ N

$Y^{o}_{XA/NH_4\text{-}N} = 0.142$ g MLVSS (g $NH_4$-N)$^{-1}$

$Y^{o}_{XH/NO_3\text{-}N} = 1.2$ g MLVSS (g $NO_3$-N)$^{-1}$

1. Calculation of the volume of the aerobic reactor.

The ammonium balance at the mixing point M (see Fig. 10.14) is:

$$Q_0 \cdot S_{NH_4\text{–}N,0} + Q_R \cdot S_{NH_4\text{–}N} + Q_{RN} \cdot S_{NH_4\text{–}N} = Q_M \cdot S_{NH_4\text{–}N,M} \tag{10.74}$$

$S_{NH_4\text{–}N,M} = 8.75$ mg $L^{-1}$ N.

In the anoxic reactor there is no oxidation of ammonium, so we balance ammonium on the aerobic reactor:

$$0 = Q_M \cdot S_{NH_4\text{–}N,M} - Q_M \cdot S_{NH_4\text{–}N} - \frac{\mu_{max,NS} X_{NS}}{Y^{o}_{XA/NH_4\text{–}N}} \cdot \frac{S_{NH_4\text{–}N}}{K_{NH_4\text{–}N} + S_{NH_4\text{–}N}} V_{ae} \tag{10.75}$$

Applying the given coefficients, we obtain the aerobic reactor volume:

$$\begin{aligned} V_{ae} &= (Q_M \cdot S_{NH_4\text{–}N,M} - Q_M \cdot S_{NH_4\text{–}N}) \cdot \frac{Y^{o}_{XA/NH_4\text{–}N}}{\mu_{max} X_{NS}} \cdot \frac{K_{NH_4\text{–}N} + S_{NH_4\text{–}N}}{S_{NH_4\text{–}N}} \\ &= (600 \cdot 0.00875 - 600 \cdot 0.0005) \cdot \frac{0.142}{0.48 \cdot 0.05} \cdot \frac{0.5 + 0.5}{0.5} = 58.6 \text{ m}^3 \end{aligned} \tag{10.76}$$

Equation (10.76) results in the hydraulic retention time $t_R$ of the aerobic reactor related to the influent flow rate $Q_0$:

$$t_R = \frac{V_{ae}}{Q_0} = \frac{58.6}{100} \frac{\text{m}^3}{\text{m}^3\,\text{d}^{-1}} = 0.586 \text{ d} = 14 \text{ h} \tag{10.77}$$

2. Calculation of the volume of the anoxic reactor.

From the nitrate balance at the mixing point M:

$$Q_0 \cdot S_{NO_3\text{–}N,0} + Q_R \cdot S_{NO_3\text{–}N,e} + Q_{RN} \cdot S_{NO_3\text{–}N,e} = Q_M \cdot S_{NO_3\text{–}N,M} \tag{10.78}$$

$S_{NO_3\text{–}N,M} = 7.9$ mg $L^{-1}$ N

We balance nitrate on the anoxic reactor:

$$0 = (Q_M \cdot S_{NO_3\text{–}N,M} - Q_M \cdot S_{NO_3\text{–}N,ax}) - \frac{\mu_{max,D} X_D}{Y^{o}_{XH/NO_3\text{–}N}} \cdot \frac{S_{NO_3\text{–}N,ax}}{K_{NO_3\text{–}N} + S_{NO_3\text{–}N,ax}} V_{ax} \tag{10.79}$$

Applying the given coefficients, we obtain the anoxic reactor volume:

$$V_{ax} = (600 \cdot 0.0079 - 600 \cdot 0.001) \cdot \frac{1.2}{2.6 \cdot 0.2} \cdot \frac{0.14 + 1}{1} = 10.9 \text{ m}^3 \tag{10.80}$$

Equation (10.80) results in hydraulic retention time $t_R$ of the anoxic reactor:

$$t_R = \frac{V_{ax}}{Q_0} = \frac{10.9}{100} \frac{\text{m}^3}{\text{m}^3\,\text{d}^{-1}} = 0.109 \text{ d} = 2.61 \text{ h} \tag{10.81}$$

*Note:* In this system without aerobic C removal, the concentration of denitrifying bacteria is relativ low, resulting in a relative large denitrification hydraulic retention time.

## PROBLEM 10.2

At the WWTP Waßmannsdorf (schematic in Fig. 10.11a), the ammonium loads show a pronounced daily variation. In the morning, the load of ammonium is lower than in the afternoon. For both cases, the ammonium is already completely oxidized to nitrate in the first or second aerobic zone with only a very low amount of nitrite accumulation (Fig. 10.13). Now we consider the aeration efficiency of the aerobic zone. As shown in Fig. 10.15, the dissolved oxygen concentration fluctuates in the aerobic zones.

There is potential to save energy consumed for aeration. What measures could improve this? Discuss the possibilities to improve the efficiency and to save operating costs.

### Solution

There are four possible improvements:

1. Reducing energy costs for aeration. The cost of aeration is the main factor determining the operating costs of a WWTP. At the concentrations occurring in the morning, ammonium is completely oxidized to nitrate after the first aerobic zone, which means that no aeration is necessary after this point. A remarkable energy savings for aeration in the second and third aerobic zones is be expected. This is also true for the afternoon.

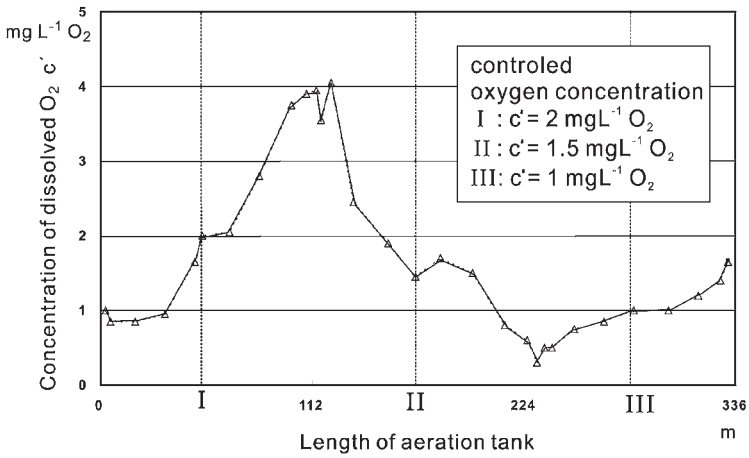


**Fig. 10.15** Oxygen concentration profiles in aerobic zones of BB-M (I), WWTP Waßmannsdorf, 23.2.2000, $14^{50}$–$15^{40}$, $O_2$ concentration is automatically controlled at three points I, II and III (Schuchardt 2005).

2. Online measurement of ammonium and nitrate is needed to control their concentration profiles and to regulate the aeration accordingly.
3. Precise regulation of dissolved oxygen concentration c′ is necessary (Fig. 10.15). The number of c′ control points should be increased through all zones.
4. Higher c′ can not only cause high energy costs but also reduce the specific oxygenation capacity described by the constant $k_L a$ (see Eq. 5.10).

Do you have further ideas to improve the process control and to optimize the process?

## References


Abeling, U.; Seyfried, C.F. **1992**, Anaerobic–aerobic treatment of high-strength ammonium wastewater – nitrogen removal via nitrite. *Water Sci. Technol.* 26, 1007–1015.

AbwV **2004**, *Verordnung über Anforderungen an das Einleiten von Abwasser in Gewässer*, Abwasserverordnung 17 June 2004.

Adam, C. **2004**, *Weitgehende Phosphor- und Stickstoffelimination in einer Membranbelebung mit nachgeschalteter Denitrifikationsstufe, VDI-Forschungsberichte, Reihe 15*, 250, ISBN 3-18-325015-2.

Adam, C.: Gnirß, R.; Lesjean, B.; Buisson, H.; Kraume, M. **2002**, Enhanced biological phosphorus removal in membrane bioreactors. *Water Sci. Technol.* 46, 281–286.

Ante, A.; Voß, H. **1995**, Mikrokinetisches dynamisches Model der Bio-P, *Veröff. Inst. Siedlungswasserwirtsch. Abfalltechn. Univ. Hannover* 92, 15.

Anthonisen, A.C.; Loehr, R.C.; Prakasam, T.B.S.; Srinath, E.G. **1976**, Inhibition of nitrification by ammonia and nitrous acid, *J. Water Pollut. Control Fed.* 48, 835–852.

Antileo, C.; Roeckel, M.; Wiesmann, U. **2003**, High nitrite buildup during nitrification in a rotating disk reactor, *Water Environ. Res.* 75, 151–162.

Bardard, J.L. **1973**, Biological denitrification, *J. Water Pollut. Control Fed.* 72, 705.

Batchelor, B. **1982**, Kinetic analysis of alternative configurations for single-sludge nitrification/denitrification, *J. Water Pollut. Control Fed.* 54, 1493.

Beller, H.R.; Madrid, V.; Hudson, G.B.; McNab, W.W.; Carlsen, T. **2004**, Biogeochemistry and natural attenuation of nitrate in groundwater at an explosives test facility. *Appl. Geochem.* 19, 1483–1494.

Bergeron, P. **1978**, Untersuchungen zur Kinetik der Nitrifikation, Karlsruher Ber. Ing. Biol. 12.

Bernet, N.; Dangcong, P.; Delgenes, J.P.; Moletta, R. **2001**, Nitrification at low oxygen concentration in a biofilm reactor. *J. Environ. Eng.* 127, 266–271.

BWB **2004**, *Purification Results in Ruhleben*, Berliner Wasserbetriebe, available at: http://www.bwb.de/englisch/abwasser/purification_results_ruhleben.html.

Carrera, J.; Baeza, J.A.; Vicent, T.; Lafuente, J. **2003**, Biological nitrogen removal of high-strength ammonium industrial wastewater with two sludge system, *Water Res.* 37, 4211–4221.

CEEP **1998**, Phosphates – a sustainable future in recycling, Centre Européen d'Études des Polyphosphates leaflet, CEFIC.

Choi, I. S. **2005**, *Aerobic degradation of surfactant and nitrification in a membrane bioreactor (MBR) with $CO_2$ and $O_2$ gas analysis, VDI-Forschungsberichte, Reihe 3*, Nr. 838, ISBN 3-18-383803-6.

De Renzo D.J. **1978**, *Nitrogen Control And Phosphorous Removal In Sewage Treatment*, Noyes Data Corp., Park Ridge, N.J., ISBN 0-8155-0711-9.

Dombrowski, T. **1991**, *Kinetik der Nitrifikation und Reaktionstechnik der Stickstoffeliminierung aus hochbelasteten Abwässern, VDI-Forschungsberichte, Reihe 15*, Nr. 87, ISBN 3-18-148715-5.

EU **1991a**, *Urban Waste Water Treatment*, Directive 91/676/EEC.

EU **1991b**, *Urban Waste Water Treatment*, Directive 91/271/EEC.

Foerst, W. **1965**, Sprengstoffe, Dynamit, in: *Ullmanns Encyklopädie der technischen Chemie*, vol 16, Urban & Schwarzenberg, Berlin, p. 92.

Fuhs, G.W.; Chen, M. **1975**, Phosphate removal in the activated sludge process, *Microb. Ecol.* 2, 119.

Fux, C.; Siegrist, H. **2004**, Nitrogen removal from sludge digester liquids by nitrification/denitrification or partial nitritation/anammox: environmental and economical considerations, *Water Sci. Technol.* 50, 19–26.

Fux, C.; Boehler, M.; Huber, P.; Brunner, I.; Siegrist, H. **2002**, Biological treatment of ammonium-rich wastewater by partial nitritation and subsequent anaerobic ammonium oxidation (anammox) in a pilot plant, *J. Biotechnol.* 99, 295–306.

Gao, Y. **1995**, Beitrag zur Stöchiometrie und Kinetik der biologischen Phosphateliminierung, *VDI-Forschungsberichte, Reihe 15*, 144.

Garrido, J.M.; van Benthum, W.A.J.; van Loosdrecht, M.C.M.; Heijnen, J.J. **1997**, Influence of dissolved oxygen concentration on nitrite accumulation in a biofilm airlift suspension reactor, *Biotechnol. Bioeng.* 53, 168–178.

Gerardi G.: Michael H. **2002**, *Wastewater Microbiology: Nitrification And Denitrification In The Activated Sludge Process*, John Wiley and Sons, New York.

Grady, C.P.;Li, JR.; Daigger, G.T.; Lim, H.C. **1999**, *Biological Wastewater Treatment*, Marcel Dekker, New York.

Green, M.; Ruskol, Y.; Shaviv, A.; Tarre, S. **2002**, The effect of $CO_2$ concentration on a nitrifying chalk reactor, *Water Res.* 36, 2147–2151.

Halling-Sørensen, B.; Jørgensen, S.E. **1993**, The removal of nitrogen compounds from wastewater, Elsevier Science, ISBN 0-444-89152-8.

Hascoet, M.C.; Florentz, M. **1985**, Influence of nitrate on biological phosphorus removal from wastewaters, *Water S.A.* 11, 1–8.

Hellinga, C.; Schellen, A.A.J.C.; Mulder, J.W.; van Loosdrecht, M.C.M.; Heijen, J.J. **1998**, The Sharon process: an innovative method for nitrogen removal from ammonium-rich waste water. *Water Sci. Technol.* 37, 135–142.

Helmer, C.; Tromm, C.; Hippen, A.; Rosenwinkel, K-H.; Seyfried, C.F.; Kunst, S. **2001**, Single stage biological nitrogen removal by nitrification and anaerobic ammonium oxidation in biofilm systems. *Water Sci. Technol.* 43, 311–320.

Henze, M.; Gujer, W.; Mino, T.; Matsuo, T.; Wentzel, M.C.; Marais, G. v. R. **1995**, *Activated Sludge Model No. 2*, IAWQ Scientific and Technical Report No. 3, IAWQ, London.

Henze, M.; Harremoës P.; Jansen J.L.C.; Arvin E. **2002**, Wastewater treatment, biological and chemical processes, 3rd edn, Springer-Verlag, ISBN 3-540-42228-5.

Hopwood, A.P.; Downing, A.L. **1965**, Factors affecting the rate of production and properties of activated sludge and plants treating domestic sewage, *J. Proc. Inst. Sewage Purif.* 64, 435–452.

Horn, H.; Hempel, D.C. **1996**, Modellierung von Substratumsatz und Stofftransport in Biofilmsystemen, *GWF Wasser Abwasser* 137, 293–301.

IAWPRC **1986**, *Activated Sludge Model*, Final report of a task group on mathematical modelling for design and operation of biological wastewater treatment. IAWPRC Scientific And Technical Reports No 1.

Jetten, M.S.M.; Strous, M.; van de Pas-Schoonen, K.T.; Schalk, J.; van Dongen, U.G.J.M.; van de Graaf, A.A.; Logemann, S.; Muyzer, G.; van Loosdrecht, M.C.M.; Kuenen, J.G. **1998**, The anaerobic oxidation of ammonium. *FEMS Microbiol. Rev.* 22, 421–437.

Klein, G. **1988**, Seensanierung in Berlin, *Wasser-Kalender*, 1988, 47–74.

Klinger, J. **1999**, Analytische Bestimmung organischer Phosphonsäuren und deren Verhalten im Prozess der Trinkwasseraufbereitung, Veröffentlichung Forschung im TZW 6, *Ergebnisse von Dissertationen zu aktuellen Fragen im Wasserfach* 1999, 9–88.

Knowles, G.; Downing, A.L.; Barret, M.J. **1965**, Determination of kinetic constants for nitrifying bacteria in mixed cultures with the aid of electronic computer. *J. Genet. Microbiol.* 38, 263–278.

Kraume, M.; Bracklow, U.; Vocks, M.; Drews, A. **2005**, Nutrient removal in MBRs for municipal wastewater treatment. *Water Sci. Technol.* 51, 391–402.

Kuai, L.; Verstraete, W. **1998**, Ammonium removal by the oxygen-limited autotrophic nitrification-denitrification system. *Appl. Environ. Microbiol.* 64, 4500–4506.

Larsen-Vefring, W. **1993**, *Simulation der Nitrifikation und anderer bakterieller Stoffwandlungen im Biofilm, VDI-Forschungsberichte, Reihe 15*, 104, ISBN 3-18-140415-2.

Lawrence, A.W.; McCarty, P.L. **1969**, Kinetics of methane fermentation in anaerobic treatment, *J. W.P.C.F.* 41, 2.

Lesjean, B.; Gnirß, R.; Adam, C.; Kraume, M.; Luck, F. **2003**, Enhanced biological phosphorous removal process implemented in membrane bioreactors to improve phosphorous recovery and recycling, *Water Sci. Technol.* 48, 87–94.

Lijmbach, D.; Driver, J.E.; Schipper, W. **2002**, Phosphorous recycling potentials, in: *Water Recycling And Resource Recovery In Industry: Analysis, Technologies And Implimentation*, IWA Publishing, ISBN 1-84339-005-1, p. 511–523.

Lindemann, J. **2002**, *Stickstoffeliminierung in Rotationsscheiben-Biofilmreaktoren, VDI-Forschungsberichte, Reihe 3*, 758, ISBN 3-18-375803-2.

Lompe, D. **1992**, *Kinetik und Reaktionstechnik der biologischen Denitrifikation* (PhD thesis), TU Berlin.

Ludzack, F.J.; Ettinger M.B. **1962**, Controlling operation to minimize activated sludge effluent nitrogen. *J. Water Pollut. Control Fed.* 34, 920–931.

Maurer, M.; Muncke, J.; Larsen T.A. **2002**, Technologies for nitrogen recovery and reuse, in: *Water Recycling And Resource Recovery In Industry: Analysis, Technologies And Implementation*, IWA Publishing, p. 491–510, ISBN 1-84339-0005-1.

McKinney, R.E.; Conway, R.A. **1957**, Chemical oxygen in biological waste treatment, *Sewage Ind. Wastes* 29, 1097–1106.

Mulder, A. **1992**, *Anoxic Ammonium Oxidation*, US patent 427849(507884).

Mulder, A.; van de Graaf, A.A.; Robertson, L.A.; Kuenen, J. G. **1995**, Anaerobic ammonium oxidation discovered in a denitrifying fluidised bed reactor, *FEMS Microb. Ecol.* 16, 177–183.

Nyhius, G. **1985**, Beitrag zu den Möglichkeiten der Abwasserbehandlung bei Abwässern mit erhöhten Stickstoffkonzentrationen. *Veröff. TU Hannover* 1985, 61.

Okabe, S.; Nielsen, P.H.; Characklis, W.G. **1995**, Rate and stoichiometry of microbial sulfate reduction by *Desulfovibrio desulfuricans* in biofilms, *Biofouling* 9, 63–83.

Painter, H.A.; Loveless, J.E. **1983**, Effect of temperature and pH value on the growth rate constants of nitrifying bacteria in the activated sludge process, *Water Res.* 17, 237–248.

Payne, W.J. **1973**, Reduction of nitrogenous oxides by microorganisms, *Bacteriol. Rev.* 37, 409–452.

Pirsing, A. **1996**, *Reaktionstechnische Untersuchungen und mathematische Modellierung der Nitrifikation in hochbelasteten Abwässern, VDI-Forschungsberichte*, ISBN 3-18-315615-6.

Randall, C.W.; Barnard, J.L.; David Stensel, H. **1992**, *Design And Retrofit Of Wastewater Treatment Plants For Biological Nutrient Removal* (Water quality management library, vol 5), Technomic Publishing, ISBN 87762-922-6.

Romanski, J. **1999**, *Biologische Phosphatelimination, Kinetische Untersuchungen zur Erstellung eines reaktionstechnischen Modells, VDI-Forschungsberichte, Reihe 15*, 621, ISBN 3-18-362103-7.

Schuchardt, A. **2005**, *Bestimmung des dynamischen Sauerstoffeintrags in nitrifizierende Belebtschlammreaktoren einer kommunalen Kläranlage, VDI-Forschungsberichte, Reihe 3*, 842.

Schuchardt, A.; Handschag, J.; Sahlmann, C.; Libra, J.; Wiesmann, U. **2002**, *Vergleich der Leistungsfähigkeit von Keramik- und Membranbelüftern des Klärwerks Waßmannsdorf und Optimierung der Prozessführung*, Abschlussbericht, Institut für Verfahrenstechnik, TU-Berlin im Auftrag der Berliner Wasserbetriebe.

Schulze-Rettmer, R. **1993**, Stickstoffeliminierung aus hochbelasteten Abwässern durch chemische Fällung. Stickstoffeliminierung aus höher belasteten Abwässern, *Kolloquium an der TU Berlin*, 1992, p. 49–64.

Sherrad, J.H. **1977**, Kinetics and stochiometry of completely mixed activated sludge. *J. W.P.C.F.* 49, 1968.

Steen, I. **1998**, Phosphorous availability in the 21st century: Management of a non renewable resource, *Phosphorus and Potassium* 1998, 25–31.

STOWA **1996**, Treatment of nitrogen-rich return flows of sewage treatment plants, Single reactor system for removal of ammonium over nitrite (in Dutch), STOWA Report 96-01.

STOWA **2001**, Hrgebruik van fosfaatreststoffen uit rwzi's, STOWA Report 2001/08, ISBN 90.5773.117.7.

Strous, M.; Heijnen, J.J.; Kuenen, J.G.; Jetten, M.S.M. **1998**, The sequencing batch reactor as a powerful tool to study very slowly growing micro-organisms, *Appl. Microbiol. Biotechnol.* 50, 589–596.

Sümer, E.; Benckiser, G.; Ottow, J.C.G. **1996**, Lachgas (N2O)-Freisetzung aus Belebungsbecken von Kläranlagen in Abhängigkeit von den Abwassereigenschaften, in: *Ökologie der Abwasserorganismen*, ed. Flemming, L.G., Springer-Verlag, Berlin.

Suzuki, I.; Kwok, S.C.; Dular, U. **1974**, Ammonia or ammonium ion as substrate for oxidation by nitrosomonas cells and extracts, *J. Bacteriol.* 120, 555.

Tsuno, H.; Somiya, I.; Matsuoto, M. **1987**, A kinetic model for biological phosphorous removal incorporating intracellular organics and phosphorous pools, in: *Proceedings of an IAWPRC Specialised Conference*, Adv. Water Pollut. Control, 99–110

Ueno, Y.; Fujii, M. **2001**, *Three years of operating experience selling recovered struvite from full scale plant*, Paper presented at the 2nd International Conference on Recovery of Phosphates from Sewage and Animal Wastes, Noordwijkerhout.

US EPA **1993**, *Process Design Manual For Nitrogen Control* (EPA/625/R-93/010), U.S. Environmental Protection Agency, Washington, D.C.

Vacker, D.; Connell, C.H.; Wells, W.N. **1967**, Phosphate removal through municipal wastewater treatment at San Antonio, Texas, *J. Water Pollut. Control Fed.* 39, 750–771.

Van de Graaf, A.A.; de Bruijn, P.; Robertson, L.A.; Jetten, M.S.M.; Kuenen, J.G. **1996**, Autotrophic growth of anaerobic ammonium-oxidizing micro-organisms in a fluidized bed reactor, *Microbiology* 142, 2187–2196.

Van Dongen, U.; Jetten, M.S.M.; Van Loosdrecht, M. **2001**, The Sharon–Anammox process for treatment of ammonium rich wastewater, *Water Sci. Technol.* 44, 153–160.

Van Kempen, R.; Mulder, J.W.; Uijterlinde, C.A.; Loosdrecht, M.C.M. **2001**, Overview: full scale experience of the SHARON process for treatment of rejection water of digested sludge dewatering, *Water Sci. Technol.* 44, 145–152.

Wentzel, M.C.; Lötter, R.E.; Loewenthal, R.E.; Marais, G.v.R. **1986**, Metabolic behaviour of *Acinetobacter* ssp. in enhanced biological phosphorous removal – a biochemical model, *Water S.A.* 12, 209–224.

Wentzel, M.C.; Dold, P.L.; Loewenthal, R.E.; Ekama, G.A.; Marais, G.v.R. **1987**, Experiments towards establishing the kinetics of biological excess phosphorous removal, in: *Biological Phosphate Removal From Wastewater*, ed. Ramadori, R., Pergamon Press, Oxford, p. 79–97.

Wentzel, M.C.; Lötter, L.H:; Ekama, G.A.; Loewenthal, R.E.; Marais, G.V.R. **1991**, Evaluation of biochemical models for biological excess phosphorous removal, *Water Sci. Technol* 23, 567–576.

Wheatland, A.B.; Barnett, M.J.; Bruce, A.M. **1959**, Some observations on denitrification in rivers and estuaries, *Inst. Sewage Purif. J. Proc.* 149.

Wiesmann, U. **1994**, Biological nitrogen removal from wastewater. *Adv. Biochem. Eng. Biotechnol.* 51, 113–154.

Wiesmann, U.; Libra, J. **1999**, Special aerobic wastewater and sludge treatment processes, in: *Environmental Processes* (*Biotechnology*, vol 11a), Wiley-VCH, Weinheim, p. 373–415.

# 11
# Modelling of the Activated Sludge Process

## 11.1
## Why We Need Mathematical Models

We address the need for mathematical models in this chapter only in reference to treatment processes in biological wastewater technology. The main compounds which must be removed from water during treatment are:

- Organics, dissolved molecules, colloids and solid particles.
- Inorganic, dissolved compounds containing nitrogen ($NH_4^+$, $NO_2^-$, $NO_3^-$) and phosphorus ($PO_4^{3-}$).

All these compounds are removable in the activated sludge process in different parts of the reactor (see Chapters 6 and 10):

- The organics in the anaerobic, anoxic and aerobic sections.
- $NH_4^+$ and $NO_2^-$ in the aerobic section.
- $NO_3^-$ and $NO_2^-$ in the anoxic section.
- $PO_4^{3-}$ in the anoxic and aerobic sections by the formation of polyphosphates or, if chemical precipitation is used, by the formation of undissolved phosphatohydroxy compounds with iron or aluminium.

Flow rates and concentrations change over time, in the aerobic part air must be dispersed, oxygen dissolved and wastewater and also sludge must be recycled. The entire process has to be controlled continously to ensure adherence with legal regulations and to minimize costs, especially for energy.

A mathematical model describing the process in whole or in part provides some of the following advantages for design and operation:

- To find the best construction for the basins, mixing and aeration system.
- To optimize the process design and the process controls.
- To develop automatic process controls.
- To use a program for training the staff.

In Chapters 5 and 6, some kinetic and reaction engineering fundamentals of modelling are discussed. In this chapter various models of the activated sludge process, their structure and their application are explained.

*Fundamentals of Biological Wastewater Treatment*. Udo Wiesmann, In Su Choi, Eva-Maria Dombrowski

ISBN: 978-3-527-31219-1

## 11.2
## Models Describing Carbon and Nitrogen Removal

### 11.2.1
### Carbon Removal

The first model will be discussed in its simplest form, which is typified by the following assumptions:

- The reactor is completely mixed and operated in steady state.
- Oxygen is used only for carbon removal.
- The bacterial growth rate is high compared to its decay rate.
- The concentrations of $HCO_3^-$ and $CO_3^{2-}$ do not change during $CO_2$ production.
- The oxygen/carbon content of bacteria $y_{XO/XC}$ is known and constant.

The balance of substrates takes the form of:

$$0 = Q_0 (S_0 - S) - r_{SC} V \tag{11.1}$$

Substrate concentration is measured as dissolved organic carbon (DOC). From Eq. (11.1) we obtain:

$$S = S_0 - r_{SC} \frac{V}{Q_0} = S_0 - r_{SC} t_R \tag{11.2}$$

where $r_{SC}$ is the rate of carbon (DOC) removal and $t_R$ is the retention time.

Is it possible to calculate S by measuring $O_2$ and $CO_2$ concentrations in the effluent air?

The following two equations must be valid:

$$r_{SC} = r_{XC} + r_{CO_2-C} \tag{11.3}$$

$$r_{O_2} = 2\, r_{XO} + 2\, r_{CO_2-O} \tag{11.4}$$

where $r_{XC}$ is the rate of carbon consumption for bacterial growth (mol $L^{-1}$ $h^{-1}$ C), $r_{XO}$ is the rate of oxygen consumption for bacterial growth (mol $L^{-1}$ $h^{-1}$ O), $r_{O_2}$ is the respiration rate (mol $L^{-1}$ $h^{-1}$ $O_2$), $r_{CO_2-C}$ is the rate of carbon consumption for the formation of $CO_2$ (mol $L^{-1}$ $h^{-1}$ C) and $r_{CO_2-O}$ is the rate of oxygen consumption for the formation of $CO_2$ (mol $L^{-1}$ $h^{-1}$ O).

Our aim is to calculate $r_{SC}$ from the measured $r_{O_2}$. Therefore, we introduce:

$$r_{CO_2-C} = 2\, r_{CO_2-O} \tag{11.5}$$

inserting Eqs. (11.4) and (11.5) into Eq. (11.3), one obtains:

$$r_{SC} = r_{XC} + r_{O_2} - 2\, r_{XO} \tag{11.6}$$

with the C/O yield of bacteria:

$$y_{XC/XO} = \frac{r_{XC}}{r_{XO}} \tag{11.7}$$

and the true yield coefficient:

$$Y^{o}_{XC/SC} = \frac{r_{XC}}{r_{SC}} \tag{11.8}$$

$r_{XC}$ and $r_{XO}$ can be replaced and $r_{SC}$ eliminated, giving:

$$r_{SC} = \frac{r_{O_2}}{1 - Y^{o}_{XC/SC}(1 - 2\,y_{XO/XC})} \tag{11.9}$$

If we know the values of the coefficients $Y^{o}_{XC/SC}$ (assumed constant) and $y_{XO/XC} = y^{-1}_{XC/XO}$, we are able to calculate $r_{SC}$ from the measured rate $r_{O2}$, assuming that bacterial decay, endogenous respiration and nitrification can be neglected.

### 11.2.2
### Carbon Removal and Bacterial Decay

Starting again from the substrate balance in Eq. (11.1), we now have to consider a carbon removal rate $r_{SC}$ which is different from that in Eq. (11.1) as a result of the reduction of bacterial concentration by decay (bacterial death and mass reduction by endogenous respiration). In addition, the oxygen consumption rate is higher than that of Eq. (11.4) due to endogenous respiration. Instead of Eqs. (11.3) and (11.4), we must now write:

$$r_{SC} = r_{XC,\Sigma} + r_{CO_2\text{–}C,\Sigma} \tag{11.10}$$

$$r_{O_2,\Sigma} = 2\,r_{XO,\Sigma} + 2\,r_{CO_2\text{–}O,\Sigma} \tag{11.11}$$

with:

$$r_{XC,\Sigma} = r_{XC} + r_{XC,d} \tag{11.12}$$

$$r_{O,\Sigma} = r_{O_2} + r_{O_2,e} \tag{11.13}$$

where $r_{XC,d}$ is the decay rate of bacteria by bacterial death and endogenous respiration and $r_{O_2,e}$ is the rate of endogenous respiration.

Defining a real yield coefficient:

$$Y_{XC/SC} = \frac{r_{XC,\Sigma}}{r_{SC}} \tag{11.14}$$

and using:

$$Y_{XC/SC} = Y^{o}_{XC/SC} \cdot \left(1 - \frac{k_d}{\mu}\right) \tag{4.34}$$

from Chapter 4 and assuming the same C/O yield of bacteria, the result is:

$$r_{SC} = \frac{r_{O2,\Sigma}}{1 - Y^{o}_{XC/SC} \cdot \left(1 - \frac{k_d}{\mu}\right)(1 - 2\,y_{XO/XC})} \tag{11.15}$$

For the same measured $r_{O_2,\Sigma} = r_{O_2}$ compared with that of Section 11.2.1, $r_{SC}$ must be lower compared to Eq. (11.9) as a result of bacterial decay $k_d$ (death rate and endogenous respiration). $r_{SC}$ can be quite low, particularly for low substrate concentrations (low specific growth rates μ), in spite of relatively high oxygen uptake rates.

### 11.2.3
### Carbon Removal and Nitrification Without Bacterial Decay

In addition to the balance of substrate (see Eq. 11.1), we now have to consider the balance of ammonia:

$$O = Q_0 (S_{NH_4-N,0} - S_{NH_4-N}) - r_{NH_4-N} V \tag{11.16}$$

The aim of the following reflections is to replace $r_{SC}$ and $r_{NH_4\text{-}N}$ with $r_{O_2,\Sigma}$. We will learn that we also need to measure $r_{CO_2\text{-}C,\Sigma}$ in addition to $r_{O_2,\Sigma}$.

We start with the following equations:

$$r_{SC} = r_{XC} + r_{CO_2-C} \tag{11.3}$$

$$r_{O_2,\Sigma} = 2\, r_{XO} + 2\, r_{CO_2-O,\Sigma} + 2\, r_{NH_4-O_2} \tag{11.17}$$

$$r_{CO_2-C,\Sigma} = r_{CO_2-C} + 2\, r_{CO_2-N} \tag{11.18}$$

$r_{CO_2-N}$ is explained a little later. We will assume that there is complete nitrification without enrichment of $NO_2^-$ (see Chapter 10):

$$NH_4^+ + 2\, O_2 \rightarrow NO_3^- + 2\, H^+ + H_2O \tag{11.19}$$

resulting in:

$$r_{NH_4-N} = 2\, r_{NH_4-O_2} \tag{11.20}$$

The $NH_4^+$ needed for the nitrifiers' anabolism is neglected. The pH is stabilized by the addition of $HCO_3^-$:

$$2\, HCO_3^- + 2\, H^+ \rightarrow 2\, H_2O + 2\, CO_2 \tag{11.21}$$

We can assume that $CO_2$ is completely degassed by aeration. Therefore, we can consider:

$$2\, r_{CO_2-N} = r_{NH_4-N} \tag{11.22}$$

In Eqs. (11.5), (11.18) and (11.20), the following rates are used: $r_{NH_4-O_2}$ is the rate of oxygen consumption for the catabolism of nitrification (mol $L^{-1}$ $h^{-1}$ $O_2$), $r_{CO_2-N}$ is the rate of $CO_2$ formation by neutralization of $H^+$ with $HCO_3^-$ (mol $L^{-1}$ $h^{-1}$ C), $r_{CO_2-O}$ is the rate of oxygen use forming $CO_2$ (mol $L^{-1}$ $h^{-1}$ O) and $r_{CO_2-C}$ is the rate of the carbon use forming $CO_2$ (mol $L^{-1}$ $h^{-1}$ C).

With the help of Eq. (11.7), we obtain $r_{SC}$ from Eq. (11.3) considering:

$$Y^o_{CO_2-C/SC} = \frac{r_{CO_2-C}}{r_{SC}} \tag{11.23}$$

$$r_{SC} = r_{XO}\, y_{XC/XO} + r_{SC}\, Y^{o}_{CO_2-C/SC} \tag{11.24}$$

$$\text{or: } r_{SC} = \frac{r_{XO}\, y_{XC/XO}}{Y^{o}_{XC/SC}} \tag{11.25}$$

$r_{XO}$ follows from Eqs. (11.17) and (11.20):

$$r_{XO} = \frac{1}{2}\,(r_{O_2,\Sigma} - r_{CO_2-C,\Sigma} - r_{NH_4-N}) \tag{11.26}$$

and after introduction into Eq. (11.25), we obtain:

$$r_{SC} = \frac{(r_{O_2,\Sigma} - r_{CO_2-C,\Sigma} - r_{NH_4-N})\, y_{XC/XO}}{2\, Y^{o}_{X-C/SC}} \tag{11.27}$$

$r_{NH_4-N}$ is obtained using Eqs. (11.17) and (11.20):

$$r_{NH_4-N} = r_{O_2,\Sigma} - 2\, r_{XO} - 2\, r_{CO_2-C,\Sigma} = r_{O_2,\Sigma} - 2\,\frac{r_{XC}}{y_{XC/XO}} - r_{CO_2-C,\Sigma} \tag{11.28}$$

and with Eq. (11.3):

$$r_{NH_4-N} = r_{O_2,\Sigma} - 2\,\frac{r_{SC} - r_{CO_2-C}}{y_{XC/XO}} - r_{CO_2-C,\Sigma} \tag{11.29}$$

By applying Eqs. (11.17) and (11.20), Eq. (11.29) can be written as:

$$r_{NH_4-N} = \frac{r_{O_2,\Sigma}\, y_{XC/XO} - 2\, r_{SC}}{2 + y_{XC/XO}} + r_{CO_2-C,\Sigma} \tag{11.30}$$

Equations (11.27) and (11.30) are two equations with two unknown parameters $r_{SC}$ and $r_{NH_4-N}$, which can both be solved.

As such methods have only recently become known, balances and waste gas analysis have seldom been used for the process control of activated sludge plants. However, we are convinced that the importance of such methods will increase during the next decades.

## 11.3 Models for Optimizing the Activated Sludge Process

### 11.3.1 Preface

The models discussed in Section 11.2 can only be used for process control via off-gas measurements. If we want to find the best process and equipment design with the help of models, we further have to introduce a known formula available for the specific growth rate of bacteria:

$$r_X = \mu X = \mu(S, c', T, pH)\, X \tag{11.31}$$

in bacterial balances and to couple it with the substrate removal rate:

$$r_{SC} = \frac{\mu X}{Y^{o}_{XC/SC}} \tag{11.32}$$

and the oxygen consumption rate:

$$r_{O_2} = \frac{\mu X}{Y^{o}_{XC/O_2}} \tag{11.33}$$

The next step is to find the best equation for Eq. (11.31) (see Chapters 6 and 10).

The construction of such models will be demonstrated in the next Sections 11.3.2 and 11.3.3, starting with a relative simple model consisting of only three balances and ending with the activated sludge model (ASM) 1 with 13 balances. Further models will be mentioned briefly in Section 13.3.5.

### 11.3.2
### Modelling the Influence of Aeration on Carbon Removal

The assumptions for this model are:

- CSTR in steady state.
- Only carbon removal.
- Monod kinetics (considering S and c′ as substrates).
- No bacterial decay.
- Bacteria concentration is measured as g $L^{-1}$ COD.

Three balances must be considered, the balance for substrate (as COD; Fig. 6.3):

$$0 = \frac{Q_M (S_M - S)}{V} - \frac{\mu_{max}}{Y^{o}_{X/S}} \frac{S}{K_S + S} \frac{c'}{K' + c'} X \tag{11.34}$$

the balance for heterotrophic bacteria (here as COD; see Fig. 6.3):

$$0 = \frac{Q_M (X_M - X)}{V} + \mu_{max} \frac{S}{K_S + S} \frac{c'}{K' + c'} X \tag{11.35}$$

and the overall balance for oxygen (liquid and gas):

$$0 = \frac{Q_G (c_{O_2,o} - c_{O_2})}{V} - \frac{\mu_{max}}{Y^{o}_{X/O_2}} \frac{S}{K_S + S} \frac{c'}{K' + c'} X \tag{11.36}$$

The three reaction rates on the right-hand part of the balances differ only in the yield coefficients: in the substrate balance $Y^{o}_{X/S}$, in the oxygen balance $Y^{o}_{X/O_2}$ and the factor 1 in the bacterial balance.

This fact can be written using a simple matrix (Henze et al. 1987a), considering (see Table 11.1):

$$\frac{1}{Y^{o}_{X/O_2}} = \frac{Y^{o}_{O_2/S}}{Y^{o}_{X/S}} = \frac{1 - Y^{o}_{X/S}}{Y^{o}_{X/S}} \tag{11.37}$$

**Table 11.1** Simple model matrix for an activated sludge reactor, only carbon removal, see Eqs. (11.34) to (11.36).

| Component | X | S | c′ | Kinetic formation |
|---|---|---|---|---|
| Process | Bacteria | Substrate | Dissolved $O_2$ | Growth rate |
| Aerobic growth of heterotrophs | 1 | $\frac{1}{Y^{o}_{X/S}}$ | $\frac{1-Y^{o}_{X/S}}{Y^{o}_{X/S}}$ | $\mu_{max}\,\frac{S}{K_S+S}\,\frac{c'}{K'+c'}\,X$ |

with:

$$1 = Y^{o}_{O_2/S} + Y^{o}_{X/S}\ ^{1)} \tag{11.38}$$

Equation (11.38) means that the substrate is partly used for catabolism ($Y^{o}_{O_2/S}$) and for anabolism ($Y^{o}_{X/S}$)

We want to discuss some solutions to Eqs. (11.34) to (11.36). We replace the oxygen consumption rate $Q_G\,(c_{O_2,o}-c_{O_2})/V$ by the specific oxygen mass transfer rate using an oxygen balance of the dispersed air:

$$Q_G\,(c_{O_2,o}-c_{O_2})/V = k_L a\,(c^*-c') \tag{11.39}$$

With Eqs. (11.36), (11.37) and (11.39), the balance of oxygen is:

$$0 = k_L a\,(c^*-c') - \frac{1-Y^{o}_{X/S}}{Y^{o}_{X/S}}\,\mu_{max}\,\frac{S}{K_S+S}\cdot\frac{c'}{K'+c'}\,X \tag{11.40}$$

It is possible to define dimensionless numbers which provide several advantages: to minimize the number of parameters and to be free of units. We will use:

- The dimensionless concentration of dissolved $O_2$, $C' = \frac{c'}{K'}$ (11.41)
- The dimensionless concentration of the substrate, $S^* = \frac{S}{K_S}$ (11.42)
- The dimensionless concentration of bacteria, $X^* = \frac{X}{K'}$ (11.43)

Introducing Eqs. (11.41) to (11.43) into Eq. (11.40), we obtain:

$$0 = \frac{k_L a}{\mu_{max}}\left(\frac{c^*}{K'} - C'\right) - \frac{1-Y^{o}_{X/S}}{Y^{o}_{X/S}}\,\frac{S^*}{1+S^*}\cdot\frac{C'}{1+C'}\,X^* \tag{11.44}$$

with:

$$\frac{k_L a}{\mu_{max}} = Sm \triangleq \text{Semenow number} \tag{11.45}$$

and $\frac{c^*}{K'}$ as the dimensionless oxygen saturation concentration.

---

[1)] Note: X is measured as g $L^{-1}$ COD.

For high Sm numbers, there is only a very low concentration gradient of dissolved $O_2$ near the bubble surface and the reaction is controlled by growth kinetics of bacteria; for low Sm numbers, $c'$ is very low ($c^* - c' \approx c^*$) and the reaction is controlled by the mass transfer rate. In a similar manner, the balances of substrate in Eq. (11.34) and bacteria in Eq. (11.35) can be written in dimensionless form (see Section 6.2), with $Da = \mu_{max} t_R$ as the Damköhler number, $n_R = Q_R/Q_0$ as the recirculation of sludge, $n_E = X_D/X_a$ as the thickening ratio and $Mo = S_0/K_S$ as the Monod number (Mehring, 1979).

Figure 11.1 demonstrates some solutions as:

$$S/K_S = f\,(Da, Sm = \text{parameter}) \tag{11.46}$$

for Mo = 10 ($K_S$ = 50 mg $L^{-1}$ COD, $S_0$ = 500 mg $L^{-1}$ COD). The other constant parameters are given in Figure 11.1.

For $Da \leq 0.2$ ($S^* = Mo = 10$), the mean retention time is low and all bacteria are washed out, even though the substrate concentration is high. Due to the low oxygen consumption rate (low $t_R$), no influence of Sm (or $k_La$) can be observed for $0.2 < Da < 0.25$.

For $Da > 2.5$, the oxygen consumption rate is again very low because of the very low substrate concentration. Only in the middle region ($0.25 < Da < 2.5$) can a large influence of Sm (or $k_La$) be observed. For $Sm \geq 100$, carbon removal and bacterial growth are not dependent on aeration intensity.

For Sm = 25 and a substrate removal of 90% ($S^* = 1$ for $S_0^* = Mo = 10$), a Da = 0.5 is needed if an aeration system is to be used effectively (Fig. 11.1). The reaction is limited by dissolved oxygen. Using pure oxygen ($c^*/K' = 475$), the mean retention time $t_R$ can be reduced by about a factor of 2 and oxygen limitation is avoided nearly completely (Fig. 11.2).

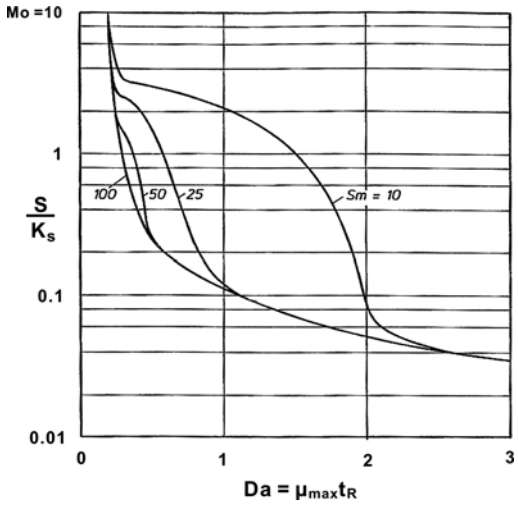


**Fig. 11.1** Influence of dimensionless mean retention time $Da = \mu_{max} t_R$ and dimensionless specific mass transfer rate $Sm = k_L a/\mu_{max}$ on dimensionless effluent substrate concentration $S/K_S$. Constant parameters: $Mo = S_0/K_2 = 10$, $n_R = 0.45$, $n_E = 3$, $c^*/K' = 95$ (aeration).

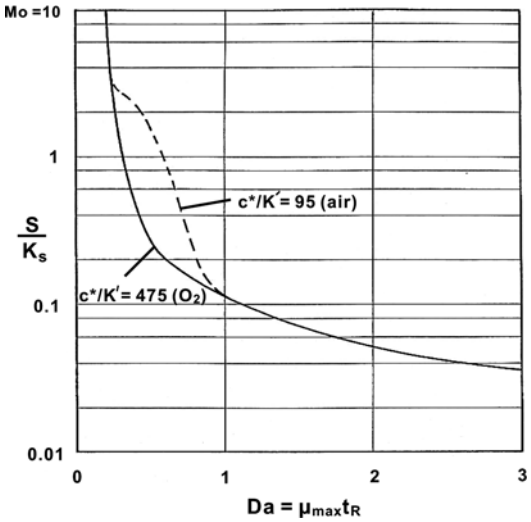


**Fig. 11.2** Influence of dimensionless mean retention time $Da = \mu_{max} t_R$ and dimensionless saturation concentration $c^*/K' = 95$ (air) and 475 (pure oxygen) on dimensionless effluent substrate concentration $S/K_S$. Constant parameters: $Mo = S_0/K_S = 10$, $n_R = 0.45$, $n_E = 3$, $Sm = 25$.

11.3.3
### Activated Sludge Model 1 (ASM 1)

This model describes the relatively complex process of aerobic and anoxic C and N removal from municipal wastewater. It is based on the post-doctoral work of Gujer (1985) and the work of Henze et al. (1987a, b). In order to present the model in its fundamental form, it is shown as a matrix which contains only reaction terms as sources (positive) or sinks (negative). This matrix is normally published without further explanations or is explained only briefly (Grady et al. 1999; Henze et al. 2000). In this section, we try to give an introduction to provide a better understanding.

The model can be fit to:

- Primary models describing different kinds of reactor configurations (anoxic/aerobic; aerobic/anoxic).
- Models describing different kinds of reactors (CSTR in one stage or as a cascade, plug flow or flow with axial dispersion, see Chapter 6).

The very simple matrix in Table 11.1 consists of only three different substances (bacteria, substrate and oxygen) and only one process (aerobic growth of heterotrophs and removal of organic substrates). ASM 1 consists of 13 different substances and eight different processes. At the beginning, we will give an overview of these 13 substances (Table 11.2).

**Table 11.2** The 13 substance concentrations of ASM 1. Units for symbols 1–7: mol $L^{-1}$ COD; units for symbol 8: –mol $L^{-1}$ COD; units for symbols 9–12: mol $L^{-1}$ N; units for symbol 13: mol $L^{-1}$.

| No. | Symbol | Substance |
|---|---|---|
| 1 | $S_I$ | Soluble inert organic matter |
| 2 | $S_S$ | Readily biodegradable substrate |
| 3 | $X_I$ | Particulate inert organic matter |
| 4 | $X_S$ | Slowly biodegradable substrate |
| 5 | $X_H$ | Active heterotrophic biomass |
| 6 | $X_A$ | Active autotrophic biomass |
| 7 | $X_P$ | Particulate products from biomass decay |
| 8 | c′ | Dissolved oxygen |
| 9 | $S_{NO}$ | Nitrate and nitrite nitrogen |
| 10 | $S_{NH_4}$ | Ammonium and amonia nitrogen |
| 11 | $S_{NS}$ | Soluble degradable organic nitrogen |
| 12 | $X_{ND}$ | Particulate degradable organic nitrogen |
| 13 | $S_{Alk}$ | Alkalinity |

It should be emphasized that, besides the readily biodegradable substances $S_S$, slowly biodegradable substances $X_S$ are considered as solid particles, which must first be hydrolyzed by exoenzymes. $X_I$ is the corresponding inert organic matter which cannot be disregarded, as we will see below. Particulate products $X_P$ result from the lysis of bacteria or remain as insoluble solids.

The eight processes are summarized in Table 11.3.

The matrix of the ASM 1 model consists, therefore, of a 13×8 matrix for the 13 substances in the columns and eight processes in the rows.

For a CSTR in non-steady condition, 13 balances must be taken into account, each of which is written in the same way as Eq. (11.47):

$$\frac{dS}{dt} = \frac{Q_M}{V}\,(S_M - S) + r_S \tag{11.47}$$

eight for different dissolved components (7 S + c′) and five for different undissolved components X. Only the reaction terms $r_{Si}$ are arranged in the matrix.

The reaction terms should be discussed in some detail before the matrix is constructed (see Table 11.4).

We will begin with the reaction terms for soluble inert organic matter.

**Table 11.3** The eight processes of ASM 1.

| No. | Process |
|---|---|
| 1 | Aerobic growth of heterotrophs |
| 2 | Anoxic growth of heterotrophs |
| 3 | Aerobic growth of autotrophs |
| 4 | Decay of heterotrophs |
| 5 | Decay of autotrophs |
| 6 | Ammonification of soluble organic nitrogen |
| 7 | Hydrolysis of particulate organics |
| 8 | Hydrolysis of particulate organic nitrogen |

**Table 11.4** Process kinetics and stoichiometric parameters of the activated sludge model ASM 1 plotted in a matrix form (13 parameters, 8 processes; Henze et al. 2000)

| | ***Component (i)*** → | ***1*** | ***2*** | ***3*** | ***4*** | ***5*** | ***6*** | ***7*** | ***8*** | ***9*** | ***10*** | ***11*** | ***12*** | ***13*** | |
|---|---|---|---|---|---|---|---|---|---|---|---|---|---|---|---|
| j ↓ | Process (j) | $S_i$ | $S_S$ | $X_i$ | $X_S$ | $X_H$ | $X_A$ | $X_P$ | c' | $S_{NO_3}$ | $S_{NH_4}$ | $S_{ND}$ | $X_{ND}$ | $S_{Alk}$ | Process rate $r_j\ [ML^{-3}T^{-1}]$ |
| 1 | Aerobic growth of heterotrophs | | $\frac{1}{Y^o_{XH/SS}}$ | | | 1 | | | $\frac{1-Y^o_{XH/SS}}{Y^o_{XH/SS}}$ | | $i_{XB}$ | | | $\frac{i_{XB}}{14}$ | $\mu_{max,H}\frac{S_S}{K_S+S_S}\frac{c'}{K'_H+c'}X_H$ |
| 2 | Anoxic growth of heterotrophs | | $\frac{1}{Y^o_{XH/SS}}$ | | | 1 | | | | $\frac{1-Y^o_{XH/SS}}{2.86\ Y^o_{XH/SS}}$ | $i_{XB}$ | | | $\frac{1-Y^o_{XH/SS}}{14\cdot 2.86\ Y^o_{XH/SS}}$ $\frac{i_{XB}}{14}$ | $\mu_{max,H}\,\eta\frac{S_S}{K_S+S_S}\frac{K_{i0}}{K_{i0}+c'}$ $\frac{S_{NO_3}}{K_{NO}+S_{NO}}X_H$ |
| 3 | Aerobic growth of autotrophs | | | | | | 1 | | $\frac{4.57-Y^o_{XA/NH_4}}{Y^o_{XA/NH_4}}$ | $Y^o_{NO_3/XA}$ | $i_{XB}-\frac{1}{Y^o_{XA/NH_4}}$ | | | $\frac{i_{XB}}{14}-\frac{1}{7\ Y^o_{XA/NH_4}}$ | $\mu_{max,A}\frac{S_{NH_4}}{K_{SA}+S_{NH_4}}\cdot$ $\frac{c'}{K'_A+c'}X_A$ |
| 4 | Decay of heterotrophs | | | | $1-f_i$ | −1 | | $f_P$ | | | | | $i_{XB}-f_P i_{XP}$ | | $k_{dH}X_H$ |
| 5 | Decay of autotrophs | | | | $1-f_i$ | | −1 | $f_P$ | | | | | $i_{XB}-f_P i_{XP}$ | | $k_{dA}X_A$ |
| 6 | Ammonification of soluble organic nitrogen | | | | | | | | | | 1 | 1 | | $\frac{1}{14}$ | $k_a S_{ND} X_H$ |
| 7 | Hydrolysis of particulate organics | | | | 1 | | | | | | | | | | $k_H\frac{X_S/X_H}{K_X+(X_S/X_H)}\left(\frac{c'}{K'_H+c'}\right.$ $\left.+\eta_n\frac{K_{i0}}{K_{i0}+c'}\frac{S_{NO_3}}{K_{NO}+S_{NO_3}}\right)X_H$ |
| 8 | Hydrolysis of particulate organic nitrogen | | | | | | | | | | | 1 | 1 | | $k_{en}(X_{ND}/X_S)$ |

### *i* = 1, $S_i$ – Soluble Inert Organic Matter

$$r_{Si} = 0$$

This assumption is a simplification made by ASM 1. In reality, such dissolved inert substances (non-biodegradable) can be formed by the hydrolysis or lysis of solid particles or other dissolved substances or they can be adsorbed on solid surfaces.

### *i* = 2, $S_S$ – Readily Biodegradable Substrate

$$r_{SS} = -\frac{1}{Y^{o}_{XH/SS}}\ \mu_{max,H}\ \frac{S_S}{K_S + S_S}\left(\frac{c'}{K'_H + c'} + \eta\ \frac{K_{i0}}{K_{i0} + c'}\ \frac{S_{NO_3}}{K_{NO} + S_{NO_3}}\right) X_H \tag{11.48}$$

$r_{SS}$ is the rate of COD removal by aerobic and anoxic bacteria.

The measured COD is:

$$S_{S\Sigma} = S_i + S_S \tag{11.49}$$

and $S_S$ can only be determined if $S_i$ is known. $\eta$ is the ratio of $\mu_{max,H}$ values for anoxic and aerobic bacteria (Henze 1986).

### *i* = 3, $X_i$ – Particulate Inert Organic Matter

$$r_{Xi} = 0$$

Nearly the same remarks are valid as those above (see *i* = 1, $S_i$). Nevertheless, $X_i$ is needed for the definition of $f_i$ (see Eq. 11.52) and for the formation of the balance describing non-steady state transport:

$$\frac{dX_i}{dt} = \frac{Q_M}{V}\ (X_{iM} - X_i) \tag{11.50}$$

### *i* = 4, $X_S$ – Slowly Biodegradable Substrate

$$r_{XS} = \underbrace{(1-f_i)\ k_{dH} X_H}_{\text{formation from decay of heterotrophs}} + \underbrace{(1-f_i)\ k_{dA} X_A}_{\text{formation from decay of autotrophs}} \underbrace{- k_H\ \frac{X_S/X_H}{K_X + X_S/X_H}\left(\frac{c'}{K'_H + c'} + \eta\ \frac{K_{i0}}{K_{i0} + c'}\ \cdot\ \frac{S_{NO_3}}{K_{NO} + S_{NO_3}}\right) X_H}_{\text{hydrolysis of entrapped organics by aerobic and anoxic bacteria}} \tag{11.51}$$

$$f_i = \frac{X_i}{X_H + X_A + X_i + X_S} \tag{11.52}$$

$$1 - f_i = \frac{X_H + X_A + X_S}{X_H + X_A + X_i + X_S} \tag{11.53}$$

$$\eta = \frac{r_{H,Ax}}{r_{H,Ae}}\ \frac{\text{hydrolysis by anoxic bacteria}}{\text{hydrolysis by aerobic bacteria}} \tag{11.54}$$

**$i = 5$, $X_H$ – Active Heterotrophic Biomass**

$$r_{XH} = \underbrace{\mu_{max,H}\,\frac{S_S}{K_S + S_S}\left(\frac{c'}{K'_H + c'} + \eta\,\frac{K_{i0}}{K_{i0} + c'}\,\frac{S_{NO_3}}{K_{NO} + S_{NO_3}}\right) X_H}_{\text{growth of aerobic and anoxic bacteria}}$$

$$\underbrace{-\,k_{dH}\,X_H}_{\text{decay of heterotrophs}} \tag{11.55}$$

**$i = 6$, $X_A$ – Active Autotrophic Biomass**

$$r_{XA} = \underbrace{\mu_{max,A}\,\frac{S_{NH_4}}{K_{SA} + S_{NH_4}}\,\frac{c'}{K'_A + c'}\,X_A}_{\text{growth of autotrophs}} - \underbrace{k_{dA}\,X_A}_{\text{decay of autotrophs}} \tag{11.56}$$

**$i = 7$, $X_P$ – Particulate Products from Biomass Decay**

$$r_{XP} = \underbrace{f_P\,k_{dH}\,X_H + f_P\,k_{dA}\,X_A}_{\text{production rate by decay}} \tag{11.57}$$

$$f_P = \frac{X_P}{X_H + X_A} \tag{11.58}$$

**$i = 8$, $c'$ – Dissolved Oxygen**

$$\begin{aligned} r_{O_2} = &- Y^{o}_{O_2/XH}\,\mu_{max,H}\,\frac{S_S}{K_S + S_S}\,\frac{c'}{K'_H + c'}\,X_H \\ &- Y^{o}_{O_2/XA}\,\mu_{max,A}\,\frac{S_{NH_4}}{K_{SA} + S_{NH_4}}\,\frac{c'}{K'_A + c'}\,X_A \end{aligned} \tag{11.59}$$

reflects oxygen consumption (or COD removal) by aerobic heterotrophs and autotrophs. Therefore, the units of $r_{O_2}$ are g $m^{-3}$ $h^{-1}$ COD.

$Y^{o}_{O_2/XH}$ follows from:

$$\underbrace{Y^{o}_{XH/SS}}_{\text{anabolism}} + \underbrace{Y^{o}_{O_2/SS}}_{\text{catabolism}} = 1^{1)} \tag{11.60}$$

$$\text{and: } Y^{o}_{O_2/XH} = \frac{Y^{o}_{O_2/SS}}{Y^{o}_{XH/SS}} = \frac{1 - Y^{o}_{XH/SS}}{Y^{o}_{XH/SS}} \tag{11.61}$$

[1)] See remarks on Eq. (11.38).

For autotrophic nitrifiers one can write:

$$Y^{o}_{O_2/XA} = \frac{Y^{o}_{O_2/NH_4}}{Y^{o}_{XA/NH_4}} \tag{11.62}$$

and:

$$\underbrace{Y^{o}_{O_2/NH_4}}_{\text{catabolism}} = Y^{o}_{O_2/NH_4-N,\Sigma} - \underbrace{Y^{o}_{XA/NH_4}}_{\text{anabolism}} \tag{11.63}$$

as well as:

$$Y^{o}_{O_2/NH_4-N,\Sigma} = \frac{r_{O_2}}{r_{NH_4-N,\Sigma}} = \frac{64}{14} = 4.57\ \frac{g\ O_2}{g\ NH_4-N} \tag{11.64}^{2)}$$

$$\text{and: } Y^{o}_{O_2/XA} = \frac{4.57 - Y^{o}_{XA/NH_4}}{Y^{o}_{XA/NH_4}} \tag{11.65}$$

Finally, Eqs. (11.61) and (11.65) are introduced into the matrix of Table 11.4 (space i = 8 for j = 1, j = 3).

***i* = 9, $S_{NO_3}$ – Nitrate Nitrogen**

As already assumed for nitrifier growth (i = 6), where nearly no $NO_2$ is produced, denitrification goes directly to nitrogen and the denitrification of $NO_2$ is not considered (Chapter 10).

$$r_{NO_3} = \underbrace{-\,Y^{o}_{NO_3/XH}\,\mu_{max,H}\,\eta\,\frac{S_S}{K_S+S_S}\,\frac{K_{i0}}{K_{i0}+c'}\,\frac{S_{NO_3}}{K_{NO}+S_{NO_3}}\,X_H}_{\text{reduction of } NO_3 \text{ by denitrification}}$$

$$\underbrace{+\,Y^{o}_{NO_3/XA}\,\mu_{max,A}\,\frac{S_{NH_4}}{K_{SA}+S_{NH_4}}\,\frac{c'}{K'_A+c'}\,X_A}_{\text{formation of } NO_3 \text{ by nitrification}} \tag{11.66}$$

Writing:

$$Y^{o}_{NO_3/XH} = \frac{Y^{o}_{O_2/XH}}{\Delta Y^{o}_{O_2/NO_3}} \tag{11.67}$$

$\Delta Y^{o}_{O_2/NO_3}$ is the oxygen savings by denitrification after nitrification and can be calculated using:

$$\Delta Y^{o}_{O_2/NO_3} = Y^{o}_{O_2/NH_4} - Y^{o}_{O_2/NO_3} \tag{11.68}$$

$Y^{o}_{O_2/NH_4-N,\Sigma} = 4.57\ g\ O_2\ (g\ NH_4-N)^{-1}$ follows from Eq. (11.64).

---

2) Note: $NH_4^+ + 2\,O_2 = NO_3^- + H_2O + 2\,H^+$ and
$Y^{o}_{O_2/NH4} = Y^{o}_{O_2/XA} \cdot Y^{o}_{XA/NH_4}$

For the calculation of $Y^{\circ}_{O_2/NO_3}$ we have to use the catabolic production of $NO_3^-$ by nitrification:

$$6\,NH_4^+ + 12\,O_2 \rightarrow 6\,NO_3^- + 6\,H_2O + 12\,H^+ \tag{11.69a}$$

and the consumption of $NO_3^-$ by denitrification using methanol as an energy source:

$$6\,NO_3^- + 5\,CH_3OH \rightarrow 3\,N_2 + 5\,CO_2 + 7\,H_2O + 6\,OH^- \tag{11.69b}$$

in comparision with the aerobic oxydation of methanol:

$$7.5\,O_2 + 5\,CH_3OH \rightarrow 5\,CO_2 + 10\,H_2O \tag{11.70}$$

For nitrification of 6 $NH_4^+$ (using 5 $CH_3OH$ for denitrification), 24 moles O are needed; for aerobic oxydation of the same amount of 5 $CH_3OH$, 15 moles O must be used. Therefore, the difference of both follows to:

$$Y^{\circ}_{O_2/NO_3} = \frac{24-15}{6} = 1.5\,\frac{g\,O}{g\,NO_3^-} = 1.5\,\frac{16}{14}\,\frac{mol\,O}{mol\,N} = 1.71\,\frac{mol\,O}{mol\,N}$$

Considering Eq. (11.68), one obtains:

$$\Delta Y^{\circ}_{O_2/NO_3} = Y^{\circ}_{O_2/NH_4} - Y^{\circ}_{O_2/NO_3} = 4.57 - 1.71 = 2.86\ g\ O_2\ (g\ NO_3 - N)^{-1}$$

From Eqs. (11.67) and (11.61), it follows (i=9, j=2):

$$Y^{\circ}_{NO_3/XH} = \frac{1-Y^{\circ}_{XH/SS}}{2.86\,Y^{\circ}_{XH/SS}} \tag{11.71}$$

***i = 10*, $S_{NH_4}$ – Ammonium Nitrogen**

$$r_{NH_4} = \underbrace{-\,i_{XB}\,\mu_{max,H}\,\frac{S_S}{K_S+S_S}\,\frac{c'}{K'_H+c'}\,X_H}_{NH_4\text{ uptake by aerobic heterotrophs}}$$

$$\underbrace{-\,i_{XB}\cdot\eta\,\mu_{max,H}\,\frac{S_S}{K_S+S_S}\,\frac{K_{i0}}{K_{i0}+c'}\,\frac{S_{NO_3}}{K_{NO}+S_{NH_3}}\,X_H}_{NH_4\text{ uptake by anoxic heterotrophs}}$$

$$\underbrace{-\left(i_{XB}+\frac{1}{Y^{\circ}_{XA/NH_4}}\right)\mu_{max,A}\,\frac{S_{NH4}}{K_{SA}+S_{NH_4}}\,\frac{c'}{K'_A+c'}\,X_A}_{NH_4\text{ uptake and }NH_4\text{ oxidation by autotrophs}} \tag{11.72}$$

$$\underbrace{+\,k_a\,S_{ND}\,X_H}_{\substack{NH_4\text{ formation by anoxic}\\ \text{hydrolysis of heterotrophs}}}$$

### *i* = 11, $S_{ND}$ – Soluble Degradable Organic Nitrogen

$$r_{ND} = \underbrace{-k_a S_{ND} X_H}_{\substack{NH_4 + NH_3 \\ \text{uptake by} \\ \text{heterotrophs}}} + \underbrace{k_{en} X_{ND}/X_S}_{\substack{\text{formation of} \\ \text{organic nitrogen} \\ \text{by hydrolysis}}} \tag{11.73}$$

### *i* = 12, $X_{ND}$ – Particulate Degradable Organic Nitrogen

$$r_{ND} = \underbrace{(i_{XB} - f_P i_{XP})\, k_{dH} X_H}_{\substack{\text{formation from} \\ \text{decay of heterotrophs}}} + \underbrace{(i_{XB} - f_P i_{XP})\, k_{dA} X_A}_{\substack{\text{formation from} \\ \text{decay of autotrophs}}} - \underbrace{k_{en} X_{ND}/X_S}_{\text{hydrolysis}} \tag{11.74}$$

$$i_{XB} = \frac{X_N}{X_H + X_A + X_S} = \frac{\text{nitrogen in bacteria}}{\text{mass of bacteria + slowly biodegradable substrate}} \tag{11.75}$$

$$i_{XP} = \frac{X_N}{X_i} = \frac{\text{nitrogen in bacteria}}{\text{particulate inert organic matter in bacteria}} \tag{11.76}$$

$$i_{XB} - f_P i_{XP} = \frac{\text{biodegradable organic nitrogen}}{\text{particulate organic matter}} \tag{11.77}$$

$f_P$ see Eq. (11.58).

### *i* = 13, $S_{Alk}$ – Alkalinity

$$S_{Alk} = S_{HCO_3^-} + S_{CO_3^{2-}} + S_{NO_3^-} + S_{OH^-} \tag{11.78}$$

$S_{Alk}$ is the concentration of anions (alkalinity). The balance:

$$\frac{dS_{Alk}}{dt} = \frac{Q_M}{V}\,(S_{Alk,0} - S_{Alk}) \pm r_{Alk} \tag{11.79}$$

describes the change of pH. For $S_{Alk} \gg S_{Alk,0}$ the pH increases and vice versa. The pH influences some equilibria ($NH_4^+/NH_3$, $NO_3^-/HNO_3$) and the activity of bacteria. In wastewater with a low $S_{Alk,0}$ and nitrification, $r_{Alk}$ cannot be neglected. The balance of anions is written in moles.

$$r_{Alk} = \underbrace{-\frac{i_{XB}}{14}\,\mu_{max,H}\,\frac{S_S}{K_S + S_S}\,\frac{c'}{K'_H + c'}\,X_H}_{\substack{\text{use of } NO_3^- \text{ for growth of aerobic heterotrophs}}}$$

$$\underbrace{-\left(\frac{i_{XB}}{14} - \frac{1 - Y^{\circ}_{XH/SS}}{14 \cdot 2.86\, Y^{\circ}_{XH/SS}}\right)\mu_{max,H} \cdot \eta\,\frac{S_S}{K_S + S_S}\,\frac{K_{i0}}{K_{i0} + c'}\,\frac{S_{NO_3}}{K_{NO} + S_{NO_3}}\,X_H}_{\substack{\text{use of } NO_3^- \text{ for growth of heterotrophs and production} \\ \text{of } HCO_3^- \text{ by denitrification}}}$$

$$\underbrace{-\left(\frac{i_{XB}}{14}+\frac{1}{7\,Y^{o}_{XA/NH_4}}\right)\mu_{max,A}\,\frac{S_{NH_4}}{K_{SA}+S_{NH_4}}\,\frac{c'}{K'_A+c'}\,x_A}_{\text{use of } NO_3^- \text{ for growth of autotrophs and use of } HCO_3^- \text{ for } H^+ \text{ uptake during nitrification}}+\underbrace{\frac{1}{14}\,k_{en}\,\frac{X_{ND}}{X_S}}_{\text{production of } NO_3^- \text{ by hydrolysis of particular orgaic nitrogen}} \tag{11.80}$$

The production of $HCO_3^-$ during denitrification is described by the stoichiometry for catabolism and anabolism using $CH_3OH$ as an energy source (see Eqs. 10.43 and 10.44).

As follows from the catabolism of nitrification without $NO_2^-$ enrichment:

$$NH_4^+ + 2\,O_2 \rightarrow NO_3^- + H_2O + 2\,H^+ \tag{10.6}$$

and with the use of $HCO_3^-$ as an electron acceptor:

$$2\,H^+ + 2\,HCO_3^- \rightarrow 2\,H_2CO_3 \tag{11.81}$$

$12\,HCO_3^-$ are needed for $6\,NH_4^+$, these are 6 more moles anions than those recovered by denitrification (see Eq. (11.69) and consider $OH^- + CO_2 = HCO_3^-$).

Because: $Y^{o}_{HCO_3^-/NH_4^+} = 2$, we write for the rate of $HCO_3^-$ consumption by nitrification (Table 11.4, space i = 13, j = 3 in the matrix):

$$\frac{Y^{o}_{HCO_3^-/NH_4^+}}{14\,Y^{o}_{XA/SS}}\,r_{NH_4}=\frac{1}{7\,Y^{o}_{XA/SS}}\,r_{NH_4} \tag{11.82}$$

The ASM 1 model makes it possible to simulate different loadings of municipal activated sludge plants in steady and non-steady state without biological phosphorous removal. It can be used as the basis for a training program for the staff of wastewater treatment plants and for design calculation of the plant and optimization of the processes.

After intensive study of the model, the reader of the matrix (see Table 11.4) will see the advantage in using the matrix in combination with a computer program.

### 11.3.4 Application of ASM 1

Grady et al. (1999) published some examples for applications of the ASM 1. It is necessary to first determine values for all 19 coefficients compiled in Table 11.5.

Some of them have been chosen from mean values from many kinetic measurements; some of them are still unreliable. The processes 6 (ammonification of soluble organic nitrogen) and 8 (hydrolysis of entrapped organic nitrogen) are neglected.

In addition to the parameters in Table 11.5, some characteristics of a domestic wastewater following primary sedimentation were considered (Table 11.6).

A large number of questions can be answered using this model. One interesting question is: what is the oxygen requirement $Q_G\,\Delta c_{O_2}$ in dependence on sludge retention time $t_{RX}$? The model was calculated for a steady-state condition and $X_A + X_H$; and then $X_H$ and $Q_G\,\Delta c_{O_2}$ were both plotted versus sludge age (Fig. 11.3).

**Table 11.5** Typical parameter values at neutral pH and 20 °C for domestic wastewater (Grady et al. 1999, p. 199).

| Symbol | Units | Value |
|---|---|---|
| **Stoichiometric coefficients** | | |
| $Y^{o}_{XH/SS}$ | mg biomass COD formed per mg COD removed | 0.60 |
| $f_P$ | mg debris COD (mg biomass COD)$^{-1}$ | 0.08 |
| $i_{XB}$ | mg N (mg COD)$^{-1}$ in active biomass | 0.086 |
| $i_{XP}$ | mg N(mg COD)$^{-1}$ in biomass debris | 0.06 |
| $Y^{o}_{XA/NH_4}$ | mg biomass COD formed per mg N oxidized | 0.24 |
| **Kinetic parameters** | | |
| $\mu_{max,H}$ | $h^{-1}$ | 0.25 |
| $K_S$ | mg $L^{-1}$ COD | 20 |
| $K'_H$ | mg $L^{-1}$ $O_2$ | 0.10 |
| $K_{NO}$ | mg $L^{-1}$ N | 0.20 |
| $k_{dH}$ | $h^{-1}$ | 0.017 |
| $\eta$ | Dimensionless | 0.8 |
| $\eta_h$ | Dimensionless | 0.4 |
| $k_a$ | L (mg biomass COD h)$^{-1}$ | 0.0067 |
| $k_H$ | mg COD (mg biomass COD h)$^{-1}$ | 0.092 |
| $K_X$ | mg COD (mg biomass COD)$^{-1}$ | 0.15 |
| $\mu_{max,A}$ | $h^{-1}$ | 0.032 |
| $K_{NO}$ | mg $L^{-1}$ N | 1.0 |
| $K'_A$ | mg $L^{-1}$ $O_2$ | 0.75 |
| $k_{dA}$ | $h^{-1}$ | 0.004 |

**Table 11.6** Characteristics of a domestic wastewater of the USA after primary sedimentation (Grady et al. 1999, p. 214; Bidstrup and Grady 1988).

| Symbol | Component | Concentration (mg $L^{-1}$) |
|---|---|---|
| $X_i$ | Inert particulate organic matter (COD) | 35.0 |
| $X_S$ | Slowly biodegradable substrate (COD) | 150.0 |
| $S_S$ | Readily biodegradable substrate (COD) | 115.0 |
| c′ | Oxygen ($O_2$) | 0.0 |
| $S_{NO}$ | Soluble nitrate N | 0.0 |
| $S_{NH}$ | Soluble ammonia N | 25.0 |
| $S_{NS}$ | Soluble biodegradable organic N | 6.5 |
| $X_{ND}$ | Particulate biodegradable organic N | 8.5 |

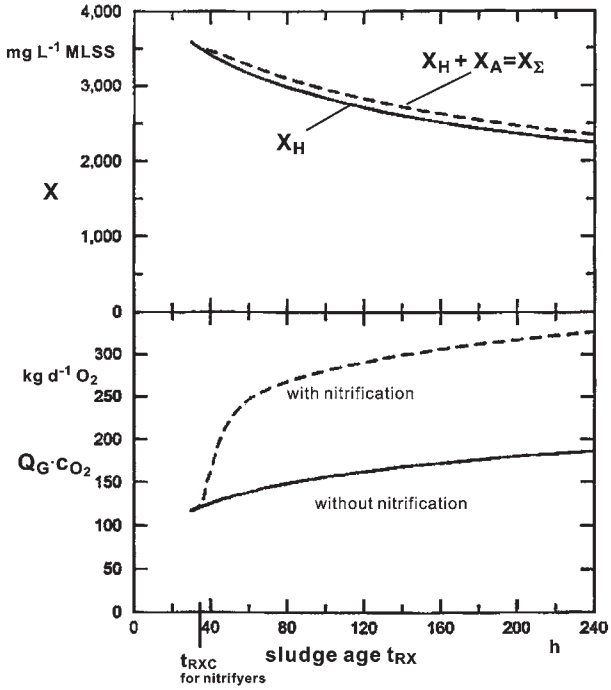


**Fig. 11.3** Effect of sludge age $t_{RX}$ on bacterial concentration $X_H$ and $X_H + X_A$ as well as oxygen demand in a CSTR with $t_{RX}/t_R = 20$. Parameter values given in Tables 11.5 and 11.6. $c' = 4.0$ mg $L^{-1}$ (Grady et al. 1999, p. 214).

The sludge age can be calculated using:

$$t_{RX} = \frac{V\,(X_A + X_H)}{Q_{ex} X_R} \tag{11.83}$$

where $Q_{ex}$ is the excess sludge flow rate ($m^3\ d^{-1}$) and $X_R$ is the concentration of excess sludge (kg $m^{-3}$).

For a sludge age of $t_{RX} \leq 35$ h, the nitrifiers are washed out. Their growth rate is too low compared with their dilution time in the system consisting of reactor and secondary clarifier. For $t_{RX} \geq 148$ h = 7 d, the oxygen demand increases mainly as a result of endogenous respiration; nitrogen and carbon are removed to a greater extent.

### 11.3.5
### More Complicated Models and Conclusions

ASM 1 does not describe biological or chemical phosphorus removal. It was necessary to expand it to 19 balances for 19 components and 12 processes. The reaction terms consist of up to 7 Monod parts. The expanded model, called ASM 2 (Henze

et al. 2000), will not be described here. ASM 2 models biological phosphorous accumulation by organisms of two fractions, one of which is able to nitrify.

ASM 3 was developed to correct some ASM 1 problems:

- Limitations of nitrogen and alkalinity on growth rate of heterotrophic organisms.
- Inclusion of soluble and particulate organic nitrogen.
- The elimination of a differentiation between inert organic material, inert particles, influent or biomass decay compared to ASM 1.

All together, ten points were mentioned (Henze et al. 2000), showing that the ASM 1 model is too simple to accurately describe the activated sludge process. Therefore, a completely new model was generated, ASM 3, which will not be described or discussed here.

There is no single model which describes all the qualities and properties of a plant-scale activated sludge process. The power of modern computer systems tempts us to construct more and more complex models. But we should not forget that an activated sludge plant in non-steady operation is not only influenced by the complicated reaction terms of the ASM models. The fluid dynamics and the mass transfer in activated sludge plants influence the substrate removal and nitrification just as much if not more than do the micro-kinetics. We model completely mixed tanks and nothing else. Frequently, it is not easy to describe the measurements of retention time distributions mathematically. But there are only a few plants that have been studied with such measurements. For most basins, we do not have these results and we are not able to conclude whether we need a cascade model with six stages or only two. We should never forget such considerations when applying simple models or one of the ASM models!

**PROBLEM 11.1**

In a completely mixed activated sludge reactor with an influent concentration of $S_0 = 200$ g m$^{-3}$ DOC, a 95% DOC reduction should be realized within $t_R = 6$ h. Calculate the necessary oxygen uptake rate $r_{O_2}$.

Given:

$$y_{XO/XC} = \frac{20}{50}\,\frac{\text{g O}}{\text{g C}} = \frac{20}{50}\,\frac{12}{16}\,\frac{\text{mol O}}{\text{mol C}} = 0.3\,\frac{\text{mol O}}{\text{mol C}}$$

and:

$$Y^{o}_{XC/SC} = 0.5\,\frac{\text{mol X}-\text{C}}{\text{mol S}-\text{C}}$$

**Solution**

The carbon removal rate $r_{SC}$ follows from the C balance in Eq. (11.2):

$$r_{SC} = \frac{S_0 - S}{t_R} = \frac{190}{6} = 31.67 \text{ g m}^{-3}\text{ h}^{-1} \text{ DOC}$$

Using Eq. (11.9), we obtain the oxygen uptake rate:

$$r_{O_2} = r_{SC}\left(1 - Y^{\circ}_{XC/SC}\left(1 - 2\, y_{XO/XC}\right)\right)$$

$$= 31.67\left(1 - 0.5\,\frac{\text{mol C}}{\text{mol C}}\left(1 - 2 \cdot 0.3\,\frac{\text{mol O}}{\text{mol C}}\right)\right)$$

$$= 31.67 \cdot 0.8\ \text{g m}^{-3}\ \text{h}^{-1}\ \text{DOC}\ \frac{\text{mol O}}{\text{mol C}}$$

$$= 25.34 \cdot 0.5\ \text{g m}^{-3}\ \text{h}^{-1}\ \text{DOC}\ \frac{\text{mol O}_2}{\text{mol C}} = 12.67\ \text{g m}^{-3}\ \text{h}^{-1}\ \text{DOC}\ \frac{32\ \text{g O}_2}{12\ \text{g C}}$$

$$r_{O2} = 33.78\ \text{g m}^{-3}\ \text{h}^{-1}\ O_2$$

## PROBLEM 11.2

The same wastewater described in Problem 11.1 is to be nitrified. The $NH_4$-N concentration of $S_{NH_4\text{–}N,o} = 50$ mg $L^{-1}$ must be reduced down to 1 mg $L^{-1}$. Oxygen utilization in the airflow is about 20%, $c_{O_2,0} = 0.232$ kg $m^{-3}$ $O_2$, V = 5000 $m^3$. We will assume that the nitrifiyers are not washed out.

1. Calculate the oxygen uptake rate and the required air flow rate.
2. Calculate the needed specific mass transfer coefficients with ($c' = 2$ mg $L^{-1}$) and without nitrification ($c' = 1$ mg $L^{-1}$).

### Solution

1. To calculate the required air flow rate, we start with an oxygen balance:

$$Q_G\left(c_{O_2,0} - c_{O_2}\right) = r_{O_2,\Sigma}\, V$$

$$Q_G = \frac{r_{O_2,\Sigma}\, V}{c_{O_2,0} - c_{O_2}}$$

with 20% oxygen utilization $c_{O_2,0} - c_{O_2} = 0.046$ kg $m^{-3}$. Starting from an $NH_4$ balance:

$$r_{NH_4\text{–}N} = \frac{\left(S_{NH_4\text{–}N,0} - S_{NH_4\text{–}N}\right)}{t_R} = \frac{49}{6} = 8.17\ \text{mg L}^{-1}\ \text{h}^{-1}$$

$$= \frac{8.17}{14} = 0.584\ \text{mmol L}^{-1}\ \text{h}^{-1}\ NH_4\text{-N}$$

can be calculated.

As $NH_4^+ + 2\,O_2 \rightarrow NO_3^- + 2\,H^+ + H_2O$, the oxygen consumption rate of nitrification is:

$$r_{O_2,N} = 2 \cdot 0.584 = 1.17 \text{ mmol } L^{-1}\,h^{-1}$$
$$= 1.17 \cdot 32 = 37.44 \text{ mg } L^{-1}\,h^{-1}\,O_2$$

$$r_{O_2,\Sigma} = r_{O_2,N} + r_{O_2,C}$$
$$= 37.44 + 33.78 \text{ (see: problem 11.1)}$$
$$= 71.22 \text{ g } m^{-3}\,h^{-1}\,O_2$$

For the flow rate we obtain:

$$Q_G = \frac{71.22 \cdot 5000}{0.046} = \frac{\text{g m}^3\,\text{m}^3}{\text{m}^3\,\text{h kg}} = 7741 \text{ m}^3\,h^{-1}$$

2. The concentration of dissolved oxygen must be increased from $c' = 1$ mg $L^{-1}$ (only carbon removal) to 2 mg $L^{-1}$ (carbon removal with nitrification).

What is the old and what do we select for the new specific mass transfer coefficient $k_La$ of the aeration system? Saturation concentration $c^* = 9$ mg $L^{-1}$ $O_2$.

(a) Only C-removal

$$k_La\,(c^* - c') = r_{O_2}$$

$$k_La = \frac{33.78}{8} = 4.2\ h^{-1}$$

(b) C-removal with nitrification

$$k_La\,(c^* - c') = r_{O_2\Sigma}$$

$$k_La = \frac{71.22}{7} = 10.2\ h^{-1}$$

The aeration system must be selected according to these requirements.

## References


Bidstrup, S.M.; Grady Jr., C.P.L. **1988**, SSSP – Simulation of single-sludge processes, *Journal Water Pollution Control Federation* 60, 351–361.

Grady, C.P.L.; Daigger, G.T.; Lim, H.C. **1999**, *Biological Wastewater Treatment*, Marcel Dekker, New York.

Gujer, W. **1985**, Ein dynamisches Modell für die Simulation von komplexen Belebtschlammverfahren, *Habilitationsschrift*, Institut für Gewässerschutz und Wassertechnologie, ETH Zürich.

Henze, M. **1986**, Nitrate versus oxygen utilization rates in wastewater and activated sludge systems, *Water Science and Technology* 18, 115–122.

Henze, M.; Grady Jr., C.P.L.; Gujer, W.; Marais, G.v.R.; Matsuo, T. **1987a**, Activated sludge model no. 1, *IAWPRC Scientific and Technical Reports* 1.

Henze, M.; Grady Jr., C.P.L.; Gujer, W.; Marais, G.v.R.; Matsuo, T. **1987b**, A general model for single-sludge wastewater treatment systems, *Water Research* 21, 505–515.

Henze, M.; Grady Jr., G.P.L.; Gujer, W.; Marais, G.v.R.; Matsuo, T. **2000**, Activated Sludge Model No. 1, in: Activated Sludge Models ASM 1, ASM 2, ASM 2 d and ASM 3, *Scientific and Technical Report No. 9*, IWA Publishing.

Mehring, A. **1979**, Zur Berechnung des Belebtschlammreaktors als ein- und mehrstufiges Mischbecken unter Berücksichtigung der Sauerstoffbilanz (PhD thesis), Technical University Berlin.

# 12
# Membrane Technology in Biological Wastewater Treatment

## 12.1
## Introduction

The high performance of membrane technology has been proven in recent years in a wide range of fields, such as chemical industry, medical technology, drinking water treatment, biotechnology and environmental technology. The German work groups of the DWA (ATV-DVWK 2000a, b, 2002a, b; DWA 2005) have provided excellent reports on the application of membranes in the field of wastewater treatment. Also, the Chemical Engineering School at the RWTH Aachen has provided important knowledge of fundamentals and applications in the whole area of membrane technology (Rautenbach and Albrecht 1981, 1989; Melin and Rautenbach 2004).

The continuous development of membrane materials and membrane design on the one hand and the knowledge of operational management on the other hand have fostered the growth of membrane technology in wastewater treatment. Many questions have yet to be answered, however, especially in activated sludge systems:

- How can we best implement membranes in activated sludge systems?
- Do we need primary settlers if we use a membrane activated sludge process?
- Which membrane modules and operating modes are effective and energy efficient?
- Is it possible to perform nitrification and phosphate elimination in combination with membrane processes?

The number of membrane processes installed for the treatment of municipal wastewater is rather low but steadily increasing. In Germany, several large membrane processes for wastewater treatment plants (>11 000 inhabitants) are in operation or being planned (MUNLV 2003). The largest one (for 80 000 inhabitants; about 1900 $m^3\ h^{-1}$) has been in operation since 2004 in the wastewater treatment plant (WWTP) at Nordkanal (DWA 2005). The biggest industrial membrane process in biological wastewater treatment for a flow rate of about 200 $m^3\ h^{-1}$ has been in operation near Dortmund since 2004 for the treatment of wastewater from the pharmaceutical production plant of Schering AG (Achtabowski and Neuhaus 2005).

*Fundamentals of Biological Wastewater Treatment*. Udo Wiesmann, In Su Choi, Eva-Maria Dombrowski

ISBN: 978-3-527-31219-1

Industrial wastewater treatment plants are often characterized by low flow rates and high pollutant concentrations. The benefit of using membranes is the possibility to reuse water in different qualities and the gain of reusable material as well as environmental aspects integrated in the production process. Examples for treatment of water and wastewater with membranes are given in Table 12.1.

Membrane processes have different targets, such as meeting the guidelines of wastewater quality standards, the recovery of components or the reuse of the treated water. In the field of municipal wastewater treatment, micro- and ultrafiltration processes are predominantly applied with the target of avoiding the need for a secondary clarifier, increasing the bacterial concentration in activated sludge process or producing an effluent free from suspended solids. In industrial wastewater treatment and water reuse, nanofiltration and reverse osmosis are preferentially used.

**Table 12.1** Examples of membrane processes in wastewater and polluted river water treatment (MUNLV 2003).

| | **Municipal, commercial and industrial applications** |
|---|---|
| Micro- and ultrafiltration | MBR for treatment of:<br>– municipal, pharmaceutical<br>– rendering plant<br>– food industry wastewater<br>– landfill leachate<br>Tertiary filtration of treated wastewater<br>Treatment of distillery wastewater<br>Treatment of electro dip coating water, oil-in-water emulsions and degreasing-processes in metal industries<br>Reuse of concentrated water-soluble lacquers<br>Pretreatment for production of boiler feed water<br>Treatment of polluted river water with integrated precipitation<br>Elimination of phosphate, iron and manganese |
| Nanofiltration | Elimination of specific compounds like EDS in wastewater<br>Desalination of wastewater<br>Discoloring of wastewater in textile and cellulose industries<br>Concentration of landfill leachate |
| Reverse osmosis | Concentration of $CaSO_4$ from mine-drainage water<br>Recycling of silver from washing water in photo industry<br>Treatment of wastewater in textile-dye industry<br>Concentration of washing water in cellulose industries<br>Reuse of phosphor acid<br>Treatment of chlorine water<br>Treatment of landfill leachate<br>Desalination<br>Reuse of water |

## 12.2
## Mass Transport Mechanism

### 12.2.1
### Membrane Characteristics and Definitions

Membranes are flat, semi-permeable structures that are permeable for at least one component and are impermeable for others. According to the nomenclature of membrane technology, various membrane processes are characterized according to the molar mass or diameter of the transported component, the aggregate state on the two sides of the membrane as well as the separation principle. The transport can be caused by gradients of concentration or pressure. Pressure-driven membrane processes like micro-, ultra- and nanofiltration as well as reverse osmosis are used in wastewater treatment.

Figure 12.1 shows the classification of membrane processes based on the average particle diameter or molar mass, with a few examples of wastewater components. Note that the ranges of the separation processes overlap with respect to the particle diameter and the driving pressure.

The functional principle behind membrane processes used in wastewater treatment are filtration or sorption and diffusion, whereby the wastewater feed is divided into a cleaned part, i.e. the filtrate or permeate, and a concentrated part, i.e. the concentrate or retentate (Fig. 12.2).

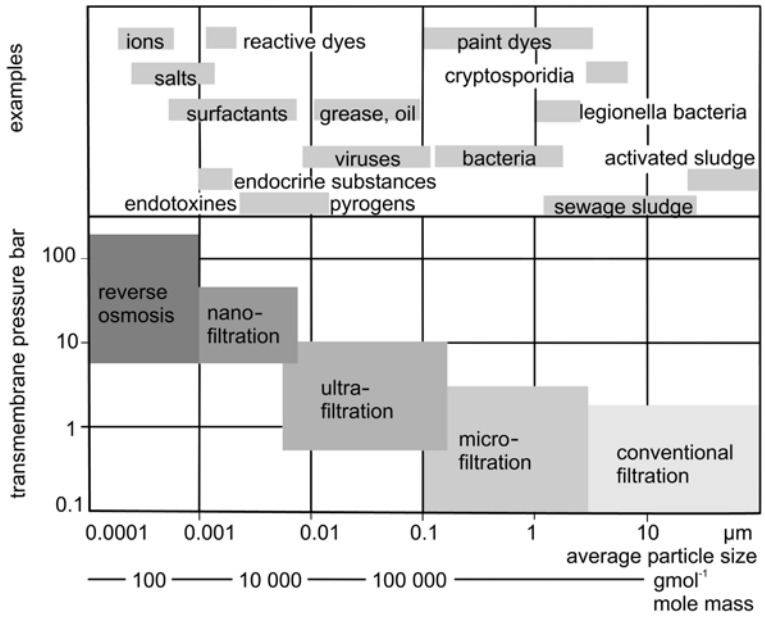


**Fig. 12.1** Classification of membrane processes used in wastewater treatment (MUNLV 2003; Rautenbach 1997).

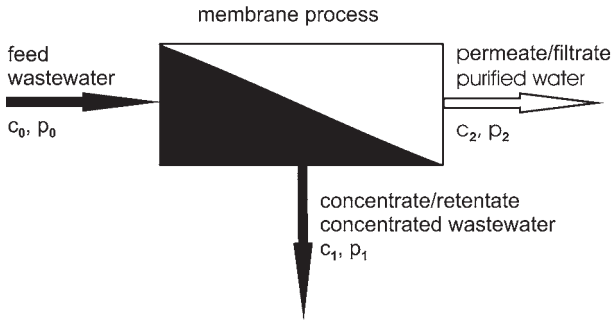


**Fig. 12.2** Scheme showing the principle of the membrane process.

The performance of a membrane filtration unit is determined by the following main parameters:

- The selectivity of the membrane is the capability to separate between components like oil and water or salt and water. Low selectivity can only be compensated with an expensive multi-stage process. For aqueous systems of a solvent and a solute the retention coefficient or retention R is a measure of the selectivity. The solute is retained while the solvent, most often water, passes through the membrane; the retention R is given by:

$$R = \frac{c_0 - c_2}{c_0} = 1 - \frac{c_2}{c_0} \tag{12.1}$$

  where $c_0$ is the concentration of the pollutant in the feed and $c_2$ is the concentration of the pollutant in the permeate.
  The true retention achieved with the membrane is higher because the concentration of the retained component increases at the surface of membrane $c_3$ as a result of concentration polarization (Section 12.3).

$$R_t = 1 - \frac{c_2}{c_3} \tag{12.2}$$

  In the field of biological wastewater treatment, one main component often has to be eliminated; and the feed and permeate concentrations are given, for example, as suspended solids in g $L^{-1}$ MLSS.

- The relative volume flux $J_{p0}$ characterizes the hydrodynamic permeability:

$$J_{p0} = \frac{Q_p}{\Delta p_{TM}\, A_m} \ \mathrm{m^3\ m^{-2}\ h^{-1}\ bar^{-1}} \tag{12.3}$$

  where $Q_p$ is the permeate volume flow rate, $\Delta p_{TM}$ is the transmembrane pressure and $A_m$ is the membrane area.

- The gradient of trans-membrane pressure, i.e. the driving force, is given by:

$$\Delta p' = \frac{p_0 + p_1}{2} - p_2 \tag{12.4}$$

  which takes into account the pressure drop along the cross-section of the membrane $p_0 - p_1$.

- Mechanical stability and resistance to fouling and scaling must be considered as other important factors.

Low permeability of a given membrane can be compensated by increasing the membrane surface area. The permeate flux $J_p$ or the permeate velocity $w_p$ is given by:

$$J_p = w_p = \frac{Q_p}{A_m} \quad m^3\, m^{-2}\, h^{-1} \tag{12.5}$$

The flux and the retention coefficients R and $R_t$ are not constant along the surface area of a membrane, even if there is no variability in the quality of the membrane material. The concentration of the retained component increases continuously and affects the flux and retention coefficients.

In wastewater treatment, transmembrane pressure $\Delta p_{TM}$ varies from 0.1 bar up to 120 bar. The characteristic cut-off of a membrane corresponds either to the particle diameter (in microns) or to the molar mass (measured in Dalton) of the largest retained substance.

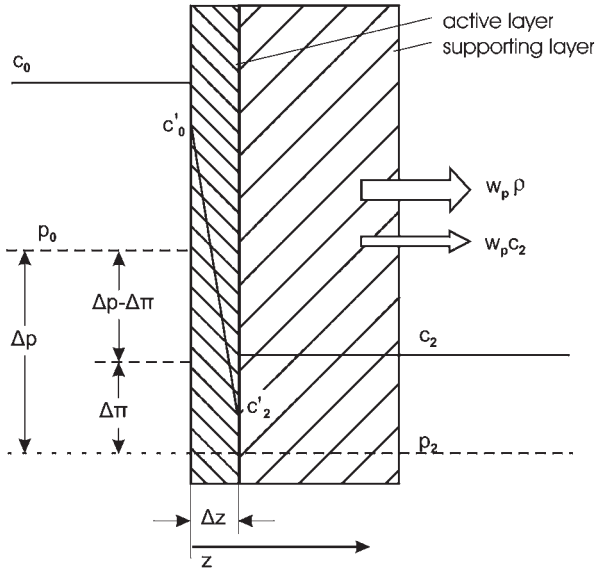


**Fig. 12.3** Concentration and pressure gradients through a solution-diffusion membrane. We have to distinguish Δp′ of Eq. (12.4) from Δp of Figure 12.3.

The cut-off of a membrane is determined as the molar mass of macro-molecules and dissolved substances with a retention coefficient of 90% or 95%. It is determined experimentally by the fractional separation curves for ultrafiltration membranes with different substances (Rautenbach 1997) and is often used for the characterization of membrane processes with the exception of microfiltration.

Various transport models are employed when studying the selectivity of different membranes and their transport mechanisms (Rautenbach 1997):

- A black-box model resulting from a large base of experimental results from real systems of combinations of treated fluids and membranes.
- Semi-empirical models for the real system with regard to physical and chemical parameters (solution-diffusion and pore model).
- Structural models in fundamental research.

Here we use semi-empirical models because it is common engineering practice to utilize the understanding of physical properties together with results of investigating process parameters. The solution–diffusion model (reverse osmosis and partly nanofiltration) and the pore model (ultra- and microfiltration) can be used with the physical and chemical background information to reduce the required number of experiments for studies and to quantitatively optimize membrane filtration operation in the area of wastewater treatment.

The design and layout of biological wastewater treatment plants with membrane bioreactor (MBR) technology has to focus on the requirements of the activated sludge process. The first guidelines were formulated by ATV-DVWK (2000b) with special regard to reactor volume, oxygen transfer rate, pre-treatment of wastewater, sludge disposal and, of course, membrane performance and cleaning (Section 12.3).

First we will focus on the most common mechanistic models of mass transport through membranes. They are based on diffusion and convection. Then we will consider resistances to mass transfer, like concentration polarization as well as the combination of transport mechanisms and resistances. A further combination of models, e.g. the solution–diffusion model and the pore model, is necessary when using membranes with an active, deep layer, a porous carrier layer or if a gel-layer is formed.

### 12.2.2 Mass Transport Through Non-porous Membranes

The solution–diffusion model describes reverse osmosis in ideal membranes as well as nanofiltration processes in non-porous membranes.

The transport of a component through a non-porous membrane is only possible by dissolution and diffusion. In this idealized model of mass transport, the membrane is treated like a liquid. Figure 12.3 shows the concentration and pressure gradients for an asymmetric membrane, where the active layer is responsible for separation and the supporting layer for mechanical stability.

The specific mass transfer rate of diffusion is described by Fick's first law:

$$J_D = -D\nabla c' \tag{12.6}$$

where $c'$ is the concentration of the dissolved component and D is the diffusion coefficient.

The diffusion coefficient D is idealized to be independent of concentration. That means D is constant and not affected by location in the membrane or by concentration. For one-dimensional diffusion, the diffusive flux follows as:

$$J_D = -D\frac{dc'}{dz}\ g\ m^{-2}\ h^{-1} \tag{12.7}$$

or (see Fig. 12.3):

$$J_D = -D\frac{c'_0 - c'_2}{\Delta z} \tag{12.8}$$

This is a solution for the steady-state mass balance for diffusion across two planes (e.g. through a thin plate membrane at the points z and z + dz):

$$0 = -\frac{dJ_D}{dz} \tag{12.9}$$

and considering Eq. (12.7):

$$0 = \frac{d}{dz}\left(D\frac{dc'}{dz}\right) = D\frac{d^2c'}{dz^2} \tag{12.10}$$

According to Henry's law, we obtain for ideal systems with linear sorption characteristics with respect to the dissolved impurity concentration in the membrane $c'$:

$$c = Hc' \tag{5.6}$$

$$J_D = \frac{D}{\Delta zH}(c_0 - c_2) = B(c_0 - c_2) \tag{12.11}$$

with:

$$B = \frac{D}{\Delta zH} \tag{12.12}$$

The membrane constant for the dissolved impurity B is independent of pressure but is a function of temperature because H and D vary with temperature.

The diffusive water flux follows in analogy to (12.8):

$$J_{DW} = D_W\frac{c'_{0W} - c'_{2W}}{\Delta z} \tag{12.13}$$

Because of the water surplus, the absorption equilibrium can be described via (partial) pressure:

$$c'_W = H'_W p \tag{12.14}$$

and the water flux follows taken together with Eq. (12.13):

$$J_{DW} = \frac{D_W H'_W}{\Delta z} (p_0 - p_2) \tag{12.15}$$

Usually, the water flux is written as a function of the pressure difference:

$$J_{DW} = \rho A (p_0 - p_2) \tag{12.16}$$

with:

$$A = \frac{D_W H'_W}{\rho \Delta z} \tag{12.17}$$

as the membrane constant A and $\rho$ as the density of water. Note that, in contrast to the dimensionless H (see Eq. 5.6), $H'_w$ has the dimension g $(m^3\ bar)^{-1}$ (Eq. 12.14).

The membrane constant A for the solvent (here water) is a function of temperature as well as a function of membrane properties [$D_w(T)$, $H'_w(T)$] and the thickness of the active layer $\Delta z$.

Equation (12.16) is valid if the osmotic pressure $\Pi$ is negligible. Otherwise the diffusive flux is:

$$J_{DW} = \rho A (p_0 - p_2 - \Delta\Pi) \tag{12.18}$$

with:

$$\Pi = - \frac{RT \ln a_i}{V_i} \tag{12.19}$$

it follows:

$$\Delta\Pi = \frac{RT}{V_i} (\ln a_{i,o} - \ln a_{i,2}) \tag{12.20}$$

$$a_i = \gamma_i x_i = \gamma_i (1 - x_j) \tag{12.21}$$

where $a_i$ is the solvent activity, $\gamma_i$ is the activity coefficient, $x_i$ is the mole fraction, $x_j$ is the mole fraction of the solute, $V_i$ is the molar volume of the solvent and R is the gas constant.

For ideal mixtures or for very low solute concentrations ($x_j << 1$) the activity coefficient $\gamma_i$ is unity (Mulder 2000) and the activity becomes:

$$\ln a_i = \ln x_i = \ln (1 - x_j) \approx -x_j \tag{12.22}$$

Thus, using the equation for the state of ideal gases for diluted solutions the molar concentration follows according to the amount of moles $N_j$ and $N_\Sigma$:

$$c_j = \frac{N_j}{V} = \frac{x_j N_\Sigma}{V} \approx \frac{x_j}{V_j} \tag{12.23}$$

At least the osmotic pressure difference between membranes follows:

$$\Delta\Pi = RT (c_0 - c_2) \tag{12.24a}$$

respectively for dissociating compounds, including the osmotic coefficient $\beta$:

$$\Delta\Pi = \beta RT (c_0 - c_2) \tag{12.24b}$$

where $c_0$ is the feed molar concentration of the solute, $c_2$ is the permeate molar concentration of the solute and $\beta$ is the osmotic coefficient for the change in numbers of moles by dissociation, depending on the degree and stoichiometrics of the dissociation reaction (Rautenbach and Albrecht 1981).

From Eqs. (12.23) and (12.24) it follows that $\Delta\Pi$ is high for high values of $c_0$ and for low values of $c_2$. Considering concentration polarization, the solute concentration at the membrane surface is $c_3 > c_0$ (Section 12.3).

The membrane constants A and B depend on temperature according to exponential functions (Rautenbach 1997) because of its influence on D and H (B in Eq. 12.12) and on $D_W$ and $H'_W$ [A in Eq. (12.17)]. Yet the temperature dependency of B is often neglected for practical purpose. A and B have to be determined experimentally. They characterize the permeability of the membrane; the quotient A/B is a degree for the selectivity of the system. For a low A/B the selectivity is high.

Often the designer's aim is to calculate:

- The flow rate of the water through membrane $w_p$.
- The permeate concentration $c_2$.

With the flow rate of permeate $w_p$ (Fig. 12.3), we obtain the mass flux $J_D$ for the solute with $c_2$:

$$J_D = w_p c_2 \tag{12.25}$$

and for water:

$$J_{DW} = w_p \rho \tag{12.26}$$

From Eqs. (12.18) and (12.26), the permeate flow rate can be calculated:

$$w_p = \frac{J_{DW}}{\rho} = A\,(p_0 - p_2 - \Delta\Pi) \tag{12.27}$$

From Eqs. (12.25) and (12.11), considering the flow rate according to Eq. (12.27), we obtain:

$$c_2 = \frac{J_D}{w_p} = \frac{B\,(c_0 - c_2)}{A\,(p_0 - p_2 - \Delta\Pi)} \tag{12.28}$$

and finally the result for the permeate concentration $c_2$:

$$c_2 = \frac{B\,c_0}{A\,(p_0 - p_2 - \Delta\Pi) + B} \tag{12.29}$$

For $p_0 - p_2 = \Delta\Pi$, no water is transported through the reverse osmosis membrane but the dissolved compound is transported, giving finally $c_2 = c_0$.

At the membrane surface, some important effects may occur, e.g. concentration polarization and fouling processes that have to be taken into consideration (Section 12.3). In reverse osmosis and nanofiltration processes osmotic pressure is important, but even in ultrafiltration processes osmotic pressure can have an effect. At high fluxes and high retention values, the concentration of macromolecules at membrane surface becomes quite high (see Problem 12.1).

### 12.2.3 Mass Transport Through Porous Membranes

The pore model is based on the assumption that the membrane pores are much smaller than the diameter of the retained particles but are permeable to water. In contrast to the solution–diffusion model, water does not diffuse through the pores; rather it flows under the influence of pressure and frictional forces. The pore system is ideally straight and parallel; and each pore has the same circular size. As a result of the small capillary diameter, laminar flow conditions are given and Hagen–Poiseuille's law is valid. For pores with diameter d and length L, one can write in dimensionless notation:

$$\xi = \frac{64}{\mathrm{Re}} \tag{12.30}$$

with Reynolds number:

$$\mathrm{Re} = \frac{w_{po}\, d}{\nu} \tag{12.31}$$

and resistance number $\xi$:

$$\xi = \frac{\Delta p}{{}^{1}/_{2}\, \rho\, w_{po}^{2}} \frac{d}{L} \tag{12.32}$$

with $w_{po}$ as the flow rate in a capillary pore.

In reality, the length of pores L is greater than the membrane thickness $\Delta z$. Therefore, a mean tortousity $\mu$ is defined:

$$\mu = \frac{L}{\Delta z} \tag{12.33}$$

The flow rate of permeate $w_p$ is now given by Hagen–Poiseuille's law (using Eqs. 12.30 to 12.33) with porosity $\varepsilon$:

$$w_p = w_{po}\, \varepsilon = \frac{\Delta p}{32\, \eta} \frac{d^2 \varepsilon}{\mu \Delta z} \tag{12.34}$$

Carman and Kozeny's pore model (Carman 1956) assumes a pore system formed of equally sized spheres in a packed bed. With permeate flux:

$$J_p = w_p = \frac{\Delta p\, \varepsilon^3}{2\, \eta\, (1-\varepsilon)^2\, a_v^2\, \mu \Delta z} \tag{12.35}$$

$$a_v = \frac{A_{po}}{V} \tag{12.36}$$

the hydraulic diameter $d_h$ for packed beds is introduced (Rautenbach and Albrecht 1981):

$$d_h = \frac{4\, \varepsilon}{(1-\varepsilon)\, a_v} \tag{12.37}$$

where $a_v$ is the volume-specific surface area.

Equation (12.35) is known as the Carman–Kozeny equation. For sphere-packed beds, the tortousity is given as μ=25/12 (Rautenbach and Albrecht 1989). With the membrane constant $A^*$:

$$A^* = \frac{\varepsilon^3}{2\eta(1-\varepsilon)^2 a_v^2 \mu \Delta z} \tag{12.38}$$

the equation shows the linear dependence of permeate flux on the driving force, i.e. the pressure gradient across the membrane:

$$J_P = A^* \Delta p \tag{12.39}$$

Comparing the diffusive water flux according to Eq. (12.16), $A^*$ corresponds to the product of the density and the membrane constant A used in the solution–diffusion model.

The linear behavior of $J_P$ in relation to Δp depends only on the membrane constant $A^*$ of a given membrane. $A^*$ must be determined experimentally because it depends on viscosity, which is a function of temperature. Figure 12.4 shows the membrane-controlled flux.

This model fits micro- and ultrafiltration processes, but in practice a gel layer at the surface of the membrane and a depositing of particles also affects mass transport (see Section 12.3).

## 12.3 Mass Transfer Resistance Mechanisms

### 12.3.1 Preface

In pressure-controlled membrane filtration (e.g. in the field of wastewater treatment), mass transfer across the membrane is affected by multiple resistances before and behind the membrane surface. In the case of asymmetric membranes used in ultrafiltration and reverse osmosis, one has a combination of local transport resistances. The resistance of the active layer is mostly rate-limiting. In reverse osmosis and in some cases of ultrafiltration, permeate fluxes are low and concentration polarization is insignificant because of the high diffusive back-flow of the small molecules. All components, even those at the surface of the membrane, remain soluble; here the membrane itself controls the mass transfer.

In every case where a concentration polarization profile can occur the effect can be controlled more or less by the flow conditions along the surface of membrane and it is therefore influenced by membrane module design (Section 12.4).

We will now discuss resistances to mass transfer and the most common model for the calculation of the concentration $c_3$ at the membrane surface in combination with mass transport mechanisms for solution–diffusion and the pore model.

### 12.3.2 Mass Transfer Resistances

Membrane-controlled mass transfer provides the simplest operational condition for porous membrane systems with pressure as the driving force. Equation (12.39) is often written in the form of Darcy's Law (Darcy 1856):

$$J_p = \frac{\Delta p}{\eta R_m} \tag{12.40}$$

with:

$$R_m = \frac{2(1-\varepsilon)^2 a_v^2 \mu \Delta z}{\varepsilon^3} = \eta \cdot A^{*-1}\, m^{-1} \tag{12.41}$$

for laminar flow as resistance of membrane $R_m$. $J_p$ is only controlled by the clean, non-blocked membrane and shows linear behavior (Fig 12.4). A further hydraulic resistance due to pore blocking and adsorption $R_f$ can be considered:

$$J_p = \frac{\Delta p}{\eta (R_m + R_f)} \tag{12.42}$$

During a membrane filtration process, the solute concentration at the membrane surface rises; and when the concentration $c_3$ exceeds the solubility limit crystallization occurs. A gel layer, also known as a sludge cake, is formed by the deposit of solids as well as by the growth of bacteria (see Fig. 12.5 in the next section and Fig. 12.9 in Section 12.4.3). Practice normally shows non-linear behavior because the gel layer controls mass transport (Fig. 12.4).

Gel layer or sludge cake formation is often found above a so-called critical flux (see Section 12.5). The accumulated material simply adds a further resistance $R_c$ for the sludge cake to the resistance of the free or blocked membrane:

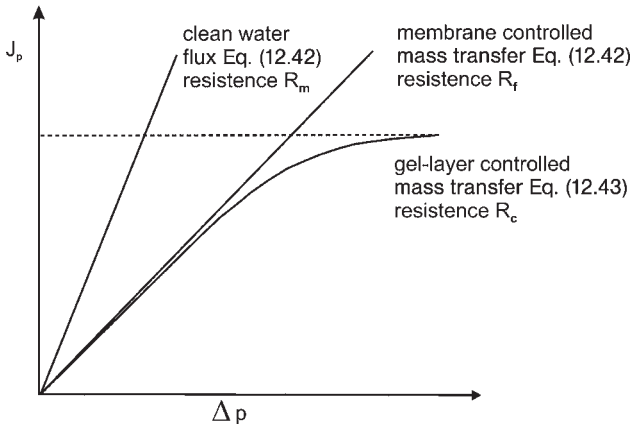


**Fig. 12.4** Permeate flux plot as a function of pressure difference.

$$J_P = \frac{\Delta p}{\eta (R_m + R_f + R_c)} \tag{12.43}$$

respectively:

$$J_P = \frac{\Delta p}{\eta R_\Sigma} \tag{12.44}$$

### 12.3.3 Concentration Polarization Model

The classic concentration polarization model describes the fluxes according to convective flow and retransfer of the solute, i.e. back diffusion through concentration boundary layer dependent on the concentration gradient between the bulk region and the surface of the membrane (Fig. 12.5).

One solution to the mass balance in the boundary layer with thickness δ is obtained at steady state conditions, $dJ_\Sigma/dz = 0$. There are two parts of the total flux: the flux of the solute counter to the z-direction, $-w_p c$, and the back diffusion of the solute, $-D\,dc/dz$. Assuming that the permeate velocity is independent of the z-coordinate it follows that:

$$J_\Sigma = -w_p c - D\frac{dc}{dz} \tag{12.45}$$

After differentiation of Eq. (12.45), we obtain at steady-state conditions:

$$0 = w_p \frac{dc}{dz} + D\frac{d^2 c}{dz^2} \tag{12.46}$$

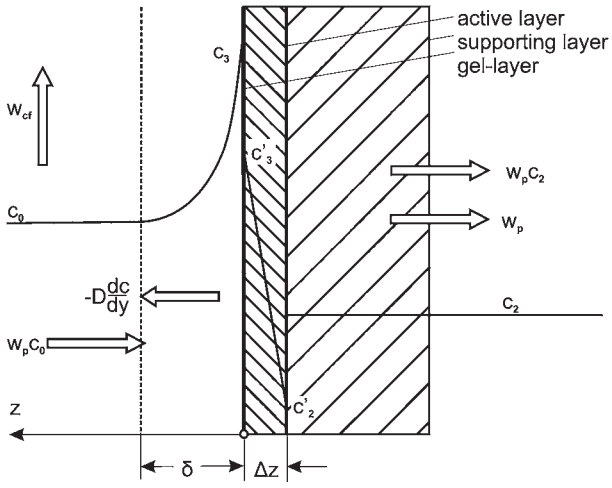


**Fig. 12.5** Concentration polarization on the feed side and boundary layer.

A possible solution of Eq. (12.46) is the exponential function:

$$c = a_1 + a_2 \exp(a_3 z) \tag{12.47}$$

and after differentiating Eq. (12.47):

$$\frac{dc}{dz} = a_3 a_2 \exp(a_3 z) \tag{12.48}$$

$$\frac{d^2 c}{dz^2} = a_3^2 a_2 \exp(a_3 z) \tag{12.49}$$

Three boundary conditions are necessary to determine the constants $a_1$, $a_2$ and $a_3$. According to Fig. 12.5: (1) at the boundary layer with thickness $\delta$, the concentration is the same as in the bulk flow $c_0$, (2) the highest concentration $c_3$ is attained at the surface of membrane at $z = 0$, and finally, (3) the condition for the permeate flux of the solute is the equality of the sum of convective flux and the back diffusive flux at the membrane surface:

$$z = \delta, \quad c = c_0 \tag{12.50}$$

$$z = 0, \quad c = c_3 \tag{12.51}$$

$$z = 0, \quad -w_p c_2 = -w_p c_3 - D \left.\frac{dc}{dz}\right|_{z=0} \tag{12.52}$$

From Eqs. (12.48) and (12.49) in Eq. (12.46) we obtain:

$$0 = w_p a_3 a_2 \exp(a_3 z) + D\, a_3^2 a_2 \exp(a_3 z) \tag{12.53}$$

and finally for the constant $a_3$:

$$a_3 = -\frac{w_p}{D} \tag{12.54}$$

From Eqs. (12.52) and (12.51) we obtain:

$$-w_p c_2 = -w_p c_3 - D\, a_3 a_2 \tag{12.55}$$

or with Eq. (12.54):

$$a_2 = c_3 - c_2 \tag{12.56}$$

Finally, considering condition Eq. (12.50), then Eq. (12.47) gives:

$$c_0 = a_1 + (c_3 - c_2) \exp\left(-\frac{w_p}{D}\,\delta\right) \tag{12.57}$$

respectively:

$$a_1 = c_0 - (c_3 - c_2) \exp\left(-\frac{w_p}{D}\,\delta\right) \tag{12.58}$$

Now, all three integration constants are known and the concentration profile near membrane ($0 \le z \le \delta$) follows to:

$$c = c_0 - (c_3 - c_2)\exp\left(-\frac{w_p}{D}\delta\right) + (c_3 - c_2)\exp\left(-\frac{w_p}{D}z\right) \tag{12.59}$$

Considering Eq. (12.51), a simple result describes the dimensionless concentration polarization as a function of velocity $w_p$ and diffusion coefficient D of the retained component at the membrane surface z = 0 according to Eq. (12.59):

$$\frac{c_3 - c_2}{c_0 - c_2} = \exp\left(\frac{w_p}{D}\delta\right) \tag{12.60}$$

The permeate flow rate $w_p$ is then given by:

$$w_p = k_L \ln\left(\frac{c_3 - c_2}{c_0 - c_2}\right) \tag{12.61}$$

with the mass transfer coefficient:

$$k_L = \frac{D}{\delta} \tag{12.62}$$

The mass transfer coefficient can be expressed by dimensionless numbers with $w_{cf}$ as the cross-flow rate:

Sherwood number: $$Sh = \frac{k_L d}{D} \tag{12.63}$$

Schmidt number: $$Sc = \frac{\nu}{D} \tag{12.64}$$

Reynolds number: $$Re = \frac{w_{cf} d}{\nu} \tag{12.65}$$

These numbers and L/d result from a dimensional analysis of the problem. The determination of the relation between the Sherwood, Schmidt and Reynolds numbers as well as L/d is based on the analogy between heat and mass transport (Table 12.2). For laminar flow and simple geometric conditions, they can be calculated by solving mass and momentum balances. The relations presented are

**Table 12.2** Sherwood number for different flow conditions experimentally proved for mass transport by Linton and Sherwood (1950) and Rautenbach and Albrecht (1981).

| | **Sherwood number** | **Flow condition** |
|---|---|---|
| Tube | $Sh = 1.62\,(Re\,Sc\,d/L)^{1/3}$ | Laminar |
| | $Sh = 0.023\,Re^{7/8}\,Sc^{1/4}$ | Turbulent |
| | $Sh = 0.04\,Re^{3/4}\,Sc^{1/3}$ | Turbulent |
| Canal with rectangular cross-section | $Sh = 1.85\,(Re\,Sc\,d_h/L)^{1/3}$ | Laminar |
| | $Sh = Sh_{tube}$ | Turbulent<br>$Re\,Sc\,d_h/L > 10^2$ |

proven experimentally for mass transport by convection and diffusion in tubes for laminar and turbulent flow conditions (Linton and Sherwood 1950) and in channels for laminar flow conditions (Rautenbach and Albrecht 1981).

From steady-state laminar flow in tubes of diameter d and length L as well as $d/L \ll 1$:

$$Sh = 1.62 \left( Re\, Sc\, \frac{d}{L} \right)^{1/3} \tag{12.66}$$

is valid. After calculation of $k_L$ from Eq. (12.66) and introduction into Eq. (12.61), the permeate rate follows:

$$w_p = 1.62 \left( \frac{D^2 w_{cf}}{dL} \right)^{1/3} \ln \left( \frac{c_3 - c_2}{c_0 - c_2} \right) \tag{12.67}$$

We must determine not only the concentrations but also the diffusive coefficient D. A possible approximation for D is given by the Stokes Einstein equation in Eq. (5.4) as a function of absolute temperature T, solute radius R, dynamic viscosity η and with the Boltzmann constant K (Section 5.1; Mulder 2000):

$$D = \frac{K\,T}{6\,\pi\,\eta\,R} \tag{5.4}$$

Deviations arise if D and v become dependant on concentration, as observed in the ultrafiltration of macromolecules, or when the cross flow rate rises for small values of d/L (Rautenbach 1997). This occurs particularly in ultrafiltration processes in the field of wastewater treatment if suspended solids are present which accumulate at the boundary layer.

### 12.3.4
### Solution–diffusion Model and Concentration Polarization

The aim is now to calculate $w_p$ and $c_2$ as well as $\Delta\Pi$. Thus, we need three independent equations. Considering the increasing concentration $c_3$ at the membrane surface for the calculation of $\Delta\Pi$ and $J_D$, we obtain Eqs. (12.68) and (12.69) from Eq. (12.24b), respectively Eq. (12.11) and (12.12).

$$\Delta\Pi = \beta\, RT\, (c_3 - c_2) \tag{12.68}$$

$$J_D = B\, (c_3 - c_2) \tag{12.69}$$

For the solution diffusion model (reverse osmosis and nanofiltration) $w_p$ follows according to Eqs. (12.27) and (12.68):

$$w_p = A\left(p_0 - p_2 - \beta\, RT\, (c_3 - c_2)\right) \tag{12.70}$$

Equations for the concentration of the retained component $c_3$ and the permeate $c_2$ are given for $c_2$ according to Eqs. (12.29) and (12.27):

$$c_2 = \frac{B\, c_3}{w_p + B} \tag{12.71}$$

The third independent equation is given by elimination of $c_3$ from Eq. (12.61):

$$c_3 = c_2 + (c_0 - c_2) \exp \frac{w_p}{k_L} \tag{12.72}$$

After introducing Eq. (12.72) in Eq. (12.71), $c_3$ and $c_2$ can be eliminated:

$$c_2 = \frac{B\, c_0 \exp \frac{w_p}{k_L}}{w_p + B \exp \frac{w_p}{k_L}} = \frac{B\, c_0}{w_p \exp\left(-\frac{w_p}{k_L}\right) + B} \tag{12.73}$$

$c_3$ follows from Eq. (12.72).

With Eqs. (12.72) and (12.73) in Eq. (12.70), we finally obtain an implicit equation for $w_p$:

$$w_p = A \left( \Delta p - \beta\, RT\, \frac{w_p c_0 \exp \frac{w_p}{k_L}}{w_p + B \exp \frac{w_p}{k_L}} \right) \tag{12.74}$$

Equation (12.74) can only be solved by graphical or numerical methods after determination of $k_L$ using one of the empirical equations in Table 12.3 (see Section 12.4.1). With these solutions, $c_3$ and $c_2$ can be calculated using Eqs. (12.72) and (12.73).

There is, however, a correlation between the true retention coefficient $R_t$ and $c_3$, the concentration at the surface of the membrane according to Eq. (12.2). With Eqs. (12.70) and (12.71), we obtain the true retention coefficient $R_t$ which can be calculated using Eqs. (12.72) and (12.73):

$$R_t = 1 - \frac{B}{A\left(p_0 - p_2 - \beta\, RT\,(c_3 - c_2)\right) + B} \tag{12.75}$$

Explicit solutions of Eq. (12.74) are possible for some specific cases:

1. If concentration polarization does not occur, $c_3 = c_0$, $\exp(w_p/k_L) = 1$ follows from Eqs. (12.60) and (12.62). Solving the quadratic equation we obtain:

$$w_p = A \left( \Delta p - \beta\, RT \frac{w_p c_0}{w_p + B} \right) \tag{12.76}$$

2. Furthermore, if the membrane is not permeable for the solute ($B = 0$), the permeate specific flow rate is:

$$w_p = A\,(\Delta p - \beta\, RT\, c_0) \tag{12.77}$$

3. In the case of low feed concentration $c_0$, then $\Delta\Pi$ can be neglected:

$$w_p = A\,\Delta p \tag{12.78}$$

### 12.3.5
### The Pore Model and Concentration Polarization

The permeate flow rate is determined with the pore model via the resistance in series models, as described in Sections 12.3.2.

Different authors use the resistance in a series of models and describe mathematical approaches as well as experimental investigations for estimation of the resistances used in Eq. (12.43) (Fu and Dempsey 1998; Melin et al. 2001; Geissler et al. 2003; Wintgens et al. 2003). For example, resistances were summarized by Chang et al. (2002) for microfiltration in MBR with $R_m = 3–22 \cdot 10^{11}\ m^{-1}$, $R_c = 3–48 \cdot 10^{11}\ m^{-1}$ and $R_f = 10^{-11}\ m^{-1}$ for different membrane materials. In ultrafiltration processes for the reuse of surfactants $R_m = 5 \cdot 10^{12}\ m^{-1}$ and $R_f = 5–9.1 \cdot 10^{12}\ m^{-1}$ was experimentally determined for PES membranes for various surfactants (Goers 2000).

The resistance of the sludge cake $R_c$ is a function of the concentration at the membrane surface. It follows from Eq. (12.43) according to the concentration polarization model.

Chang and Fane (2000) describe the shear stress on micro and ultrafiltration membrane surfaces from air bubbling of submerged hollow fibers by slug flow conditions, i.e. based on two-phase flow conditions influenced by the formation of Taylor bubbles. Melin et al. (2001) and Wintgens et al. (2003) use the same model of slug flow conditions, considering concentration polarization and hydrodynamic effects. They use experimental data from the full-scale wastewater treatment plant Rödingen in Germany to obtain coefficients for their model. Further investigations are summarized by Stephenson et al. (2000).

## 12.4
## Performance and Module Design

### 12.4.1
### Membrane Materials

The efficiency of membrane filtration processes in wastewater treatment is decisively influenced by the selection of the membrane material for the wastewater to be treated with regard to the particles and dissolved compounds it contains. Therefore, the membrane material has to be chosen carefully by the supplier in cooperation with the plant engineers. It is usually necessary to perform investigations in laboratory or pilot scale and to test different membrane materials and modules. Table 12.3 presents an overview of common membrane materials.

Depending on the composition and properties of the wastewater to be treated as well as on the membrane's mechanical stability, it is possible to use either organic or inorganic solid materials. Once commonly used, cellulose membranes are now used less often in recent times compared to polymer membranes, like polysulfone PS, polyacrylonitrile PAN and polyethersulfone PES. Because of their resistance to high temperatures and chemical stress, the use of inorganic materials like ceramics, aluminum, refined steel and glass is becoming more important (MUNLV 2003).

**Table 12.3** Common membrane materials and membrane structures used in membrane processes (according to ATV-DVWK 2002a).

| | Membrane structure | Membrane material | Active layer material |
|---|---|---|---|
| Microfiltration | Symmetric, porous | Polymer and ceramic | Polypropylene PP<br>Polyvinylidenfluoride PVDF<br>Polysulphone PSU<br>Aluminium oxide<br>Refined steel<br>Titanium dioxide<br>Zirconium dioxide |
| Ultrafiltration | Asymmetric, porous | Polymer phase inversion, composite membrane and ceramic | Polysulphone PSU<br>Reg. cellulose<br>Polyacrylnitrile PAN<br>Polyethersulphone PES<br>Titanium dioxide<br>Zirconium dioxide<br>Polyvinylidenfluoride PVDF |
| Nanofiltration | Asymmetric, dense | Polymer phase inversion, composite membrane | Polyamide PA<br>(Zirconium dioxide)<br>Polyethersulphone PES<br>Cellulose acetate CA |
| Reverse osmosis | Asymmetric, dense | Polymer phase inversion, composite membrane | Polyamide PA 95%<br>Cellulose acetate AC 5% |

Membranes are either symmetric or asymmetric in structure. That means they exhibit a homogenous or inhomogeneous dispersion of material. An asymmetric membrane is constructed by two layers of one material with different porosities (a phase inversion membrane), or by two layers of different materials (a composite membrane).

The very thin and dense active layer of about 1 µm on the feed side is responsible for the membrane's performance and permeability. The porous second layer is the supporting structure. Higher fluxes are attainable, especially for solution diffusion membrane processes, with asymmetric membranes. Both composite and phase inversion membranes can be constructed as porous or non-porous membranes (Rautenbach 1997).

## 12.4.2 Design and Configuration of Membrane Modules

### 12.4.2.1 Preliminary Remarks

The following informations are valid generally for all possible applications. There are several very different ways to construct membrane modules by the arrangement of the inlet and outlet streams. For example, a three-end module for cross-flow configuration consists of a frame construction for the selected membrane

**Table 12.4** Characteristics, advantages and disadvantages of plate and tubular membrane modules (MUNLV 2003; VDMA 2005).

| | **Tubular membranes** | | | **Plate membranes** | | |
|---|---|---|---|---|---|---|
| | **Tubular module** | **Capillary module** | **Hollow fiber module** | **Plate and frame module** | **Spiral wound module** | **Membrane cushion** |
| Active layer | Inside | Out-/inside | Out-/inside | Outside | Outside | Outside |
| Internal diameter | 5.5–25 mm | 0.25–5.5 mm | 0.04–0.25 mm | | | |
| Membrane surface area–volume ratio | ca. 80 $m^2\ m^{-3}$ | ca. 1000 $m^2\ m^{-3}$ | ca. 10000 $m^2\ m^{-3}$ | 40–100 $m^2\ m^{-3}$ | ca. 1000 $m^2\ m^{-3}$ | 400 $m^2\ m^{-3}$ |
| Configuration | Cross flow | Dead end/cross flow | Dead end | Cross flow | Dead end/cross flow | Dead end/cross flow |
| Advantages | Low blocking, low pressure drop, gel layer controlled | High surface area–volume ratio, low design costs, permeate back-washing | Very high surface area–volume ratio, low specific membrane costs, stable against high pressure | Simple exchange of membranes, low blocking | High surface area–volume ratio, fewer seals, low design costs | Low pressure drop, low fouling |
| Disadvantages | Low surface area–volume ratio | Low compression strength | Blockage, pressure drop | Many seals, low surface area–volume ratio | Long permeate ways, no mechanical cleaning, high blockage danger | Low surface area–volume ratio, many seals |

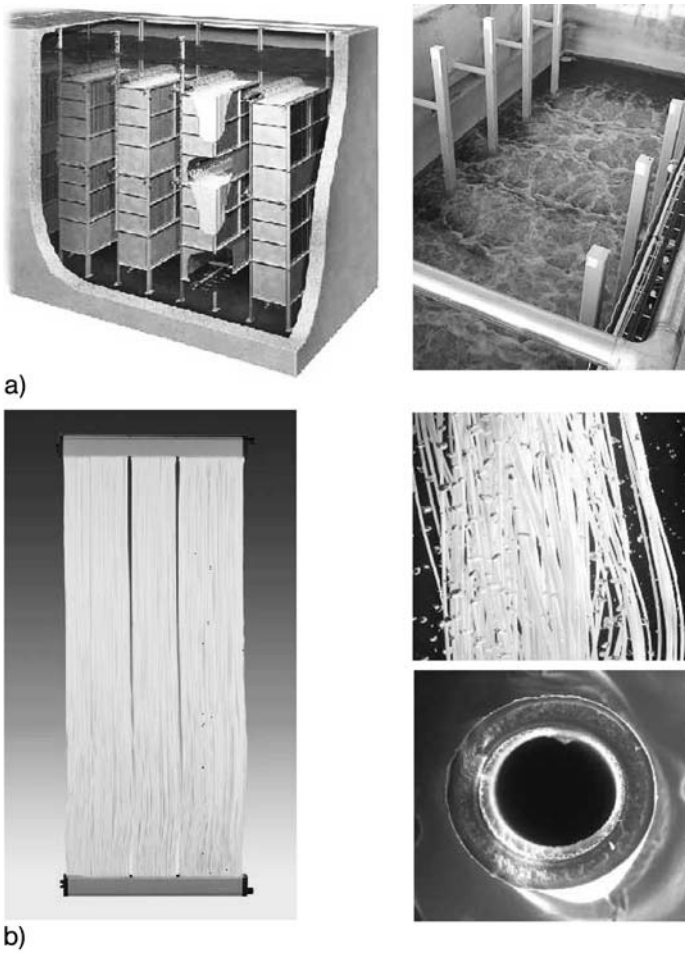


**Fig. 12.6** Membrane modules in submerged mode. (a) Kubota flat panel, submerged in an unit with bubble diffusor. (b) Zenon hollow fiber module, with air bubbling and a hollow fiber in detail.

material with connections to one inlet (feed) and two outlet streams (permeate and concentrate) and a pump providing the driving pressure. Modules with tubular or plate membranes are described in Table 12.4.

Five principle configurations are commonly found (Stephenson et al. 2000):

- Plate-and-frame modules, commonly known from electrolysis stacks, are often used for micro- and ultrafiltration and less often for reverse osmosis (e.g. Kubota flat panel; Fig. 12.6a). Similarly, there are membrane cushions with permeate spacers and support plates welded together with the plate membranes.
- Spiral-wound modules are the standard configuration for reverse osmosis and nanofiltration modules.

- Membrane cushions are although used in ultra- and nanofiltration modules.
- Hollow fine fiber (Zenon; Fig. 12.6b) and capillary membranes are self-supporting membranes with out-to-in flow direction for hollow fibers and in-to-out flow direction for capillary ones.
- Tubular membranes are used for high turbulence and good cleaning characteristics (Berghof 2005; Fig. 12.7a). An example for a complete process is the Wehrle ultrafiltration plant in Fig. 12.7b.

Module design has to fulfil the following requirements:

- High ratio of membrane area to module bulk volume.
- Low pressure drop, low energy demand.
- High degree of turbulence on the feed side to promote mass transfer.
- Low costs per unit membrane area.
- Good cleaning management.

a)

b)

**Fig. 12.7** Membrane modules in cross-flow mode. (a) Berghof tubular module and membranes. (b) Wehrle, MBR, ultrafiltration plant for the food industry.

For the treatment of a feed with a high suspended solids concentration, the demands for a high membrane area : volume ratio together with a design that facilitates cleaning is inconsistent and a compromise is necessary. Furthermore, hydrophilic behavior, attainable permeate volume flux, cut-off and operational life of the membrane have to be taken into account. Configurations such as dead-end, submerged and cross-flow mode are used for ultra- and microfiltration.

### 12.4.2.2 **Dead-end Configuration**

In the dead-end filtration process, the flow of the wastewater stream is orthogonal to the membrane and no retentate stream is produced. A two-end module is needed (Fig. 12.8a).

As a consequence, the retained colloids and macromolecules build a layer on the membrane surface which has to be removed periodically. This configuration results in an unsteady process which demands a two-end module and is only suitable if the feed suspended solids concentration is low.

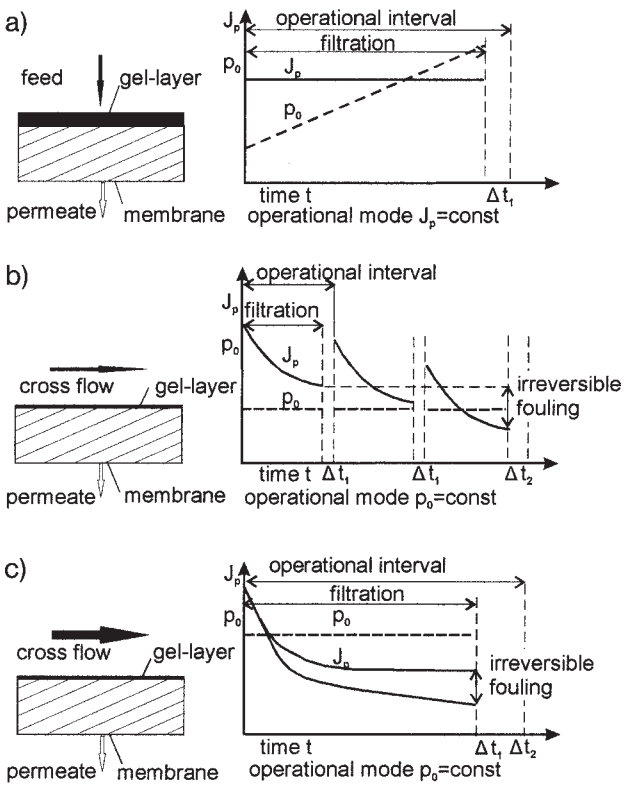


**Fig. 12.8** Configuration of membrane filtration modules:
(a) dead-end mode, (b) submerged mode, (c) cross-flow mode.
$\Delta t_1$ = backwashing period; $\Delta t_2$ = chemical enhanced cleaning period.

#### 12.4.2.3 Submerged Configuration

A special configuration of a two-end module is the submerged mode because a cross flow near membrane surface is applied without producing an additional stream (Fig. 12.8b). To minimize the building of a sludge cake layer and to avoid the high energy cost for high turbulence cross flow, a submerged system is used. The membranes are immersed directly in the activated sludge tank, where intensified aeration produces cross flow at the membrane surface (see Fig. 12.6b). Investigations have been performed on the influence of shear stress induced by bubbles (see Section 12.3.5). Permeate is removed by vacuum at transmembrane pressures of about 0.05 bar to 0.6 bar (Günder 1999; ATV-DVWK 2002b).

Transmembrane pressure is remarkably lower than 1 bar because of the drop in pressure which results from the water column above the submerged membrane. The rejected biomass remains in the bioreactor and the purified water passes through the membranes, usually from the outside in. Hollow fibers are flexible and move slightly to reduce gel layer formation because they are slightly longer than the module length and are therefore free to move (see Fig. 12.8b).

One significant characteristic of the submerged system is its operation in quasi steady state, in contrast to dead-end mode, and its higher frequency of back washing. Compared to the cross-flow configuration, there is less energy used (per $m^3$ permeate) but a greater membrane surface area is needed because of the low attainable fluxes in submerged systems. Recently, submerged systems have become highly significant in the field of aerobic biological wastewater treatment. The advantages and disadvantages of dead-end and submerged mode are summarized in Table 12.5.

Enhanced permeate flux was proven to be a result of two-phase flow. Gas-sparged ultrafiltration with tubular membranes has been investigated experimentally with different suspensions as well as with river water (Chang and Fane 2000; Cabbasud et al. 2001) although computational fluid dynamics (CFD) were used to model this two-phase flow conditions (Taha and Cui 2002).

#### 12.4.2.4 Cross-flow Configuration

In cross-flow filtration, the wastewater flow is parallel to the membrane (Fig. 12.8c). There is a continuous retentate stream in addition to the feed and permeate stream; and a three-end module is necessary. The retained material builds a layer on the surface of the membrane which can be influenced by the cross-flow rate. Thus the process is in continuous operation (see Table 12.5).

The reversible gel layer can be controlled by cross-flow conditions, while an irreversible gel layer has to be removed by a cleaning procedure. Gel layer-controlled filtration helps to protect microfiltration membranes from pore blockage. In general, there are two methods to control the severity of the reversible gel layer. When high turbulence at the membrane surface is realized by higher cross-flow rate with or without air injection, it leads to high energy costs. Higher turbulence can be obtained, though, by the use of smaller hydraulic diameters of membrane canals in tubular or flat membranes. This, however, increases the risk of blockage. Some examples of alternative methods to produce higher turbulence are the modules with rotor and stator system, e.g. VRM-Modul in WWTP Knautnaundorf (Stein 2003).

**Table 12.5** Advantages and disadvantages of dead-end (unsteady and submerged mode) and cross-flow mode in membrane filtration of wastewater (Chang and Fane, 2000; ATV-DVWK 2002b; Melin and Rautenbach 2004).

| Configuration of MBR | Advantages and disadvantages |
|---|---|
| Dead-end mode | Unsteady state process<br>Requires low suspended solids in feed stream<br>Low specific energy costs of 0.1–0.5 kWh $m^{-3}$<br>Module and membrane blocking<br>Back-washing if stable versus compression<br>Long filtration intervals<br>Periodic cleaning management<br>Final filtration of wastewater |
| Submerged mode | Quasi-steady state<br>High suspended solids in the feed treatable<br>Low specific energy costs of 0.3–0.7 kWh $m^{-3}$<br>Low fluxes of about 10–30 L $m^{-2}$ $h^{-1}$<br>Less stress for biomass<br>Two-phase flow pattern for hydrodynamical influence on deposits, permanent bubbling<br>High investment, low operational costs<br>Back-washing with and without air<br>Short filtration intervals<br>Periodic cleaning management |
| Cross-flow mode in steady state | Requires reversible gel layer for steady state process<br>High suspended solids treatable<br>Highest specific energy costs of 2.5–6.0 kWh $m^{-3}$<br>High fluxes of about 100 L $m^{-2}$ $h^{-1}$<br>With cross-flow of $w_{cf}$ 3–6 m $s^{-1}$<br>High stress for biomass<br>Low investment but high operational costs<br>Back-washing with and without air<br>Periodic cleaning management |

Another way to control gel layer formation is to use interval back flushing but with the disadvantage of a poor water recovery rate in the range of 80–90% of the feed flow. Intervals for back-flushing and chemically enhanced cleaning depend greatly on water quality and are often necessary in the case of river water processing (Dietze 2004).

## 12.4.3 Membrane Fouling and Cleaning Management

### 12.4.3.1 Types of Fouling Processes

The major symptoms of fouling are a decline in flux over operating time, increasing transmembrane pressure, sludge cake formation and changes to the retention coefficient $R_t$ (see Eq. 12.75). Stationary filtration behavior is not possible. Fouling

occurs if a critical flux is exceeded. Chang et al. (2002) defined the critical flux as the highest flux for which the transmembrane pressure remains constant based on data from a step-by-step increase in flux, depending on the type of membrane material, MLSS and cross-flow velocity. However, there is a transition between concentration polarization and stagnant cake formation (Chen et al. 1997). For a relatively high $c_3$, polymerization and precipitation can occur, resulting in solid cakes. To a certain extent, nearly every feed component leads to membrane fouling.

The formation of surface deposits on membranes is influenced by feed composition, flow conditions, the chemical nature of the membrane and interactions between components and the membrane. The type of fouling depends on the nature of deposit components (Fleming 1995). We distinguish:

- Scaling or mineral fouling is the deposit of inorganic material with crystal structures like salts.
- Organic fouling is the deposit of organic material like grease, oil, surfactants, proteins and humic substances.
- Colloidal fouling is the deposit of particles like clay and metal-oxides or hydroxides.
- Bio-fouling is the formation of bio-films by microorganisms captured and growing at the surface. A secondary phenomenon is the excretion of enzymes and extracellular polymeric substances (EPS) which influence the gel layer.

Deposits which can be detached by cleaning processes, like back-flushing and mechanical cleaning, are called reversible fouling and cause a reversible gel layer formation. Deposits which lead to an irreversible gel layer formation can only be removed by chemical cleaning procedures and are called irreversible fouling (Rautenbach and Albrecht 1989). Therefore, fouling can be controlled only to a certain degree by hydrodynamics.

Different fouling mechanisms are shown in Fig. 12.9. An irreversible sludge cake layer is formed by particles, contaminants and agglomerates of contaminants which are bigger than the pore size of the membrane.

Due to the heterogeneous nature of bioreactors, mixed liquor fouling is difficult to predict and control in a MBR. Factors affecting fouling are (Chang et al. 2002; Lee et al. 2003; Rosenberger 2003; Shon et al. 2004):

- The membrane material hydrophobicity, porosity and pore size and distribution.
- The mass of microorganism MLSS and of extra-cellular polymeric substances EPS, floc structure, dissolved matter and floc size.
- The operating conditions e.g. configuration, cross flow velocity, aeration, hydraulic and solid retention time and trans-membrane pressure.

#### 12.4.3.2 **Membrane Cleaning Strategies**

To reduce the two negative influences of concentration polarization and decreasing flux rates which result from fouling, a cleaning strategy has to be developed together with the membrane suppliers which is adapted to the wastewater characteristics, the membrane material and the configuration of the membrane filtration

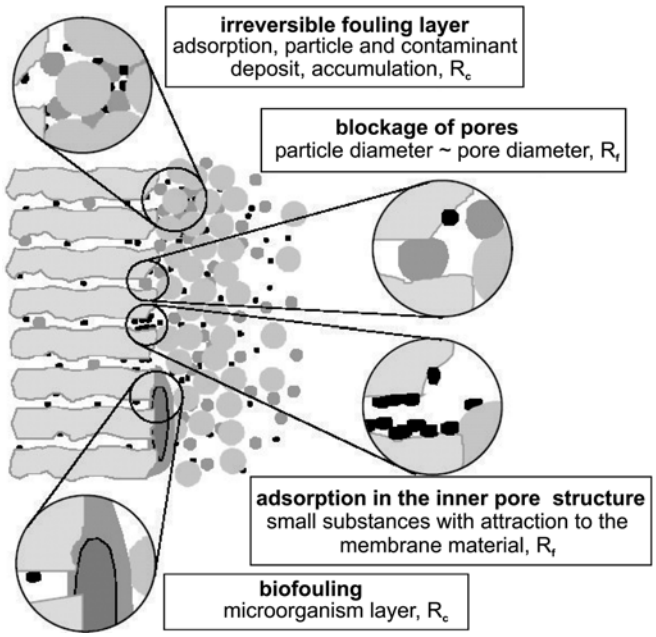


**Fig. 12.9** Fouling mechanisms, adapted from Melin and Rautenbach (2004).

process. In general, process integrated back-flushing during the filtration process is used to maintain a constant flux. Periodically *in situ* cleaning with chemicals and intensive washing with chemicals *ex situ* are necessary to remove irreversible deposits.

MBR processes in submerged or cross-flow mode often use fixed-interval back-washing or back-flushing with permeate, whereby reverse flow is used to wash-out reversible fouling. Usually, a filtration process cycle of about 10 min is followed by a back-washing time of 1 min, resulting in a water recovery of at least 90% as shown in Fig. 12.8. Experiments are necessary to optimize two factors: (a) permeate loss by back-washing and (b) the slight decrease in permeate flux which requires maintenance cleaning to recover 100% flux. In submerged systems, intensified aeration in a range of 0.21–3.0 $m^3\ m^{-2}\ h^{-1}$ is also used to prevent fouling (Benedek and Côté 2003; Cornel et al. 2001).

Maintenance cleaning is done at longer intervals with various chemicals. The chemicals used and the interval chosen must be specifically adapted to the range of application to avoid membrane damage or the formation of harmful substances (ATV-DVWK 2002b). Chemical cleaning usually restores the permeate flux but produces a certain amount of contaminated water.

*In situ* chemically enhanced cleaning procedures (intermediate cleaning) are used in MBR processes if the flux decreases by about 20% down to 100 $L\ m^{-2}\ h^{-1}\ bar^{-1}$, or as dictated by a cleaning management time table.

Acidic solutions are used particularly for the elimination of inorganic fouling causing substances and alkaline solutions for the oxidation of organic foulants. Disinfectants may be used to eliminate microorganisms. Commonly used commercial purifiers contain active chlorine concentrations between 300 mg $L^{-1}$ (Wehrle Umwelt 2005) and 2000 mg $L^{-1}$ (MUNLV 2003), or may contain special mixtures of acids, leaching agents, surfactants, active enzymes (Berghof 2005) or hydrogen peroxide (AV Aggerwasser 2005). Tests are also often performed with citric acid, NaOH, HCL, oxalic acid (Wozniak 2003) and nitro-hydrochloric acid. Sodium hypochlorite is known to recover total permeability, but its use is decreasing because of the damage caused to microorganisms at high concentrations (MUNLV 2003). Heating of the purifiers, sometimes in a separate tank, may be necessary to reach the required cleaning temperature of 35–40 °C.

An intensive *ex situ* cleaning (main cleaning) is necessary at least twice a year. The typical cleaning management program combines alternating chemical cleaning and clean water rinsing for neutralization and a reaction procedure enhanced with chemicals.

## 12.5 Membrane Bioreactors

### 12.5.1 Final Treatment (Behind the Secondary Clarifier)

The methods of industrial and municipal wastewater treatment have already achieved a high standard by combining biological and mechanical processes and additional treatment steps for the elimination of phosphorus and nitrogen (see Chapter 10). However, the microbiological quality of effluents is still a burden for surface waters. Pathogens like bacteria, viruses and parasites are a problem, particularly for bathing waters in summer, or in areas with drinking water reservoirs. There are different standards in effect, such as the EU Water Framework Directive (EU 2000) with the aim to reach a high ecological water quality by 2015, or the EEC Council Directive 76/160/EEC of 8 December 1975 concerning the quality of bathing waters (EEC 1991; Table 12.6).

Ultra- and microfiltration are of high interest as a post-treatment method after sedimentation, and recently, as an alternative to the traditional gravity settlers used in municipal wastewater treatment to meet the quality standards mentioned above.

The high efficiency of membrane systems as a final treatment in municipal WWTP was investigated and proven by Altmann et al. (1995) in Berlin–Ruhleben. In pilot-scale experiments, five different membrane systems were investigated in combination with phosphate precipitation. Microorganisms were found to be eliminated by a factor of several orders of magnitude and viruses were typically adsorbed on suspended solids, which were eliminated (see Fig. 12.10 in Section 12.5.2). An alternative is to couple biological treatment with sand filtration.

**Table 12.6** Requirements for post treatment of effluents from WWTP Microbiological Standard in EEC Council Directive 76/160/EEC of 8 December 1975 concerning the quality of bathing water (EEC 1991).

| Parameter | Imperative value | Guide value |
|---|---|---|
| Total coliform bacteria (cells/100 mL) | 500 | 10 000 |
| Fecal coliform bacteria (cells/100 mL) | 100 | 2 000 |
| *Streptococcus faecalis* (cells/100 mL) | 100 | – |
| Salmonella (cells/1 L) | – | 0 |
| Bowel viruses (PFU/10 L) | – | 0 |

### 12.5.2 Membrane Bioreactors in Aerobic Wastewater Treatment

The combination of biological and membrane filtration processes is known as a membrane bioreactor (MBR) system. The benefits of MBR systems in submerged or external cross-flow mode are (ATV-DVWK, 2000b; DWA 2005):

- High microbiological quality of effluent water resulting from the high removal efficiency of suspended solids, microorganisms and viruses.
- Greater freedom to vary process parameters, like the reduction of excess sludge or the concentration of slowly growing organisms because MBR systems are independent on the sedimentation behavior of sludge.
- Volume reduction of the activated sludge tank because of higher biomass concentration and elimination of the sedimentation tank, both resulting in a reduction of the total plant footprint (Côté and Liu 2003).

The financial success of MBR is largely determined by the processes used to restore decreased flux caused by fouling. The resulting disadvantages of MBR are the high investment cost for the needed membrane surface area and/or high operating costs for cleaning management and the energy demand for cross-flow mode on top of the cost for supplying oxygen to microorganisms (Choi 2005; DWA 2005).

The discharge of harmful substances, like endocrine-disrupting substances (EDS) into municipal and industrial wastewater and their passage through WWTP has also been investigated (Filali-Meknassi et al. 2004). Reverse osmosis and nanofiltration processes are able to reject EDS (Fig. 12.1), but sorption was found to be the main elimination process in sewage and industrial wastewater treatment, hence the elimination efficiency was high for MBR (Kunst 2002; Gallenkemper et al. 2003; Schäfer et al. 2003; Oschmann et al. 2005).

Recently, submerged membranes have been applied in large-scale activated sludge plants more and more often because of the economical advantages of low pressure processes. By 2004, several commercial municipal WWTP in Germany had been built with submerged MBR systems for more than 100 000 inhabitants; and common permeate fluxes are 8–30 L $(m^2\ h)^{-1}$. The percentage of submerged systems is still increasing, evidently for small-scale systems (Bischof et al. 2005; Brinkmeyer et al. 2005).

Figure 12.10 gives an overview of the membrane filtration process in comparison with conventional wastewater treatment.

In cross-flow mode (Fig. 12.10c), the higher operational pressure of about 3 bar is provided by pressure pumps and a loop or recycling stream is used to increase shear at the membrane surface to attain high fluxes (e.g. BIOMEMBRAT used in activated sludge plants of food industries). Air bubbling and periodic back-flushing is possible. To date, no application of cross-flow mode in municipal WWTPs has been realized.

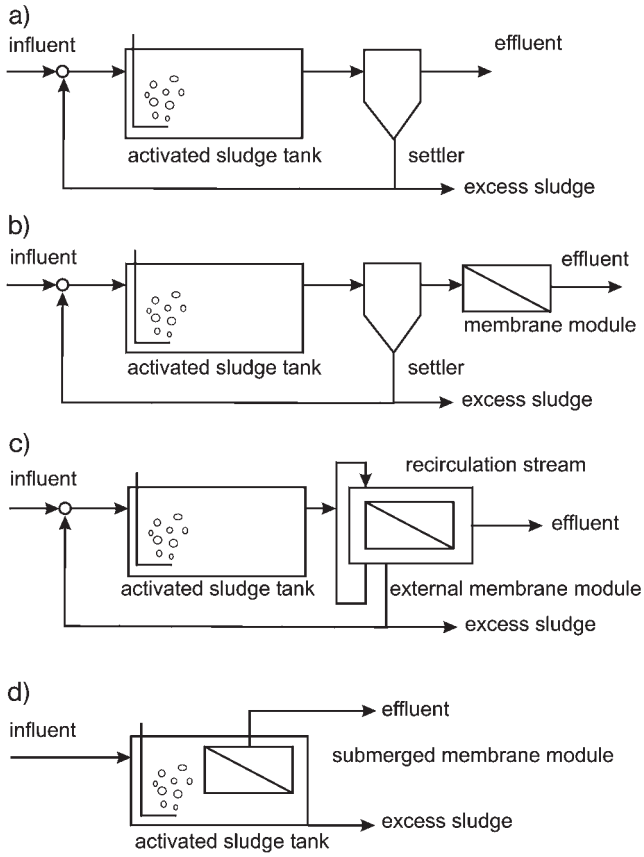


**Fig. 12.10** MBR systems, external and submerged mode in comparison with a conventional activated sludge system.

**Table 12.7** Performance characteristic of conventional activated sludge process and MBR (Günder 1999; ATV-DVWK 2000b; Cornel et al. 2001; Côté and Liu 2003; MUNLV 2003).

| Parameter | | Conventional WWTP | MBR |
|---|---|---|---|
| X | g $L^{-1}$ MLSS | <5 | 8.0–16.0 |
| $t_{RX}$ | d | 15 | 15.0 |
| $t_R$ | h | 23 | 3.6–8.0 |
| $B_X$ | kg $BSB_5$ $kg^{-1}$ $d^{-1}$ MLSS | <0.08 | <0.08 |
| $\alpha$, $O_2$ transfer ratio | – | 0.6 | 0.6 |
| *Effluent data* | | | |
| S | mg $L^{-1}$ COD | 40–50 | <30.0 |
| $N_{ges}$ | mg $L^{-1}$ | <13 | <13.0 |
| $P_{ges}$ | mg $L^{-1}$ | 0.8–1.0 | <0.3 |
| $X_e$ | mg $L^{-1}$ MLSS | 10–15 | 0 |
| Microbiological quality | – | Hygienically critical | Bathing water quality |

In the submerged mode (Fig. 12.10d), the membrane modules are directly installed in the activated sludge bioreactor or immersed in an aerated separate container (e.g. ZeeWeed-Cassettes; Cornel et al. 2001). Air bubbling plays a significant role in attaining high fluxes (Section 12.4.3) and periodic back-flushing is used to reduce fouling.

The retention efficiency of the separation process is not influenced by gas bubbles, floating sludge or bulky flocs with lower density. Performance characteristics of MBR systems are given in Table 12.7 in comparison with conventional WWTP. The minimum solid retention time with nitrification is 15 d for both systems, according to ATV-DVWK (2000a).

In the case of a MBR, the retention time of the sludge is unaffected by sedimentation behavior (Fig. 12.10c, d) and very high sludge ages (see Section 6.2.3) can be reached; but for municipal WWTP sludge ages of 15 d and sludge concentration of 8–16 g $L^{-1}$ MLSS are common (Table 12.8). Activated sludge with such high concentration exhibits non-Newtonian behavior, the apparent viscosity is a function of g $L^{-1}$ MLSS as well as shear gradient and affects both oxygen mass transfer and the degree of mixing (Rosenberger 2003; Kubin 2004; Choi 2005). The relative oxygen transfer ratio $\alpha_w$ (see Eq. 5.12) for different WWTP under operational conditions is found to be in the range of 0.25 to 0.8 for X and the range of 1–17 g $L^{-1}$ MLSS (Cornel et al. 2001; Drews and Kraume 2005; DWA 2005).

Removal efficiency rises with increasing MLSS concentration, but a maximum removal of 96–97% cannot be exceeded. COD removal efficiency was summarized by Kubin (2004) and Drews and Kraume (2005).

We summarize data for some German MBRs in the field of municipal wastewater treatment in Table 12.8. These all operate with submerged membrane modules. The positive experience gained over several years of operation has led to fur-

**Table 12.8** Membrane bioreactors in municipal wastewater treatment plants, submerged mode (Engelhardt 2003; Stein 2003; Voßenkaul et al. 2003; MUNLV 2003; Wozniak 2003; De Wilde et al. 2005; Roest et al. 2005; Rondi and Montagnoli 2005).

| Year | WWTP operator | Company, membrane, configuration, submerged mode | Q $m^3h^{-1}$) | $A_M$ ($10^3$ $m^2$) |
|---|---|---|---|---|
| 1999 | Rödingen Erftverband | Zenon, hollow fiber | 135 | 4.846 |
| 2004 | Nordkanal Erftverband | Zenon, hollow fiber | 1881 | 85 |
| 1999 | Büchel Aggerverband | Kubota, plate membrane | 40 | 0.96 |
| 2004 | Seelscheid Aggerverband | Kubota, plate membrane | 356 | 12.48 |
| 2000 | Markranstädt kommunale Wasserwerke Leipzig | Zenon, hollow fiber | 180 | 8.8 |
| 2002 | Knautnaundorf kommunale Wasserwerke Leipzig | Martin System AG, rotating plate membrane | 23 | 0.756 |
| 2004 | Markkleeberg kommunale Wasserwerke Leipzig | Zenon, hollow fiber | 710 | 28.4 |
| 2003 | Simmerath Wasserverbd. Eifel-Ruhr | Puron, hollow fiber | Bypass | 1.0 |
| 2003 | Monheim Stadt Monheim | Zenon, hollow fiber | 288 | 12.32 |
| 2004 | Waldmössingen Stadtwerke Schramberg | Zenon, hollow fiber | 90 | 5.3 |
| 2003 | Schilde (Belgium) | Zenon, hollow fiber | 355 | 10.56 |
| 2003 | Brescia (Italy) | Zenon, hollow fiber | 1750 | – |
| 2004 | Varsseveld (The Netherlands) | Zenon, hollow fiber | 755 | 20.16 |

ther applications. For example, in WWTP Markranstädt (Stein 2003) the hollow fiber membrane filtration modules are located in the upper part of the nitrification tank. Mixing units are installed together with aeration to reduce fouling. An *ex situ* cleaning shaft located between the nitrification lines is in place to take up the modules for the cleaning procedures. Another concept is followed with separated membrane filtration containers in WWTP Büchel (Wozniak 2003) and WWTP Rödingen (Engelhardt 2003). These filtration containers are aerated and the wastewater is recycled between the nitrification and denitrification tanks and the filtration containers, where nitrification also takes place.

Experience with the WWTPs mentioned above has shown the importance of an intensive pre-treatment of wastewater by filtration. To reduce membrane fouling by the deposit of particles, it is necessary to perform additional pre-treatment of wastewater with a grid or a sieve <1 mm (Engelhardt 2003; Stein 2003; DWA 2005). Especially the fibrous components of the untreated wastewater leave deposits in the upper part of hollow fiber modules.

The costs associated with MBR systems operating in cross-flow and submerged mode have been analyzed by Melin and Rautenbach (2004), who showed in estimated overall operating cost of 0.57 € $m^{-3}$ for cross-flow mode and 0.56 € $m^{-3}$ for submerged mode in sewage WWTP at small scales with volume rates of 100 $m^3$ $h^{-1}$. Overall operational costs for existing MBRs in wastewater treatment in the food industries were found to be 0.90 € $m^{-3}$ (Wienands and Streif 2005), while the highest costs of cross-flow mode come from the energy consumption and the highest costs for submerged mode result from the investment in the membrane. The energy consumption of submerged systems has been measured between 0.8 kWh $m^{-3}$ and 4 kWh $m^{-3}$. Optimization of the aeration management leads to a reduction of energy consumption by about 35% and a consumption of less than 1 kWh $m^{-3}$ has been predicted (Engelhardt 2003).

### 12.5.3
### Membrane Bioreactors and Nutrient Removal

To achieve nitrogen removal with a MBR system, aerobic–anoxic operation conditions are necessary as in the conventional process (see Section 10.4.2). A MBR offers good nitrification conditions because of the high retention of sludge allowed. Therefore, even slowly growing nitrifying bacteria have an excellent chance to establish themselves in the aerated tank. Nitrogen removal with preliminary denitrification (see Fig. 10.9a) and with post-denitrification (see Fig. 12.11b) is in operation with MBRs (Brepols et al. 2005). Investigations have also been performed in small-scale applications with post-denitrification without dosage of a carbon source (Gnirß 2005; Maas 2005).

The high oxygen transfer associated with submerged membranes creates a need for a larger denitrification zone (Engelhardt 2003; Gnirß et al. 2003; MUNLV 2003). In the case of post-denitrification, the membrane modules are located in a separate container behind the anoxic zone with optiomal aeration to avoid sludge cake formation (Adam 2004; Drews et al. 2005).

Phosphorus elimination by simultaneous precipitation is a well known technique in conventional wastewater treatment and is also used in MBR. The high MLSS retention efficiency of the membrane process significantly reduces the discharge of coagulant chemicals and leads, therefore, to less loading of rivers. In surface water processing, Dietze (2004) achieved low phosphate concentrations (<15 µg $L^{-1}$ $PO_4$-P) in permeate using phosphorus flocculation and membrane filtration while reducing the coagulant and salts discharge, compared to traditional flocculation and sand filtration.

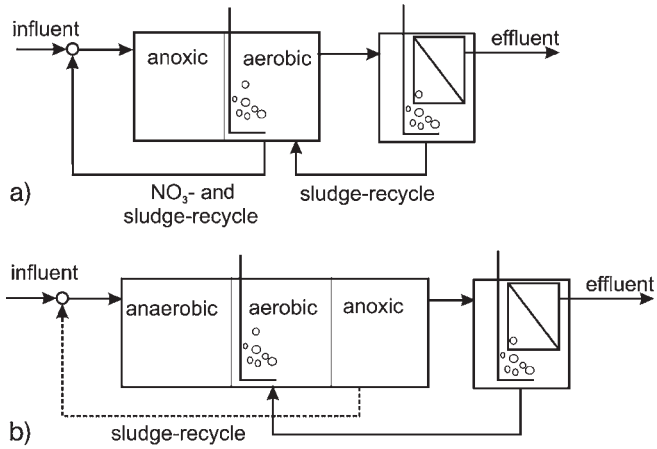


**Fig. 12.11** MBR and nutrient removal with submerged membranes with: (a) preliminary denitrification, (b) post-denitrification without substrate dosage and with biological phosphorus removel.

Investigations have been conducted to combine biological phosphorus elimination with an anaerobic zone, not only in WWTP (Section 10.4.3, Fig. 10.9a) but also in the MBR process to reduce the use of chemicals like $FeCl_3$. The question remains whether the high sludge ages used in MBR yield higher phosphorus elimination capacities. The high retention of MLSS and the prevention of phosphorus release caused by the high oxygen concentration in the MBR system lead to a high efficiency (Gnirß et al. 2003). Orthophosphates from release cannot be retained by ultrafiltration membranes (Adam 2004).

**PROBLEM 12.1**

When do we have to consider the impact of osmotic pressure?
Calculate the osmotic pressure for two aqueous solutions, considering complete retention ($c_2 = 0$ mg $L^{-1}$) and neglecting concentration polarization. The feed contains 15 g $L^{-1}$ NaCl and 15 g $L^{-1}$ glucose (T = 288.2 K, R = 8.31 J $mol^{-1}$ $K^{-1}$).

**Solution**

NaCl, molar mass M = 58 g $mol^{-1}$, the osmotic pressure increases as a result of dissociation as the number of moles increases (Rautenbach and Albrecht 1981). For complete dissociation of NaCl β = 2 follows, we obtain from Eq. (12.24b):

$$\Delta\Pi = \frac{2 \cdot 15 \cdot 8.31 \cdot 288.2}{58} \frac{\text{g J mol K}}{\text{L g mol K}} = 12.4 \frac{10^5 \text{ J}}{\text{m}^3} = 12.4 \frac{10^5 \text{ N}}{\text{m}^2} = 12.4 \text{ bar}$$

Glucose, molar mass M = 181 g mol$^{-1}$. At the cut-off of nanofiltration membranes, we obtain from Eq. (12.24a):

$$\Delta\Pi = \frac{15 \cdot 8.31 \cdot 288.2}{181} \frac{\text{g J mol K}}{\text{L g mol K}} = 198 \frac{\text{J}}{\text{L}} = 2 \frac{10^5 \text{ J}}{\text{m}^3} = 2 \frac{10^5 \text{ N}}{\text{m}^2} = 2 \text{ bar}$$

Considering concentration polarization and increasing concentration of the feed in the direction of flow, the osmotic pressure increases. For particles like bacteria or colloids >10 000 g mol$^{-1}$, the influence of osmotic pressure is negligible.

## PROBLEM 12.2

What membrane surface area is required for a WWTP for 100 000 inhabitants, considering permeate fluxes $J_{p10}$ at 10 °C? ($J_{p8}$ = 25 L m$^{-2}$ h$^{-1}$)
The common design method of a WWTP is based on ATV-DVWK-Arbeitsblatt A 131 (ATV-DVWK 2000a). The maximum flow rate $Q_m$ is determined by the dry-weather flow $Q_s$ and the average wastewater from other areas $Q_f$. According to ATV-DVWK-Arbeitsblatt A 198 (ATV-DVWK 1992), the flow rate is given by:

$$Q_m \geq 2\,Q_s + Q_f \text{ L s}^{-1} \tag{12.79}$$

To determine the maximum inlet flow rate $Q_m$ we choose:

$$Q_m = 3.5\,Q_s + Q_f \tag{12.80}$$

$Q_s$ is the average sewage flow rate according to the median discharge per household, commercial and industrial wastewater, here for 100 000 inhabitants, with a specific volume rate of inhabitants (inh.) of 130 L (inh. d)$^{-1}$.
$Q_f$ is annual average extrameous wastewater from other areas, here we choose 6000 m$^3$ d$^{-1}$.

### Solution

For 100 000 inhabitants, $Q_m$ is given by:

$$Q_m = \frac{3.5 \cdot 130 \cdot 100\,000 \cdot 10^{-3} + 6000}{24} \frac{\text{L inh. d}}{\text{inh. d h}} \cdot \frac{\text{m}^3 \text{ d}}{\text{d h}} = 2146 \text{ m}^3 \text{ h}^{-1}$$

while the average daily flow rate $Q_d$ (dry-weather flow) is:

$$Q_d = Q_s + Q_f \tag{12.81}$$

The required permeate flow rate of a membrane module has to equal the maximum volume rate $Q_m$; and the required membrane surface area $A_M$ can be determined from permeate flux of common membrane modules. At 8 °C, a flux of $J_{p8}$ = 25 L m$^{-2}$ h$^{-1}$ is given. For higher temperatures (here 10 °C) the flux is about 15% higher than at 8 °C (MUNLV 2003), resulting in:

$$J_{p10} = 1.15 \cdot 25 \text{ L m}^{-2} \text{ h}^{-1} = 28.75 \text{ L m}^{-2} \text{ h}^{-1}$$

According to Eq. (12.5), the required membrane surface area $A_M$ follows:

$$A_m = \frac{Q_m}{J_{p10}} = \frac{2146}{28.75} \cdot \frac{m^3\ m^2\ h}{L\ h} = 74\,638\ m^2$$

For maintenance cleaning twice a year, the complete membrane area is taken out of operation. Each cleaning procedure lasts about 1 day; the effective membrane area is in operation, therefore, only 363 days year$^{-1}$ or about 99% of the time. To realize the required flux, the total membrane surface area $A_t$ must be 101% of $A_M$.

$$A_t = A_M + 0.01\ A_M = 75.4 \cdot 10^3\ m^2$$

**PROBLEM 12.3**

How different are the volumes of a MBR and an activated sludge tank, for the same treatment task with nitrification?
Conditions with full nitrification require sludge ages of more than 15 days (ATV-DVWK 2000). The common method for a single-step activated sludge process is based on the sludge loading rate $B_X$ (Günder 1999):

$$B_X = \frac{S\ Q_d}{V\ X}\ \text{kg BOD}_5\ (\text{kg MLSS d})^{-1} \tag{12.82}$$

where $B_X$ is the sludge loading rate, $Q_d$ is the dry-weather flow rate according to Eq. (12.81) = 19 000 m$^3$ d$^{-1}$, X is the concentration of bacteria and S is the concentration of substrate (we choose 400 mg L$^{-1}$ $BOD_5$). For the MBR we choose $B_X$ = 0.03 kg $BOD_5$ (kg MLSS · d)$^{-1}$ and for a conventional plant a higher loading rate of 0.06 kg $BOD_5$ (kg MLSS · d)$^{-1}$.

**Solution**

Under the assumptions of no oxygen limitation and identical percentage of living bacteria, an approach for processes with and without membrane is given by:

1. With the membrane, the concentration of microorganisms is in the range of 8–16 g L$^{-1}$ MLSS. We choose X = 12 g L$^{-1}$ MLSS (Table 12.7). The volume of the aerated sludge tank for MBR follows from Eq. (12.82):

$$V = \frac{S\ Q_d}{X\ B_X} = \frac{0.4 \cdot 19\,000}{12 \cdot 0.03} \frac{m^3\ kg\ m^3\ kg\ d}{kg\ m^3\ d\ kg} = 21.1 \cdot 10^3\ m^3$$

2. In the conventional activated sludge process under the same conditions of S and $Q_d$, the attainable concentration of microorganisms is X = 3 g L$^{-1}$ MLSS and a higher sludge loading rate of 0.06 kg $BOD_5$ (kg MLSS d)$^{-1}$ (Table 12.7) is possible. The volume of the single-step activated sludge tank is:

$$V = \frac{S\ Q_d}{X\ B_X} = \frac{0.4 \cdot 19\,000}{3 \cdot 0.06} \frac{m^3\ kg\ m^3\ kg\ d}{kg\ m^3\ d\ kg} = 42.2 \cdot 10^3\ m^3$$

## References


Achtabowski, A., Neuhaus, O. **2005**, Das PAA-Membranbelebungsverfahren – Konzeption und erste Betriebserfahrungen mit der großtechnischen Anlage, *10th Aachen Membrane Colloquium*.

Adam, C. **2004**, Weitgehende Phosphor- und Stickstoffelimination in einer Membranbelebung mit nachgeschalteter Denitrifikationsstufe, *VDI-Forschungsberichte, Reihe 15*, 250.

Altmann H.-J., Dittrich J., Gnirß R., Peter-Fröhlich A., Sarfert F. **1995**, Mikrofiltration von kommunalem Abwasser zur Keim- und P-Entfernung, *Korrespondenz Abwasser*, 42, 758–769.

ATV-DVWK **1992**, Arbeitsblatt A 198 (Abwassertechnische Vereinigung – Deutsche Vereinigung für Wasserwirtschaft, Abwasser und Abfall e.V.), *Vereinheitlichung und Herleitung von Bemessungswerten für Abwasseranlagen*, Gesellschaft zur Förderung der Abwassertechnik GFA, St. Augustin.

ATV-DVWK **2000a**, Arbeitsblatt A 131 (Abwassertechnische Vereinigung – Deutsche Vereinigung für Wasserwirtschaft, Abwasser und Abfall e.V.), *Bemessung von einstufigen Belebungsanlagen*, Abwassertechnische Vereinigung, Hennef.

ATV-DVWK **2000b**, (Abwassertechnische Vereinigung – Deutsche Vereinigung für Wasserwirtschaft, Abwasser und Abfall e.V.), Membranbelebungsverfahren, *Arbeitsbericht des ATV-DVWK Fachausschuss KA-7, KA-Wasserwirtschaft, Abwasser, Abfall*, 47, 1547–1553.

ATV-DVWK **2002a**, (Abwassertechnische Vereinigung – Deutsche Vereinigung für Wasserwirtschaft, Abwasser und Abfall e.V.), Aufbereitung von Industrieabwasser und Prozesswasser mit Membranverfahren und Membranbelebungsverfahren, *Arbeitsbericht der ATV-DVWK-Arbeitsgruppe IG 5.5, Membrantechnik, Teil 1: Membranverfahren, KA-Wasserwirtschaft, Abwasser, Abfall*, 49, 1423–1431.

ATV-DVWK **2002b**, (Abwassertechnische Vereinigung- deutsche Vereinigung für Wasserwirtschaft, Abwasser und Abfall e.V.), Aufbereitung von Industrieabwasser und Prozesswasser mit Membranverfahren und Membranbelebungsverfahren, *Arbeitsbericht der ATV-DVWK-Arbeitsgruppe IG 5.5, Membrantechnik, Teil 2: Aerobe Membranbelebungsverfahren, KA-Wasserwirtschaft, Abwasser, Abfall*, 49, 1563–1571.

AV Aggerwasser **2005**, AWK Membrantechnik, chemische Reinigung, *Firmenmitteilung*, AV Aggerwasser GmbH.

Benedek, A., Côté, P. **2003**, Long term experience with hollow fibre membrane bioreactors, *International Desalination Association* BAH03-180, 1–5.

Berghof **2005**, Berghof Filtrations- und Anlagentechnik, Reinigungs- und Konservierungsanleitung für Berghof Rohrmodule mit Stützrohr und austauschbaren Membranen zur cross-flow Filtration, *Firmenmitteilung*.

Bischof, F.; Meuler, S.; Hackner, T.; Reber, R. **2005**, Einsatz und Erfahrung mit Membranbiologien im ländlichen Raum-Praxiserfahrungen mit Kleinkläranlagen, *KA-Abwasser, Abfall*, 52, 164–169.

Brepols, C.; Schäfer, H.; Engelhardt, N. **2005**, Hinweise zur verfahrenstechnischen Integration getauchter Membranfilter in kommunalen Membranbelebungsanlagen, *KA-Abwasser, Abfall*, 52, 45–50.

Brinkmeyer, J.; Rosenwinkel, K.-H.; Flasche, K.; Koppmann, M.; Austermann-Haun, U. **2005**, Einsatz und Erfahrungen mit Membranbiologien im ländlichen Raum-Bedeutung und Chancen für die Verwendung in Kleinkläranlagen, *KA-Abwasser, Abfall*, 52, 158–163.

Cabbasud C.; Laborie S.; Durand-Bourlier L.; Laine J.M. **2001**, Air sparging in ultrafiltration hollow fibres: relationship between flux enhancement, cake characteristics and hydrodynamic parameters, *Journal of Membrane Science*, 181, 57–69.

Carman, P.C. **1956**, *Flow of Gases Through Porous Media*, Butterworths Scientific Publications, London.

Chang I. S.;Fane A.G. **2000**, Filtration of biomass with axial inter-fibre upward slug flow: performance and mechanism, *Journal of Membrane Science*, 180, 57–68.

Chang, I. S.; Clech, P.; Jefferson, B.; Judd, S. **2002**, Membrane fouling in membrane bioreactors for wastewater treatment, *Journal of Environmental Engineering*, 2002, 1018–1029.

Chen, V., Fane, A.G., Madaeni, S., Wenten, I.G. **1997**, Particle deposition during membrane filtration of colloids: transition between concentration polarization and cake formation, *Journal of Membrane Science*, 125, 109–122.

Choi, I. S. **2005**, Aerobic degradation of surfactant and nitrification in a membrane bioreactor (MBR) with $CO_2$ and $O_2$ gas analysis, *VDI-Forschungsberichte, Reihe 3*, 838.

Cornel, P.; Wagner, M.; Krause, S. **2001**, Sauerstoffeintrag in Membranbelebungsanlagen, *4. Aachener Tagung Siedlungswasserwirtschaft und Verfahrenstechnik, Membrantechnik in der Wasseraufbereitung und Abwasserbehandlung*, Aachen, A14.

Côté, P; Liu, M. **2003**, Immersed membranes options for water reuse, *International Desalination Association* BAH03-066, 1–14.

Darcy, H. **1856**, *Distribution d'Eau, le Fountaines Publiques de la Ville de Dijon*, Paris.

De Wilde W.; Thoeye, C.; De Gueldre, G. **2005**, Operational experiences and optimisations two years after star-up of the first full-scale MBR for domestic wastewater treatment in the Benelux, *6. Aachener Tagung Siedlungswasserwirtschaft und Verfahrenstechnik, Membrantechnik in der Wasseraufbereitung und Abwasserbehandlung*, Aachen, A5.

Dietze, A. **2004**, Oberflächenwasseraufbereitung durch Membranfiltration: Einsatz der Fällung/Flockung mit anschließender Ultrafiltration zur Phosphateliminierung, *VDI-Forschungsberichte, Reihe 3*, 813.

Drews, A.; Kraume, M. **2005**, Process improvement by application of membrane bioreactors, *Chemical Engineering Research and Design*, 83, 1–9.

Drews, A., Vocks, M.; Iversen, V., Lesjean, B., Kraume, M. **2005**, Fouling in Membranbelebungsreaktoren: Erfahrungen beim Betrieb mit diskontinuierlichem Schlammabzug, *Chemie Ingenieur Technik*, 77, 593–599.

DWA **2005**, Membranbelebungsverfahren, 2. Arbeitsbericht des DWA Fachausschuss KA-7, *KA-Abwasser, Abfall*, 52, 322, draft.

EEC **1991**, *EEC Council Directive 76/160/EWG des Rates über die Qualität von Badegewässern* vom 8. Dezember 1975, ABl EG vom 5.2.1976 Nr. L31 S. 1, ABl EG vom 31.12.1991 Nr. L377 S. 48, in der Fassung vom 23. Dezember 1991.

Engelhardt, N. **2003**, Membranbelebungsverfahren – eine beherrschbare und erfolgreiche Technik – Erfahrungen nach vierjährigem Betrieb, *5. Aachener Tagung Siedlungswasserwirtschaft und Verfahrenstechnik, Membrantechnik in der Wasseraufbereitung und Abwasserbehandlung*, Aachen, A1.

EU **2000**, *EU Water Framework Directive 2000/60/EG des Europäischen Parlaments und des Rates* vom 23. Oktober 2000 zur Schaffung eines Ordnungsrahmens für Maßnahmen der Gemeinschaft im Bereich der Wasserpolitik, L327 S. 1, ABl EG vom 22.12. 2000.

Filali-Meknassi, Y.; Tyagi, R. D.; Surampalli, R. Y.; Barata, C.; Riva, M. C. **2004**, Endocrine-disrupting compounds in wastewater, sludge-treatment process, and receiving waters, *Overview, Practice Periodical of Hazardous, Toxic, and Radioactive Waste Management, ASCE*, 8, 39–56.

Fleming, H.-C. **1995**, *Biofouling bei Membranprozessen*, Springer-Verlag, Berlin, Heidelberg.

Fu, L.F.; Dempsey, B.A. **1998**, Modelling the effect of particle size and charge on the structure of the filter cake in ultrafiltration, *Journal of Membrane Science*, 149, 221–240.

Gallenkemper, M.; Salehi, F.; Melin, T. **2003**, Rückhalt endokrin wirksamer Substanzen mittels NF – Betriebsparameter und Modellierung, *5. Aachener Tagung Siedlungswasserwirtschaft und Verfahrenstechnik, Membrantechnik in der Wasseraufbereitung und Abwasserbehandlung*, Aachen, P8.

Geissler, S.; Melin, T.; Zhou, H.; Zytner, R. **2003**, Vorhersagemöglichkeiten im Hinblick auf die Filtrationsleistung von Membranbelebungsanlagen, *5. Aachener Tagung Siedlungswasserwirtschaft und Verfahrenstechnik, Membrantechnik in der Wasseraufbereitung und Abwasserbehandlung*, Aachen, A13.

Gnirß, R. **2005**, Semi-zentrale Erschließung eines Berliner Siedlungsgebietes mit einer Membranbelebungsanlage – Das Projekt ENREM, Vortrag auf der *5. Wasserwerk-*

*statt, Kolloquium des Kompetenzzentrums Wasser*, Berlin.

Gnirß, R.; Lesjean, B.; Buisson, H. **2003**, Biologische Phosphorentfernung mit einer nachgeschalteten Denitrifikation im Membranbelebungsverfahren, *5. Aachener Tagung Siedlungswasserwirtschaft und Verfahrenstechnik, Membrantechnik in der Wasseraufbereitung und Abwasserbehandlung*, Aachen, A17.

Goers, B. **2000**, Spülwassermanagement und Tensidrückgewinnung in Mehrproduktanlagen mit Membranverfahren, *VDI-Forschungsberichte, Reihe 3*, 671.

Günder, B. **1999**, Das Membranbelebungsverfahren in der kommunalen Abwasserreinigung, *Stuttgarter Berichte zur Siedlungswasserwirtschaft, 45*, Oldenbourg-Verlag, Munich.

Kubin, K. **2004**, Einfluss unterschiedlicher Verfahrenskonzepte auf Substratabbau und Nährstoffverwertung in Membranbelebungsanlagen zur kommunalen Abwasserreinigung (PhD thesis), TU Berlin.

Kunst, S. **2002**, Endokrin wirksame Substanzen in Kläranlagen – Vorkommen, Verbleib und Wirkung, *KA-Wasserwirtschaft, Abwasser, Abfall*, 49, 1572–1577.

Lee, W.; Kang, S.; Shin, H. **2003**, Sludge characteristics and their contribution to microfiltration in submerged membrane bioreactors, *Journal of Membrane Science*, 216, 217–227.

Linton, W.H.; Sherwood, T.K. **1950**, Mass transfer from solid phase to water in streamline and turbulent flow, *Chemical Engineering Progress*, 46, 258–264.

Maas, D. B2005, Life and Life+ – EU-Förderung auch für Projekte im Abwasserbereich, *KA-Abwasser, Abfall*, 52, 28–30.

Melin, T.; Rautenbach, R. **2004**, Membranverfahren, Grundlagen der Modul- und Anlagenauslegung, 2. Auflage, Springer-Verlag, Berlin, Heidelberg.

Melin, T.; Wintgens, T.; Rosen, J. **2001**, Ansätze zur Modellierung und Simulation von Membranbelebungsanlagen, *4. Aachener Tagung Siedlungswasserwirtschaft und Verfahrenstechnik, Membrantechnik in der Wasseraufbereitung und Abwasserbehandlung*, Aachen, P16.

Mulder, M. **2000**, *Basic Principles of Membrane Technology*, 2nd ed., Kluwer Academic Publishers, Dordrecht, ISBN 0-7923-4247-X (HB).

MUNLV **2003**, Ministerium für Umwelt und Naturschutz, Landwirtschaft und Verbraucherschutz des Landes Nordrhein-Westfalen, *Abwasserreinigung mit Membrantechnik, Membraneinsatz im kommunalen und industriellen Bereich*, Hrsg. MUNLV, Düsseldorf.

Oschmann, N.; Nghiem, L.D.; Schäfer, A.I. **2005**, Fouling mechanism of submerged ultrafiltration membranes in greywater recycling, *Desalination* 179, 215–233.

Rautenbach, R. **1997**, *Membranverfahren, Grundlagen der Modul- und Anlagenauslegung*, Springer-Verlag, Berlin, Heidelberg.

Rautenbach, R.; Albrecht, R. **1981**, *Membrantrennverfahren, Ultrafiltration und Umkehrosmose*, Salle+Sauerländer.

Rautenbach, R.; Albrecht, R. **1989**, *Membrane Processes*, John Wiley & Sons, Chichester, New York, Brisbane, Toronto, Singapore.

Roest van der, H.F.; Bentem van, A.G.N.; Schyns, Ir.P.; Petri, C. **2005**, Uijterlinde, Varsseveld: Dutch full scale demonstration of MBR-progress, *6. Aachener Tagung Siedlungswasserwirtschaft und Verfahrenstechnik, Membrantechnik in der Wasseraufbereitung und Abwasserbehandlung*, Aachen, A4.

Rondi, S.; Montagnoli, T. **2005**, Two years of operation of a 42,000 $m^3$/d MBR process: the case of ASM Brescia (Italy), *6. Aachener Tagung Siedlungswasserwirtschaft und Verfahrenstechnik, Membrantechnik in der Wasseraufbereitung und Abwasserbehandlung*, Aachen, A2.

Rosenberger, S. **2003**, Charakterisierung von belebtem Schlamm in Membranbioreaktoren zur Abwasserreinigung, *VDI-Forschungsberichte, Reihe 3*, 769.

Schäfer, A.; Wintgens, T.; Gallenkemper, M.; Melin, T. **2003**, Rückhalt hormonell wirksamer Spurenschadstoffe durch Membranverfahren, *5. Aachener Tagung Siedlungswasserwirtschaft und Verfahrenstechnik, Membrantechnik in der Wasseraufbereitung und Abwasserbehandlung*, Aachen, A16.

Shon, H.K.; Vigneswaran, S.; Kim, I.S.; Cho, J.; Ngo, H.H. **2004**, Effect of pretreatment on the fouling of membranes: application in biologically treated sewage effluent, *Journal of Membrane Science*, 234, 111–120.

Stein, S. **2003**, Betriebserfahrungen mit unterschiedlichen Membrantechniken ZeeWeed und VRM, *5. Aachener Tagung Siedlungswasserwirtschaft und Verfahrenstechnik, Membrantechnik in der Wasseraufbereitung und Abwasserbehandlung*, Aachen, A6.

Stephenson, T.; Judd, S.; Jefferson, B.; Brindle K. **2000**, *Membrane Bioreactors for Wastewater Treatment*, IWA Publishing, London.

Taha T.; Cui Z.F. **2002**, CFG modelling of gas sparged ultrafiltration in tubular membranes, *Journal of Membrane Science*, 210, 13–27.

VDMA **2005**, VDMA-Einheitsblatt, *Membrananlagen in der Wasser- und Abwassertechnik Hinweise für die Auswahl, Projektierung und Ausrüstung*, VDMA 24653, Beuth Verlag, Berlin.

Voßenkaul, K.; Schäfer, S.; Kullmann, C. **2003**, Das Puron-Membran-System – neue Konzepte für die membrangestützte Wasseraufbereitung und Abwasserbehandlung, *5. Aachener Tagung Siedlungswasserwirtschaft und Verfahrenstechnik, Membrantechnik in der Wasseraufbereitung und Abwasserbehandlung*, Aachen, A7.

Wehrle Umwelt **2005**, Wehrle Umwelt GmbH, *Firmenmitteilung*.

Wienands, H., Streif, G. **2005**, *KA-Wasserwirtschaft, Abwasser, Abfall*, 52, 58–62.

Wintgens, T.; Rosen, J.; Melin, T.; Brepols, C.; Drensla, K.; Engelhardt, N. **2003**, Modelling of a membrane bioreactor system for municipal wastewater treatment, *Journal of Membrane Science*, 216, 55–65.

Wozniak, T. **2003**, Ergebnisse der Untersuchungen zum Membranbelebungsverfahren auf der KA Büchel, *5. Aachener Tagung Siedlungswasserwirtschaft und Verfahrenstechnik, Membrantechnik in der Wasseraufbereitung und Abwasserbehandlung*, Aachen, A4.

# 13
# Production Integrated Water Management and Decentralized Effluent Treatment

## 13.1
## Introduction

Until now, the main point of interest in this book has been biological wastewater treatment. In this chapter we want to expand our perspective to the development of new production processes with reduced consumption levels of water and raw materials and with reduced production of wastewater. For this purpose, we have to direct our interest towards an entire production process and we have to consider new methods to save water and different, mostly non-biological ways to treat water.

Figure 13.1 provides a systematic view to make the following discussions in this chapter more readily understood.

It is necessary to limit the problem to a single state and it is also prudent to discuss the problem with respect to water while keeping in mind that water as well as all impurities may change their state.

Water pollution and wastewater treatment are typically divided into the two different fields of application, i.e. industrial and municipal wastewater. In this chapter, we will consider the production and treatment of industrial wastewater (Fig. 13.1).

*Process integrated water management* is characterized by three management procedures:

1. Minimization of water use may already be an important aim, but it may be that water reuse is not possible or the cases are restricted and the advantages are too small. Only if two or three processes have coupled, multiple use of water can offer a chance for considerable saving. Therefore, a separate discussion of point 1 is necessary.
2. The development of new processes and the optimization of existing or new ones with the aim of saving water, materials and energy must be the first step of water management. The price for fresh water, the costs for wastewater treatment and the charges for discharging into surface waters must be considered to find the best way for a *sustainable development* which is a balance of economical success, environmental protection and social acceptance (Fig. 13.2)
3. The regeneration and recycling of water should be taken into account where there is a short supply of fresh water, which makes it necessary to close water cycles at least partly. Point 3 should be discussed together with point 1.

*Fundamentals of Biological Wastewater Treatment*. Udo Wiesmann, In Su Choi, Eva-Maria Dombrowski

ISBN: 978-3-527-31219-1

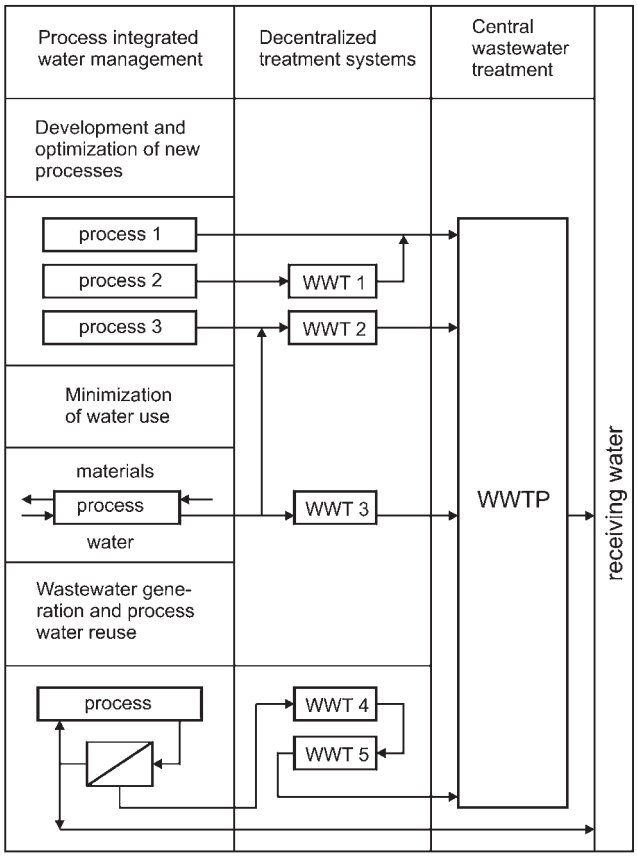


**Fig. 13.1** Schematic of industrial water management as process integrated water management, distributed treatment systems and central wastewater treatment.

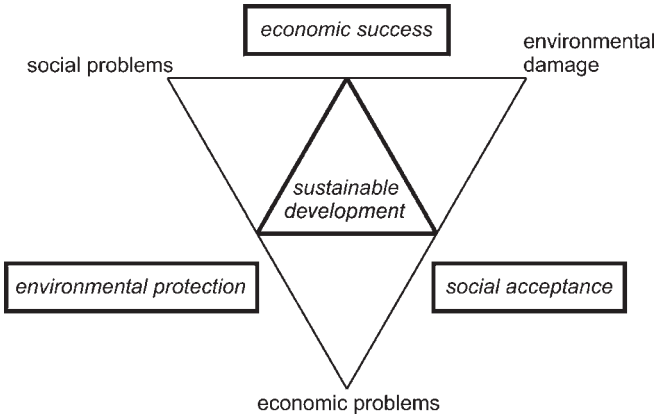


**Fig. 13.2** Sustainability (Christ 1996, 1999).

Decentralized effluent treatment systems can be divided in those with and those without reuse. There are two motivations to treat effluents in a decentralized manner:

- The water is only loaded by components which can be separated easily at low cost, which makes it possible to discharge the treated water directly into a river at no additional cost. The costs may be significantly lower than the amount which would have to be paid to the central WWTP. Another case may be applicable for a highly loaded effluent which can be treated anaerobically without significant sludge production and without aeration costs. It may be cheaper to treat this effluent anaerobically together with several similarly loaded effluents in comparison to a single aerobic stage.
- Following decentralized treatment, the water may be reused in further processes which do not need water with freshwater quality or it can be sent to a larger aerobic industrial or municipal WWTP.

In this chapter, we will explain what process integrated water management and decentralized effluent pretreatment are and how they can be applied in specific industries such as the chemical, pharmaceutical, food, textile, drinks, paper and cellulose, iron and steel industries. To these topics anual meetings take place at University Bremen, Germany (Räbiger 1999). We find the most examples for process integrated water management within the chemical industry. Therefore, this industry is suitable to give examples for the following discussion.

## 13.2
## Production Integrated Water Management in the Chemical Industry

### 13.2.1
### Sustainable Development and Process Optimization

#### 13.2.1.1 Primary Points of View

For a simple and clear overview, we want to discuss the following problems arising during technical-scale chemical synthesis, using an example of a one-step reaction in water:

$$A + B \rightarrow C + D \tag{13.1}$$

It may be possible to produce a mixture of the main product C and the byproduct D in water under *laboratory conditions*. Additionally, we are often left with remaining educts A and B as a result of an incomplete reaction and/or a non-stoichiometric addition. For a homogeneously catalyzed reaction:

$$A + B \xrightarrow[\text{catalysts}]{\text{surfactants}} C + D \tag{13.2}$$

the catalyst is a part of the effluent which also contains an auxiliary, such as a surfactant.

Furthermore, the target or byproduct can be converted during a subsequent reaction, producing a further byproduct E:

$$C + D \rightarrow E \tag{13.3}$$

In a *technical-scale synthesis* large amounts of raw materials are used which frequently contain impurities that can also be transformed by reactions ($N_1 \rightarrow N_1'$, $N_2$ inert). The wastewater produced contains all these materials; and the product C must therefore be separated. Complete separation of C is not economical and thus the target product also contributes additional pollution left in the wastewater. Chemical companies are often interested in changing this situation by developing new processes or by optimizing existing ones, particularly if they were developed several decades ago.

It may be possible to use:

- New ways of chemical synthesis.
- Enzymatic methods or conversions by microorganisms.
- New raw materials with lower impurities content.
- New catalysts with higher selectivity.
- New conditions for the reaction (T, p, pH).
- New methods for saving water (Sections 13.2.2 and 13.2.3) as well as relieving end-of-pipe treatment.
- More effective methods of product seperation from all other materials.

Modernization of existing processes or development of new ones along these lines is not only done to lower the cost of production and waste management but also to obtain products of higher purity and to reduce side-effects of pharmacological products.

#### 13.2.1.2 **Material Flow Management**

The aims described in Section 13.2.1.1 can only be reached if material and energy balances are studied for existing processes and for new concepts. We restrict the following discussion, thus, to a *material (or mass) flow analysis*. Some fundamentals of mass balances were already explained in the section above. This analysis can be divided into several steps:

1. All influent and effluent flow rates in the liquid, solid and gas state must be determined.
2. The concentration of all important components must be measured in these different streams: the influent raw materials A and B and the effluent components C and D (Eq. 13.1), the catalysts and auxiliaries (Eq. 13.2), the byproduct E (Eq. 13.3) and all important impurities $N_1$, $N_2$ and $N_1'$.
3. Do these components change their state by crystallization, condensation or evaporation?
4. Write mass balances for all components and test them by using measurements.

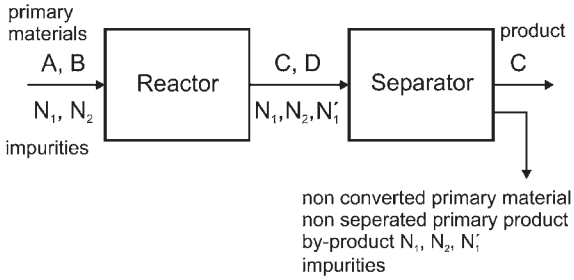


**Fig. 13.3** General schematic of a production process.

After successful tests, the calculation of some characteristic parameters can start. In order to achieve a simpler analysis

- All flow rates are summarized $Q_\Sigma = \Sigma Q_i$.
- We assume there is no change of state.
- Mean concentrations are calculated from mass balances at mixing points, i.e. for the influent:

$$c_{oi} = \frac{\sum_{i=1}^{n} Q_i c_i}{Q_o} \tag{13.4}$$

Figure 13.3 presents a simple scheme describing this situation.

The following considerations follow explanations by Christ (1999), who used masses $m_i = c_i V_i$.

### Stoichiometric Yields

In taking the discussion further, we will introduce stoichiometric coefficients into Eq. (13.1). Normalized to 1 mol A, we obtain:

$$A + Y^o_{B/A} B \rightarrow Y^o_{C/A} C + Y^o_{D/A} D \tag{13.5}$$

$Y^o_{C/A}$ mol C/mol A is the *stoichiometric yield* of the target product C relative to the educt A. It can be calculated from measured values for the converted mass of A $m_A$ and the mass of C formed $m_C$. Using the molar masses of A and C we have:

$$Y^o_{C/A} = \frac{m_C M_A}{m_A M_C} \frac{\text{mol C}}{\text{mol A}} \tag{13.6}$$

The stoichiometric yield has some disadvantages. It gives no information about:

- Other educts contained in Eq. (13.5).
- Other raw materials which may be contained in the total influent mass.
- Subsequent products which may be produced by further reactions.
- Auxiliary materials present, e.g. solvents, surfactants, etc.

Thus, further yield coefficients must be defined.

**Consideration of Secondary Materials**

B, the second educt in Eq. (13.5), gives:

$$Y^{o}_{C/A+B} = \frac{m_C/M_C}{\frac{m_A}{M_A} + \frac{m_B}{M_B}} \frac{\text{mol C}}{\text{mol A} + \text{mol B}} \tag{13.7}$$

$Y^{o}_{C/A+B}$ is smaller than $Y^{o}_{C/A}$ and is decreased remarkably if a larger number of primary raw materials is used:

$$Y^{o}_{C/\Sigma PM} = \frac{m_C/M_C}{\sum_{i=1}^{n} \frac{m_i}{M_i}} \tag{13.8}$$

With Eq. (13.7) or Eq. (13.8), only the first of the four points mentioned above can be considered.

Further definitions regarding the kind and amount of the secondary materials $N_1$ and $N_2$ will be introduced which frequently can only be measured using the units of mass instead of moles. Some of these components are often unknown and their number may be high.

For the *real balance yield*, the result is:

$$Y_{C/A+B+\Sigma N} = \frac{m_C}{m_A + m_B + m_{N1} + m_{N2}} \frac{g}{g} \frac{C}{(A + B + \Sigma N)} \tag{13.9}$$

For higher masses of $N_1$ and $N_2$, the result is remarkably low compared to $Y^{o}_{C/A+B}$. The relation of both is given by the specific real balance yield:

$$Y_{spec} = \frac{Y_{C/A+B+\Sigma N}}{Y^{o}_{C/A+B}} \frac{g\ C\ (\text{mol A} + \text{mol B})}{g\ (A + B + \Sigma N)\ \text{mol C}} \tag{13.10}$$

and indicates the influences of all secondary materials. For $\Sigma N \gg A + B$, the specific real balance yield may be for example $Y_{spec} = 0.15$, influenced by the high amount of secondary raw materials present. From an economical and ecological point of view, a different raw material with a lower amount of secondary substances should be used.

Altogether, there are three important points which should be considered when assessing raw materials: the quality, the price and the cost for environmental protection.

### 13.2.1.3 Production of Naphthalenedisufonic Acid

Aromatic sulfonic acids are produced in large scale plants and are used as surfactants. Naphthalenedisulfonic acids are important intermediate substances for the production of azo dyes (see Section 9.5). Most can only be biodegraded with great difficulty and naphthalene-1,5-disulfonic acid is not biodegradable at all (Krull and Hempel 1994). Only after chemical oxidation with ozone can mineralization by a subsequent aerobic biological treatment be successful (Breithaupt et al. 2003).

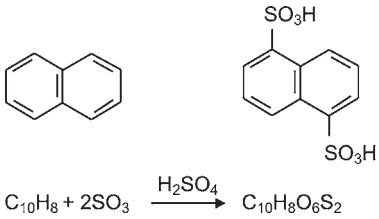


**Fig. 13.4** Formation of 4,8-naphthalenedisulfonic acid.

Some fundamental microbiological studies were published by Nörtemann and Knackmus (1988) and some important biotechnological research by Krull et al. (1991). The following example is discussed in detail by Christ (1999). During the technical synthesis of a desired naphthalenedisulfonic acid (i.e. 4-8-NDSA; Fig. 13.4), temperature, concentration of $H_2SO_4$ and $SO_3$ as well as mean retention time are optimized to obtain the target product at a concentration as high as possible. Nevertheless, some other undesired derivates of NDSA are formed and increase the wastewater load after separation of the desired product.

This process is presented by Fig. 13.5a. Naphthalene is treated with $H_2SO_4$ and $SO_3$ at 50–60 °C. After addition of NaOH and $Na_2SO_4$, NSA precipitates as a sodium salt and can be filtered out.

Besides the target product, several other sodium salts of NSA remain in the filtrate as byproducts. Yet a large amount of different derivates from NSA and NDSA

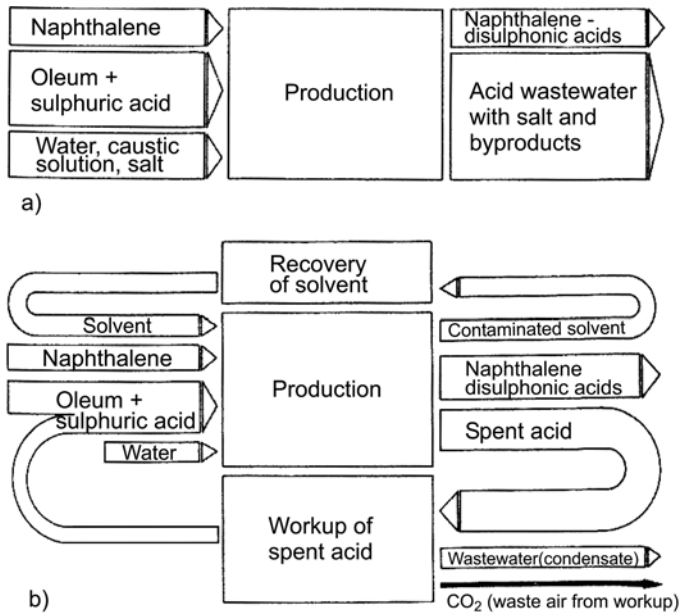


**Fig. 13.5** Bayer AG processes for naphthalenedisulfonic acid production: (a) old process (before 1989, 3000 t $a^{-1}$ COD); (b) new process (after 1989, 3 t $a^{-1}$ COD; Christ 1999).

remained in the filtrate and increased the COD load of the wastewater remarkably, to levels of 3000 t $a^{-1}$ COD.

Only a small amount of this COD could be mineralized in the biological end-of-pipe treatment plant. A modification of the process was absolutely necessary.

The first step for developing a new process was to find a catalyst with a higher selectivity in favor of the product 4-8-DNSA (Bueb et al. 1990). A team from Bayer AG succeeded by replacing the formerly used iron chloride–sulfur catalyst with an iron chloride catalyst. The result was the production of fewer byproducts. But the use of this new catalyst was only possible if sulphuric acid was no longer used as the reaction medium.

The new solvent for naphthalene and $SO_3$, a chlorinated hydrocarbon, allowed a reduction of the reaction temperature. The dehydrating action of $SO_3$ led to the formation of higher molecular structures. The anhydride bridges must be hydrolyzed in the next step by adding the reaction mixture to water. This results in an aqueous sulfonic acid solution, the organic solvent can be separated, and the free sulfuric acid is precipitated by addition of sulfonic acid followed by cooling. After filtration of the precipitated product, the remaining "mother liquor" is regenerated as spent sulfuric acid and recycled.

In the old process, wastewater was produced which contained:

- A high concentration of nafthalene disulfonic acids as byproducts,
- Excess sulfonic acid,
- Inorganic salts for the salting out of the product with subsequent filtration, resuspension and spray drying.

In the new process:

- The portion of the desired product is increased by using a new catalyst with a higher selectivity.
- An organic solvent for naphthalene and $SO_3$ replaces the sulfonic acid which can be regenerated and recycled.
- A portion of the acid used is cleaned by distillation and recycled.
- The salting-out is replaced by a membrane, yielding a dye-free permeate and a concentrate which is spray-dried.

The permeate can be reused as feed water; and its COD is reduced about 80% in comparison to the filtrate of the former process. The condensed vapor of this distillation process is the only wastewater, with a COD load of only 3 t $a^{-1}$. The costs of production are reduced because of the reduced costs for wastewater treatment; and the yield and product quality are somewhat higher than before.

#### 13.2.1.4 **Methodology of Process Improvement**

A systematic approach is necessary if an old process is to be changed to reduce its high costs, such as the costs of wastewater treatment, exhaust gas handling and solid waste disposal. This will be explained using Table 13.1.

**Table 13.1** Different points which must be considered when a new process is to be developed.

| Point | Consideration |
|---|---|
| 1 | New biotechnological process? |
| | 1.1 Catalyzed by an immobilized enzyme? |
| | 1.2 Converted by suspended or immobilized microorganisms? |
| 2 | New chemical process? |
| | 2.1 New method of synthesis<br>Different raw materials<br>Different catalyst with reduced amount of by-products<br>Different reaction conditions (T, p, pH)<br>Other solvent (organics instead of water) |
| | 2.2 New methods of product recovery<br>• Precipitation, filtration<br>• Distillation, condensation<br>• Concentration, spray drying<br>• Ultrafiltration, reverse osmosis |
| | 2.3 Recycling of solvent (water, organics) after removal of impurities<br>Recycling of concentrates with remaining product, primary materials, and catalysts |
| | 2.4 Recovery of a by-product to use as a starting material in a further process<br>Recovery of an auxiliary for reuse |

For a high wastewater flow rate and a high COD concentration, an estimation of the treatment costs lets us know whether it is better to treat it in an end-of-pipe plant or in a decentralized effluent treatment system.

### 13.2.2 Minimization of Fresh Water Use

#### 13.2.2.1 Description of the Problem

A number of different processes must be supplied with water. This water may be used

- for heat transfer processes (cooling, evaporation, condensation, etc.),
- for mass transfer processes (washing, absorption/desorption, distillation/condensation, reaction, etc.).

The rising costs of energy, fresh water and wastewater treatment make it necessary to save both energy and water (Pauli 1997). The following considerations are to be made for water management.

The problem is presented by Fig. 13.6, showing four different water-using processes in parallel, each of them using water for mass transfer processes.

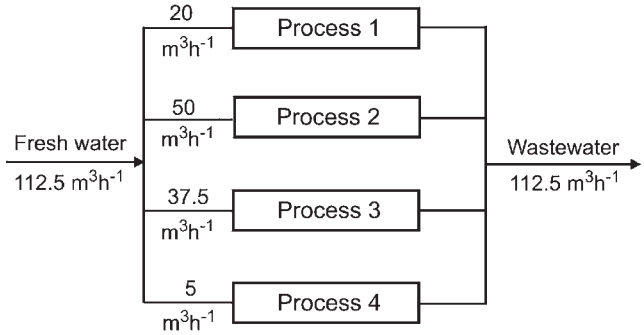


**Fig. 13.6** Fresh water use in each of the four processes leading to a fresh water flow rate of 112.5 $m^3\ h^{-1}$.

Following the discussion of Wang and Smith (1995), Smith et al. (1994) and Baetens (2002), we will at first assume that 112.5 t $h^{-1}$ fresh water are used for all four processes. The mass transfer data are given in Table 13.2.

**Table 13.2** Example for process data of the process of Fig. 13.7.

| Process No. j | Mass load of contaminant $Q\ c_{out}$ (kg $h^{-1}$) | Concentrations $c_{in}$ (kg $m^{-3}$) | $c_{out}$ (kg $m^{-3}$) | Water flow rate Q ($m^3\ h^{-1}$) |
|---|---|---|---|---|
| 1 | 2 | 0 | 0.1 | 20 |
| 2 | 5 | 0 | 0.1 | 50 |
| 3 | 30 | 0 | 0.8 | 37.5 |
| 4 | 4 | 0 | 0.8 | 5 |
| | Σ 41 | | | Σ 112.5 |

For process 1 with a given contaminant mass load of $Q_1\, c_{1,out} = 2$ kg $h^{-1}$ impurities and a given concentration of $c_{1,out} = 0.1$ kg $m^{-3}$, a flow rate of $Q_1 = 20\ m^3\ h^{-1}$ results. Correspondingly for the mass loads of processes 2, 3 and 4 (Table 13.2), given as 5, 30 and 4 kg $h^{-1}$, flow rates of 50, 37.5 and 5 $m^3\ h^{-1}$ can be calculated, which yields a sum of:

$$\sum_{j=1}^{4} Q_j = 112.5\ m^3\ h^{-1} \tag{13.11}$$

How much water do we need if we do not operate the four processes in parallel and look for a more economical water use?

### 13.2.2.2 The Concentration/Mass Flow Rate Diagram and the Graphical Solution

In a water-using mass transfer process, different components are transported to the water (Fig. 13.7a). In the following, we will study only one component. The index i for different compounds can now be omitted.

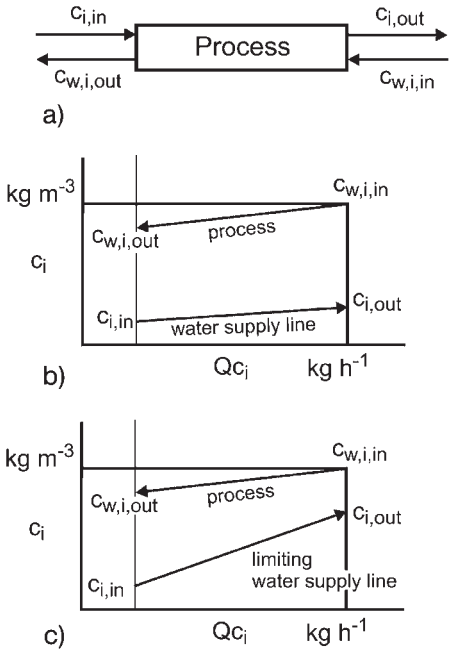


**Fig. 13.7** Concentration/mass flow rate diagram. (a) Schematic of a water using process for impurity. (b) A water-using process in a concentration/mass flow rate diagram, with the water profile not limited for one impurity. (c) The water profile is limited (one impurity).

The concentration of this component (the impurity) decreases inside the process system and increases in the water. This can be demonstrated using a concentration/mass flow rate diagram (Fig. 13.7b). The slopes of the straight lines are the reverse of the flow rate Q. The water flow rate is very high, resulting in a low increase in the concentration $c_i$. In Fig. 13.7c, the water flow rate Q is reduced down to the lowest possible value which is still sufficient to meet the required reduction of $c_{in}$ to $c_{out}$. The lower straight lines are called *water supply lines* and the limiting line in Fig. 13.7c is the *limiting water supply line*. Any water supply line which is below the limiting water supply line will satisfy the process requirements. However, there are also possibilities to save water. How we can find a method to save the greatest possible amount of fresh water without reducing the transferred impurities if there are four processes with different $c_{in}$ and flow rates $Q_j$?

We want to approach the solution step by step. The first step is to construct a concentration/mass flow rate diagram as in Fig. 13.7, one for each of the four processes presented by Fig. 13.6 and Table 13.2.

All four water supply lines start at the point ($c_j = 0$, $Q_j c_j = 0$), but they end at different points $c_{j,out}$, showing different slopes $Q_j$ (Fig. 13.8 and Table 13.2). The total water flow rate is $\Sigma Q_j = 112.5\ m^3\ h^{-1}$.

The next step is a discussion with the process operators which may result in higher permissible $c_{in}$ values for processes 2, 3 and 4 (Table 13.3).

If such a system of process water management is to be realized, the total water flow rate would have to be increased to 170 $m^3\ h^{-1}$ (Table 13.3), much more than if using fresh water for each process (112.5 $m^3\ h^{-1}$, Table 13.2). However, the following considerations will show a way to reduce this water flow rate remarkably.

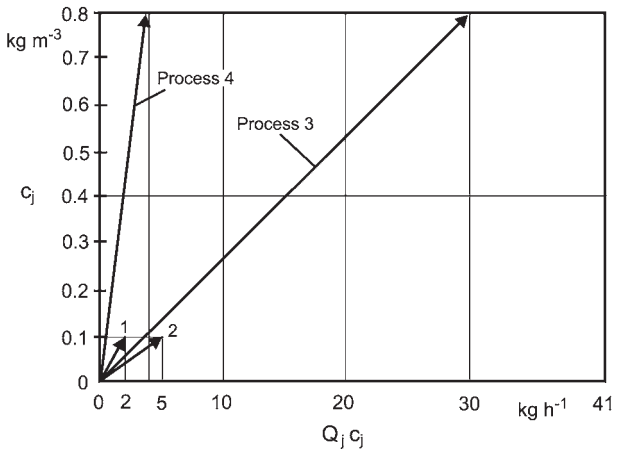


**Fig. 13.8** The four processes j connected in parallel with a fresh water use of 112.5 $m^3\ h^{-1}$ presented in a concentration/mass flow rate diagram.

**Table 13.3** Example for limiting process data (see Fig. 13.9a).

| Process No. j | Mass load of contaminant $Q_j\ c_{out}$ (kg $h^{-1}$) | Concentrations $c_{in}$ (kg $m^{-3}$) | $c_{out}$ (kg $m^{-3}$) | Water flow rate $Q_j$ ($m^3\ h^{-1}$) |
|---|---|---|---|---|
| 1 | 2 | 0 | 0.1 | 20 |
| 2 | 5 | 0.05 | 0.1 | 100 |
| 3 | 30 | 0.05 | 0.8 | 40 |
| 4 | 4 | 0.4 | 0.8 | 10 |
| | Σ 41 | | | Σ 170 |

As a part of the analysis we constructed *one* concentration/mass flow rate diagram for the *four* processes, but there are still no connections between the straight lines (Fig. 13.9a).

The discontinuities in concentrations can be avoided by connecting the points as follows (Fig. 13.9b, based on Table 13.3).

The water for *process 1* must be clean ($c_{1,in} = 0$ kg $m^{-3}$). So the first straight line will not be changed but the second straight line for *process 2*, starting at $c_{2,in} = 0.05$ kg $m^{-3}$, meets the first line at $Qc_{2,in} = 1.0$ kg $h^{-1}$. The straight line for process 3 follows from Table 13.3, by calculating the slope using $\Delta c_j = 0.4 - 0.1 = 0.3$ kg $m^{-3}$ and $\Delta Q_j c_j = 21 - 9 = 12$ kg $h^{-1}$, giving slope = 0.3/12 h $m^{-3}$ and thus Q = 1/slope = 40 $m^3\ h^{-1}$. Figure 13.9b presents the concentration/mass flow rate diagram for a system of four processes characterized by requirements presented by Table 13.3. This curve is called the *limiting composite curve*.

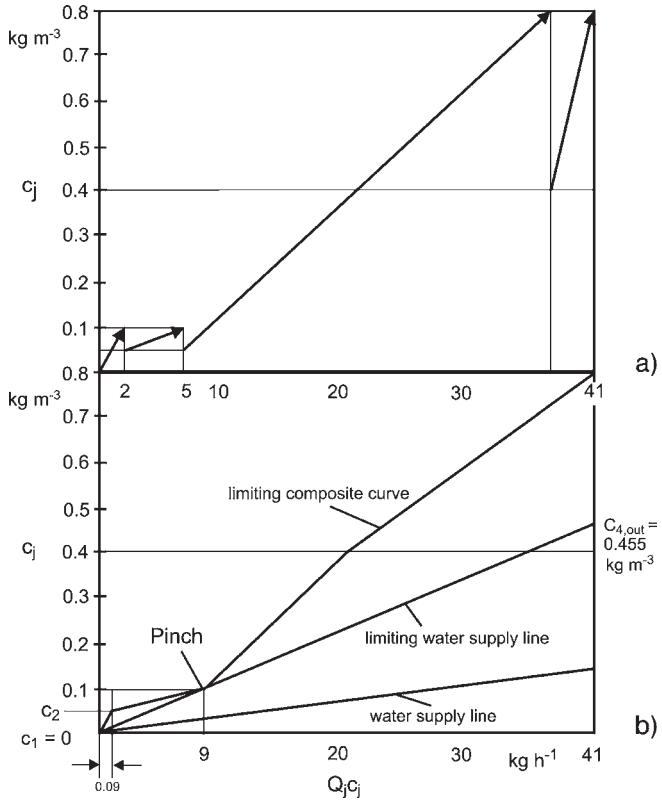


**Fig. 13.9** Limiting composite curve. (a) Limiting water profile. (b) Limiting composite curve with water supply line defining the minimum water flow rate.

In analogy to Fig. 13.7, which presents the concentration/mass flow rate diagram for only one process, it is very interesting to find the limiting water supply line. The straight line with the lower slope plotted in Fig. 13.9b shows a water supply with a relatively high flow rate Q. The lowest possible flow rate $Q_{min}$ can be calculated from the limiting water supply line which touches the limiting composite curve without crossing the line. This point is called a *pinch* (Wang and Smith 1994).

The slope of this limiting water supply line can be calculated using $c_{in}$ = 0 kg $m^{-3}$ and $c_{out,max} = (41 \cdot 0.1)/9 = 0.455$ kg $m^{-3}$.

$$\frac{c_{out,max} - c_{in}}{Q_{min} \cdot c_{out,max}} = \frac{0.455}{41} \text{ m}^{-3}\text{ h} \qquad (13.12)$$

$$Q_{min} = 90 \text{ m}^3\text{ h}^{-1}$$

If we compare this optimized water demand with that of processes connected in parallel we would save:

$$\frac{112.5-90}{112.5} = 20\% \qquad \text{if using clean water and}$$

$$\frac{170-90}{170} = 47\% \qquad \text{if using partly polluted water}$$

But what network of processes do we have to build in order to save this amount of water?

### 13.2.3 The Network Design Method

The inlet and outlet concentrations of the impurity $c_{in}$ and $c_{out}$ and the concentration/mass flow rate diagram with the pinch point form the basis of the recommendations for the network design (see Table 13.3), which yields a minimum wastewater flow rate of 90 $m^3\,h^{-1}$ (Fig. 13.9b). This form of data is used for the construction of a network (Fig. 13.10). Note that there may be more than one way to design a network.

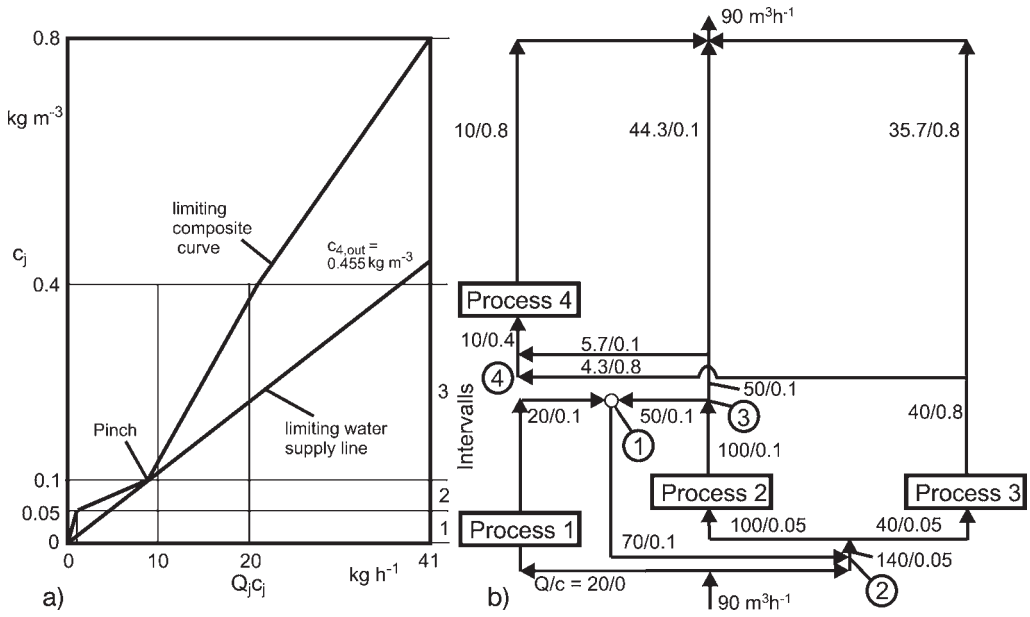


**Fig. 13.10** The design of the water management system. (a) Limiting composite curve with limited water supply line for Q = 90 $m^3\,h^{-1}$. (b) Final design of the wastewater network with four processes for Q = 90 $m^3\,h^{-1}$.

We distinguish three intervals. For the following considerations, we must conform to Table 13.3 and Fig. 13.10.

**Interval 1 (0–0.05 kg m$^{-3}$)**
Only process 1 is considered within interval 1. As follows from Table 13.3, the concentration increases from $c_{1,in} = 0$ to $c_{1,out} = 0.1$ kg m$^{-3}$, giving a water flow rate $Q_1 = 20$ m$^3$ h$^{-1}$, with 70 m$^3$ h$^{-1}$ flowing directly to segment 2.

**Interval 2 (0.05–0.1 kg m$^{-3}$)**
There are two processes located in interval 2. As follows from Table 13.3, the influent concentration of both processes 2 and 3 should be $c_{2,in} = c_{3,in} = 0.05$ kg m$^{-3}$. However, the concentration coming from interval 1 is 0 kg m$^{-3}$ and the flow rate is 70 m$^3$ h$^{-1}$. In order to get 0.05 kg m$^{-3}$, the same flow rate of 70 m$^3$ h$^{-1}$ and an effluent concentration of process 1 and 2 of 0.1 kg m$^{-3}$ must be recycled. After mixing 70/0 with 70/0.1, 140/0.05 is obtained, which is then divided into 100/0.05 for process 2 and 40/0.05 for process 3. Fundamentally, at each of the mixing points 1, 2, 3 and 4, the balances for water (the equation of continuity) and for the impurity (mass balance) can be formulated and solved to calculate the unknown flow rate or concentration. The relatively simple example presented in Fig. 13.10 makes a simpler solution possible.

**Interval 3 (0.1–0.4 kg m$^{-3}$)**
Only process 4 is located in interval 3. The water flow rate for this process is 10 m$^3$ h$^{-1}$ and the influent concentration is 0.4 kg m$^{-3}$ (Table 13.3). We only get these conditions after mixing portions of the effluents from process 2 and process 3. For this purpose, we need two balances for water and for the impurity, as mentioned above:

$$Q'_2 + Q'_3 = Q_4 \tag{13.13}$$

Impurity:

$$Q'_2 c_{2,out} + Q'_3 c_{3,out} = Q_4 c_{4,in} \tag{13.14}$$

where $c_{2,out} = 0.1$ kg m$^{-3}$, $c_{3,out} = 0.8$ kg m$^{-3}$, $c_{4,in} = 0.4$ kg m$^{-3}$. $Q_2$ follows to:

$$Q_2 = \frac{Q_4 c_{4,in} - Q_3 c_{3,out}}{c_{2,out}} \tag{13.15}$$

$$Q_3 = Q_4 - Q_2 \tag{13.16}$$

$$Q_2 = \frac{Q_4 (c_{4,in} - c_{3,out})}{c_{2,out} - c_{3,out}} \tag{13.17}$$

## 13.3 Decentralized Effluent Treatment

### 13.3.1 Minimization of Treated Wastewater

#### 13.3.1.1 Description of the Problem

We assume that a production unit of a factory generates four wastewater streams which are polluted by nearly the same components, giving a COD which can be removed by the same method or type of treatment. The treatment must take place before discharging the treated water into an end-of-pipe treatment plant (WWTP). The COD must be removed down to $c_e$. An example of such a situation is given in Fig. 13.11, showing WWTP 1, 2, 3 and 4 as a situation of a development for a decentralized treatment system. It is assumed that the costs of the pretreatment are proportional to the flow rate. Therefore, the aim of the optimization is to minimize the treated flow rate. This assumption is only one of several possible objectives. However, it makes it easier to explain the procedure. In Fig. 13.11, four different ways to reach the objective are discussed.

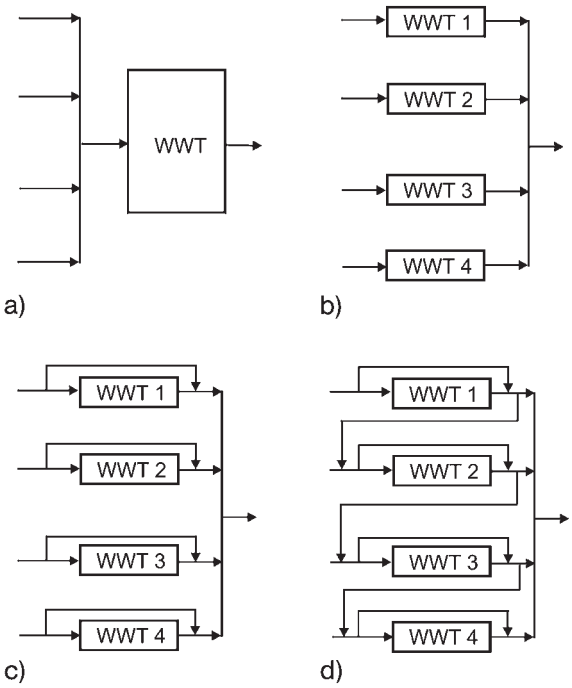


**Fig. 13.11** Decentralized effluent pretreatment systems. (a) One treatment process. (b) Four parallel treatment processes. (c) Four parallel treatment processes with bypasses. (d) Four treatment processes partly connected in parallel, partly in series with bypasses.

In Fig. 13.11a, the streams flow into one treatment plant, where they are mixed and treated together. This method is problematic because a stream with a high flow rate and a low concentration may be mixed with a stream with a low flow rate and a very high concentration.

A better way may be to treat the four streams separately (Fig. 13.11b). The retention time in treatment plant 1 (TP 1) can now be lower because of the low COD and the high flow rate. In contrast, it may be possible to treat another stream in TP 2 or TP 3 using a higher retention time. But there are several reasons to be dissatisfied with this treatment concept and we have not decreased the reactor volume.

This is possible if we reduce the COD in each TP below $c_e$, pumping only part of the four streams each in parallel to the TPs and mixing them all together to obtain the required $c_e$ (Fig. 11.13c).

A further way to reduce the reactor volume is presented by Fig. 13.11d. The TPs are connected in parallel and in series. The part of the wastewater which is treated in parallel can be decreased by increasing the part being treated in series. Several possibilities are given to optimize this treatment process. The part of the recycled wastewater in WWT 1 can influence that of the following WWTs. A strategy is necessary to find an optimized solution to a given problem. The method described in the next section was published by Wang and Smith (1994).

### 13.3.1.2 Representation of Treatment Processes in a Concentration/ Mass Flow Rate Diagram

Initially, we want to discuss the influence of a bypass on only one treatment plant. The lower line in Fig. 13.12 shows the wastewater stream with an influent concentration $c_{in}$, for example, in g $L^{-1}$ COD and a lower flow rate Q.

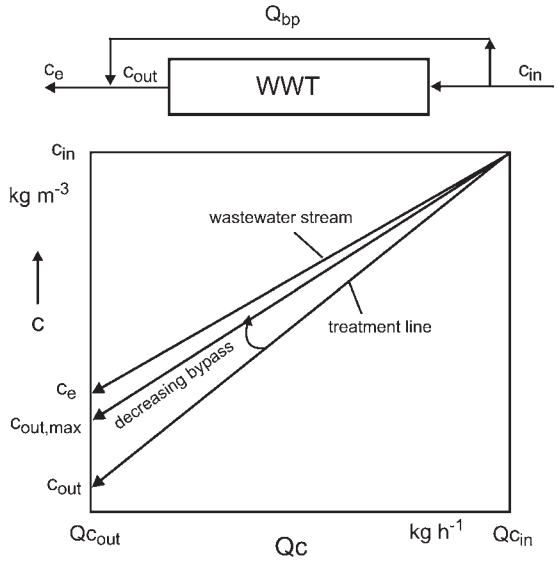


**Fig. 13.12** Concentration/ mass flow rate diagram for one treatment plant with bypass.

An effluent concentration $c_e$ is given. The rest of the flow rate flows through the bypass. The concentration $c_{out}$ before mixing with the bypass wastewater is relative low owing to the relative high mean retention time inside the reactor. With decreasing bypass, $c_{out}$ increases and finally reaches $c_{out,max}$, the highest allowed effluent concentration, which should not be exceeded. $c_{out,max}$ can be calculated using a mass balance and the given concentration $c_e$.

In the next step, several treatment plants either without bypass (Fig. 13.11b) or with bypass (Fig. 13.11c) are connected in parallel. The concentration/mass flow rate diagrams for four plants are presented in Fig. 13.13. In Fig. 13.13a, the effluent concentrations are lower than $c_e$ in three of the four plants because all the wastewater goes directly through the treatment plants. By adjusting bypass flow rates, the situation presented in Fig. 13.13b can be obtained: the effluent concentrations in all four treatment systems agree at $c_e$.

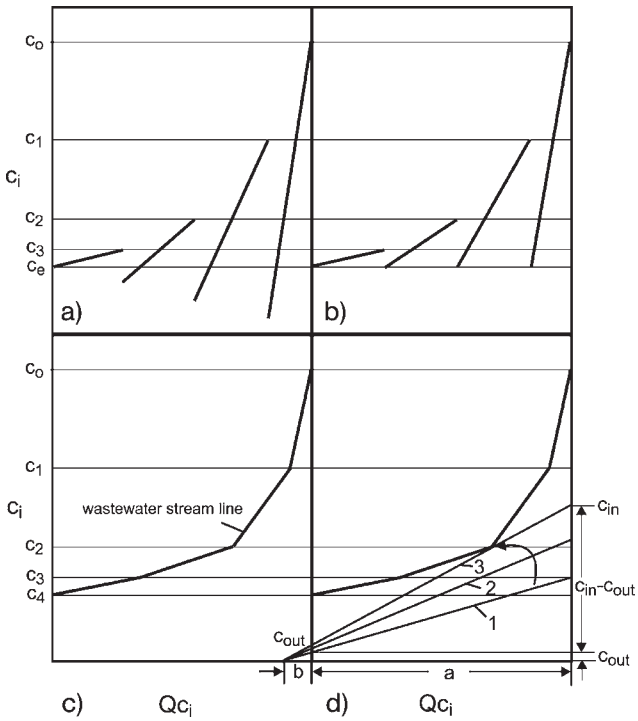


**Fig. 13.13** Decentralized effluent pretreatment process in the concentration/mass flow rate diagram. (a) (Treatment in) parallel plants, partly with lower effluent concentration than the required $c_e$. (b) (Treatment in) parallel plants, all with the required effluent concentrations $c_e$. (c) (Treatment by) using the parallel/series portion and the bypasses of all four plants. (d) Construction of the treatment lines for higher flow rates (curve 1 and curve 2) and for the lowest possible flow rate Q (curve 3).

Up to here, all WWTs have been connected in parallel. Now, we wish to combine the lowest points in Fig. 13.13b by connecting the highest point of the first plant with the lowest point of the second plant. To do this, we will change: (a) the parallel/series portion and (b) the bypass of all four plants. This changes the flow rates in each of the plants as well as the concentrations of the influent wastewater, giving $c_1$, $c_2$, $c_3$ and $c_4$ (Fig. 13.13c).

#### 13.3.1.3 The Lowest Wastewater Flow Rate to Treat

Now we search for the treatment line with the lowest flow rate. To achieve this, we have to know the desired degree of removal:

$$\alpha = \frac{c_{in} - c_{out}}{c_{in}} \tag{13.18}$$

The highest removal $\alpha$ follows from curve 3:

$$\frac{c_{in} - c_{out}}{c_{in}} = \frac{a}{a+b} = \alpha = \text{const} \tag{13.19}$$

it characterises the three triangle in Fig. 13.13d. The lowest treatment line 1 and the middle line 2 are possible solutions of the wastewater treatment, but the flow rates $Q_1$ and $Q_2$, the reciprocal inclinations, are relatively high. Only treatment line 3, which touches the wastewater stream line, represents a solution of the problem using the lowest possible flow rate $Q_3$ (Fig. 13.13d). A straight line with a larger slope crosses the wastewater stream line at two points (not plotted here). It represents an impossible solution because mass balances are not fulfilled (Wang and Smith 1994).

After obtaining the fundamental solution for $Q_{min}$, $c_{in}$ and $c_{out}$, a study of the design of the treatment system must follow. We will not go further into details here and will take up this question in Problem 13.2. We are convinced that there is a need to use this type of method to save water in industry.

### 13.3.2 Processes for Decentralized Effluent Treatment

The target of this optimization procedure is to reduce the amount of wastewater to the lowest possible level. This can be performed

- for continuous production processes and
- for batch processes with large storage tanks which can be employed to realize nearly constant flow rates during filling.

Often, discontinuous treatment processes must be used and other optimization methods are needed. Physico-chemical processes are especially suited (Bueb et al. 1990, Kollatsch 1990), e.g.:

- stripping
- distillation, rectification
- extraction
- adsorption, absorption
- precipitation, flocculation
- wet oxidation
- evaporation
- incineration, etc.

In future, some membrane technology processes will become useful alone or in combination with a bioreactor (Chapter 12) or with one of the processes mentioned above. Fundamentally, all biological treatment processes discussed in detail in Chapters 5 to 11 may be interesting, if the cost is low compared with other treatment processes.

**PROBLEM 13.1**

For a reaction given by Eq. (13.5), the masses and molar masses of the educts A and B and the product C are:

$m_A = 50$ kg, $M_A = 70$ g mol$^{-1}$
$m_B = 22$ kg, $M_B = 140$ g mol$^{-1}$
$m_C = 45$ kg, $M_C = 74$ g mol$^{-1}$

The masses of the secondary materials $N_1$ and $N_2$ are:

$m_{N1} = 25$ kg and $m_{N2} = 17$ kg

Calculate the stoichiometric yields, $Y^o_{C/A}$ and $Y^o_{C/A+B}$, the real balance yield $Y_{C/A+B+\Sigma N}$ and the specific real balance yield $Y_{spec}$.

**Solution**

$$Y^o_{C/A} = \frac{m_C M_A}{m_A M_C} = \frac{45 \cdot 70}{74 \cdot 50} \frac{\text{mol C}}{\text{mol A}} = 0.942 \triangleq 94.2\%$$

$$Y^o_{C/A+B} = \frac{m_C/M_C}{\frac{m_A}{M_A} + \frac{m_B}{M_B}} = 0.698 \triangleq 69.8\%$$

$$Y^o_{C/A+B+\Sigma N} = \frac{m_C}{m_A + m_B + m_{N1} + m_{N2}} = \frac{45}{50 + 22 + 25 + 17} = 0.395 \triangleq 39.5\%$$

$$Y_{spec} = \frac{Y_{C/A+B+\Sigma N}}{Y^o_{C/A+B}} = \frac{0.395}{0.698} = 0.566 \triangleq 56.6\%$$

Results:

- 69.8% of the moles from both educts are obtained as product C;
- 39.4% of the mass from all primary and secondary materials are obtained as product C;
- the specific real balance yield $Y_{spec}$ can be increased by using better raw materials from 56.6% up to 100%.

## PROBLEM 13.2

The calculation of stoichiometric relations is surely a very simple example for the first part of material flow management. The next part is the study of the main mass balances, i.e. the foundation for process optimization.

For this problem, the flow rates and inlet concentrations for three effluent streams are given in Table 13.4 (Wang and Smith 1994). The total flow rate is 90 $m^3\ h^{-1}$.

The limit effluent concentration must be $c_e = 20\ mg\ L^{-1}$ DOC. Only a part of this wastewater is to be treated to a removal degree of $\alpha = 0.99$ and as low a flow rate as possible should be treated. The composite curve with the three wastewater streams is shown in Fig. 13.14.

The total mass flow rate in the influent is $Qc_{in} = 17.8\ kg\ h^{-1}$ DOC. The limiting wastewater stream line goes through the pinch (0.1/5.8) and forms two similar triangles with the ordinate and abscissa of Fig. 13.14.

Calculate the limit flow rate of the treated water and design a network for the water system.

**Table 13.4** Wastewater streams for Problem 13.2 (Wang and Smith 1994).

| Stream No. j | Flow rate $Q_j$ ($m^3\ h^{-1}$) | Concentration $c_j$ ($kg\ m^{-3}$) |
|---|---|---|
| 1 | 40 | 0.4 |
| 2 | 30 | 0.1 |
| 3 | 20 | 0.03 |

### Solution

Comparing the largest and the smallest triangle in Fig. 13.14 and using $c_{out} = 0.01 \cdot c_{in}$, it follows that:

$$\frac{c_{in}}{17.8 + a} = \frac{c_{out}}{a} = \frac{0.01\, c_{in}}{a}$$

and it can be calculated that: $a = 0.18\ kg\ h^{-1}$ COD.

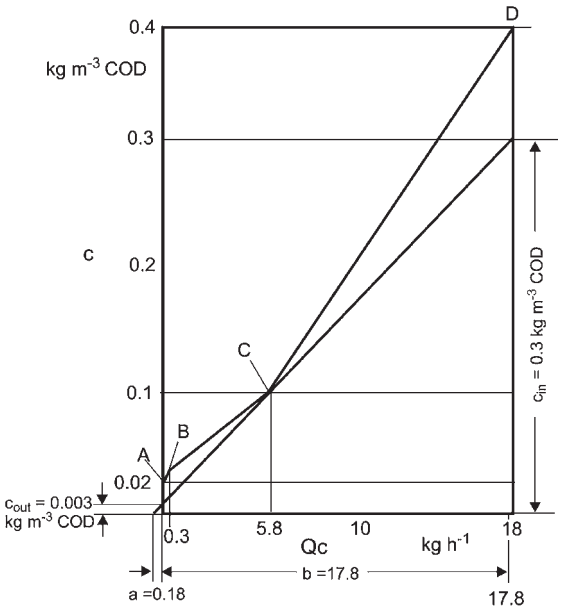


**Fig. 13.14** Construction of the limiting water supply line for a given removal $\alpha = 0.99$ (and three processes).

From the upper smaller and the largest triangles:

$$\frac{c_{in}-0.1}{17.8-5.8} = \frac{c_{in}}{17.8+0.18}$$

$c_{in} = 0.300$ kg m$^{-3}$ COD is obtained as the allowed influent concentration for the flow rate of:

$$Q = \frac{17.8}{0.3} = 59.33 \text{ m}^3 \text{ h}^{-1}$$

Only $59.33 \approx 60$ m$^3$ h$^{-1}$, respectively ~ 66.6% must be treated.

An obvious solution would be to treat the effluent from process 1. But the flow rate is too low and the concentration is too high. A better strategy is to use a part of the effluent from process 2 for mixing with the effluent of process 1 and a second part for mixing with the effluent from process 3 (Fig. 13.15).

Starting with $c_{in} = 0.3$ kg m$^{-3}$ DOC and $\alpha = 0.99$, $c_{out}$ is obtained from:

$$\alpha = \frac{c_{in}-c_{out}}{c_{in}}, \; c_{out} = c_{in}\,(1-\alpha), \; c_{out} = 0.003 \text{ kg m}^{-3}$$

To obtain $Q_{1,2}$, the flow rate from process 2 is mixed with that of process 1; and a further mass balance at mixing point M1 is:

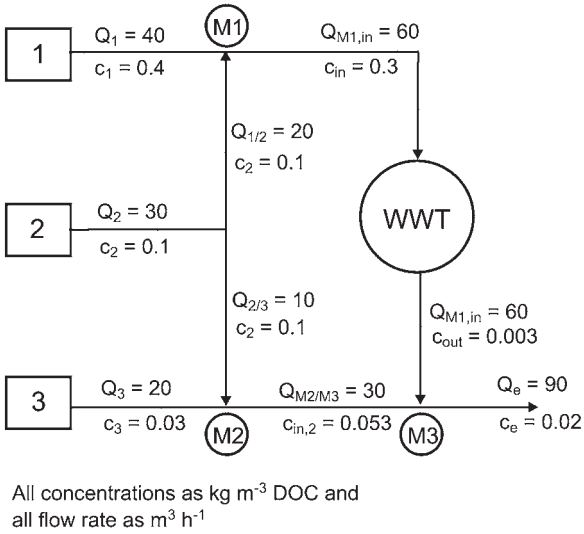


**Fig. 13.15** Construction of a water network considering the results of Fig. 13.14

$$Q_1 c_1 + Q_{1/2} c_2 = Q_{M1,in} c_{in}$$

giving:

$$Q_{1/2} = \frac{Q_{M1,in} c_{in} - Q_1 c_1}{c_2}$$

with:

$c_2 = 0.1$ kg m$^{-3}$ DOC.

It then follows that: $Q_{1/2} = 20$ m$^3$ h$^{-1}$.

With two further mass balances, we are able to test whether the limit of $c_e = 0.020$ kg m$^{-3}$ DOC is upheld:

1. The concentration after mixing effluent from processes 2 and 3 at mixing point M2 is:

$$20 \cdot 0.03 + 10 \cdot 0.1 = 30 \cdot c_{in,2}$$

$$c_{in,2} = \frac{20 \cdot 0.03 + 10 \cdot 0.1}{30} = 0.053 \text{ kg m}^{-3} \text{ DOC}$$

2. The concentration after mixing at mixing point M3 is:

$$30 \cdot 0.053 + 60 \cdot 0.003 = 90 \cdot c_e$$

$$c_e = \frac{30 \cdot 0.053 + 60 \cdot 0.003}{90} = 0.019 \approx 0.020 \text{ kg m}^{-3} \text{ DOC}$$

The proposed network for the treatment of three wastewater streams is suitable to undercut the required limit of:

$c_e = 0.020 \text{ kg m}^{-3} \text{ DOC} > 19 \text{ mg L}^{-1} \text{ DOC}$

Thus, 30 $m^3$ of the wastewater must not be treated.

## References


Baetens, D. **2002**, Water pinch analysis: minimisation of water and wastewater in the process industry, Water Recycling and Resource Recovery in Industry, Lens, P., L. H. Wilderer, P. and Asano, T. (Eds.), IMA Publishing, 207–222.

Breithaupt, T.; Reemtsma, T.; Jekel, M.; Storm, T.; Wiesmann, U. **2003**, Combined biological treatment/ozonation of wastewater for the mineralization of non-biodegradable naphtholine-1,5-disulfonic acid, *Acta Biotechnology* 23, 321–333.

Bueb, M.; Finzenhagen, M.; Mann, T.; Müller, K. **1990**, Verminderung der Abwasseremission in der chemischen Industrie durch Verfahrensumstellungen und Teilstrombehandlungen, *Korrespondenz Abwasser* 37, 542–558

Christ, C. **1996**, Integrated environmental protection reduces environmental impact, *Chemical Technology Europe* 3, 19.

Christ, C. (ed) **1999**, *Production Integrated Environmental Protection and Waste Management in the Chemical Industry*, Wiley-VCH, Weinheim.

Kollatsch, D. **1990**, Industrielles Wassersparen und Abwasserreinigen schaffen neue Dimensionen, *Korrespondenz Abwasser* 37, 560–564.

Krull, R.; Hempel, D.C. **1994**, Biodegradation of naphtaline sulfonic acid-containing sewage in a two-stage treatment plant, *Bioprocess Engineering* 10, 229–234.

Krull, R.; Nörtemann, B.; Kuhm, A.; Hempel, D.C.; Knackmuss, H.-J. **1991**, Der bakterielle Abbau von 2,6-Naphtalindisulfonsäure mit immobilisierten Mikroorganismen, *gwf Wasser-Abwasser* 132, 352–354.

Nörtemann, B.; Knackmuss, H.-J. **1988**, Abbau sulfonierter Aromaten, *gwf Wasser-Abwasser* 129, 75–79.

Pauli, G. **1997**, Zero emissions: the ultimate goal of cleaner production, *J. Cleaner Prod.* 5, 109–113.

Räbiger, N. **1999**, Future Aspects – Clean Production, Biotechnology Vol. 11a, Environmental Processes I, J. Winter (ed.), Wiley-VCH, Weinheim, 561–577.

Smith, R.; Petela, E.; Wang, Y.P. **1994**, Water, water everywhere ..., *The Chemical Engineer* 12, 21–24.

Wang, Y.-P.; Smith, R. **1994**, Design of distributed effluent treatment systems, *Chem. Eng. Sci.* 49, 3127–3145.

Wang, Y.P.; Smith, R. **1995**, Wastewater minimization with flowrate constraints, *Trans. IchemE.* 73, 889.

# Subject Index



*Fundamentals of Biological Wastewater Treatment*. Udo Wiesmann, In Su Choi, Eva-Maria Dombrowski

ISBN: 978-3-527-31219-1

## *Related Titles*

P. Quevauviller, M.-F. Pouet, O. Thomas, A. Van Der Berken (Eds.)

**Wastewater Quality Monitoring**

**On-line Methods**

2007. ISBN 978-0-471-49929-9

B. Kamm, P. R. Gruber, M. Kamm (Eds.)

**Biorefineries – Industrial Processes and Products**

**Status Quo and Future Directions**

2006. ISBN 978-3-527-31027-2

F. J. Keil (Ed.)

**Modeling of Process Intensification**

2006. ISBN 978-3-527-31143-9

L. Puigjaner, G. Heyen (Eds.)

**Computer Aided Process and Product Engineering**

2006. ISBN 978-3-527-30804-0

K. Sundmacher, A. Kienle, A. Seidel-Morgenstern (Eds.)

**Integrated Chemical Processes**

**Synthesis, Operation, Analysis, and Control**

2005. ISBN 978-3-527-30831-6

G. Bitton

**Wastewater Microbiology**

2005. ISBN 978-0-471-65071-3

V. Hessel, S. Hardt, H. Löwe, A. Müller, G. Kolb

**Chemical Micro Process Engineering**

**2 Volumes**

2005. ISBN 978-3-527-31407-2

V. Hessel, H. Löwe, A. Müller, G. Kolb

**Chemical Micro Process Engineering**

**Processing and Plants**

2005. ISBN 978-3-527-30998-6

M. H. Gerardi, M. C. Zimmerman

**Wastewater Pathogens**

2004. ISBN 978-0-471-20692-7

Wiley-VCH (Ed.)

**Ullmann's Processes and Process Engineering**

2004. ISBN 978-3-527-31096-8